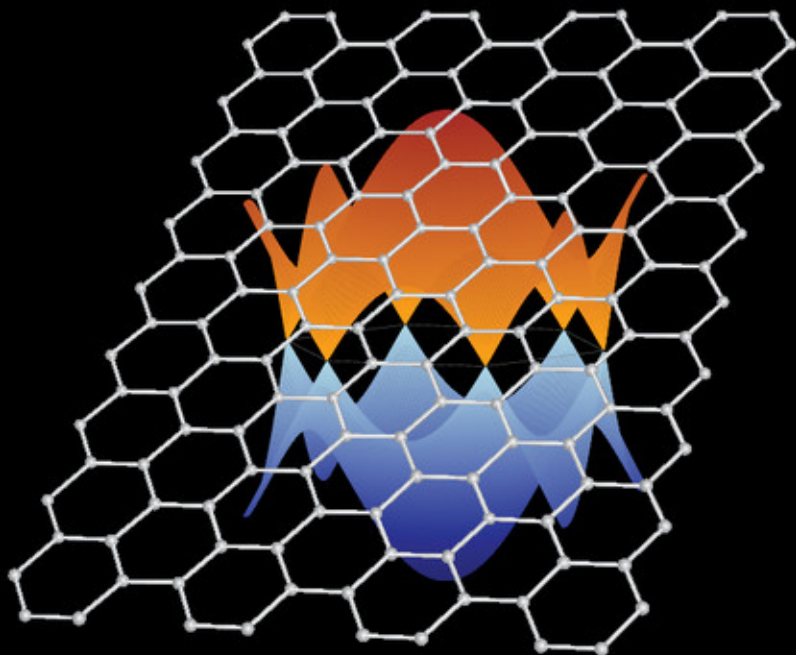


Thomas Wolfram and Sinași Ellialtıoğlu

# Applications of Group Theory to Atoms, Molecules and Solids



CAMBRIDGE



## APPLICATIONS OF GROUP THEORY TO ATOMS, MOLECULES, AND SOLIDS

The majority of all knowledge concerning atoms, molecules, and solids has been derived from applications of group theory. Taking a unique, applications-oriented approach, this book gives readers the tools needed to analyze any atomic, molecular, or crystalline solid system.

Using a clearly defined, eight-step program, this book helps readers to understand the power of group theory, what information can be obtained from it, and how to obtain it. The book takes in modern topics, such as graphene, carbon nanotubes, and isotopic frequencies of molecules, as well as more traditional subjects: the vibrational and electronic states of molecules and solids, crystal-field and ligand-field theory, transition-metal complexes, space groups, time-reversal symmetry, and magnetic groups.

With over a hundred end-of-chapter exercises, this book is invaluable for graduate students and researchers in physics, chemistry, electrical engineering, and materials science.

THOMAS WOLFRAM is a former Chairman and Professor of the Department of Physics and Astronomy, University of Missouri-Columbia. He has founded a science and technology laboratory for a major company and started a company that manufactured diode-pumped, fiber-optic transmitters and amplifiers.

ŞİNASİ ELLİALTIOĞLU is a former Chairman and Professor of Physics at the Middle East Technical University in Ankara, Turkey. He has been a recipient of Humboldt and Fulbright Fellowships. Currently he is a Professor of Physics and Director of Basic Sciences at TED University in Ankara.



# APPLICATIONS OF GROUP THEORY TO ATOMS, MOLECULES, AND SOLIDS

THOMAS WOLFRAM

*Formerly of the University of Missouri-Columbia*

ŞİNASİ ELLİALTIOĞLU

*TED University, Ankara*

*Formerly of Middle East Technical University, Ankara*



CAMBRIDGE  
UNIVERSITY PRESS

CAMBRIDGE  
UNIVERSITY PRESS

University Printing House, Cambridge CB2 8BS, United Kingdom

Published in the United States of America by Cambridge University Press, New York

Cambridge University Press is part of the University of Cambridge.

It furthers the University's mission by disseminating knowledge in the pursuit of education, learning, and research at the highest international levels of excellence.

[www.cambridge.org](http://www.cambridge.org)

Information on this title: [www.cambridge.org/9781107028524](http://www.cambridge.org/9781107028524)

© T. Wolfram and Ş. Ellialtıoğlu 2014

This publication is in copyright. Subject to statutory exception and to the provisions of relevant collective licensing agreements, no reproduction of any part may take place without the written permission of Cambridge University Press.

First published 2014

Printed in the United Kingdom by CPI Group Ltd, Croydon CR0 4YY

*A catalogue record for this publication is available from the British Library*

*Library of Congress Cataloguing in Publication data*

Wolfram, Thomas, 1936–

Applications of group theory to atoms, molecules, and solids / Thomas Wolfram, Şinasi Ellialtıoğlu.  
pages cm

ISBN 978-1-107-02852-4 (hardback)

1. Solids – Mathematical models. 2. Molecular structure. 3. Atomic structure. 4. Group theory.  
I. Title.

QC176.W65 2013

530.4'1015122–dc23

2013008434

ISBN 978-1-107-02852-4 Hardback

Cambridge University Press has no responsibility for the persistence or accuracy of URLs for external or third-party internet websites referred to in this publication, and does not guarantee that any content on such websites is, or will remain, accurate or appropriate.

# Contents

<i>Preface</i>	<i>page xi</i>
1 Introductory example: Squarene	1
1.1 In-plane molecular vibrations of squarene	1
1.2 Reducible and irreducible representations of a group	12
1.3 Eigenvalues and eigenvectors	27
1.4 Construction of the force-constant matrix from the eigenvalues	30
1.5 Optical properties	31
References	34
Exercises	35
2 Molecular vibrations of isotopically substituted $AB_2$ molecules	39
2.1 Step 1: Identify the point group and its symmetry operations	39
2.2 Step 2: Specify the coordinate system and the basis functions	39
2.3 Step 3: Determine the effects of the symmetry operations on the basis functions	41
2.4 Step 4: Construct the matrix representations for each element of the group using the basis functions	41
2.5 Step 5: Determine the number and types of irreducible representations	42
2.6 Step 6: Analyze the information contained in the decompositions	42
2.7 Step 7: Generate the symmetry functions	43
2.8 Step 8: Diagonalize the matrix eigenvalue equation	50
2.9 Constructing the force-constant matrix	50
2.10 Green's function theory of isotopic molecular vibrations	52
2.11 Results for isotopically substituted forms of $H_2O$	60

References	62
Exercises	62
3 Spherical symmetry and the full rotation group	66
3.1 Hydrogen-like orbitals	66
3.2 Representations of the full rotation group	68
3.3 The character of a rotation	72
3.4 Decomposition of $D^{(l)}$ in a non-spherical environment	75
3.5 Direct-product groups and representations	76
3.6 General properties of direct-product groups and representations	79
3.7 Selection rules for matrix elements	83
3.8 General representations of the full rotation group	85
References	88
Exercises	88
4 Crystal-field theory	90
4.1 Splitting of $d$ -orbital degeneracy by a crystal field	90
4.2 Multi-electron systems	95
4.3 Jahn–Teller effects	116
References	119
Exercises	119
5 Electron spin and angular momentum	123
5.1 Pauli spin matrices	123
5.2 Measurement of spin	126
5.3 Irreducible representations of half-integer angular momentum	127
5.4 Multi-electron spin–orbital states	129
5.5 The $L$ – $S$ -coupling scheme	130
5.6 Generating angular-momentum eigenstates	132
5.7 Spin–orbit interaction	138
5.8 Crystal double groups	150
5.9 The Zeeman effect (weak-magnetic-field case)	153
References	155
Exercises	156
6 Molecular electronic structure: The LCAO model	158
6.1 $N$ -electron systems	158
6.2 Empirical LCAO models	162
6.3 Parameterized LCAO models	163
6.4 An example: The electronic structure of squareene	168
6.5 The electronic structure of $\text{H}_2\text{O}$	182



References	188
Exercises	189
7 Electronic states of diatomic molecules	193
7.1 Bonding and antibonding states: Symmetry functions	193
7.2 The “building-up” of molecular orbitals for diatomic molecules	198
7.3 Heteronuclear diatomic molecules	206
Exercises	209
8 Transition-metal complexes	211
8.1 An octahedral complex	211
8.2 A tetrahedral complex	227
References	237
Exercises	237
9 Space groups and crystalline solids	239
9.1 Definitions	239
9.2 Space groups	244
9.3 The reciprocal lattice	246
9.4 Brillouin zones	247
9.5 Bloch waves and symmorphic groups	249
9.6 Point-group symmetry of Bloch waves	252
9.7 The space group of the $\mathbf{k}$ -vector, $g_{\mathbf{k}}^s$	258
9.8 Irreducible representations of $g_{\mathbf{k}}^s$	259
9.9 Compatibility of the irreducible representations of $g_{\mathbf{k}}$	260
9.10 Energy bands in the plane-wave approximation	265
References	276
Exercises	276
10 Application of space-group theory: Energy bands for the perovskite structure	280
10.1 The structure of the $ABO_3$ perovskites	280
10.2 Tight-binding wavefunctions	282
10.3 The group of the wavevector, $g_{\mathbf{k}}$	283
10.4 Irreducible representations for the perovskite energy bands	284
10.5 LCAO energies for arbitrary $\mathbf{k}$	298
10.6 Characteristics of the perovskite bands	300
References	301
Exercises	302

11 Applications of space-group theory: Lattice vibrations	304
11.1 Eigenvalue equations for lattice vibrations	305
11.2 Acoustic-phonon branches	309
11.3 Optical branches: Two atoms per unit cell	314
11.4 Lattice vibrations for the perovskite structure	320
11.5 Localized vibrations	327
References	334
Exercises	334
12 Time reversal and magnetic groups	337
12.1 Time reversal in quantum mechanics	337
12.2 The effect of $\mathbb{T}$ on an electron wavefunction	340
12.3 Time reversal with an external field	341
12.4 Time-reversal degeneracy and energy bands	342
12.5 Magnetic crystal groups	346
12.6 Co-representations for groups with time-reversal operators	350
12.7 Degeneracies due to time-reversal symmetry	357
References	361
Exercises	361
13 Graphene	363
13.1 Graphene structure and energy bands	363
13.2 The analogy with the Dirac relativistic theory for massless particles	368
13.3 Graphene lattice vibrations	369
References	381
Exercises	381
14 Carbon nanotubes	383
14.1 A description of carbon nanotubes	384
14.2 Group theory of nanotubes	386
14.3 One-dimensional nanotube energy bands	393
14.4 Metallic and semiconducting nanotubes	401
14.5 The nanotube density of states	403
14.6 Curvature and energy gaps	406
References	407
Exercises	407
<i>Appendix A</i> Vectors and matrices	410
<i>Appendix B</i> Basics of point-group theory	415

<i>Appendix C</i>	Character tables for point groups	430
<i>Appendix D</i>	Tensors, vectors, and equivalent electrons	442
<i>Appendix E</i>	The octahedral group, $O$ and $O_h$	449
<i>Appendix F</i>	The tetrahedral group, $T_d$	455
<i>Appendix G</i>	Identifying point groups	462
<i>Index</i>		465



## Preface

The majority of all knowledge accumulated in physics and chemistry concerning atoms, molecules, and solids has been derived from applications of group theory to quantum systems.

My (T.W.) first encounter with group theory was as an undergraduate in physics, struggling to understand Wigner's *Group Theory and Its Application to the Quantum Mechanics of Atomic Spectra* (1959). I felt there was something magical about the subject. It was amazing to me that it was possible to analyze a physical system knowing only the symmetry and obtain results that were absolute, independent of any particular model. To me it was a miracle that it was possible to find some exact eigenvectors of a Hamiltonian by simply knowing the geometry of the system or the symmetry of the potential.

Many books devote the initial chapters to deriving abstract theorems before discussing any of the applications of group theory. We have taken a different approach. The first chapter of this book is devoted to finding the molecular vibration eigenvalues, eigenvectors, and force constants of a molecule. The theorems required to accomplish this task are introduced as needed and discussed, but the proofs of the theorems are given in the appendices. (In later chapters the theorems needed for the analysis are derived within the discussions.) By means of this applications-oriented approach we are able to immediately give a general picture of how group theory is applied to physical systems. The emphasis is on the process of applying group theory. The various steps needed to analyze a physical system are clearly delineated. By the end of the first chapter the reader should have an appreciation for the power of group theory, what information can be obtained, and how to obtain it. That is, the "magic" of group theory should already be apparent.

In addition to the essential, traditional topics, there are new topics, including the electronic and vibrational properties of graphene and nanotubes, the vibrations of isotopically substituted molecules, localized vibrations, and discussions of the axially symmetric lattice dynamics model. The energy bands and vibrational

normal modes of crystals with the perovskite structure are also discussed in detail.

The material in this book was developed in part from group-theory courses and from a series of lectures presented in courses on special topics at the University of Missouri-Columbia. It is appropriate for science and engineering graduate students and advanced undergraduate seniors. The ideal reader will have had a course in quantum mechanics and be familiar with eigenvalue problems and matrix algebra. However, no prerequisite knowledge of group theory is necessary.

This book may be employed as a primary text for a first course in group theory or as an auxiliary book for courses in quantum mechanics, solid-state physics, physical chemistry, materials science, or electrical engineering. It is intended as a self-teaching tool and therefore the analyses in the early chapters are given in some detail. Each chapter includes a set of exercises designed to reinforce and extend the material discussed in the chapter.

Thomas Wolfram  
and  
Şinasi Ellialtıoğlu

# 1

## Introductory example: Squarene

In this chapter we illustrate the solution of a simple physical problem in order to familiarize the reader with the procedures used in the group-theoretical analysis. Since this is the initial chapter, we shall give nearly all of the details involved in the analysis. Some readers familiar with group theory may find that the discussion includes too much detail, but we would rather be clear than brief. In later chapters less detail will be required since the reader will by then be familiar with the analysis method.

Theorems from group theory are stated and discussed when employed in the analysis, but the proofs of the theorems are not presented in this chapter. Readers interested in the proofs can find them in Appendix B or refer to a number of excellent standard group-theory texts [1.1].

The procedures employed in this chapter are simple but somewhat tedious and not the most efficient way to analyze the simple example discussed. However, these procedures will prove extremely valuable when we are faced with more complex problems. Therefore the reader is encouraged to work through the details of the chapter and the exercises at the end of the chapter.

### 1.1 In-plane molecular vibrations of squarene

As an introductory example we consider a fictitious square molecule we shall call “squarene”. The squarene molecule, shown in Fig. 1.1, lies in the plane of the paper with identical atoms at each corner of a square. Our aim in this chapter is to use group theory to assist in determining the vibrational frequencies and motions of the normal modes (eigenvalues and eigenvectors) of the molecule.

In general the molecular vibration problem may be cast into the form of a matrix eigenvalue problem,

$$\mathbb{F} \xi = \omega^2 \mathbb{M} \xi,$$

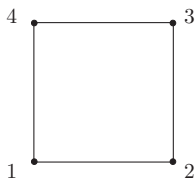


Figure 1.1 The squarene molecule.

where  $\mathbb{F}$  is a matrix of “force constants” and  $\xi$  is a column vector whose components are the vibrational displacements of the atoms. The matrix  $\mathbb{M}$  is a diagonal mass matrix,  $\mathbb{M}_{ij} = m_i \delta_{ij}$  where  $m_i$  is the mass of the atom with coordinate component  $\xi_i$  and  $\omega$  is the angular frequency of vibration. This equation may be transformed to a standard eigenvalue form,

$$\mathbb{F}' \eta = \omega^2 \eta,$$

with  $\mathbb{F}' = \mathbb{M}^{-1/2} \mathbb{F} \mathbb{M}^{-1/2}$  and  $\eta = \mathbb{M}^{1/2} \xi$ .

In the case of squarene all the masses are the same, so  $\mathbb{M}$  can be replaced by a scalar,  $m$ , the common mass of the four atoms. Therefore the eigenvalue equation we are concerned with is the  $8 \times 8$  matrix equation

$$\mathbb{F} \xi = m \omega^2 \xi. \quad (1.1)$$

Solutions of (1.1) consist of a set of eight eigenvalues,  $m(\omega^k)^2$ , and a set of eight associated eigenvectors,  $\xi^k$  ( $k = 1, 2, \dots, 8$ ), that specify the relative displacements of the atoms. The solutions of (1.1) will include three “body modes”, namely translation in the  $x$ -direction, translation in the  $y$ -direction, and rotation about an axis perpendicular to the plane of the molecule at the center of the square. The angular frequencies of these three body modes may be taken as zero because there are no “restoring forces” when a molecule is translated or rotated as a unit. Therefore, for our two-dimensional squarene molecule there will be five vibrational modes and three zero-frequency, body modes.

One approach to the molecular vibrations of squarene would be to postulate a force-constant model,  $\mathbb{F}$ , and solve the resulting eigenvalue problem. In its most general form,  $\mathbb{F}$  will have 64 non-zero matrix elements. If no simplifications are made, the diagonalization of an  $8 \times 8$  matrix could be daunting without the use of a computer. If approximations are employed to simplify  $\mathbb{F}$ , it will not be evident whether the results are constrained by symmetry or by the assumptions made in the postulated force-constant model. The use of group theory not only greatly simplifies the analysis, but also yields the most general form possible for  $\mathbb{F}$  and provides physical insight into the nature of the normal modes of vibration.



Often, the normal-mode frequencies can be measured by spectroscopic means; infrared or Raman spectroscopy, for example. However, the force constants (the matrix elements of  $\mathbb{F}$ ) **can not** be measured directly. They are usually inferred by using a specific model and choosing the constants so that the eigenfrequencies match the observed frequencies. This method does not always produce a unique set of force constants, and other spectroscopic data must be employed; for example, the frequencies of isotopically substituted molecules and/or elastic constants.

In Chapter 2 we shall investigate how group theory can be used to predict isotopic frequency shifts. In fact, in some cases the frequencies of an isotopic molecule can be expressed in terms of frequencies of the non-isotopic molecule [1.2] without ever having to specify the force-constant matrix.<sup>1</sup>

There is a general order to the way in which group theory is employed to analyze an eigenvalue problem. We shall label the various steps as “Step 1” through “Step 8”.

### 1.1.1 Step 1: Identify the point group and its symmetry operations

At rest, the squarene molecule has the symmetry of a square. For simplicity we confine our discussion to the two dimensions of the plane of the molecule. (There is no loss of generality in this assumption because the in-plane vibrational modes do not mix with the motions perpendicular to the plane of the molecule (see Exercise 1.16).) The operations that rotate or reflect an object into a configuration indistinguishable from its original configuration are called the *covering operations* and constitute a group. For squarene these operations are *rotations* about an axis perpendicular to the plane of the molecule and *reflections* through lines in the plane of the molecule. For example we can rotate the square by 90 degrees or any multiple of 90 degrees about an axis perpendicular to the plane passing through the center of the square. So there are four rotations: 90-degree, 180-degree, 270-degree, and 360-degree rotations. Rotation by 360 degrees is taken to be the same as “doing nothing”. The “doing-nothing” operation is usually called the “identity” operation and denoted by the symbol  $E$ . There are seven other symmetry operations. If we draw a diagonal line across the square and reflect the corners through this line, the square remains unchanged. There are two different diagonal lines that pass through the center and two corners of the square. Another pair of reflection lines passes through the middle of the square and bisects two opposite sides. These symmetry operations are shown schematically in Fig. 1.2. The point group corresponding to these operations is “ $C_{4v}$ ”. (In three dimensions the group is  $D_{4h}$ .

<sup>1</sup> Assuming harmonic motions and neglecting very small changes in the force constants due to isotope substitution.

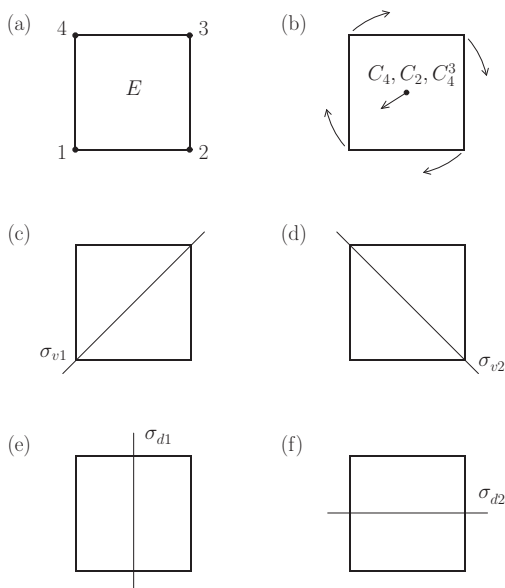


Figure 1.2 The square molecule and its symmetry elements.

Methods for identifying the group of a molecule are discussed in Appendix G.) For  $C_{4v}$  there are in total eight symmetry elements.<sup>2</sup>

- (1)  $E$  = a 0-degree or 360-degree rotation.
- (2)  $C_4$  = a 90-degree rotation.
- (3)  $C_2$  = a 180-degree rotation.
- (4)  $C_4^3$  = a 270-degree rotation.
- (5)  $\sigma_{v1}$  = reflection in a diagonal line.
- (6)  $\sigma_{v2}$  = reflection in a diagonal line.
- (7)  $\sigma_{d1}$  = reflection in a line cutting the sides of the square.
- (8)  $\sigma_{d2}$  = reflection in a line cutting the sides of the square.

For the remainder of this chapter we shall regard the symbols  $E$ ,  $C_4$ ,  $\sigma_{v1}$  etc. as symmetry operators that act on the molecule, not the coordinate system.<sup>3</sup> Thus, for example  $C_4$  rotates the molecule and its nuclear displacement by 90 degrees in a clockwise manner.

The formal definition of a group is given in Theorem 1.1.

<sup>2</sup> Inversion through the center of the square (i.e.,  $\mathbf{r} \rightarrow -\mathbf{r}$ ) is a symmetry operation. However, the effect of inversion is the same as the effect of a  $C_2$  rotation in this case and so may be omitted.

<sup>3</sup> There is a distinction between the symmetry elements and the symmetry operators, but the group of the operators is isomorphic to the group of the elements, which means that the two groups are equivalent group theoretically.

**Theorem 1.1** (Definition of a group)

1. A group is a set of elements that are closed under group multiplication. That is, the product of any two elements in the group produces another element of the group. If  $A$  and  $B$  are in the group then so is  $AB$ .
2. The associative law holds:  $A(BC) = (AB)C$ .
3. There is a unit or identity element,  $E$ , such that  $EA = AE = A$ .
4. Every element in the group has an inverse element that is also in the group. If  $A$  is an element then  $A^{-1}$  is also an element in the group, and  $AA^{-1} = A^{-1}A = E$ .
5. The word “operator” may be substituted for the word “element” in items 1 through 4 to define a group based on the operators associated with the elements.

A bit later we shall verify that the eight symmetry elements identified above satisfy all of the conditions of a group as defined in Theorem 1.1.

**1.1.2 Step 2: Specify the coordinate system and basis functions**

The coordinate system to be employed in the analysis is often a set of Cartesian coordinates,<sup>4</sup> but there are many other choices; Euler angles, internal coordinates, cylindrical coordinates, and spherical coordinates, to name a few. In general the choice of basis functions depends on the physical phenomena to be analyzed. In the case of molecular vibrations we are concerned with the motions of each of the atoms comprising the molecule. Therefore an appropriate choice of basis functions is the atomic displacement vectors. To measure the displacements of each atom from its equilibrium position we label the corner positions of the square (not the atoms of the molecule) and construct  $X$ – $Y$  Cartesian coordinate systems anchored to these corner positions as shown in Fig. 1.3(a).

**1.1.3 Step 3: Determine the effects of the symmetry operations on the basis functions**

We consider how a vector representing the displacement of one of the atoms is transformed when the molecule is subjected to one of the symmetry operations. Note that the  $X$ – $Y$  coordinate systems as well as the position numbers of the corners are fixed. Imagine the molecule placed on top of the square in Fig. 1.3(a) and rotated or reflected under the action of a symmetry operation. If we rotate the molecule clockwise by 90 degrees (the  $C_4$  operation) the atoms of the molecule move to different corner positions as indicated by Table 1.1.

<sup>4</sup> In chemistry texts internal coordinates are often used. See reference [1.3].

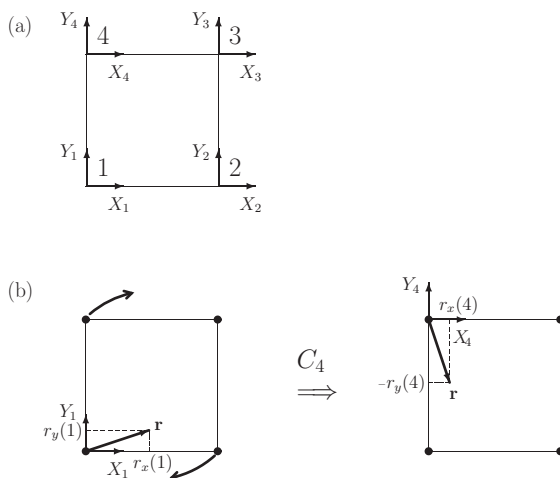


Figure 1.3 (a) The coordinate system. Here 1, 2, 3, and 4 label the fixed corners of the square, and  $X_i$  and  $Y_i$  label the fixed coordinate axes. (b) The effect of  $C_4$  rotation on the displacement vector,  $\mathbf{r}$ , on an atom initially at corner 1.

Table 1.1 *The effect of  $C_4$  on squarene*

Atom's initial corner	Atom's final corner
1	4
2	1
3	2
4	3

Consider a vector displacement  $\mathbf{r}$  of an atom initially located at corner 1. The components of this vector in the  $X_1$ – $Y_1$  coordinate system are  $r_x$  and  $r_y$ , respectively, as shown in Fig. 1.3(b). After rotation the displacement vector  $\mathbf{r}$  (anchored to the atom) is now centered on the  $X_4$ – $Y_4$  coordinate system associated with corner 4. In the  $X_4$ – $Y_4$  coordinate system, the  $X_4$  component is  $r_y$  and the  $Y_4$  component is  $-r_x$ . In symbolic notation,

$$C_4 r_x(1) \rightarrow -r_y(4),$$

$$C_4 r_y(1) \rightarrow r_x(4),$$

meaning that the  $C_4$  operation transforms the component of  $\mathbf{r}$  along the  $X_1$  axis into a component along the  $-Y_4$  axis and transforms the component of  $\mathbf{r}$  along the  $Y_1$  axis into a component along the  $X_4$  axis. The displacement vector of any of the atoms of squarene will transform in the same way, so, in general,

$$C_4 r_x(i) \rightarrow -r_y(f),$$

$$C_4 r_y(i) \rightarrow r_x(f),$$

where “ $i$ ” and “ $f$ ” refer to the initial and final corners given in Table 1.1.

Table 1.2 *The effect of  $\sigma_{v1}$  on squarene*

Atom's initial corner	Atom's final corner
1	1
2	4
3	3
4	2

Table 1.3 *The action table for squarene*

	$E$	$C_4$	$C_2$	$C_4^3$	$\sigma_{v1}$	$\sigma_{v2}$	$\sigma_{d1}$	$\sigma_{d2}$
$r_x$	$r_x$	$-r_y$	$-r_x$	$r_y$	$r_y$	$-r_y$	$-r_x$	$r_x$
$r_y$	$r_y$	$r_x$	$-r_y$	$-r_x$	$r_x$	$-r_x$	$r_y$	$-r_y$
1	1	4	3	2	1	3	2	4
2	2	1	4	3	4	2	1	3
3	3	2	1	4	3	1	4	2
4	4	3	2	1	2	4	3	1

Next consider the action of the reflection operation,  $\sigma_{v1}$ . For this symmetry operator we have the results shown in Table 1.2. For  $\sigma_{v1}$  the displacements are transformed so that  $r_x(i) \rightarrow r_y(f)$  and  $r_y(i) \rightarrow r_x(f)$ . Symbolically,

$$\sigma_{v1} r_x(i) \rightarrow r_y(f),$$

$$\sigma_{v1} r_y(i) \rightarrow r_x(f),$$

where the initial and final corner numbers are given in Table 1.2.

A convenient device for determining the effects of symmetry operations is the *action table* shown in Table 1.3. The columns are labeled by the group operators. The rows are labeled by  $r_x$  and  $r_y$  and the corner numbers. The intersection of a column and a row is the action of the column operator on the displacements (first two rows) and the corner labels (last four rows). The table makes it easy to generate the effect of any operator. For example, consider  $\sigma_{d1}$  acting on the displacement vector initially at corner 2. From the table (column 7) we see that under action of  $\sigma_{d1}$  corner 2  $\rightarrow$  corner 1,  $r_x \rightarrow -r_x$ , and  $r_y \rightarrow r_y$ . Therefore,  $r_x(2) \rightarrow -r_x(1)$  and  $r_y(2) \rightarrow r_y(1)$ . Using the action table the effect of any operator of the group on the basis functions can be determined.

Another useful device is the *group multiplication table* shown in Table 1.4. In this table the rows and columns are labeled by the operators of the group,  $O_i$  ( $i = 1, 2, \dots, 8$ ). The intersection of the  $i$ th row with the  $j$ th column is the operator obtained by the sequential application of the operators in the order  $O_i O_j$ . The order is important because  $O_i O_j$  is often different from  $O_j O_i$ . The group

Table 1.4 *The group multiplication table for  $C_{4v}$* 

$C_4$	$E$	$C_4$	$C_2$	$C_4^3$	$\sigma_{v1}$	$\sigma_{v2}$	$\sigma_{d1}$	$\sigma_{d2}$
$E$	$E$	$C_4$	$C_2$	$C_4^3$	$\sigma_{v1}$	$\sigma_{v2}$	$\sigma_{d1}$	$\sigma_{d2}$
$C_4$	$C_4$	$C_2$	$C_4^3$	$E$	$\sigma_{d2}$	$\sigma_{d1}$	$\sigma_{v1}$	$\sigma_{v2}$
$C_2$	$C_2$	$C_4^3$	$E$	$C_4$	$\sigma_{v2}$	$\sigma_{v1}$	$\sigma_{d2}$	$\sigma_{d1}$
$C_4^3$	$C_4^3$	$E$	$C_4$	$C_2$	$\sigma_{d1}$	$\sigma_{d2}$	$\sigma_{v2}$	$\sigma_{v1}$
$\sigma_{v1}$	$\sigma_{v1}$	$\sigma_{d1}$	$\sigma_{v2}$	$\sigma_{d2}$	$E$	$C_2$	$C_4$	$C_4^3$
$\sigma_{v2}$	$\sigma_{v2}$	$\sigma_{d2}$	$\sigma_{v1}$	$\sigma_{d1}$	$C_2$	$E$	$C_4^3$	$C_4$
$\sigma_{d1}$	$\sigma_{d1}$	$\sigma_{v2}$	$\sigma_{d2}$	$\sigma_{v1}$	$C_4^3$	$C_4$	$E$	$C_2$
$\sigma_{d2}$	$\sigma_{d2}$	$\sigma_{v1}$	$\sigma_{d1}$	$\sigma_{v2}$	$C_4$	$C_4^3$	$C_2$	$E$

multiplication table is easily generated from the action table. For example,  $C_4$  transforms  $r_x, r_y, 1, 2, 3, 4$  into  $-r_y, r_x, 4, 1, 2, 3$ , respectively. If we now apply  $\sigma_{d1}$  to this result then  $-r_y, r_x, 4, 1, 2, 3$  is transformed into  $-r_y, -r_x, 3, 2, 1, 4$ . Therefore,  $\sigma_{d1}C_4$  transforms  $r_x, r_y, 1, 2, 3, 4$  into  $-r_y, -r_x, 3, 2, 1, 4$ . On looking at the action table, we see that this is the same action as  $\sigma_{v2}$ . Thus  $\sigma_{d1}C_4 = \sigma_{v2}$ . This result may be seen as the operation at the intersection of the row labeled  $\sigma_{d1}$  and the column labeled  $C_4$  in the group multiplication table. Similarly, one may see from the same table that  $C_4\sigma_{d1} = \sigma_{v1}$ , which shows that with a change of order in multiple operations one does not necessarily obtain the same result.

The action table can also be applied to products such as  $r_x(1)r_y(2)$ ,  $[r_x(1)]^2$ , or products of more than two displacements. For example,  $C_4 r_x(1)r_y(2) \rightarrow -r_y(4)r_x(1)$  and  $C_4 [r_x(1)]^2 \rightarrow [r_y(4)]^2$ .

#### 1.1.4 Step 4: Construct matrix representations for each element of the group using the basis functions

It will prove useful to employ an eight-component column vector so that we can show the effect of a symmetry operation on all the atomic displacement vectors at the same time. To do this, we use, as the components of the 8-vector, the  $r_x$  and  $r_y$  displacement components of all four atoms. Using the action table we have, in our symbolic notation,

$$C_4 \begin{bmatrix} r_x(1) \\ r_y(1) \\ r_x(2) \\ r_y(2) \\ r_x(3) \\ r_y(3) \\ r_x(4) \\ r_y(4) \end{bmatrix} \Rightarrow \begin{bmatrix} r_y(2) \\ -r_x(2) \\ r_y(3) \\ -r_x(3) \\ r_y(4) \\ -r_x(4) \\ r_y(1) \\ -r_x(1) \end{bmatrix}. \quad (1.2)$$

The rows of the column vectors in (1.2) are labeled from top to bottom by  $\mathbf{e}_x(1)$ ,  $\mathbf{e}_y(1)$ ,  $\mathbf{e}_x(2)$ ,  $\mathbf{e}_y(2)$ ,  $\mathbf{e}_x(3)$ ,  $\mathbf{e}_y(3)$ ,  $\mathbf{e}_x(4)$ , and  $\mathbf{e}_y(4)$ , unit vectors along the fixed Cartesian coordinates in Fig. 1.3(a). It is important to understand the meaning of (1.2). The rows of the column vectors are labeled by the unit vectors of the **fixed** coordinate system. Therefore a column vector such as

$$\begin{pmatrix} 0 \\ 0 \\ 0 \\ c \\ 0 \\ 0 \\ 0 \\ 0 \end{pmatrix}$$

is a displacement of length  $c$  for the  $y$ -component on corner 2. The column vector

$$\begin{pmatrix} d \\ 0 \\ 0 \\ 0 \\ 0 \\ 0 \\ 0 \\ 0 \end{pmatrix}$$

is a displacement of length  $d$  for the  $x$ -component on corner 1. What equation (1.2) means is that a clockwise rotation,  $C_4$ , rotates the molecule so that the  $x$ -component of the molecular displacement on corner 1 after rotation appears as the  $-y$ -component on corner 4. In other words, we assign to the new vector (right-hand side) the value  $-r_x(1)$  for its  $y$ -component on corner 4. This is indicated by the arrow in (1.2). Similarly, we assign to the new vector the value  $r_y(4)$  for its  $x$ -component on corner 3. In more compact notation,

$$\Gamma(C_4) \mathbf{V}_i = \mathbf{V}_f, \quad (1.3)$$

where  $\Gamma(C_4)$  is an  $8 \times 8$  matrix.<sup>5</sup> The eight-dimensional column vector,  $\mathbf{V}_i$ , has as its components the entries of the column on the left-hand side of (1.2). The components of the column vector,  $\mathbf{V}_f$ , are the entries of the right-hand side of (1.2).

$\Gamma(C_4)$  can easily be constructed. For example, (1.2) shows that  $r_x(1)$  is transformed to  $-r_y(4)$ , therefore the first column of  $\Gamma(C_4)$  has only one entry, namely

<sup>5</sup> An equally valid method of describing the group and its representations is to fix the molecule and rotate the coordinate framework. Clearly, rotating the coordinate axes *counter-clockwise* with the molecule fixed is equivalent to fixing the coordinate axes and rotating the molecule clockwise. However, the usual convention in most texts is rotation of the molecule or function rather than the coordinate axes.

a “−1” in the eighth row. Similarly,  $r_y(3)$  is transformed to  $r_x(2)$ , so the sixth column of  $\Gamma(C_4)$  has a single entry, a “+1” in the third row. Proceeding in this way produces the  $8 \times 8$  matrix

$$\Gamma(C_4) = \begin{array}{c|cccccccc} & & & & 1 & & & \\ & & -1 & & & & & \\ & & & & & 1 & & \\ & & & & -1 & & & \\ & & & & & & & 1 \\ & & & & & & -1 & \\ & & 1 & & & & & \\ -1 & & & & & & & \end{array}$$

Matrix multiplication of  $\mathbf{V}_i$  by  $\Gamma(C_4)$  produces the vector  $\mathbf{V}_f$ . Using the action table we can readily construct matrices for each of the eight operations of the  $C_{4v}$  group. These matrices are shown in Table 1.5.

The eight matrices in Table 1.5 form a **matrix representation** of the  $C_{4v}$  group. In the parlance of group theory we say that the displacements  $r_x(j)$  and  $r_y(j)$  ( $j = 1, 2, 3$ , and 4) are basis functions for an eight-dimensional representation of the group  $C_{4v}$ . The symbols  $r_x$  and  $r_y$  without regard to the corner numbers form a two-dimensional representation of  $C_{4v}$ . Finally, we note that the corner numbers (the last four rows in Table 1.3) form the basis for a four-dimensional representation of  $C_{4v}$ .

From the group multiplication table we can find the inverse of any representation matrix by finding the intersection that produces the identity element. For example, the inverse of  $C_4$  is  $C_4^3$  and the reflection operators are their own inverses.

Inspection of the representation matrices in Table 1.5 reveals a number of properties. (1) All of the matrices are unitary, meaning that the inverse,  $\Gamma(O_i)^{-1}$ , is the transpose, complex conjugate of  $\Gamma(O_i)$ , where  $O_i$  denotes the  $i$ th operator of the group. Since, in this case, all the matrix elements are real, the inverse is simply the transpose. (2) The rows (or columns) of  $\Gamma(O_i)$  are orthogonal to each other; that is,

$$\sum_{s=1}^h \Gamma(O_i)_{rs} \Gamma(O_i)_{ts} = \sum_{s=1}^h \Gamma(O_i)_{sr} \Gamma(O_i)_{st} = \delta_{rt},$$

where  $h$ , the *order* of the group, is the number of elements in the group and  $\Gamma(O_i)_{rs}$  is the  $rs$  matrix element of  $\Gamma(O_i)$ . (3) The determinant of each matrix is +1. The results (2) and (3) are consequences of (1), namely of the matrices being unitary.



Table 1.5 Matrix representations of the group  $C_{4v}$ : (a) through (h), representation matrices based on the displacement coordinates of squareene(a)  $\Gamma(E) =$ 

1							
	1						
		1					
			1				
				1			
					1		
						1	
							1

(b)  $\Gamma(C_4) =$ 

			1				
		-1					
				1			
			-1				
						1	
					-1		
	1						
-1							

(c)  $\Gamma(C_2) =$ 

			-1				
				-1			
					-1		
						-1	
-1							
	-1						
		-1					
			-1				

(d)  $\Gamma(C_4^3) =$ 

						1	-1
							1
	-1						
1							
		-1					
		1					
				-1			
			1				

(e)  $\Gamma(\sigma_{v2}) =$ 

				-1			
			-1				
		-1					
	-1						
-1							
						-1	
					-1		

(f)  $\Gamma(\sigma_{v1}) =$ 

	1						
1							
						1	
					1		
			1				
		1					
	1						

(g)  $\Gamma(\sigma_{d1}) =$ 

		-1					
			1				
-1							
	1						
				-1			
						1	
			-1				
				1			

(h)  $\Gamma(\sigma_{d2}) =$ 

					1		
						-1	
			1				
				-1			
	1						
		-1					
1							
	-1						

To verify that the matrices in Table 1.5 form a proper representation of the group, one can simply multiply them together to show that they obey the properties of a group representation given in Theorem 1.2.

**Theorem 1.2** (Properties of a matrix representation)

1. For any operators  $A$ ,  $B$ , and  $C$  in the group there are associated matrices  $\Gamma(A)$ ,  $\Gamma(B)$ , and  $\Gamma(C)$  such that if  $AB = C$  then  $\Gamma(A)\Gamma(B) = \Gamma(AB) = \Gamma(C)$ . (This requires that  $\Gamma(A)^{-1} = \Gamma(A^{-1})$ .)
2. For every point group there exists a representation consisting of unitary matrices. Unitary matrices are square matrices for which  $\Gamma(A)^{-1}$  is the complex conjugate, transpose of  $\Gamma(A)$ .

It follows from Theorem 1.2 that matrices given in Table 1.5 obey the same group multiplication table (Table 1.4) as do the operators with  $\Gamma(O_i)$  instead of  $O_i$  labeling the rows and columns.

## 1.2 Reducible and irreducible representations of a group

A group can have many matrix representations. If we perform the same similarity transformation,  $\mathbb{T}^{-1} \Gamma(O_i) \mathbb{T}$ , on all of the matrices of Table 1.5 we will obtain a different set of  $8 \times 8$  matrices,  $\Gamma^{(a)}(O_i)$ , that also represents the group. (This could be written as  $\mathbb{T}^{-1} \Gamma \mathbb{T} = \Gamma^{(a)}$ , where it is understood that the similarity transformation,  $\mathbb{T}$ , is applied to all of the representation matrices.) Two representations related by a similarity transformation are said to be **equivalent**. If we use different basis functions we may obtain a representation whose dimensionality is different from that of  $\Gamma$ . For example, we could base a representation on how the atoms of the molecule move without regard to atomic displacements. That would generate  $\Gamma^{(b)}$ , a  $4 \times 4$  matrix representation of  $C_{4v}$ . Finally we could combine all these representations into a  $20 \times 20$  representation by placing  $\Gamma(O_i)$ ,  $\Gamma^{(a)}(O_i)$ , and  $\Gamma^{(b)}(O_i)$  as blocks along the diagonal to form the matrix  $\Gamma^{(c)}(O_i)$ . This process is shown schematically in Fig. 1.4(a).  $\Gamma$ ,  $\Gamma^{(a)}$ ,  $\Gamma^{(b)}$ , and  $\Gamma^{(c)}$  are all valid representations of the group.  $\Gamma^{(c)}$  is composed of three uncoupled representations (unconnected blocks of matrices). If an arbitrary similarity transformation were performed on  $\Gamma^{(c)}$ , the block-diagonal form would usually be lost even though the transformed representation would be equivalent to  $\Gamma^{(c)}$ .

We see from the previous paragraph how larger representation matrices can be composed from smaller ones. The reverse process can also be accomplished. Given an  $N \times N$  matrix representation,  $\Gamma^N$ , it may be possible to transform all its matrices into block-diagonalized forms by a similarity transformation  $\Gamma = \mathbb{S}^{-1} \Gamma^N \mathbb{S}$ . That

$$\begin{aligned}
\text{(a)} \quad \Gamma^{(c)} &= \begin{pmatrix} \boxed{\begin{matrix} \Gamma \\ (8 \times 8) \end{matrix}} & & 0 \\ & \boxed{\begin{matrix} \Gamma^{(a)} \\ (8 \times 8) \end{matrix}} & \\ 0 & & \boxed{\begin{matrix} \Gamma^{(b)} \\ (4 \times 4) \end{matrix}} \end{pmatrix} \\
\text{(b)} \quad \Gamma^N(O_i) &= \begin{pmatrix} a_{11} & a_{12} & \dots & a_{1N} \\ a_{21} & a_{22} & \dots & a_{2N} \\ \vdots & \vdots & & \vdots \\ a_{N1} & a_{N2} & \dots & a_{NN} \end{pmatrix} \\
\text{(c)} \quad \mathbb{S}^{-1} \Gamma^N(O_i) \mathbb{S} &= \begin{pmatrix} \boxed{\Gamma^{(1)}(O_i)} & & 0 \\ & \boxed{\Gamma^{(2)}(O_i)} & \\ & & \ddots \\ 0 & & & \boxed{\Gamma^{(m)}(O_i)} \end{pmatrix}
\end{aligned}$$

Figure 1.4 (a) The  $(20 \times 20)$  representation  $\Gamma^{(c)} = \Gamma + \Gamma^{(a)} + \Gamma^{(b)}$ , (b) the  $N \times N$  representation  $\Gamma^N$ , and (c) decomposition of  $\Gamma^N$  into smaller representations by a similarity transformation.

is, by a similarity transformation we can **decompose** the  $\Gamma^N$  representation into smaller representations. Symbolically, we have

$$\Gamma^N \equiv \Gamma^{(1)} \oplus \Gamma^{(2)} \oplus \dots \oplus \Gamma^{(m)}. \quad (1.4)$$

Equation (1.4) is an equivalence statement meaning that there exists a similarity transformation that will decompose  $\Gamma^N$  into the series of uncoupled blocks shown on the right-hand side. In more detail,

$$\Gamma^N(O_i) = \Gamma^{(1)}(O_i) \oplus \Gamma^{(2)}(O_i) \oplus \cdots \oplus \Gamma^{(m)}(O_i) \quad (i = 1, 2, \dots, h).$$

The symbol  $\oplus$  means that *the matrix representation which follows is a block along the diagonal of  $\Gamma^N$  after a suitable similarity transformation*. The order of representations on the right-hand side of (1.4) is irrelevant. Each of the representation matrices  $\Gamma^N(O_i)$  consists of  $m$  uncoupled blocks or submatrices. Such a transformation is shown schematically in Fig. 1.4(c). For simplicity the decomposition formula of (1.4) is often written as

$$\Gamma^N = \Gamma^{(1)} + \Gamma^{(2)} + \cdots + \Gamma^{(m)}, \quad (1.5)$$

with the understanding that simple matrix addition is **not** implied. We will use this notation when there is no chance for confusion.

Since each  $\Gamma^{(i)}$  appearing in (1.5) is itself a representation, it may be possible to decompose it into smaller blocks. Eventually, minimum-sized blocks must be achieved. These minimal blocks are said to be **irreducible representations**. (We shall use the abbreviation “IR” for “irreducible representation” throughout this book.)

**Theorem 1.3** (Definitions of reducible and irreducible representations)

- *A representation that can be reduced or decomposed by a similarity transformation into smaller, uncoupled, submatrix representations is a reducible representation.*
- *Conversely, a representation that can not be reduced by any similarity transformation into smaller, uncoupled, submatrix representations is an irreducible representation.*

For most science problems the basis functions normally employed to describe the system are bases for a reducible representation,  $\Gamma$ . The role of group theory is to provide a method of finding the matrix  $\mathbb{S}$  such that the similarity transformation  $\mathbb{S}^{-1} \Gamma \mathbb{S} = \Gamma^{\mathbb{S}}$  produces a representation that has only IRs along the diagonal of each  $\Gamma^{\mathbb{S}}(O_i)$ . *The notation  $\mathbb{S}^{-1} \Gamma \mathbb{S} = \Gamma^{\mathbb{S}}$  is symbolic. It means that the same similarity transformation is applied to every representation matrix of  $\Gamma$ , that is  $\mathbb{S}^{-1} \Gamma(O_i) \mathbb{S} = \Gamma^{\mathbb{S}}(O_i)$  ( $i = 1, 2, \dots, h$ ), and every  $\Gamma^{\mathbb{S}}(O_i)$  has the same block-diagonal form consisting of submatrices that are irreducible representation matrices.*

The columns of  $\mathbb{S}$  or the rows of  $\mathbb{S}^{-1}$  are the **symmetry functions** for the system. These symmetry functions are linear combinations of the original basis functions. When a physical problem is expressed in terms of its symmetry functions the eigenvalue equation is block-diagonal and a great simplification of the mathematics usually results. A method for deriving the symmetry functions is discussed in “Step 7” below in Subsection 1.2.6.

Symmetry functions are usually not eigenfunctions. If the decomposition of the representation based on the physical coordinates contains the same IR  $r$  times, then there will be  $r$  sets of symmetry functions for that IR and the eigenfunctions will be linear combinations of these symmetry functions. On the other hand, if the decomposition contains a particular IR only once, then the basis functions for that IR are also eigenfunctions. This is a rather amazing result. It means that some of the eigenfunctions of a physical system may be entirely determined by symmetry, independently of the details of the system's Hamiltonian or force-constant matrix.<sup>6</sup> We shall see examples of this as we proceed with the analysis of the vibrations of squareene.

### 1.2.1 Step 5. Determine the number and types of irreducible representations

The matrix representation,  $\Gamma$ , we have constructed for squareene is reducible into unconnected IR blocks by the similarity transformation  $\mathbb{S}^{-1} \Gamma \mathbb{S}$ , where  $\mathbb{S}$  is the matrix of symmetry functions. The reduction of  $\Gamma$  to diagonal blocks need not result in distinct IRs, and in many cases the same (or equivalent) IR will occur more than once among the diagonal blocks. The number and types of IRs that occur among the diagonal blocks depend on the basis functions used to generate  $\Gamma$ .

What is the connection between the IRs of the  $C_{4v}$  group and the physical problem of the molecular vibrations? The connection is this: The similarity transformation  $\mathbb{S}$  which block-diagonalizes the reducible representation  $\Gamma$  will also block-diagonalize the matrix  $\mathbb{F}$  of (1.1).

To determine the number and type of IRs contained in  $\Gamma$  we need to explore a few other properties of a group.

### 1.2.2 Classes of a group

An important feature of a group is its **classes**. The definition of a class is given in Theorem 1.4.

**Theorem 1.4** (Definition of a class)

- Two operators,  $A$  and  $B$ , are conjugate if  $A = CBC^{-1}$ , where  $C$  is any member of the group. A class is a set of all of the distinct operators of a group that are conjugate to each other.
- From the definition of a representation, Theorem 1.2, it follows that two representation matrices  $\Gamma(A)$  and  $\Gamma(B)$  belong to the same class if  $\Gamma(A) = \Gamma(C) \Gamma(B) \Gamma(C)^{-1}$ , where  $\Gamma(C)$  is a matrix representation of any operator of the group.

<sup>6</sup> A valid Hamiltonian is not arbitrary. It must commute with the operations of the group. Similarly,  $\mathbb{F}$  must commute with the operations of the group.

To find the classes of  $C_{4v}$  we can make use of the group multiplication table (Table 1.4). The inverse of any operation can be found from the table by observing which product produces the identity,  $E$ :

$$\begin{aligned} E^{-1} &= E, \\ C_4^{-1} &= C_4^3, \\ C_2^{-1} &= C_2, \\ (C_4^3)^{-1} &= C_4. \end{aligned}$$

Also it is evident that any reflection operator is its own inverse; that is,  $\sigma_i^{-1} = \sigma_i$ . Clearly,  $E$  is in a class by itself since  $A E A^{-1} = E$  for all  $A$  in the group. To find the other classes we start with  $C_4$  and form the products  $O_i C_4 O_i^{-1}$  ( $i = 1, 2, \dots, h$ ). This procedure yields

$$\begin{aligned} E C_4 E &= C_4, & \sigma_{v1} C_4 \sigma_{v1} &= \sigma_{v1} \sigma_{d2} = C_4^3, \\ C_4 C_4 C_4^{-1} &= C_4, & \sigma_{v2} C_4 \sigma_{v2} &= \sigma_{v2} \sigma_{d1} = C_4^3, \\ C_2 C_4 C_2^{-1} &= C_2 C_4 C_2 = C_4, & \sigma_{d1} C_4 \sigma_{d1} &= \sigma_{d1} \sigma_{v2} = C_4^3, \\ C_4^3 C_4 (C_4^3)^{-1} &= C_4^3 C_4 C_4 = C_4, & \sigma_{d2} C_4 \sigma_{d2} &= \sigma_{d2} \sigma_{v1} = C_4^3. \end{aligned}$$

Therefore  $C_4$  and  $C_4^3$  form a class. Continuing this procedure with the other elements of the group shows that there are five classes. They are as follows:  $\{E\}$ ;  $\{C_4, C_4^3\}$ ;  $\{C_2\}$ ;  $\{\sigma_{d1}, \sigma_{d2}\}$ ; and  $\{\sigma_{v1}, \sigma_{v2}\}$ . Similarly, for the representation matrices the classes are  $\{\Gamma(E)\}$ ;  $\{\Gamma(C_4), \Gamma(C_4^3)\}$ ;  $\{\Gamma(C_2)\}$ ;  $\{\Gamma(\sigma_{d1}), \Gamma(\sigma_{d2})\}$ ; and  $\{\Gamma(\sigma_{v1}), \Gamma(\sigma_{v2})\}$ .

### 1.2.3 The character of a representation matrix

Another important property of a representation matrix is its **trace**. The trace of a matrix is the sum of the diagonal elements of the matrix. The trace of a representation matrix is called its **character**. The usual symbol for a character is  $\chi$  and the character of  $\Gamma^\alpha(O_i)$  is denoted by  $\chi^\alpha(O_i)$  or  $\chi_i^\alpha$ .

If  $A$  and  $B$  are in the same class then  $A = C B C^{-1}$  for some element  $C$  in the group. This requires that  $\Gamma(A) = \Gamma(C) \Gamma(B) \Gamma(C)^{-1}$  and therefore  $\Gamma(A)$  and  $\Gamma(B)$  are related by a similarity transformation. The trace of a matrix is unchanged by a similarity transformation and therefore the character of  $\Gamma(A)$  must be equal to the character of  $\Gamma(B)$ . From this result it follows that *all representation matrices belonging to the same class have the same character*.

The **character table** for the  $C_{4v}$  group is given in Table 1.6. The first column of the table lists the names of the IRs of the  $C_{4v}$  group. The next five columns give the characters (the  $\chi$ s) of the classes of  $C_{4v}$  for the five different IRs. The last row lists the results for  $\Gamma$ , our  $8 \times 8$  representation for squarene obtained from

Table 1.6 The character table for  $C_{4v}$ 

$\Gamma$ (IR name)	Classes					Basis functions
	$E$ $\chi(E)$	$2C_4$ $\chi(C_4)$	$C_2$ $\chi(C_2)$	$2\sigma_v$ $\chi(\sigma_v)$	$2\sigma_d$ $\chi(\sigma_d)$	
$A_1$	1	1	1	1	1	$z, x^2 + y^2, z^2$
$A_2$	1	1	1	-1	-1	$R_z$
$B_1$	1	-1	1	1	-1	$x^2 - y^2$
$B_2$	1	-1	1	-1	1	$xy$
$\mathcal{E}$	2	0	-2	0	0	$(x, y), (xy, yz), (R_x, R_y)$
$\Gamma(8 \times 8)$	8	0	0	0	0	$(r_x(i), r_y(i)), i = 1 \text{ to } 4.$

the traces of the representations in Table 1.5. A shorthand notation is used in the character table. Instead of listing all of the elements of a class, only one element is given and the number of elements in the class is specified. For example, the class  $\{C_4, C_4^3\}$  is denoted by  $2C_4$ , meaning that there are two elements in the class to which  $C_4$  belongs. Since all the members of a class have the same character, it is not necessary to specify each element. The last column of Table 1.6 lists a few functions that can serve as basis functions for the corresponding IR. Character tables for the different point groups are given in Appendix C.

The character table for  $C_{4v}$  gives all the information we need to determine the number and types of IRs of our  $8 \times 8$  representation,  $\Gamma$ . However, to find the decomposition of  $\Gamma$  and to construct the  $\mathbb{S}$  matrix that block-diagonalizes the eigenvalue equation we need a few more results from group theory.

#### 1.2.4 Orthogonality of the characters of an irreducible representation

$C_{4v}$  has five classes. If the characters of the classes of a given IR of  $C_{4v}$  are considered as components of a five-dimensional unit vector, five normalized vectors can be constructed, one for each of the IRs of  $C_{4v}$ . We define the  $k$ th component of such vectors by

$$e_k^\alpha = \sqrt{\frac{N_k}{h}} \chi_k^\alpha, \quad (1.6)$$

where  $k = 1, 2, \dots, 5$  denotes the class,  $N_k$  is the number of elements for the  $k$ th class,  $\chi_k^\alpha$  is the character of the  $k$ th class of the  $\alpha$ th IR, and  $h$  is the number of elements in the group. The vectors are

$$\begin{aligned}
\mathbf{e}^{A_1} &= \frac{1}{\sqrt{8}} \begin{pmatrix} 1 \\ \sqrt{2} \\ 1 \\ \sqrt{2} \end{pmatrix}, & \mathbf{e}^{A_2} &= \frac{1}{\sqrt{8}} \begin{pmatrix} 1 \\ \sqrt{2} \\ 1 \\ -\sqrt{2} \end{pmatrix}, \\
\mathbf{e}^{B_1} &= \frac{1}{\sqrt{8}} \begin{pmatrix} 1 \\ -\sqrt{2} \\ 1 \\ \sqrt{2} \end{pmatrix}, & \mathbf{e}^{B_2} &= \frac{1}{\sqrt{8}} \begin{pmatrix} 1 \\ -\sqrt{2} \\ 1 \\ -\sqrt{2} \end{pmatrix}, & \mathbf{e}^{\mathcal{E}} &= \frac{1}{\sqrt{8}} \begin{pmatrix} 2 \\ 0 \\ -2 \\ 0 \\ 0 \end{pmatrix},
\end{aligned} \tag{1.7}$$

where the order of the components (top to bottom) is the same as the order of the classes in the character table.

It is easily verified that these vectors are orthogonal to each other, meaning that the scalar product (dot product) of any two different vectors is zero,  $(\mathbf{e}^\alpha, \mathbf{e}^\beta) = (1/h) \sum_{k=1}^{\mathcal{N}_c} N_k (\chi_k^\alpha)^* \chi_k^\beta = \delta_{\alpha\beta}$ . The orthogonality of the characters of the IRs is a general feature of a group. A statement of this property is given in Theorem 1.5.

**Theorem 1.5** (Orthogonality of the characters of irreducible representations) *The characters of the representation matrices of the IRs of a group are orthogonal to one another:*

$$\frac{1}{h} \sum_{i=1}^h (\chi_i^\alpha)^* \chi_i^\beta = \delta_{\alpha\beta}, \tag{GT1.5a}$$

where  $\chi_i^\alpha$  is the character of  $\Gamma^\alpha(O_i)$  and  $h$  is the number of elements in the group.

Since operations belonging to the same class have the same character,

$$\frac{1}{h} \sum_{k=1}^{\mathcal{N}_c} N_k (\chi_k^\alpha)^* \chi_k^\beta = \delta_{\alpha\beta}, \tag{GT1.5b}$$

where  $N_k$  is the number of elements in the  $k$ th class and  $\mathcal{N}_c$  is the number of classes in the group.

Theorem 1.5 is the general statement of the result we found for the characters in (1.7). To proceed with our analysis we also need the results from group theory given in Theorem 1.6.

**Theorem 1.6** (Properties of irreducible representations)

1. The number of different irreducible representations of a group is equal to  $\mathcal{N}_c$ , the number of classes.



2. The sum of the squares of the dimensions of all the distinct IRs of a group is equal to the number of elements in the group:

$$\sum_{i=1}^{\mathcal{N}_c} l_i^2 = h,$$

where  $l_i$  is the dimension of the  $i$ th IR and  $h$  is the number of elements in the group.

We see from the character table for  $C_{4v}$  that there are five IRs. Since the character  $E$  is equal to the dimensionality of the IR, it is clear the first four IRs are one-dimensional and the last is two-dimensional. The first result quoted in Theorem 1.6 tells us that there are five IRs since there are five classes for  $C_{4v}$ . The second result of Theorem 1.6 tells us that the sum of the squares of the dimensions of the five IRs must be 8. There can't be a three-dimensional IR (since  $3^2 = 9$  is already greater than 8) and the smallest dimension possible has  $l_i = 1$ . So we need five integers, all of which are either 1 or 2 and whose squares add up to 8. The only solution is  $1^2 + 1^2 + 1^2 + 1^2 + 2^2 = 8$ .

Our next step is to determine the number and types of IRs contained in our  $8 \times 8$  representation,  $\Gamma$ . In general, if  $\Gamma$  is any representation of the group we know that there exists a similarity transformation,  $\mathbb{S}^{-1}\Gamma(O_i)\mathbb{S} = \Gamma'(O_i)$ , where  $\Gamma'(O_i)$  is block-diagonal with various IR matrices along the diagonal. The character of  $\Gamma'(O_i)$  is equal to the sum of the traces of the IR blocks along the diagonal. Since the trace of  $\Gamma(O_i)$  is unchanged by the similarity transformation, its trace is equal to the trace of  $\Gamma'(O_i)$ . Therefore, it follows that

$$\chi_i^\Gamma = \sum_{\alpha=1}^{\mathcal{N}_c} n^\alpha \chi_i^\alpha \quad (i = 1, 2, \dots, h), \quad (1.8)$$

where  $\chi_i^\Gamma$  is the character of the representation matrix  $\Gamma(O_i)$  and  $\chi_i^\alpha$  is the character of the  $\alpha$ th IR representing the operation  $O_i$ . The coefficients  $n^\alpha$  are the number of times the  $\alpha$ th IR occurs among the diagonal blocks of  $\Gamma'(O_i)$ . Notice that the  $n^\alpha$  coefficients are the same for all of the different operations  $O_i$ . This is what is meant when it is stated that  $\mathbb{S}^{-1}\Gamma\mathbb{S}$  block-diagonalizes all of the representation matrices in the same way.

If we multiply both sides of (1.8) by the factor  $(1/h)(\chi_i^\beta)^*$  and sum over all of the operations of the group, we obtain

$$\frac{1}{h} \sum_{i=1}^h (\chi_i^\beta)^* \chi_i^\Gamma = \sum_{\alpha=1}^{\mathcal{N}_c} n^\alpha \frac{1}{h} \sum_{i=1}^h (\chi_i^\beta)^* \chi_i^\alpha = \sum_{\alpha=1}^{\mathcal{N}_c} n^\alpha \delta_{\alpha\beta} = n^\beta. \quad (1.9)$$

To obtain the final result in (1.9) we used the equation (GT1.5a) from Theorem 1.5. Equation (1.9) can be rewritten in terms of the characters of the classes:

$$n^\beta = \frac{1}{h} \sum_{k=1}^{\mathcal{N}_c} N_k (\chi_k^\beta)^* \chi_k^\Gamma, \quad (1.10)$$

where the sum of  $k$  is over the classes,  $N_k$  is the number of elements in the  $k$ th class,  $\mathcal{N}_c$  is the number of classes,  $\chi_k^\Gamma$  is the character of the  $k$ th class of  $\Gamma$ , and  $\chi_k^\beta$  is the character of the  $k$ th class of the  $\beta$ th IR.

To see how (1.10) works, we apply it to our representation for squarene. With the help of the character table (Table 1.6), we find that

$$\begin{aligned} n^\alpha &= \frac{1}{h} [\chi_E^* \chi_E^\alpha + 2(\chi_{C_4}^* \chi_{C_4}^\alpha) + \chi_{C_2}^* \chi_{C_2}^\alpha + 2(\chi_{\sigma_v}^* \chi_{\sigma_v}^\alpha) + 2(\chi_{\sigma_d}^* \chi_{\sigma_d}^\alpha)], \\ n^{A_1} &= \frac{1}{8} [8 \times 1 + 2(0 \times 1) + 0 \times 1 + 2(0 \times 1) + 2(0 \times 1)] = 1, \\ n^{A_2} &= \frac{1}{8} [8 \times 1 + 2(0 \times 1) + 0 \times 1 + 2(0 \times -1) + 2(0 \times -1)] = 1, \\ n^{B_1} &= \frac{1}{8} [8 \times 1 + 2(0 \times -1) + 0 \times 1 + 2(0 \times 1) + 2(0 \times -1)] = 1, \\ n^{B_2} &= \frac{1}{8} [8 \times 1 + 2(0 \times -1) + 0 \times 1 + 2(0 \times -1) + 2(0 \times 1)] = 1, \\ n^\mathcal{E} &= \frac{1}{8} [8 \times 2 + 2(0 \times 0) + 0 \times -2 + 2(0 \times 0) + 2(0 \times 0)] = 2. \end{aligned} \quad (1.11)$$

The decomposition of  $\Gamma$  into IRs is then, symbolically,

$$\Gamma = \Gamma^{A_1} + \Gamma^{A_2} + \Gamma^{B_1} + \Gamma^{B_2} + 2\Gamma^\mathcal{E}. \quad (1.12)$$

Since the  $\mathcal{E}$  IR is two-dimensional, it requires two basis functions. That is,  $\mathbb{S}^{-1}$  will have two rows of symmetry functions for each  $\mathcal{E}$  IR. To distinguish the two functions they are called the “row-1” and “row-2” basis functions of  $\mathcal{E}$ . (An  $N$ -dimensional IR will have  $N$  rows of symmetry functions.) For squarene  $\mathcal{E}$  occurs twice in the decomposition, so there will be two different row-1 and two different row-2 symmetry functions in  $\mathbb{S}^{-1}$ .

### 1.2.5 Step 6: Analyze the information contained in the decomposition

One of the most important results of group theory is the result stated below in Theorem 1.7.

**Theorem 1.7** (Matrix elements of a commuting operator) *If  $\mathbb{H}$  is a Hermitian operator that commutes with the operations of the group, the matrix elements of  $\mathbb{H}$  vanish between basis functions for different IRs or between basis functions for different rows of  $\mathbb{S}^{-1}$  (or columns of  $\mathbb{S}$ ) of the same IR.*

*Let  $\mathbf{V}_j^\alpha$  be a basis vector for the  $j$ th row of the  $\alpha$ th IR and  $\mathbf{W}_k^\beta$  be a basis vector for the  $k$ th row of the  $\beta$ th IR, then*

$$\langle \mathbf{V}_j^\alpha | \mathbb{H} | \mathbf{W}_k^\beta \rangle = \mathbb{M}_{VW} \delta_{jk} \delta_{\alpha\beta},$$

*where  $\mathbb{M}_{VW}$  is a constant that depends on the two functions.*

*Note that  $\mathbf{V}$  and  $\mathbf{W}$  can both be basis functions for the same row of the same IR even if they are different functions.*

For our vibration problem Theorem 1.7 tells us that there are no non-zero matrix elements of  $\mathbb{F}$  between symmetry functions that belong to different IRs or to different rows of  $\mathbb{S}^{-1}$  (or columns of  $\mathbb{S}$ ) of the same IR.

A great deal of information can be gleaned from the decomposition of  $\Gamma$  (Eq. (1.12)). First, we note that  $\Gamma^{A_1}$ ,  $\Gamma^{A_2}$ ,  $\Gamma^{B_1}$ , and  $\Gamma^{B_2}$  are one-dimensional IRs and  $\Gamma^{\mathcal{E}}$  is a two-dimensional IR. The number of degrees of freedom is  $(4 \times 1 + 2 \times 2) = 8$ . We know that the similarity transformation  $\mathbb{S}$  which block-diagonalizes  $\Gamma$  must also block-diagonalize the force-constant matrix,  $\mathbb{F}$ , of (1.1). Thus  $\mathbb{S}^{-1}\mathbb{F}\mathbb{S}$  will have four  $1 \times 1$  blocks. Since, according to Theorem 1.7, there can be no matrix elements between basis functions for different IRs, the columns of  $\mathbb{S}$  corresponding to these one-dimensional blocks must be eigenvectors. For these four normal modes the eigenvectors are the same as the symmetry functions and are completely determined, independently of the values of the force constants. The eigenvalues (mass times frequencies squared), of course, depend on the force constants, since they are diagonal matrix elements of  $\mathbb{S}^{-1}\mathbb{F}\mathbb{S}$  corresponding to the  $A_1$ ,  $A_2$ ,  $B_1$ , and  $B_2$  vibrations.

We also know that  $\mathbb{S}^{-1}\mathbb{F}\mathbb{S}$  has two  $(2 \times 2)$   $\mathcal{E}$ -representations. Since  $\mathcal{E}$  appears twice in the decomposition of  $\Gamma$ , there will be two different symmetry functions that are the bases for row 1 and two that are the bases for row 2 of  $\mathcal{E}$ . There can be matrix elements between two functions that are bases for the same row of the same IR. Therefore  $\mathbb{S}^{-1}\mathbb{F}\mathbb{S}$  could have what appears to be a  $4 \times 4$  block.

### 1.2.6 Step 7: Generate the symmetry functions

In order to determine the  $\mathbb{S}$  matrix we need to find the symmetry functions. Group-theoretical results can be used to generate the symmetry functions starting from an arbitrary function of the displacement coordinates. The theorem that allows us to do this is given below in Theorem 1.8.

**Theorem 1.8** (The symmetry-function-generating machine: The projection operator) *Let  $\mathbf{V}$  be an arbitrary column vector and generate the vector  $\mathbf{V}_m^\alpha$  according to the rule*

$$\mathbf{V}_m^\alpha = \sum_{k=1}^h \Gamma_{mm}^\alpha(O_k) [\Gamma(O_k) \mathbf{V}]. \quad (\text{GT1.8})$$

*Then  $\mathbf{V}_m^\alpha$  is a basis function for row  $m$  of the  $\alpha$ th IR or a null vector.*

In Eq. (GT1.8),  $\Gamma_{mm}^\alpha(O_k)$  is the  $m$ th diagonal matrix element of the  $\alpha$ th IR for the  $k$ th operator of the group and  $\Gamma(O_k)\mathbf{V}$  is the function obtained by multiplying the function  $\mathbf{V}$  by the matrix  $\Gamma(O_k)$ . If we choose  $\mathbf{V}$  to be any linear function of the displacement coordinates for squarene,  $\mathbf{V}_m^\alpha$  (when normalized) will be a symmetry function that is a basis for row  $m$  of the  $\alpha$ th IR. *Therefore Theorem 1.8 provides a direct method for obtaining the symmetry functions that are needed in order to block-diagonalize the eigenvalue matrix equation of (1.1).*

To simplify the notation we shall use  $\mathbf{V}_{xk}$  ( $\mathbf{V}_{yk}$ ) to indicate a column vector having a single entry of “1” in the row corresponding to  $x$  ( $y$ ) displacement on the  $k$ th corner.

As an example we generate the symmetry coordinate that transforms according to the  $B_1$  irreducible representation.  $\Gamma^{B_1}$  is one-dimensional, so the matrix elements are the same as the characters listed in Table 1.6. We select as our arbitrary column vector,  $\mathbf{V}_{x3}$ , where

$$\mathbf{V}_{x3} = \begin{bmatrix} 0 \\ 0 \\ 0 \\ 0 \\ 1 \\ 0 \\ 0 \\ 0 \end{bmatrix}.$$

Using the action table (Table 1.3) and character table (Table 1.6), we have

$$\begin{aligned} \mathbf{V}^{B_1} \propto & \left[ (1)\Gamma(E) + (-1)\Gamma(C_4) + (1)\Gamma(C_2) + (-1)\Gamma(C_4^3) \right. \\ & \left. + (-1)\Gamma(\sigma_{d1}) + (-1)\Gamma(\sigma_{d2}) + (1)\Gamma(\sigma_{v1}) + (1)\Gamma(\sigma_{v2}) \right] \mathbf{V}_{x3}. \end{aligned} \quad (1.13)$$

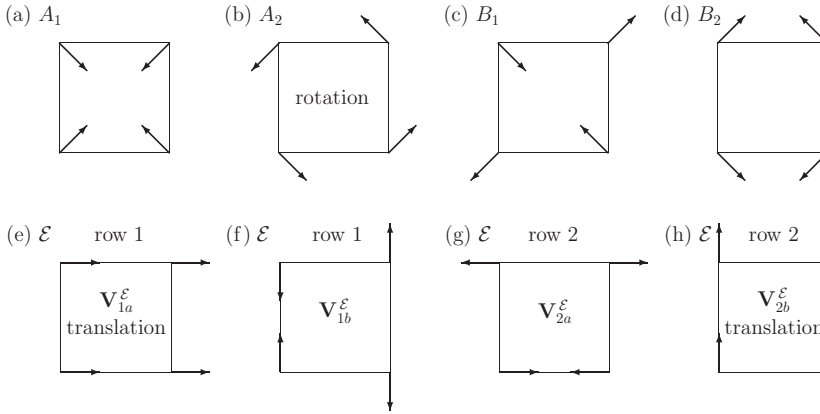


Figure 1.5 The squareene molecule and its symmetry functions.

Expressing  $\mathbf{V}^{B_1}$  as a normalized column vector, we have

$$\mathbf{V}^{B_1} = \frac{1}{\sqrt{8}} \begin{bmatrix} -1 \\ -1 \\ -1 \\ 1 \\ 1 \\ 1 \\ 1 \\ -1 \end{bmatrix}. \quad (1.14)$$

We could have chosen different displacements for  $\mathbf{V}$  and generated the same result. Since  $\Gamma^{B_1}$  appears only once in the decomposition,  $\mathbf{V}^{B_1}$  must be an eigenvector of the molecular vibration problem of (1.1). Figure 1.5(c) shows schematically the relative motions of the atoms for this normal mode.

Now let us find the symmetry functions that transform according to  $\mathcal{E}$ . The representation is two-dimensional and, according to (1.12), it is contained twice in the decomposition of  $\Gamma$ . This means that there must be four symmetry functions (2 IRs  $\times$  2 rows). To use the symmetry-function-generating machine we need the diagonal matrix elements of the IR for  $\mathcal{E}$ . According to the character table (the last column of Table 1.6)  $X$  and  $Y$  (or the displacements  $r_x$  and  $r_y$ ) can be used as basis functions for a two-dimensional  $\mathcal{E}$  representation.

We have already done the work for this representation. The first two rows of Table 1.3 show how  $r_x$  and  $r_y$  transform under the group operations. We have, for example, that

$$\begin{aligned} C_4 r_x &\rightarrow -r_y, \\ C_4 r_y &\rightarrow r_x, \end{aligned}$$

Table 1.7 IR matrices for the  $\mathcal{E}$  representation

$\Gamma^{\mathcal{E}}(E) = \begin{bmatrix} 1 & 0 \\ 0 & 1 \end{bmatrix}$	$\Gamma^{\mathcal{E}}(C_4) = \begin{bmatrix} 0 & 1 \\ -1 & 0 \end{bmatrix}$
$\Gamma^{\mathcal{E}}(C_2) = \begin{bmatrix} -1 & 0 \\ 0 & -1 \end{bmatrix}$	$\Gamma^{\mathcal{E}}(C_4^3) = \begin{bmatrix} 0 & -1 \\ 1 & 0 \end{bmatrix}$
$\Gamma^{\mathcal{E}}(\sigma_{d1}) = \begin{bmatrix} -1 & 0 \\ 0 & 1 \end{bmatrix}$	$\Gamma^{\mathcal{E}}(\sigma_{d2}) = \begin{bmatrix} 1 & 0 \\ 0 & -1 \end{bmatrix}$
$\Gamma^{\mathcal{E}}(\sigma_{v1}) = \begin{bmatrix} 0 & 1 \\ 1 & 0 \end{bmatrix}$	$\Gamma^{\mathcal{E}}(\sigma_{v2}) = \begin{bmatrix} 0 & -1 \\ -1 & 0 \end{bmatrix}$

from which it follows that  $C_4$  has the  $2 \times 2$  IR,

$$\Gamma^{\mathcal{E}}(C_4) = \begin{bmatrix} 0 & 1 \\ -1 & 0 \end{bmatrix}.$$

All of the  $2 \times 2$  matrices for the  $\mathcal{E}$  representation are shown in Table 1.7.

To generate a row-1 symmetry function we proceed as we did in finding  $\mathbf{V}^{B_1}$ , except now we use the diagonal elements,  $\Gamma^{\mathcal{E}}(O_i)_{11}$ , instead of the characters to generate the function. The matrix elements are given in Table 1.7. Since there are several coordinates, we shall label these vectors according to the IR **and** the row of the matrix element used to generate the function. Using  $\mathbf{V}_{x1}$  as our arbitrary function and the first-row diagonal matrix elements, we obtain

$$\begin{aligned} \mathbf{V}_{1a}^{\mathcal{E}} &\propto \left[ (1)\Gamma(E) + (-1)\Gamma(C_2) + (-1)\Gamma(\sigma_{d1}) + (1)\Gamma(\sigma_{d2}) \right] \mathbf{V}_{x1} \\ &= \left[ \mathbf{V}_{x1} + \mathbf{V}_{x2} + \mathbf{V}_{x3} + \mathbf{V}_{x4} \right] \end{aligned}$$

and the normalized vector is

$$\mathbf{V}_{1a}^{\mathcal{E}} = \frac{1}{2} \begin{bmatrix} 1 \\ 0 \\ 1 \\ 0 \\ 1 \\ 0 \\ 1 \\ 0 \end{bmatrix}.$$

The physical motion represented by this vector is translation in the  $x$ -direction as shown in Fig. 1.5(e). If we use  $\mathbf{V}_{y1}$  to generate a symmetry function, we find

$$\mathbf{V}_{1b}^{\mathcal{E}} = \frac{1}{2} \begin{bmatrix} 0 \\ 1 \\ 0 \\ -1 \\ 0 \\ 1 \\ 0 \\ -1 \end{bmatrix}.$$

$\mathbf{V}_{1a}^{\mathcal{E}}$  and  $\mathbf{V}_{1b}^{\mathcal{E}}$  are the two row-1 symmetry functions. The vectors are orthogonal to each other. The remaining two  $\mathcal{E}$ -functions transform according to the row-2 symmetry functions of the  $\mathcal{E}$  irreducible representation. For the row-2 vectors we use the (2,2) diagonal elements with  $\mathbf{V}_{x1}$  and  $\mathbf{V}_{y1}$  as the generating functions. We obtain

$$\mathbf{V}_{2a}^{\mathcal{E}} = \frac{1}{2} \begin{bmatrix} 1 \\ 0 \\ -1 \\ 0 \\ 1 \\ 0 \\ -1 \\ 0 \end{bmatrix}, \quad \mathbf{V}_{2b}^{\mathcal{E}} = \frac{1}{2} \begin{bmatrix} 0 \\ 1 \\ 0 \\ 1 \\ 0 \\ 1 \\ 0 \\ 1 \end{bmatrix}. \quad (1.15)$$

The vector  $\mathbf{V}_{2b}^{\mathcal{E}}$  represents a translation in the  $y$ -direction.

Using  $\mathbf{V}_{x1}$  as the arbitrary function, we find the  $A_2$  symmetry function to be

$$\mathbf{V}^{A_2} = \frac{1}{\sqrt{8}} \begin{bmatrix} 1 \\ -1 \\ 1 \\ 1 \\ -1 \\ 1 \\ -1 \\ -1 \end{bmatrix}.$$

The motion associated with  $\mathbf{V}^{A_2}$ , shown in Fig. 1.5(b), is a rotation about a  $z$ -axis through the center of the square.<sup>7</sup> This result could have been anticipated from the

<sup>7</sup> The  $\mathbf{V}^{A_2}$  mode represents a rotation in the limit of small displacements.

Table 1.8 *The  $\mathbb{S}$  matrix. The top row labels the symmetry functions according to the IR to which they belong. The left-most column lists the displacement coordinates and the bottom row lists the normalization factors. The center  $8 \times 8$  is the  $\mathbb{S}$  matrix.*

	$\mathbf{V}^{A_1}$	$\mathbf{V}^{A_2}$	$\mathbf{V}^{B_1}$	$\mathbf{V}^{B_2}$	$\mathbf{V}_{1a}^{\mathcal{E}}$	$\mathbf{V}_{1b}^{\mathcal{E}}$	$\mathbf{V}_{2a}^{\mathcal{E}}$	$\mathbf{V}_{2b}^{\mathcal{E}}$
$r_{x1}$	1	1	-1	1	1	0	1	0
$r_{y1}$	1	-1	-1	-1	0	1	0	1
$r_{x2}$	-1	1	-1	-1	1	0	-1	0
$r_{y2}$	1	-1	1	-1	0	-1	0	1
$r_{x3}$	-1	-1	1	-1	1	0	1	0
$r_{y3}$	-1	1	1	1	0	1	0	1
$r_{x4}$	1	-1	1	1	1	0	-1	0
$r_{y4}$	-1	-1	-1	1	0	-1	0	1
Normalization factor	$1/\sqrt{8}$	$1/\sqrt{8}$	$1/\sqrt{8}$	$1/\sqrt{8}$	$\frac{1}{2}$	$\frac{1}{2}$	$\frac{1}{2}$	$\frac{1}{2}$

character table (Table 1.6), which lists  $R_z$  (rotation about the  $z$ -axis) as the basis function (last column) for the  $A_2$ . All of the symmetry functions for squarene are shown schematically in Fig. 1.5.

The symmetry functions can be used to construct the  $\mathbb{S}$  and  $\mathbb{S}^{-1}$  matrices needed for the similarity transformation that block-diagonalizes the eigenvalue matrix equation (1.1). The  $8 \times 8$  matrix  $\mathbb{S}$  is given in Table 1.8. The inverse,  $\mathbb{S}^{-1}$ , is simply the transpose of  $\mathbb{S}$ .

### 1.2.7 Step 8. Block-diagonalize the eigenvalue matrix equation

A vibrational normal mode must leave the center of mass stationary. This can be expressed by the conditions

$$\sum_i m_i \mathbf{r}_i = 0, \quad (1.16)$$

where  $\mathbf{r}_i$  is the vector displacement of the  $i$ th atom with mass  $m_i$ . It can be seen from Fig. 1.5 that for squarene all of the symmetry functions except the translations leave the center of mass unchanged. Often, however (see Exercise 1.8), Eq. (1.16) can be applied as a constraint to assist in the analysis.

#### Center-of-mass considerations

The similarity transformation carries the  $\mathbb{F}$  matrix of (1.1) into the block-diagonal form. We shall denote this block-diagonal matrix by the symbol,  $\mathfrak{F}$ , where



$\mathfrak{F} = \mathbb{S}^{-1} \mathbb{F} \mathbb{S}$ . Since the  $A_1$ ,  $A_2$ ,  $B_1$ , and  $B_2$  irreducible representations are one-dimensional, the diagonal matrix elements must be the eigenvalues. Thus, the first four diagonal entries in  $\mathfrak{F}$  are  $m(\omega^{A_1})^2$ ,  $m(\omega^{A_2})^2$ ,  $m(\omega^{B_1})^2$ , and  $m(\omega^{B_2})^2$ . We have identified the  $A_2$  mode as rotation and therefore  $\omega^{A_2} = 0$ . For the two  $2 \times 2$  blocks we use the fact that the eigenvectors must be linear combinations of the symmetry functions that transform according to the same row of the same IR. However, in this case, one of the row-1 symmetry functions,  $\mathbf{V}_{1a}^{\mathcal{E}}$ , corresponds to translation of the molecule in the  $x$ -direction. The vibrational frequencies are unaffected by translation of the molecule as a unit and therefore we may assume that there is no mixing of the two symmetry functions. Similarly,  $\mathbf{V}_{2b}^{\mathcal{E}}$  corresponds to translation in the  $y$ -direction and hence the mixing of it with  $\mathbf{V}_{2a}^{\mathcal{E}}$  may be taken to be zero also.

From Fig. 1.5 it is clear that the vibrational motions represented by  $\mathbf{V}_{1b}^{\mathcal{E}}$  and  $\mathbf{V}_{2a}^{\mathcal{E}}$  are equivalent physically. In fact, application of the operator  $C_4^3$  to  $\mathbf{V}_{1b}^{\mathcal{E}}$  produces  $\mathbf{V}_{2a}^{\mathcal{E}}$  and therefore, according to Theorem 1.9, these two normal modes must be degenerate; that is,  $\omega^{\mathcal{E}}(1b) = \omega^{\mathcal{E}}(2a) \equiv \omega^{\mathcal{E}}$ . The last four diagonal elements of  $\mathfrak{F}$  are 0,  $m(\omega^{\mathcal{E}})^2$ ,  $m(\omega^{\mathcal{E}})^2$ , and 0. Therefore,  $\mathfrak{F}$  is completely diagonal.

**Theorem 1.9** *Let  $\mathbb{H}$  be a Hermitian matrix that commutes with the elements of the group. If  $\mathbf{V}^{\lambda}$  is an eigenvector of  $\mathbb{H}$  with eigenvalue  $\lambda$ , then  $O_i \mathbf{V}^{\lambda}$  is also an eigenvector with eigenvalue  $\lambda$ , where  $O_i$  is any element of the group.*

### 1.3 Eigenvalues and eigenvectors

In the symmetry analysis of an eigenvalue equation of the type  $\mathbb{H}\psi = \lambda\psi$ , it is common for the same IR to occur more than once in the decomposition of  $\Gamma$ . Consider the case for which  $\Gamma^{\alpha}$  is an  $m \times m$  IR that occurs  $p$  times in the decomposition of  $\Gamma$ . There will be  $p \times m$  symmetry functions:  $p$  symmetry functions for each of the  $m$  rows. The  $p$  ( $m \times m$ ) submatrices on the diagonal of  $\Gamma' = \mathbb{S}^{-1} \Gamma \mathbb{S}$  will be uncoupled from one another. However, *it does not follow that  $\mathbb{H}' = \mathbb{S}^{-1} \mathbb{H} \mathbb{S}$  will automatically be block-diagonal since there can be non-zero matrix elements between the same rows of the same IR and each row of  $\Gamma^{\alpha}$  occurs  $p$  times*. The problem is easily corrected by rearranging the rows and columns of  $\mathbb{H}'$  so that all  $p$  functions belonging to a given row are grouped together. The rearrangement does not change the eigenvalues, but simply changes the order in which we list the symmetry functions. After rearrangement  $\mathbb{H}'$  will have  $m$  ( $p \times p$ ) blocks, even though  $\Gamma' = \mathbb{S}^{-1} \Gamma \mathbb{S}$  has  $p$  ( $m \times m$ ) blocks. This type of rearrangement is illustrated in Fig. 1.6 for a case where  $p = 3$  and  $m = 2$ .

Each of the  $m$  submatrices of  $\mathbb{H}'$  will produce  $p$  eigenvalues when diagonalized. There is no requirement of degeneracy among these  $p$  eigenvalues of one of the  $p \times p$  matrices. **However, each of the  $m$  submatrices will yield the same set of**

(a) Three  $2 \times 2$ 

$$\Gamma' = \mathbb{S}^{-1} \Gamma \mathbb{S} =$$

	1a	2a	1b	2b	1c	2c
1a	×	×				
2a	×	×				
1b			×	×		
2b			×	×		
1c					×	×
2c					×	×

(b) Matrix elements between same rows

$$\mathbb{H}' = \mathbb{S}^{-1} \mathbb{H} \mathbb{S} =$$

	1a	2a	1b	2b	1c	2c
1a	×		×		×	
2a		×		×		×
1b	×		×		×	
2b		×		×		×
1c	×		×		×	
2c		×		×		×

(c) Two  $3 \times 3$ 

$$\mathbb{H}'_{\text{Rearranged}} =$$

	1a	1b	1c	2a	2b	2c
1a	×	×	×			
1b	×	×	×			
1c	×	×	×			
2a				×	×	×
2b				×	×	×
2c				×	×	×

Figure 1.6 Block-diagonal forms. (a)  $\mathbb{S}^{-1} \Gamma \mathbb{S}$ . The first-row functions are labeled 1a, 1b, and 1c. The second-row functions are labeled 2a, 2b, and 2c. (b)  $\mathbb{H}' = \mathbb{S}^{-1} \mathbb{H} \mathbb{S}$  before rearrangement. (c)  $\mathbb{S}^{-1} \mathbb{H} \mathbb{S}$  after rearranging same-row functions adjacent to one another.

**eigenvalues. Consequently each of the  $p$  eigenvalues will be  $m$ -fold degenerate.**

For example, for squarene the two first-row eigenfunctions have eigenvalues of 0 and  $m(\omega^{\mathcal{E}})^2$  and the second-row functions yield exactly the same eigenvalues. In principle, the two first-row (or the two second-row) symmetry functions for the  $\mathcal{E}$  IR could be mixed to form the eigenvectors. However, no mixing occurs for squarene because  $\mathbf{V}_{1a}$  is a translation of the molecule in the  $x$ -direction and therefore does not mix with the  $\mathbf{V}_{1b}$  vibrational mode. Similarly  $\mathbf{V}_{2b}$  is a translation in the  $y$ -direction and therefore does not mix with the  $\mathbf{V}_{2a}$  vibrational mode.

If an IR occurs more than once in the decomposition  $\Gamma$ , the eigenvectors and eigenvalues of the final sub-blocks of  $\mathbb{H}' = \mathbb{S}^{-1} \mathbb{H} \mathbb{S}$  usually can not be determined

by group theory alone (unlike in the case of squareness). However, the eigenvectors must be linear combinations of the symmetry functions that belong to the same row of the same IR. This allows us to form eigenvectors in terms of mixing parameters. For example, if we have an uncoupled  $2 \times 2$  block associated with the symmetry functions  $\mathbf{V}_{1a}^\alpha$  and  $\mathbf{V}_{1b}^\alpha$ , the eigenvectors  $\psi_{1r}^\alpha$  and  $\psi_{1s}^\alpha$  may be written as orthogonal linear combinations,

$$\begin{aligned}\psi_{1r}^\alpha &= \frac{1}{\sqrt{1+|a|^2}} [\mathbf{V}_{1a}^\alpha + a\mathbf{V}_{1b}^\alpha], \\ \psi_{1s}^\alpha &= \frac{1}{\sqrt{1+|a|^2}} [-a^*\mathbf{V}_{1a}^\alpha + \mathbf{V}_{1b}^\alpha],\end{aligned}\tag{1.17}$$

where  $a$  is a “mixing” parameter that specifies the amount of mixing of the two symmetry functions which is needed in order to form the eigenvectors. Equation (1.17) defines a transformation,  $\mathbf{t}$ , given by

$$\mathbf{t} = \frac{1}{\sqrt{1+|a|^2}} \begin{bmatrix} 1 & a \\ -a^* & 1 \end{bmatrix}\tag{1.18}$$

that diagonalizes the  $2 \times 2$  submatrix of  $\mathbb{H}'$ . In general,  $a$  will not be zero and may be complex. In the case of molecular vibrations  $a$  is sometimes determined by the requirement that the translations have zero frequencies or that the center of mass of the molecule be stationary. In other cases the mixing parameter can be determined from experimentally observed frequencies.

Suppose  $\mathbb{H}'$  has the  $2 \times 2$  submatrix  $\mathbb{R}$ , with elements  $R_{11}$ ,  $R_{12}$ ,  $R_{21}$ , and  $R_{22}$ . (Because the submatrix must be Hermitian,  $R_{21}$  must be the complex conjugate of  $R_{12}$ .) The similarity transformation  $\mathbf{t}^{-1}\mathbb{R}\mathbf{t}$  leads to a diagonal submatrix for the proper choice of  $a$ ,

$$\mathbf{t}^{-1}\mathbb{R}\mathbf{t} = \begin{bmatrix} \lambda^r & 0 \\ 0 & \lambda^s \end{bmatrix},\tag{1.19}$$

where  $\lambda^r$  and  $\lambda^s$  are the eigenvalues of  $\psi_{1r}^\alpha$  and  $\psi_{1s}^\alpha$ , respectively. For molecular vibrational analysis these eigenvalues would be mass-weighted, squared frequencies,  $\lambda^r = m(\omega^r)^2$  and  $\lambda^s = m(\omega^s)^2$ . The matrix,  $\mathbb{R}$ , can then be expressed in terms of the eigenvalues and the mixing parameter,

$$\begin{aligned}\mathbb{R} &= \mathbf{t} \begin{bmatrix} \lambda^r & 0 \\ 0 & \lambda^s \end{bmatrix} \mathbf{t}^{-1} = \frac{1}{\sqrt{1+|a|^2}} \begin{pmatrix} \lambda^r + |a|^2\lambda^s & a\lambda^s - a^*\lambda^r \\ a^*\lambda^s - a\lambda^r & \lambda^s + |a|^2\lambda^r \end{pmatrix} \\ &= \begin{bmatrix} R_{11} & R_{12} \\ R_{12}^* & R_{22} \end{bmatrix}.\end{aligned}$$

Table 1.9 *The  $\mathfrak{F}$  matrix is diagonal with four distinct eigenvalues:  $m(\omega^{A_1})^2$ ,  $m(\omega^{B_1})^2$ ,  $m(\omega^{B_2})^2$ , and  $m(\omega^\mathcal{E})^2$ . The zero-eigenvalues  $\mathfrak{F}_{22}$ ,  $\mathfrak{F}_{55}$ , and  $\mathfrak{F}_{88}$  correspond to rotation ( $A_2$ ), translation in the  $x$ -direction ( $\mathbf{V}_{1a}^\mathcal{E}$ ) and translation in the  $y$ -direction ( $\mathbf{V}_{2b}^\mathcal{E}$ ), respectively.*

$m(\omega^{A_1})^2$							
	0						
		$m(\omega^{B_1})^2$					
			$m(\omega^{B_2})^2$				
				0			
					$m(\omega^\mathcal{E})^2$		
						$m(\omega^\mathcal{E})^2$	
							0

The point of this discussion is that it is often useful to express the matrix elements of  $\mathbb{H}$  in terms of the eigenvalues and symmetry-function mixing parameters.

#### 1.4 Construction of the force-constant matrix from the eigenvalues

Our symmetry analysis of squarene shows that there are at most four distinct vibrational frequencies. Group theory can not tell us what these frequencies are, and to carry the analysis further we have two choices: (1) construct a model for the force-constant matrix  $\mathbb{F}$  and determine the frequencies in terms of the force constants, or (2) use experimentally measured frequencies to calculate the set of force constants that will yield these frequencies. Since the force constants are not observable, we prefer to use the second approach.

The diagonalized  $\mathfrak{F}$  matrix is given in Table 1.9. Now that we know the elements of  $\mathfrak{F}$  and the  $\mathbb{S}$  matrix we can construct the  $\mathbb{F}$  matrix in terms of the vibrational frequencies since  $\mathbb{S}\mathfrak{F}\mathbb{S}^{-1} = \mathbb{F}$ . Recalling that  $\mathbb{S}^{-1}$  is simply the transpose of  $\mathbb{S}$  and carrying out the matrix multiplication yields the force-constant matrix given in Table 1.10.

There are 64 force-constant matrix elements, but only four independent parameters, the frequencies,  $m(\omega^{A_1})^2$ ,  $m(\omega^{B_1})^2$ ,  $m(\omega^{B_2})^2$ , and  $m(\omega^\mathcal{E})^2$ . The form of  $\mathbb{F}$  given in Table 1.10 is the most general form that (1) is consistent with symmetry requirements, (2) commutes with all of the operations of the group, and (3) has zero frequencies for the translation and rotation modes.

The alternate approach to analyzing the vibrational problem is to construct an empirical force-constant model and then diagonalize the matrix to find its

Table 1.10 *The force-constant matrix deduced from vibrational frequencies*

$r + v$	$s$	$-t - v$	$u$	$-r + v$	$-s$	$t - v$	$-u$
	$r + v$	$-u$	$t - v$	$-s$	$-r + v$	$u$	$t - v$
		$r + v$	$-s$	$t - v$	$u$	$-r + v$	$s$
			$r + v$	$-u$	$-t - v$	$s$	$-r + v$
				$r + v$	$s$	$-t - v$	$u$
	$F_{ji} = F_{ij}$				$r + v$	$-u$	$t - v$
						$r + v$	$-s$
							$r + v$

$$\begin{aligned}
r &= \frac{1}{8}m[(\omega^{A_1})^2 + (\omega^{B_1})^2 + (\omega^{B_2})^2], & s &= \frac{1}{8}m[(\omega^{A_1})^2 - (\omega^{B_1})^2 + (\omega^{B_2})^2], \\
t &= \frac{1}{8}m[(\omega^{A_1})^2 + (\omega^{B_1})^2 - (\omega^{B_2})^2], & u &= \frac{1}{8}m[(\omega^{A_1})^2 - (\omega^{B_1})^2 - (\omega^{B_2})^2], \\
v &= \frac{1}{2}m(\omega^{\mathcal{E}})^2.
\end{aligned}$$

eigenvalues. The force constants can then be adjusted until the eigenvalues achieve a best fit to the observed frequencies. However, special constraints must be employed in order to ensure that the translation and rotation modes have zero frequencies. Chemists often use *internal coordinates* [1.3] rather than Cartesian coordinates; for example, “bending” (changes in the angles between adjacent sides) and “stretching” (changes in distances between atoms) coordinates. This approach leads to a more complex form of the eigenvalue problem. Use of internal coordinates does, however, reduce the size of the eigenvalue equation. Some scientists find the description physically appealing because the “stretching” and “bending” force constants for a particular chemical bond are roughly the same for different molecules with similar bonds.

## 1.5 Optical properties

### *Infrared active normal modes*

We can determine which of the vibrational modes are infrared active and/or Raman active. To do this we consider Theorem 1.7 and the result

$$\langle V_j^\alpha | \mathbb{H} | W_k^\beta \rangle = \mathbb{M}_{VW} \delta_{jk} \delta_{\alpha\beta}. \quad (1.20)$$

If  $\mathbb{H}$  is a constant, say unity, then (1.20) gives

$$\langle V_j^\alpha | W_k^\beta \rangle = \mathbb{M}_{VW} \delta_{jk} \delta_{\alpha\beta}, \quad (1.21)$$

which means that vectors belonging to different IRs or to different rows of the same IR are orthogonal.

When a molecule in its ground state absorbs optical radiation a vibrational mode may be excited if the photon energy is approximately equal to the vibrational energy. Usually, the vibrational frequency is in the infrared spectral range. Whether or not a given vibrational mode can be excited depends largely upon the symmetry of the eigenvector.

A normal mode of molecular vibration involves the displacements of the nuclei from their equilibrium positions. When the nuclei move they may create an electric dipole due to the redistribution of electronic charge. The absorption of infrared radiation may occur when the electric dipole moment for the entire molecule due to nuclear displacements is non-zero. The electric dipole moment for the molecule is

$$\mu = \sum_i^N q_i \mathbf{r}_i,$$

where  $N$  is the number of atoms of the molecule,  $q_i$  is the effective charge, and  $\mathbf{r}_i$  is the displacement of the  $i$ th atom. The electric dipole moment  $\mu$  is a vector and its components  $\mu_x$ ,  $\mu_y$ , and  $\mu_z$  will transform under the operations of the group according to the IRs whose basis functions are  $x$ ,  $y$ , and  $z$ . It follows that the components of  $\mu$  belong to the same IRs as the translation modes of the molecule. For squarene (in two dimensions) the character table (Table 1.6) indicates that  $\mu_x$  and  $\mu_y$  belong to the  $\mathcal{E}$  IR of the  $C_{4v}$  group.

The quantum-mechanical probability of a transition from the molecular ground state to a state with one quantum of vibrational energy is proportional to [1.3]

$$\sum_{\alpha} \sum_k |\langle \mathbf{V}_0 | \mu | \mathbf{V}_k^{\alpha} \rangle|^2, \quad (1.22)$$

where  $\mathbf{V}_0$  is the molecular vibrational ground state,  $\mu$  is the dipole moment operator for the molecule, and  $\mathbf{V}_k^{\alpha}$  is the eigenvector for the state with one quantum of energy in the normal mode that belongs to the  $k$ th row of the  $\alpha$ th IR. The vibrational ground state,  $\mathbf{V}_0$ , transforms under the operations of the group as a constant, so for the purpose of determining whether the integral vanishes we need only know whether  $\langle \mu | \mathbf{V}_k^{\alpha} \rangle$  vanishes due to symmetry. Therefore (1.21) requires that  $\mathbf{V}_k^{\alpha}$  belongs to a translation IR, since otherwise the matrix element must vanish. Since  $\mu$  is antisymmetric with respect to the center of symmetry, we can also see the  $\langle \mu | \mathbf{V}_k^{\alpha} \rangle$  must vanish unless  $\mathbf{V}_k^{\alpha}$  is also antisymmetric. That is, a dipole transition from the ground state (symmetric) must be to an antisymmetric vibration. In general a dipole transition can occur only if the initial and final vibration states are opposite in parity. In addition, if the total electric dipole moment is zero the transition is forbidden.

**Theorem 1.10** (Infrared-active vibration mode) *For single quantum excitations from the vibrational ground state to a final vibrational state, a vibrational mode can not be infrared active unless it belongs to the same IR as  $x$  or  $y$  or  $z$ . If the total electric dipole moment due to the mode is zero, the transition is forbidden. The final state must be antisymmetric with respect to the center of symmetry if one exists.*

This rule is called the **selection rule** for infrared absorption. It is almost trivial to apply. In the case of squareene the functions labeled  $\mathbf{V}_{1b}^{\mathcal{E}}$  and  $\mathbf{V}_{2a}^{\mathcal{E}}$  are the only modes that belong to the same IR as a translation mode. Therefore  $\mathbf{V}_{1b}^{\mathcal{E}}$  and  $\mathbf{V}_{2a}^{\mathcal{E}}$  could **possibly** be infrared active. However, they are **not** because the dipole moment itself vanishes in this case; that is,  $\mu = \sum q_i \mathbf{r}_i = q \sum \mathbf{r}_i = 0$  for all of the vibrational modes.

### *Raman-active normal modes*

If the optical radiation incident on a molecule has energy greater than the energy of the normal modes of the molecule it is still possible for a vibrational transition to occur. If the optical radiation has angular frequency  $\omega_0$  and a normal mode has angular frequency  $\omega_1$ , in some cases the scattered optical radiation is observed to have angular frequencies  $\omega_0 \pm \omega_1$ . In this Raman process the light excites a normal mode (Stokes) or absorbs (anti-Stokes) the energy of a thermally excited normal mode.

For the Raman (Stokes) process the quantum-mechanical probability of the scattered light having frequency  $\omega_0 + \omega_1$  is proportional to [1.3]

$$\sum_{\alpha} \sum_k |\langle \mathbf{V}_0 | \alpha_p | \mathbf{V}_k^{\alpha} \rangle|^2. \quad (1.23)$$

The operator  $\alpha_p$  is the polarizability tensor. Symmetry-wise its elements behave as the symmetric (under inversion) bilinear products of the coordinates, such as  $x^2$ ,  $y^2$ ,  $z^2$ ,  $xy$ ,  $xz$ , and  $yz$ . In our two-dimensional example there is no  $z$ -coordinate so the relevant bilinear products are just  $x^2$ ,  $y^2$ , and  $xy$ . Again,  $\mathbf{V}_0$ , the vibrational ground state, can be treated as a constant and the question is whether  $\langle \alpha_p | \mathbf{V}_k^{\alpha} \rangle$  vanishes due to symmetry. According to (1.21), a non-vanishing result requires that  $\mathbf{V}_k^{\alpha}$  belong to the same IR as at least one of the products,  $x^2$ ,  $y^2$ , and  $xy$ , of  $\alpha_p$ . This information can be gleaned from the character table. For  $C_{4v}$  the far-right column of the character table (Table 1.6) lists the basis functions for the IRs. We see that the  $A_1$ ,  $B_1$ ,  $B_2$ , and  $\mathcal{E}$  vibrational modes have basis functions that contain such bilinear products. However, the  $\mathcal{E}$  modes do not have basis functions that transform as  $x^2$ ,  $y^2$ , or  $xy$ , and therefore can not be Raman active. Another way to see this is that the  $\mathcal{E}$  modes are antisymmetric under inversion, while  $\alpha_p$  is symmetric.

**Theorem 1.11** (Raman-active normal mode) *A normal vibration mode can not be Raman active unless it belongs to an IR that has basis functions that are symmetric under inversion and transform as bilinear functions of the spatial coordinates.*

Selection rules that forbid transitions such as those stated in Theorem 1.10 and Theorem 1.11 are always true. However, the converse statements need not always be valid. That is because the rules use only the IR label, but the row label of the IR as well as other factors must also be considered in order to say that a matrix element does not vanish. A more complete discussion of selection rules is given in Chapter 3.

### Center of symmetry

If a molecule is unchanged by inversion ( $\mathbf{r} \rightarrow -\mathbf{r}$ ) through a center of symmetry, the normal modes can be classified as odd or even. Even modes are unchanged by inversion and odd modes go into the negative of themselves under inversion. (The usual notation is *g* (*gerade*) for even modes and *u* (*ungerade*) for odd modes.) Clearly, the dipole-moment operator is odd under inversion because it is linear in the displacement coordinates. Therefore any normal mode that is infrared active must also be odd under inversion.

In the Raman case, the operator,  $\alpha_p$ , involves binary products of the displacements and is even under inversion. Therefore Raman-active normal modes must also be even under inversion. *We can conclude that, for a molecule having an inversion center, no normal mode can be both infrared active and Raman active.*

Our brief discussion of optical transitions included only transitions from the ground state to some excited vibrational state with a single quantum of energy. Other sorts of transitions are possible. For example, transitions from the ground state to more than one excited state, absorption of more than one quantum of vibrational energy, or even transitions from one excited state to another. These other types of transitions tend to be weaker in intensity, but can yield valuable spectroscopic information. Whatever the nature of the transition, the selection rule can be determined group-theoretically if the symmetry of the transition operator, the initial state, and the final state are specified.

### References

- [1.1] M. Tinkham, *Group Theory and Quantum Mechanics* (New York: McGraw-Hill Book Company, 1964);  
 D. M. Bishop, *Group Theory and Chemistry* (New York: Dover Publications, Inc., 1993);  
 E. P. Wigner, *Group Theory and Its Application to the Quantum Mechanics of Atomic Spectra* (New York: Academic Press, 1959).



- [1.2] R. E. DeWames and T. Wolfram, “Vibrational analysis of substituted and perturbed molecules I. The exact isotope rule for molecules”, *J. Chem. Phys.* **40**, 853–860 (1964).
- [1.3] E. B. Wilson, J. C. Decius, and P. C. Cross, *Molecular Vibrations: The Theory of Infrared and Raman Spectra* (New York: Dover Publications, 1980).

### Exercises

- 1.1 Consider a square, planar molecule (e.g.,  $\text{XeF}_4$ ) with four atoms of mass  $m_1$  on the corners of the square and an atom of mass  $m_2$  at the center of the square as shown in Fig. 1.7.

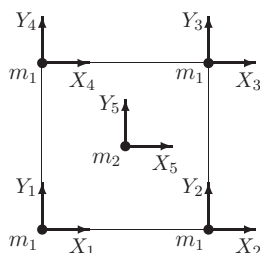


Figure 1.7

The mass matrix of (1.1) can not be taken as a scalar since there are two different masses. Show that the eigenvalue equation can be rewritten as

$$\mathbb{F}' \eta = \omega^2 \eta, \quad (\text{E1.1})$$

where  $\mathbb{F}' = \mathbb{M}^{-1/2} \mathbb{F} \mathbb{M}^{-1/2}$ ,  $\mathbb{M}^{1/2}$  is the square root of the diagonal mass matrix, and  $\eta = \mathbb{M}^{1/2} \xi$ .

- 1.2 Assuming  $\mathbb{F}$  is a Hermitian matrix, show that  $\mathbb{F}' = \mathbb{M}^{-1/2} \mathbb{F} \mathbb{M}^{-1/2}$  is also a Hermitian matrix; that is,  $\mathbb{F}'_{ij} = (\mathbb{F}'_{ji})^*$ . (Since  $\mathbb{F}'$  is Hermitian we can use all of the results of Chapter 1 to solve the new matrix eigenvalue equation, (E1.1).)
- 1.3 Using the coordinate system shown in Fig. 1.7, construct the  $10 \times 10$  representation matrices  $\Gamma(O_i)$  ( $i = 1, 2, \dots, 8$ ) for the operations of the group of the molecule. Use the fact that the central atom can only be transformed into itself.
- 1.4 For the representation matrices in Exercise 1.3, show that the decomposition into IRs is  $\Gamma = \Gamma^{A_1} + \Gamma^{A_2} + \Gamma^{B_1} + \Gamma^{B_2} + 3\Gamma^{\mathcal{E}}$ .
- 1.5 For the molecule of Exercise 1.1, use the symmetry-function-generating machine operating on the functions  $r_x(1) + r_x(5)$  and  $r_y(1) + r_y(5)$  to construct the  $A_1$ ,  $A_2$ ,  $B_1$ , and  $B_2$  symmetry functions. Why are these

symmetry functions the same as those of squarene? Are these symmetry functions eigenfunctions?

- 1.6 For the molecule of Exercise 1.1, use the symmetry-function-generating machine operating on the functions  $r_x(1)$ ,  $r_x(5)$ ,  $r_y(1)$ , and  $r_y(5)$  to construct three row-1 and three row-2  $\mathcal{E}$ -symmetry functions.
  - 1.7 For the molecule of Exercise 1.1, construct the  $x$ -translation and  $y$ -translation vectors  $\xi_{T_x}$  and  $\xi_{T_y}$ . Use these vectors to form  $\eta_{T_x}$  and  $\eta_{T_y}$ .
  - 1.8 The decomposition of  $\Gamma$  (Exercise 1.4) contains the  $\mathcal{E}$  IR three times. Therefore there are three symmetry functions for each row. One of the row-1 symmetry functions is the translation function  $\eta_{T_x}$ . The two remaining row-1 symmetry functions correspond to vibrations. (1) The *displacements* ( $\xi$ -functions) of these two row-1 functions must leave the center-of-mass stationary, and (2) the corresponding  $\eta$ -functions must be orthogonal to all of the other  $\eta$  symmetry functions.
- (a) Show that the row-1 and row-2  $\eta$ -functions for the  $\mathcal{E}$  vibrations satisfying conditions (1) and (2) are

<u>row-1 functions</u>	<u>row-2 functions</u>
$\eta_{1\alpha} = \frac{1}{\sqrt{N_{1\alpha}}} \begin{bmatrix} 1 \\ 0 \\ 1 \\ 0 \\ 1 \\ 0 \\ 1 \\ 0 \\ -\mu \\ 0 \end{bmatrix},$	$\eta_{2\alpha} = \frac{1}{\sqrt{N_{1\alpha}}} \begin{bmatrix} 0 \\ 1 \\ 0 \\ 1 \\ 0 \\ 1 \\ 0 \\ 1 \\ 0 \\ -\mu \end{bmatrix},$

$\eta_{1\beta} = \frac{1}{\sqrt{5}} \begin{bmatrix} 0 \\ 1 \\ 0 \\ -1 \\ 0 \\ 1 \\ 0 \\ -1 \\ 0 \\ 0 \end{bmatrix},$	$\eta_{2\beta} = \frac{1}{\sqrt{5}} \begin{bmatrix} 1 \\ 0 \\ -1 \\ 0 \\ 1 \\ 0 \\ -1 \\ 0 \\ 0 \\ 0 \end{bmatrix},$
--	--

where  $N_{1\alpha} = \sqrt{4 + \mu^2}$  and  $\mu = 4\sqrt{m_1/m_2}$ .

- (b) For the  $\mathcal{E}$  IR, make a sketch of the components of each of the six  $\eta$ -functions and give the relative amplitudes of the displacements.
- (c) Make a sketch of the sum of  $\eta_{1\alpha}$  and  $\eta_{1\beta}$  and the sum of  $\eta_{2\alpha}$  and  $\eta_{2\beta}$ .
- 1.9 Show that  $\eta_{T_x}$ ,  $\eta_{T_y}$ ,  $\eta_{1\alpha}$ ,  $\eta_{2\alpha}$ ,  $\eta_{1\beta}$ , and  $\eta_{2\beta}$  found in Exercise 1.8 form a set of mutually orthogonal vectors. Which of these vectors could be mixed to form eigenvectors? What symmetry functions are already eigenvectors?
- 1.10 Eigenvectors  $\psi_k$  satisfy the equation

$$\mathbb{H} \psi_k = \lambda_k \psi_k,$$

where  $\mathbb{H}$  is Hermitian and commutes with the operations of the group. Show that, if  $\psi_k$  is an eigenvector with eigenvalue  $\lambda_k$ , then  $\phi = O_i \psi_k$  is also an eigenvector with eigenvalue  $\lambda_k$ , where  $O_i$  is any operation of the group.

- 1.11 Make a sketch of the block-diagonalized portion of  $\mathbb{S}^{-1} \mathbb{F}' \mathbb{S}$  for the  $\mathcal{E}$ -mode block if  $\mathbb{S}$  is based on the symmetry functions of Exercise 1.8. Explain why the two  $2 \times 2$  blocks must have the same eigenvalues.
- 1.12 For an arbitrary group  $G$ , form a set of  $h$  matrices by application of the following rules. (i) Rearrange the group multiplication table so that  $E$  appears only on the diagonal. (ii) The representation matrix for  $\Gamma(R_i)$  is obtained by replacing  $R_i$  in the rearranged multiplication table by unity and all other entries by 0.

For example, for the group  $C_4$  the rearranged multiplication table is

	$E$	$C_2$	$C_4$	$C_4^3$
$E$	$E$	$C_2$	$C_4$	$C_4^3$
$C_2$	$C_2$	$E$	$C_4^3$	$C_4$
$C_4^3$	$C_4^3$	$C_4$	$E$	$C_2$
$C_4$	$C_4$	$C_4^3$	$C_2$	$E$

$$\Gamma(C_4) =$$

		1	
			1
	1		
1			

$$\Gamma(C_2) =$$

	1		
1			
			1
		1	

Prove, for any group, that the matrices constructed by application of rules (i) and (ii) form a representation of  $G$ . This representation is called the *regular*

*representation.* (Hint: The columns are labeled by  $R_i$  and the rows are labeled by  $R_j^{-1}$ , so  $\Gamma(R_a)_{ij}$  can be written as  $\Gamma(R_a)_{R_i^{-1}, R_j} \cdot$ )

- 1.13 For the operator  $C_{4v}$  use the regular representation (Exercise 1.12) to show explicitly that  $\Gamma(C_4)^{-1} = \Gamma(C_4^{-1})$ .
- 1.14 Let  $\mathcal{G}$  be the set of all the operators of the group  $G$  (the order of the operators is irrelevant). Show that  $R\mathcal{G} = \mathcal{G}$ , where  $R$  is any operator of the group  $G$ . This is called the *rearrangement theorem* because the only effect of multiplying  $\mathcal{G}$  by a member of  $G$  is to rearrange the order of the operators in  $\mathcal{G}$ .
- 1.15 Prove that a molecule with three atoms has no out-of-plane vibrational modes. (Hint: Consider the translation and rotation modes.)
- 1.16 For the planar molecule, squareene, it is also true that the out-of-plane motions do not mix with the in-plane vibrational modes. The displacements  $r_z(i)$  can be used to form a representation of  $C_{4v}$ .
  - (a) Find the characters for the operations and decompose the representation. Identify which IRs corresponds to body modes and which to vibrations.
  - (b) Considering the symmetry of the out-of-plane vibration, argue why there are no matrix elements between this mode and the in-plane modes.

## 2

# Molecular vibrations of isotopically substituted $AB_2$ molecules

In this chapter we illustrate how group theory can be used to find the normal mode frequencies of isotopically substituted molecules. We consider triatomic molecules of the  $AB_2$  type with isotopic substitutions for either the  $A$  atom or the  $B$  atom, or both. In particular, we analyze and derive numerical results for  $H_2O$  when deuterium or tritium is substituted for hydrogen and when  $^{18}O$  is substituted for  $^{16}O$ . We begin by analyzing the vibrational modes of the  $AB_2$  molecule, and then go on to discuss the vibrational modes of isotopically substituted  $AB_2$  molecules.

### 2.1 Step 1: Identify the point group and its symmetry operations

A schematic representation of an  $AB_2$  molecule is shown in Fig. 2.1(a). In two dimensions the only symmetry operations are the identity,  $E$ , and 180-degree rotation about an axis through the  $A$  site, bisecting the  $B-B$  line. Reflection in the line of the  $C_2$  axis gives the same result as  $C_2$  in two dimensions. The group is  $C_2$ . In three dimensions, the elements include  $C_2$ , a reflection in the plane perpendicular to the plane of the paper and containing the  $C_2$  axis,  $\sigma_v$ , and reflection in the plane of the paper,  $\sigma'_v$ . In three dimensions the group is  $C_{2v}$ . Since the  $AB_2$  molecule has no out-of-plane vibrational modes (Exercise 1.15), we shall use the smaller  $C_2$  group for analysis.

### 2.2 Step 2: Specify the coordinate system and the basis functions

The coordinate system, shown in Fig. 2.1(b), consists of  $Y-Z$  Cartesian coordinates erected at each corner of the triangle. (We use  $y-z$  instead of  $x-y$  because it is customary for the  $C_2$  axis to be chosen to lie along the  $z$ -axis). The displacement vectors,  $\mathbf{r}_i$  ( $i = 1, 2$ , and  $3$ ), of the atoms are the basis functions for the molecular vibrational eigenvalue problem,

$$\mathbb{F} \xi = \mathbb{M} \omega^2 \xi, \quad (2.1)$$

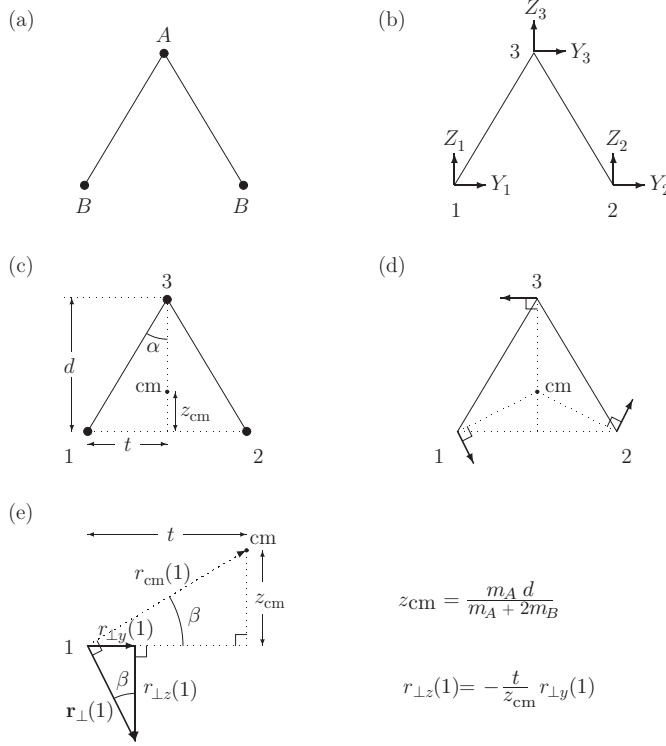


Figure 2.1 (a) The  $AB_2$  molecule. (b) The coordinate system. (c) The geometry and center of mass. (d) Rotation about the center of mass. (e) Displacements are perpendicular to the lines from the atom to the center of mass.

where  $\mathbb{F}$  is a  $(6 \times 6)$  force-constant matrix, and  $\xi$  is a 6-vector whose components are the  $r_{y_i}$  and  $r_{z_i}$  displacements of the atoms. The subscripts are as follows:  $i = 1$  is  $r_{y1}$ ,  $i = 2$  is  $r_{z1}$ ,  $i = 3$  is  $r_{y2}$ ,  $i = 4$  is  $r_{z2}$ ,  $i = 5$  is  $r_{y3}$ , and  $i = 6$  is  $r_{z3}$ . The matrix  $\mathbb{M}$  is a  $6 \times 6$  diagonal matrix whose elements are  $M_{ii} = m_B$  for  $i = 1, 2, 3, 4$ , and  $m_A$  for  $i = 5$  or  $6$ , where  $m_A$  and  $m_B$  are the masses of atoms  $A$  and  $B$  respectively. As discussed in Chapter 1, the eigenvalue problem can be transformed to the standard form

$$\mathfrak{F} \eta = \omega^2 \eta, \quad (2.2)$$

where

$$\mathfrak{F} = \mathbb{M}^{-1/2} \mathbb{F} \mathbb{M}^{-1/2},$$

$$\eta = \mathbb{M}^{1/2} \xi.$$

Here,  $\eta$  is a 6-vector whose components are mass-weighted displacements,  $\eta_i = (m_i)^{1/2} \xi_i$ , where  $m_i$  is the mass of the atom whose displacement component is  $\xi_i$

Table 2.1 The action table for the  $AB_2$  molecule

	$E$	$C_2$
$r_y$	$r_y$	$-r_y$
$r_z$	$r_z$	$r_z$
1	1	2
2	2	1
3	3	3

( $m_A$  or  $m_B$ ). The 6-vector  $\eta$  transforms under the symmetry operations in the same way as  $\xi$ .

Since the eigenvalue equation in  $\eta$ -space is in normal form, the eigenvectors form an orthogonal set of functions, but the  $\xi$ -space functions do not, unless  $\mathbb{M}$  is a scalar.

### 2.3 Step 3: Determine the effects of the symmetry operations on the basis functions

The action table for the displacements of the  $AB_2$  molecule is given in Table 2.1. Using this table, we have

$$C_2 \begin{bmatrix} r_{y1} \\ r_{z1} \\ r_{y2} \\ r_{z2} \\ r_{y3} \\ r_{z3} \end{bmatrix} \Rightarrow \begin{bmatrix} -r_{y2} \\ r_{z2} \\ -r_{y1} \\ r_{z1} \\ -r_{y3} \\ r_{z3} \end{bmatrix}. \quad (2.3)$$

### 2.4 Step 4: Construct the matrix representations for each element of the group using the basis functions

The  $6 \times 6$  matrix representation for  $C_2$  is

$$C_2 = \begin{bmatrix} & & -1 & & & \\ & & & 1 & & \\ -1 & & & & & \\ & 1 & & & & \\ & & & & -1 & \\ & & & & & 1 \end{bmatrix}.$$

Table 2.2 The character table for  $C_2$ 

$\Gamma$	$E$	$C_2$	Basis functions	Basis functions
$\mathcal{A}$	1	1	$R_z, z$	$x^2, y^2, z^2, xy$
$\mathcal{B}$	1	-1	$x, y, R_x, R_y$	$xz, yz$
$\Gamma(6 \times 6)$	6	0	$r_{yi}, r_{zi}, (i = 1, 2, 3)$	

The identity is the unit matrix,

$$E = \begin{array}{|c|c|c|c|c|c|} \hline 1 & & & & & \\ \hline & 1 & & & & \\ \hline & & 1 & & & \\ \hline & & & 1 & & \\ \hline & & & & 1 & \\ \hline & & & & & 1 \\ \hline \end{array}.$$

We shall refer to these matrices as the  $\Gamma$  representation.

## 2.5 Step 5: Determine the number and types of irreducible representations

The character table for  $C_2$  is given in Table 2.2. To find the decomposition of  $\Gamma$  into the irreducible representations we employ (1.10) with  $\mathcal{N}_c = 2$ ,  $\mathcal{N}_k = 1$ , and  $h = 2$ ,

$$n^\beta = \frac{1}{2} \sum_{i=1}^2 (\chi_i^\beta)^* \chi_i = \frac{1}{2} \sum_{i=1}^2 \chi_i^* \chi_i^\beta, \quad (2.4)$$

where  $n^\beta$  is the number of times the  $\beta$ th IR occurs,  $\chi_i$  is the character of the  $i$ th element of  $\Gamma$ , and  $\chi_i^\beta$  is the character of the  $i$ th element of the  $\beta$ th IR. The results of (2.4) are obvious from the character table,  $n^{\mathcal{A}} = 3$ , and  $n^{\mathcal{B}} = 3$ ; that is,  $\Gamma = 3\Gamma^{\mathcal{A}} + 3\Gamma^{\mathcal{B}}$ .

## 2.6 Step 6: Analyze the information contained in the decompositions

There are six modes. Three modes belong to the  $\mathcal{A}$  representation and three to the  $\mathcal{B}$  representation. Both  $\mathcal{A}$  and  $\mathcal{B}$  IRs are one-dimensional. We know that there are three body modes:  $T_y$ , translation in the  $y$ -direction;  $T_z$ , translation in the  $z$ -direction; and  $R_x$ , rotation of the molecule about an  $x$ -axis through the center of mass of the molecule. From the list of basis functions in the character table it is clear that  $T_y$  and  $R_z$  both belong to  $\mathcal{B}$ , while  $T_z$  belongs to  $\mathcal{A}$ . Therefore, there must be one  $\mathcal{B}$  and two  $\mathcal{A}$  vibrational modes. According to the optical selection rules discussed in Chapter 1, all three normal modes are infrared-active because each belongs to an IR of a translation mode. All of the vibrational modes are also Raman-active since both the  $\mathcal{A}$  and the  $\mathcal{B}$  IRs have basis functions that are binary in the displacements and there is no center of symmetry.



	$\eta_a^A$	$\eta_b^A$	$\eta_3^B$	$\eta_{T_y}^B$	$\eta_{T_z}^A$	$\eta_{R_x}^B$
$\eta_a^A$	$\times$	$\times$				
$\eta_b^A$	$\times$	$\times$				
$\eta_3^B$			$\omega_3^2$			
$\eta_{T_y}^B$				0		
$\eta_{T_z}^A$					0	
$\eta_{R_x}^B$						0

Figure 2.2 The block-diagonal form of  $\mathfrak{F}' = \mathbb{S}^{-1}\mathfrak{F}\mathbb{S}$ . The “ $\times$ ” signs indicate the possible non-zero matrix elements. The “0” entries indicate the zero-frequency body modes. The “ $\eta$ ” terms are the symmetry functions. The  $\mathcal{B}$  vibrational frequency is designated as  $\omega_3$ . The two vibrational  $\mathcal{A}$  symmetry functions are designated as  $\eta_a^A$  and  $\eta_b^A$ .

The decomposition of  $\Gamma$  determines the block diagonal form  $\mathfrak{F}' = \mathbb{S}^{-1}\mathfrak{F}\mathbb{S}$ , where  $\mathbb{S}$  is the matrix of the symmetry functions. The body modes,  $T_y$ ,  $T_z$ , and  $R_x$ , will have zero frequencies and do not mix with any of the vibrational modes. Therefore the  $3 \times 3$  block corresponding to the  $\mathcal{B}$  IRs is completely diagonal. Figure 2.2 shows the form of the block diagonal  $\mathfrak{F}'$  matrix. The last three rows and columns have been rearranged for convenience in the order  $\eta_{T_y}^B$ ,  $\eta_{T_z}^A$ , and  $\eta_{R_x}^B$ .

In Fig. 2.2, the rows and columns are labeled by the symmetry functions.  $\eta_a^A$  and  $\eta_b^A$  are the symmetry functions for the two vibrational modes belonging to  $\mathcal{A}$ . These two symmetry functions are mixed to form the eigenvectors of the two  $\mathcal{A}$  vibrational modes.  $\eta_3^B$  is the symmetry function for the  $\mathcal{B}$  vibrational mode, and we designate its frequency as  $\omega_3$ .  $\eta_{R_x}^B$  is the symmetry function for rotation, while  $\eta_{T_y}^B$  and  $\eta_{T_z}^A$  are the symmetry functions for translations. Figure 2.2 shows that obtaining the eigenvectors and eigenvalues will require the diagonalization of a  $2 \times 2$  matrix.

## 2.7 Step 7: Generate the symmetry functions

### 2.7.1 The body modes

The translation symmetry functions are easily obtained. They correspond to unit displacements of each of the atoms in the  $y$ -direction or in the  $z$ -direction,

$$\xi_{T_y} = \frac{1}{\sqrt{3}} \begin{bmatrix} 1 \\ 0 \\ 1 \\ 0 \\ 1 \\ 0 \end{bmatrix}, \quad \xi_{T_z} = \frac{1}{\sqrt{3}} \begin{bmatrix} 0 \\ 1 \\ 0 \\ 1 \\ 0 \\ 1 \end{bmatrix}.$$

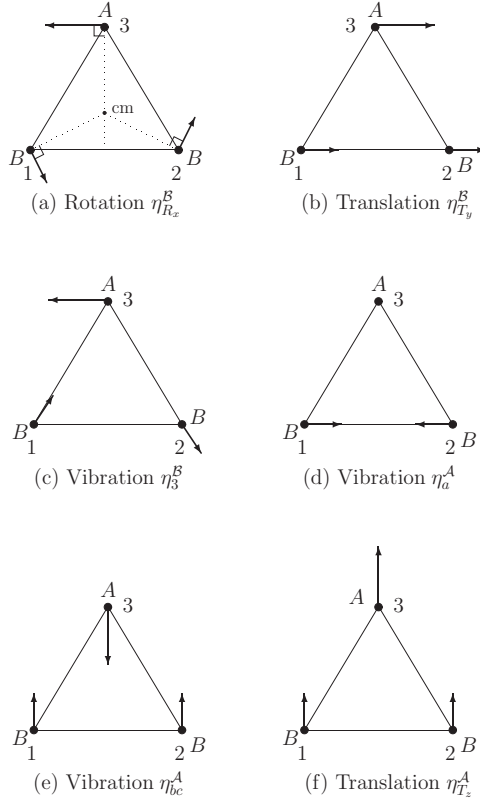


Figure 2.3 Symmetry functions and normal modes for  $AB_2$  molecules.  $\mathbf{r}(i)$ ,  $i = 1, 2$ , and  $3$  are displacement vectors in  $\xi$ -space for the atoms at the sites labeled  $1, 2$ , and  $3$ .  $\eta_a^A$  and  $\eta_{bc}^A$  are mixed to form two vibrational eigenfunctions. Other functions are eigenvectors. (a) Rotation,  $\eta_{R_x}^B$ ,  $|r(3)_y/r(1)_y| = -2m_B/m_A$ ,  $|r(1)_z/r(1)_y| = \tan \alpha / (m_A d_1^2)$ . (b) Translation in the  $y$ -direction,  $\eta_{T_y}^B$ , equal displacement in  $\xi$ -space. (c) Vibration symmetry function,  $\eta_3^B$ ,  $|r(3)_y/r(1)_y| = 2m_B/m_A$ ,  $|r(1)_z/r(1)_y| = \cot \alpha$ . (d) Vibration symmetry function,  $\eta_a^A$ , equal and opposite displacements. (e) Vibration symmetry function,  $\eta_{bc}^A$ ,  $|r(3)_y/r(1)_y| = 2m_B/m_A$ . (f) Translation  $\eta_{T_z}^A$ , equal displacements in  $\xi$ -space.

On transforming these to  $\eta$ -space and normalizing the vectors, we obtain

$$\eta_{T_y} = \frac{1}{\sqrt{m_A + 2m_B}} \begin{bmatrix} \sqrt{m_B} \\ 0 \\ \sqrt{m_B} \\ 0 \\ \sqrt{m_A} \\ 0 \end{bmatrix}, \quad (2.5)$$

$$\eta_{T_z} = \frac{1}{\sqrt{m_A + 2m_B}} \begin{bmatrix} 0 \\ \sqrt{m_B} \\ 0 \\ \sqrt{m_B} \\ 0 \\ \sqrt{m_A} \end{bmatrix}. \quad (2.6)$$

Our next task is to find the symmetry function,  $\eta_{R_x}^B$ , for rotation. The axis of rotation for  $R_x$  must pass through the center of mass of the molecule. For  $AB_2$  molecules the center of mass lies on the  $C_2$ -axis a distance  $z_{\text{cm}}$  above the line joining the  $B$  atoms, as shown in Fig. 2.1(c). To determine  $z_{\text{cm}}$ , we require that  $m_A(d - z_{\text{cm}}) = 2m_B z_{\text{cm}}$ , or

$$z_{\text{cm}} = \left( \frac{m_A}{m_A + 2m_B} \right) d. \quad (2.7)$$

If we draw a line from the center of mass to each of the corners of the molecule the displacement vectors for  $R_x$  must be perpendicular to these lines, as shown in Fig. 2.1(d). The vector from atom  $B$  at corner 1 to the center of mass is  $\mathbf{r}_{\text{cm}}(1) = t\mathbf{e}_{y1} + z_{\text{cm}}\mathbf{e}_{z1}$ , where  $\mathbf{e}_{y1}$  and  $\mathbf{e}_{z1}$  are unit vectors along the  $Y_1$  and  $Z_1$  coordinate directions, and  $t$  is half the  $B$ - $B$  length. A vector perpendicular to  $\mathbf{r}_{\text{cm}}(1)$  is  $\mathbf{r}_{\perp}(1) = z_{\text{cm}}\mathbf{e}_{y1} - t\mathbf{e}_{z1}$ . Similarly,  $\mathbf{r}_{\perp}(2) = z_{\text{cm}}\mathbf{e}_{y2} + t\mathbf{e}_{z2}$ . We can express the displacements of  $\mathbf{r}_{\perp}(2)$  in terms of the  $y$ -component of the displacement  $r_{\perp}(1)_y$ :

$$\begin{aligned} r_{\perp}(2)_y &= r_{\perp}(1)_y, \\ r_{\perp}(1)_z &= -\left( \frac{t}{z_{\text{cm}}} \right) r_{\perp}(1)_y, \\ r_{\perp}(2)_z &= \left( \frac{t}{z_{\text{cm}}} \right) r_{\perp}(2)_y = \left( \frac{t}{z_{\text{cm}}} \right) r_{\perp}(1)_y. \end{aligned}$$

In order for the molecule to rotate about the center of mass

$$\sum_i M_i \mathbf{r}_{\perp}(i) = 0. \quad (2.8)$$

This requires that

$$\begin{aligned} m_A r_{\perp}(3)_y &= -2m_B r_{\perp}(1)_y, \\ r_{\perp}(2)_z &= -r_{\perp}(1)_z = -\left( \frac{t}{z_{\text{cm}}} \right) r_{\perp}(1)_y. \end{aligned} \quad (2.9)$$

From the geometry in Fig. 2.1(c) it follows that the length  $t = d \tan \alpha$ , where  $\alpha$  is one-half of the apex angle. Therefore,

$$r_{\perp}(2)_z = \left( \frac{\tan \alpha}{m_A d_1^2} \right) r_{\perp}(1)_y, \quad (2.10)$$

with

$$d_1 = \frac{1}{\sqrt{2m_B + m_A}}. \quad (2.11)$$

Now we can obtain the rotation function  $\xi_{R_x}$ ,

$$\xi_{R_x} \propto \begin{bmatrix} 1 \\ -\tan \alpha / (m_A d_1^2) \\ 1 \\ \tan \alpha / (m_A d_1^2) \\ -2m_B / m_A \\ 0 \end{bmatrix}. \quad (2.12)$$

The proportionality sign is used in (2.12) because the vector is not normalized to unity. Since  $\eta = M^{1/2}\xi$ , we can find the symmetry function (also the eigenfunction),  $\eta_{R_x}$ ,

$$\eta_{R_x} \propto \sqrt{m_B} \begin{bmatrix} 1 \\ -\tan \alpha / (m_A d_1^2) \\ 1 \\ \tan \alpha / (m_A d_1^2) \\ -2\sqrt{m_B / m_A} \\ 0 \end{bmatrix}. \quad (2.13)$$

The vector can be normalized to unity by dividing by the square root of the sum of the squares of its components, with the result

$$\eta_{R_x} = \frac{d_1 d_2}{\sqrt{2}} \begin{bmatrix} m_A C_\alpha \\ -S_\alpha / d_1^2 \\ m_A C_\alpha \\ S_\alpha / d_1^2 \\ -2\sqrt{m_A m_B} C_\alpha \\ 0 \end{bmatrix}, \quad (2.14)$$

where  $d_1 = (2m_B + m_A)^{-1/2}$ ,  $d_2 = (m_A + 2m_B S_\alpha^2)^{-1/2}$ ,  $S_\alpha \equiv \sin \alpha$ , and  $C_\alpha \equiv \cos \alpha$ .

## 2.7.2 Vibration symmetry functions

### *B symmetry functions*

We can make use of the symmetry-function-generating machine described in Chapter 1.

Let  $f$  be an arbitrary function and generate the vector,  $f_m^\alpha$ , according to the rule

$$f_m^\alpha = \sum_{k=1}^h \Gamma_{mm}^\alpha(O_k) [O_k f], \quad (\text{GT1.8})$$

then  $f_m^\alpha$  is an (un-normalized) basis function for the  $m$ th row of the  $\alpha$ th irreducible representation. In (GT 1.8),  $\Gamma_{mm}^\alpha(O_k)$  is the  $mm$  diagonal matrix element of the  $\alpha$ th IR for the  $O_k$  operation.

For the  $\mathcal{B}$  symmetry functions we use  $r_{y1}$ ,  $r_{z1}$ , and  $r_{y3}$ , separately as the “arbitrary” functions to obtain

$$\begin{aligned} E(r_{y1}) - C_2(r_{y1}) &= r_{y1} + r_{y2}, \\ E(r_{z1}) - C_2(r_{z1}) &= r_{z1} - r_{z2}, \\ E(r_{y3}) - C_2(r_{y3}) &= r_{y3} + r_{y3}. \end{aligned} \quad (2.15)$$

The three (orthogonal and normalized)  $\mathcal{B}$  symmetry functions are

$$\begin{aligned} \eta_a^{\mathcal{B}} &= \frac{1}{\sqrt{2m_B}} \begin{bmatrix} \sqrt{m_B} \\ 0 \\ \sqrt{m_B} \\ 0 \\ 0 \\ 0 \end{bmatrix} = \frac{1}{\sqrt{2}} \begin{bmatrix} 1 \\ 0 \\ 1 \\ 0 \\ 0 \\ 0 \end{bmatrix}, \\ \eta_b^{\mathcal{B}} &= \frac{1}{\sqrt{2m_B}} \begin{bmatrix} 0 \\ \sqrt{m_B} \\ 0 \\ -\sqrt{m_B} \\ 0 \\ 0 \end{bmatrix} = \frac{1}{\sqrt{2}} \begin{bmatrix} 0 \\ 1 \\ 0 \\ -1 \\ 0 \\ 0 \end{bmatrix}, \\ \eta_c^{\mathcal{B}} &= \frac{1}{\sqrt{m_A}} \begin{bmatrix} 0 \\ 0 \\ 0 \\ 0 \\ \sqrt{m_A} \\ 0 \end{bmatrix} = \begin{bmatrix} 0 \\ 0 \\ 0 \\ 0 \\ 1 \\ 0 \end{bmatrix}. \end{aligned} \quad (2.16)$$

We already have two of the three  $\mathcal{B}$  symmetry functions, namely  $\eta_{T_y}$  (Eq. (2.5)) and  $\eta_{R_x}$  (Eq. (2.14)).

The third symmetry function, the vibrational symmetry function,  $\eta_3^B$ , must be orthogonal to  $\eta_{T_y}$  and  $\eta_{R_x}$ , and this requirement is sufficient to determine the eigenvector  $\eta_3^B$ . We can express  $\eta_3^B$  as a linear combination of  $\eta_a^B$ ,  $\eta_b^B$ , and  $\eta_c^B$ ,

$$\eta_3^B = \mu \eta_a^B + \nu \eta_b^B + \rho \eta_c^B, \quad (2.17)$$

where  $\mu$ ,  $\nu$ , and  $\rho$  are coefficients to be determined by orthogonality and normalization conditions,

$$\begin{aligned} \mu^2 + \nu^2 + \rho^2 &= 1 & (\text{normalization}), \\ \mu &= -\sqrt{\frac{m_A}{2m_B}} \rho & (\text{orthogonal to } \eta_{T_y}), \\ \mu &= \left( \frac{\tan \alpha}{m_A d_1^2} \right) \nu + \sqrt{\frac{2m_B}{m_A}} \rho & (\text{orthogonal to } \eta_{R_x}). \end{aligned} \quad (2.18)$$

After a bit of algebra we find that

$$\begin{aligned} \mu &= \sqrt{m_A} d_2 S_\alpha, \\ \nu &= \sqrt{m_A} d_2 C_\alpha, \\ \rho &= -\sqrt{2m_B} d_2 S_\alpha, \end{aligned} \quad (2.19)$$

and

$$\eta_3^B = \sqrt{m_B} d_2 S_\alpha \eta_a^B + \sqrt{m_A} d_2 C_\alpha \eta_b^B - \sqrt{2m_B} d_2 S_\alpha \eta_c^B, \quad (2.20)$$

or, as a column vector,

$$\eta_3^B = \sqrt{\frac{m_A}{2}} d_2 \begin{bmatrix} S_\alpha \\ C_\alpha \\ S_\alpha \\ -C_\alpha \\ -2\sqrt{m_B/m_A} S_\alpha \\ 0 \end{bmatrix}. \quad (2.21)$$

A sketch of this vibration mode is shown in Fig. 2.3(c). Note that  $r(1)$  and  $r(2)$  lie along the lines joining the  $A$  and  $B$  atoms. It is easily verified that this mode leaves the center of mass stationary.

Since  $\eta_{R_x}^B$ ,  $\eta_{T_y}^B$ , and  $\eta_3^B$  are eigenfunctions of  $\mathfrak{F}$ , we have succeeded in completely diagonalizing the  $3 \times 3$   $\mathcal{B}$ -block eigenvalue problem. Next we look at the  $3 \times 3$ ,  $\mathcal{A}$ -block problem.

*A symmetry functions*

We start by finding a set of symmetry functions using each of  $r_{y1}$ ,  $r_{z1}$ , and  $r_{z3}$  as “arbitrary” functions. Applying the symmetry-function-generating machine gives

$$E(r_{y1}) + C_2(r_{y1}) = r_{y1} - r_{y2},$$

$$E(r_{z1}) + C_2(r_{z1}) = r_{z1} + r_{z2},$$

$$E(r_{z3}) + C_2(r_{z3}) = r_{z3} + r_{z3}.$$

The corresponding symmetry functions are

$$\begin{aligned} \eta_a^A &= \frac{1}{\sqrt{2m_B}} \begin{bmatrix} \sqrt{m_B} \\ 0 \\ -\sqrt{m_B} \\ 0 \\ 0 \\ 0 \end{bmatrix} = \frac{1}{\sqrt{2}} \begin{bmatrix} 1 \\ 0 \\ -1 \\ 0 \\ 0 \\ 0 \end{bmatrix}, \\ \eta_b^A &= \frac{1}{\sqrt{2m_B}} \begin{bmatrix} 0 \\ \sqrt{m_B} \\ 0 \\ \sqrt{m_B} \\ 0 \\ 0 \end{bmatrix} = \frac{1}{\sqrt{2}} \begin{bmatrix} 0 \\ 1 \\ 0 \\ 1 \\ 0 \\ 0 \end{bmatrix}, \\ \eta_c^A &= \frac{1}{\sqrt{m_A}} \begin{bmatrix} 0 \\ 0 \\ 0 \\ 0 \\ 0 \\ \sqrt{m_A} \end{bmatrix} = \begin{bmatrix} 0 \\ 0 \\ 0 \\ 0 \\ 0 \\ 1 \end{bmatrix}. \end{aligned} \quad (2.22)$$

The translation symmetry function can be expressed in terms of these three symmetry functions,

$$\eta_{T_z}^A = d_1 \left[ \sqrt{2m_B} \eta_b^A + \sqrt{m_A} \eta_c^A \right]. \quad (2.23)$$

The remaining two  $\mathcal{A}$  modes are vibration modes, so they must be formed from symmetry functions that are orthogonal to the translation function. The function  $\eta_a^A$  is already orthogonal to  $\eta_{T_z}^A$ , and we can form the last function,  $\eta_{bc}^A$ , as the linear combination

$$\eta_{bc}^A = d_1 \left[ \sqrt{m_A} \eta_b^A - \sqrt{2m_B} \eta_c^A \right]. \quad (2.24)$$

Table 2.3 The  $\mathbb{S}$  matrix:  $a$  is the mixing parameter,

$C = (1 + |a|^2)^{1/2}$ ,  $C_\alpha = \cos \alpha$ ,  $S_\alpha = \sin \alpha$ ,  $d_1 = (m_A + 2m_B)^{-1/2}$ ,  
 $d_2 = (m_A + 2m_B S_\alpha^2)^{-1/2}$ ,  $r = 1/(\sqrt{2}C)$ ,  $t = (m_A/2)^{1/2}d_2$ ,  
 $u = m_A^{1/2}d_1$ ,  $s = m_B^{1/2}d_1$ , and  $p = (2m_B)^{1/2}d_2$

	$\eta_1^A$	$\eta_2^A$	$\eta_3^B$	$\eta_{T_y}^B$	$\eta_{T_z}^A$	$\eta_{R_x}^B$
$\eta_1^A$	$r$	$-ar$	$-tS_\alpha$	$s$	$0$	$tuC_\alpha$
$\eta_2^A$	$aur$	$ur$	$-tC_\alpha$	$0$	$s$	$-tu^{-1}S_\alpha$
$\eta_3^B$	$-r$	$ar$	$-tS_\alpha$	$s$	$0$	$tuC_\alpha$
$\eta_{T_y}^B$	$aur$	$ur$	$tC_\alpha$	$0$	$s$	$tu^{-1}S_\alpha$
$\eta_{T_z}^A$	$0$	$0$	$pS_\alpha$	$u$	$0$	$-puC_\alpha$
$\eta_{R_x}^B$	$-2asr$	$-2sr$	$0$	$0$	$u$	$0$

These two symmetry functions ( $\eta_a^A$  and  $\eta_{bc}^A$ ) are mixed to form the two vibration normal modes (i.e., the eigenfunctions). According to (1.17) of Chapter 1, we can write the two vibrational eigenfunctions as

$$\begin{aligned}\eta_{\text{vib1}}^A &= \eta_1^A = \frac{1}{C} (\eta_a^A + a \eta_{bc}^A), \\ \eta_{\text{vib2}}^A &= \eta_2^A = \frac{1}{C} (-a \eta_a^A + \eta_{bc}^A),\end{aligned}\tag{2.25}$$

where

$$C = \sqrt{1 + |a|^2}.$$

## 2.8 Step 8: Diagonalize the matrix eigenvalue equation

The similarity transformation  $\mathbb{S}^{-1} \mathfrak{F} \mathbb{S}$  produces a block-diagonal matrix,  $\mathfrak{F}_d$ , where  $\mathbb{S}$  is the matrix with the symmetry functions as columns. The  $\mathbb{S}$  matrix is shown in Table 2.3. Since all of our symmetry functions are also eigenvectors of  $\mathfrak{F}$ , the transformed matrix  $\mathfrak{F}_d$  is completely diagonal as shown in Table 2.4. The diagonal elements of  $\mathfrak{F}_d$  are the eigenvalues of  $\mathfrak{F}$ , that is, the squares of the normal-mode angular frequencies.

## 2.9 Constructing the force-constant matrix

The force-constant matrix can be obtained by reversing the similarity transformation:  $\mathbb{S} \mathfrak{F}_d \mathbb{S}^{-1} = \mathfrak{F}$ , where  $\mathfrak{F}_d$  is the diagonal matrix shown in Table 2.4.



Table 2.4 The diagonal matrix  $\mathfrak{F}_d = \mathbb{S}^{-1} \mathfrak{F} \mathbb{S}$ :  $\omega_1 = \omega_1^A$ ,  $\omega_2 = \omega_2^A$ , and  $\omega_3 = \omega_3^B$ . The column labels are the same as in Table 2.3.

$\omega_1^2$					
	$\omega_2^2$				
		$\omega_3^2$			
			0		
				0	
					0

Table 2.5 The force-constant matrix,  $\mathfrak{F}$ :  $C = (1 + |a|^2)^{1/2}$ ,  $C_\alpha = \cos \alpha$ ,  $S_\alpha = \sin \alpha$ ,  $d_1 = (m_A + 2m_B)^{-1/2}$ ,  $d_2 = (m_A + 2m_B S_\alpha^2)^{-1/2}$ ,  $r = 1/(\sqrt{2}C)$ ,  $t = (m_A/2)^{1/2}d_2$ ,  $u = m_A^{1/2}d_1$ ,  $s = m_B^{1/2}d_1$ ,  $p = (2m_B)^{1/2}d_2$ ,  $v = (m_A m_B)^{1/2}d_2^2$ ,  $K \equiv a^2\omega_1^2 + \omega_2^2$ ,  $L \equiv \omega_1^2 + a^2\omega_2^2$ , and  $M \equiv \omega_1^2 - \omega_2^2$

$r^2 L$ $+ t^2 S_\alpha^2 \omega_3^2$	$aur^2 M$ $+ t^2 S_\alpha C_\alpha \omega_3^2$	$-r^2 L$ $+ t^2 S_\alpha^2 \omega_3^2$	$aur^2 M$ $- t^2 S_\alpha C_\alpha \omega_3^2$	$-v S_\alpha^2 \omega_3^2$	$-2asr^2 M$
	$u^2 r^2 K$ $+ t^2 C_\alpha^2 \omega_3^2$	$-aur^2 M$ $+ t^2 S_\alpha C_\alpha \omega_3^2$	$u^2 r^2 K$ $- t^2 C_\alpha^2 \omega_3^2$	$-v S_\alpha C_\alpha \omega_3^2$	$-2usr^2 K$
		$r^2 L$ $+ t^2 S_\alpha^2 \omega_3^2$	$-aur^2 M$ $- t^2 S_\alpha C_\alpha \omega_3^2$	$-v S_\alpha^2 \omega_3^2$	$2asr^2 M$
			$u^2 r^2 K$ $+ t^2 C_\alpha^2 \omega_3^2$	$v S_\alpha C_\alpha \omega_3^2$	$-2usr^2 K$
	$\mathfrak{F}_{ij} = \mathfrak{F}_{ji}$			$p^2 S_\alpha^2 \omega_3^2$	0
					$4s^2 r^2 K$

The  $\mathbb{S}$  matrix is given in Table 2.3 and  $\mathbb{S}^{-1}$  is the transpose of  $\mathbb{S}$ . The resulting force-constant matrix is shown in Table 2.5.

It can be concluded that the most general form of the force-constant matrix for an  $AB_2$  molecule is a  $6 \times 6$  matrix with 34 non-zero force constants. However, there can be at most four independent parameters:  $\omega_1$ ,  $\omega_2$ ,  $\omega_3$ , and the mixing parameter,  $a$ . Since  $\mathbb{F} = \mathbb{M}^{1/2} \mathfrak{F} \mathbb{M}^{1/2}$ , the force-constant matrix in  $\xi$ -space is easily obtained. The matrix elements of  $\mathbb{F}$  are

$$\mathbb{F}_{rs} = \mathfrak{F}_{rs}(m_r m_s)^{1/2}. \quad (2.26)$$

We have now achieved a complete analysis of the normal modes of vibration of  $AB_2$  molecules. In the next section we discuss how the frequencies of isotopically substituted forms of  $AB_2$  molecules can be obtained.

### 2.10 Green's function theory of isotopic molecular vibrations

Consider an arbitrary, isotopically substituted, molecule. The matrix  $N \times N$  eigenvalue equation that determines the vibrational frequencies is

$$\mathbb{F} \xi = \omega^2 \mathbb{M}^{(i)} \xi,$$

where  $\mathbb{M}^{(i)}$  is the diagonal matrix of the masses of the molecule with isotopically substituted masses. We can write

$$\mathbb{M}^{(i)} = \mathbb{M} + \Delta\mathbb{M}^{(i)}, \quad (2.27)$$

with  $\mathbb{M}$  the matrix of the normal masses and  $\Delta\mathbb{M}^{(i)} = \mathbb{M}^{(i)} - \mathbb{M}$ . The eigenvalue equation may be rewritten in the form

$$[\mathfrak{F} - \omega^2 \mathbb{I} - \omega^2 \Delta\mathfrak{M}^{(i)}] \eta = 0, \quad (2.28)$$

with

$$\mathfrak{F} = \mathbb{M}^{-1/2} \mathbb{F} \mathbb{M}^{-1/2}, \quad (2.29)$$

$$\Delta\mathfrak{M}^{(i)} = \mathbb{M}^{-1/2} \Delta\mathbb{M}^{(i)} \mathbb{M}^{-1/2}, \quad (2.30)$$

$$\eta = \mathbb{M}^{1/2} \xi. \quad (2.31)$$

Since both  $\mathbb{M}^{-1/2}$  and  $\Delta\mathbb{M}^{(i)}$  are diagonal, it follows that  $\Delta\mathfrak{M}^{(i)}$  is also diagonal. Its matrix elements are given by

$$[\Delta\mathfrak{M}^{(i)}]_{rs} = \delta_{rs} (\Delta m_r / m_r), \quad (2.32)$$

where  $\Delta m_r$  is the difference between the isotopic and normal mass of the atom whose coordinate corresponds to  $\xi_r$ . Equation (2.28) can be rewritten in the form

$$(\mathfrak{F} - \omega^2 \mathbb{I}) [\mathbb{I} - \omega^2 G(\omega^2) \Delta\mathbb{M}^{(i)}] \eta = 0, \quad (2.33)$$

where

$$G(\omega^2) = (\mathfrak{F} - \omega^2 \mathbb{I})^{-1}, \quad (2.34)$$

with  $\mathbb{I}$  an  $N \times N$  unit matrix and  $G(\omega^2)$  the molecular Green's function. The eigenvalues are determined by the vanishing of the determinant,

$$\det\{(\mathfrak{F} - \omega^2 \mathbb{I}) [\mathbb{I} - \omega^2 G(\omega^2) \Delta\mathbb{M}^{(i)}]\} = 0, \quad (2.35)$$

where the notation  $\det \mathbb{A}$  indicates the determinant of the matrix  $\mathbb{A}$ . Since  $\det \mathbb{A}\mathbb{B} = \det \mathbb{A} \det \mathbb{B}$ , (2.35) yields two conditions,

$$\det \{(\mathfrak{F} - \omega^2 \mathbb{I})\} = 0, \quad (2.36)$$

$$\det \{[\mathbb{I} - \omega^2 G(\omega^2) \Delta \mathbb{M}^{(i)}]\} = 0. \quad (2.37)$$

Equation (2.36) is satisfied for  $\omega^2 = (\omega_k)^2$  ( $k = 1, 2, \dots, N$ ), where  $\omega_k$  is the  $k$ th frequency of the normal molecule. The roots of (2.37) are the isotopically shifted frequencies,  $\omega^2 = (\omega_k^{(i)})^2$ . To make use of (2.37), we need the Green's function matrix elements.

### 2.10.1 Green's function for molecular vibrations

Let  $\mathbb{U}$  be the  $N \times N$  matrix constructed with the eigenvectors of  $\mathfrak{F}$  as the columns of the matrix. Then  $\mathbb{U}^{-1} \mathfrak{F} \mathbb{U}$  is completely diagonal, with matrix elements

$$\{\mathbb{U}^{-1} \mathfrak{F} \mathbb{U}\}_{rs} = \delta_{rs} \omega_r^2. \quad (2.38)$$

The molecular Green's function is also diagonal when transformed by  $\mathbb{U}$ ,

$$\mathcal{G} = \{\mathbb{U}^{-1} \mathbb{G}(\omega^2) \mathbb{U}\}_{rs} = -\frac{\delta_{rs}}{\omega_r^2 - \omega^2}. \quad (2.39)$$

It follows that

$$\mathbb{G}(\omega^2) = \mathbb{U} \mathcal{G} \mathbb{U}^{-1}, \quad (2.40)$$

$$\begin{aligned} \{\mathbb{G}(\omega^2)\}_{rs} &= \sum_k \sum_p U_{rk} [\omega (AB_2)_k^2 - \omega^2]^{-1} \delta_{kp} U_{ps}^{-1} \\ &= \sum_k \frac{U_{rk} U_{ks}}{\omega_k^2 - \omega^2}. \end{aligned} \quad (2.41)$$

In the first part of this chapter we obtained the eigenvectors for the molecular vibrations of an  $AB_2$  molecule in terms of the normal vibrational frequencies,  $\omega_1^2$ ,  $\omega_2^2$ , and  $\omega_3^2$ , and the mixing parameter,  $a$ . Equation (2.40) or Eq. (2.41) can be used to construct the Green's function for the  $AB_2$  molecule. In this case, the matrix of eigenvectors,  $\mathbb{U}$ , is the same as the  $\mathbb{S}$  matrix given in Table 2.3. The diagonal Green's function,  $\mathcal{G}$ , is shown in Table 2.6.

The Green's function in  $\eta$ -space is  $\mathbb{G}(\omega^2) = \mathbb{U} \mathcal{G} \mathbb{U}^{-1} = \mathbb{S} \mathcal{G} \mathbb{S}^{-1}$ , where the  $\mathbb{S}$  matrix is given in Table 2.3. Carrying out the matrix multiplication gives the Green's function shown in Table 2.7.

Table 2.6 *The diagonal form of the molecular Green's function,  $\mathcal{G}(\omega^2)$ . Empty squares indicate matrix elements whose values are zero.*

$(\omega_1^2 - \omega^2)^{-1}$					
	$(\omega_2^2 - \omega^2)^{-1}$				
		$(\omega_3^2 - \omega^2)^{-1}$			
			$-(\omega^2)^{-1}$		
				$-(\omega^2)^{-1}$	
					$-(\omega^2)^{-1}$

### 2.10.2 Isotopic frequencies of $A^{(i)}B_2$ , $B^{(i)}AB^{(i)}$ , and $B^{(i)}A^{(i)}B^{(i)}$ molecules

There are three types of symmetrically substituted molecules: (1)  $A^{(i)}B_2$ , (2)  $B^{(i)}AB^{(i)}$ , and (3)  $B^{(i)}A^{(i)}B^{(i)}$ , where  $A^{(i)}$  or  $B^{(i)}$  indicates the isotopic masses  $m_A^{(i)}$  and  $m_B^{(i)}$ , respectively. For example, the normal (most abundant) form of the water molecule has  $m_H = 1$  and  $m_O = 16$  in atomic mass units. Isotopically substituted forms include molecules with  $m_H = 2$  (deuterium) or 3 (tritium) and  $m_O = 18$ . We shall indicate the normal water molecule by  $H_2O$ . For the hydrogen isotopes we will use the symbols D (for deuterium) and T (for tritium). Employing the observed frequencies of  $H_2O$  and one of the frequencies of an isotopically substituted molecule allows us to determine all of the parameters in the theory. Once that has been accomplished, the force-constant matrix (Table 2.5) and the Green's function (Table 2.7) are determined. Using the Green's function, the vibrational frequencies of all types of isotopic substitutions can be calculated from (2.37).

#### $A^{(i)}B_2$ molecules

For the isotopically substituted species  $A^{(i)}B_2$  the matrix  $\Delta\mathbb{M}^{(i)}$  has only two non-zero elements:

$$(\Delta\mathbb{M}^{(i)})_{55} = (\Delta\mathbb{M}^{(i)})_{66} = \frac{m_A^{(i)} - m_A}{m_A} = \frac{m_A^{(i)}}{m_A} - 1 \equiv \epsilon. \quad (2.42)$$

Equation (2.37) gives

$$\det\{\mathbb{I} - \omega^2 \mathbb{G}(\omega^2) \Delta\mathbb{M}^{(i)}\} = [1 - \epsilon\omega^2 G(5, 5)][1 - \epsilon\omega^2 G(6, 6)] - \epsilon^2\omega^2 G(5, 6)^2 = 0. \quad (2.43)$$

Since  $G(5, 6) = 0$  (Table 2.7), the equations that determine the isotopic frequencies are

$$1 - \epsilon\omega^2 G(5, 5) = 0 \quad (\mathcal{B} \text{ vibrational modes}) \quad (2.44)$$

Table 2.7 *Green's function,  $\mathbb{G}(\omega^2)$ , for  $AB_2$  molecules. The parameters are as follows:  $\lambda_1 = 1/(\omega_1^2 - \omega^2)$ ,  $\lambda_2 = 1/(\omega_2^2 - \omega^2)$ ,  $\lambda_3 = 1/(\omega_3^2 - \omega^2)$ ,  $\Lambda_1 = (\lambda_1 + a^2\lambda_2)$ ,  $\Lambda_2 = (a^2\lambda_1 + \lambda_2)$ ,  $X_1 = (\lambda_1 - \lambda_2)$ ,  $X_2 = (\lambda_1 + \lambda_2)$ ,  $X_3 = (\lambda_3 + 1/\omega^2)$ ,  $C_\alpha = \cos \alpha$ ,  $S_\alpha = \sin \alpha$ ,  $C = 1/(1 + |a|^2)^{1/2}$ ,  $r = 1/(\sqrt{2}C)$ ,  $d_1^2 = 1/(m_A + 2m_B)$ ,  $d_2^2 = 1/(m_A + 2m_B S_\alpha^2)$ ,  $t^2 = (m_A/2)d_2^2$ ,  $u^2 = m_A d_1^2$ ,  $s^2 = m_B d_1^2$ ,  $p^2 = (2m_B)d_2^2$ , and  $v^2 = (m_A m_B)d_2^4$ .*

$r^2 \Lambda_1$ $+ t^2 S_\alpha^2 \lambda_3$ $- \frac{s^2 + t^2 u^2 C_\alpha^2}{\omega^2}$	$aur^2 X_1$ $+ t^2 S_\alpha C_\alpha X_3$	$-r^2 \Lambda_1$ $+ t^2 S_\alpha^2 \lambda_3$	$aur^2 X_1$ $- t^2 S_\alpha C_\alpha X_3$	$-v S_\alpha^2 \lambda_3$ $- \frac{u(s - uv C_\alpha^2)}{\omega^2}$	$-2asr^2 X_1$
	$r^2 u^2 \Lambda_2$ $+ t^2 C_\alpha^2 \lambda_3$ $- \frac{s^2 + (t/u)^2 S_\alpha^2}{\omega^2}$	$-aur^2 X_1$ $+ t^2 S_\alpha C_\alpha X_3$	$r^2 u^2 \Lambda_2$ $- t^2 C_\alpha^2 \lambda_3$ $- \frac{s^2 - (t/u)^2 S_\alpha^2}{\omega^2}$	$-v S_\alpha C_\alpha X_3$	$-2usr^2 \Lambda_2$ $- su/\omega^2$
		$r^2 \Lambda_1$ $+ t^2 S_\alpha^2 \lambda_3$ $- \frac{(s^2 + t^2 u^2 C_\alpha^2)}{\omega^2}$	$aur^2 X_1$ $- t^2 S_\alpha C_\alpha X_3$	$-v S_\alpha^2 \lambda_3$ $- \frac{u(s - uv C_\alpha^2)}{\omega^2}$	$2asr^2 X_1$
			$u^2 r^2 \Lambda_2$ $+ t^2 C_\alpha^2 \lambda_3$ $- \frac{s^2 + (t/u)^2 S_\alpha^2}{\omega^2}$	$v S_\alpha C_\alpha X_3$	$-2asr^2 \Lambda_2$ $- su/\omega^2$
	$\mathbb{G}(i, j) = \mathbb{G}(j, i)$			$p^2 S_\alpha^2 \lambda_3$ $- \frac{u^2(1 + p^2)C_\alpha^2}{\omega^2}$	0
					$4s^2 r^2 \Lambda_2$ $- u^2/\omega^2$

and

$$1 - \epsilon \omega^2 G(6, 6) = 0 \quad (\mathcal{A} \text{ vibrational modes}). \quad (2.45)$$

Equation (2.45) takes the form

$$2m_B + m_A - 2m_B \frac{\epsilon \omega^2}{C^2} \left( \frac{a^2}{\omega_1^2 - \omega^2} + \frac{1}{\omega_2^2 - \omega^2} \right) + \epsilon m_A = 0. \quad (2.46)$$

With a bit of algebra (2.46) can be rewritten as a quadratic equation in the variable  $\omega^2$ :

$$(\omega^2)^2 - A \omega^2 + B = 0. \quad (2.47)$$

It follows that the sum of the roots of (2.47) is equal to  $A$  and the product of the roots is  $B$ ,

$$\begin{aligned} (\omega_1^{(i)})^2 + (\omega^{(i)})^2 &= \frac{m_A}{m_A^{(i)}} \left\{ \omega_1^2 + \omega_2^2 \right. \\ &\quad \left. + \frac{\epsilon}{C^2} \frac{2m_B (\omega_1^2 + a^2 \omega_2^2) + m_A C^2 (\omega_1^2 + \omega_2^2)}{2m_B + m_A} \right\}, \end{aligned} \quad (2.48)$$

$$(\omega_1^{(i)})^2 (\omega^{(i)})^2 = \frac{m_A}{m_A^{(i)}} (\omega_1^2 \omega_2^2) \frac{2m_B + m_A^{(i)}}{2m_B + m_A}, \quad (2.49)$$

$$\epsilon = \frac{m_A^{(i)}}{m_A} - 1, \quad (2.50)$$

where  $\omega_1^{(i)}$  and  $\omega_2^{(i)}$  are the  $A$  vibrational mode frequencies of the  $A^{(i)}B_2$  molecule, and  $\omega_1$  and  $\omega_2$  are those of the normal  $AB_2$  molecule. Equation (2.49) is the well-known Teller–Redlich product rule [2.1] for isotopic substitution. The remaining isotopic frequency ( $B$  vibrational mode) is obtained from (2.44). That equation gives

$$[1 - \epsilon \omega^2 G(5, 5)] = 1 - \epsilon \left[ \frac{2\omega^2 m_B d_2^2 S_\alpha^2}{\omega_3^2 - \omega^2} - m_A d_1^2 - 2m_B d_1^2 m_A d_2^2 C_\alpha^2 \right] = 0. \quad (2.51)$$

The solution of (2.51) gives  $(\omega_3^{(i)})^2$ ,

$$(\omega_3^{(i)})^2 = \omega_3^2 \frac{\epsilon m_A d_2^2 + 1}{1 + \epsilon} = \omega_3^2 \frac{m_A}{m_A^{(i)}} \frac{m_A^{(i)} + 2m_B S_\alpha^2}{m_A + 2m_B S_\alpha^2}, \quad (2.52)$$

where  $\epsilon = m_A^{(i)}/m_A - 1$ .

### $B^{(i)}AB^{(i)}$ molecules

The isotopic frequencies of  $B^{(i)}AB^{(i)}$  molecules are easily obtained from those of  $BA^{(i)}B$  molecule discussed in the previous section. Consider a molecule  $B^{(i)}XB^{(i)}$  with  $m_X = (m_B^{(i)}/m_B)m_A$ . Such a molecule is the same as the normal  $AB_2$  molecule except that the masses are all scaled by the factor  $m_B^{(i)}/m_B$ . Therefore the frequencies for this molecule are related to those of the normal molecule by

$$(\omega_k^2)_{B^{(i)}XB^{(i)}} = \frac{m_B}{m_B^{(i)}} (\omega_k^2)_{BAB}, \quad k = 1, 2, \text{ and } 3.$$

If we now substitute a normal  $A$  atom for the  $X$  atom, we arrive at the  $B^{(i)}AB^{(i)}$  molecule and we may apply the results of the previous section with the following rules:

- (a)  $m_A$  is replaced by  $(m_B^{(i)}/m_B)m_A$
- (b)  $m_A^{(i)}$  is replaced by  $m_A$
- (c)  $(\omega_k^2)$  is replaced  $(m_B/m_B^{(i)})(\omega_k^2)$
- (d)  $m_B$  is replaced by  $m_B^{(i)}$ .

Making these replacements gives us the following results:

$$(\omega_1^{(i)})^2 + (\omega_2^{(i)})^2 = \omega_1^2 + \omega_2^2 + \frac{\epsilon}{C^2} \frac{2m_B(\omega_1^2 + a^2\omega_2^2) + m_A C^2(\omega_1^2 + \omega_2^2)}{2m_B + m_A}, \quad (2.53)$$

$$(\omega_1^{(i)})^2 (\omega_2^{(i)})^2 = \frac{m_B}{m_B^{(i)}} (\omega_1^2 \omega_2^2) \frac{m_A + 2m_B^{(i)}}{m_A + 2m_B}, \quad (2.54)$$

$$(\omega_3^{(i)})^2 = \omega_3^2 \frac{m_B}{m_B^{(i)}} \frac{m_A + 2m_B^{(i)} S_\alpha^2}{m_A + 2m_B S_\alpha^2}, \quad (2.55)$$

$$\epsilon = \frac{m_B}{m_B^{(i)}} - 1. \quad (2.56)$$

#### $B^{(i)}A^{(i)}B^{(i)}$ molecules

The frequencies of the final symmetrically substituted form  $B^{(i)}A^{(i)}B^{(i)}$  can be obtained by the same method as was applied to  $B^{(i)}AB^{(i)}$ . For  $B^{(i)}A^{(i)}B^{(i)}$  we make the following replacements in (2.48)–(2.50):

- (a)  $m_A$  is replaced by  $(m_B^{(i)}/m_B)m_A$
- (b)  $(\omega_k^2)$  is replaced  $(m_B/m_B^{(i)})(\omega_k^2)$
- (c)  $m_B$  is replaced by  $m_B^{(i)}$ .

This gives

$$(\omega_1^{(i)})^2 + (\omega_2^{(i)})^2 = \frac{m_A}{m_A^{(i)}} \left\{ \omega_1^2 + \omega_2^2 + \frac{\epsilon}{C^2} \frac{2m_B(\omega_1^2 + a^2\omega_2^2) + m_A C^2(\omega_1^2 + \omega_2^2)}{2m_B + m_A} \right\}, \quad (2.57)$$

$$(\omega_1^{(i)})^2 (\omega_2^{(i)})^2 = (\omega_1^2 \omega_2^2) \frac{2m_B^{(i)} + m_A^{(i)}}{2m_B + m_A}, \quad (2.58)$$

$$(\omega_3^{(i)})^2 = \omega_3^2 \frac{m_A m_B}{m_A^{(i)} m_B^{(i)}} \frac{m_A^{(i)} + 2m_B^{(i)} S_\alpha^2}{m_A + 2m_B S_\alpha^2}, \quad (2.59)$$

$$\epsilon = \frac{m_B m_A^{(i)}}{m_B^{(i)} m_A} - 1. \quad (2.60)$$

### 2.10.3 Asymmetric isotopic substitution for $B^{(i)}AB$ molecules

For the isotopic molecule  $B^{(i)}AB$  we have two non-zero matrix elements for  $\Delta M^{(i)}$ ,

$$(\Delta M^{(i)})_{11} = (\Delta M^{(i)})_{22} = \frac{m_B^{(i)} - m_B}{m_B} = \frac{m_B^{(i)}}{m_B} - 1 = \epsilon. \quad (2.61)$$

Equation (2.36) yields

$$[1 - \epsilon\omega^2 G(1, 1)][1 - \epsilon\omega^2 G(2, 2)] - [\epsilon\omega^2 G(1, 2)]^2 = 0. \quad (2.62)$$

The Green's function matrix elements and parameters are given in Table 2.7:

$$\begin{aligned} G(1, 1) &= r^2 \Lambda_1 + t^2 S_\alpha^2 \lambda_3 - \frac{s^2 + t^2 u^2 C_\alpha^2}{\omega^2}, \\ G(2, 2) &= r^2 u^2 \Lambda_2 + t^2 C_\alpha^2 \lambda_3 - \frac{s^2 + (t/u)^2 S_\alpha^2}{\omega^2}, \\ G(1, 2) &= r^2 a u X_1 + t^2 S_\alpha C_\alpha X_3. \end{aligned}$$

Equation (2.62) leads to a cubic equation in the variable  $\omega^2$  from which the isotopic frequencies can be calculated. The details are not presented here, but may be found in reference [2.2].

#### The mixing parameter

The square of the mixing parameter,  $a^2$ , can easily be obtained from the results for the  $B^{(i)}AB^{(i)}$  molecule. Use is made of (2.53) to solve for  $(\omega_2^{(i)})^2$  in terms of  $(\omega_1^{(i)})^2$ .  $(\omega_2^{(i)})^2$  can then be eliminated from (2.54) and the equation solved for  $C^2$  ( $= 1 + |a|^2$ ). The result is

$$C^2 = \frac{2\epsilon m_B (\omega_1^2 - \omega_2^2)}{(\omega_1^{(i)})^2 + \omega_1^2 \omega_2^2 / (\omega_1^{(i)})^2 - (\omega_1^2 + \omega_2^2)(2m_B + m_A + \epsilon m_A) - 2m_B \epsilon \omega_2^2}, \quad (2.63)$$

where

$$\epsilon = \left( \frac{m_B}{m_B^{(i)}} \right) - 1.$$



Knowledge of the normal molecular frequencies,  $\omega_1$  and  $\omega_2$ , of  $\text{H}_2\text{O}$  and one of the isotopic frequencies,  $\omega_1^{(i)}$  or  $\omega_2^{(i)}$ , of  $\text{D}_2\text{O}$  is sufficient to determine the square of the mixing parameter via (2.63). The sign of the parameter  $a$  is not determined for symmetrical substitution. However, it is determined in the case of asymmetrical isotopic substitution since  $a$  appears linearly in  $G(1, 2)^2$ . Therefore knowledge of  $\omega_1$ ,  $\omega_2$ ,  $\omega_3$ , and one of the frequencies,  $\omega_1^{(i)}$  or  $\omega_2^{(i)}$ , of the  $B^{(i)}AB$  molecule is sufficient to determine all of the frequencies of all of the isotopically substituted forms of  $\text{H}_2\text{O}$ . There is no need to construct any type of force-constant matrix. On the other hand, if one wishes to construct the force-constant matrix, it is completely determined (Table 2.5) in terms of the frequencies of the normal molecule and the mixing parameter  $a$ .

#### 2.10.4 The sum and product rules for $AB_2$ and its isotopically substituted species

Equation (2.62) can be expressed as a cubic equation in  $x = \omega^2$  of the form  $x^3 + A_2 x^2 + A_3 = 0$ , where  $A_2$  and  $A_3$  are constants. In this form the constant  $A_3$  gives the product of the roots. That is,  $A_3 = [\omega_1^{(i)} \omega_2^{(i)} \omega_3^{(i)}]^2$ . This result is equivalent to the Teller–Redlich product rule for  $B^{(i)}AB$  isotopic frequencies. A sum rule relating the sums of the frequencies of  $BAB$ ,  $B^{(i)}AB$ , and  $B^{(i)}AB^{(i)}$  can also be obtained [2.3]. This rule states that

$$\sum \omega_k^2(BAB) + \sum \omega_k^2(B^{(i)}AB^{(i)}) = 2 \sum \omega_k^2(B^{(i)}AB). \quad (2.64)$$

In (2.64) the symbol  $\omega_k^2(BAB)$  indicates the frequencies of the normal molecule. The symbols  $\omega_k^2(B^{(i)}AB^{(i)})$  and  $\omega_k^2(B^{(i)}AB)$  indicate frequencies of the isotopic molecules  $B^{(i)}AB^{(i)}$  and  $B^{(i)}AB$ , respectively. This sum rule may be obtained using the Green's function method; however, the calculation is rather messy. There is another way to obtain the sum rule of (2.64), which we will now discuss. The force-constant matrix in diagonal form is given by (2.37),

$$\{\mathbb{U}^{-1} \mathfrak{F} \mathbb{U}\}_{rs} = \delta_{rs} (\omega_r)^2.$$

Therefore,  $\text{Tr}\{\mathbb{U}^{-1} \mathfrak{F} \mathbb{U}\} = \sum_k \omega_k^2$ , but, since the trace of a matrix is not changed by a similarity transformation or a unitary transformation, it follows that  $\text{Tr} \mathfrak{F} = \sum (\mathfrak{F})_{kk} = \sum \omega_k^2$ . The matrix  $\mathfrak{F}$  is related to  $\mathbb{F}$  by the relation  $\mathbb{F} = \mathbb{M}^{1/2} \mathfrak{F} \mathbb{M}^{1/2}$ . The matrix  $\mathbb{F}$  is the force-constant matrix in coordinate space and its elements **do not change with isotopic substitutions** (this is not true for  $\mathfrak{F}$ ). The diagonal elements of  $\mathfrak{F}$  are

$$(\mathfrak{F})_{kk} = (\mathbb{M}^{1/2} \mathbb{F} \mathbb{M}^{1/2})_{kk} = m_k \mathbb{F}_{kk}.$$

Therefore we can write

$$\sum m_k \mathbb{F}_{kk} = \sum \omega_k^2. \quad (2.65)$$

To make this clearer we rewrite (2.65) in the form

$$\sum m_k(XYZ) \mathbb{F}_{kk} = \sum \omega_k^2(XYZ), \quad (2.66)$$

where, for our  $AB_2$  molecule and its isotopically substituted species,  $XYZ$  can be  $BAB$ ,  $BA^{(i)}B$ ,  $B^{(i)}AB$ , or  $B^{(i)}AB^{(i)}$ . Note that the matrix elements  $\mathbb{F}_{kk}$  are the same for all of the molecules being considered. On applying (2.66) we obtain

$$\begin{aligned} \sum m_k(BAB) \mathbb{F}_{kk} &= \sum \omega_k^2(BAB) \\ &= m_B(F_{11} + F_{22} + F_{33} + F_{44}) + m_A(F_{55} + F_{66}), \\ \sum m_k(B^{(i)}AB^{(i)}) \mathbb{F}_{kk} &= \sum \omega_k^2(B^{(i)}AB^{(i)}) \\ &= m_B^{(i)}(F_{11} + F_{22} + F_{33} + F_{44}) + m_A(F_{55} + F_{66}), \\ \sum m_k(B^{(i)}AB) \mathbb{F}_{kk} &= \sum \omega_k^2(B^{(i)}AB) \\ &= m_B^{(i)}(F_{11} + F_{22}) + m_B(F_{33} + F_{44}) \\ &\quad + m_A(F_{55} + F_{66}). \end{aligned}$$

Because of the symmetry of the molecules we are considering,  $F_{11} = F_{33}$  and  $F_{22} = F_{44}$  (see Table 2.5). Therefore,

$$\begin{aligned} \sum \omega_k^2(BAB) &= 2m_B(F_{11} + F_{22}) + m_A(F_{55} + F_{66}), \\ \sum \omega_k^2(B^{(i)}AB^{(i)}) &= 2m_B^{(i)}(F_{11} + F_{22}) + m_A(F_{55} + F_{66}), \\ \sum \omega_k^2(B^{(i)}AB) &= m_B^{(i)}(F_{11} + F_{22}) + m_B(F_{11} + F_{22}) + m_A(F_{55} + F_{66}), \end{aligned}$$

from which it follows that

$$\sum \omega_k^2(BAB) + \sum \omega_k^2(B^{(i)}AB^{(i)}) = 2 \sum \omega_k^2(B^{(i)}AB).$$

## 2.11 Results for isotopically substituted forms of $H_2O$

In this section we apply the theory developed above to obtain results for isotopically substituted variants of  $H_2O$ . The physical and spectroscopic data needed to apply the theory are

$$\begin{aligned} \nu_1(H_2O) &= 3825.32 \text{ cm}^{-1}, & m_A(H_2O) &= 16, & m_A(H_2^{(18)}O) &= 18, \\ \nu_2(H_2O) &= 1653.91 \text{ cm}^{-1}, & m_B(H_2O) &= 1, & \alpha(H_2O) &= 105^\circ, \\ \nu_3(H_2O) &= 3935.59 \text{ cm}^{-1}, & m_B(D_2O) &= 2, & a &= -0.74141, \\ \nu_1(D_2O) &= 2758.06 \text{ cm}^{-1}, & m_B(T_2O) &= 3, & \omega &= 2\pi\nu. \end{aligned}$$

Table 2.8 Experimentally observed and calculated frequencies for isotopically substituted variants of H<sub>2</sub>O. All theoretical values are derived using the observed H<sub>2</sub>O frequencies and  $\omega_1$  from D<sub>2</sub>O (frequencies with asterisks are the input data). The calculated value for  $a(\text{H}_2\text{O})$  is  $-0.741\,41$ . The angle  $\alpha(\text{H}_2\text{O}) = 105^\circ$ , and the atomic masses are  $m_A = 16$ ,  $m_B(\text{H}) = 1$ ,  $m_B(\text{D}) = 2$ , and  $m_B(\text{T}) = 3$ . Frequencies are in units of  $\text{cm}^{-1}$ . To convert to frequency in Hz, multiply by the velocity of light,  $2.9978 \times 10^{10} \text{ cm/s}$ .

Molecule [Reference]	Frequencies in $\text{cm}^{-1}$		
	$\nu_1$ Calculated experimental	$\nu_2$ Calculated experimental	$\nu_3$ Calculated experimental
H <sub>2</sub> O	3825*	1654*	3936*
[2.6]	3825	1654	3936
D <sub>2</sub> O	2758*	1209	2925
[2.6]	2758	1210	2884
[2.7]	2669	1178	2788
HDO	2819	1451	3883
[2.8]	2824	1440	3890
[2.9]	2724	1403	3707
T <sub>2</sub> O	2299	1017	2436
[2.10]		1017	2438
[2.7]	2234	995	2367
HTO	2363	1373	3882
[2.10]		1359	3895
D <sub>2</sub> O <sup>(18)</sup>	2746	1202	2862
[2.8]	2784	1206	2889

Using the above data, we find from (2.67) that  $a^2 = 0.5497$ . Calculations of asymmetric substitution show that  $a$  is negative. The calculated frequencies for H<sub>2</sub>O with various substitutions of deuterium (D) and tritium (T) are shown in Table 2.8 and compared with experimental data. The mixing parameter,  $a^2$ , and the frequencies of various isotopically substituted forms of H<sub>2</sub>O, D<sub>2</sub>O, H<sub>2</sub>S, and D<sub>2</sub>S are available [2.2]. Isotopically substituted XY<sub>3</sub> molecules [2.4] and ethylene [2.5] have also been analyzed using the Green's function method.

### 2.11.1 The force-constant matrix for H<sub>2</sub>O

Using the value of  $C^2$  and the experimental frequencies listed in Table 2.8 for H<sub>2</sub>O, we can calculate the numerical values of the force constants. Evaluation of the elements in Table 2.5 gives the force-constant matrix in Table 2.9.

Table 2.9 The force-constant matrix ( $\mathfrak{F}$  in  $\eta$ -space) for  $H_2O$ . The force constants are in units of  $4\pi^2 \times 10^6 \text{ cm}^{-2}$ .

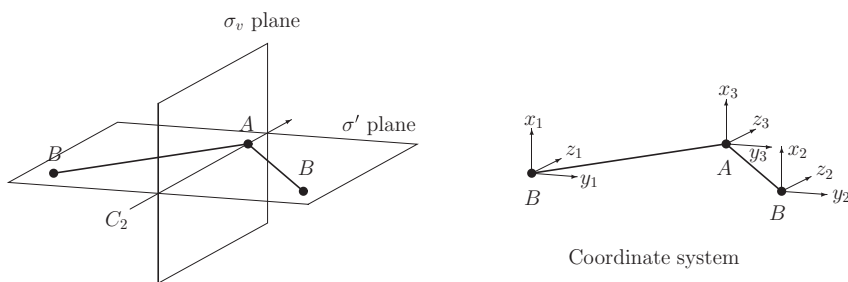
11.678	−4.417	1.247	−0.948	−3.236	1.341
	3.556	0.948	2.626	0.867	−1.546
		11.678	4.417	−3.236	−1.341
			3.556	−0.867	−1.546
	$F_{ij} = F_{ji}$			1.618	0.000
					0.773

### References

- [2.1] O. Redlich, “Eine allgemeine Beziehung zwischen den Schwingungsfrequenzen isotoper Moleküln (nebst Bemerkungen über die Berechnung harmonischer Kraftkonstanten)”, *Z. Phys. Chem. B* **28**, 371–382 (1935).
- [2.2] R. E. DeWames and T. Wolfram, “Vibrational analysis of substituted and perturbed molecules I. The exact isotope rule for molecules”, *J. Chem. Phys.* **40**, 853–860 (1964).
- [2.3] J.C. Decius and E.B. Wilson Jr., “Sum rules for the vibration frequencies of isotopic molecules”, *J. Chem. Phys.* **19**, 1409–1412 (1951).
- [2.4] C.D. Bass, L. Lynds, T. Wolfram, and R. E. DeWames, “Vibrational analysis of substituted and perturbed molecules. II. Planar  $XY_3$  molecules; application to  $BCl_3$ – $HBCl_2$ – $DBCl_2$ ”, *J. Chem. Phys.* **40**, 3611–3619 (1964).
- [2.5] T. Wolfram and A. Asgharian, “Generalized isotope rules for molecular vibrations with application to  $A_2B_4$  planar molecules”, *J. Chem. Phys.* **74**, 1661–1676 (1981).
- [2.6] G. Herzberg, *Infrared and Raman Spectra of Polyatomic Molecules* (New York: D. Van Nostrand, Inc., 1945).
- [2.7] R. Lemus, “Vibrational excitations in  $H_2O$  in the framework of a local model”, *J. Mol. Spectrosc.* **225**, 73–92 (2004). P.F. Bernath, “The spectroscopy of water vapour: Experiment, theory and applications”, *Phys. Chem. Chem. Phys.* **4**, 1501–1509 (2002).
- [2.8] W.S. Benedict, N. Gailar, and E.K. Plyler, “Rotation–vibration spectra of deuterated water vapor”, *J. Chem. Phys.* **24**, 1139–1165 (1956).
- [2.9] A. Janca, K. Tereszchuk, P.F. Bernath, N.F. Zobov, S. V. Shirin, O.L. Polyansky, and J. Tennyson, “Emission spectrum of hot HDO below  $4000 \text{ cm}^{-1}$ ”, *J. Mol. Spectrosc.* **210**, 132–135 (2003).
- [2.10] P.A. Staats, H.W. Morgan, and J.H. Goldstein, “Infrared spectra of  $T_2O$ ,  $THO$ , and  $TDO$ ”, *J. Chem. Phys.* **24**, 916–917 (1956).

### Exercises

Consider the  $AB_2$  molecule in three dimensions (Fig. 2.4). For simplicity use  $C_{2v}$  as the covering group. The operations and character table for the group are shown in Fig. 2.4.



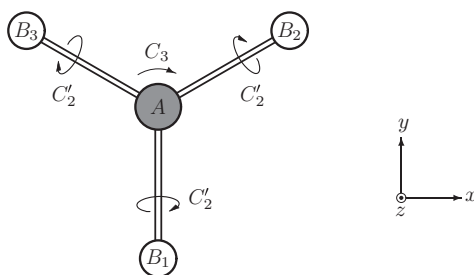
$\Gamma$	$E$	$C_2$	$\sigma_v$	$\sigma'_v$
$A_1$	1	1	1	1
$A_2$	1	1	-1	-1
$B_1$	1	-1	1	-1
$B_2$	1	-1	-1	1

Character table for  $C_{2v}$ 

Figure 2.4

- 2.1 Construct the action table for the atomic displacements  $r_x$ ,  $r_y$ , and  $r_z$ , and the atomic positions 1, 2, and 3.
- 2.2 Use the action table to find the characters of the operations of  $C_{2v}$  for a representation
  - (a) based on  $r_{xi}$  ( $i = 1, 2$ , and  $3$ ),
  - (b) based on  $r_{yi}$  and  $r_{zi}$  ( $i = 1, 2$ , and  $3$ ), and
  - (c) based on  $r_{xi}$ ,  $r_{yi}$ , and  $r_{zi}$  ( $i = 1, 2$ , and  $3$ ).
- 2.3 Decompose each of the representations (a), (b), and (c) in Exercise 2.2 into the IRs of  $C_{2v}$ .
- 2.4 Using the results of Exercise 2.3, explain why the in-plane symmetry functions do not mix with the out-of-plane (i.e., perpendicular to the plane of the molecule) symmetry functions.
- 2.5 Find the out-of-plane symmetry functions using the symmetry-function-generating machine.
  - (a) Use  $r_{x1}$  and  $r_{x3}$  as the generating functions.
  - (b) Identify the symmetry function for the rotation  $R_z$  (about the  $C_2$ -axis).
  - (c) Construct the translation  $T_x$  for translation in the  $x$ -direction.
  - (d) Transform the three symmetry functions to  $\eta$ -space and normalize them.
  - (e) Express  $T_x$  in  $\eta$ -space.
  - (f) Find the second  $B_1$ , out-of-plane, normal mode by requiring it to be orthogonal to  $R_z$  and  $T_x$ .

- (g) Show that the mode in part (f) corresponds to a rotation about a  $y$ -axis passing through the center of mass.
- (h) Sketch the three out-of-plane modes.
- 2.6 Consider a molecule with three atoms. The three atomic positions define a plane. By considering the body modes, prove that a triatomic molecule has no out-of-plane vibration modes.
- 2.7 The vibration frequencies of  $H_2S$  are  $\omega_1 = 2,714 \text{ cm}^{-1}$ ,  $\omega_2 = 1,215 \text{ cm}^{-1}$ , and  $\omega_3 = 2,732 \text{ cm}^{-1}$ , and the square of the mixing parameter is  $c^2 = 0.8978$ . Calculate the isotopic frequencies for the  $D_2S$  molecule.
- 2.8 Consider the planar molecule  $AB_3$  for which the  $B$  atoms are at the vertices of an equilateral triangle and the  $A$  atom is at the center of the triangle as shown in Fig. 2.5. The covering group is  $D_{3h}$ ; however, for this problem you may use the  $D_3$  group.



$D_3$	$E$	$2C_3$	$3C_2'$	
$A_1$	1	1	1	
$A_2$	1	1	-1	$R_z, z$
$\mathcal{E}$	1	-1	0	$R_x, R_y$

Figure 2.5

- (a) Decompose the representation  $\Gamma(Z)$  based on the four out-of-plane displacements,  $r_{zi} = Z_i$  ( $i = 1, 2, 3$ , and 4) into the IRs of  $D_3$ .
- (b) Identify the IRs for the body modes and the vibrations.
- (c) Find the eigenvectors for the three body modes.
- (d) Determine the out-of-plane, vibration eigenvector using orthogonality requirements.
- 2.9 Show that the isotopic frequencies of  $A^{(i)}B_3$  are given by

$$1 - \omega^2 G_{44}(\omega^2) \epsilon = 0,$$

with  $\epsilon = M_A^{(i)} / M_A - 1$ , and  $G_{44}(\omega^2) = [(\mathbb{F} - \omega^2)^{-1}]_{44}$ .

The matrix indices designated as  $i = 1, 2$ , and  $3$  refer to the out-of-plane displacements of the  $B_i$  atoms, and  $i = 4$  refers to the out-of-plane displacement of the  $A$  atom.

- 2.10 Find an expression for the out-of-plane frequency of the  $A^{(i)}B_3$  molecule in terms of the out-of-plane frequency of the  $AB_3$  molecule.

# 3

## Spherical symmetry and the full rotation group

### 3.1 Hydrogen-like orbitals

The full rotation group,  $O(3)$ , consists of all the real orthogonal transformations that leave a sphere invariant. The group includes proper rotations and inversion. The number of elements in the full rotation group is infinite, but the operators form a group that satisfies the definition given in Chapter 1 by Theorem 1.1. To work with the full rotation group, it is useful to have basis functions for the irreducible representations. One set of basis functions is the set of eigenfunctions for the hydrogen-like atom.

Hydrogen-like functions are eigenstates of Schrödinger's equation for a single electron bound to a nucleus whose charge is  $+Ze$ . Similar functions are also obtained as one-electron, approximate solutions for a many-electron atom. In this case the charge  $Ze$  is the (effective) average charge experienced by the electron, including the “shielding” of the nuclear charge by the other electrons.

Schrödinger's equation in the eigenvalue form is

$$(\mathbb{H}^0 - E_{\mathbf{k}}) \Psi_{\mathbf{k}}(\mathbf{r}) = 0,$$

with

$$\mathbb{H}^0 = -\frac{\hbar^2}{2m_e} \nabla^2 - \frac{Ze^2}{r} + V_{\text{eff}}(r), \quad r = |\mathbf{r}|,$$

where  $\mathbb{H}^0$  is a one-electron Hamiltonian and  $\Psi_{\mathbf{k}}(\mathbf{r})$  is an eigenstate whose eigenvalue is  $E_{\mathbf{k}}$ . The Hamiltonian consists of the electron's kinetic energy, the effective nuclear Coulomb attraction, and an effective (spherically symmetric) potential,  $V_{\text{eff}}$ .

The hydrogen-like eigenstates, called orbitals, are characterized by three quantum numbers,  $n$ ,  $l$ , and  $m$ . The principal quantum number,  $n$ , can take on the values  $1, 2, 3, \dots$ . The quantity  $l$  is the angular-momentum quantum number, and its range



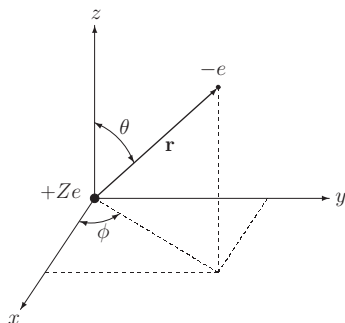


Figure 3.1 The coordinate system for the hydrogenic orbitals.

of values for a given  $n$  is  $l = 1, 2, \dots, n - 1$ . Finally,  $m$ , the magnetic quantum number, takes on integral values between  $-l$  and  $+l$ . The energy corresponding to  $\Psi_{nlm}$  depends on the value of  $n$ , but not on  $l$  and  $m$ . (If spin-orbit interactions are considered the energy will also depend on  $l$ , but not on  $m$ ). For our purposes it is sufficient that the energy does not depend on  $m$ .

The orbitals can be separated into a radial function,  $R_{nl}(r)$ , and an angular function,  $Y_l^m(\theta, \phi)$ ,

$$\Psi_{nlm}(\mathbf{r}) = R_{nl}(r) Y_l^m(\theta, \phi),$$

where  $n = 1, 2, 3, \dots$ ;  $l = 1, 2, 3, \dots, n - 1$ ; and  $m = 0, \pm 1, \pm 2, \dots, \pm l$ .

The coordinate system defining the variables  $r$ ,  $\theta$ , and  $\phi$  is shown in Fig. 3.1.

$R_{nl}(r)$  determines the radial shape of the wavefunction. The number of radial nodes is  $n$ . The principal quantum number,  $n$ , determines the energy (eigenvalue) of the orbital, and orbitals having the same value of  $n$  are said to belong to the same “shell”. The angular function,  $Y_l^m(\theta, \phi)$ , is one of an infinite set of orthogonal functions known as the spherical harmonics. The quantum number  $l$  determines the angular shape of the orbital. The  $s$ -orbitals have  $l = 0$ , the  $p$ -orbitals have  $l = 1$ , and the  $d$ -orbitals have  $l = 2$ . The magnetic quantum number  $m$  determines the orientation of the orbital with respect to the  $z$ -axis. Since  $m$  ranges from  $-l$  to  $+l$  in integral steps, it takes on  $(2l + 1)$  integral values. Each of the spherical harmonic functions can be separated into a product of two functions:

$$Y_l^m(\theta, \phi) = P_l^m(\cos \theta) e^{im\phi},$$

where  $P_l^m(\cos \theta)$  is an associated Legendre polynomial. The functions for  $l = 0$ , 1, and 2 are given in Table 3.1.

Table 3.1 Spherical harmonic functions for  $l = 0, 1$ , and 2

$Y_0^0(\theta, \phi) = \frac{1}{2}\sqrt{1/\pi}$	$Y_2^{-2}(\theta, \phi) = \frac{1}{4}\sqrt{15/(2\pi)} \sin^2 \theta e^{-2i\phi}$
$Y_1^{-1}(\theta, \phi) = \frac{1}{2}\sqrt{3/(2\pi)} \sin \theta e^{-i\phi}$	$Y_2^{-1}(\theta, \phi) = \frac{1}{2}\sqrt{15/(2\pi)} \sin \theta \cos \theta e^{-i\phi}$
$Y_1^0(\theta, \phi) = \frac{1}{2}\sqrt{3/\pi} \cos \theta$	$Y_2^0(\theta, \phi) = \frac{1}{4}\sqrt{5/\pi} (3 \cos^2 \theta - 1)$
$Y_1^1(\theta, \phi) = -\frac{1}{2}\sqrt{3/(2\pi)} \sin \theta e^{i\phi}$	$Y_2^1(\theta, \phi) = -\frac{1}{2}\sqrt{15/(2\pi)} \sin \theta \cos \theta e^{i\phi}$
	$Y_2^2(\theta, \phi) = \frac{1}{4}\sqrt{15/(2\pi)} \sin^2 \theta e^{2i\phi}$

### 3.2 Representations of the full rotation group

In the previous chapters we used the operators  $O_R$  to subject the nuclear displacements to a rotation,  $R$ , with the convention that a rotation was clockwise. We rotated the function(s) and kept the coordinate axes fixed. We also noted that the same matrix representation of the group could be obtained by fixing the function and rotating the axes in a counter-clockwise manner.

We now need to define a symmetry operator more generally. The conventional symbol for an operator that operates on a function of the coordinates is  $P_R$ . Its action on a function  $f(\mathbf{x})$  is defined by the equation

$$P_R f(\mathbf{x}) = f(R^{-1}\mathbf{x}), \quad (3.1)$$

where  $\mathbf{x}$  represents a system of orthogonal coordinates, e.g.,  $(X, Y, Z)$ , or, as in the case of square,  $(X_1, Y_1, X_2, Y_2, \dots, Y_4)$ .  $P_R f(\mathbf{x})$  is clockwise rotation of the function  $f(\mathbf{x})$  with the coordinates fixed and  $f(R^{-1}\mathbf{x})$  is the function expressed in the counter-clockwise-rotated coordinate system.

If  $R, S, T, \dots$  are the elements of a group  $G$ , the operators  $P_R, P_S, P_T, \dots$  form a group that is isomorphic to  $G$ . This means that, if  $RS = T$ , then  $P_R P_S f(\mathbf{x}) = P_T f(\mathbf{x}) = f((RS)^{-1}\mathbf{x}) = f(S^{-1}R^{-1}\mathbf{x})$ . *Note the order of the operators after the last equals sign. It is easy to make the erroneous argument that  $P_R P_S f(\mathbf{x}) = P_R f(S^{-1}\mathbf{x}) = f(R^{-1}S^{-1}\mathbf{x})$  (which is **incorrect**).*

The appearance of  $R^{-1}$  on the right-hand side of (3.1) may seem a bit strange at first. However, this definition of the action of the operator is consistent with the method used in previous chapters. A simple example may serve to clarify this point. Consider a vector  $\mathbf{r}$  in the  $x$ - $y$  plane as shown in Fig. 3.2(a).  $R$  is a rotation by  $\pi/2$  about the  $z$ -axis (out of the plane of the paper). In the case of Fig. 3.2(a) we rotate the vector  $\mathbf{r}$  clockwise with the coordinate axes fixed. This is the method used in Chapters 1 and 2. For this operation the  $x$ -component of  $\mathbf{r}$  before rotation becomes the negative  $y$ -component of  $\mathbf{r}$  after rotation. Similarly, the  $y$ -component before

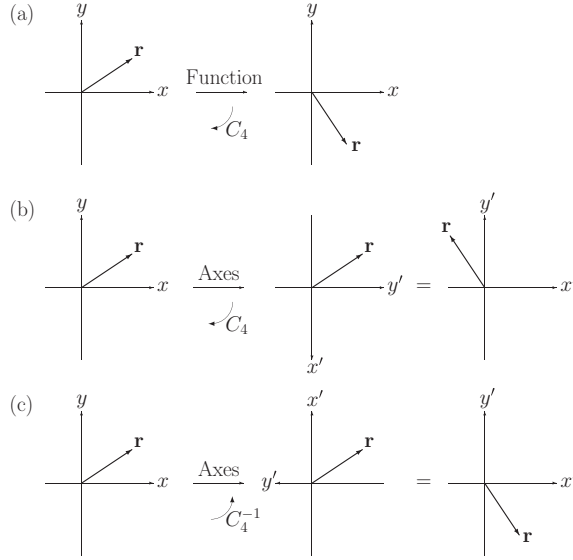


Figure 3.2 Rotation of a function versus rotation of the axes. (a) Clockwise rotation of  $\mathbf{r}$  by  $\pi/2$  with the coordinate axes fixed. (b) Clockwise rotation by  $\pi/2$  of the axes with  $\mathbf{r}$  fixed. (c) Counter-clockwise rotation by  $\pi/2$  of the axes with  $\mathbf{r}$  fixed. The components  $r_x$  and  $r_y$  in (a) are the same as  $r_{x'}$  and  $r_{y'}$ , respectively, in (c).

rotation becomes the  $x$ -component after rotation. The matrix that accomplishes this is

$$\begin{pmatrix} 0 & 1 \\ -1 & 0 \end{pmatrix}. \quad (3.2)$$

If we rotate the axes clockwise (Fig. 3.2(b)), we are making a change of coordinates described by  $\mathbf{x}' = R\mathbf{x}$ ; that is,

$$\begin{aligned} x' &= R_{11}x + R_{12}y, \\ y' &= R_{21}x + R_{22}y, \end{aligned} \quad (3.3)$$

in which the  $x'$ -axis is  $-y$  and the  $y'$ -axis is  $x$ . Clearly, the transformation coefficients are  $R_{11} = R_{22} = 0$ ,  $R_{12} = -1$ , and  $R_{21} = 1$ . The matrix for this operation is

$$\begin{pmatrix} 0 & -1 \\ 1 & 0 \end{pmatrix}. \quad (3.4)$$

In Fig. 3.2(c), we rotate the axes counter-clockwise. This gives  $x' = y$  and  $y' = -x$ , so the matrix representing this transformation is

$$\begin{pmatrix} 0 & 1 \\ -1 & 0 \end{pmatrix}. \quad (3.5)$$

From these different cases we can conclude that a rotation of the function clockwise with the axes fixed produces the same representation matrix as a counter-clockwise rotation of the axes with the function fixed. In the above example we see that the matrix for clockwise rotation of the axes is the inverse of the matrix for counter-clockwise rotation. This relationship is always true since if we rotate clockwise through an angle and then counter-clockwise through the same angle we have changed nothing. That is,  $R(\text{cw}) R(\text{ccw}) = E$ , from which it follows that  $R(\text{ccw}) = R(\text{cw})^{-1}$ .

Returning to our discussion of the operator,  $P_R$ , we see from its definition in (3.1) that  $P_R$  operating on  $f(\mathbf{x})$  has the same matrix representation as rotating the function clockwise, since  $R^{-1}$  is a clockwise rotation of the axes.

Now let us look at the effect  $P_R$  has on the spherical harmonic functions. The function  $Y_l^m$  has the property that if the polar axis is rotated the new function can be expressed as a linear combination of the old functions,

$$P_R Y_l^m(\theta, \phi) = \sum_{m'=-l}^{+l} D_{m'm}^{(l)}(R) Y_l^{m'}(\theta, \phi). \quad (3.6)$$

The matrices  $D_{m'm}^{(l)}(R)$  form a representation of the group of rotations, as we shall show below. Let  $\Psi$  be a linear combination of spherical harmonic functions,

$$\Psi = \sum_m C_m Y_l^m,$$

where  $C_m$  is a constant coefficient in the expansion. We can represent  $\Psi$  as a column vector with  $(2l + 1)$  rows:

$$\begin{pmatrix} C_l \\ C_{l-1} \\ C_{l-2} \\ \vdots \\ C_{-l} \end{pmatrix}.$$

In this case the rows of the column vector are the coefficients of the functions,  $Y_l^l, Y_l^{l-1}, Y_l^{l-2}, \dots, Y_l^{-l}$ . So the  $Y_l^m$ s act as the unit vectors of a coordinate space with  $(2l + 1)$  dimensions. If we operate on  $\Psi$ , we have

$$\begin{aligned} P_R \Psi &= \sum_m C_m P_R Y_l^m = \sum_m \sum_{m'} C_m D_{m'm}^{(l)}(R) Y_l^{m'} \\ &= \sum_{m'} \left( \sum_m D_{m'm}^{(l)}(R) C_m \right) Y_l^{m'} = \sum_{m'} C_{m'}' Y_l^{m'}, \end{aligned} \quad (3.7)$$

where

$$\sum_m D_{m'm}^{(l)}(R) C_m = C'_{m'}. \quad (3.8)$$

Equation (3.8) written out in matrix form for  $l = 1$  is

$$\begin{pmatrix} D_{11}^{(1)}(R) & D_{10}^{(1)}(R) & D_{1-1}^{(1)}(R) \\ D_{01}^{(1)}(R) & D_{00}^{(1)}(R) & D_{0-1}^{(1)}(R) \\ D_{-11}^{(1)}(R) & D_{-10}^{(1)}(R) & D_{-1-1}^{(1)}(R) \end{pmatrix} \begin{pmatrix} C_1 \\ C_0 \\ C_{-1} \end{pmatrix} = \begin{pmatrix} C'_1 \\ C'_0 \\ C'_{-1} \end{pmatrix}. \quad (3.9)$$

Equation (3.9) is the same form as we had for the representation matrices in Chapter 1, namely,

$$\Gamma(R) \mathbf{V}_i = \mathbf{V}_f, \quad (3.10)$$

where  $\mathbf{V}_i$  is the initial vector,  $\Gamma(R)$  is the representation matrix for  $R$ , and  $\mathbf{V}_f$  is the final vector (after rotating the function clockwise). In Chapter 1 we rotated the function, not the axes. In (3.9)  $D^{(1)}(R)$  rotates the axes counter-clockwise, which produces the same matrix representation as rotating the function clockwise.

A word about notation is needed. We shall reserve the symbol  $D^{(l)}(R)$  for the representation of  $P_R$  based on the  $(2l + 1)$  spherical harmonic functions. Other representations of  $P_R$  will be denoted by  $D(R)$  ( $D$  without a superscript  $(l)$ ), or by  $\Gamma(R)$  or  $\Gamma^\alpha(R)$ .

In general, if  $f_j$  is one of a set of functions ( $j = 1, 2, \dots, N$ ) for which

$$P_R f_j = \sum_{r=1}^N D_{rj}(R) f_r, \quad (3.11)$$

then  $D(R)$  is a matrix representation of  $P_R$  (not necessarily an IR). The order of the indices is essential in (3.11) if  $D(R)$  is to form a representation of the group under ordinary matrix multiplication. For the set of basis functions,

$$\begin{aligned} P_S P_R f_j &= \sum_k D(R)_{kj} P_S f_k = \sum_k \sum_m D(R)_{kj} D(S)_{mk} f_m \\ &= \sum_m \left\{ \sum_k D(S)_{mk} D(R)_{kj} \right\} f_m = \sum_m D(SR)_{mj} f_m. \end{aligned} \quad (3.12)$$

In (3.12)  $k$  and  $m$  take on the values  $1, 2, \dots, N$ , where  $N$  is the number of basis functions. Equation (3.12) confirms that the  $D(R)$  matrices of (3.11) satisfy the requirements of a matrix representation of the  $P_R$  operators.

The spherical harmonic functions,  $Y_l^m$ , provide basis functions for an IR of the operators of the full rotation group. There is an infinite number of such

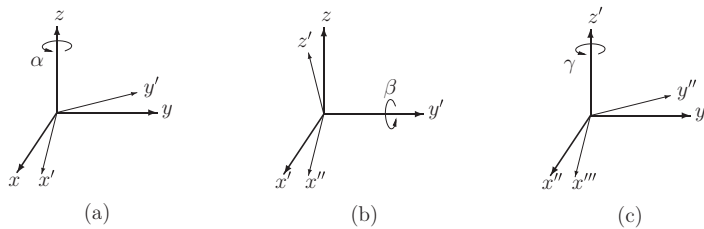


Figure 3.3 Euler-angle rotations: (a) rotation about the  $z$ -axis by  $\alpha$ , (b) rotation about the  $y'$ -axis by  $\beta$ , and (c) rotation about the  $z'$ -axis by  $\gamma$ . The sequence (a) to (c) corresponds to the operations in the order  $R_{z'}(\gamma) R_{y'}(\beta) R_z(\alpha)$ . The axes are positioned in each figure so that the  $z$ - or  $z'$ -axis is vertical.

representations, one for each value of  $l$ , and each is an IR. The dimensionality of the representations,  $(2l + 1)$ , is always an odd integer. Even-dimensional representations are discussed in Section 3.8.

**Theorem 3.1** *The  $(2l + 1)$ -dimensional representations of the full rotation group,  $D^{(l)}(R)$ , based on the spherical harmonic functions  $Y_l^m(\theta, \phi)$ ,  $m = \pm l, \pm(l - 1), \pm(l - 2), \dots, 0$ , are irreducible. There are no other inequivalent irreducible representations.*

The connection between the quantum numbers of the hydrogen-like orbitals and the representations is apparent. Each angular quantum number,  $l$ , is the name of an IR of the rotation group. Each magnetic quantum number is the name of a partner function of the IR; that is,  $Y_l^m$  is the  $m$ th-row function for the  $l$ th IR.

### 3.3 The character of a rotation

It is useful to use Euler angles  $\alpha$ ,  $\beta$ , and  $\gamma$  to describe a rotation. The Eulerian rotations, illustrated in Fig. 3.3, are defined as counter-clockwise rotations as follows: start with the  $x$ - $y$ - $z$  axes then perform (a) a rotation about the  $z$ -axis through an angle  $\alpha$  carrying  $x \rightarrow x'$ ,  $y \rightarrow y'$ , and  $z \rightarrow z$ , followed by (b) a rotation about the  $y'$ -axis through an angle  $\beta$ , carrying  $x' \rightarrow x''$ ,  $y' \rightarrow y'$  and  $z \rightarrow z'$ , followed by (c) a rotation about the  $z'$ -axis through an angle  $\gamma$ , carrying  $x'' \rightarrow x'''$ ,  $y' \rightarrow y''$ , and  $z' \rightarrow z'$ .

The IR in terms of the Euler angles is denoted by  $D^{(l)}(\alpha, \beta, \gamma)$ , and (3.6) takes the form

$$P_{(\alpha, \beta, \gamma)} Y_l^m = \sum_{m'=-l}^{+l} D^{(l)}(\alpha, \beta, \gamma)_{m'm} Y_l^{m'}. \quad (3.13)$$

The Eulerian system has the property that the same rotated vector can be achieved by applying the rotations in the reverse order about **fixed** axes: start with the  $x$ - $y$ - $z$  axes, then perform (1) a rotation about the  $z$ -axis through an angle  $\gamma$ , followed by (2) a rotation about the  $y$ -axis through an angle  $\beta$ , followed by (3) a rotation about the  $z$ -axis through an angle  $\alpha$ . The final rotated vector is the same as produced by the Euler rotations of Fig. 3.3. Stated mathematically,

$$R_z(\alpha) R_y(\beta) R_z(\gamma) = R_{z'}(\gamma) R_{y'}(\beta) R_z(\alpha), \quad (3.14)$$

where the rotations on the left operate on a vector in the fixed  $x$ - $y$ - $z$  axes system. For  $\gamma = 0$ , we have

$$R_z(\alpha) R_y(\beta) = R_{y'}(\beta) R_z(\alpha). \quad (3.15)$$

If (3.15) is substituted into (3.14), we obtain

$$R_z(\gamma) = R^{-1} R_{z'}(\gamma) R, \quad (3.16)$$

where  $R = [R_{y'}(\beta) R_z(\alpha)]$ . Recalling that elements  $A$  and  $B$  belong to the same class if they are related by  $A = R^{-1} B R$ , where  $R$  is any member of the group (Chapter 1, Theorem 1.3) we can conclude that  $R_z(\gamma)$  and  $R_{z'}(\gamma)$  are in the same class. But, since we can choose the angles  $\alpha$  and  $\beta$  at will, the axis  $z'$  can be arbitrarily chosen. Therefore all rotations by an angle  $\gamma$  belong to the same class regardless of the axis of rotation.

Now suppose we choose a rotation about the  $z$ -axis through an angle  $\alpha$  with  $\beta = \gamma = 0$ . The operator  $P_{(\alpha,0,0)}$  acts only on the  $\phi$ -dependent part of  $Y_l^m(\theta, \phi)$ ,

$$P_{(\alpha,0,0)} Y_l^m(\theta, \phi) = P_{lm}(\cos \theta) [P_{(\alpha,0,0)} e^{im\phi}] = e^{-im\alpha} Y_l^m(\theta, \phi). \quad (3.17)$$

The negative sign in the exponential results because  $P_{(\alpha,0,0)}$  rotates the function clockwise, that is, takes  $\phi$  into  $\phi - \alpha$ . We see that  $P_{(\alpha,0,0)}$  acting on  $Y_l^m$  produces a multiple of the same function. Therefore the representation matrix  $D^{(l)}(\alpha, 0, 0) \equiv D^{(l)}(\alpha)$  is diagonal,

$$D^{(l)}(\alpha)_{m,m'} = e^{-im\alpha} \delta_{m,m'}, \quad (3.18)$$

and for the character of the matrix we have

$$\chi^{(l)}(\alpha) = \sum_{m=-l}^{+l} e^{-im\alpha} = \frac{\sin[(l+1/2)\alpha]}{\sin(\alpha/2)}. \quad (3.19)$$

Since all rotations by an angle  $\alpha$  about any axis are in the same class, it follows that the characters of all such rotations are the same. Therefore, in finding the

character of the matrix representing a rotation it is not necessary to specify the axis of rotation; only the angle need be specified. We may then write

$$\chi^{(l)}(A) = \frac{\sin[(l + 1/2)A]}{\sin(A/2)}, \quad (3.20)$$

where  $\chi^{(l)}(A)$  is the character of the representation matrix for a rotation of the function through an angle  $A$  in radians about any axis. We note that the character of a rotation by  $A$  is the same as that for a rotation by  $-A$ . Therefore the **character** is the same irrespective of whether we rotate the function or the coordinates. However, the matrix  $D^{(l)}$  depends on the sign of  $A$ , and incorrect results may be obtained if one does not consistently use a single convention. We shall consistently use the convention that  $P_R$  rotates the function clockwise as implied by (3.1).

Approximate solutions of Schrödinger's equation for atoms with many electrons may be built up from combinations of hydrogen-like, one-electron orbitals. The wavefunction may be, for example, a Slater determinant (or a linear combination of Slater determinants) whose elements are one-electron, hydrogenic orbitals. As mentioned previously, the energies of the orbitals do not depend on the magnetic quantum number,  $m$ . This means that orbitals for a particular  $l$  are  $(2l + 1)$ -fold degenerate in a spherically symmetric environment. Since all the partner functions (basis functions for the rows of  $D^{(l)}$ ) have the same energy, linear combinations of these functions also have the same energy. Certain linear combinations of the spherical harmonics are more convenient to work with than others. In particular, it is useful to take combinations that are real functions. The usual choices for these functions are given in Table 3.2.

The combinations of  $Y_l^m$  in Table 3.2 are symmetry coordinates for IRs of the octahedral group,  $O$ .

Table 3.2 *The s, p, and d hydrogen-like orbitals*

$s = Y_0^0 = \sqrt{1/(4\pi)}$	$d_{z^2} = Y_2^0 = \sqrt{5/(16\pi)} (3z^2 - r^2)/r^2$
	$d_{x^2} = \sqrt{\frac{1}{2}}(Y_2^2 + Y_2^{-2})$ $= \sqrt{15/(16\pi)} (x^2 - y^2)/r^2$
$p_x = -\sqrt{\frac{1}{2}}(Y_1^1 - Y_1^{-1}) = \sqrt{3/(4\pi)} x/r$	$d_{xy} = -i\sqrt{\frac{1}{2}}(Y_2^2 - Y_2^{-2}) = \sqrt{15/(4\pi)} xy/r^2$
$p_y = i\sqrt{\frac{1}{2}}(Y_1^1 + Y_1^{-1}) = \sqrt{3/(4\pi)} y/r$	$d_{xz} = \sqrt{\frac{1}{2}}(Y_2^1 + Y_2^{-1}) = \sqrt{15/(4\pi)} xz/r^2$
$p_z = Y_1^0 = \sqrt{3/(4\pi)} z/r$	$d_{yz} = \sqrt{\frac{1}{2}}(Y_2^1 - Y_2^{-1}) = \sqrt{15/(4\pi)} yz/r^2$



### 3.4 Decomposition of $D^{(l)}$ in a non-spherical environment

For a given value of  $l$  the hydrogen-like orbitals  $Y_l^m(\theta, \phi)$  are basis functions for a  $(2l + 1)$ -dimensional matrix representation of the rotation group. All of the partner functions (those functions corresponding to different values of  $m$ ) are degenerate eigenfunctions of the hydrogen-like Hamiltonian in (3.1).

If the environment of the atom is changed so that it is no longer spherically symmetric, some of the degeneracies may be lifted. Examples of changes in environment include application of an electric or magnetic field or imbedding the atom in a crystal or molecule. In a non-spherical environment the symmetry is reduced, and the group of the covering operations is no longer the full rotation group.

Suppose  $G$ , a group for a non-spherical environment, consists of the elements  $R_1, R_2, R_3, \dots, R_h$ . The matrices  $D^{(l)}(R_1)_{mm'}, D^{(l)}(R_2)_{mm'}, D^{(l)}(R_3)_{mm'}, \dots, D^{(l)}(R_h)_{mm'}$  of (3.6) form a valid representation of  $G$ , but the representation might not be an IR. To find out whether it is, we can decompose  $D^{(l)}$  into the IRs of the group  $G$  in the usual way (Chapter 1, Eq. (1.10)),

$$n^\beta = \frac{1}{h} \sum_{k=1}^{\mathcal{N}_c} N_k \chi^l(R_k)^* \chi^\beta(R_k), \quad (3.21)$$

where  $n^\beta$  is the number of times the  $\beta$ th IR of  $G$  appears in the decomposition of  $D^{(l)}$ ,  $\mathcal{N}_c$  is the number of classes of  $G$ , and  $N_k$  is the number of elements in the  $k$ th class. As an example, consider an atom in a crystal at a site of octahedral symmetry. The character table for the octahedral group  $O$  is given in Table 3.3.

The last row of Table 3.3 shows the characters for the  $D^{(l)}$  representation derived from (3.20) for  $A = 2\pi/n$ . For the  $d$ -orbitals,  $l = 2$  and we have  $\chi^{(2)}(C_2) = \chi^{(2)}(\pi) = S_2^{(2)} = 1$ ,  $\chi^{(2)}(C_3) = \chi^{(2)}(2\pi/3) = S_3^{(2)} = -1$ , and  $\chi^{(2)}(C_4) = \chi^{(2)}(\pi/2) = S_4^{(2)} = -1$ . The decomposition of  $D^{(2)}$  is as follows:

$$\begin{aligned} n^{A_1} &= \frac{1}{24} [1 \times 5 \times 1 + 8 \times -1 \times 1 + 3 \times 1 \times 1 + 6 \times 1 \times 1 + 6 \times -1 \times 1] = 0, \\ n^{A_2} &= \frac{1}{24} [1 \times 5 \times 1 + 8 \times -1 \times 1 + 3 \times 1 \times 1 + 6 \times 1 \times -1 + 6 \times -1 \times -1] = 0, \\ n^{\mathcal{E}} &= \frac{1}{24} [1 \times 5 \times 2 + 8 \times -1 \times -1 + 3 \times 1 \times 2 + 6 \times 1 \times 0 + 6 \times -1 \times 0] = 1, \\ n^{T_1} &= \frac{1}{24} [1 \times 5 \times 3 + 8 \times -1 \times 0 + 3 \times 1 \times -1 + 6 \times 1 \times -1 + 6 \times -1 \times 1] = 0, \\ n^{T_2} &= \frac{1}{24} [1 \times 5 \times 3 + 8 \times -1 \times 0 + 3 \times 1 \times -1 + 6 \times 1 \times 1 + 6 \times -1 \times -1] = 1, \\ D^{(2)} &= \mathcal{E} + T_2. \end{aligned} \quad (3.22)$$

Table 3.3 *The character table for the octahedral group,  $O$ . The last row shows the characters for a reducible representation of  $O$  based on the spherical harmonic functions,  $Y_l^m(\theta, \phi)$ .  $S_n^{(l)} = \sin[(l + 1/2)2\pi/n]/\sin(\pi/n)$ .*

IR name	$E$	$8C_3$	$3C_2$	$6C_2'$	$6C_4$	Basis functions
$A_1$	1	1	1	1	1	$x^2 + y^2 + z^2$
$A_2$	1	1	1	-1	-1	$xyz$
$\mathcal{E}$	2	-1	2	0	0	$\{(x^2 - y^2), (3z^2 - r^2)\}$
$T_1$	3	0	-1	-1	1	$\{x, y, z\}; \{R_x, R_y, R_z\}$
$T_2$	3	0	-1	1	-1	$\{xy, xz, yz\}$
$D^{(l)}$	$2l+1$	$S_3^{(l)}$	$S_2^{(l)}$	$S_2^{(l)}$	$S_4^{(l)}$	

The decomposition shows that in an octahedral environment the five-fold degenerate  $d$ -orbitals split into two groups: a doubly degenerate  $\mathcal{E}$  group and a triply degenerate  $T_2$  group. Since each IR in the decomposition is contained once only, the symmetry functions constructed from linear combinations of the spherical harmonics will be eigenfunctions of a Hamiltonian having spherical or octahedral symmetry. (The energies of  $E_g$  and  $T_{2g}$  functions are degenerate for spherical symmetry, but are split in octahedral symmetry.)

The  $d$ -orbitals listed in Table 3.2 are bases for IRs of the  $O$  group. The functions  $d_{z^2}$  and  $d_{x^2}$  are the basis functions for the  $\mathcal{E}$  IR, and  $d_{xy}$ ,  $d_{xz}$ , and  $d_{yz}$  are the basis functions for the  $T_2$  IR.

### 3.5 Direct-product groups and representations

Consider two groups,  $G_a$  and  $G_b$ , that have no common elements other than the identity and whose elements commute with one another. We can form a larger, composite group denoted by  $G_a \times G_b$ . If  $G_a$  has elements  $R_{aj}$ ,  $j = 1, 2, 3, \dots, h_a$ , and  $G_b$  has elements  $R_{bk}$ ,  $k = 1, 2, 3, \dots, h_b$ , then the elements of the direct-product group,  $G_a \times G_b$ , are of the form  $R_{aj}R_{bk}$ . The total number of elements in  $G_a \times G_b$  is  $h_a h_b$ . Such product groups are useful when the operators of the two groups operate on different kinds of coordinates, or to extend a group to include new elements. The first case occurs, for example, when dealing with vibronic states,  $\Psi(r, X) = \phi(r)\psi(X)$ , where  $\phi(r)$  is a function of the electronic coordinates and  $\psi(X)$  is a function of the nuclear displacements. In this case, the operators corresponding to  $G_a$  operate on electronic coordinates and the operators corresponding to  $G_b$  operate on the nuclear displacements. The groups  $G_a$  and  $G_b$  can be identical, but the operators operate on different types of coordinates. An

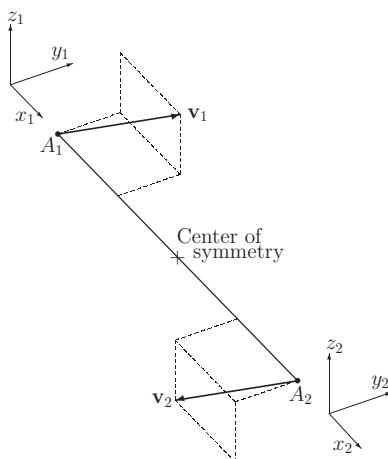


Figure 3.4 A molecule with a center of symmetry. The atoms at  $A_1$  and  $A_2$  are of the same type and in symmetry-equivalent positions. Under inversion a displacement  $\mathbf{v}$  at  $A_1$  becomes a displacement  $-\mathbf{v}$  at  $A_2$ .

example using the direct product to enlarge a group is the addition of the inversion operator,  $i$ , to a group that does not contain  $i$  or an operation equivalent to  $i$ .

### 3.5.1 Inversion

The operation of inversion, denoted by the symbol “ $i$ ”, carries a vector  $\mathbf{r}$  into  $-\mathbf{r}$ . For a molecule with a center of symmetry, “ $i$ ” carries equivalent atoms  $A_1$  and  $A_2$  into one another. The displacement vector,  $\mathbf{v}_1$ , of  $A_1$  is carried into  $\mathbf{v}_2$  of  $A_2$ , where  $\mathbf{v}_1 = -\mathbf{v}_2$  as shown in Fig. 3.4.

The inversion operation will be a member of the covering group when a “center of inversion” or “center of symmetry” exists for the system being analyzed. However, in some cases the inversion operation may produce the same effect as a rotation or reflection, and as a result some groups do not explicitly contain the inversion-operation symbol. For example, in Chapter 1 we considered the group  $C_{4v}$  of the covering operations of a square. In that case the inversion operation (in two dimensions) was equivalent to a rotation by  $180^\circ$  about an axis perpendicular to the plane of the square and the inversion operation is not explicitly included in  $C_{4v}$ , but  $C_{4v} \times i$  would contain redundant operations.

The octahedral group,  $O$ , has 24 elements. When the inversion operation is included the extended group,  $O_h = O \times i$ , has 48 elements. The set of corresponding operators,  $P_{R_k}$  and  $P_{iR_k}$ , forms a group isomorphic to  $O_h$ .

If  $G$  is a group with elements  $R_k$  ( $k = 1, 2, \dots, h$ ), and none of the elements is equivalent to  $i$ , then a larger group can be formed, whose elements are  $R_k$  and

Table 3.4 *The character table for the inversion group*

IR	$E$	$i$
$\Gamma^g$	1	1
$\Gamma^u$	1	-1

Table 3.5 *The character table for  $O_h = O \times i$* 

	IR	$R$					$iR$					Basis functions
		$E$	$8C_3$	$3C_2$	$6C'_2$	$6C_4$	$i$	$8iC_3$	$3iC_2$	$6iC'_2$	$6iC_4$	
$\Gamma_g$	$A_{1g}$	1	1	1	1	1	1	1	1	1	1	$x^2 + y^2 + z^2$
	$A_{2g}$	1	1	1	-1	-1	1	1	1	-1	-1	
	$\mathcal{E}_g$	2	-1	2	0	0	2	-1	2	0	0	$(x^2 - y^2), (3z^2 - r^2)$
	$T_{1g}$	3	0	-1	-1	1	3	0	-1	-1	1	$(x, y, z); (R_x, R_y, R_z)$
	$T_{2g}$	3	0	-1	1	-1	3	0	-1	1	-1	$(xy, xz, yz)$
$\Gamma_u$	$A_{1u}$	1	1	1	1	1	-1	-1	-1	-1	-1	
	$A_{2u}$	1	1	1	-1	-1	-1	-1	-1	1	1	$xyz$
	$\mathcal{E}_u$	2	-1	2	0	0	-2	1	-2	0	0	
	$T_{1u}$	3	0	-1	-1	1	-3	0	1	1	-1	$(x, y, z)$
	$T_{2u}$	3	0	-1	1	-1	-3	0	1	-1	1	

$iR_k$  ( $k = 1, 2, \dots, h$ ). Clearly the larger group has twice as many elements as the original group. Inversion and the identity form a group by themselves that is denoted by the symbol  $i$  or  $S_2$ . The character table for the  $i$  group is given in Table 3.4.

It is common to write that  $G_h = G \times i$ , which means that  $G_h$  is the *direct product* of the groups  $G$  and  $i$ . A basis function of an IR of  $G_h$  is labeled “ $g$ ” or “ $u$ ” depending upon whether it is even or odd under the inversion operation. For  $g$ -functions,  $P_i f(\mathbf{r}) = f(\mathbf{r})$ ; for  $u$ -functions  $P_i f(\mathbf{r}) = -f(\mathbf{r})$ .

The character table for  $O_h = O \times i$  is easily obtained from the character tables of  $O$  and  $i$ . It is essentially the direct product of the character tables of  $G$  and  $i$ , as can be seen in Table 3.5.

The inversion operation that carries  $\mathbf{r}$  into  $-\mathbf{r}$  can be accomplished by a rotation by  $\pi$  about an axis through the origin, perpendicular to any plane containing  $\mathbf{r}$ . Therefore the character of  $i$  for the spherical harmonic representation is  $\sin[(l + 1/2)\pi]/\sin(\pi/2) = (-1)^l$ . As a result, the spherical harmonic functions for a given  $l$  are symmetric ( $g$ ) under inversion for even values of  $l$  and antisymmetric ( $u$ ) under inversion for odd values of  $l$ .

A useful theorem from group theory is that the character of the direct-product representation is the product of the characters,  $\chi(iR) = \chi(i)\chi(R)$ . (We shall prove a more general result a bit later in this chapter.) Therefore,

$$\chi^l(iR) = \chi^l(R) \quad \text{for } l \text{ even}, \quad (3.23)$$

$$\chi^l(iR) = -\chi^l(R) \quad \text{for } l \text{ odd}. \quad (3.24)$$

Equations (3.23) and (3.24) can be used to assign “g” or “u” labels to the decomposition of  $D^{(l)}$  into the IRs of  $O_h$ . A few results are

$$s\text{-orbitals} \quad D^{(0)} = A_{1g}, \quad (3.25)$$

$$p\text{-orbitals} \quad D^{(1)} = T_{1u}, \quad (3.26)$$

$$d\text{-orbitals} \quad D^{(2)} = T_{2g} + \mathcal{E}_g, \quad (3.27)$$

$$f\text{-orbitals} \quad D^{(3)} = A_{2u} + T_{1u} + T_{2u}. \quad (3.28)$$

From (3.26) and (3.27) we see that at a site of octahedral symmetry the  $p$ -orbitals remain three-fold degenerate, but the  $d$ -orbitals split into two-fold degenerate  $\mathcal{E}_g$  states and three-fold degenerate  $T_{2g}$  states. This information is available in the character table for the  $O_h$  group (Table 3.5), which shows that  $d_{xy}$ ,  $d_{xz}$ , and  $d_{yz}$  are the basis functions for the different rows of the  $T_{2g}$  IR and that  $d_{z^2}$  and  $d_{x^2}$  are basis functions for the different rows of the  $\mathcal{E}_g$  IR.

No IR appears more than once in the decomposition of  $D^{(2)}$ , therefore the symmetry functions for the  $T_{2g}$  or those for the  $\mathcal{E}_g$  IRs are *eigenstates* of the original  $O(3)$ -**Hamiltonian** plus any potential having octahedral symmetry. We know they are eigenstates because there can be no non-zero matrix elements of the Hamiltonian (including octahedrally symmetric terms) between bases for different IRs or between bases belonging to different rows of the same IR.

The above conclusions are valid only if the octahedral environment is represented by a potential. For a molecule or solid, the octahedral environment is due to the surrounding ligands. If the orbitals of the ligands that create the octahedral environment are included in the analysis there usually will be combinations of the ligand orbitals that belong to the  $T_{2g}$  (and  $\mathcal{E}_g$ ) IRs. If so, these combinations will be mixed with the  $d$ -orbitals to form the eigenstates. In either case the  $T_{2g}$  and  $\mathcal{E}_g$  states are not mixed so long as the symmetry of the system is spherical,  $O$  or  $O_h$ .

### 3.6 General properties of direct-product groups and representations

In general we can have the direct product of two groups if the operations of one commute with the operations of the other and they have no elements in common other than the identity. If the operators corresponding to the two groups operate on

$$\begin{pmatrix} A_{11} & A_{12} \\ A_{21} & A_{22} \end{pmatrix} \times \begin{pmatrix} B_{11} & B_{12} & B_{13} \\ B_{21} & B_{22} & B_{23} \\ B_{31} & B_{32} & B_{33} \end{pmatrix} = \left( \begin{array}{c|ccc} A_{11}B & A_{12}B & & \\ \hline A_{21}B & A_{22}B & & \end{array} \right)$$

$$= \left( \begin{array}{ccc|ccc} A_{11}B_{11} & A_{11}B_{12} & A_{11}B_{13} & A_{12}B_{11} & A_{12}B_{12} & A_{12}B_{13} \\ A_{11}B_{21} & A_{11}B_{22} & A_{11}B_{23} & A_{12}B_{21} & A_{12}B_{22} & A_{12}B_{23} \\ A_{11}B_{31} & A_{11}B_{32} & A_{11}B_{33} & A_{12}B_{31} & A_{12}B_{32} & A_{12}B_{33} \\ \hline A_{21}B_{11} & A_{21}B_{12} & A_{21}B_{13} & A_{22}B_{11} & A_{22}B_{12} & A_{22}B_{13} \\ A_{21}B_{21} & A_{21}B_{22} & A_{21}B_{23} & A_{22}B_{21} & A_{22}B_{22} & A_{22}B_{23} \\ A_{21}B_{31} & A_{21}B_{32} & A_{21}B_{33} & A_{22}B_{31} & A_{22}B_{32} & A_{22}B_{33} \end{array} \right)$$

Figure 3.5 The direct product of two matrices:  $[A \times B]_{ss',tt'} = A_{st} B_{s't'}$ .

different kinds of coordinates, they do not have common operators even if the two groups are the same.

Consider the direct-product group  $G_a \times G_b$  with elements  $A_i B_j$  and corresponding operators  $P_{A_i} P_{B_j} = P_{A_i B_j}$ . If  $\Gamma^a$  is a matrix representation of the operators of  $G_a$  and  $\Gamma^b$  is a matrix representation of the operators of  $G_b$ , then  $\Gamma^a \times \Gamma^b$  is a matrix representation of the operators of the direct-product group  $G_a \times G_b$ . This statement is a brief way of saying that

$$\Gamma^{(a \times b)}(A_i B_j) = \Gamma^a(A_i) \times \Gamma^b(B_j), \quad (3.29)$$

for all of the operators of  $G_a \times G_b$ . The matrix elements are defined as follows:

$$[\Gamma^{(a \times b)}(A_i B_j)]_{ss',tt'} = [\Gamma^a(A_i)]_{st} [\Gamma^b(B_j)]_{s't'}. \quad (3.30)$$

The direct product of two matrices is illustrated in Fig. 3.5.

Direct-product matrix multiplication is also similar to regular matrix multiplication, but the sum on the index is now a sum on a pair of indices:

$$\begin{aligned}
& [\Gamma^{(a \times b)}(A_i B_j) \Gamma^{(a \times b)}(A_{i'} B_{j'})]_{nn',mm'} \\
&= \sum_k \sum_{k'} [\Gamma^a(A_i)]_{nk} [\Gamma^b(B_j)]_{n'k'} [\Gamma^a(A_{i'})]_{km} [\Gamma^b(B_{j'})]_{k'm'} \\
&= \left\{ \sum_k [\Gamma^a(A_i)]_{nk} [\Gamma^a(A_{i'})]_{km} \right\} \left\{ \sum_{k'} [\Gamma^b(B_j)]_{n'k'} [\Gamma^b(B_{j'})]_{k'm'} \right\} \\
&= [\Gamma^a(A_i A_{i'})]_{nm} [\Gamma^b(B_j B_{j'})]_{n'm'} = [\Gamma^{(a \times b)}(A_i A_{i'})(B_j B_{j'})]_{nn',mm'}. \quad (3.31)
\end{aligned}$$

The diagonal elements of  $[\Gamma(A_i B_j)]_{nn',mm'}$  are obtained when  $m = n$  and  $m' = n'$ ,

$$[\Gamma^{(a \times b)}(A_i B_j)]_{nn',nn'} = [\Gamma^a(A_i)]_{nn} [\Gamma^b(B_j)]_{n'n'}. \quad (3.32)$$

The character of  $\Gamma^{(a \times b)}(A_i B_j)$ , a quantity denoted by  $\chi^{(a \times b)}(A_i B_j)$ , is the sum of the diagonal elements,

$$\begin{aligned}\chi^{(a \times b)}(A_i B_j) &= \sum_n \sum_{n'} [\Gamma^{(a \times b)}(A_i B_j)]_{nn', nn'} \\ &= \sum_n [\Gamma^a(A_i)]_{nn} \sum_{n'} [\Gamma^b(B_j)]_{n'n'} \\ &= \chi^{\Gamma^a}(A_i) \chi^{\Gamma^b}(B_j).\end{aligned}\tag{3.33}$$

Equation (3.33) shows that the character of the matrix representation of  $P_{A_i B_j}$  for the direct-product group  $G_a \times G_b$  is the product of the characters of the matrix representation of  $P_{A_i}$  and the matrix representation of  $P_{B_j}$ . Thus we can find the characters of the direct-product representations from the characters of the individual representations. Some important properties of direct products are summarized in Theorem 3.2.

**Theorem 3.2** (Properties of direct-product representations)

*Notation and definitions*

$$G^{(a \times b)} = G_a \times G_b.$$

- The elements of  $G_a$  are  $A_i$  and the corresponding operators are  $P_{A_i}$ .
- The elements of  $G_b$  are  $B_j$  and the corresponding operators are  $P_{B_j}$ .
- The elements of  $G_a \times G_b$  are  $A_i B_j$  and the corresponding operators are  $P_{A_i} P_{B_j} = P_{A_i B_j}$ .
- $\Gamma^a(A_i)$  is a matrix representation of  $P_{A_i}$  and  $\Gamma^b(B_j)$  is a matrix representation of  $P_{B_j}$ .
- $\Gamma^{(a \times b)}(A_i B_j)$  is a matrix representation of the direct-product operator  $P_{A_i B_j}$ .
- $\chi^{(a \times b)}(A_i B_j)$  is the character of the matrix representing  $P_{A_i B_j}$ .
- $\chi^{\Gamma^a}(A_i)$  is the character of the matrix representing  $P_{A_i}$  and  $\chi^{\Gamma^b}(B_j)$  is the character of the matrix representing  $P_{B_j}$ .

*Theorem 3.2a.*  $\Gamma^{(a \times b)} = \Gamma^a \times \Gamma^b$ . This means that  $\Gamma^{(a \times b)}(A_i^a B_j^b) = \Gamma^a(A_i^a) \times \Gamma^b(B_j^b)$  for all  $A_i^a$  and  $B_j^b$ . The direct product of two representations is a representation of the direct-product group.

*Theorem 3.2b.* The direct product of two IRs is an IR of the direct-product group. That is, if  $\Gamma^a$  is an IR of  $G_a$  and  $\Gamma^b$  an IR of  $G_b$ , then  $\Gamma^a \times \Gamma^b$  is an IR of  $G_a \times G_b$ .

*Theorem 3.2c.* The number of classes in  $G_a \times G_b$  is the product of the number of classes in  $G_a$  times the number of classes in  $G_b$ .

*Theorem 3.2d.* The character of a direct-product matrix representation is the product of the characters of the two representations:  $\chi^{(a \times b)}(A_i B_j) = \chi^{\Gamma^a}(A_i) \chi^{\Gamma^b}(B_j)$ .

**Theorem 3.2e.** *If  $C_1$  is a class of  $G_1$  and  $C_2$  is a class of  $G_2$ , then  $C_1 \times C_2$  is a class of  $G_1 \times G_2$ .*

### 3.6.1 Direct products of groups whose operators operate on different types of coordinates

Let  $\xi_1, \xi_2, \dots, \xi_N$  be basis functions for a representation  $\Gamma^a$  of  $G_a$  whose elements are  $A_i$ , and let  $\zeta_1, \zeta_2, \dots, \zeta_M$  be basis functions for a representation  $\Gamma^b$  of  $G_b$  whose elements are  $B_j$ . The operators  $P_{A_i}$  operate only on the  $\xi$ -functions and the operators  $P_{B_j}$  operate only on the  $\zeta$ -functions. The  $NM$  functions,  $\xi_s \zeta_{s'}$  ( $s = 1, 2, \dots, N$ ;  $s' = 1, 2, \dots, M$ ), are basis functions for a representation of the direct-product group,  $\Gamma^{(a \times b)}$ . Consider

$$\begin{aligned} P_{A_i B_j} \xi_t \zeta_{t'} &= (P_{A_i} \xi_t)(P_{B_j} \zeta_{t'}) = \sum_s \sum_{s'} \Gamma(A_i)_{st} \Gamma(B_j)_{s't'} (\xi_s \zeta_{s'}) \\ &= \sum_s \sum_{s'} \Gamma^{(a \times b)}(A_i B_j)_{ss', tt'} (\xi_s \zeta_{s'}). \end{aligned} \quad (3.34)$$

For the last equality in (3.34) we used the definition of the matrix element  $\Gamma_{ss', tt'}^{(a \times b)}$  in (3.30). Note the order of the indices in (3.34). The rows are  $s$  and  $s'$  and the columns are  $t$  and  $t'$ .

Equations (3.30) and (3.34) show that  $\Gamma^{(a \times b)}$  is a matrix representation of  $G_a \times G_b$  with basis functions  $\xi_s \zeta_{s'}$ .

There is an aspect of the direct product that should be noted. Theorem 3.2b tells us that if  $\Gamma^a$  and  $\Gamma^b$  are IRs of  $G_a$  and  $G_b$ , respectively, then  $\Gamma^a \times \Gamma^b = \Gamma^{(a \times b)}$  is an IR of  $G_a \times G_b$ . However,  $\Gamma^{(a \times b)}$  is also a representation of  $G_a$  (or  $G_b$ ), but it is a *reducible* representation with respect to  $G_a$  (or  $G_b$ ).

### 3.6.2 Direct products of representations of the same group

A common use of the direct product of representations of the same group is in the analysis of multi-electron problems and selection rules for transitions between two states of a system. For example, for a two-electron system the wavefunction may be composed of products of one-electron functions,  $\varphi_\lambda(\mathbf{r}_1) \varphi_\nu(\mathbf{r}_2)$ , where  $\lambda$  and  $\nu$  represent the quantum numbers. The group of the Hamiltonian for the system is  $G^H$  and its operators  $P_R^H$  operate on the coordinates of  $\varphi_\lambda(\mathbf{r}_1) \varphi_\nu(\mathbf{r}_2)$ . Explicitly,  $P_R^H \varphi_\lambda(\mathbf{r}_1) \varphi_\nu(\mathbf{r}_2) = \varphi_\lambda(R^{-1}\mathbf{r}_1) \varphi_\nu(R^{-1}\mathbf{r}_2)$ . If  $\varphi_\lambda(\mathbf{r}_1)$  is a basis function for the representation  $\Gamma^1$  of  $G^H$  and  $\varphi_\nu(\mathbf{r}_2)$  is a basis function for the representation  $\Gamma^2$  of  $G^H$ , then the product,  $\varphi_\lambda(\mathbf{r}_1) \varphi_\nu(\mathbf{r}_2)$ , is a basis function for the direct product of these representations,  $\Gamma^1 \times \Gamma^2$ . The two matrix representations  $\Gamma^1$  and  $\Gamma^2$  are



representations of the *same* group,  $G^H$ .  $\Gamma^1 \times \Gamma^2$  is usually a reducible representation even if  $\Gamma^1$  and  $\Gamma^2$  are both IRs of  $G^H$ . For example, if  $G^H$  is the octahedral group,  $O$ ,  $\Gamma^1 = T_1$  and  $\Gamma^2 = T_2$ , then  $T_1 \times T_2$  decomposes into the following IRs of  $O$ :  $A_2 + \mathcal{E} + T_1 + T_2$ . What does this decomposition mean with regard to the function  $\varphi_\lambda(\mathbf{r}_1) \varphi_\nu(\mathbf{r}_2)$ ? It means we can be certain that no part of  $\varphi_\lambda(\mathbf{r}_1) \varphi_\nu(\mathbf{r}_2)$  transforms according to any IR **not** contained in the decomposition. Applying the symmetry-function-generating machine to  $\varphi_\lambda(\mathbf{r}_1) \varphi_\nu(\mathbf{r}_2)$  will generate linear combinations of products that transform according to the IRs in the decomposition or produce a null function.

It is important to distinguish between the direct-product representation  $\Gamma^{(\alpha \times \beta)} = \Gamma^\alpha(G) \times \Gamma^\beta(G)$  of the same group,  $G$ , and a representation  $\Gamma^{(G_a \times G_b)}$  of two groups,  $G_a$  and  $G_b$ , whose operators are distinct (except for the identity) and commute with each other. If  $\varphi^\alpha(\mathbf{r}_1)$  is a basis function for the  $\alpha$ th IR of  $G_a$  and  $\varphi^\beta(\mathbf{r}_2)$  is a basis function for the  $\beta$ th IR of  $G_b$ , then  $\varphi_\alpha(\mathbf{r}_1) \varphi_\beta(\mathbf{r}_2)$  is a basis function for an IR of  $G_a \times G_b$ . On the other hand, if both  $\varphi^\alpha(\mathbf{r}_1)$  and  $\varphi^\beta(\mathbf{r}_2)$  are basis functions for IRs of the same group  $G$ , then  $\varphi_\alpha(\mathbf{r}_1) \varphi_\beta(\mathbf{r}_2)$  is usually not a basis function for an IR of  $G$ . That is,  $\Gamma^{(\alpha \times \beta)}$  is usually a reducible representation. (Note that the elements of  $G \times G$  do not form a group.)

### 3.7 Selection rules for matrix elements

As we have discussed previously in connection with the optical transitions, the question of whether a transition is forbidden by symmetry depends on a matrix element of the type

$$\langle f_k^\alpha(\xi) | f_{\text{op}}(\xi) | f_j^\beta(\xi) \rangle = \int f_k^\alpha(\xi)^* f_{\text{op}}(\xi) f_j^\beta(\xi) d\xi, \quad (3.35)$$

where  $f_k^\alpha(\xi)$  is the initial state and  $f_j^\beta(\xi)$  is the final state. In (3.35)  $f_k^\alpha(\xi)$  and  $f_j^\beta(\xi)$  are eigenstates of a Hamiltonian or Hermitian operator whose covering group is  $G$ . Here  $f_k^\alpha$  belongs to the  $k$ th row of the  $\alpha$ th IR and  $f_j^\beta$  belongs to the  $j$ th row of the  $\beta$ th IR of  $G$ . The operator  $f_{\text{op}}(\xi)$  could be, for example, the electric dipole of a molecule or the Raman tensor. In the most general case,  $f_{\text{op}}$  could be any function of  $\xi$ . If the matrix element vanishes due to symmetry considerations, the transition from the initial to the final state is said to be symmetry-forbidden or just forbidden.

Let us begin with a simple case for which  $f_{\text{op}}(\xi) = f_i^\gamma$  is a basis function for the  $i$ th row of the  $\gamma$ th IR of  $G$ . For convenience let us arbitrarily group the functions together in the following way:

$$\langle f_k^\alpha(\xi) | F(\xi) \rangle, \quad (3.36)$$

where

$$F(\xi) = [f_i^\gamma(\xi) f_j^\beta(\xi)]. \quad (3.37)$$

From (1.21) we know that the matrix element will vanish unless  $F(\xi)$  belongs to the same row of the same IR as  $f_k^\alpha(\xi)$ , that is, the  $k$ th row of the  $\alpha$ th IR.

The function  $F(\xi) = f_i^\gamma(\xi) f_j^\beta(\xi)$  is a basis function for the direct-product representation  $\Gamma^\gamma \times \Gamma^\beta$ . We can determine whether the function has the **possibility** of belonging to the  $\alpha$ th IR of  $G$  by decomposing  $\Gamma^\gamma \times \Gamma^\beta$  into the IRs of  $G$ . If the decomposition does **not** contain  $\Gamma^\alpha$  then we can definitely say that the matrix element vanishes due to symmetry considerations. If the decomposition does contain  $\Gamma^\alpha$  we can **not** conclude that the matrix element is symmetry-allowed. To say that the matrix element is symmetry-allowed requires that  $F(\xi)$  not only contains  $\Gamma^\alpha$  but also contains a part that transforms as the  $k$ th row of  $\Gamma^\alpha$ . How can we determine whether  $F(\xi)$  belongs to the  $k$ th row of the  $\alpha$ th IR? One method is to apply the symmetry-function-generating machine to  $F(\xi)$ . In this case we need to consider

$$\sum_{R_i} \Gamma^\alpha(R_i)_{kk}^* \{P_{R_i} F(\xi)\}, \quad (3.38)$$

where the sum over  $R_i$  is over all of the elements of the group  $G$ .

If the result of (3.38) is not zero, then the matrix element is not required by symmetry to vanish. If the result is zero, the matrix element is required by symmetry to vanish.

Care must be taken when employing symmetry arguments to matrix elements. Selection rules are usually only in terms of the IRs with no consideration for the row requirement. On the other hand, *the negative statement is always valid*. That is, if  $\Gamma^\gamma \times \Gamma^\beta$  does not contain  $\Gamma^\alpha$  the matrix element certainly vanishes. Another way to express the selection rule is that a non-vanishing matrix element requires that

$$\Gamma^\alpha \times \Gamma^\beta \times \Gamma^\gamma \text{ must contain the totally symmetric IR of } G. \quad (3.39)$$

In the case of the  $O_h$  group the totally symmetric IR is  $A_{1g}$ .

A simple example serves to illustrate the problem. Consider the case where  $f_k^\alpha = x$ ,  $f_j^\beta = z$ , and  $f_i^\gamma = y$ . These functions are all basis functions for the  $T_1$  IR of the  $O$  group. The product  $f_i^\gamma f_k^\beta$  is a basis function for the direct-product representation,  $T_1 \times T_1 = A_1 + \mathcal{E} + T_1 + T_2$ . Since  $T_1 \times T_1$  contains  $T_1$  and  $f_k^\alpha$  belongs to  $T_1$  we would conclude that the matrix element does not vanish because of symmetry if we considered only the direct-product decomposition. By contrast, if the symmetry-function-generating machine is applied to  $f_i^\gamma f_k^\beta$  in an attempt to generate a  $k$ th-row  $T_1$ -function we would obtain zero. It is easy to see why. The product  $f_i^\gamma f_k^\beta = yz$  is the basis function for one of the rows of  $T_2$  and therefore

it provides no basis for the  $T_1$  representation of  $G$ . Thus in this example the matrix element must be zero due to symmetry considerations despite the fact that it passes the IR selection-rule test.

### 3.8 General representations of the full rotation group

Representations of the full rotation group based on the spherical harmonic functions provide the IRs for the full rotation group for integral values of the angular momentum, i.e., for  $l = 0, 1, 2, 3, \dots$ . Quantum systems with spin have total angular momentum  $j = l + s$  that can take on half-integral values. In general,  $j$  can take on the values  $\frac{1}{2}, 1, \frac{3}{2}, 2, \frac{5}{2}, \dots$ . Therefore it is essential to have the IRs of both integral and half-integral angular momenta. The matrix representations for both integral and half-integral angular momenta are based on the work of Hermann Weyl. He developed the theory of continuous groups based on matrix representations during the period from 1923 to 1938. His method for finding the IRs of the rotation group is based on establishing a homomorphism between  $2 \times 2$  unitary matrices and the  $3 \times 3$  matrices representing three-dimensional rotations. We will not delve into the details of the theory, but will simply state the results. More details may be found elsewhere [3.1, 3.2].

**Theorem 3.3** *The IR matrices of the rotation group for a given integral or half-integral value of  $j$  are*

$$D^{(j)}(\alpha, \beta, \gamma)_{m', m} = e^{-im'\alpha} e^{-im\gamma} \times \sum_{\kappa} \frac{(-1)^{\kappa} \sqrt{(j+m)!(j-m)!(j+m')!(j-m')!}}{\kappa!(j+m-\kappa)!(j-m'-\kappa)!(\kappa+m'-m)!} \times \left( \cos\left(\frac{\beta}{2}\right) \right)^{2j-2\kappa-m'+m} \left( -\sin\left(\frac{\beta}{2}\right) \right)^{2\kappa+m'-m}.$$

$D^{(j)}(\alpha, \beta, \gamma)_{m', m}$  is a matrix element of the  $m'$ th row and  $m$ th column of the  $j$ th IR for a rotation characterized by the Euler angles  $\alpha$ ,  $\beta$ , and  $\gamma$ . In Theorem 3.3 the sum on the index  $\kappa$  includes only the integral values of  $\kappa$  that lie between (a) the larger of zero or  $m - m'$  and (b) the smaller of  $j - m'$  and  $j + m$ . The resulting representation matrices for  $j = 0, \frac{1}{2}, 1, \frac{3}{2}$ , and 2 are given in Table 3.6. These matrices rotate the basis functions of the IRs in clockwise manner through the Euler angles  $-\alpha$ ,  $-\beta$ , and  $-\gamma$ . For integral values of  $j$  the basis functions are the spherical harmonics discussed previously in this chapter. For the half-integral values of  $j$  the basis functions are linear combinations of spin or spinor functions.

In Section 3.3 we showed that all rotations through the same angle about any axis belong to the same class and therefore have the same character. We consider

a rotation about the  $z$ -axis so that  $\beta = \gamma = 0$ . For diagonal elements ( $m = m'$ ) all of the terms of Theorem 3.3 vanish except the term for which  $\kappa = 0$ . For that term,  $(-\sin(\beta/2))^{2\kappa+m'-m} = (-\sin(\beta/2))^{2\kappa} = (-\sin(\beta/2))^0 = 1$  and the factorial coefficient is also 1. Therefore we have

$$D^{(j)}(\alpha, 0, 0)_{mm} = e^{-im\alpha}, \quad (3.40)$$

where  $m$  takes on values from  $j$  to  $-j$  in unit steps. The trace or character is then

$$\chi^{(j)}(\alpha) = \sum_{m=-j}^j D^{(j)}(\alpha, 0, 0)_{mm} = \frac{\sin[(j+1/2)\alpha]}{\sin(\alpha/2)}. \quad (3.41)$$

Equation (3.41) holds for integer or half-integer  $j$  (it differs from (3.23) only in that  $l$  is replaced by  $j$ ). Since (3.41) applies to all rotations through an angle  $\alpha$  about any axis, in general we have

$$\chi^{(j)}(A) = \frac{\sin[(j+1/2)A]}{\sin(A/2)}, \quad (3.42)$$

where  $A$  is the angle of rotation in radians about any axis.

This result, (3.42), is not immediately obvious from the matrices given in Table 3.6. The reason why it is not apparent is that the angle,  $A$ , is about an axis that will produce the same rotation as the three Euler rotations. To determine  $A$  from  $\alpha$ ,  $\beta$ , and  $\gamma$  is a problem in spherical trigonometry that we shall not pursue here. However, the plausibility of (3.42) is evident from a few special cases. Consider the character of  $D^{(1/2)}(\alpha, \beta, \gamma)$ . From Table 3.6 we have

$$\begin{aligned} \chi^{(1/2)}(\alpha, \beta, \gamma) &= e^{-i(\alpha+\gamma)/2} \cos(\beta/2) + e^{i(\alpha+\gamma)/2} \cos(\beta/2) \\ &= 2 \cos[(\alpha + \gamma)/2] \cos(\beta/2). \end{aligned} \quad (3.43)$$

If  $\beta = 0$  then

$$\chi^{(1/2)}(\alpha, 0, \gamma) = 2 \cos[(\alpha + \gamma)/2] = \frac{\sin(\alpha + \gamma)}{\sin[(\alpha + \gamma)/2]}. \quad (3.44)$$

In this case the two rotations are about the  $z$ -axis so that  $A = \alpha + \gamma$ . Equation (3.44) agrees with Eq. (3.41) when  $A$  is replaced by  $\alpha + \gamma$ . If  $\alpha = \gamma = 0$ , then

$$\chi^{(1/2)}(0, \beta, 0) = 2 \cos(\beta/2) = \frac{\sin(\beta)}{\sin(\beta/2)}, \quad (3.45)$$

which agrees with (3.42) for  $A = \beta$ .

The matrices for half-integral  $j$  ( $j = n + 1/2, n = 0, 1, 2, \dots$ ) are double-valued in that  $D^{(n+1/2)}(R + 2\pi) = -D^{(n+1/2)}(R)$ , but  $D^{(n+1/2)}(R + 4\pi) = +D^{(n+1/2)}(R)$ , where  $R$  is any rotation. These matrices represent rotations of spinor objects such as the spin of an electron or neutron or any total half-integer momentum vector  $j$ , for which a rotation by  $4\pi$  is required in order to return the object to its original state.

Table 3.6 *IRs of the full rotation group. Note that the integral representations can be expressed in terms of the angle  $\beta$ , while the half-integral representations are dependent on the angle  $\beta/2$  and hence are double-valued.*

$\bullet D^{(0)} = 1$   
 $\bullet D^{(1/2)}(\alpha, \beta, \gamma)_{m'm} = e^{-im'\alpha} e^{-im\gamma} M^{(1/2)}(\beta)_{m'm}$

$m = \frac{1}{2}$	$m = -\frac{1}{2}$	$m'$
$C$	$-S$	$\frac{1}{2}$
$S$	$C$	$-\frac{1}{2}$

with  $C = \cos(\beta/2)$ ,  $S = \sin(\beta/2)$

$\bullet D^{(1)}(\alpha, \beta, \gamma)_{m'm} = e^{-im'\alpha} e^{-im\gamma} M^{(1)}(\beta)_{m'm}$

$m = 1$	$m = 0$	$m = -1$	$m'$
$\frac{1}{2}(1+C)$	$-(1/\sqrt{2})S$	$\frac{1}{2}(1-C)$	1
$(1/\sqrt{2})S$	$C$	$-(1/\sqrt{2})S$	0
$\frac{1}{2}(1-C)$	$(1/\sqrt{2})S$	$\frac{1}{2}(1+C)$	-1

with  $C = \cos \beta$ ,  $S = \sin \beta$

$\bullet D^{(3/2)}(\alpha, \beta, \gamma)_{m'm} = e^{-im'\alpha} e^{-im\gamma} M^{(3/2)}(\beta)_{m'm}$

$m = \frac{3}{2}$	$m = \frac{1}{2}$	$m = -\frac{1}{2}$	$m = -\frac{3}{2}$	$m'$
$C^3$	$-\sqrt{3}C^2S$	$\sqrt{3}CS^2$	$-S^3$	$\frac{3}{2}$
$\sqrt{3}C^2S$	$(C^3 - 2CS^2)$	$(S^3 - 2C^2S)$	$\sqrt{3}CS^2$	$\frac{1}{2}$
$\sqrt{3}CS^2$	$-(S^3 - 2C^2S)$	$(C^3 - 2CS^2)$	$-\sqrt{3}C^2S$	$-\frac{1}{2}$
$S^3$	$\sqrt{3}CS^2$	$\sqrt{3}C^2S$	$C^3$	$-\frac{3}{2}$

with  $C = \cos(\beta/2)$ ,  $S = \sin(\beta/2)$

$\bullet D^{(2)}(\alpha, \beta, \gamma)_{m'm} = e^{-im'\alpha} e^{-im\gamma} M^{(2)}(\beta)_{m'm}$

$M^{(2)}(\beta)_{m'm} =$

$m = 2$	$m = 1$	$m = 0$	$m = -1$	$m = -2$	$m'$
$\frac{1}{4}(1+C)^2$	$-\frac{1}{2}(1+C)S$	$\frac{1}{2}\sqrt{\frac{3}{2}}S^2$	$-\frac{1}{2}(1-C)S$	$\frac{1}{4}(1-C)^2$	2
$\frac{1}{2}(1+C)S$	$\frac{1}{4}[(1+C)^2 - 3S^2]$	$-\sqrt{\frac{3}{2}}CS$	$-\frac{1}{4}[(1-C)^2 - 3S^2]$	$-\frac{1}{2}(1-C)S$	1
$\frac{1}{2}\sqrt{\frac{3}{2}}S^2$	$\sqrt{\frac{3}{2}}CS$	$\frac{1}{2}(3C^2 - 1)$	$-\sqrt{\frac{3}{2}}CS$	$\frac{1}{2}\sqrt{\frac{3}{2}}S^2$	0
$\frac{1}{2}(1-C)S$	$-\frac{1}{4}[(1-C)^2 - 3S^2]$	$\sqrt{\frac{3}{2}}CS$	$\frac{1}{4}[(1+C)^2 - 3S^2]$	$-\frac{1}{2}(1+C)S$	-1
$\frac{1}{4}(1-C)^2$	$\frac{1}{2}(1-C)S$	$\frac{1}{2}\sqrt{\frac{3}{2}}S^2$	$\frac{1}{2}(1+C)S$	$\frac{1}{4}(1+C)^2$	-2

with  $C = \cos \beta$ ,  $S = \sin \beta$

The  $D^{(l)}(\alpha, \beta, \gamma)$  matrices assume the phase convention  $Y_l^{|m|} = (-1)^m Y_l^{-|m|}$  used in Table 3.1.  $D^{(l)}(\alpha, \beta, \gamma)$  acting on  $Y_l^m$  produces a clockwise (positive) rotation of the function in a fixed coordinate system.

### References

- [3.1] E.P. Wigner, *Group Theory and its Application to the Quantum Mechanics of Atomic Spectra* (New York: Academic Press, 1959).  
 [3.2] M. Tinkham, *Group Theory and Quantum Mechanics* (New York: McGraw-Hill, 1969).

### Exercises

- 3.1 Express the functions listed below in terms of  $d_{x^2}$  and  $d_{z^2}$  orbitals defined in Table 3.2:  
 (a)  $(3x^2 - r^2)/r^2$ ,  
 (b)  $(2y^2 - x^2 - z^2)/r^2$ ,  
 (c)  $(z^2 - y^2)/r^2$ .  
 3.2 (a) Use Table 3.1 to show for the  $l = 1$  spherical harmonics that

$$\begin{aligned}
 Y_1^0 &= \sqrt{\frac{3}{4\pi}} \frac{z}{r}, \\
 Y_1^1 &= -\sqrt{\frac{3}{8\pi}} \frac{x + iy}{r}, \\
 Y_1^{-1} &= \sqrt{\frac{3}{8\pi}} \frac{x - iy}{r}, \\
 \sqrt{\frac{3}{4\pi}} \frac{x}{r} &= -\frac{1}{\sqrt{2}} (Y_1^1 - Y_1^{-1}), \\
 \sqrt{\frac{3}{4\pi}} \frac{y}{r} &= \frac{i}{\sqrt{2}} (Y_1^1 + Y_1^{-1}), \\
 \sqrt{\frac{3}{4\pi}} \frac{z}{r} &= Y_1^0.
 \end{aligned}$$

- (b) Find the matrix elements of  $120^\circ$  rotation about an axis along the  $(1, 1, 1)$  direction for a representation based on the  $l = 1$  spherical harmonics.  
 3.3 Show that the real part of  $Y_2^2$  is a basis function for the  $\mathcal{E}_g$  and that the imaginary part is a basis function for the  $T_{2g}$  for the  $O_h$  group.  
 3.4 Every group has a totally symmetric IR wherein every element is represented by unity. The totally symmetric IR is usually named  $\Gamma^{A_1}$  or simply  $A_1$ . Assume the characters are real and show that  $\Gamma^\alpha \times \Gamma^\beta$  contains the  $A_1$  representation if and only if  $\alpha = \beta$ .  
 3.5 Show that the requirement that  $\Gamma^\alpha \times \Gamma^\beta$  contain  $\Gamma^\delta$  is equivalent to the requirement that  $\Gamma^\alpha \times \Gamma^\beta \times \Gamma^\delta$  contains the  $A_1$  representation for groups for which the characters are real.

- 3.6 Determine the degeneracies for  $l = 0, 1$ , and  $2$  of the spherical harmonic functions,  $Y_l^m$ , in an environment whose symmetry is  $D_4$ . The character table for  $D_4$  is given below.

$D_4$	$E$	$C_2 = C_4^2$	$2C_4$	$2C_2'$	$2C_2''$	Basis functions
$A_1$	1	1	1	1	1	$x^2 + y^2, z^2$
$A_2$	1	1	1	-1	-1	$R_z, z$
$B_1$	1	1	-1	1	-1	$x^2 - y^2$
$B_2$	1	1	-1	-1	1	$xy$
$\mathcal{E}$	2	-2	0	0	0	$(xz, yz)$ $\left\{ \begin{array}{l} (x, y) \\ (R_x, R_y) \end{array} \right.$

- 3.7 Decompose the direct product of  $D^{(2)} \times D^{(1)}$  into the IRs of  $D_4$ .
- 3.8 To what representation of  $O_h$  does the operator  $\nabla^2 = \partial^2/\partial x^2 + \partial^2/\partial y^2 + \partial^2/\partial z^2$  belong?
- 3.9 (a) Use the symmetry-function-generating machine to find the three partner functions of the  $T_1(O)$  representation starting with the function  $(x^3 + y^3 + z^3)$ . The matrix elements of the  $T_1$  IR are given in Appendix E.  
 (b) To which IR of  $O_h$  do the partner functions belong?
- 3.10 (a) The electric-dipole operator is a *polar* vector  $e \mathbf{R} = e(X, Y, Z)$  in Cartesian coordinates. Find the matrix that rotates  $\mathbf{R}$  by an angle  $\alpha$  about the  $z$ -axis.  
 (b) Find the matrix that rotates  $\mathbf{R}$  by an angle  $\alpha$  about the  $z$ -axis and subjects the vector to the inversion operation.  
 (c) What is the trace (character) of the combined rotation–inversion matrix?  
 (d) To what IR of  $O_h$  does  $R$  belong?
- 3.11 The magnetic-dipole operator is an axial vector  $\mu \propto \mathbf{R} \times d\mathbf{R}/dt$  (vector cross product) Since  $\mu$  is a vector (a pseudo-vector) the rotation matrix of Exercise 3.10 applies.  
 (a) What is the combined rotation–inversion matrix for  $\mu$ ?  
 (b) What is the character of the matrix?  
 (c) To what IR of  $O_h$  does  $\mu$  belong?

## 4

# Crystal-field theory

### 4.1 Splitting of $d$ -orbital degeneracy by a crystal field

As we saw in the previous chapter the  $s$ - and  $p$ -orbital degeneracies are unaffected when an atom or ion is placed in a site of octahedral symmetry. On the other hand, the  $d$ - and  $f$ -orbital degeneracies are changed. Transition metal ions of Ti, Fe, Ni, and Co, for example, have  $3d$  electrons in their outer unfilled shells and exist as positively charged ions in solids and molecular complexes. Most frequently, the transition metal ion is coordinated with six neighboring ligands at a site of octahedral symmetry. The second most common situation is tetrahedral coordination with four neighboring ligands. Many of these transition metal solids and molecular complexes are colored and many are magnetic. The colors are attributed to vibronic (electronic plus vibration) transitions between the  $d$ -orbital groups that are split in energy by the non-spherical potential of the ligands. When the ligand orbitals are included in determining the splitting, the procedure is called ligand-field theory. Splitting due to adjacent ligands is discussed in Chapter 6.

Crystal-field theory was developed by Bethe [4.1] and Van Vleck [4.2] to explain the optical spectra of transition metal complexes and to understand their magnetic properties. In its simplest form the crystal-field model represents the ligands surrounding a metal ion as point charges that interact with the transition metal ion only through an electrostatic potential. This is, of course, a very crude approximation, since the orbitals of the ligands usually form electronic bonds with the metal ion's  $d$ -electrons. However, the type of splitting that occurs depends only on the symmetry of the environment. Therefore, crystal-field theory can be applied as a semi-empirical model with the strength of the interaction taken as an adjustable parameter to be determined by experiment.



### 4.1.1 Splitting of the $d^1$ configuration

As an example, consider a metal ion with a single electron in its  $d$ -electron shell in a site of octahedral symmetry. The ion could, for example, be in an octahedral site in a metal oxide such as  $n$ -type  $\text{SrTiO}_3$  or an ion in a chemical complex such as  $[\text{Ti}(\text{H}_2\text{O})_6]^{3+}$ .

The crystal-field Hamiltonian for a  $d$ -electron in the octahedral environment is

$$\mathbb{H}_{\text{oct}} = \mathbb{H}^0 + V_{\text{oct}}, \quad (4.1)$$

$$\mathbb{H}^0 = -\frac{\hbar^2}{2m_e} \nabla^2 - \frac{e^2 Z}{r} + V_{\text{eff}}(r), \quad r = |\mathbf{r}|, \quad (4.2)$$

where  $\mathbb{H}^0$  is the Hamiltonian for a spherically symmetric environment and  $V_{\text{oct}}$  is the octahedrally symmetric point-charge potential. The arrangement of the point-charges shown in Fig. 4.1(a) produces an electrostatic potential given by

$$V_{\text{oct}}(r) = e^2 Z_{\text{ligand}} \sum_{j=1}^6 \frac{1}{|\mathbf{r} - \mathbf{R}_j|}, \quad (4.3)$$

where  $e Z_{\text{ligand}}$  is the effective negative point charge representing one of the ligands,  $e$  is the electron charge, and  $\mathbf{R}_j$  is the vector from the  $d$ -ion to the  $j$ th point charge. If the potential is expanded in a Taylor's series (for  $|\mathbf{r}| < t$ , see Fig. 4.1(a)) the lowest-order, non-spherically symmetric term is

$$V_{\text{oct}} = D \left( x^4 + y^4 + z^4 - \frac{3}{5} r^4 \right), \quad (4.4)$$

$$D = \frac{35}{4} \frac{e^2 Z_{\text{ligand}}}{t^5}, \quad (4.5)$$

where  $|\mathbf{R}_j| = t$  is the distance between the metal ion and any one of the equidistant ligand charges as shown in Fig. 4.1(a). There are higher-order terms in the expansion of  $V_{\text{oct}}$ , but they make no contribution to the energy splitting of the  $d$ -orbitals (see Exercise 4.1).

We have already established in Chapter 3 that the  $d$ -orbitals of Table 4.1 are eigenstates both of the spherically symmetric Hamiltonian,  $\mathbb{H}^0$ , and of  $\mathbb{H}_{\text{oct}} = \mathbb{H}^0 + V_{\text{oct}}$ . The eigenstates are degenerate in the absence of  $V_{\text{oct}}$ , so

$$\int \int \int \psi_d^* \mathbb{H}^0 \psi_d r^2 \sin \theta d\theta d\phi dr = E^0, \quad (4.6)$$

where  $E^0$  is the energy due to the spherically symmetric Hamiltonian and  $\psi_d$  is any one of the  $d$ -orbitals listed in Table 4.1. We can calculate the relative splitting

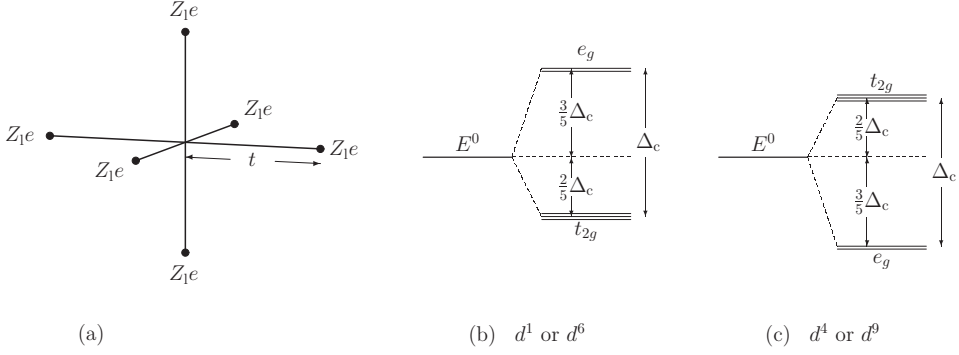


Figure 4.1 (a) The crystal-field model. The six ligands have charge  $eZ_{\text{ligand}}$  (written  $Z_1e$  in part (a)) and each is a distance  $t$  from the central ion. (b) Splitting of a  $d^1$  configuration term into two-fold-degenerate  $\mathcal{E}_g$  states and three-fold-degenerate  $T_{2g}$  states. The splitting is  $\Delta_c = 10Dq$ .  $E^0$  is the energy in the absence of the crystal-field potential. (c) Splitting for the  $d^4$  or  $d^9$  configuration corresponding to a hole in a closed-shell configuration.

of the  $T_{2g}$  and  $\mathcal{E}_g$  energy levels due to the octahedral potential of (4.4). For the  $d_{xz}$  state the crystal-field energy is given by

$$\begin{aligned}
 \Delta(T_{2g}) &= \int \int \int d_{xz}^* D \left( x^4 + y^4 + z^4 - \frac{3}{5} r^4 \right) d_{xz} r^2 \sin \theta d\theta d\phi dr \\
 &= DI_{\text{rad}} \int_0^{2\pi} d\phi \int_0^\pi \sin \theta d\theta \frac{15}{4\pi} (S_\theta C_\phi C_\theta)^2 \\
 &\quad \times \left\{ \left[ S_\theta^4 C_\phi^4 + S_\theta^4 S_\phi^4 + C_\theta^4 \right] - \frac{3}{5} \right\} \\
 &= DI_{\text{rad}} \left( \frac{11}{21} - \frac{3}{5} \right) = -DI_{\text{rad}} \frac{8}{105},
 \end{aligned} \tag{4.7}$$

where

$$I_{\text{rad}} = \int_0^\infty r^4 |R_{nd}(r)|^2 r^2 dr = \langle r^4 \rangle_{\text{avg}} \tag{4.8}$$

is the average value of  $r^4$  for the  $d$ -orbitals. The same result is obtained for the  $d_{xy}$  and  $d_{yz}$  orbitals.

For the  $d_{z^2}$  orbital we have

$$\begin{aligned}
 \Delta(\mathcal{E}_g) &= \int \int \int d_{z^2}^* D \left( x^4 + y^4 + z^4 - \frac{3}{5} r^4 \right) d_{z^2} r^2 \sin \theta d\theta d\phi dr \\
 &= DI_{\text{rad}} \int_0^{2\pi} d\phi \int_0^\pi \sin \theta d\theta \frac{5}{16\pi} (3C_\theta^2 - 1)^2 \left\{ \left[ S_\theta^4 C_\phi^4 + S_\theta^4 S_\phi^4 + C_\theta^4 \right] - \frac{3}{5} \right\} \\
 &= DI_{\text{rad}} \left( \frac{15}{21} - \frac{3}{5} \right) = +DI_{\text{rad}} \frac{12}{105}.
 \end{aligned} \tag{4.9}$$

Table 4.1 The  $d$ -orbitals,  $\psi_d$ , are degenerate eigenstates of the hydrogen-like Hamiltonian,  $\mathbb{H}^0$ . The  $\mathcal{E}_g$  states ( $d_{z^2}$  and  $d_{x^2}$ ) and the  $T_{2g}$  states ( $d_{xy}$ ,  $d_{xz}$ , and  $d_{yz}$ ) are also eigenstates of  $\mathbb{H}_{\text{oct}}$ , but they have different energies.  $R_{n2}(r)$  is the radial part of the wavefunction for principal quantum number  $n$  and angular momentum  $l = 2$ .

$\mathcal{E}_g$ orbitals	$T_{2g}$ orbitals
$d_{z^2} = \sqrt{\frac{5}{16\pi}} \frac{3z^2 - r^2}{r^2} R_{n2}(r)$	$d_{xy} = \sqrt{\frac{15}{4\pi}} \frac{xy}{r^2} R_{n2}(r)$
$d_{x^2} = \sqrt{\frac{15}{16\pi}} \frac{x^2 - y^2}{r^2} R_{n2}(r)$	$d_{xz} = \sqrt{\frac{15}{4\pi}} \frac{xz}{r^2} R_{n2}(r)$
	$d_{yz} = \sqrt{\frac{15}{4\pi}} \frac{yz}{r^2} R_{n2}(r)$

The same result is obtained for  $d_{x^2}$ . The total splitting is usually defined as  $\Delta_c$  or  $10Dq$ . It is given by

$$10Dq = \Delta(\mathcal{E}_g) - \Delta(T_{2g}) = 10D \left\{ I_{\text{rad}} \frac{2}{105} \right\}, \quad (4.10)$$

from which it follows that  $\Delta(\mathcal{E}_g) = 6Dq$  and  $\Delta(T_{2g}) = -4Dq$ , with  $q = (2/105)I_{\text{rad}} = (2/105)\langle r^4 \rangle_{\text{avg}}$ . The splitting is shown schematically in Fig. 4.1(b). The  $\mathcal{E}_g$  states are higher in energy than the  $T_{2g}$  states because the maximum charge density of the  $\mathcal{E}_g$  orbitals, roughly speaking, “points” directly into the repulsive crystal-field charges, whereas the maximum charge density of the  $T_{2g}$  orbitals points between the crystal-field charges.

We can make a crude estimate of  $10Dq$  for a  $\text{Ti}^{3+}$  ion in an octahedral crystal field.  $\text{Ti}^{3+}$  has a single  $d$ -electron outside its argon closed-shell configuration. For a hydrogen-like  $3d$  orbital

$$\langle r^4 \rangle_{\text{avg}} = 336 \left( \frac{3a_0}{2Z_{\text{nucleus}}} \right)^3 \langle r \rangle_{\text{avg}}, \quad (4.11)$$

where  $a_0 = 0.53 \text{ \AA}$  is the Bohr radius. Using  $Z_{\text{nucleus}} = 3$ , (4.11) gives  $\langle r^4 \rangle_{\text{avg}}$  approximately equal to  $6.25\langle r \rangle_{\text{avg}}$ . If we take  $\langle r \rangle_{\text{avg}}$  to be the ionic radius for  $\text{Ti}^{3+}$  ( $0.67 \text{ \AA}$ ) then we have  $\langle r^4 \rangle_{\text{avg}}$  approximately equal to  $4.19 \text{ \AA}^4$ . We assume  $t = 2 \text{ \AA}$  (a typical metal–oxygen distance) and, because of charge neutrality,  $Z_{\text{ligand}} = 1/2$  (so that  $6eZ_{\text{ligand}} = 3$  electron charges). Using all of these estimates we have

$$\begin{aligned}
10Dq &= 10 \left( \frac{2}{105} \right) \left( \frac{35}{4} \right) \frac{e^2 Z_{\text{ligand}}}{r^5} \langle r^4 \rangle_{\text{avg}} \\
&= \frac{5}{3} (14.3942 \text{ eV } \text{\AA}) \frac{1}{2} \frac{4.19}{32} = 1.57 \text{ eV} = 12,668 \text{ cm}^{-1}.
\end{aligned}$$

The experimentally observed absorption peak for the complex  $[\text{Ti}(\text{H}_2\text{O})_6]^{3+}$  occurs at about  $20,300 \text{ cm}^{-1}$ . So our crude estimate is of the correct order of magnitude but off by nearly a factor of two. Typical values of  $10Dq$  for ions in solution range from  $6,000$  to  $30,000 \text{ cm}^{-1}$ .

Visible light has a wavelength ranging roughly from about  $380 \text{ nm}$  to  $750 \text{ nm}$  or energy of  $1.65$  to  $3.26$  electron volts or  $13,333$  to  $26,300 \text{ cm}^{-1}$ . The crystal-field splitting of the electron levels of transition metal complexes often lies within this range. Therefore these complexes absorb part of the white-light spectrum, causing the material (in a solid or in solution) to appear colored.

It should be noted that direct transitions among the  $d$ -levels are forbidden because the selection rules for electric-dipole transitions require the initial and final states to have opposite parity. Since all  $d$ -levels are “ $g$ ”, a transition between two  $d$ -levels is forbidden. The actual transitions are likely vibronic, meaning that both electron and vibrational states are involved. The parity of the initial or final state is the product of the parity of the electronic state times the parity of the vibrational state. Since the  $d$ -levels are all “ $g$ ”, this type of transition requires that the vibrational mode be “ $u$ ” (antisymmetric under the inversion operation).

#### 4.1.2 Filled and half-filled atomic shells

If each of the  $(2l + 1)$  hydrogen-like states are occupied by one electron the total charge density,  $\rho$ , is spherically symmetric. For example, for the  $d$ -states

$$\begin{aligned}
\rho(d^5, r, \theta, \phi) &= e |R_{n2}(r)|^2 \{ |Y_2^0|^2 + |Y_2^1|^2 + |Y_2^{-1}|^2 + |Y_2^2|^2 + |Y_2^{-2}|^2 \} \\
&= e |R_{n2}(r)|^2 \{ |d_{xy}|^2 + |d_{xz}|^2 + |d_{yz}|^2 + |d_{z^2}|^2 + |d_{x^2}|^2 \} \\
&= e |R_{n2}(r)|^2 \frac{5}{4\pi}.
\end{aligned} \tag{4.12}$$

A half-filled shell ( $d^5$  with one electron in each of the different  $d$ -orbitals) has spherically symmetric charge density and so does a completely filled shell ( $d^{10}$  with each of the two spin states occupied). If there are four electrons occupying four of the five different  $d$ -orbitals, the charge density will be

$$\rho(d^4, r, \theta, \phi) = \rho(d^5, r, \theta, \phi) - e |R_{n2}(r)|^2 |d_\alpha|^2, \tag{4.13}$$

where  $d_\alpha$  is the empty  $d$ -orbital.

The spherically symmetric charge density,  $\rho(d^5, r, \theta, \phi)$ , can be incorporated into the effective potential,  $V_{\text{eff}}$ , of the Hamiltonian. The non-spherically symmetric charge is the same as that of a single electron in the  $d_\alpha$  orbit except the charge is  $-e$  (positive). Therefore, under the operations of the rotation group the symmetry properties of a half-filled shell minus one electron ( $d^4$ ) or a completely filled shell minus one electron ( $d^9$ ) are the same as those of a single electron with a positive charge (i.e., a hole). Similarly, considering only the orbital momentum, the symmetry properties of a half-filled shell plus one additional electron ( $d^6$ ) are the same as those of a single electron.

Because the effective charges of the  $d^4$  and  $d^9$  hole states are positive, the splitting is reversed from the  $d^1$  case. For  $d^4$  and  $d^9$  the  $\mathcal{E}_g$  hole states lie below the  $T_{2g}$  states, as illustrated in Fig. 4.1(c). The lowest energy state is that with the hole occupying an  $\mathcal{E}_g$  orbital. From the electron point of view this is equivalent to removing one electron from the upper  $\mathcal{E}_g$  state in Fig. 4.1(b).

## 4.2 Multi-electron systems

The preceding analysis of crystal-field splitting applies to the states of a single  $d$ -electron or single  $d$ -hole. For a multi-electron system the electronic states are characterized by several schemes that specify how the orbital and spin momenta should be combined. For example, for light atoms ( $Z < 30$  or so) the spin-orbit interaction is small compared with the crystal-field splitting (10% or so) and the **L**–**S** coupling scheme can be employed. With the **L**–**S** scheme the individual orbital momenta are combined to form **L** and the spin momenta are combined to form **S**. For heavier atoms, particularly for the rare earths, where the spin-orbit interaction is larger, **j**–**j** coupling should be employed. In this case the orbital and spin momenta of the  $k$ th electron are added to form **j**<sub>*k*</sub>. The total angular momentum is  $\mathbf{J} = \sum \mathbf{j}_k$ .

For a multi-electron atom or ion the electronic *configuration* is specified by indicating which types of atomic orbitals are occupied. For example, for two  $3d$ -electrons outside of closed shells the *configuration* would be indicated as  $1s^2 2s^2 2p^6 3s^2 3p^6 3d^2$ . From a group-theoretical point of view, the filled shells are unimportant because they have spherically symmetric charge densities and are invariant under all of the operations of the rotation group. The outer electrons determine the symmetry properties and therefore the *configuration* is abbreviated as  $3d^2$  or just  $d^2$  if the principal quantum number is unimportant. Given a particular *configuration*, the vector model from atomic physics can be used to determine how to add the orbital and spin momenta of the two electrons to form different *terms*. With **L**–**S** coupling of two  $d$ -electrons the orbital angular momentum,  $M_L = \sum m_l$ , and the spin,  $S = \sum s_i$ , are obtained by assigning the two electrons to any of the

$m = 0, \pm 1, \pm 2$   $d$ -states consistent with the Pauli exclusion principle. In this case,  $M_L$  can be 0,  $\pm 1$ ,  $\pm 2$ ,  $\pm 3$ , or  $\pm 4$ . There may be more than one assignment that results in the same value of  $M_L$ . For example,  $m_1 = 2$  and  $m_2 = 0$  have the same  $M_L$  as  $m_1 = 1$  and  $m_2 = 1$ . The eigenstates are formed from a linear combination of states with the same  $M_L$  determined by the requirement that the eigenvalue of  $M_L^2 = L(L + 1)$ . The possible values of  $L$  can be determined by the decomposition of the direct product:  $D^{(2)} \times D^{(2)} = D^{(0)} + D^{(1)} + D^{(2)} + D^{(3)} + D^{(4)}$  (see Eq. (4.18) below). Thus two  $d$ -electrons can form  $S$ ,  $P$ ,  $D$ ,  $F$ , and  $G$  terms. The assignment of spins to the various one-electron  $d$ -states must be done in such a manner that the total wavefunction is antisymmetric under the interchange of the electron and spin coordinates of the two electrons. For terms with even  $L$  (0, 2, 4, ... or  $S$ ,  $D$ ,  $G$ , ...) the spatial function is symmetric under the interchange of the spatial coordinates and therefore the spin function must be antisymmetric. For two electrons that requires zero total spin,  $S = s_1 + s_2 = 0$  (antisymmetric spin state). Conversely, for odd  $L$  (1, 3, 5, ... or  $P$ ,  $F$ ,  $H$ , ...) the spatial function is antisymmetric, so the spin function must be symmetric. For two electrons that requires  $S = 1$ . The convention is to label a term with a left-hand superscript that gives the spin multiplicity,  $2S + 1$ . For the  $d^2$  configuration the terms appear as  $^1S$ ,  $^3P$ ,  $^1D$ ,  $^3F$ , and  $^1G$ . A further specification of the term is given by placing the value of  $J$  as a right-hand subscript. The complete identification is then  $^{(2S+1)}L_J$ . The value of  $J$  can range from  $|M_L - S|$  to  $|M_L + S|$  in integer steps.

In the following sections we examine how the ground-state term of a  $d^2$  configuration is split by an octahedral crystal field.

#### 4.2.1 Crystal-field splitting for a $d^2$ configuration

In a spherically symmetric environment  $Y_l^m(r)$  is a basis function for the  $D^{(l)}$  IR. The orbitals for a two-electron wavefunction involve the products of the type  $Y_l^m(r) Y_{l'}^{m'}(r')$ . For such products there are  $2l+1$  functions of  $r$  and  $2l'+1$  functions of  $r'$  and therefore a total of  $(2l+1)(2l'+1)$  products. These product functions form the basis for the direct-product representation,  $D^{(l)}(R) \times D^{(l')}(R)$ , and therefore the characters of the direct-product representation are the products of the characters of the two representations  $D^{(l)}(R)$  and  $D^{(l')}(R)$  (see Theorem 3.2c).

However, it is important to recognize that the covering group for the Hamiltonian of a two-electron (or any many-electron) system is **not** the direct-product group. The Hamiltonian contains electrostatic interactions of the form  $e^2/|r - r'|$  and therefore is invariant only under operations that are applied to both coordinates of the product basis functions. The Hamiltonian is invariant only under the diagonal elements of the direct-product group,  $P_{R_i}(r) R_{R_i}(r')$ . An off-diagonal element such as  $P_{R_i}(r) R_{R_j}(r')$ , with  $i$  unequal to  $j$ , is an operation under which  $e^2/|r - r'|$  is

not invariant. The group of the diagonal elements is in fact just the group of the covering operations of the Hamiltonian. The direct-product representation  $D^{(l)} \times D^{(l')}$  is a reducible representation of the group of the Hamiltonian even if it is a direct product of the one-electron IRs.

With the understanding that an operation  $R$  is applied to all of the relevant coordinates ( $r$  and  $r'$ ), we shall write  $P_R f(r) g(r')$  to mean  $P_R f(r) P_R g(r')$ . The character of the direct-product representation matrix is the product of the characters of the two representations, so  $\chi^{(D^{(l)} \times D^{(l')})}(R) \equiv \chi^{(l \times l')}(R) = \chi^{(l)}(R) \chi^{(l')}(R)$ . The character of a rotation by an angle  $A$  about any axis is the same as the character of a rotation about the  $z$ -axis through an angle  $A$  and therefore

$$\begin{aligned} \chi^{(l \times l')}(A) &= \sum_{m=-l}^{+l} e^{-imA} \sum_{m'=-l'}^{+l'} e^{-im'A} = \sum_{k=|l-l'|}^{l+l'} \left\{ \sum_{M=-k}^{+k} e^{-iMA} \right\} \\ &= \sum_{k=|l-l'|}^{l+l'} \chi^{(k)}(A). \end{aligned} \quad (4.14)$$

Equation (4.14) tells us that the character for a rotation through an angle of  $A$  of the direct-product representation matrix is the sum of characters of  $D^{(k)}(A)$  from  $k = |l - l'|$  to  $(l + l')$  (see Exercise 4.5). This result suggests that the direct product decomposes into a sum of  $D^{(l)}$ s. In fact, the decomposition is as shown in Theorem 4.1.

**Theorem 4.1** *Decomposition of the direct product into the IRs of the rotation group:*

$$D^{(l)} \times D^{(l')} = \sum_{k=|l-l'|}^{l+l'} D^{(k)}. \quad (\text{GT4.1})$$

Some examples of the decomposition of the direct products of the IRs of the rotation group are

$$D^{(0)} \times D^{(l')} = D^{(l')}, \quad (4.15)$$

$$D^{(1)} \times D^{(1)} = D^{(0)} + D^{(1)} + D^{(2)}, \quad (4.16)$$

$$D^{(1)} \times D^{(2)} = D^{(1)} + D^{(0)} + D^{(2)} + D^{(3)}, \quad (4.17)$$

$$D^{(2)} \times D^{(2)} = D^{(0)} + D^{(1)} + D^{(2)} + D^{(3)} + D^{(4)}. \quad (4.18)$$

For integral values of  $l$ ,  $D^{(l)}(R)$  and  $D^{(l)}(R)^*$  have the same basis functions and the same characters. The effect of the complex conjugation is simply to interchange the  $m$ th-row and  $-m$ th-row functions. Therefore,  $\chi^{(l)}(R)^* = \chi^{(l)}(R)$ , so the character of  $D^{(l)}(R)^* \times D^{(l')}(R) = \chi^{(l)}(R) \chi^{(l')}(R)$ . As a consequence, the decomposition of  $D^{(l)*} \times D^{(l')}$  is the same as that of  $D^{(l)} \times D^{(l')}$ .

According to Theorem 4.1 each IR on the right-hand side appears only once. Therefore, the two-electron basis functions,  $Y_l^m Y_{l'}^{m'}$ , for these IRs will be eigenfunctions of a hydrogen-like Hamiltonian  $\mathbb{H}(r, r') = \mathbb{H}^0(r) + \mathbb{H}^0(r')$ , where  $\mathbb{H}^0$  is given by (4.2).

#### 4.2.2 The group-theoretical basis for the vector model of atomic physics

The results of Theorem 4.1 serve as a theoretical basis for the vector model used in atomic physics to determine the possible spectroscopic terms. Consider an electron in an  $np$ -orbital and a second electron in an  $n'p$ -orbital ( $n \neq n'$ ). Each orbital transforms according to  $D^{(1)}$ . The multi-electron wavefunction (a Slater determinant, for example) will contain products of the type  $R_{n1}(r) Y_1^m(r, \theta, \phi) R_{n'1}(r') Y_1^m(r', \theta', \phi')$ , where  $R_{n1}$  is the radial part of the orbital. These products serve as basis functions for the direct product  $D^{(1)} \times D^{(1)}$ . Equation (GT4.1) specifies the angular-momentum terms that result when the direct product is reduced to the IRs of the group of the Hamiltonian. We have  $D^{(1)} \times D^{(1)} = D^{(0)} + D^{(1)} + D^{(2)}$ , so the two  $p$ -electrons can form  $S$ ,  $P$ , and  $D$  spectroscopic terms. The spin states are determined by  $D^{(1/2)} \times D^{(1/2)} = D^{(0)} + D^{(1)}$ , which corresponds to a singlet ( $S = 0$ ) and a triplet ( $S = 1$ ). Therefore the possible terms are  $^1S$ ,  $^1P$ ,  $^1D$ ,  $^3S$ ,  $^3P$ , and  $^3D$ .

The total wavefunction must be antisymmetric under the interchange of space and spin coordinates of the two electrons. The spin-triplet states are symmetric and the spin-singlet state is antisymmetric under the interchange of the spin variables. Therefore, the  $^3S$ ,  $^3P$ , and  $^3D$  states must have antisymmetric spatial wavefunctions, and the  $^1S$ ,  $^1P$ , and  $^1D$  states must have symmetrical spatial wavefunctions.

In the case of two equivalent  $p$  electrons ( $n = n'$ ) only the  $^3P$ ,  $^1S$ , and  $^1D$  terms are permitted by the Pauli exclusion principle (see Chapter 5 for more detail).

#### Hund's rules for determining the ground state

1. Of the terms arising from the electron configuration, the term with maximum spin multiplicity,  $2S + 1$  ( $\sum s_i = S$ ), lies lowest in energy.
2. Among the terms of the same spin multiplicity, the term with the largest-value angular momentum,  $M_L = \sum m'_i$  (consistent with the Pauli exclusion principal), has the lowest energy.
3. For a given term, if the outer sub-shell is half-filled or less, then the level with the smallest  $J$  lies lowest in energy. If the sub-shell is more than half-filled, then the level with the largest  $J$  lies lowest. ( $J$  takes on the integer values from  $|M_L - S|$  to  $|M_L + S|$ .)

Note: These rules apply only to the ground state and assume that the repulsion between the electrons is much greater than the spin-orbit interaction.



For the case of a  $d^2$  configuration we use the Russell–Saunders coupling so  $M_L$  is the sum of the  $m$ -values, and  $S$  is the sum of the spins. The possible terms resulting from two  $d$ -electrons are  $S$ ,  $P$ ,  $D$ ,  $F$ , and  $G$ , corresponding to the  $D^{(0)}$ ,  $D^{(1)}$ ,  $D^{(2)}$ ,  $D^{(3)}$ , and  $D^{(4)}$  IRs on the right-hand side of (4.18). We can determine the ground state using Hund’s rules. We have five  $d$ -orbital states, which can be filled with either an  $\alpha$  (spin  $1/2$ ) or a  $\beta$  (spin  $-1/2$ ) or two electrons in the same spatial orbital with spin  $\alpha$  or  $\beta$ . However, the Pauli exclusion principle requires that no two electrons can have the same orbital and spin states. For two  $d$ -electrons outside of a closed shell, Hund’s rules require the electrons to be assigned (a) to give the maximum value for the sum of the spins and then (b) the maximum for the sum of the  $m_i$  values. Therefore the ground state has the configuration  $(m = 2, s = \alpha)(m' = 1, s' = \alpha)$ . With this configuration we have  $M_L = \sum m_i = 3$  and  $S = \sum s_i = 1$ . According to Hund’s rules the value of  $\mathbf{J}$  to be assigned to this configuration is  $|M_L - S| = 3 - 1 = 2$  since the  $d$ -shell is less than half-filled. Therefore the ground-state term is  $^{(2S+1)}F_J = {}^3F_2$ . The  $F$  term will have  $(2M_L + 1) = 7$  states that are degenerate in a spherical environment.

We want to determine how the orbital degeneracy of this seven-fold-degenerate ground state is affected when the system is in an octahedral crystal field. The expected type of splitting can immediately be determined by decomposing the  $F(D^{(3)})$  term into the IRs of the  $O$  or  $O_h$  groups. Since the basis functions of the direct product  $D^{(2)} \times D^{(2)}$  are products of functions that are symmetric under inversion, the decomposition must be into “ $g$ ” IRs. In the octahedral environment  $D^{(3)} = A_2 + T_1 + T_2$ , or, under  $O_h$ ,  $D^{(3)} = A_{2g} + T_{1g} + T_{2g}$ . Therefore, we see that the seven-fold degeneracy of the  $F$  ground state splits into a non-degenerate  $A_{2g}$  and two triply degenerate groups,  $T_{1g}$  and  $T_{2g}$ . Note that the one-electron  $f$ -orbitals are antisymmetric under inversion, so in an octahedral environment  $D^{(3)}$  decomposes into  $A_{2u} + T_{1u} + T_{2u}$  (Eq. (3.38)). Here the basis functions are symmetric under inversion and hence the decomposition is into “ $g$ ” states. To determine the details of these splittings we must first find the appropriate two-electron basis functions and then calculate the matrix elements of the crystal-field potential between these states.

### 4.2.3 Basis functions for the ground state

Our task is to find the basis functions for the  ${}^3F$  ground state of two electrons. The basis functions should be eigenfunctions of the operator  $M_L^2$  with eigenvalue  $3(3 + 1)$  ( $F$  state with  $L = 3$ ), and the eigenvalues of  $M_L = \sum m_i$  are  $-3, -2, -1, 0, 1, 2$ , and  $3$ , corresponding to the  $(2M_L + 1) = 7$  partner functions for an  $F(D^{(3)})$  representation.

We can use  $d$ -orbital Slater determinants to construct states that are antisymmetric for the interchange of space and spin variables. We define

$$|m, \alpha; m', \alpha'\rangle = \sqrt{\frac{1}{2}} \det \begin{bmatrix} \Phi_m(r) \alpha & \Phi_m(r') \alpha' \\ \Phi_{m'}(r) \alpha & \Phi_{m'}(r') \alpha' \end{bmatrix},$$

where  $\Phi_m(r) = R_d(r) Y_2^m(r, \theta, \phi)$  and  $\Phi_{m'}(r') = R_d(r') Y_2^{m'}(r', \theta', \phi')$ . Expansion of the determinant gives

$$\begin{aligned} |m, \alpha; m', \alpha'\rangle &= \sqrt{\frac{1}{2}} R_d(r) R_d(r') \\ &\times \left[ Y_2^m(r, \theta, \phi) Y_2^{m'}(r', \theta', \phi') - Y_2^{m'}(r, \theta, \phi) Y_2^m(r', \theta', \phi') \right] \alpha \alpha' \\ &= |m, m'\rangle \alpha \alpha', \end{aligned} \quad (4.19)$$

where  $|m, m'\rangle$  is the determinant of the spatial functions.

The two-electron state,  $|m, m'\rangle \alpha \alpha'$ , is “*g*” under the inversion operation and is antisymmetric in the interchange of  $\mathbf{r}, \alpha$  with  $\mathbf{r}', \alpha'$ .<sup>1</sup> The aim is now to find linear combinations of Slater determinants with same  $M_L$  that are also eigenstates of  $M_L^2$ .

Consider the determinantal states shown in Table 4.2. These functions have eigenvalues of  $M_L = 3, 2, 1, 0, -1, -2$ , and  $-3$ , but are not all eigenfunctions of  $M_L^2$ . To find the effect of  $M_L^2$  on the states in Table 4.2, we can use the following operator result for two-electron states:<sup>2</sup>

$$\begin{aligned} M_L^2 |m, m'\rangle &= [l(l+1) + l'(l'+1) + 2mm'] |m, m'\rangle \\ &+ [(l-m)(l+m+1)(l'+m')(l'-m'+1)]^{1/2} |m+1, m'-1\rangle \\ &+ [(l+m)(l-m+1)(l'-m')(l'+m'+1)]^{1/2} |m-1, m'+1\rangle, \end{aligned} \quad (4.20)$$

where the angular-momentum quantum numbers are  $l$  and  $l'$ , and the magnetic quantum numbers are  $m$  and  $m'$ . For two  $d$ -electrons ( $l = 2$  and  $l' = 2$ ) (4.20) reduces to

$$\begin{aligned} M_L^2 |m, m'\rangle &= [12 + 2mm'] |m, m'\rangle \\ &+ \{[6 - m(m+1)][6 - m'(m'-1)]\}^{1/2} |m+1, m'-1\rangle \\ &+ \{[6 - m(m-1)][6 - m'(m'+1)]\}^{1/2} |m-1, m'+1\rangle. \end{aligned} \quad (4.21)$$

<sup>1</sup> With three or more electrons the states can not be described by the product of a single spatial function times a single spin function (see Exercise 4.10).

<sup>2</sup> For the general operator formulas see Chapter 5 or references [4.3, 4.4].

Table 4.2 Slater determinant states. The first column is the Slater determinant. The second column is  $M_L = \sum m_i$ . The third column is the eigenvalue of  $M_L^2$ . If no eigenvalue is given the state is not an eigenstate of  $M_L^2$ . The last column lists the states that are coupled by the  $M_L^2$  operator (4.21). Linear combinations of the coupled states must be used to construct eigenstates of  $M_L^2$ .

Slater determinant $ m, m'\rangle$	$M_L = m + m'$	$M_L^2$	Coupled by $M_L^2$ operator
$ 1, 2\rangle$	3	$3(3 + 1)$	
$ 2, 0\rangle$	2	$3(3 + 1)$	
$ 2, -1\rangle$	1		$ 1, 0\rangle$
$ 1, 0\rangle$	1		$ 2, -1\rangle$
$ 1, -1\rangle$	0		$ 2, -2\rangle$
$ 2, -2\rangle$	0		$ 1, -1\rangle$
$ 1, -2\rangle$	-1		$ -1, 0\rangle$
$ -1, 0\rangle$	-1		$ 1, -2\rangle$
$ -2, 0\rangle$	-2	$3(3 + 1)$	
$ -2, -1\rangle$	-3	$3(3 + 1)$	

In calculating  $M_L^2|m, m'\rangle$  note that  $|m, m\rangle = 0$  (two electrons in identical states) and  $|m', m\rangle = -|m, m'\rangle$  (a property of an antisymmetric wavefunction). For example, for the state  $|2, 1\rangle$  we have

$$\begin{aligned} M_L^2|2, 1\rangle &= (12 + 4)|2, 1\rangle + 4|1, 2\rangle \\ &= 16|2, 1\rangle - 4|2, 1\rangle = 3(3 + 1)|2, 1\rangle. \end{aligned} \quad (4.22)$$

Therefore  $|2, 1\rangle$  is an eigenstate of  $M_L^2$  with eigenvalue  $L(L + 1) = 3(3 + 1)$ . For  $|2, 0\rangle$  we have

$$M_L^2|2, 0\rangle = (12 + 0)|2, 0\rangle + 4|1, 1\rangle = 12|2, 0\rangle = 3(3 + 1)|2, 0\rangle. \quad (4.23)$$

The first two states and the last two states of Table 4.2 are suitable basis functions because they are eigenstates of  $M_L^2$ . However, if we calculate  $M_L^2|2, -1\rangle$ , we find that it is not an eigenstate, but is coupled to the state  $|1, 0\rangle$ ,

$$M_L^2|2, -1\rangle = 8|2, -1\rangle + 2\sqrt{6}|1, 0\rangle, \quad (4.24)$$

$$M_L^2|1, 0\rangle = 6|1, 0\rangle + 2\sqrt{6}|2, -1\rangle. \quad (4.25)$$

In order to achieve basis functions that are eigenstates of  $M_L^2$  we must take linear combinations of the coupled states. Consider the coupled states  $|2, -1\rangle$  and  $|1, 0\rangle$ . We take the linear combination,  $c|2, -1\rangle + d|1, 0\rangle$ , and require that

$$M_L^2[c|2, -1\rangle + d|1, 0\rangle] = \lambda[c|2, -1\rangle + d|1, 0\rangle]. \quad (4.26)$$

Using (4.24) and (4.25) in (4.26), we obtain

$$[(8 - \lambda)c + 2\sqrt{6}d]|2, -1\rangle + [2\sqrt{6}c + (6 - \lambda)d]|1, 0\rangle = 0, \quad (4.27)$$

or, written as an eigenvalue matrix equation,

$$\begin{pmatrix} 8 - \lambda & 2\sqrt{6} \\ 2\sqrt{6} & 6 - \lambda \end{pmatrix} \begin{pmatrix} c \\ d \end{pmatrix} = 0. \quad (4.28)$$

The vanishing of the determinant requires that

$$(8 - \lambda)(6 - \lambda) - 24 = 0, \quad (4.29)$$

or

$$\lambda^2 - 14\lambda + 24 = (\lambda - 2)(\lambda - 12) = 0. \quad (4.30)$$

The two eigenvalues are obviously  $\lambda = 2 = 1(1 + 1)$  and  $\lambda = 12 = 3(3 + 1)$ . The first eigenvalue leads to a linear combination associated with a  $P$  term. The second eigenvalue corresponds to an  $F$  term and is the desired result. The coefficients are determined by substituting the eigenvalue into (4.28) and finding the ratio of  $c$  to  $d$ . This gives  $c/d = \sqrt{6}/2$  and the normalized basis function

$$(3/5)^{1/2}|2, -1\rangle + (2/5)^{1/2}|1, 0\rangle. \quad (4.31)$$

For the coupled states  $|1, -1\rangle$  and  $|2, -2\rangle$ , we have

$$M_L^2|1, -1\rangle = 10|1, -1\rangle + 4|2, -2\rangle, \quad (4.32)$$

$$M_L^2|2, -2\rangle = 4|2, -2\rangle + 4|1, -1\rangle. \quad (4.33)$$

On taking a linear combination of the two states we find that the state with  $M_L^2 = 3(3 + 1)$  is

$$(4/5)^{1/2}|1, -1\rangle + (1/5)^{1/2}|2, -2\rangle. \quad (4.34)$$

Following the above procedure for the coupled states gives us the set of seven functions shown in Table 4.3.

Table 4.3 *Basis functions based on linear combinations of Slater determinants. The notation  $\Phi(m_L)$  is defined in the first column.*

Eigenfunctions of $M_L$ and $M_L^2$	Eigenvalue of $M_L$	Eigenvalue of $M_L^2$
$\Phi(3) =  2, 1\rangle$	3	$3(3 + 1)$
$\Phi(2) =  2, 0\rangle$	2	$3(3 + 1)$
$\Phi(1) = (2/5)^{1/2} 1, 0\rangle + (3/5)^{1/2} 2, -1\rangle$	1	$3(3 + 1)$
$\Phi(0) = (4/5)^{1/2} 1, -1\rangle + (1/5)^{1/2} 2, -2\rangle$	0	$3(3 + 1)$
$\Phi(-1) = (2/5)^{1/2} -1, 0\rangle + (3/5)^{1/2} -2, 1\rangle$	-1	$3(3 + 1)$
$\Phi(-2) =  -2, 0\rangle$	-2	$3(3 + 1)$
$\Phi(-3) =  -2, -1\rangle$	-3	$3(3 + 1)$

In Table 4.3 we have introduced a simplified notation for the states  $\Phi(M_L)$ ,  $M_L = 3, 2, 1, 0, -1, -2$ , and  $-3$ .

Our next task is to calculate the matrix elements of the crystal-field potential between the basis functions in Table 4.3. The Hamiltonian for the two-electron system (ignoring for the moment the electron–electron interactions) is

$$\mathbb{H}(r, r') = \mathbb{H}^0(r) + \mathbb{H}^0(r') + V_{\text{oct}}(r) + V_{\text{oct}}(r'), \quad (4.35)$$

where

$$\mathbb{H}^0 = -\frac{\hbar^2}{2m_e} \nabla^2 - \frac{e^2 Z}{r} + V_{\text{eff}}(r), \quad (4.36)$$

$$V_{\text{oct}}(r) = D \left( x^4 + y^4 + z^4 - \frac{3}{5} r^4 \right), \quad (4.37)$$

$$D = \frac{35}{4} \frac{e^2 Z_{\text{ligand}}}{r^5}. \quad (4.38)$$

$V_{\text{eff}}(r)$  includes any effective spherical potential due to the filled-shell electrons, but excludes the crystal-field potential and the electron–electron interactions between the  $d$ -electrons. The two-electron states listed in Table 4.3 are composed of linear combinations of products such as  $Y_2^m(r) Y_2^{m'}(r')$  and are therefore degenerate eigenstates of  $H^0(r, r') = \mathbb{H}^0(r) + \mathbb{H}^0(r')$ . That is,

$$\mathbb{H}^0(r, r') \Phi(M_L) = 2E^0 \Phi(M_L). \quad (4.39)$$

As a consequence, we need only calculate the matrix elements of the crystal-field potential  $V(r, r')_{\text{oct}} = V_{\text{oct}}(r) + V_{\text{oct}}(r')$  between the various  $\Phi(M_L)$  states.

#### 4.2.4 Calculation of the matrix elements of the crystal field for $d^2$

Since  $V(r, r')_{\text{oct}} = V_{\text{oct}}(r) + V_{\text{oct}}(r')$  is a sum of one-electron operators (there are no terms involving both  $r$  and  $r'$ ), it follows that

$$\begin{aligned} \langle m, m' | V(r, r')_{\text{oct}} | n, n' \rangle &= \langle m | V(r) | n \rangle \delta_{m', n'} + \langle m' | V(r') | n' \rangle \delta_{m, n} \\ &\quad - \langle m' | V(r) | n \rangle \delta_{m, n'} - \langle m | V(r') | n' \rangle \delta_{m', n}, \end{aligned} \quad (4.40)$$

where  $\langle m |$  is the one-electron wavefunction,  $R_d(r) Y_2^m(r, \theta, \phi)$ . Using (4.40) for  $\Phi(3)$ , for example, gives

$$\begin{aligned} \langle \Phi(3) | V_{\text{oct}}(r) + V_{\text{oct}}(r') | \Phi(3) \rangle &= \langle 2, 1 | V_{\text{oct}}(r) + V_{\text{oct}}(r') | 2, 1 \rangle \\ &= \langle 2 | V_{\text{oct}}(r) | 2 \rangle + \langle 1 | V_{\text{oct}}(r) | 1 \rangle. \end{aligned} \quad (4.41)$$

Table 4.4 *One-electron integrals:  $\langle m|V_{\text{oct}}(r)|m'\rangle$  in units of  $Dq$* 

$m$	$m'$				
	2	1	0	-1	-2
2	1	0	0	0	5
1	0	-4	0	0	0
0	0	0	6	0	0
-1	0	0	0	-4	0
-2	5	0	0	0	1

Written out in detail,

$$\begin{aligned}
 \langle \Phi(3)|V_{\text{oct}}(r) + V_{\text{oct}}(r')|\Phi(3)\rangle &= D \int |R_{n2}(r)|^2 r^2 dr \int d\phi \int d\theta \sin\theta \\
 &\quad \times \{|Y_2^2|^2 + |Y_2^1|^2\} \left( x^4 + y^4 + z^4 - \frac{3}{5}r^4 \right). \quad (4.42)
 \end{aligned}$$

Table 4.4 gives the results for the integrals of the crystal-field potential between the different spherical harmonics. Using this table we can quickly calculate all of the various matrix elements.

For example, to calculate  $\langle \Phi(3)|V_{\text{oct}}(r) + V_{\text{oct}}(r')|\Phi(3)\rangle = \langle 2|V_{\text{oct}}(r)|2\rangle + \langle 1|V_{\text{oct}}(r)|1\rangle$  we use Table 4.4 to obtain

$$\langle \Phi(3)|V_{\text{oct}}(r) + V_{\text{oct}}(r')|\Phi(3)\rangle = Dq(1 - 4) = -3Dq. \quad (4.43)$$

For  $\langle \Phi(1)|V_{\text{oct}}(r) + V_{\text{oct}}(r')|\Phi(1)\rangle$ , we have

$$\begin{aligned}
 &\left[ \sqrt{\frac{2}{5}}\langle 1, 0| + \sqrt{\frac{3}{5}}\langle 2, -1| \right] |V_{\text{oct}}(r) + V_{\text{oct}}(r')| \left[ \sqrt{\frac{2}{5}}|1, 0\rangle + \sqrt{\frac{3}{5}}|2, -1\rangle \right] \\
 &= \frac{2}{5} \left[ \langle 1|V_{\text{oct}}(r)|1\rangle + \langle 0|V_{\text{oct}}(r)|0\rangle \right] + \frac{3}{5} \left[ \langle 2|V_{\text{oct}}(r)|2\rangle + \langle -1|V_{\text{oct}}(r)|-1\rangle \right] \\
 &= \frac{2}{5}(-4 + 6)Dq + \frac{3}{5}(1 - 4)Dq = \left( \frac{4}{5} - \frac{9}{5} \right) = -Dq. \quad (4.44)
 \end{aligned}$$

The crystal-field matrix elements of the two-electron functions of Table 4.3 are shown in Table 4.5.

Now that we have all the matrix elements of the proper basis functions we must solve the matrix eigenvalue equation

$$\begin{aligned}
 &\langle \Phi(m)|H^0(r) + H^0(r') + V_{\text{oct}}(r) + V_{\text{oct}}(r') - E|\Phi(m')\rangle \\
 &= \langle \Phi(m)|\{(2E^0 - E)\delta_{mm'} + V_{\text{oct}}(r) + V_{\text{oct}}(r')\}|\Phi(m')\rangle = 0. \quad (4.45)
 \end{aligned}$$

Table 4.5 *Matrix elements of the crystal-field potential,  $V_{\text{oct}}(r) + V_{\text{oct}}(r')$ , for two-electron  ${}^3F$  states in units of  $Dq$ . Blank spaces indicate that the integral is zero.*

	$\Phi(3)$	$\Phi(2)$	$\Phi(1)$	$\Phi(0)$	$\Phi(-1)$	$\Phi(-2)$	$\Phi(-3)$
$\Phi(3)$	-3				$\sqrt{15}$		
$\Phi(2)$		7				5	
$\Phi(1)$			-1				$\sqrt{15}$
$\Phi(0)$				-6			
$\Phi(-1)$	$\sqrt{15}$				-1		
$\Phi(-2)$		5				7	
$\Phi(-3)$			$\sqrt{15}$				-3

On grouping the coupled rows and columns together, we have the secular equation

	$\Phi(3)$	$\Phi(-1)$	$\Phi(-3)$	$\Phi(1)$	$\Phi(2)$	$\Phi(-2)$	$\Phi(0)$
$\Phi(3)$	$-3Dq - \lambda$	$\sqrt{15}Dq$					
$\Phi(-1)$	$\sqrt{15}Dq$	$-Dq - \lambda$					
$\Phi(-3)$			$-3Dq - \lambda$	$\sqrt{15}Dq$			
$\Phi(1)$			$\sqrt{15}Dq$	$-Dq - \lambda$			
$\Phi(2)$					$7Dq - \lambda$	$5Dq$	
$\Phi(-2)$					$5Dq$	$7Dq - \lambda$	
$\Phi(0)$							$-6Dq - \lambda$

$$\det = 0, \quad (4.46)$$

where  $\lambda = E - 2E^0$ . The eigenvalues of the upper two  $2 \times 2$ s are  $\lambda = 2Dq$  and  $\lambda = -6Dq$ . The eigenvalues of the lower  $2 \times 2$  are  $\lambda = 2Dq$  and  $\lambda = 12Dq$ . The lower  $1 \times 1$  gives  $\lambda = -6Dq$ . To find the eigenvectors we can treat each of the uncoupled blocks separately. For the upper block with the eigenvalue  $-6Dq$ , the upper row requires that  $+3a + \sqrt{15}b = 0$ , where  $a$  and  $b$  are the amplitudes of  $\Phi(3)$  and  $\Phi(-1)$ , respectively. This relation determines the ratio of  $a$  to  $b$ , and normalization yields another condition so that the coefficients  $a$  and  $b$  are completely determined. The normalized state is  $(5/8)^{1/2}\Phi(3) - (3/8)^{1/2}\Phi(-1)$ . Proceeding in this manner we have the terms and levels given in Table 4.6.

Since the  $F$  representation decomposes into  $A_{2g} + T_{1g} + T_{2g}$ , it is clear that the non-degenerate eigenvalue belongs to the  $A_{2g}$  representation. However, both  $T_{1g}$

Table 4.6 *Terms and levels for the  $^3F$  crystal-field states*

(a) $T_{1g}$ : A triple degeneracy	States
	$\Phi(0)$
$E = 2E^0 - 6Dq$	$(5/8)^{1/2}\Phi(3) - (3/8)^{1/2}\Phi(-1)$ $(5/8)^{1/2}\Phi(-3) - (3/8)^{1/2}\Phi(1)$
(b) $T_{2g}$ : A triple degeneracy	States
	$(3/8)^{1/2}\Phi(3) + (5/8)^{1/2}\Phi(-1)$ $(3/8)^{1/2}\Phi(-3) + (5/8)^{1/2}\Phi(1)$ $(1/2)^{1/2}[\Phi(2) - \Phi(-2)]$
(c) $A_{2g}$ : A non-degenerate state	State
$E = 2E^0 + 12Dq$	$(1/2)^{1/2}[\Phi(2) + \Phi(-2)]$

and  $T_{2g}$  are three-fold degenerate representations. In order to assign the states in (a) and (b), we must look at their symmetry properties. The functions listed in parts (a) and (b) of Table 4.6 are the bases for three-dimensional IRs. We can calculate the trace of the matrix representing rotations using these functions. From the traces we can identify which is  $T_{1g}$  and which is  $T_{2g}$ .

Consider a rotation  $C_4$  or  $(\pi/2)$  about the  $z$ -axis. If we operate on a Slater determinant  $|m, n\rangle$  we find

$$\begin{aligned}
 R_{(\pi/2)}|m, n\rangle &= [R_{n2}(r) R_{n2}(r')] \\
 &\times \frac{1}{\sqrt{2}} \left\{ Y_2^m \left( r, \theta, \phi + \frac{\pi}{2} \right) Y_2^n \left( r', \theta', \phi' + \frac{\pi}{2} \right) \right. \\
 &\quad \left. - Y_2^m \left( r', \theta', \phi' + \frac{\pi}{2} \right) Y_2^n \left( r, \theta, \phi + \frac{\pi}{2} \right) \right\} \\
 &= e^{i(m+n)\pi/2} |m, n\rangle = i^{m+n} |m, n\rangle.
 \end{aligned} \tag{4.47}$$

(Here  $R_{(\pi/2)}$  operates both on  $\mathbf{r}$  and on  $\mathbf{r}'$ .) Using this rule, we find that

$$R_{(\pi/2)}\Phi(M) = i^M \Phi(M). \tag{4.48}$$

For the functions in part (a) of Table 4.6 we have

$$R_{(\pi/2)}\Phi(0) = \Phi(0), \tag{4.49}$$

$$\begin{aligned}
 R_{(\pi/2)} \left[ \sqrt{\frac{5}{8}} \Phi(3) - \sqrt{\frac{3}{8}} \Phi(-1) \right] &= i^3 \sqrt{\frac{5}{8}} \Phi(3) + i \sqrt{\frac{3}{8}} \Phi(-1) \\
 &= -i \left[ \sqrt{\frac{5}{8}} \Phi(3) - \sqrt{\frac{3}{8}} \Phi(-1) \right],
 \end{aligned} \tag{4.50}$$



$$\begin{aligned}
 R_{(\pi/2)} \left[ \sqrt{\frac{5}{8}} \Phi(-3) - \sqrt{\frac{3}{8}} \Phi(1) \right] &= i^{-3} \sqrt{\frac{5}{8}} \Phi(-3) - i \sqrt{\frac{3}{8}} \Phi(1) \\
 &= +i \left[ \sqrt{\frac{5}{8}} \Phi(-3) - \sqrt{\frac{3}{8}} \Phi(1) \right]. \quad (4.51)
 \end{aligned}$$

Therefore, the representation matrix for  $R_{(\pi/2)}$  is diagonal. The trace of the matrix representing  $R_{(\pi/2)}$  is the character,  $\chi^{(a)}(\pi/2)$ , of the representation. It is just the sum of the eigenvalues:  $1 - i + i = +1$ . Repeating this procedure for group (b) in Table 4.6 yields  $\chi^{(b)}(\pi/2) = -1$ . From the character table for  $O$  we see that the character for  $C_4$  is  $+1$  for  $T_1$  and  $-1$  for  $T_2$ . Therefore we can identify group (a) as  $T_{1g}$  and group (b) as  $T_{2g}$ . The spin is  $S = 1$  for all of these states, so the spin multiplicity is  $2S + 1 = 3$ , and therefore we can label the states as triplets:  ${}^3A_{2g}$ ,  ${}^3T_{1g}$ , and  ${}^3T_{2g}$ . The splitting is shown schematically in Fig. 4.2.

One might suppose that we could use the above two-electron results to deduce the behavior of the  $d^3$  or  $d^8$  states, since the  $d$ -shell would have two holes. The electronic (Hund's rules) ground-state term is  ${}^4F_{3/2}$ , corresponding to  $S = 3/2$ . In the case of three  $d$ -electrons not all of the spin-orbitals can be represented by a single Slater determinant (see Exercise 4.10). Consequently, the "hole" picture is more complex. In the most studied case ( $\text{Cr}^{3+}$  in ruby) the lowest crystal-field level is the  ${}^4A_{2g}$  state. For the  $d^8$  configuration ( $\text{Ni}^{2+}$ ) the lowest crystal-field level is  ${}^3A_{2g}$ . This is what one might expect from the "two-hole" argument, since the highest level for the  $d^2$  configuration is  $A_{2g}$ .

We have explored the splitting of the  ${}^3F$  ground state of the  $d^2$  configuration in detail above without regard to electron–electron interactions and the other higher-lying terms. In the octahedral environment higher-lying terms may have a level with the same symmetry as one of the  ${}^3F$  levels. Levels with the same symmetry will interact with one another. For example, the  ${}^3P$  term has a group of

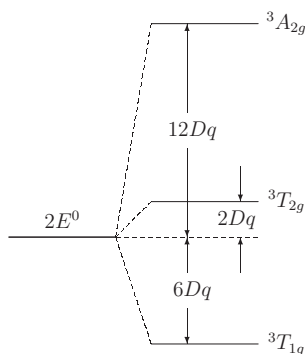


Figure 4.2 Crystal-field splitting of the two- $d$ -electron  ${}^3F$  term.

$T_{1g}$  states that will interact with the  $T_{1g}$  states of the  ${}^3F$  term. We have neglected the  $d$ – $d$ -electron interactions, but in a more complete treatment [4.5, 4.6, 4.7] of the crystal-field theory the potential,  $e^2/|\mathbf{r} - \mathbf{r}'|$ , is included explicitly in the two-electron Hamiltonian. We shall consider the effects of the electron–electron interactions in Section 4.2.6 below.

#### 4.2.5 The strong-crystal-field case

If the crystal field is very large compared with the electrostatic, orbit–orbit, and spin–orbit interactions, the eigenstates can be characterized by the IRs of the crystal-field symmetry. For a strong octahedral crystal field,  $d$ -electron configurations are more appropriately specified in terms of the number of electrons occupying the  $T_{2g}$  and  $\mathcal{E}_g$  states. An outer-electron configuration is therefore of the form  $t^m e^n$ , meaning that there are  $m$  electrons assigned to  $T_{2g}$  orbitals and  $n$  electrons in  $\mathcal{E}_g$  orbitals. For the case of two  $d$ -electrons there are three possible configurations:  $t^2$ ,  $e^2$ , and  $te$ . The terms resulting from these configurations are determined by the direct-product decompositions.

In the case of the  $te$  states one electron resides in a  $t$  orbital and the other in an  $e$  orbital. The spins may therefore be parallel or antiparallel, so both triplets ( ${}^3T_{1g}$ ,  ${}^3T_{2g}$ ) and singlets ( ${}^1T_{1g}$ ,  ${}^1T_{2g}$ ) are permissible. For the  $e^2$  and  $t^2$  the terms involving doubly occupied orbitals can not have parallel spins, and some triplet states are forbidden.

The symmetry-function-generating machine can be used to generate the basis functions for the various IRs listed in the decompositions of Table 4.7. For the one-dimensional IRs,  $A_{1g}$  and  $A_{2g}$ , all that is required is the character table for the  $O$  group. (All the spatial functions must be “ $g$ ” since they are constructed from the product of two  $d$ -functions.) As an example, we generate an  $e^2$  function belonging to the  $A_{1g}$  IR using  $d_{x^2}(r) d_{x^2}(r')$  as the starting function (see Table 4.2 for definitions of the  $d$ -orbitals). In this case the generating machine takes the form

$$F^{A_{1g}}(r, r') \propto \sum_R \chi^{A_{1g}}(R) P_R[d_{x^2}(r) d_{x^2}(r')] = \sum_R P_R[d_{x^2}(r) d_{x^2}(r')], \quad (4.52)$$

Table 4.7 Strong-crystal-field configurations and  $O_h$  terms

Configuration	Direct product	Decomposition into the IRs of $O_h$
$t^2$	$T_{1g} \times T_{1g}$	$A_{1g} + \mathcal{E}_g + T_{1g} + T_{2g}$
$te$	$T_{1g} \times \mathcal{E}_g$	$T_{1g} + T_{2g}$
$e^2$	$\mathcal{E}_g \times \mathcal{E}_g$	$A_{1g} + A_{2g} + \mathcal{E}_g$

where the sum is over all of the operations of  $O$ , and the characters of the  $A_1$  representation are all equal to unity. The effect of  $P_R$  on the various  $d$ -electron functions is given in Appendix E. This procedure gives

$$F^{A_{1g}}(r, r') \propto [d_{x^2}(r) d_{x^2}(r') + d_{z^2}(r') d_{z^2}(r)]. \quad (4.53)$$

The function is symmetric upon interchange of the spatial coordinates and therefore the spin state must be antisymmetric. The normalized spin-orbital function is

$$\Phi(r, r', s, s') = \frac{1}{2} [d_{x^2}(r) d_{x^2}(r') + d_{z^2}(r') d_{z^2}(r)] [\alpha(s)\beta(s') - \alpha(s')\beta(s)], \quad (4.54)$$

where  $\alpha$  and  $\beta$  are the spin  $+1/2$  and  $-1/2$  states, respectively.

For the  $\mathcal{E}_g$ ,  $T_{1g}$ , and  $T_{2g}$  terms it is necessary to have the matrix elements of the IRs. The symmetry-function-generating machine gives

$$F^\Gamma(r, r')_j \propto \sum_R \Gamma(R)_{jj} P_R[d_a(r) d_b(r')], \quad (4.55)$$

where  $F^\Gamma(r, r')_j$  is a function that belongs to the  $j$ th row of the  $\Gamma$  IR and  $\Gamma(R)_{jj}$  is the  $j$ th diagonal matrix element of the IR. In (4.55)  $d_a$  and  $d_b$  are any of the  $d$ -orbitals or linear combinations of the  $d$ -orbitals listed in Table 4.1. The IR matrix elements,  $\Gamma(R)_{ij}$ , for the IRs of  $O$  are given in Appendix E. Table 4.8 gives the wavefunctions for the  $t^2$ ,  $e^2$ , and  $te$  configurations calculated using (4.55). The wavefunctions are eigenstates of the crystal-field Hamiltonian in the absence of the electrostatic potential,  $e^2/|\mathbf{r} - \mathbf{r}'|$ . The functions  $F^\Gamma(r, r')_j$  must be symmetrized and normalized appropriately. For symmetric spin functions ( $S = 1$ ), if  $F^\Gamma(r, r')_j$  is not antisymmetric in the interchange of  $r$  and  $r'$  it is replaced by  $[F^\Gamma(r, r')_j - F^\Gamma(r', r)_j]$ , and then normalized. For antisymmetric spin functions ( $S = 0$ ), if  $F^\Gamma(r, r')_j$  is not symmetric in the interchange of  $r$  and  $r'$  it is replaced by  $[F^\Gamma(r, r')_j + F^\Gamma(r', r)_j]$ , and then normalized.

#### 4.2.6 The effect of electron–electron interactions on crystal-field splitting

In the strong-crystal-field case, the zeroth-order energy (in the strong-field limit) for a  $T_{2g}$ -electron state is  $10Dq$  lower than that of an  $\mathcal{E}_g$ -electron state. It is customary to choose the zero of energy as the  $te$  configuration. With that choice, the  $e^2$  configuration's energy is  $+10Dq$  and the  $t^2$  configuration's energy is  $-10Dq$  as shown on the right-hand side of Fig. 4.3 on p. 115.

The states listed in Table 4.8 are the symmetry functions for the levels of the  $d^2$ -configuration terms. They are eigenstates of  $\mathbb{H}^0(r, r') = \mathbb{H}^0(r) + \mathbb{H}^0(r') + V_{\text{oct}}(r) + V_{\text{oct}}(r')$ . To obtain the energies in the presence of the electron–electron interactions we must solve the eigenvalue equation  $(\mathbb{H} - 2E^0 - \lambda^\alpha)\Psi^\alpha(r, r') = 0$ ,

Table 4.8 *Symmetry functions for the terms of the  $t^2$ ,  $e^2$ , and  $te$  configurations of two  $d$ -electrons in a strong octahedral crystal field. Each row function of the triplets has the three spin states listed on the right. Each singlet has one spin state listed on the right. These functions are eigenstates in the absence of the  $e^2/|\mathbf{r} - \mathbf{r}'|$  interaction in a spherical or octahedral environment.*

$t^2$ terms		
$^3T_{1g}, S = 1$	Spatial part of the eigenstate	Spin eigenstates
$ t^2, ^3T_{1g}, 1\rangle$	$[a(r)b(r') - b(r)a(r')]/\sqrt{2}$	$S^1(1), S^1(0), S^1(-1)$
$ t^2, ^3T_{1g}, 2\rangle$	$[a(r)c(r') - b(r)c(r')]/\sqrt{2}$	$S^1(1), S^1(0), S^1(-1)$
$ t^2, ^3T_{1g}, 3\rangle$	$[b(r)c(r') - b(r)c(r')]/\sqrt{2}$	$S^1(1), S^1(0), S^1(-1)$
$^1T_{2g}, S = 0$		
$ t^2, ^1T_{2g}, 1\rangle$	$[b(r)c(r') + c(r)b(r')]/\sqrt{2}$	$S(0)$
$ t^2, ^1T_{2g}, 2\rangle$	$[a(r)c(r') + c(r)a(r')]/\sqrt{2}$	$S(0)$
$ t^2, ^1T_{2g}, 3\rangle$	$[a(r)b(r') + b(r)a(r')]/\sqrt{2}$	$S(0)$
$^1E_g, S = 0$		
$ t^2, ^1E_g, 1\rangle$	$[b(r)b(r') - c(r)c(r')]/\sqrt{2}$	$S(0)$
$ t^2, ^1E_g, 2\rangle$	$[2a(r)a(r') - b(r)b(r') - c(r)c(r')]/\sqrt{6}$	$S(0)$
$^1A_{1g}, S = 0$		
$ t^2, ^1A_{1g}, 1\rangle$	$[a(r)a(r') + b(r)b(r') + c(r)c(r')]/\sqrt{3}$	$S(0)$
$e^2$ terms		
$^1A_{1g}, S = 0$	Spatial part of the eigenstate	Spin eigenstates
$ e^2, ^1A_{1g}, 1\rangle$	$[x^2(r)x^2(r') + z^2(r)z^2(r')]/\sqrt{2}$	$S(0)$
$^3A_{2g}, S = 1$		
$ e^2, ^3A_{2g}, 1\rangle$	$[x^2(r)z^2(r') - z^2(r)x^2(r')]/\sqrt{2}$	$S^1(1), S^1(0), S^1(-1)$
$^1E_g, S = 0$		
$ e^2, ^1E_g, 1\rangle$	$[x^2(r)z^2(r') + z^2(r)x^2(r')]/\sqrt{2}$	$S(0)$
$ e^2, ^1E_g, 2\rangle$	$[x^2(r)x^2(r') - z^2(r)z^2(r')]/\sqrt{2}$	$S(0)$
$te$ terms		
$^1T_{1g}, S = 0$	Spatial part of the eigenstate	Spin eigenstates
$ te, ^1T_{1g}, 1\rangle$	$\{c(r)[x^2(r') + \sqrt{3}z^2(r')] + c(r')[x^2(r) + \sqrt{3}z^2(r)]\}/\sqrt{8}$	$S(0)$
$ te, ^1T_{1g}, 2\rangle$	$\{b(r)[x^2(r') - \sqrt{3}z^2(r')] + b(r')[x^2(r) - \sqrt{3}z^2(r)]\}/\sqrt{8}$	$S(0)$
$ te, ^1T_{1g}, 3\rangle$	$\{a(r)x^2(r') + a(r')x^2(r)\}/\sqrt{2}$	$S(0)$

Table 4.8 (cont.)

${}^3T_{1g}, S = 1$		
$ te, {}^3T_{1g}, 1\rangle$	$\{c(r)[x^2(r') + \sqrt{3}z^2(r')] - c(r')[x^2(r) + \sqrt{3}z^2(r)]\}/\sqrt{8}$	$S^1(1), S^1(0), S^1(-1)$
$ te, {}^3T_{1g}, 2\rangle$	$\{b(r)[x^2(r') - \sqrt{3}z^2(r')] - b(r')[x^2(r) - \sqrt{3}z^2(r)]\}/\sqrt{8}$	$S^1(1), S^1(0), S^1(-1)$
$ te, {}^3T_{1g}, 3\rangle$	$\{a(r)x^2(r') - a(r')x^2(r)\}/\sqrt{2}$	$S^1(1), S^1(0), S^1(-1)$
${}^1T_{2g}, S = 0$		
$ te, {}^1T_{2g}, 1\rangle$	$\{a(r)z^2(r') + a(r')z^2(r)\}/\sqrt{2}$	$S(0)$
$ te, {}^1T_{2g}, 2\rangle$	$\{b(r)[z^2(r') + \sqrt{3}x^2(r')] + b(r')[z^2(r) + \sqrt{3}x^2(r)]\}/\sqrt{8}$	$S(0)$
$ te, {}^1T_{2g}, 3\rangle$	$\{c(r)[z^2(r') - \sqrt{3}x^2(r')] + c(r')[z^2(r) - \sqrt{3}x^2(r)]\}/\sqrt{8}$	$S(0)$
${}^3T_{2g}, S = 1$		
$ te, {}^3T_{2g}, 1\rangle$	$\{a(r)z^2(r') - a(r')z^2(r)\}/\sqrt{2}$	$S^1(1), S^1(0), S^1(-1)$
$ te, {}^3T_{2g}, 2\rangle$	$\{b(r)[z^2(r') + \sqrt{3}x^2(r')] - b(r')[z^2(r) + \sqrt{3}x^2(r)]\}/\sqrt{8}$	$S^1(1), S^1(0), S^1(-1)$
$ te, {}^3T_{2g}, 3\rangle$	$\{c(r)[z^2(r') - \sqrt{3}x^2(r')] - c(r')[z^2(r) - \sqrt{3}x^2(r)]\}/\sqrt{8}$	$S^1(1), S^1(0), S^1(-1)$

$|nm, {}^p\Gamma, q\rangle$  :  $nm$  is the octahedral configuration ( $t^2$ ,  $te$ , or  $e^2$ ),  $\Gamma$  is the IR of  $O_h$ ,  $q$  is the row of  $\Gamma$ , and  $p$  is the spin multiplicity. The total spatial eigenfunction is  $R_{n2}(r) R_{n2}(r') |nm, {}^p\Gamma, q\rangle$ .  $z^2(r) = d_{z^2}(r)$ ,  $x^2(r) = d_{x^2}(r)$ ,  $a(r) = d_{xy}(r)$ ,  $b(r) = d_{xz}(r)$ ,  $c(r) = d_{yz}(r)$ .  $S(0) = [\alpha(s)\beta(s') - \beta(s)\alpha(s')]/\sqrt{2}$ , where  $\alpha$  is spin up and  $\beta$  is spin down,  $S^1(1) = \alpha(s)\alpha(s')$ , and  $S^1(0) = [\alpha(s)\beta(s') + \beta(s)\alpha(s')]/\sqrt{2}$ , and  $S^1(-1) = \beta(s)\beta(s')$ .

where  $\mathbb{H} = \mathbb{H}^0(r, r') + e^2/|\mathbf{r} - \mathbf{r}'|$ . The eigenstates  $\Psi^\alpha(r, r')$  will be linear combinations of the symmetry functions in Table 4.8 that belong to the same row of the same IR. For example, there are  $A_{1g}$  states both for the  $t^2$  and for the  $e^2$  configurations. These two same-symmetry states will be mixed to form the final  $A_{1g}$  eigenstates. Therefore we need the matrix elements of  $e^2/|\mathbf{r} - \mathbf{r}'|$  between the symmetry functions of the same type. *Note that  $e^2/|\mathbf{r} - \mathbf{r}'|$  is invariant under all of the operations of the group because  $P_R$  rotates both  $\mathbf{r}$  and  $\mathbf{r}'$  in the same way and the quantity  $|\mathbf{r} - \mathbf{r}'|$  is unchanged by the rotational operations. Therefore,  $e^2/|\mathbf{r} - \mathbf{r}'|$  belongs to the totally symmetric  $A_{1g}$  representation. Consequently, there can be no non-zero matrix elements between different IRs or between different rows of the same IR.* This feature greatly simplifies the calculations of the matrix elements.  $e^2/|\mathbf{r} - \mathbf{r}'|$  does not involve the spins, so its matrix element between two states vanishes unless  $S = S'$ .

When calculating the electrostatic interactions there are two important mathematical results that are useful. The first is

$$\frac{1}{|\mathbf{r}_1 - \mathbf{r}_2|} = \sum_{k=0}^{\infty} \frac{r_{<}^k}{r_{>}^{k+1}} P_k(\cos \gamma), \quad (4.56)$$

where  $r_{<}$  is the smaller of  $r_1$  and  $r_2$  and  $r_{>}$  is the larger of  $r_1$  and  $r_2$ . The angle  $\gamma$  is the angle between  $\mathbf{r}_1$  and  $\mathbf{r}_2$ , and  $P_k$  is the  $k$ th Legendre polynomial.

The second result, called the “addition theorem”, is

$$P_k(\cos \gamma) = \frac{4\pi}{2k+1} \sum_{m=-k}^k Y_k^m(\theta_1, \phi_1)^* Y_k^m(\theta_2, \phi_2). \quad (4.57)$$

These two mathematical results can be used to evaluate the electrostatic interaction between electrons. A general interaction matrix element is of the form

$$\left\langle n_1, n_2, l_1, l_2, m_1, m_2 \left| \frac{e^2}{|\mathbf{r}_a - \mathbf{r}_b|} \right| n_3, n_4, l_3, l_4, m_3, m_4 \right\rangle, \quad (4.58)$$

where  $n$ ,  $l$ , and  $m$  are the principal, angular-momentum, and magnetic quantum numbers, respectively.

In detail the matrix element (4.58) is

$$\begin{aligned} & \int r_1^2 dr_1 \int r_2^2 dr_2 \int d\theta_1 \sin \theta_1 \int d\theta_2 \sin \theta_2 \int d\phi_1 \int d\phi_2 \\ & \times \left[ R_{n_1}(r_1) R_{n_2}(r_2) Y_{l_1}^{m_1}(\theta_1, \phi_1) Y_{l_2}^{m_2}(\theta_2, \phi_2) \right]^* \\ & \times \left[ \sum_{k=0}^{\infty} \frac{r_{<}^k}{r_{>}^{k+1}} \frac{4\pi}{2k+1} \sum_{m=-k}^k Y_k^m(\theta_2, \phi_2)^* Y_k^m(\theta_1, \phi_1) \right] \\ & \times \left[ R_{n_3}(r_1) R_{n_4}(r_2) Y_{l_3}^{m_3}(\theta_1, \phi_1) Y_{l_4}^{m_4}(\theta_2, \phi_2) \right]. \end{aligned} \quad (4.59)$$

This is a formidable-appearing result, but it can be simplified in application. The matrix element involves the products

$$\begin{aligned} & \left[ \int d\phi_1 \int d\theta_1 \sin \theta_1 Y_{l_1}^{m_1}(\theta_1, \phi_1)^* Y_k^m(\theta_1, \phi_1) Y_{l_3}^{m_3}(\theta_1, \phi_1) \right] \\ & \times \left[ \int d\phi_2 \int d\theta_2 \sin \theta_2 Y_{l_2}^{m_2}(\theta_2, \phi_2)^* Y_k^m(\theta_2, \phi_2) Y_{l_4}^{m_4}(\theta_2, \phi_2) \right]. \end{aligned} \quad (4.60)$$

The integrals over  $\phi_1$  and  $\phi_2$  can be carried out immediately, with the result

$$\begin{aligned} & \int_0^{2\pi} e^{i(-m_1+m+m_3)\phi_1} d\phi_1 \int_0^{2\pi} e^{i(-m_2-m+m_4)\phi_2} d\phi_2 \\ & \propto \delta(-m_1 + m + m_3) \delta(-m_2 - m + m_4), \end{aligned} \quad (4.61)$$

which requires  $m_1 + m_2 = m_3 + m_4$ . Therefore the matrix element vanishes unless the total orbital momenta of the two states are equal. Furthermore, the direct-product selection rules tell us that the integrals vanish except for  $k$  simultaneously in the range of both  $|l_1 - l_2| \leq k \leq l_1 + l_2$  and  $|l_3 - l_4| \leq k \leq l_3 + l_4$ . For two  $d$ -electrons, this requires that  $k \leq 4$ . Thus, of the infinite number of terms in (4.59) only the first four terms of the sum over the index  $k$  contribute a non-zero result.

It is important to note that the matrix element of (4.58) is not between the symmetry functions listed in Table 4.8. However, the matrix elements of the symmetry functions will consist of a sum of these types of integrals.

For our two- $d$ -electron problem there are at most two different symmetry functions belonging to a given row of the same IR, as can be seen from Table 4.8. Let  $f_j^\alpha$  and  $g_j^\alpha$  be two different functions both belonging to  $j$ th row of the  $\alpha$ th IR of  $O_h$ . The matrix elements of  $e^2/|\mathbf{r}_1 - \mathbf{r}_2|$  are given by

$$\begin{aligned} M_{11} &= \langle f_j^\alpha | \frac{e^2}{|\mathbf{r}_1 - \mathbf{r}_2|} | f_j^\alpha \rangle, \\ M_{22} &= \langle g_j^\alpha | \frac{e^2}{|\mathbf{r}_1 - \mathbf{r}_2|} | g_j^\alpha \rangle, \\ M_{21} &= M_{12} = \langle f_j^\alpha | \frac{e^2}{|\mathbf{r}_1 - \mathbf{r}_2|} | g_j^\alpha \rangle. \end{aligned} \quad (4.62)$$

The results are independent of which row (which  $j$ ) is used to evaluate the integral. The matrix elements between functions belonging to different IRs or different row functions vanish. The elements of  $\mathbb{M}$  for the various IRs of  $O_h$  have been compiled by Tanabe and Sugano [4.7]. Those for the  $d^2$  symmetry functions listed in Table 4.8 are given in Table 4.9.

The constants  $B$  and  $C$  are combinations of integrals over the radial coordinates of the hydrogen-like atomic states [4.8]. Treating these constants as adjustable parameters allows one to explore how the levels change as the ratio of the crystal-field strength to the electron–electron-interaction strength varies.

For the  $V^{3+}$  ion, approximate values are  $Dq = 1,800 \text{ cm}^{-1}$ ,  $B = 860 \text{ cm}^{-1}$ , and  $C = 3,800 \text{ cm}^{-1}$ . Using Table 4.9, we can calculate the energies of the interacting states. For example, consider the  ${}^3T_{1g}$  eigenvalue secular equation (the first row of Table 4.9). The eigenvalues for these states are obtained from the  $2 \times 2$ -matrix equation,

$$\begin{pmatrix} -5B - 10Dq - \lambda & 6B \\ 6B & 4B - \lambda \end{pmatrix}, \quad (4.63)$$

where  $\lambda = E - 2E^0$ .

For  $V^{3+}$  ( $d^2$  configuration) this gives  $\lambda({}^3T_{1g}) = 4,436 \text{ cm}^{-1}$  and  $-23,296 \text{ cm}^{-1}$ . If we solve (4.63) with  $Dq = 0$  then we obtain the energies of the terms in the

Table 4.9 *Electron–electron matrix elements for the terms of the  $d^2$  configuration*

IR of the states	Strong-field configuration	$M_{11}$ (upper) $M_{21}$ (lower)	$M_{12}$ (upper) $M_{22}$ (lower)
$^3T_{1g}$	$t^2$	$-5B - 10Dq$	$6B$
	$te$	$6B$	$4B$
$^1T_{2g}$	$t^2$	$B + 2C - 10Dq$	$2\sqrt{3}B$
	$te$	$2\sqrt{3}B$	$2C$
$^1E_g$	$t^2$	$B + 2C - 10Dq$	$-2\sqrt{3}B$
	$e^2$	$-2\sqrt{3}B$	$2C + 10Dq$
$^1A_{1g}$	$t^2$	$10B + 5C - 10Dq$	$\sqrt{6}(2B + C)$
	$e^2$	$\sqrt{6}(2B + C)$	$8B + 4C + 10Dq$
$^3A_{2g}$	$t^2$	$-8B + 10Dq$	
$^1T_{1g}$	$te$	$4B + 2C$	
$^3T_{2g}$	$te$	$-8B$	

weak-field limit. They are  $\lambda(^3T_{1g}) = 6,020\text{ cm}^{-1}$  and  $-6,880\text{ cm}^{-1}$ . We can also trace the evolutions from the weak-field case to the strong-field case by allowing  $Dq$  to continuously increase from zero to its value of  $1,800\text{ cm}^{-1}$ . Proceeding in this manner for all of the terms listed in Table 4.9 allows us to correlate the weak-field terms with the terms for the strong crystal field. The results are shown schematically in Fig. 4.3. The eigenvalues for  $Dq = 0$  and  $Dq = 1,800\text{ cm}^{-1}$  are given in Table 4.10.

#### 4.2.7 Book keeping

For the free ion with two  $d$ -electrons we determine the states from  $D^{(2)} \times D^{(2)} = D^{(0)} + D^{(1)} + D^{(2)} + D^{(3)} + D^{(4)}$  or  $S + P + D + F + G$ . Since all of these states are constructed from the product of two  $d$  orbitals, they must be “ $g$ ” under inversion. If we then decompose these IRs into those of  $O_h$ , we obtain

$$\begin{aligned}
 S &= A_{1g}, \\
 P &= T_{1g}, \\
 D &= E_g + T_{2g}, \\
 F &= A_{2g} + T_{2g} + T_{1g}, \\
 G &= E_g + T_{1g} + T_{2g} + A_{1g}.
 \end{aligned} \tag{4.64}$$

Conversely, if we start from the strong-field limit the configurations are  $t^2$ ,  $e^2$ , and  $te$ , and the terms are derived from the direct products,  $T_{2g} \times T_{2g}$ ,  $E_g \times E_g$ , and  $E_g \times T_{2g}$ . These direct products are



## Crystal-field theory

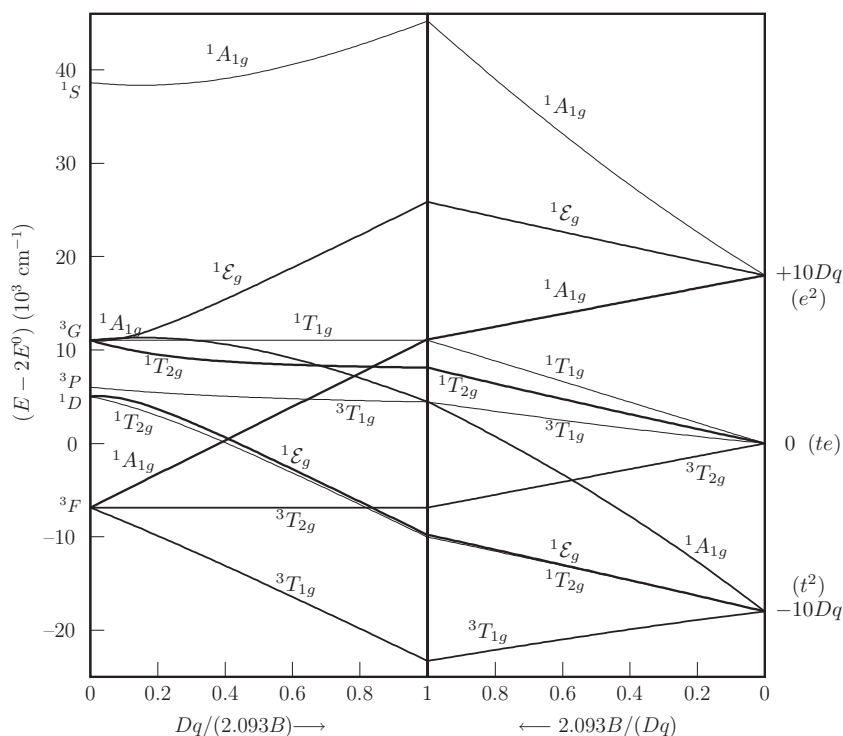


Figure 4.3 A correlation diagram using the values of the parameters for  $V^{3+}$ :  $B = 860 \text{ cm}^{-1}$ ,  $C/B = 4.42$ , and  $Dq = 1,800 \text{ cm}^{-1}$ . Terms derived from  $t^2$ ,  $e^2$ , and  $te$  configurations asymptotically approach  $-10Dq$ ,  $10Dq$ , and  $0$ , respectively, as  $B/Dq \rightarrow 0$ .

$$\begin{aligned}
 T_{2g} \times T_{2g} &= A_{1g} + E_g + T_{1g} + T_{2g}, \\
 E_g \times E_g &= A_{1g} + A_{2g} + E_g, \\
 E_g \times T_{2g} &= T_{1g} + T_{2g} + T_{1g} + T_{2g}.
 \end{aligned}
 \tag{4.65}$$

On comparing the terms on the right-hand side of (4.64) with those of (4.65) we find that they are exactly the same.

A schematic representation of the evolution of the terms on going from the weak-field to the strong-field case is shown in Fig. 4.3. On the extreme left the energies are those for  $Dq = 0$ . On the extreme right the energies are for  $Dq \rightarrow \infty$ . In this limit terms derived from the  $t^2$  configuration merge to  $-10Dq$ , while those derived from the  $e^2$  configuration merge to  $+10Dq$ . The terms from the  $te$  configuration tend to  $0$  (by virtue of the choice of the origin of energy).

Table 4.10  $d^2$  States. Energy  $\lambda = E - 2E^0$ . Results for  $Dq = 0$  and  $Dq = 1,800 \text{ cm}^{-1}$  with  $B = 860 \text{ cm}^{-1}$  and  $C = 3,800 \text{ cm}^{-1}$ . The “observed” energy levels of  $[V(\text{H}_2\text{O})_6]^{3+}$  are given in the fourth column and the last column gives the calculated values.  $E_1 = E(-23,296 \text{ cm}^{-1})$  is the lowest  ${}^3F$  state for  $Dq = 1,800 \text{ cm}^{-1}$ .

Free-ion terms	Levels: Weak crystal field $Dq = 0 \text{ cm}^{-1}$	Eigenvalues $O_h$ symmetry $Dq = 1,800 \text{ cm}^{-1}$	Observed $E - E_1$ (approximate values) ( $\text{cm}^{-1}$ )	Calculated $E - E_1$ ( $\text{cm}^{-1}$ )
${}^1S$	${}^1A_{1g}$ 38,640	45,214		
${}^1G$	${}^1A_{1g}$ 11,040	4,466		
${}^1G$	${}^1E_g$ 11,040	25,851		
${}^1G$	${}^1T_{1g}$ 11,040	11,040		
${}^1G$	${}^1T_{2g}$ 11,040	8,103		
${}^3P$	${}^3T_{1g}$ 6,020	4,436	${}^3T_{1g}(P) \rightarrow {}^3T_{1g}(F)$ 25,000	27,732
${}^1D$	${}^1T_{2g}$ 5,020	-10,043		
${}^1D$	${}^1E_g$ 5,020	-9,791		
${}^3F$	${}^3A_{2g}$ -6,880	11,120	${}^3A_{2g}(F) \rightarrow {}^3T_{1g}(F)$ 37,000	34,416
${}^3F$	${}^3T_{1g}$ -6,880	-23,296		
${}^3F$	${}^3T_{2g}$ -6,880	-6,880	${}^3T_{2g}(F) \rightarrow {}^3T_{1g}(F)$ 17,700	16,416

### 4.3 Jahn–Teller effects

The Jahn–Teller distortion (or Jahn–Teller effect) refers to the tendency of a molecule whose ground state is degenerate to distort structurally. For example, the complex ion  $[\text{Ti}(\text{H}_2\text{O})_6]^{3+}$  would be expected to consist of a  $\text{Ti}(d^1)$  ion surrounded by an octahedron of water molecules. Since all of the six water molecules are equivalent, there is no apparent reason why any one axis should be singled out to be different. However, experimentally the complex is observed to be compressed along one axis (arbitrarily designated as the  $z$ -axis), resulting in  $D_{4h}$  rather than  $O_h$  symmetry. By contrast,  $[\text{Cu}(\text{H}_2\text{O})_6]^{2+}(d^9)$  is elongated along the  $z$ -axis as shown schematically in Fig. 4.4.

Jahn and Teller [4.9] put forward the following theorem: “Any non-linear molecular system in a degenerate electronic state will be unstable and will undergo distortion to form a system of lower symmetry and lower energy, thereby removing the degeneracy”.

The Jahn–Teller distortion is most often observed with transition metal ions in what would be expected to be an octahedral environment. The effect is found to be most pronounced when an odd number of electrons occupy (doubly degenerate)  $E_g$  orbitals. The effect occurs for electrons occupying degenerate  $T_{2g}$  orbitals as well, but is much weaker.

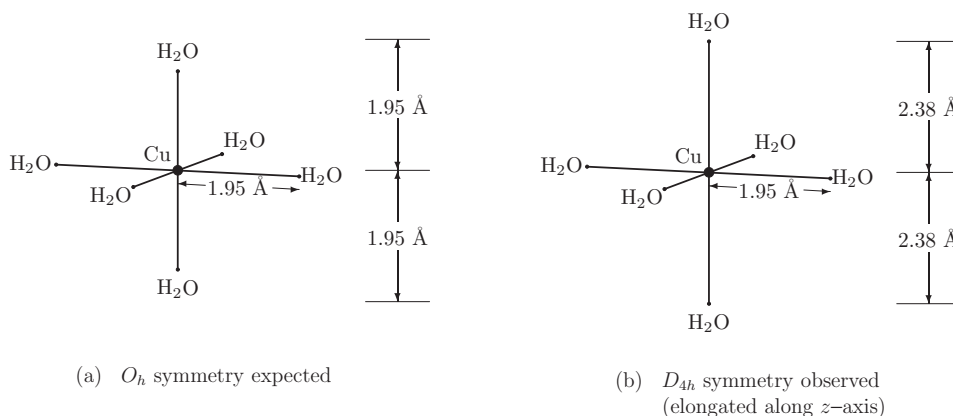


Figure 4.4 The complex  $[\text{Cu}(\text{H}_2\text{O})_6]^{2+}$ : (a) the octahedral structure expected in the absence of the Jahn–Teller effect and (b) the observed structure. The complex is elongated along the  $z$ -axis due to the Jahn–Teller effect. The resulting structure has  $D_{4h}$  symmetry.

To see why a distortion might reduce the ground-state energy of a complex, start with a  $d$ -ion surrounded by a perfect octahedron of ligands. A change in the ion–ligand bond length along the  $z$ -axis changes the symmetry from  $O_h$  to  $D_{4h}$ . For a  $d^1$  configuration the octahedral ground state is a triply degenerate  $T_{2g}$  level. For a single  $d$ -hole ( $d^9$ ) the ground state is the  $\mathcal{E}_g$  level. The  $\mathcal{E}_g$  and  $T_{2g}$  IRs of  $O_h$  are reducible representations of the  $D_{4h}$  group. Since the  $d$ -orbitals are symmetric under inversion, we need only consider the decomposition of  $\mathcal{E}$  and  $T_2$  into the IRs of  $D_4$ . The character table for  $D_4$  is given in Table 4.11, together with the characters of the  $\mathcal{E}(O)$ ,  $T_2(O)$ , and  $T_1(O)$  IRs of the  $O$  group. The correspondences of the classes of the two groups are  $8C_3(O) \rightarrow \text{none in } D_4$ ,  $3C_2(O) \rightarrow C_2(D_4) + 2C_2'(D_4)$ ,  $6C_2(O) \rightarrow 2C_2''(D_4)$ , and  $6C_4(O) \rightarrow 2C_4(D_4)$ .

Using Table 4.11, we find that the  $T_2(O)$  IR splits into a doubly degenerate  $\mathcal{E}(D_4)$  and a non-degenerate  $B_2(D_4)$  as shown in Fig. 4.5. The  $\mathcal{E}(O)$  IR splits into a non-degenerate  $A_1(D_4)$  and a non-degenerate  $B_1(D_4)$  level. For a  $d^1$  configuration the distortion produces a lower energy level for the  $d$ -electron to reside in. For the  $d^9$  configuration a similar argument can be made regarding the hole. The  $d^1$  electron occupies the  $\mathcal{E}_g(D_{4h})$  for elongation or the  $B_{2g}(D_{4h})$  for compression (e.g.,  $[\text{Ti}(\text{H}_2\text{O})_6]^{3+}$ ). In either case the ground-state energy is lowered.

There are, of course, opposing reactions to a Jahn–Teller distortion, including elastic, dipolar, and other changes in the electronic structure of the complex due to distortion. The occurrence of the Jahn–Teller distortion implies that the  $d$ -electron splitting energy is dominant. The  $d^9$  configuration, which is typical of many Cu-containing molecules and solids, has an  $\mathcal{E}_g$  (hole in the  $d_{x^2}$  level) ground state, and the Jahn–Teller effect generally results in an elongation along the  $z$ -axis.

Table 4.11 The character table for the symmetry elements of  $D_4$  and IRs of  $O$ . The upper segment is the character table for  $D_4$ . The lower segment shows the decomposition of  $\mathcal{E}$ ,  $T_2$ , and  $T_1$  of  $O$  into the IRs of  $D_4$ .

IR	$E$	$C_2$	$2C_4$	$2C'_2$	$2C''_2$	Basis functions
$A_1$	1	1	1	1	1	$x^2 + y^2, z^2$
$A_2$	1	1	1	-2	-2	$R_z, z$
$B_1$	1	1	-2	1	-2	$x^2 - y^2$
$B_2$	1	1	-2	-2	1	$xy$
$\mathcal{E}$	2	-2	0	0	0	$(xy, yz); (R_x, R_y)$
Decomposition $O \rightarrow D_4$						
$\mathcal{E}(O)$	2	2	0	2	0	$A_1 + B_1$
$T_2(O)$	3	-2	-2	-2	1	$B_2 + \mathcal{E}$
$T_1(O)$	3	-2	1	-2	-2	$A_2 + \mathcal{E}$

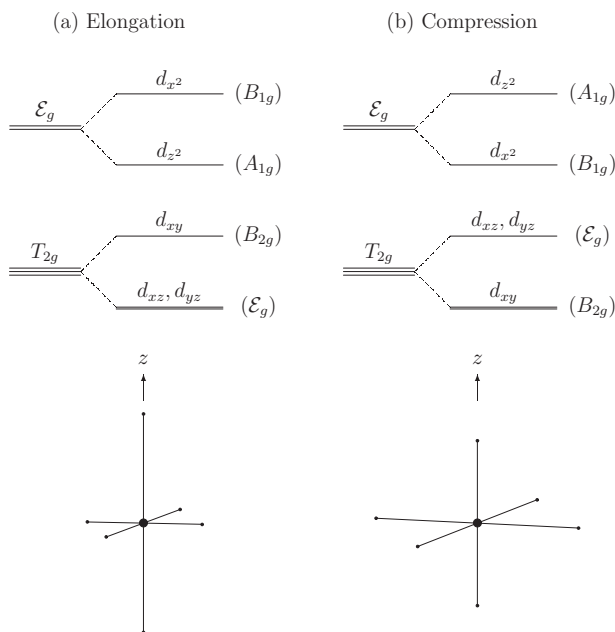


Figure 4.5 Jahn–Teller splitting of the  $d$ -orbital energies: (a) elongation and (b) compression.

There are two other closely related effects that can lead to structural distortion. The first is the dynamic Jahn–Teller effect. This effect may occur when there are several different structural distortions that are separated by small energy barriers. Quantum-mechanical tunneling between the different structures can occur with the assistance of phonons of the proper symmetry. There is experimental evidence for

the dynamic Jahn–Teller effect in molecules and solids. It is conjectured that the phenomenon may play a role in explaining high-temperature superconductivity in the cuprate compounds.

A second effect, called the second-order Jahn–Teller effect, occurs when an excited state of a system is very close in energy to the ground state. A distortion of the structure may allow the states to mix, resulting in a lower ground-state configuration. This effect is believed to be involved in stereochemical non-rigidity.

### References

- [4.1] H. Bethe, “Termaufspaltung in Kristallen”, *Ann. Phys.* **3**, 133–206 (1929).
- [4.2] J. H. Van Vleck, “The group relation between the Mulliken and Slater–Pauling theories of valence”, *J. Chem. Phys.* **3**, 803–807 (1935).  
J. H. Van Vleck, “Valence strength and the magnetism of complex salts”, *J. Chem. Phys.* **3**, 807–814 (1935).
- [4.3] H. Eyring, J. Walter, and G. E. Kimball, *Quantum Chemistry* (New York: Wiley, 1944).
- [4.4] E. U. Condon and G. H. Shortley, *The Theory of Atomic Spectra* (Cambridge: Cambridge University Press, 1963).
- [4.5] T. M. Dunn, D. S. McClure, and R. G. Pearson, *Some Aspects of Crystal Field Theory* (New York: Harper & Row, 1965). (Note that there are errors in some of the formulas on pages 18 and 20. These have been corrected in our discussion.)
- [4.6] D. S. McClure, “Electronic spectra of molecules and ions in crystals. II. Spectra of ions in crystals”, *Solid State Phys.* **9**, 399–525 (1958).
- [4.7] Y. Tanabe and S. Sugano, “On the absorption spectra of complex ions I”, *J. Phys. Soc. Japan* **9**, 753–766 (1954).  
Y. Tanabe and S. Sugano, “On the absorption spectra of complex ions II”, *J. Phys. Soc. Japan* **9**, 766–779 (1954).
- [4.8] G. Racah, “Theory of complex spectra II”, *Phys. Rev.* **62**, 438–462 (1942).
- [4.9] H. A. Jahn and E. Teller, “Stability of polyatomic molecules in degenerate electronic states. I. Orbital degeneracy”, *Proc. Royal Soc. London A* **161** (no. 905), 220–235 (1937).

### Exercises

- 4.1 The spherical harmonics form a complete, orthogonal set and therefore the crystal field can be expanded in these functions:

$$\begin{aligned}
 V_{\text{oct}} &= \sum_{l=0}^{\infty} \sum_{m=-l}^l f_l^m(r) Y_l^m(\theta, \phi) \\
 &= \frac{7eZ_{\text{ligand}}}{3r^5} \left[ Y_4^0 + \frac{5}{14} (Y_4^4 + Y_4^{-4}) \right] + \text{terms with } l > 4,
 \end{aligned}$$

where  $r$  is the magnitude of the vector  $\mathbf{r}$ . Use the direct-product rules to show that the terms with  $l > 4$  make no contribution to the matrix elements of the crystal field for  $d$ -orbitals.

- 4.2 An ion at the origin is surrounded by four equidistant ligands, each having negative charge  $Z_{\text{ligand}}e$  ( $Z_1e$  in Fig. 4.6).

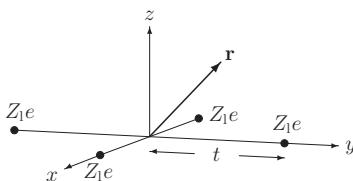


Figure 4.6

- (a) Identify the symmetry group for the three-dimensional configuration.  
 (b) Using a Taylor's-series expansion of the potential (for  $r < t$ ) show that the lowest-order non-spherical term is

$$e^2 Z_{\text{ligand}} \frac{3(x^2 + y^2) - 2r^2}{t^3}.$$

- (c) From Table 4.11 identify the IR corresponding to the potential.  
 (d) Determine the type of splitting of a  $d$ -electron due to the potential.
- 4.3 Consider a single  $d$ -electron and the  $d$ -states,  $d_{xy}$ ,  $d_{xz}$ ,  $d_{yz}$ ,  $d_{x^2}$ , and  $d_{z^2}$ .
- (a) Identify to which IR of  $D_4$  each  $d$ -state belongs.  
 (b) The matrix elements of the potential in Exercise 4.2 between the  $d$ -states can be written symbolically as  $\langle \Gamma^a(D_4) | A_1(D_4) | \Gamma^b(D_4) \rangle$ . Use direct-product arguments to show that the off-diagonal matrix elements are zero.  
 (c) Calculate the crystal-field splitting between the  $B_2(D_4)$  and  $\mathcal{E}(D_4)$  levels in terms of the parameter  $\gamma = e^2 Z_{\text{ligand}} \langle r^2 \rangle_{\text{avg}} / t^3$ , where

$$\langle r^2 \rangle_{\text{avg}} = \int_0^\infty r^2 [r^2 R_{nd}(r)^2] dr.$$

- 4.4 Use Hund's rules to find the ground states of the elements  $\text{Sc}(d^1)$ ,  $\text{Ti}(d^2)$ ,  $\text{V}(d^3)$ ,  $\text{Cr}(d^5s)$ ,  $\text{Mn}(d^5)$ ,  $\text{Fe}(d^6)$ ,  $\text{Co}(d^7)$ ,  $\text{Ni}(d^8)$ , and  $\text{Cu}(d^{10}s)$ .
- 4.5 Find the terms of the configuration  $f^2$  and show that the Hund ground state is  $^3H_4$ .
- 4.6 Show that, for the  $^3H_4$  ground state in Exercise 4.5 the combination of Slater determinants corresponding to  $M_L = 3$ ,  $M_L^2 = 5(5 + 1)$  is  $\Phi(3) = (3^{1/2}/2)|3, 0\rangle + (1/3)^{1/2}|2, 1\rangle$ .

- 4.7 The  $D^{(1)}$  representation based on spherical harmonics is equivalent to the  $T_1$  representation of the  $O$  group, meaning that  $D^{(1)}$  is related to  $T_1$  by a similarity transformation. Show that the decomposition of the direct product of  $D^{(1)} \times D^{(1)}$  into the IRs of  $O$  is the same as the decomposition of  $T_1 \times T_1$  into the IRs of  $O$ . Indicate whether the representations of the decompositions are “ $u$ ” or “ $g$ ”.
- 4.8 Use the formula

$$\sum_{k=0}^l x^k = \frac{1 - x^{(l+1)}}{1 - x}$$

for  $x < 1$  to show that

$$\sum_{k=-l}^l e^{-ik\alpha} = \frac{\sin(l + 1/2)\alpha}{\sin(\alpha/2)}.$$

- 4.9 Prove that

$$\chi^{(l)}(R)\chi^{(l')}(R) = \sum_{k=|l-l'|}^{l+l'} \chi^{(k)}(R),$$

where  $\chi^{(l)}$  is the character of  $D^{(l)}(R)$  and  $\chi^{(l)} = \sum_{m=-l}^l e^{-im\theta(R)}$ , where  $\theta(R)$  is the angle associated with the operation  $R$ .

- 4.10 Find the ground state for a  $d^3$  configuration using Hund’s rules (Exercise 4.4,  $V^{2+}(d^3)$ ).
- (a) Write a Slater determinant wavefunction,

$$\Phi(n, l_1, m_1, s_{1z}; n, l_2, m_2, s_{2z}; n, l_3, m_3, s_{3z}),$$

for three  $d$ -electrons with  $M_L = 3$  and  $S_z = 3/2$  in terms of hydrogen-like spin-orbitals.

- (b) The spin-lowering operator,  $S^-$ , lowers the spin of the state it operates on by 1 (in units of  $\hbar$ ):

$$\begin{aligned} & S^- \Phi_1(l_1, m_1, s_{1z}; l_2, m_2, s_{2z}; \dots; n_k, l_k, m_k, s_{kz}; \dots; l_N, m_N, s_{Nz}) \\ &= \sum_{k=1}^N \{(l_k + m_k)(l_k - m_k + 1)\}^{1/2} \times \\ & \quad \times \Phi(n_1, l_1, m_1, s_{1z}; n_2, l_2, m_2, s_{2z}; \dots; n_k, l_k, m_k, (s_{kz} - 1); \dots; \\ & \quad l_N, m_N, s_{Nz}), \end{aligned}$$

where  $\Phi$  is a Slater determinant of spin-orbitals with quantum numbers  $n, l, m$ , and  $s_z$ , and  $S^-$  operating on a state with  $s_{kz} = -1/2$  gives zero. Use  $S^-$  on the  $S_z = 3/2$  state of (a) to generate the  $S_z = 1/2, -1/2$ , and  $-3/2$  states. (Note: The spin  $\pm 1/2$  states can not be separated into a single Slater determinant of spatial functions times a product of spin functions.)



## 5

### Electron spin and angular momentum

Unlike orbital angular momentum, the total spin of a system can be integral or half-integral. Fermions such as electrons, positrons, neutrinos, and quarks possess intrinsic angular momentum or spin with a measurable value of  $\pm 1/2$  (in units of  $\hbar$ ). Composite particles such as protons and neutrons also have measurable spin of  $\pm 1/2$  and atomic nuclei can have half-integral spin values ( $1/2, 3/2, 5/2, \dots$ ). The “spinor” function for half-integral spin is unusual in that rotation by  $2\pi$  transforms it into the negative of itself. A rotation by  $4\pi$  is required in order to transform the spin function into itself. While this may at first glance seem unreasonable, there are simple examples that display this property.

Take a strip of paper and form a Möbius strip by twisting one end  $180^\circ$  and joining it to the other end. Start at any point on the strip and trace a line through  $360^\circ$ . You do not end up at the starting point, but rather on the other side of the paper strip, as shown in Fig. 5.1. Continue tracing along the surface for another  $360^\circ$  and you will return to the original starting point.

Early spectroscopic experiments on hydrogen and hydrogen-like atoms revealed that there were twice as many states as predicted by the solutions of Schrödinger’s equation. The idea that an electron could have intrinsic angular momentum (spin) with two possible states was proposed by Kronig, Uhlenbeck, and Goudsmit [5.1] in 1925. Later, Dirac [5.2] developed a theory revealing that spin was a natural consequence of requiring the electron wavefunction to be consistent with relativity theory.

#### 5.1 Pauli spin matrices

The spin state of an electron can be represented as a two-component spinor. The Pauli matrices [5.3] for spin  $1/2$  are matrices that represent the three-dimensional spin-vector operator in terms of matrices that operate on the two-component

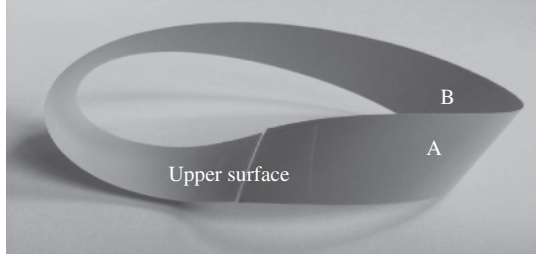


Figure 5.1 Consider a paper model of a Möbius strip. On the right-hand side of the paper, mark the upper surface with an A and the other side of the paper with a B. Starting from A, trace a line through  $360^\circ$  counter-clockwise on the Möbius strip, arriving at B on the other side of the paper. To return to A requires another  $360^\circ$  around the Möbius strip.

spinors. The Pauli  $\sigma$ -matrices are related to the spin-vector operator by  $\mathbf{s}_x = (\hbar/2)\sigma_x$ ,  $\mathbf{s}_y = (\hbar/2)\sigma_y$ , and  $\mathbf{s}_z = (\hbar/2)\sigma_z$ , where

$$\sigma_x = \begin{pmatrix} 0 & 1 \\ 1 & 0 \end{pmatrix}, \quad (5.1)$$

$$\sigma_y = \begin{pmatrix} 0 & -i \\ i & 0 \end{pmatrix}, \quad (5.2)$$

$$\sigma_z = \begin{pmatrix} 1 & 0 \\ 0 & -1 \end{pmatrix}. \quad (5.3)$$

The Pauli matrices anticommute, meaning that  $\sigma_i\sigma_j + \sigma_j\sigma_i = \{\sigma_i, \sigma_j\} = 0$  for  $i \neq j$ . For  $i = j$ ,  $\{\sigma_i, \sigma_j\} = 2I$ , where  $I$  is the unit matrix.

The eigenvectors of Pauli matrices correspond to the spin states with the spin vector aligned parallel or antiparallel to the direction of the  $x$ ,  $y$ , or  $z$  spatial axis. The spin eigenvalues are always  $\pm(\hbar/2)$ . This is easily verified by diagonalizing the  $\sigma$ -matrices. The eigenvectors and eigenvalues of  $s_x$ ,  $s_y$ , and  $s_z$  are

$$\chi_x^+ = \frac{1}{\sqrt{2}} \begin{pmatrix} 1 \\ 1 \end{pmatrix}, \text{ eigenvalue } +\frac{1}{2}, \text{ spin aligned along the } +x\text{-axis}, \quad (5.4)$$

$$\chi_x^- = \frac{1}{\sqrt{2}} \begin{pmatrix} 1 \\ -1 \end{pmatrix}, \text{ eigenvalue } -\frac{1}{2}, \text{ spin aligned along the } -x\text{-axis}, \quad (5.5)$$

$$\chi_y^+ = \frac{1}{\sqrt{2}} \begin{pmatrix} 1 \\ i \end{pmatrix}, \text{ eigenvalue } +\frac{1}{2}, \text{ spin aligned along the } +y\text{-axis}, \quad (5.6)$$

$$\chi_y^- = \frac{1}{\sqrt{2}} \begin{pmatrix} 1 \\ -i \end{pmatrix}, \text{ eigenvalue } -\frac{1}{2}, \text{ spin aligned along the } -y\text{-axis}, \quad (5.7)$$

$$\chi_z^+ = \frac{1}{\sqrt{2}} \begin{pmatrix} 1 \\ 0 \end{pmatrix}, \text{ eigenvalue } +\frac{1}{2}, \text{ spin aligned along the } +z\text{-axis}, \quad (5.8)$$

$$\chi_z^- = \frac{1}{\sqrt{2}} \begin{pmatrix} 0 \\ 1 \end{pmatrix}, \text{ eigenvalue } -\frac{1}{2}, \text{ spin aligned along the } -z\text{-axis}. \quad (5.9)$$

For example,

$$\mathbf{s}_x \chi_x^- = \frac{\hbar}{2} \frac{1}{\sqrt{2}} \begin{pmatrix} 0 & 1 \\ 1 & 0 \end{pmatrix} \begin{pmatrix} 1 \\ -1 \end{pmatrix} = \frac{\hbar}{2} \frac{1}{\sqrt{2}} \begin{pmatrix} -1 \\ 1 \end{pmatrix} = -\frac{\hbar}{2} \chi_x^-. \quad (5.10)$$

To determine the spin operator,  $\mathbf{s}_e$ , for rotated axes we construct the dot product (scalar product) of  $\mathbf{s}$  with a unit vector,  $\mathbf{e}$ , in any arbitrary direction,

$$\mathbf{s}_e = \mathbf{s} \cdot \mathbf{e} = (e_x \mathbf{s}_x + e_y \mathbf{s}_y + e_z \mathbf{s}_z) = \frac{\hbar}{2} \begin{pmatrix} e_z & e_x - ie_y \\ e_x + ie_y & -e_z \end{pmatrix}, \quad (5.11)$$

where  $e_x$ ,  $e_y$ , and  $e_z$  are the components of  $\mathbf{e}$  along the original  $x$ -,  $y$ -, and  $z$ -axes, respectively. Note that  $\mathbf{s}_e$  is shown in bold type because it is a (scalar) operator, but it is not a vector. The eigenvectors of  $\mathbf{s}_e$ , however, are two-component spinors, that is, vectors in Pauli spin-space.

The eigenvalues of  $\mathbf{s}_e$  are obtained by requiring the determinant of  $(\mathbf{s}_e - \lambda \mathbb{I})$  to vanish, where  $\mathbb{I}$  is the  $2 \times 2$  unit matrix. We obtain

$$\det \left\{ \frac{\hbar}{2} \begin{pmatrix} e_z - 2\lambda/\hbar & e_x - ie_y \\ e_x + ie_y & -e_z - 2\lambda/\hbar \end{pmatrix} \right\} = \left[ \lambda^2 - \left( \frac{\hbar}{2} \right)^2 (e_x^2 + e_y^2 + e_z^2) \right] = 0. \quad (5.12)$$

Since  $\mathbf{e}$  is a unit vector,  $(e_x^2 + e_y^2 + e_z^2) = 1$  and the eigenvalues are  $\lambda = \pm \hbar/2$ . Therefore, the eigenvalues of the electron's spin operator are always  $\pm \hbar/2$  regardless of the orientation of the axes. The eigenvectors of  $\mathbf{s}_e$  can be found in the usual way by inserting the eigenvalue into the secular equation and solving for the ratio of the two amplitudes. When normalized the eigenstates are

$$\chi_e^+ = \frac{1}{\sqrt{2(1-e_z)}} \begin{pmatrix} e_x - ie_y \\ 1 - e_z \end{pmatrix}, \quad (5.13)$$

$$\chi_e^- = \frac{1}{\sqrt{2(1+e_z)}} \begin{pmatrix} e_x - ie_y \\ -(1 + e_z) \end{pmatrix}. \quad (5.14)$$

Equations (5.13) and (5.14) are indeterminate when  $e_z = \pm 1$  (along the  $\pm z$ -axis). For these two exceptional cases we can simply use  $\chi_z^+$  and  $\chi_z^-$  given by (5.8) and (5.9), respectively.

To determine the eigenvalue of  $\mathbf{s}^2$  for a single electron, we note that  $s_x^2 = s_y^2 = s_z^2 = (\hbar/2)^2 \mathbb{I}$ , where  $\mathbb{I}$  is a  $2 \times 2$  unit matrix. Therefore,

$$\mathbf{s}^2 = \left( \frac{\hbar}{2} \right)^2 (\sigma_x^2 + \sigma_y^2 + \sigma_z^2) = 3 \left( \frac{\hbar}{2} \right)^2 \mathbb{I} = \hbar^2 \frac{1}{2} \left( \frac{1}{2} + 1 \right) \mathbb{I}.$$

It follows that  $\mathbf{s}^2 \chi = \hbar^2(1/2)(1/2 + 1)\chi$  for every one-electron spin state.

## 5.2 Measurement of spin

According to the generally accepted postulates of quantum theory, performing a measurement of the spin along a given direction causes the spin function to “collapse” into one of the two corresponding eigenstates for that direction. Suppose the spin was initially in the eigenstate  $\chi_I^s$ . After a measurement along the direction specified by the unit vector  $\mathbf{e}$  the probability of the state being  $\chi_e^+$  plus the probability of the state being  $\chi_e^-$  is unity. According to this postulate, the measurement process destroys the initial state and puts the spin into either  $\chi_e^+$  or  $\chi_e^-$ . In general, the individual probabilities for  $\chi_f^+$  and  $\chi_f^-$  depend upon the initial eigenstate and the direction of measurement, but the sum of the probability of  $+\hbar/2$  plus the probability of  $-\hbar/2$  along  $\mathbf{e}$  is always unity.

The probability that the spin of an electron will be  $\pm\hbar/2$  along the  $\mathbf{e}$ -axis (an arbitrary axis) is given by the absolute value of the square of the projection of the spin-eigenstate state  $\chi_I$  onto the eigenstate  $\chi_e^\pm$ . The probability of measuring  $\pm\hbar/2$  along the  $\mathbf{e}$ -direction when the spin was initially in the state  $\chi_I$  is

$$|\langle\chi_I|\chi_e^+\rangle|^2 + |\langle\chi_I|\chi_e^-\rangle|^2 = 1, \quad (5.15)$$

where

$$|\langle\chi_I|\chi_e^+\rangle|^2 = \text{Probability of the spin being parallel to } \mathbf{e}, \quad (5.16)$$

$$|\langle\chi_I|\chi_e^-\rangle|^2 = \text{Probability of the spin being antiparallel to } \mathbf{e}. \quad (5.17)$$

In equations (5.15)–(5.17)  $|\langle\chi_I|\chi_e^+\rangle|^2 = (\chi_{I1} \cdot \chi_{e1}^+)^2 + (\chi_{I2} \cdot \chi_{e2}^+)^2$ . For example, suppose  $\chi_I = \chi_z^+$  and we want the probability for the spin states along the direction  $\mathbf{e} = (1/3)^{1/2}(1, 1, 1)$ . According to (5.13) the eigenvector for the spin in the positive  $\mathbf{e}$ -direction is

$$\chi_e^+ = \frac{1}{\sqrt{2(1-e_z)}} \begin{pmatrix} e_x - ie_y \\ 1 - e_z \end{pmatrix} = \frac{1/\sqrt{3}}{\sqrt{2(1-1/\sqrt{3})}} \begin{pmatrix} 1-i \\ \sqrt{3}-1 \end{pmatrix}. \quad (5.18)$$

The probability *amplitude* is given by

$$\langle\chi_z^+|\chi_e^+\rangle = \frac{1/\sqrt{3}}{\sqrt{2(1-1/\sqrt{3})}} (1 \ 0) \begin{pmatrix} 1-i \\ \sqrt{3}-1 \end{pmatrix} = \frac{1/\sqrt{3}}{\sqrt{2(1-1/\sqrt{3})}} (1-i) \quad (5.19)$$

and the probability of measuring  $+\hbar/2$  is

$$|\langle\chi_z^+|\chi_e^+\rangle|^2 = \frac{2/3}{2(1-1/\sqrt{3})} = 0.788\,675. \quad (5.20)$$

A similar calculation shows that  $|\langle\chi_z^+|\chi_e^-\rangle|^2 = (2/3)/(2+2/\sqrt{3}) = 0.211\,325$ , so the probability of measuring either  $+\hbar/2$  or  $-\hbar/2$  along the  $(1,1,1)$  axis is unity.

In general the probability of measuring either  $+\hbar/2$  or  $-\hbar/2$  along any direction is unity.

It is evident that the probabilities are reciprocal since  $|\langle\chi_z^+|\chi_e^+\rangle|^2 = |\langle\chi_e^+|\chi_z^+\rangle|^2$ . The probability of measuring  $+\hbar/2$  along the  $+z$ -direction if the state was initially along the positive (1,1,1) direction is the same as the probability of measuring  $+\hbar/2$  along the (1,1,1) direction if the state was initially along the  $+z$ -axis.

If the spin is initially in an eigenstate along the direction  $\mathbf{e}$ , the probability of measuring  $\pm\hbar/2$  in a direction *perpendicular* to  $\mathbf{e}$  is always 1/2. For example, if the spin was initially in the state  $\chi_y^+$  the probability of measuring  $-\hbar/2$  along the  $x$ -axis is 1/2:

$$\langle\chi_y^+|\chi_x^-\rangle = \frac{1}{2}(1-i)\begin{pmatrix} 1 \\ -1 \end{pmatrix} = \frac{1}{2}(1-i), \quad (5.21)$$

$$|\langle\chi_y^+|\chi_x^-\rangle|^2 = \frac{1}{2}. \quad (5.22)$$

### 5.3 Irreducible representations of half-integer angular momentum

In Chapter 3 we discussed the  $D^{(l)}$  irreducible representations for the rotation group. The matrix elements of the IR for orbital momentum  $l$  are given by Theorem 3.3. In that discussion  $l$  was an integer and the basis functions were the spherical harmonic functions. The basis functions for half-integer momentum are the spinor functions. For spin-1/2 particles the basis functions are the two-component Pauli spinors. Even though the basis functions are not spherical harmonic functions, the formula for  $D^{(l)}$  remains valid, where now  $l$  is allowed to be integral or half-integral. For the spin  $J$  the rotation of the spin vector is achieved by applying the matrix  $D^{(J)}(\alpha, \beta, \gamma)$  to the spin function. For spin 1/2, the IR matrix is

$$D^{(1/2)}(\alpha, \beta, \gamma) = \begin{pmatrix} e^{i\alpha/2} \cos(\beta/2) e^{i\gamma/2} & e^{i\alpha/2} \sin(\beta/2) e^{-i\gamma/2} \\ -e^{-i\alpha/2} \sin(\beta/2) e^{i\gamma/2} & e^{-i\alpha/2} \cos(\beta/2) e^{-i\gamma/2} \end{pmatrix}. \quad (5.23)$$

(Note that the labeling of the matrix is  $D_{11}^{(1/2)} = D_{+1/2, +1/2}^{(1/2)}$ ,  $D_{12}^{(1/2)} = D_{+1/2, -1/2}^{(1/2)}$ ,  $D_{21}^{(1/2)} = D_{-1/2, +1/2}^{(1/2)}$ , and  $D_{22}^{(1/2)} = D_{-1/2, -1/2}^{(1/2)}$ . The matrix is often written with the rows and columns interchanged from this choice. The matrix of (5.23) rotates the function clockwise. Other texts give the matrix for a “positive” rotation, namely a counter-clockwise rotation.) We define the operator  $O_R = P_R Q_R$ , where  $P_R$  is our previous operator that operates on the spatial coordinates and  $Q_R$  operates on the spin vector. A rotation of the state  $\phi(\mathbf{r}) \chi(\mathbf{s})$  is given by

$$O_R \phi(\mathbf{r}) \chi(\mathbf{s}) = P_R \phi(\mathbf{r}) Q_R \chi(\mathbf{s}) = \phi(R^{-1}\mathbf{r}) D^{(1/2)}(R) \chi(\mathbf{s}). \quad (5.24)$$

Consider a rotation by  $\beta$  about the  $y$ -axis. The result is

$$P_{(0,\beta,0)} \phi(\mathbf{r}) D^{(1/2)}(0, \beta, 0) \chi(\mathbf{s}) = \phi(R(\beta)^{-1} \mathbf{r}) D^{(1/2)}(0, \beta, 0) \chi(\mathbf{s}), \quad (5.25)$$

where  $R(\beta)^{-1}$  is a rotation about the  $y$ -axis by an angle  $\beta$  in a clockwise sense. The transformation of an arbitrary spin state due a rotation by  $\beta$  is

$$\begin{aligned} D^{(1/2)}(0, \beta, 0) \chi(s) &= \begin{pmatrix} \cos(\beta/2) & \sin(\beta/2) \\ -\sin(\beta/2) & \cos(\beta/2) \end{pmatrix} \begin{pmatrix} a \\ b \end{pmatrix} \\ &= \begin{pmatrix} a \cos(\beta/2) + b \sin(\beta/2) \\ -a \sin(\beta/2) + b \cos(\beta/2) \end{pmatrix}, \end{aligned} \quad (5.26)$$

where  $|a|^2 + |b|^2 = 1$ . For the spin state  $\chi_z^+$ ,  $a = 1$  and  $b = 0$ , so the rotated state,  $\chi_\beta$ , is

$$\chi_\beta = \begin{pmatrix} \cos(\beta/2) \\ -\sin(\beta/2) \end{pmatrix}. \quad (5.27)$$

The probability of measuring  $+\hbar/2$  along the rotated vector direction is

$$|\langle \chi_z^+ | \chi_\beta \rangle|^2 = \cos^2 \left( \frac{\beta}{2} \right), \quad (5.28)$$

and the probability of measuring  $-\hbar/2$  along the rotated vector is  $\sin^2(\beta/2)$ . For the state  $\chi_z^-$  we have  $a = 0$  and  $b = -1$ , and the rotated vector is

$$\chi_\beta = \begin{pmatrix} -\sin(\beta/2) \\ \cos(\beta/2) \end{pmatrix}, \quad (5.29)$$

$$|\langle \chi_z^+ | \chi_\beta \rangle|^2 = \sin^2 \left( \frac{\beta}{2} \right), \quad (5.30)$$

$$|\langle \chi_z^- | \chi_\beta \rangle|^2 = \cos^2 \left( \frac{\beta}{2} \right). \quad (5.31)$$

In general, we can write  $|\langle \chi^\pm | D^{(1/2)}(R) | \chi^\pm \rangle|^2$  as the probability of measuring  $\pm\hbar/2$  along the direction of the rotated vector,  $D^{(1/2)}(R) \chi^\pm$ , if the spin eigenstate was  $\chi^\pm$  before rotation, where  $R$  represents the rotation in terms of the Euler angles,  $\alpha$ ,  $\beta$ , and  $\gamma$ . In some cases, it is easier to specify the rotation in terms of the components of  $\mathbf{e}$  rather than in terms of the Euler angles.

The combination of the Pauli matrices  $(\sigma_x + i\sigma_y)/2 \equiv \sigma^+$  is a spin-raising operator. When acting on  $\chi_z^-$  it produces the state  $\chi_z^+$ . When acting on  $\chi_z^+$  it produces a null state,

$$\sigma^+ = \begin{pmatrix} 0 & 1 \\ 0 & 0 \end{pmatrix}, \quad (5.32)$$

and

$$\begin{pmatrix} 0 & 1 \\ 0 & 0 \end{pmatrix} \begin{pmatrix} 0 \\ 1 \end{pmatrix} = \begin{pmatrix} 1 \\ 0 \end{pmatrix}, \quad (5.33)$$

$$\begin{pmatrix} 0 & 1 \\ 0 & 0 \end{pmatrix} \begin{pmatrix} 1 \\ 0 \end{pmatrix} = \begin{pmatrix} 0 \\ 0 \end{pmatrix}. \quad (5.34)$$

Similarly,  $\sigma^- \equiv (\sigma_x - i\sigma_y)/2$  lowers the spin. When operating on  $\chi_z^+$  it produces  $\chi_z^-$ . When operating on  $\chi_z^-$  it produces a null state,

$$\sigma^- = \begin{pmatrix} 0 & 0 \\ 1 & 0 \end{pmatrix}, \quad (5.35)$$

and

$$\begin{pmatrix} 0 & 0 \\ 1 & 0 \end{pmatrix} \begin{pmatrix} 1 \\ 0 \end{pmatrix} = \begin{pmatrix} 0 \\ 1 \end{pmatrix}, \quad (5.36)$$

$$\begin{pmatrix} 0 & 0 \\ 1 & 0 \end{pmatrix} \begin{pmatrix} 0 \\ 1 \end{pmatrix} = \begin{pmatrix} 0 \\ 0 \end{pmatrix}. \quad (5.37)$$

#### 5.4 Multi-electron spin–orbital states

For the Russell–Saunders or  $L$ – $S$  coupling scheme [5.4] the spins combine to form a total spin vector,  $\mathbf{S} = \sum \mathbf{s}_i$ , and the orbital angular momenta combine to form a total orbital angular momentum,  $\mathbf{L} = \sum \mathbf{l}_i$ . The basis states for a multi-electron system can be built up from products of one-electron orbitals and one-spin functions. Usually the spatial orbitals used are the hydrogen-like orbitals (spherical harmonic functions) and the spinors are the Pauli two-state functions discussed in Section 5.1. For the  $L$ – $S$  scheme the built-up functions for the angular and spin variables are constructed so that they are eigenfunctions of the operators  $\mathbf{L}_z$ ,  $\mathbf{L}^2$ ,  $\mathbf{S}_z$ , and  $\mathbf{S}^2$ . A multi-electron state is labeled by the eigenvalues of these operators. Such functions are eigenstates of the hydrogen-like Hamiltonian,  $\mathbb{H}^0$ . As a consequence, there are no non-zero matrix elements of  $\mathbb{H}^0$  between two states that differ in any of the eigenvalue labels. All angular-momentum operators have units of  $\hbar$  and the squared angular-momentum operator has units of  $\hbar^2$ . It is conventional to use a set of dimensionless operators defined as follows for the total angular momenta:

$$\mathbf{M}_s = \frac{1}{\hbar} \mathbf{S}_z, \quad \mathbf{M}_s^2 = \frac{1}{\hbar^2} \mathbf{S}^2, \quad (5.38)$$

$$\mathbf{M}_L = \frac{1}{\hbar} \mathbf{L}_z, \quad \mathbf{M}_L^2 = \frac{1}{\hbar^2} \mathbf{L}^2, \quad (5.39)$$

$$\mathbf{M}_J = \frac{1}{\hbar} \mathbf{J}_z, \quad \mathbf{M}_J^2 = \frac{1}{\hbar^2} \mathbf{J}^2. \quad (5.40)$$

Table 5.1 Notation for the operators and their eigenvalues used in this chapter. Bold symbols indicate operators. Non-bold symbols are numbers. Capitalized symbols refer to multi-electron operators and uncapitalized symbols to single electrons.

Operator	Eigenvalue
$\mathbf{M}_L^2 (\mathbf{L}^2/\hbar^2)$	$L(L + 1)$ , where $L$ is a positive integer
$\mathbf{M}_{L_z} (\mathbf{L}_z/\hbar)$	$M_L$ , a positive or negative integer
$\mathbf{m}_l^2 (\mathbf{l}^2/\hbar^2)$	$l(l + 1)$ , where $l$ is a positive integer
$\mathbf{m}_{l_z} (\mathbf{l}_z/\hbar)$	$m_l$ , a positive or negative integer
$\mathbf{M}_S^2 (\mathbf{S}^2/\hbar^2)$	$S(S + 1)$ , $S$ is a positive integer or half-integer
$\mathbf{M}_{S_z} (\mathbf{S}_z/\hbar)$	$M_S$ , a positive or negative integer or half-integer
$\mathbf{m}_{s^2} (\mathbf{s}^2/\hbar^2)$	$s(s + 1)$ , where $s = 1/2$
$\mathbf{m}_{s_z} (\mathbf{s}_z/\hbar)$	$m_s, \pm 1/2$
$\mathbf{M}_J^2 (\mathbf{J}^2/\hbar^2)$	$J(J + 1)$ , $J$ is a positive integer or half-integer
$\mathbf{M}_{J_z} (\mathbf{J}_z/\hbar)$	$M_J$ , a positive or negative integer or half-integer
$\mathbf{m}_j^2 (\mathbf{j}^2/\hbar^2)$	$j(j + 1)$ , $j$ is a positive integer or half-integer
$\mathbf{m}_{j_z} (\mathbf{j}_z/\hbar)$	$m_j$ , a positive or negative integer or half-integer

The notation for the single-electron operators is

$$\mathbf{m}_s = \frac{1}{\hbar} \mathbf{s}_z, \quad \mathbf{m}_s^2 = \frac{1}{\hbar^2} \mathbf{s}^2, \quad (5.41)$$

$$\mathbf{m}_l = \frac{1}{\hbar} \mathbf{l}_z, \quad \mathbf{m}_l^2 = \frac{1}{\hbar^2} \mathbf{l}^2, \quad (5.42)$$

$$\mathbf{m}_j = \frac{1}{\hbar} \mathbf{j}_z, \quad \mathbf{m}_j^2 = \frac{1}{\hbar^2} \mathbf{j}^2. \quad (5.43)$$

The notation for the operators and their eigenvalues is given in Table 5.1.

### 5.5 The $L$ – $S$ -coupling scheme

For the  $L$ – $S$  or Russel–Saunders coupling scheme [5.4], the multi-electron states are eigenstates of  $\mathbf{M}_L^2$ ,  $\mathbf{M}_{L_z}$ ,  $\mathbf{M}_S^2$ , and  $\mathbf{M}_{S_z}$ . The multi-electron states are built up from one-electron eigenstates of the operators,  $\mathbf{m}_l^2$ ,  $\mathbf{m}_{l_z}$ ,  $\mathbf{m}_s^2$ , and  $\mathbf{m}_s$ . These one-electron spin-orbitals are products of a hydrogen-like orbital function times a Pauli spin function.

Consider the product of  $N$ , one-electron spin-orbitals:

$$\Psi = \phi(\mathbf{r}_1, \mathbf{s}_1; n_1, m_{l_1}, m_{s_1}) \phi(\mathbf{r}_2, \mathbf{s}_2; n_2, m_{l_2}, m_{s_2}) \dots \phi(\mathbf{r}_N, \mathbf{s}_N; n_N, m_{l_N}, m_{s_N}), \quad (5.44)$$

where  $n$  is the radial or principal quantum number,  $\phi(\mathbf{r}, \mathbf{s}; n, m_l, m_s) = R_{nl} Y_l^{m_l} \chi_z(m_s)$ . The eigenvalue of  $\chi_z(m_s)$  is  $m_s$ . That is,  $\mathbf{m}_s \chi_z(m_s) = m_s \chi_z(m_s)$  and  $m_s$  can have the values  $\pm 1/2$ .



For our discussions in this section we can drop some of the labels and write the product of the  $N$  one-electron states as

$$\Psi = \phi(m_{l_1}, m_{s_1}; m_{l_2}, m_{s_2}; m_{l_3}, m_{s_3}; \dots; m_{l_N}, m_{s_N}). \quad (5.45)$$

As defined,  $\Psi$  is an eigenstate of the operators,  $\mathbf{m}_l$ ,  $\mathbf{m}_s$ ,  $\mathbf{M}_L$ , and  $\mathbf{M}_S$ ,

$$\mathbf{M}_L \Psi = M_L \Psi = \left( \sum m_{lk} \right) \Psi \quad (k = 1, 2, \dots, N), \quad (5.46)$$

$$\mathbf{M}_S \Psi = M_S \Psi = \left( \sum m_{sk} \right) \Psi \quad (k = 1, 2, \dots, N). \quad (5.47)$$

Usually,  $\Psi$  is not an eigenstate of  $\mathbf{M}_L^2$  or  $\mathbf{M}_S^2$  and it is necessary to construct a linear combination of such product states in order to obtain eigenstates.

A physically allowed multi-electron state must be antisymmetric in the interchange of any two different pairs of space-spin variables. One method of forming such an antisymmetric state is to use a Slater determinant,

$$\det\{\phi(m_{l_1}, m_{s_1}; m_{l_2}, m_{s_2}; m_{l_3}, m_{s_3}; \dots; m_{l_N}, m_{s_N})\} = \frac{1}{\sqrt{N!}} \times$$

$$\begin{vmatrix} \phi(\mathbf{r}_1, \mathbf{s}_1; n_1, m_{l_1}, m_{s_1}) & \phi(\mathbf{r}_1, \mathbf{s}_1; n_2, m_{l_2}, m_{s_2}) & \dots & \phi(\mathbf{r}_1, \mathbf{s}_1; n_N, m_{l_N}, m_{s_N}) \\ \phi(\mathbf{r}_2, \mathbf{s}_2; n_1, m_{l_1}, m_{s_1}) & \phi(\mathbf{r}_2, \mathbf{s}_2; n_2, m_{l_2}, m_{s_2}) & \dots & \phi(\mathbf{r}_2, \mathbf{s}_2; n_N, m_{l_N}, m_{s_N}) \\ \vdots & \vdots & \ddots & \vdots \\ \phi(\mathbf{r}_N, \mathbf{s}_N; n_1, m_{l_1}, m_{s_1}) & \phi(\mathbf{r}_N, \mathbf{s}_N; n_2, m_{l_2}, m_{s_2}) & \dots & \phi(\mathbf{r}_N, \mathbf{s}_N; n_N, m_{l_N}, m_{s_N}) \end{vmatrix}. \quad (5.48)$$

The coordinate variables  $\mathbf{r}$  and  $\mathbf{s}$  are constant across the rows, and the state labels are constant down the columns.

It is useful to introduce antisymmetrization operator,  $\mathcal{A}$ , which is defined by its action on a product function:

$$\begin{aligned} \mathcal{A} \phi(m_{l_1}, m_{s_1}; m_{l_2}, m_{s_2}; m_{l_3}, m_{s_3}; \dots; m_{l_N}, m_{s_N}) \\ = \frac{1}{\sqrt{N!}} \det\{\phi(m_{l_1}, m_{s_1}; m_{l_2}, m_{s_2}; m_{l_3}, m_{s_3}; \dots; m_{l_N}, m_{s_N})\}. \end{aligned} \quad (5.49)$$

$\mathcal{A}$  commutes with all of the angular-momentum operators and this allows a great simplification. We can apply any of the angular-momentum operators to a product function and then apply  $\mathcal{A}$  to the result instead of having to work with the  $N!$  terms of the determinantal state. For example,

$$\begin{aligned} \mathbf{M}_L^2 \det\{\phi(m_{l_1}, m_{s_1}; m_{l_2}, m_{s_2}; m_{l_3}, m_{s_3}; \dots; m_{l_N}, m_{s_N})\} \\ = \mathbf{M}_L^2 \mathcal{A} \phi(m_{l_1}, m_{s_1}; m_{l_2}, m_{s_2}; m_{l_3}, m_{s_3}; \dots; m_{l_N}, m_{s_N}) \\ = \mathcal{A}\{\mathbf{M}_L^2 \phi(m_{l_1}, m_{s_1}; m_{l_2}, m_{s_2}; m_{l_3}, m_{s_3}; \dots; m_{l_N}, m_{s_N})\} \\ = \frac{1}{\sqrt{N!}} \det\{\mathbf{M}_L^2 \phi(m_{l_1}, m_{s_1}; m_{l_2}, m_{s_2}; m_{l_3}, m_{s_3}; \dots; m_{l_N}, m_{s_N})\}. \end{aligned} \quad (5.50)$$

Another method used to construct antisymmetrized wavefunctions is to use the product of an antisymmetric spatial state and a symmetric spin state or an antisymmetric spin state and a symmetric space state. In many instances the determinantal state can be factored into a product of a space times a spin function. A determinantal state with all spins parallel can be factored into an antisymmetric space function,  $\det[\phi_1(m_{l_1})\phi_2(m_{l_2})\dots\phi_N(m_{l_N})]$ , and a symmetric spin product,  $\sigma_1\sigma_2\dots\sigma_N$ , where all the  $\sigma_j$  are spin up or all are spin down. The two-electron state,  $(1/2)[\phi_a(1)\phi_a(2) \pm \phi_b(1)\phi_b(2)](\alpha_1\beta_2 - \beta_1\alpha_2)$ , is the product of a symmetrical space function times an antisymmetric spin function. This state can be obtained from two Slater determinants,

$$\begin{aligned} & \frac{1}{2}[\phi_a(1)\phi_a(2) \pm \phi_b(1)\phi_b(2)](\alpha_1\beta_2 - \beta_1\alpha_2) \\ &= \frac{1}{2}\{\det[\phi_a\alpha, \phi_a\beta] \pm \det[\phi_b\alpha, \phi_b\beta]\}. \end{aligned} \quad (5.51)$$

### Spin orientations in real space

In the discussions we have referred loosely to “spin-up” and “spin-down” states of an electron. However, it is worth noting that the  $\alpha$  (spin up) and  $\beta$  (spin down) eigenstates (1,0) and (0,1) do not correspond to spin vectors in real space that are aligned along the  $z$ -axis. For the  $\alpha$  state (1,0) is the eigenstate of the operator  $s_z$  with eigenvalue  $\hbar/2$ , and also the eigenstate of the operator  $\mathbf{s}^2$  with eigenvalue  $(1/2)(1/2 + 1)\hbar^2 = (3/4)\hbar^2$ . (1,0) is *not* an eigenstate of the operator  $\mathbf{s}$ . The magnitude  $|\mathbf{s}| = (3/4)^{1/2}\hbar$  and the magnitude of the component along the  $z$ -axis is  $\hbar/2$ . Therefore the spin vector in real space makes an angle with the  $z$ -axis given by  $(3/4)^{1/2} \cos \theta = 1/2$  or  $\theta = \cos^{-1}(1/\sqrt{3}) = 54.74^\circ$ .

We have spoken also of “parallel” and “antiparallel” two-electron spin states, for example,  $\alpha_1\alpha_2$  or  $\alpha_1\beta_2$ . For two  $L$ - $S$ -coupled spins, the state  $\alpha_1\alpha_2$  does not correspond to the spin vectors being parallel in real space. We have  $\mathbf{S} = \mathbf{s}_1 + \mathbf{s}_2$  and  $\mathbf{S}^2 = \mathbf{s}_1^2 + \mathbf{s}_2^2 + 2\mathbf{s}_1 \cdot \mathbf{s}_2 = \mathbf{s}_1^2 + \mathbf{s}_2^2 + 2|\mathbf{s}_1||\mathbf{s}_2|\cos\varphi$ , where  $\varphi$  is the angle between the real-space vectors  $\mathbf{s}_1$  and  $\mathbf{s}_2$ . Thus  $\cos\varphi = [\mathbf{S}^2 - (\mathbf{s}_1^2 + \mathbf{s}_2^2)]/(2|\mathbf{s}_1||\mathbf{s}_2|) = 1/3$ . This result gives  $\varphi = 70.53^\circ$ . On the other hand, for “antiparallel” spins,  $\mathbf{S}^2 = 0$ , so  $\cos\varphi = -1$  or  $\varphi = \pi$ . Therefore the real-space spins are actually antiparallel.

## 5.6 Generating angular-momentum eigenstates

We shall use the notation  $(m_{l1}, m_{s1}; m_{l2}, m_{s2}; m_{l3}, m_{s3}; \dots; m_{lN}, m_{sN})$  to indicate the product state,  $\Pi_p \phi(m_{lp}, m_{sp}) = \phi(m_{l1}, m_{s1}; m_{l2}, m_{s2}; m_{l3}, m_{s3}; \dots; m_{lN}, m_{sN})$ , and  $|m_{l1}, m_{s1}; m_{l2}, m_{s2}; m_{l3}, m_{s3}; \dots; m_{lN}, m_{sN}\rangle$  to represent the determinantal state. By construction, both the product states and the determinantal states are eigenstates of  $\mathbf{M}_{S_z}$  and  $\mathbf{M}_{L_z}$ ,

Table 5.2 Raising and lowering operators

Operator	Effect of operator
$\mathbf{m}_{sk}^{\pm} = (\mathbf{s}_{xk} \pm i\mathbf{s}_{yk})/\hbar$	$\mathbf{m}_{sk}^{\pm} \phi(m_{lk}, m_{sk}) = \phi(m_{lk}, m_{sk} \pm 1) \delta(m_{sk}, \mp 1/2)$
$\mathbf{M}_S^{\pm} = \sum_k \mathbf{m}_{sk}^{\pm}$	$\mathbf{M}_S^{\pm} \Pi_p \phi(m_{lp}, m_{sp}) = \sum_k \Pi_{p \neq k} \phi(m_{lp}, m_{sp}) \times \phi(m_{lk}, m_{sk} \pm 1) \delta(m_{sk}, \mp 1/2)$
Also	$\mathbf{M}_S^{\pm} \Phi(L, S, M_L, M_S) = \sqrt{(S \mp M_S)(S \pm M_S + 1)} \times \Phi(L, S, M_L, M_S \pm 1)$
$\mathbf{m}_{lk}^{\pm} = (\mathbf{l}_{xk} \pm i\mathbf{l}_{yk})/\hbar$	$\mathbf{m}_{lk}^{\pm} \phi(m_{lk}, m_{sk}) = \sqrt{(l \mp m_{lk})(l \pm m_{lk} + 1)} \phi(m_{lk} \pm 1, m_{sk})$
$\mathbf{M}_L^{\pm} = \sum_k \mathbf{m}_{lk}^{\pm}$	$\mathbf{M}_L^{\pm} \Pi_p \phi(m_{lp}, m_{sp}) = \sum_k \Pi_{p \neq k} \phi(m_{lp}, m_{sp}) \times \sqrt{(l \mp m_{lk})(l \pm m_{lk} + 1)} \times \phi(m_{lk} \pm 1, m_{sk})$
Also	$\mathbf{M}_L^{\pm} \Phi(L, S, M_L, M_S) = \sqrt{(L \mp M_L)(L \pm M_L + 1)} \times \Phi(L, S, M_L \pm 1, M_S)$
$\mathbf{m}_{jk}^{\pm} = (\mathbf{j}_{xk} \pm i\mathbf{j}_{yk})/\hbar$	$\mathbf{m}_{jk}^{\pm} \phi(m_{lk}, m_{sk}) = (\mathbf{m}_{lk}^{\pm} + \mathbf{m}_{sk}^{\pm}) \phi(m_{lk}, m_{sk})$
$\mathbf{M}_J^{\pm} = \sum_k \mathbf{m}_{jk}^{\pm}$	$\mathbf{M}_J^{\pm} \Pi_p \phi(m_{lp}, m_{sp}) = \sum_k (\mathbf{m}_{lk}^{\pm} + \mathbf{m}_{sk}^{\pm}) \Pi_{p \neq k} \phi(m_{lp}, m_{sp})$
Also	$\mathbf{M}_J^{\pm} \Phi(J, M_J) = \sqrt{(J \mp M_J)(J \pm M_J + 1)} \Phi(J, M_J \pm 1)$
$\Pi_p \phi(m_{lp}, m_{sp}) = \phi(m_{l1}, m_{s1}; m_{l1}, m_{s1}; \dots; m_{lN}, m_{sN})$ $= \phi(m_{l1}, m_{s1}) \phi(m_{l2}, m_{s2}) \dots \phi(m_{lN}, m_{sN})$	
$\Phi(L, S, M_L, M_S)$ is a properly normalized $LS$ eigenstate $\Phi(J, M_J)$ is a properly normalized $JM$ eigenstate	

$$\mathbf{M}_{S_z} \Psi = \left\{ \sum_k \mathbf{m}_{sk} \right\} \Psi = \left\{ \sum_k m_{sk} \right\} \Psi = M_S \Psi, \quad (5.52)$$

$$\mathbf{M}_{L_z} \Psi = \left\{ \sum_k \mathbf{m}_{lk} \right\} \Psi = \left\{ \sum_k m_{lk} \right\} \Psi = M_L \Psi, \quad (5.53)$$

where  $\Psi$  is the product state  $\phi(m_{l1}, m_{s1}; m_{l2}, m_{s2}; m_{l3}, m_{s3}; \dots; m_{lN}, m_{sN})$  or the determinantal state  $|m_{l1}, m_{s1}; m_{l2}, m_{s2}; m_{l3}, m_{s3}; \dots; m_{lN}, m_{sN}\rangle$ .

### Raising and lowering operators

The angular-momentum-raising and -lowering operators are defined in Table 5.2. We have

$$\mathbf{m}_{sk}^{\pm}(m_{lk}, m_{sk}) = (m_{lk}, (m_{sk} \pm 1)), \quad (5.54)$$

with the understanding that a state with spin  $> 1/2$  or spin  $< -1/2$  is a null state.

$\mathbf{M}_s^2$  can be expressed in terms of the one-electron raising and lowering operators

$$\begin{aligned}\mathbf{M}_s^2 &= \left( \sum_k \mathbf{m}_{sk} \right) \cdot \left( \sum_{k'} \mathbf{m}_{sk'} \right) \\ &= \sum_k (m_{sk})^2 + \sum_k \sum_{k' \neq k} \left\{ m_{sk} m_{sk'} + \frac{1}{2} (\mathbf{m}_{sk}^+ \mathbf{m}_{sk'}^- + \mathbf{m}_{sk}^- \mathbf{m}_{sk'}^+) \right\},\end{aligned}\quad (5.55)$$

where the sum is over the  $N$  electrons,  $k = 1$  to  $N$  and  $k' = 1$  to  $N$  for the double summation.

With the aid of (5.55) we can operate on a determinantal state with  $\mathbf{M}_s^2$ ,

$$\begin{aligned}\mathbf{M}_s^2 |m_{l1}, m_{s1}; m_{l2}, m_{s2}; \dots; m_{lN}, m_{sN}\rangle \\ &= \left\{ N \left( \frac{3}{4} \right) + \sum_{k'} \sum_{k > k'} 2m_{sk} m_{sk'} \right\} |m_{l1}, m_{s1}; m_{l2}, m_{s2}; \dots; m_{lN}, m_{sN}\rangle \\ &+ \sum_{k, k' < k} |m_{l1}, m_{s1}; m_{l2}, m_{s2}; \dots; m_{lk}, m_{sk+1}; \dots; m_{lk'}, m_{sk'-1}; \dots; m_{lN}, m_{sN}\rangle \\ &+ \sum_{k, k' < k} |m_{l1}, m_{s1}; m_{l2}, m_{s2}; \dots; m_{lk}, m_{sk-1}; \dots; m_{lk'}, m_{sk'+1}; \dots; m_{lN}, m_{sN}\rangle,\end{aligned}\quad (5.56)$$

where  $(m_{lk}, m_{sk} \pm 1)$  indicates that the spin is raised (lowered) by one unit.

For two electrons,

$$\mathbf{M}_s^2 = 2 \left( \frac{3}{4} \right) + 2m_{s1} m_{s2} + (\mathbf{m}_{s1}^+ \mathbf{m}_{s2}^- + \mathbf{m}_{s1}^- \mathbf{m}_{s2}^+) \quad (5.57)$$

and

$$\begin{aligned}\mathbf{M}_s^2 |m_{l1}, m_{s1}; m_{l2}, m_{s2}\rangle &= \left( \frac{3}{2} + 2m_{s1} m_{s2} \right) |m_{l1}, m_{s1}; m_{l2}, m_{s2}\rangle \\ &+ |m_{l1}, (m_{s1} + 1); m_{l2}, (m_{s2} - 1)\rangle \\ &+ |m_{l1}, (m_{s1} - 1); m_{l2}, (m_{s2} + 1)\rangle.\end{aligned}\quad (5.58)$$

For three electrons the operator is

$$\begin{aligned}\mathbf{M}_s^2 &= 3 \left( \frac{3}{4} \right) + (2m_{s1} m_{s2} + 2m_{s1} m_{s3} + 2m_{s2} m_{s3}) \\ &+ (\mathbf{m}_{s1}^+ \mathbf{m}_{s2}^- + \mathbf{m}_{s1}^- \mathbf{m}_{s2}^+) + (\mathbf{m}_{s1}^+ \mathbf{m}_{s3}^- + \mathbf{m}_{s1}^- \mathbf{m}_{s3}^+) \\ &+ (\mathbf{m}_{s2}^+ \mathbf{m}_{s3}^- + \mathbf{m}_{s2}^- \mathbf{m}_{s3}^+).\end{aligned}\quad (5.59)$$

In a similar fashion we can express the operator  $\mathbf{M}_L^2$  in terms of the one-electron operators. We define the orbital raising and lowering operators by

$$\mathbf{m}_{lk}^{\pm} = \frac{\mathbf{l}_x \pm i\mathbf{l}_y}{\hbar}. \quad (5.60)$$

Their action on a one-electron state according to Table 5.2 is

$$\mathbf{m}_{lk}^{-}(m_{lk}, m_{sk}) = \sqrt{(l_k + m_{lk})(l_k - m_{lk} + 1)} ((m_{lk} - 1), m_{sk}), \quad (5.61)$$

$$\mathbf{m}_{lk}^{+}(m_{lk}, m_{sk}) = \sqrt{(l_k - m_{lk})(l_k + m_{lk} + 1)} ((m_{lk} + 1), m_{sk}). \quad (5.62)$$

Also,

$$\mathbf{m}_{lk}^2(m_{lk}, m_{sk}) = l_k(l_k + 1)(m_{lk}, m_{sk}). \quad (5.63)$$

The value of  $l_k$  appearing on the right-hand side of (5.60)–(5.62) is the value of the angular-momentum quantum number of  $Y_l^m$  from which  $(m_{lk}, m_{sk})$  is constructed. For example, if the one-electron orbital,  $\phi_k$ , is for a  $d$ -electron state, then  $l_k = 2$ . Using these one-electron operators, we find that

$$\begin{aligned} \mathbf{M}_L^2 &= \left( \sum_k \mathbf{m}_{lk} \right) \cdot \left( \sum_{k'} \mathbf{m}_{lk'} \right) \\ &= \sum_k (m_{lk})^2 + \sum_k \sum_{k' \neq k} \left\{ 2m_{lk}m_{lk'} + \frac{1}{2}(\mathbf{m}_{lk}^{+}\mathbf{m}_{lk'}^{-} + \mathbf{m}_{lk}^{-}\mathbf{m}_{lk'}^{+}) \right\}. \end{aligned} \quad (5.64)$$

For two electrons (5.64) gives

$$\begin{aligned} \mathbf{M}_L^2 |m_{l1}, m_{s1}; m_{l2}, m_{s2}\rangle &= \{l_1(l_1 + 1) + l_2(l_2 + 1) + 2(m_{l1}m_{l2})\} |m_{l1}, m_{s1}; m_{l2}, m_{s2}\rangle \\ &\quad + \sqrt{(l_1 - m_{l1})(l_1 + m_{l1} + 1)} |(m_{l1} + 1), m_{s1}; (m_{l2} - 1), m_{s2}\rangle \\ &\quad + \sqrt{(l_2 + m_{l2})(l_2 - m_{l2} + 1)} |(m_{l1} - 1), m_{s1}; (m_{l2} + 1), m_{s2}\rangle. \end{aligned} \quad (5.65)$$

### 5.6.1 Russell–Saunders ( $L$ – $S$ ) states

For this coupling scheme, the orbital momenta of the electrons combine to form a total  $\mathbf{L} = \sum \mathbf{l}_k$  and the spins combine to form a total  $\mathbf{S} = \sum \mathbf{s}_k$ . Table 5.2 defines the raising and lowering operators that operate on the product of states or determinantal states,

$$\mathbf{M}_S^{-} = \sum_k \mathbf{m}_{sk}^{-}, \quad (5.66)$$

$$\mathbf{M}_L^{-} = \sum_k \mathbf{m}_{lk}^{-}. \quad (5.67)$$

Let  $\Phi(L, S, M_L, M_S)$  be an eigenstate of the operators  $\mathbf{L}^2$ ,  $\mathbf{S}^2$ ,  $\mathbf{L}_z$ , and  $\mathbf{S}_z$ , with eigenvalues  $L(L+1)$ ,  $S(S+1)$ ,  $M_L$ , and  $M_S$ , respectively.  $\Phi(L, S, M_L, M_S)$  may be a determinantal state or a linear combination of determinantal states. According to Table 5.2, we have

$$\mathbf{M}_S^- \Phi(L, S, M_L, M_S) = \sqrt{(S+M_S)(S-M_S+1)} \Phi(L, S, M_L, M_S-1), \quad (5.68)$$

where  $\Phi(L, S, M_L, M_S-1)$  is a properly normalized eigenstate whose  $M_S$  is lowered by 1. If we operate with  $\mathbf{M}_L^-$ ,

$$\mathbf{M}_L^- \Phi(L, S, M_L, M_S) = \sqrt{(L+M_L)(L-M_L+1)} \Phi(L, S, M_L-1, M_S), \quad (5.69)$$

where  $\Phi(L, S, M_L-1, M_S)$  is a properly normalized eigenstate with the  $M_L$  lowered by one unit. The operators  $\mathbf{M}_S^-$  and  $\mathbf{M}_L^-$  allow us to generate all of the levels of a given term. For example, consider a set of three equivalent  $d$ -electrons. The highest spin state with the highest  $M_L$  will have an  $m_{l1} = 2, m_{s1} = +1/2, m_{l2} = 1, m_{s2} = +1/2, m_{l3} = 0, m_{s3} = +1/2$  state. We simplify our notation so that  $|2^+1^+0^+\rangle$  represents the corresponding determinantal state, where the numbers are the  $m_l$  values and  $\pm$  indicates the spin state,  $\pm\hbar/2$ . Using the operators in the previous section, we find that  $|2^+1^+0^+\rangle$  is an eigenstate with  $L = 3, S = 3/2, M_L = 3$ , and  $M_S = 3/2$ . Using the notation  ${}^4F(L, M_L, S, M_S)$ , this particular state is  ${}^4F(3, 3, 3/2, 3/2)$ .<sup>1</sup>

To generate the  $2S+1$  spin states (all with  $L = 3$  and  $S = 3/2$ ), we operate on  $|2^+1^+0^+\rangle$  with  $\mathbf{M}_S^-$ . Using Table 5.2, we obtain

$$\begin{aligned} \mathbf{M}_S^- [{}^4F(3, 3, 3/2, 3/2)] &= \sqrt{3} {}^4F(3, 3, 3/2, 1/2) = \sum_k \mathbf{m}_{sk}^- |2^+1^+0^+\rangle \\ &= [|2^-1^+0^+\rangle + |2^+1^-0^+\rangle + |2^+1^+0^-\rangle]. \end{aligned} \quad (5.70)$$

Hence,

$${}^4F(3, 3, 3/2, 1/2) = \frac{1}{\sqrt{3}} [|2^-1^+0^+\rangle + |2^+1^-0^+\rangle + |2^+1^+0^-\rangle]. \quad (5.71)$$

Each application of  $\mathbf{M}_S^-$  reduces  $M_S$  by 1:

$$\mathbf{M}_S^- [{}^4F(3, 3, 3/2, 1/2)] = 2 [{}^4F(3, 3, 3/2, -1/2)].$$

Also,

$$\mathbf{M}_S^- [{}^4F(3, 3, 3/2, 1/2)] = \sum_k \mathbf{m}_{sk}^- \frac{1}{\sqrt{3}} \left\{ |2^-1^+0^+\rangle + |2^+1^-0^+\rangle + |2^+1^+0^-\rangle \right\}$$

<sup>1</sup> Note that the order of  $L, M_L, S$ , and  $M_S$  in  ${}^4F(L, M_L, S, M_S)$  is different from that used for  $\Phi(L, S, M_L, M_S)$ .

$$= \frac{1}{\sqrt{3}} \left\{ 2|2^-1^-0^+\rangle + 2|2^-1^+0^-\rangle + 2|2^+1^-0^-\rangle \right\}; \quad (5.72)$$

therefore

$${}^4F(3, 3, 3/2, -1/2) = \frac{1}{\sqrt{3}} \left\{ |2^-1^-0^+\rangle + |2^-1^+0^-\rangle + |2^+1^-0^-\rangle \right\}. \quad (5.73)$$

Then

$$\begin{aligned} \mathbf{M}_S^- [{}^4F(3, 3, 3/2, -1/2)] &= 3[{}^4F(3, 3, 3/2, -3/2)] \\ &= \sum_k \mathbf{m}_{sk}^- \frac{1}{\sqrt{3}} \left\{ |2^-1^-0^+\rangle + |2^-1^+0^-\rangle + |2^+1^-0^-\rangle \right\} \\ &= \frac{1}{\sqrt{3}} \{ 3|2^-1^-0^-\rangle \}, \end{aligned} \quad (5.74)$$

and therefore

$${}^4F(3, 3, 3/2, -3/2) = |2^-1^-0^-\rangle. \quad (5.75)$$

To generate the  $2L + 1$  orbital states (all with  $L = 3$  and  $S = 3/2$ ) we apply  $\mathbf{M}_L^-$  to the eigenstate  $|2^+1^+0^+\rangle$ :

$$\begin{aligned} \mathbf{M}_L^- [{}^4F(3, 3, 3/2, 3/2)] &= \sqrt{6}[{}^4F(3, 2, 3/2, 3/2)] = \sum_k \mathbf{m}_{lk}^- |2^+1^+0^+\rangle \\ &= \{ 2|1^+1^+0^+\rangle + \sqrt{6}|2^+0^+0^+\rangle + \sqrt{6}|2^+1^+-1^+\rangle \}. \end{aligned} \quad (5.76)$$

The determinantal states  $|1^+1^+0^+\rangle$  and  $|2^+0^+0^+\rangle$  vanish, since each has two identical rows; therefore

$${}^4F(3, 2, 3/2, 3/2) = |2^+1^+-1^+\rangle. \quad (5.77)$$

A second application of  $\mathbf{M}_L^-$  gives

$$\begin{aligned} \mathbf{M}_L^- [{}^4F(3, 2, 3/2, 3/2)] &= \sqrt{10}[{}^4F(3, 1, 3/2, 3/2)] = \sum_k \mathbf{m}_{lk}^- |2^+1^+-1^+\rangle \\ &= \left\{ 2|2^+1^+-2^+\rangle + \sqrt{6}|2^+0^+-1^+\rangle \right\}, \end{aligned} \quad (5.78)$$

so that

$${}^4F(3, 1, 3/2, 3/2) = \left\{ \sqrt{\frac{3}{5}}|2^+0^+-1^+\rangle + \sqrt{\frac{2}{5}}|2^+1^+-2^+\rangle \right\} \quad (5.79)$$

Continuing this process gives

$${}^4F(3, 0, 3/2, 3/2) = \frac{1}{\sqrt{5}}|1^+0^+-1^+\rangle + \sqrt{\frac{4}{5}}|2^+0^+-2^+\rangle, \quad (5.80)$$

$${}^4F(3, -1, 3/2, 3/2) = \sqrt{\frac{3}{5}}|1^+0^+-2^+\rangle + \sqrt{\frac{2}{5}}|2^+-1^+-2^+\rangle, \quad (5.81)$$

$$\begin{aligned} {}^4F(3, -2, 3/2, 3/2) &= \left( \sqrt{\frac{18}{50}} + \sqrt{\frac{8}{50}} \right) |1^+-1^+-2^+\rangle \\ &= |1^+-1^+-2^+\rangle, \end{aligned} \quad (5.82)$$

$${}^4F(3, -3, 3/2, 3/2) = |0^+-1^+-2^+\rangle. \quad (5.83)$$

All  $(2S+1)(2L+1) = 4 \times 7 = 28$  states of the  ${}^4F$  term can be generated in this manner by operating with both  $\mathbf{M}_L^-$  and  $\mathbf{M}_S^-$ . For example, to find the state  ${}^4F(3, -1, 3/2, 1/2)$  we can operate with  $\mathbf{M}_S^-$  on  ${}^4F(3, -1, 3/2, 3/2)$  or operate with  $\mathbf{M}_S^-\mathbf{M}_L^-$  on  ${}^4F(3, 0, 3/2, 3/2)$  to obtain

$$\begin{aligned} {}^4F(3, -1, 3/2, 1/2) &= \sqrt{\frac{3}{15}} \left\{ |1^-0^+-2^+\rangle + |1^+0^--2^+\rangle + |1^+0^+-2^-\rangle \right\} \\ &\quad + \sqrt{\frac{2}{15}} \left\{ |2^- - 1^+-2^+\rangle + |2^+-1^--2^+\rangle \right. \\ &\quad \left. + |2^+-1^+-2^-\rangle \right\}. \end{aligned} \quad (5.84)$$

## 5.7 Spin-orbit interaction

The spin-orbit effect in atomic physics arises from the interaction between the magnetic moment of the electron and the charge of the nucleus. A simple classical model serves to show how this interaction comes about. If one “sits” on the electron, the nuclear charge appears to be circling around the electron. The moving nuclear charge creates an electrical current that produces a magnetic field  $\mathbf{B} = -\mathbf{v} \times \mathbf{E}/c^2$ , where  $\mathbf{v}$  is the velocity of the electron and  $\mathbf{E}$  is the electric field due to the nuclear charge.  $\mathbf{E} = -\nabla_r V(r) = [-\partial V(r)/\partial r]\mathbf{r}/r$ , with  $V(r)$  being the electrostatic potential energy experienced by the electron due to the nuclear charge. In the case of a hydrogenic atom,  $V(r) = -Ze^2/r$ , where  $+Ze$  is the effective nuclear charge. For this case,  $[-\partial V(r)/\partial r]\mathbf{r}/r = (-Ze^2/r^2)\mathbf{r}/r$ . The angular momentum,  $\mathbf{L}$ , of the electron is given by  $\mathbf{L} = \mathbf{r} \times \mathbf{p} = m_e\mathbf{r} \times \mathbf{v}$ , so  $\mathbf{B} = 1/(m_e c^2)[(1/r)(\partial V(r)/\partial r)]\mathbf{L}$ . The magnetic moment of the electron is  $\mu_s = -(g_s\mu_B/\hbar)\mathbf{S}$ , where the  $g$ -factor,  $g_s$ , is approximately 2, and  $\mu_B$  is the



Bohr magneton. The interaction energy between the spin magnetic moment and the orbital magnetic field is

$$-\boldsymbol{\mu}_s \cdot \mathbf{B} = \mu_B \frac{g_s}{m_e c^2 \hbar} \frac{1}{r} \frac{\partial V(r)}{\partial r} \mathbf{L} \cdot \mathbf{S}. \quad (5.85)$$

This classical result differs from the correct result by a factor of 1/2. According to Dirac's relativistic quantum theory, the actual coefficient of  $\mathbf{L} \cdot \mathbf{S}$  is half that given in (5.85). For the  $N$ -electron case each electron spin interacts with its own orbit, so

$$\mathbb{H}_{\text{so}} = \sum_{k=1}^N \xi_{k(nl)}(r) \mathbf{l}_k \cdot \mathbf{s}_k, \quad (5.86)$$

$$\xi_k(r) = \frac{1}{2} \mu_B \frac{g_s}{m_e c^2 \hbar} \frac{1}{r} \frac{\partial V_k(r)}{\partial r}. \quad (5.87)$$

The result (5.86) includes only the interaction between an electron's spin and its own orbit. There are also interactions between a spin and another electron's orbital momentum. In most cases these "spin-other-orbit" interactions are much smaller than the "spin-same-orbit" interactions.

When the spin-orbit interaction is large, as it is with heavier atoms, the  $k$ th electron's spin couples with its own orbital momentum to form  $\mathbf{j}_k = \mathbf{l}_k + \mathbf{s}_k$ . For a multi-electron system,  $\mathbf{J} = \sum \mathbf{j}_k$ . As we shall show below, we can find linear combinations of one-electron spin-orbitals *that are eigenstates of  $\mathbf{j}^2$ ,  $\mathbf{l}^2$ ,  $\mathbf{s}^2$ , and  $\mathbf{j}_z$* . For these states the spin-orbit interaction is diagonal:

$$\mathbf{l}_k \cdot \mathbf{s}_k = \frac{\hbar^2}{2} [j_k(j_k + 1) - l_k(l_k + 1) - s_k(s_k + 1)]. \quad (5.88)$$

The energy associated with the spin-orbit interaction for a single-electron spin-orbital that is an eigenstate of  $\mathbf{j}^2$ ,  $\mathbf{l}^2$ , and  $\mathbf{s}^2$  is

$$\langle \mathbb{H}_{\text{so}} \rangle = \frac{\hbar^2}{2} \langle \xi_{nl} \rangle \{j(j + 1) - l(l + 1) - s(s + 1)\}, \quad (5.89)$$

where

$$\langle \xi_{nl} \rangle = \int |R_{nl}(r)|^2 \xi(r) r^2 dr. \quad (5.90)$$

The matrix elements of  $\mathbf{l} \cdot \mathbf{s}$  between states differing in any of the eigenvalues of  $\mathbf{j}^2$ ,  $\mathbf{l}^2$ ,  $\mathbf{s}^2$ , and  $\mathbf{j}_z$  vanish. From (5.89) we see that  $\langle \mathbb{H}_{\text{so}} \rangle$  is independent of the values of  $j_z$ ,  $l_z$ , and  $s_z$ . The factor  $\langle \xi_{nl} \rangle$  depends on the principal quantum number  $n$ , and on  $l$ .

For an  $N$ -electron system the spin-orbit interaction is

$$\langle \mathbb{H}_{\text{so}} \rangle = \sum_k \langle \xi_{k(nl)} \rangle \mathbf{l}_k \cdot \mathbf{s}_k = \frac{1}{2} \sum_k \langle \xi_{k(nl)} \rangle [\mathbf{j}_k^2 - \mathbf{l}_k^2 - \mathbf{s}_k^2], \quad (5.91)$$

and, for states for which  $j$ ,  $l$ , and  $s$  are “good” quantum numbers, the energy is

$$\langle \mathbb{H}_{\text{so}} \rangle = \frac{1}{2} \hbar^2 \sum_k \langle \xi_{k(nl)} \rangle \{ j_k(j_k + 1) - l_k(l_k + 1) - s_k(s_k + 1) \}. \quad (5.92)$$

### 5.7.1 Spin-orbit splitting of one-electron states

The eigenvalue of  $\mathbf{j}^2$  is  $j(j + 1)$ . For a single electron with orbital momentum  $l$ , the basis functions transform according to  $D^{(l)}$  and the spinor functions according to  $D^{(1/2)}$ ; therefore the spin-orbitals are the basis for the direct product  $D^{(l)} \times D^{(1/2)} = D^{(l-1/2)} + D^{(l+1/2)}$ . As a result,  $j$  can have two possible values, namely  $j = l + 1/2$  and  $j = l - 1/2$ , corresponding to  $\mathbf{s}$  parallel and antiparallel to  $\mathbf{l}$ . The spin-orbit energy,  $\langle \mathbb{H}_{\text{so}} \rangle$ , has two possible values, one for each eigenvalue of  $\mathbf{j}^2$ :

$$\begin{aligned} [\langle \mathbb{H}_{\text{so}} \rangle]^\pm &= \frac{\hbar^2}{2} \langle \xi_{nl} \rangle (l \pm 1/2) \{ (l \pm 1/2 + 1) - l(l + 1) - 3/4 \} \\ &= \frac{\hbar^2}{2} \langle \xi_{nl} \rangle [(l - 1/2) \pm 1/2]. \end{aligned} \quad (5.93)$$

For  $l = 0$  the spin-orbit interaction is zero, as may be seen from (5.88). Therefore each one-electron state with  $l > 0$  is split into two states by the spin-orbit interaction. This splitting is observed spectroscopically and is referred to as *fine structure*. For a hydrogenic atom the spin-orbit energy can be evaluated analytically. The result is that

$$\langle \mathbb{H}_{\text{so}} \rangle = A(n, l) Z^4 [j(j + 1) - l(l + 1) - s(s + 1)], \quad (5.94)$$

where

$$A(n, l) = \frac{\mu_0}{4\pi} \frac{n^3 a_0^3}{n^3 a_0^3} \frac{g_s \mu_B^2}{l(l + 1/2)(l + 1)}, \quad (5.95)$$

$n$  is the principal quantum number,  $l > 0$  is the angular-momentum quantum number,  $\mu_0$  is the permeability of vacuum ( $\mu_0/(4\pi) = 10^{-7} \text{ N/A}^2$ ), and  $a_0$  is the Bohr radius. The  $2p$  level ( $l = 1$ ) of hydrogen splits into  $j = 3/2$  and  $j = 1/2$  states with an energy separation of about  $4.5 \times 10^{-5} \text{ eV}$ .

### 5.7.2 $j$ - $m_j$ spin-orbitals

The one-electron spin-orbitals can be characterized by  $n$ ,  $l$ ,  $m_l$ , and  $m_s$ . We can also choose the quantum numbers  $n$ ,  $l$ ,  $j$ , and  $m_j$ . Multi-electron states can be built up from the latter spin-orbitals with the quantum numbers  $J$  and  $M_J$  (instead of  $L$  and  $M_L$ ). We have that  $\mathbf{M}_J^2 = (\sum \mathbf{m}_{jk})^2$  and  $\mathbf{M}_{Jz} = \sum \mathbf{m}_{jz} = \sum (\mathbf{m}_{lkz} + \mathbf{m}_{skz})$ , and, according to Table 5.1, the eigenvalues of  $\mathbf{M}_J^2$  and  $\mathbf{M}_{Jz}$  are  $J(J + 1)$  and  $M_J$ .

Our first task is to find one-electron states that are eigenstates of  $\mathbf{j}^2$ . The hydrogen-like spin-orbital  $\phi(n, l, m_l, m_s) = R_{nl}(r) Y_l^{m_l}(\theta, \phi) \gamma(s)$ , where  $n$  is the principal quantum number and  $l$  is the angular-momentum quantum number. The spinor function  $\gamma(s)$  is either  $\alpha$  (spin up or  $+$ ) or  $\beta$  (spin down or  $-$ ).  $\phi(n, l, m_l, m_s)$  is an eigenstate of  $\mathbf{j}_z$  but not of  $\mathbf{j}^2$ . The problem then comes down to finding linear combinations of these spin-orbitals that are eigenfunctions of  $\mathbf{j}^2$ . To simplify the notation in this section, we suppress the  $n$  and  $l$  quantum numbers and write  $\phi(n, l, m_l, m_s)$  (for a fixed  $n$  and  $l$ ) as  $\phi(m_l, m_s)$ .

Since  $\mathbf{m}_j = \mathbf{m}_l + \mathbf{m}_s$ , we have

$$\begin{aligned} \mathbf{m}_j^2 &= \mathbf{m}_l^2 + \mathbf{m}_s^2 + 2\mathbf{m}_l \cdot \mathbf{m}_s \\ &= l(l+1) + s(s+1) + 2m_l m_s + \mathbf{m}_l^+ \mathbf{m}_s^- + \mathbf{m}_l^- \mathbf{m}_s^+. \end{aligned} \quad (5.96)$$

Therefore

$$\begin{aligned} \mathbf{m}_j^2 \phi(m_l, m_s) &= [l(l+1) + s(s+1) + 2m_l m_s] \phi(m_l, m_s) \\ &\quad + \sqrt{(l-m_l)(l+m_l+1)} \phi(m_l+1, m_s-1) \\ &\quad + \sqrt{(l+m_l)(l-m_l+1)} \phi(m_l-1, m_s+1). \end{aligned} \quad (5.97)$$

Consider the spin-orbital  $\phi(l, 1/2)$ . This function has the maximum  $m_l$  ( $m_l = l$ ) and maximum  $m_s$  ( $m_s = 1/2$ ). By operating on this state with  $\mathbf{m}_j^2$  we obtain

$$\begin{aligned} \mathbf{m}_j^2 \phi(l, 1/2) &= [l(l+1) + 3/4 + l] \phi(l, 1/2) \\ &= [(l+1/2)(l+1/2+1)] \phi(l, 1/2). \end{aligned} \quad (5.98)$$

Therefore this state is an eigenstate of  $\mathbf{j}_z$  and  $\mathbf{j}^2$  with eigenvalues  $m_j = l+1/2$  and  $j = l+1/2$ . However, if we operate on the state  $\phi(l, -1/2)$  we obtain

$$\mathbf{m}_j^2 \phi(l, -1/2) = [l(l+1) + 3/4 - l] \phi(l, -1/2) + \sqrt{2l} \phi(l-1, 1/2). \quad (5.99)$$

Similarly,

$$\mathbf{m}_j^2 \phi(l-1, 1/2) = [l(l+1) + 3/4 + l-1] \phi(l-1, 1/2) + \sqrt{2l} \phi(l, -1/2). \quad (5.100)$$

Equations (5.99) and (5.100) show that neither  $\phi(l, -1/2)$  nor  $\phi(l-1, 1/2)$  is an eigenstate of  $\mathbf{j}^2$ . However, these two states are coupled only to each other, and therefore we can use a linear combination to form an eigenstate of  $\mathbf{j}^2$ . We take  $\Phi = A \phi(l, -1/2) + B \phi(l-1, 1/2)$ , where  $A$  and  $B$  are constants to be determined by requiring that  $\mathbf{j}^2 \Phi = \lambda \Phi$ . The resulting secular equation is

$$\begin{pmatrix} E_1 - l - \lambda & \sqrt{2l} \\ \sqrt{2l} & E_1 + l - 1 - \lambda \end{pmatrix} \begin{pmatrix} A \\ B \end{pmatrix} = 0, \quad (5.101)$$

where  $E_1 = l(l+1) + 3/4$ . The two solutions are  $\lambda_1 = l^2 + 2l + 3/4 = (l+1/2)(l+1/2+1)$ , corresponding to  $j = l+1/2$ , and  $\lambda_2 = l^2 - 1/4 = (l-1/2)(l-1/2+1)$ ,

corresponding to  $j = l - 1/2$ . The eigenvalue  $\lambda_1$  corresponds to  $\mathbf{s}$  parallel to  $l$  and  $\lambda_2$  corresponds to  $\mathbf{s}$  antiparallel to  $l$ . By substituting the eigenvalues for  $\lambda$  into (5.101) the ratio  $A/B$  can be determined, and hence the eigenvectors. This process yields

$$\Phi(l + 1/2, l - 1/2) = \frac{\sqrt{2l} \phi(l - 1, 1/2) + \phi(l, -1/2)}{\sqrt{2l + 1}}, \quad (5.102)$$

$$\Phi(l - 1/2, l - 1/2) = \frac{-\sqrt{2l} \phi(l, -1/2) + \phi(l - 1, 1/2)}{\sqrt{2l + 1}}. \quad (5.103)$$

Now that we have the two eigenstates corresponding to  $j = l + 1/2$  and  $j = l - 1/2$ , we can generate all of the other  $m_j$  states by applying the operator  $\mathbf{m}_j^- = \mathbf{m}_l^- + \mathbf{m}_s^-$  to these two eigenstates. Using Table 5.2, we obtain

$$\mathbf{m}_j^- \Phi(j, m_j) = \sqrt{(j + m_j)(j - m_j + 1)} \Phi(j, m_j - 1). \quad (5.104)$$

Applying this to (5.102) gives

$$\mathbf{m}_j^- \Phi(l + 1/2, l - 1/2) = \sqrt{4l} \Phi(l + 1/2, l - 3/2). \quad (5.105)$$

We can also write

$$\begin{aligned} \mathbf{m}_j^- \Phi(l + 1/2, l - 1/2) &= (\mathbf{m}_l^- + \mathbf{m}_s^-) \frac{\sqrt{2l} \phi(l - 1, 1/2) + \phi(l, -1/2)}{\sqrt{2l + 1}} \\ &= \frac{\sqrt{2l}[\sqrt{4l - 2} \phi(l - 2, 1/2) + 2\phi(l - 1, -1/2)]}{\sqrt{2l + 1}}, \end{aligned} \quad (5.106)$$

so that

$$\Phi(l + 1/2, l - 3/2) = \frac{\sqrt{2l}[\sqrt{4l - 2} \phi(l - 2, 1/2) + 2\phi(l - 1, -1/2)]}{\sqrt{4l} \sqrt{2l + 1}}. \quad (5.107)$$

Similarly,

$$\mathbf{m}_j^- \Phi(l - 1/2, l - 1/2) = \sqrt{2l - 1} \phi(l - 1/2, l - 3/2), \quad (5.108)$$

and

$$\begin{aligned} (\mathbf{m}_l^- + \mathbf{m}_s^-) \frac{-\sqrt{2l} \phi(l, -1/2) + \phi(l - 1, 1/2)}{\sqrt{2l + 1}} \\ = \frac{-(2l - 1)\phi(l - 1, -1/2) + \sqrt{4l - 2} \phi(l - 2, 1/2)}{\sqrt{2l + 1}}, \end{aligned} \quad (5.109)$$

Table 5.3  $\Phi(j, m_j)$  functions in terms of  $\phi(m_l, m_s)$  for  $l = 1$  ( $p$ -electron)

$j$	$m_j$	$\Phi(j, m_j)$ in terms of $\phi(m_l, m_s)$
3/2	3/2	(1 <sup>+</sup> )
3/2	1/2	$[\sqrt{2}(0^+) + (1^-)]/\sqrt{3}$
3/2	-1/2	$[(-1^+) + \sqrt{2}(0^-)]/\sqrt{3}$
3/2	-3/2	(-1 <sup>-</sup> )
1/2	1/2	$[(0^+) - \sqrt{2}(1^-)]/\sqrt{3}$
1/2	-1/2	$[\sqrt{2}(-1^+) - (0^-)]/\sqrt{3}$

Notation:  $(m_l^\pm) = \phi(l = 1, m_l, m_s = \pm 1/2)$

Table 5.4  $\Phi(j, m_j)$  functions in terms of  $\phi(m_l, m_s)$  for  $l = 2$  ( $d$ -electron)

$j$	$m_j$	$\Phi(j, m_j)$ in terms of $\phi(m_l, m_s)$
5/2	5/2	(2 <sup>+</sup> )
5/2	3/2	$[2(1^+) + (2^-)]/\sqrt{5}$
5/2	1/2	$[\sqrt{3}(0^+) + \sqrt{2}(1^-)]/\sqrt{5}$
5/2	-1/2	$[\sqrt{2}(-1^+) + \sqrt{3}(0^-)]/\sqrt{5}$
5/2	-3/2	$[(-2^+) + 2(-1^-)]/\sqrt{5}$
5/2	-5/2	(-2 <sup>-</sup> )
3/2	3/2	$[(1^+) - 2(2^-)]/\sqrt{5}$
3/2	1/2	$[\sqrt{2}(0^+) - \sqrt{3}(1^-)]/\sqrt{5}$
3/2	-1/2	$[\sqrt{3}(-1^+) - \sqrt{2}(0^-)]/\sqrt{5}$
3/2	-3/2	$[-2(-2^+) + (-1^-)]/\sqrt{5}$

Notation:  $(m_l^\pm) = \phi(l = 2, m_l, m_s = \pm 1/2)$

from which it follows that

$$\Phi(l - 1/2, l - 3/2) = \frac{-(2l - 1)\phi(l - 1, -1/2) + \sqrt{4l - 2}\phi(l - 2, 1/2)}{\sqrt{2l + 1}\sqrt{2l - 1}}. \quad (5.110)$$

Using the procedure outlined above, we can easily find the  $\Phi(j, m_j)$  states for any value of the orbital momentum,  $l$ . Results for  $l = 1, 2$ , and 3 are summarized in Tables 5.3–5.5.

### 5.7.3 Two-electron $j$ - $j$ spin-orbitals

Many-electron states characterized by  $j_1, j_2, J$ , and  $M_J$  can be built up for the one-electron spin-orbitals of the type in Tables 5.3–5.5 which are characterized by the eigenvalues  $j$  and  $m_j$ . In general, the eigenstates of  $\mathbf{J}^2$  involve a linear combination of products of these states with  $j_1$  and  $j_2$  fixed, but with various values of  $m_j$ . The

Table 5.5  $\Phi(j, m_j)$  functions in terms of  $\phi(m_l, m_s)$  for  $l = 3$  ( $f$ -electron)

$j$	$m_j$	$\Phi(j, m_j)$ in terms of $\phi(m_l, m_s)$
7/2	7/2	$(3^+)$
7/2	5/2	$[\sqrt{6}(2^+) + (3^-)]/\sqrt{7}$
7/2	3/2	$[\sqrt{5}(1^+) + \sqrt{2}(2^-)]/\sqrt{7}$
7/2	1/2	$[2(0^+) + \sqrt{3}(1^-)]/\sqrt{7}$
7/2	-1/2	$[\sqrt{3}(-1^+) + 2(0^-)]/\sqrt{7}$
7/2	-3/2	$[\sqrt{2}(-2^+) + \sqrt{5}(-1^-)]/\sqrt{7}$
7/2	-5/2	$[(-3^+) + \sqrt{6}(-2^-)]/\sqrt{7}$
7/2	-7/2	$(-3^-)$
5/2	5/2	$[(2^+) - \sqrt{6}(3^-)]/\sqrt{7}$
5/2	3/2	$[\sqrt{2}(1^+) - \sqrt{5}(2^-)]/\sqrt{7}$
5/2	1/2	$[\sqrt{3}(0^+) - 2(1^-)]/\sqrt{7}$
5/2	-1/2	$[2(-1^+) - \sqrt{3}(0^-)]/\sqrt{7}$
5/2	-3/2	$[\sqrt{5}(-2^+) - \sqrt{2}(-1^-)]/\sqrt{7}$
5/2	-5/2	$[\sqrt{6}(-3^+) - (-2^-)]/\sqrt{7}$

Notation:  $(m_l^\pm) = \phi(l = 3, m_l, m_s = \pm 1/2)$

reason for this is that  $\mathbf{J}^2$ ,  $\mathbf{J}^-$ , or  $\mathbf{J}^+$  operating on  $\Phi(j_1, m_{j_1}) \Phi(j_2, m_{j_2})$  does not change  $j_1$  or  $j_2$ . Because of this feature, the spin-orbit interaction energy can easily be evaluated.

A one-electron spin-orbital characterized by  $j$  will transform according to  $D^{(j)}$ , where  $j$  can have the values  $l \pm 1/2$ . A two-electron state constructed from a product of two one-electron states will transform according to the direct product  $D^{(j_1)} \times D^{(j_2)} = D^{(j_1+j_2)} + D^{(j_1+j_2-1)} + D^{(j_1+j_2-2)} + \dots + D^{|j_1-j_2|}$ . As an example consider the configuration  $npn'p$  with  $n$  unequal to  $n'$ . There are several possible pairs of  $j_1$  and  $j_2$ :  $(3/2, 3/2)$ ,  $(3/2, 1/2)$ ,  $(1/2, 3/2)$ , and  $(1/2, 1/2)$ . The following decompositions apply:

$$D_n^{(3/2)} \times D_{n'}^{(3/2)} = D^{(3)} + D^{(2)} + D^{(1)} + D^{(0)}, \quad (5.111)$$

$$D_n^{(3/2)} \times D_{n'}^{(1/2)} = D^{(2)} + D^{(1)}, \quad (5.112)$$

$$D_{n'}^{(1/2)} \times D_n^{(3/2)} = D^{(2)} + D^{(1)}, \quad (5.113)$$

$$D_n^{(1/2)} \times D_{n'}^{(1/2)} = D^{(1)} + D^{(0)}, \quad (5.114)$$

where the subscripts  $n$  and  $n'$  are reminders that the principal quantum numbers  $n$  and  $n'$  are not equal. Thus the combination of two inequivalent  $p$ -electrons leads to terms with  $J = 3, 2, 1$ , and  $0$ ;  $J = 2, 1$ ;  $J = 2, 1$ ; and  $J = 1, 0$ . Each level is  $(2J + 1)$ -fold degenerate, and therefore there is a total of 36 states. In the  $L$ - $S$  scheme we have six  $np$  spin-orbitals and six  $n'p$  spin-orbitals. The first electron can go into any of the six  $np$  states and the second into any of the six  $n'p$  states. Therefore the total number of states for  $npn'p$  is  $6 \times 6 = 36$ .

In the case of two equivalent electrons,  $(np)^2$ , the Pauli exclusion principle forbids two electrons occupying the same spin-orbital. The exclusion principle is not built into the results of (5.111)–(5.114). The effect is to forbid  $D^{(3)}$  and  $D^{(1)}$  in the  $D^{(3/2)} \times D^{(3/2)}$  decomposition and  $D^{(1)}$  in the  $D^{(1/2)} \times D^{(1/2)}$  decomposition. In addition, the terms in (5.112) and (5.113) are indistinguishable. Therefore, the permitted terms are  $J = 0$  and  $J = 2$  for  $D^{(3/2)} \times D^{(3/2)}$ ,  $J = 1$  and  $J = 0$  for  $D^{(1/2)} \times D^{(3/2)}$  and  $J = 0$  for  $D^{(1/2)} \times D^{(1/2)}$ . These terms give a total of 15 states. This result is clear in the  $L$ - $S$  scheme. The first spin-orbital can be chosen in six ways but the second can be chosen in only five ways. This reduces the number of states from  $6 \times 6 = 36$  to  $6 \times 5 = 30$ . The states  $(m_{l_1}, m_{s_1}, m_{l_2}, m_{s_2})$  are indistinguishable from the states  $(m_{l_2}, m_{s_2}, m_{l_1}, m_{s_1})$ , and this reduces the number of remaining states by a factor of 2. Therefore, the total number of distinct states for two equivalent  $p$ -electrons is 15.

It is easy to see why the  $J = 3$  for  $D^{(3/2)} \times D^{(3/2)}$  and the  $J = 1$  for  $D^{(1/2)} \times D^{(1/2)}$  are present for two inequivalent electrons but absent for the two equivalent electrons. The state  $\sqrt{2}|nl^+, n'l^+\rangle$  ( $l = 1, n \neq n'$ ) is an eigenstate of  $\mathbf{j}_1^2$ ,  $\mathbf{j}_2^2$ , and  $\mathbf{J}^2$  with eigenvalues  $j_1 = 3/2$ ,  $j_2 = 3/2$ , and  $J = 3$ . For equivalent electrons  $\sqrt{2}|nl^+, nl^+\rangle$  ( $l = 1, n = n'$ ) is clearly a null state and forbidden by the exclusion principle. Similarly, the state  $\sqrt{2}|nl^-, n'l^-\rangle$  is an eigenstate of  $\mathbf{j}_1^2$ ,  $\mathbf{j}_2^2$ , and  $\mathbf{J}^2$  with eigenvalues  $j_1 = 1/2$ ,  $j_2 = 1/2$ , and  $J = 1$ . For equivalent electrons,  $\sqrt{2}|nl^-, nl^-\rangle$  ( $l = 1, n = n'$ ) is a null state.

For two electrons the determinantal state can be written as a product of a spin and a space function. The decomposition of the direct product for the spatial representations,  $D^{(1)} \times D^{(1)} = D^{(2)} + D^{(1)} + D^{(0)}$ , where  $D^{(0)}$  and  $D^{(2)}$  correspond to symmetric spatial functions and  $D^{(1)}$  corresponds to an antisymmetric spatial function. Therefore the  $S$  and  $D$  terms are singlets, while the  $P$  term is a triplet. The spectroscopic terms are two  $^1S_0$ , one  $^3P_1$ , and two  $^1D_2$ .

As an example of how the  $j$ - $j$  states can be constructed, consider the case of two equivalent  $p$ -electrons. Our aim is to find the 15 eigenstates of the operators  $\mathbf{j}_1$ ,  $\mathbf{j}_2$ ,  $\mathbf{J}^2$ , and  $\mathbf{M}_J$ . If we use products of the spin-orbital in Table 5.3 we are assured that the basis states are eigenstates of  $\mathbf{j}_1$ ,  $\mathbf{j}_2$ ,  $\mathbf{m}_{j_1}$ , and  $\mathbf{m}_{j_2}$ . Furthermore, we know that the eigenstates of  $\mathbf{J}^2$  must be linear combinations of states having the same value

Table 5.6  $j$ - $j$ -Coupled states for  $J = 2$  for two equivalent  $p$ -electrons

$J = 2$	$(j_1, j_2) = (1/2, 1/2)$
$M_J$	$ \Phi(j_1, m_{j_1}) \Phi(j_2, m_{j_2})\rangle$
2	$ \Phi(3/2, 3/2) \Phi(1/2, 1/2)\rangle$
1	$\{\sqrt{3} \Phi(3/2, 1/2) \Phi(1/2, 1/2)\rangle +  \Phi(3/2, 3/2) \Phi(1/2, -1/2)\rangle\}/2$
0	$\{ \Phi(3/2, -1/2) \Phi(1/2, 1/2)\rangle +  \Phi(3/2, 1/2) \Phi(1/2, -1/2)\rangle\}/\sqrt{2}$
-1	$\{\sqrt{3} \Phi(3/2, -1/2) \Phi(1/2, -1/2)\rangle +  \Phi(3/2, -3/2) \Phi(1/2, 1/2)\rangle\}/2$
-2	$ \Phi(3/2, -3/2) \Phi(1/2, -1/2)\rangle$
Notation: $ \Phi(j_1, m_{j_1}) \Phi(j_2, m_{j_2})\rangle = \det\{\Phi(j_1, m_{j_1}) \Phi(j_2, m_{j_2})\}/\sqrt{2}$	
$\Phi(j, m_j)$ is defined in Table 5.3.	

for  $m_{j_1} + m_{j_2} = M_J$ . This is true because  $\mathbf{J}^2$  applied to any of the spin-orbitals may result in a sum of orbital functions, but they all have the same  $M_J$ .

As mentioned earlier, for two equivalent  $p$ -electrons  $J = 3$  does not occur. To generate the  $J = 2$  level, we start with any product function  $\Phi(j_1, m_{j_1}) \Phi(j_2, m_{j_2})$  with  $m_{j_1} + m_{j_2} = M_J = 2$ , e.g., the product  $\Phi(3/2, 3/2) \Phi(1/2, 1/2)$ , where the  $\Phi(j, m_j)$  functions are listed in Table 5.3. We operate with  $\mathbf{J}^2$  on the state, and obtain

$$\begin{aligned}
 \mathbf{J}^2 |\Phi(3/2, 3/2) \Phi(1/2, 1/2)\rangle \\
 &= \{j_1^2 + j_2^2 + 2(m_{j_1} m_{j_2}) + j_1^+ j_2^- + j_1^- j_2^+\} |\Phi(3/2, 3/2) \Phi(1/2, 1/2)\rangle \\
 &= 6 |\Phi(3/2, 3/2) \Phi(1/2, 1/2)\rangle.
 \end{aligned} \tag{5.115}$$

Therefore,  $\Phi(3/2, 3/2) \Phi(1/2, 1/2)$  is an eigenstate of  $\mathbf{J}^2$  arising from  $D^{(3/2)} \times D^{(1/2)}$ , with  $J = 2$  and  $M_J = 2$ . We can generate all of the states belonging to this term by operating with  $\mathbf{M}_J^-$ . The results are shown in Table 5.6.

Another product that yields  $M_J = 2$  is  $|\Phi(3/2, 3/2) \Phi(3/2, 1/2)\rangle$ , and

$$\begin{aligned}
 \mathbf{J}^2 |\Phi(3/2, 3/2) \Phi(3/2, 1/2)\rangle \\
 &= 9 |\Phi(3/2, 3/2) \Phi(3/2, 1/2)\rangle + 3 |\Phi(3/2, 1/2) \Phi(3/2, 3/2)\rangle \\
 &= 6 |\Phi(3/2, 3/2) \Phi(3/2, 1/2)\rangle \\
 &= 2(2 + 1) |\Phi(3/2, 3/2) \Phi(3/2, 1/2)\rangle.
 \end{aligned} \tag{5.116}$$

Therefore this state is an eigenstate with  $J = 2$  and  $M_J = 2$  arising from  $D^{(3/2)} \times D^{(3/2)}$ . Operating repeatedly on this state with  $\mathbf{M}_J^-$  gives the results shown in Table 5.7.



Table 5.7  $j$ - $j$ -Coupled states for  $J = 2$  for two equivalent  $p$ -electrons

$J = 2$	$(j_1, j_2) = (3/2, 3/2)$
$M_J$	$ \Phi(j_1, m_{j1}) \Phi(j_2, m_{j2})\rangle$
2	$ \Phi(3/2, 3/2) \Phi(3/2, 1/2)\rangle$
1	$ \Phi(3/2, 3/2) \Phi(3/2, -1/2)\rangle$
0	$\{ \Phi(3/2, 1/2) \Phi(1/2, -1/2)\rangle +  \Phi(3/2, 3/2) \Phi(3/2, -3/2)\rangle\}/\sqrt{2}$
-1	$ \Phi(3/2, 1/2) \Phi(3/2, -3/2)\rangle$
-2	$ \Phi(3/2, -1/2) \Phi(3/2, -3/2)\rangle$
Notation: $ \Phi(j_1, m_{j1}) \Phi(j_2, m_{j2})\rangle = \det\{\Phi(j_1, m_{j1}) \Phi(j_2, m_{j2})\}/\sqrt{2}$	
$\Phi(j, m_j)$ is defined in Table 5.3.	

For the  $J = 1$  states we select the product  $|\Phi(3/2, 3/2) \Phi(1/2, -1/2)\rangle$  for which  $M_J = 1$ . We find that

$$\begin{aligned} \mathbf{M}_J^2 |\Phi(3/2, 3/2) \Phi(1/2, -1/2)\rangle &= 3 |\Phi(3/2, 3/2) \Phi(1/2, -1/2)\rangle \\ &\quad + \sqrt{3} |\Phi(3/2, 1/2) \Phi(1/2, 1/2)\rangle \end{aligned} \quad (5.117)$$

and

$$\begin{aligned} \mathbf{M}_J^2 |\Phi(3/2, 1/2) \Phi(1/2, 1/2)\rangle &= 5 |\Phi(3/2, 3/2) \Phi(1/2, -1/2)\rangle \\ &\quad + \sqrt{3} |\Phi(3/2, 3/2) \Phi(1/2, -1/2)\rangle. \end{aligned} \quad (5.118)$$

To form an eigenstate of  $\mathbf{M}_J^2$  we take a linear combination of the two coupled states:

$$\Theta = A |\Phi(3/2, 3/2) \Phi(1/2, -1/2)\rangle + B |\Phi(3/2, 1/2) \Phi(1/2, 1/2)\rangle, \quad (5.119)$$

where  $A$  and  $B$  are coefficients to be selected so that  $\mathbf{M}_J^2 \Theta = \lambda \Theta$ . The eigenvalue equation is

$$\begin{pmatrix} 3 - \lambda & \sqrt{3} \\ \sqrt{3} & 5 - \lambda \end{pmatrix} \begin{pmatrix} A \\ B \end{pmatrix} = 0. \quad (5.120)$$

The vanishing of the determinant give the roots  $\lambda = 4 \pm 2$ . The lower sign gives  $\lambda = 2 = 1(1 + 1)$  and corresponds to  $J = 1$ . Substituting  $\lambda = 2$  into the secular equation determines the ratio of  $A$  to  $B$ , and the normalized state arising from  $D^{(3/2)} \times D^{(1/2)}$  is

$$\Theta = -\sqrt{3} |\Phi(3/2, 3/2) \Phi(1/2, -1/2)\rangle + |\Phi(3/2, 1/2) \Phi(1/2, 1/2)\rangle. \quad (5.121)$$

Table 5.8 *j-j-Coupled states for  $J = 1$  for two equivalent  $p$ -electrons*

$J = 1$	$(j_1, j_2) = (3/2, 1/2)$
$M_J$	$ \Phi(j_1, m_{j1}) \Phi(j_2, m_{j2})\rangle$
1	$\{ \Phi(3/2, 1/2) \Phi(1/2, 1/2)\rangle - \sqrt{3} \Phi(3/2, 3/2) \Phi(1/2, -1/2)\rangle\}/2$
0	$\{ \Phi(3/2, -1/2) \Phi(1/2, 1/2)\rangle -  \Phi(3/2, 1/2) \Phi(1/2, -1/2)\rangle\}/\sqrt{2}$
-1	$\{ \Phi(3/2, -1/2) \Phi(1/2, -1/2)\rangle - \sqrt{3} \Phi(3/2, -3/2) \Phi(1/2, 1/2)\rangle\}/2$
Notation: $ \Phi(j_1, m_{j1}) \Phi(j_2, m_{j2})\rangle = \det\{\Phi(j_1, m_{j1}) \Phi(j_2, m_{j2})\}/\sqrt{2}$	
$\Phi(j, m_j)$ is defined in Table 5.3.	

The other states for  $J = 1$  generated by use of  $\mathbf{M}_J^-$  are shown in Table 5.8.

So far we have found 13 of the 15 eigenstates. The remaining two have  $J = 0$ . As a generating function we choose  $|\Phi(3/2, 3/2) \Phi(3/2, -3/2)\rangle$ , which has  $M_J = 0$ . We have

$$\begin{aligned} \mathbf{M}_J^2 |\Phi(3/2, 3/2) \Phi(3/2, -3/2)\rangle &= 3|\Phi(3/2, 3/2) \Phi(3/2, -3/2)\rangle \\ &\quad + 3|\Phi(3/2, 1/2) \Phi(3/2, -1/2)\rangle \end{aligned} \quad (5.122)$$

and

$$\begin{aligned} \mathbf{M}_J^2 |\Phi(3/2, 1/2) \Phi(3/2, -1/2)\rangle &= 3|\Phi(3/2, 1/2) \Phi(3/2, -1/2)\rangle \\ &\quad + 3|\Phi(3/2, 3/2) \Phi(3/2, -3/2)\rangle. \end{aligned} \quad (5.123)$$

The two states  $|\Phi(3/2, 1/2) \Phi(3/2, -1/2)\rangle$  and  $|\Phi(3/2, 3/2) \Phi(3/2, -3/2)\rangle$  are coupled. On solving the secular equation we find that the  $J = 0$  state arising from  $D^{(3/2)} \times D^{(3/2)}$  is

$$\frac{1}{\sqrt{2}} \left\{ |\Phi(3/2, 3/2) \Phi(3/2, -3/2)\rangle - |\Phi(3/2, 1/2) \Phi(3/2, -1/2)\rangle \right\}. \quad (5.124)$$

The other  $J = 0$  state, namely that arising from  $D^{(1/2)} \times D^{(1/2)}$ , is

$$|\Phi(1/2, 1/2) \Phi(1/2, -1/2)\rangle. \quad (5.125)$$

Thus, by selecting product functions having the desired  $M_J$  value and using the operators  $\mathbf{M}_J^2$  and  $\mathbf{M}_J^-$ , we are able to generate all of the  $j-j$ -coupled eigenstates. These  $j-j$ -coupled states can be expressed in terms of the  $L-S$ -coupled states. In general the transformation of the  $j-j$ -coupled states to or from the  $L-S$ -coupled states is a tedious task when the number of electrons is more than two.

Table 5.9 *Spin-orbit energies of  $j$ - $j$ -coupled states with  $n = 1$  and  $J = 2$  for two equivalent  $p$ -electrons*

$j_1$	$j_2$	$\frac{1}{2} \sum \{j_k(j_k + 1) - l_k(l_k + 1) - s_k(s_k + 1)\} \xi_{knl}$	Degeneracy
3/2	3/2	$\xi_{knl}$	6
3/2	1/2	$-\xi_{knl}/2$	8
1/2	1/2	$-2\xi_{knl}$	1

With the  $j$ - $j$  coupling the spin-orbit energy is easily evaluated. For the two equivalent  $p$ -electrons  $l_k = 1$  and  $s_k = 1/2$ , and the values of  $j_k$  can be read directly from the eigenstate labels. The spin-orbit energy does not depend on  $M_J$  or  $m_j$ , and hence is constant for the various levels of a given  $J$  term.

For two equivalent  $p$ -electrons the spin-orbit energies are shown in Table 5.9. The column labeled “degeneracy” lists the number of states that have the pair  $j_1$  and  $j_2$ . We note that the  $(np)^2$  configuration is split into three equally spaced groups by the spin-orbit interaction. In addition, the sum of the spin-orbit energies times their degeneracies is equal to zero. This is a general feature of spin-orbit splitting. The “center of gravity” of the energy levels is unaffected by the spin-orbit interaction.

#### 5.7.4 The nuclear-shell model

The neutrons and protons of a nucleus are held together by very strong nuclear interactions. The binding energy or stability of a nucleon depends on the number of protons ( $Z$ ) and the number of neutrons ( $N$ ) comprising the nucleus. Imagine building a nucleus by successively adding neutrons and protons. It is experimentally observed that the binding energy of the last added nucleon is particularly large for special numbers called “magic numbers”. The magic numbers for neutrons or protons are 2, 8, 20, 28, 50, 82, and 126. In some cases both  $Z$  and  $N$  are magic numbers (not necessarily the same number), in which case the nucleus is “doubly magic” and has exceptional stability. The calcium isotopes having  $Z = 20$  and  $N = 20$  and 28 are doubly magic nuclei. These two isotopes are much more stable than the other isotopes of calcium. The occurrence of magic numbers suggests that the nucleus may have a shell structure analogous to the atomic shells for electrons. Other evidence includes the observations that (1) the stable isotopes of radioactive series all have magic numbers for  $N$  and  $Z$ , and (2) the neutron-absorption cross-section is lower for magic-numbered nuclei than for other isotopes. An empirical nuclear-shell model similar to the electronic-shell model was developed by E. P. Wigner, M. Goeppert-Mayer, and J. H. D. Jensen, who shared the Nobel prize in 1963 for their contributions.

The model accounts for the magic numbers and also predicts the total spin of nuclei [5.5]. Although there are strong similarities between the nuclear-shell model and the electronic-shell model, protons and neutrons are different particles, and each species has its own shells. Second, there is no physical, central core about which the nucleons circulate. Nevertheless, the nuclear-shell model supposes that each nucleon moves in a spherically symmetric potential due to its interactions with the other nucleons. Various empirical potentials that decay exponentially beyond the nuclear radius have been suggested, but all depend only on the magnitude of  $r$ . This assumption is essential because it allows the Schrödinger equation for a nucleon to be separated into radial and angular functions. The angular functions are the same spherical harmonics as those used for atomic states. The one-nucleon eigenstates are then characterized by angular momentum  $l$ , magnetic quantum number  $m_l$ , spin  $s$ , and  $m_s$ . Unlike in the atomic case,  $l$  is not limited by  $n$  (in the atomic case  $l$  can not exceed  $n$ .) The magic numbers are then associated with the filling of a proton or neutron shell. To obtain the correct magic numbers, a strong spin-orbit interaction must be included in the model. This means that the states must be characterized by  $j$ ,  $m_j$ ,  $J$ ,  $M_j$ , and parity (“ $g$ ” or “ $u$ ” states). The nucleons are Fermi particles, and therefore obey the Pauli exclusion principle. They can be assigned to the various shells just as one does for electrons. The filled shells have zero total  $J$ . Therefore the nucleons occupying the unfilled shells determine the value of the total angular momentum and the value of the total spin. The shell model correctly predicts the total  $J$  and spin of nuclei [5.5].

### 5.8 Crystal double groups

For the rotation group the formula for the character of a rotation through an angle  $\alpha$  given by (3.20),

$$\chi^l(\alpha) = \frac{\sin[(l + 1/2)\alpha]}{\sin(\alpha/2)}, \quad (5.126)$$

was derived from the properties of the spherical harmonic functions for integer angular momentum,  $l$ . The spinor functions that are the basis for half-integer momentum are not spherical harmonic functions; however, the same formula applies. The formula for the character can be generalized to read

$$\chi^J(\alpha) = \frac{\sin[(J + 1/2)\alpha]}{\sin(\alpha/2)}, \quad (5.127)$$

where  $J$  represents integer or half-integer angular momentum. If we now consider a rotation through an angle  $\alpha + 2\pi$  we obtain the result that

$$\begin{aligned}
& \chi^J(\alpha + 2\pi) \\
&= \frac{\sin[(J + 1/2)(\alpha + 2\pi)]}{\sin(\alpha/2 + \pi)} \\
&= \frac{\sin[(J + 1/2)\alpha] \cos[2\pi(J + 1/2)] + \cos[(J + 1/2)\alpha] \sin[2\pi(J + 1/2)]}{\sin(\alpha/2) \cos(\pi) + \cos(\alpha/2) \sin(\pi)} \\
&= \frac{\sin[(J + 1/2)\alpha] \cos[2\pi(J + 1/2)]}{\sin(\alpha/2) \cos(\pi)} = \chi^J(\alpha) \cos(2\pi J) \\
&= (-1)^{2J} \chi^J(\alpha). \tag{5.128}
\end{aligned}$$

When  $J$  is a half-integer (5.128) shows that a rotation by  $2\pi$  has the character  $-1$  and that  $\chi^J(\alpha + 2\pi)$  is the negative of  $\chi^J(\alpha)$ . However,  $\chi^J(\alpha + 4\pi) = \chi^J(\alpha)$  when  $J$  is an integer or half-integer. Since any rotation that is a multiple of  $2\pi$  has been assumed to be equivalent to  $E$ , the identity, we see that the character of a rotation for half-integer momentum is not single-valued and, in fact, the  $D^{(J)}(R)$  representation matrices for half-integer  $J$  are determined only up to a  $\pm$  sign.

A method for handling this sign ambiguity for half-integer  $J$  has been developed. The approach introduces an element,  $R$ , that corresponds to a rotation by  $2\pi$ .  $E$  corresponds to a rotation by  $4\pi$ . A new group,  $G^*$  (the crystal double group), can be constructed from the original group,  $G$ , using as elements  $C$  and  $RC$ , where  $C$  is any element of  $G$ . This results in a group that has twice as many elements and therefore additional IRs. Although there are twice as many elements, there need not be twice as many classes, and hence there need not be twice as many IRs. However, if  $\Gamma$  is an IR of  $G$  with characters  $\chi(C_i)$ , then an IR of the double group has the characters  $\chi(RC_i) = \chi(C_i)$ . Thus the characters of  $N_\kappa$  IRs of  $G^*$  are immediately determined, where  $N_\kappa$  is the number of IRs of  $G$ .

The rules for determining the class structure, originally due to Opechowski [5.6], are summarized below.

Let  $G$  be the original group and  $\{C_\alpha\}$  a class in  $G$ , then the sets  $\{C_\alpha\}$  and  $\{RC_\alpha\}$  are different classes in  $G^*$ . An exception to this rule occurs if and only if  $C_{\alpha i}$  is a rotation by  $\pi$  and there is another  $C_2$  rotation about an axis perpendicular to the symmetry axis of  $C_{\alpha i}$ . In such a case,  $C_{\alpha i}$  and  $RC_{\alpha i}$  are in the same class.

In atomic theory the basis functions for the IRs of the rotation group are spherical harmonic functions when  $J$  is an integer [5.6]. For half-integer  $J$  the basis functions are linear combinations of the spin-orbitals we have been discussing in this chapter. The double group provides the IRs needed in order to decompose the representations based on spin-orbitals in exactly the same manner as that in which the representations based on spatial orbitals are decomposed. The complexities of constructing the IRs of the double group can be found elsewhere [5.7] and will not be discussed here. As an example of a double group, the character table for the

Table 5.10  $O'$ : The crystal double group for octahedral symmetry. The  $R$  operator is a rotation by  $2\pi$  and  $E$  is a rotation by  $4\pi$ . The IRs of the  $O$  group are shown on the far right. The new IRs, namely  $\Gamma_6$ ,  $\Gamma_7$ , and  $\Gamma_8$ , are those resulting from extending the  $O$  group.

$O'$	$E$	$R$	$8C_3$	$8RC_3$	$3C_2 + 3RC_2$	$6C_2 + 6RC_2$	$6C_4$	$6RC_4$	$O$
$\Gamma_1$	1	1	1	1	1	1	1	1	$A_1$
$\Gamma_2$	1	1	1	1	1	-1	-1	-1	$A_2$
$\Gamma_3$	2	2	-1	-1	2	0	0	0	$E$
$\Gamma_4$	3	3	0	0	-1	-1	1	1	$T_1$
$\Gamma_5$	3	3	0	0	-1	1	-1	-1	$T_2$
$\Gamma_6$	2	-2	1	-1	0	0	$\sqrt{2}$	$-\sqrt{2}$	New
$\Gamma_7$	2	-2	1	-1	0	0	$-\sqrt{2}$	$\sqrt{2}$	IRs
$\Gamma_8$	4	-4	-1	1	0	0	0	0	

extended  $O$  group, denoted as  $O'$ , is presented in Table 5.10. We shall refer to the upper block ( $\Gamma_1$  through  $\Gamma_5$ ) as the “old IRs” and the lower block ( $\Gamma_6$  through  $\Gamma_8$ ) as the “new IRs”.

For integral values of  $J$ , the representation  $D^{(J)}$  has  $\chi^J(RC) = \chi^J(C)$ , while the characters of the new IRs satisfy  $\chi^{\Gamma(\text{new})}(RC) = -\chi^{\Gamma(\text{new})}(C)$ . Therefore the decomposition of  $D^{(J)}$  into the new IRs is

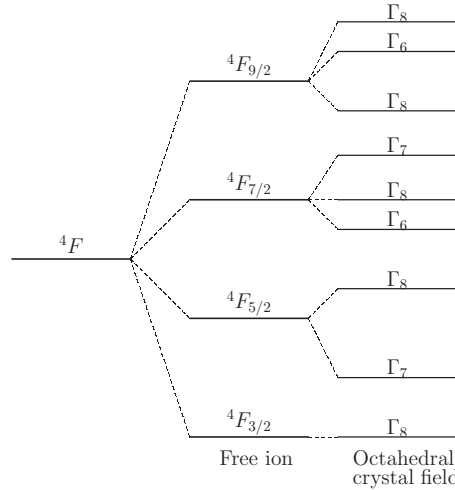
$$\begin{aligned}
 n^{\Gamma(\text{new IR})} &= \frac{1}{48} \sum \{ \chi^{\Gamma(\text{new})}(C) \}^* \chi^J(C) + \{ \chi^{\Gamma(\text{new})}(RC) \}^* \chi^J(RC) \\
 &= \frac{1}{48} \sum \{ \chi^{\Gamma(\text{new})}(C) \}^* \chi^J(C) - \{ \chi^{\Gamma(\text{new})}(C) \}^* \chi^J(C) = 0,
 \end{aligned}
 \tag{5.129}$$

where the sum is over all of the 24 operations of the  $O$  group. Equation (5.129) shows that the representations corresponding to integral  $J$  contain none of the new IRs and therefore decompose entirely into the old IRs of  $O'$ . Conversely, for half-integer  $J$ ,  $\chi(RC) = -\chi(C)$ , while the characters of the old IRs satisfy  $\chi^{\Gamma}(RC) = +\chi^{\Gamma}(C)$ . Consequently, the decomposition for a half-integer representation is entirely into the new IRs. The decomposition of  $D^{(J)}$  into the IRs of the double group corresponding to octahedral symmetry is given for several values of  $J$  in Table 5.11.

It follows from these decompositions that the  $J = 1/2$  and  $J = 3/2$  levels are not split by an octahedral field. A “ $p$ ” spin-orbital will have  $j = 3/2$  and

Table 5.11 *Decomposition of  $D^{(J)}$  into the IRs of  $O'$* 

$D^{(1/2)} = \Gamma_6$	$D^{(7/2)} = \Gamma_6 + \Gamma_7 + \Gamma_8$
$D^{(3/2)} = \Gamma_8$	$D^{(9/2)} = \Gamma_6 + 2\Gamma_8$
$D^{(5/2)} = \Gamma_7 + \Gamma_8$	$D^{(11/2)} = \Gamma_6 + \Gamma_7 + 2\Gamma_8$
$D^{(0)} = \Gamma_1$	$D^{(3)} = \Gamma_2 + \Gamma_4 + \Gamma_5$
$D^{(1)} = \Gamma_4$	$D^{(4)} = \Gamma_1 + \Gamma_3 + \Gamma_4 + \Gamma_5$
$D^{(2)} = \Gamma_3 + \Gamma_5$	$D^{(5)} = \Gamma_3 + 2\Gamma_4 + \Gamma_5$

Figure 5.2 A schematic representation of the splitting of the  ${}^4F$  term in an octahedral environment.

$j = 1/2$  levels, neither of which will be split by an octahedral crystal field. A “ $d$ ” spin-orbital will have  $j = 5/2$  and  $j = 3/2$  levels. The  $5/2$  level splits into a doublet ( $\Gamma_7$ ) and a quartet ( $\Gamma_8$ ), while the  $3/2$  level remains unsplit.

The splitting of a multi-electron term can also be easily deduced now. For example, for a  $d^3$  configuration (e.g.,  $V^{2+}$ ) the  ${}^4F$  term has  $L = 3$ ,  $S = 3/2$ .  $J$  can have integer values ranging from  $L + S$  to  $|L - S|$ . That is,  $J$  can have the values  $9/2$ ,  $7/2$ ,  $5/2$ , and  $3/2$ . From Table 5.11 we see that in an octahedral environment the  $J$  levels are split as shown in Fig. 5.2.

### 5.9 The Zeeman effect (weak-magnetic-field case)

In the presence of an external magnetic field, the orbital and spin magnetic moments interact with the field. The potential energy due to this magnetic interaction is

$$\mathbb{H}_M = -\boldsymbol{\mu} \cdot \mathbf{B} = \frac{\mu_B}{\hbar} \sum_k (\mathbf{l}_k + g_s \mathbf{s}_k) \cdot \mathbf{B} = \mu_B \sum_k (m_{l_k} + g_s m_{s_k}) B, \quad (5.130)$$

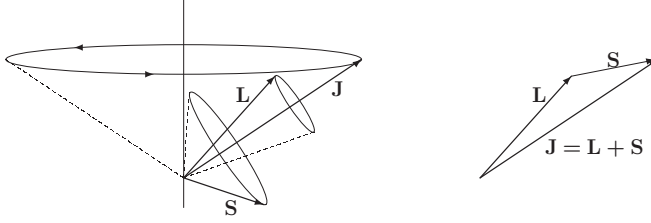


Figure 5.3 A schematic representation of the classical picture of  $L$  and  $S$  precessing about  $J$  as  $J$  precesses about the  $z$ -axis. The projection of  $J$  onto the  $z$ -axis is  $m_J$ . Since  $L$  and  $S$  precess about  $J$ , their projection onto the  $z$ -axis is not constant.

where  $\mu_B$  is the Bohr magneton,  $\mathbf{B}$  is the external magnetic field (also known as the induction, field density, or flux density). The  $g$ -factor for the spin,  $g_s = 2.002\,319$ , will for simplicity be taken as 2 in our discussion. We may assume that  $B$  is oriented along the  $z$ -axis, so for states described by the  $L$ – $S$ -coupling scheme

$$\mathbb{H}_M = \mu_B(\mathbf{L}_z + 2\mathbf{S}_z)B = \mu_B(M_L + 2M_S)B. \quad (5.131)$$

For a system with spherically symmetric electron potentials the  $(2L + 1)$  level eigenstates of  $\mathbb{H}_0$  are degenerate as are the  $(2S + 1)$  states of each level. The perturbation,  $\mathbb{H}_M$ , splits the degeneracy of the  $L$ – $S$  states.

However, often the spin–orbit interaction is larger than  $\mathbb{H}_M$ . In that case the states are best described in terms of  $J$  and  $M_J$  rather than  $L$  and  $S$ . The magnetic interaction will remove the  $(2J + 1)$  degeneracy of the  $J$  terms, but the calculation of the splitting is complicated because  $M_L$  and  $M_S$  are no longer appropriate quantum numbers. The classical picture is that the vectors  $\mathbf{L}$  and  $\mathbf{S}$  precess about  $\mathbf{J}$  as shown in Fig. 5.3.

Equation (5.130) is not useful because  $L$  and  $S$  are no longer “good” quantum numbers. Since  $L$  is precessing about  $J$ , its time-averaged value is just the projection of  $L$  onto  $J$ . The components perpendicular to  $J$  average to zero. The same argument applies to  $S$ . Therefore,

$$\langle \mathbf{L} \rangle_{\text{avg}} = \frac{(\mathbf{L} \cdot \mathbf{J})\mathbf{J}}{J^2}, \quad (5.132)$$

$$\langle \mathbf{S} \rangle_{\text{avg}} = \frac{(\mathbf{S} \cdot \mathbf{J})\mathbf{J}}{J^2}, \quad (5.133)$$

$$\begin{aligned} \mathbb{H}_M &\approx \frac{\mu_B}{\hbar} \frac{(\mathbf{L} \cdot \mathbf{J})\mathbf{J} + 2(\mathbf{S} \cdot \mathbf{J})\mathbf{J}}{J^2} \mathbf{J} \cdot \mathbf{B}, \\ &= \mu_B M_J B \frac{(\mathbf{L} \cdot \mathbf{J})\mathbf{J} + 2(\mathbf{S} \cdot \mathbf{J})\mathbf{J}}{J^2}. \end{aligned} \quad (5.134)$$



The terms  $(\mathbf{L} \cdot \mathbf{J})$  and  $(\mathbf{S} \cdot \mathbf{J})$  can be eliminated by use of the relations

$$(\mathbf{L} \cdot \mathbf{J}) = \frac{1}{2}(J^2 + L^2 - S^2) = \frac{\hbar^2}{2}[J(J+1) + L(L+1) - S(S+1)], \quad (5.135)$$

$$(\mathbf{S} \cdot \mathbf{J}) = \frac{1}{2}(J^2 - L^2 + S^2) = \frac{\hbar^2}{2}[J(J+1) - L(L+1) + S(S+1)], \quad (5.136)$$

$$\mathbf{J} \cdot \mathbf{B} = J_z B_z = \hbar M_J B. \quad (5.137)$$

On substituting (5.135)–(5.137) into (5.134) we obtain

$$\begin{aligned} \langle \mathbb{H}_M \rangle_{\text{avg}} &= \mu_B M_J B \\ &\times \frac{[J(J+1) + L(L+1) - S(S+1)] + 2[J(J+1) - L(L+1) + S(S+1)]}{2J(J+1)} \\ &= \mu_B M_J B \left\{ \frac{3}{2} + \frac{S(S+1) - L(L+1)}{2J(J+1)} \right\} = \mu_B g_L M_J B, \end{aligned} \quad (5.138)$$

where  $g_L$ , the factor enclosed in curly brackets, is called the Landé  $g$ -factor. Its value depends on  $L$  and  $S$  as well as on  $J$ .

Equation (5.138) is useful in evaluating  $\langle \mathbb{H}_M \rangle_{\text{avg}}$  for a  $J$  level belonging to an  $L$ – $S$ -coupling term. For example, the ground state of V with the  $d^3$  configuration is  $(2S+1)F_J = {}^4F_{3/2}$ , so  $J = 3/2$ ,  $L = 3$ , and  $S = 3/2$ . In a spherically symmetric environment the  $(2J+1)$  values of  $M_J$  are degenerate. In the presence of a magnetic field these levels are split. According to (5.138),

$$\langle \mathbb{H}_M \rangle_{\text{avg}} = \mu_B M_J B \left\{ \frac{3}{2} + \frac{15/4 - 12}{15/2} \right\} = \frac{2}{5} M_J \mu_B B. \quad (5.139)$$

Therefore, for  $M_J = \pm 3/2$  and  $\pm 1/2$ ,  $\langle \mathbb{H}_M \rangle_{\text{avg}} = \pm 3/5$  and  $\pm 1/5$ , respectively, in units of  $\mu_B B$ .

## References

- [5.1] S. A. Goudsmit and G. E. Uhlenbeck, “Ersetzung der Hypothese vom unmechanischen Zwang durch eine Forderung bezüglich des inneren Verhaltens jedes einzelnen Elektrons”, *Naturwissenschaften* **47**, 953–954 (1925).  
S. A. Goudsmit and G. E. Uhlenbeck, “Over het roteerende electron en de structuur der spectra”, *Physica* **6**, 273–290 (1926).
- [5.2] P. A. M. Dirac, “The quantum theory of the electron”, *Proc. Roy. Soc. A* **117**, 610–624 (1928).
- [5.3] W. Pauli, “Zur Quantenmechanik des magnetischen Elektrons”, *Z. Phys.* **43**, 601–623 (1927).
- [5.4] E. U. Condon and G. H. Shortley, *The Theory of Atomic Spectra* (Cambridge: Cambridge University Press, 1963).
- [5.5] M. Goeppert-Mayer, *Elementary Theory of Nuclear Shell Structure* (New York: Wiley, 1960). M. Goeppert-Mayer, “On closed shells in nuclei, II”, *Phys. Rev.* **75**, 1969–1970 (1949).

- [5.6] W. Opechowski, “Sur les groupes cristallographiques ‘doubles’”, *Physica* **7**, 552 (1940).  
 N. B. Backhouse, “Projective character tables and Opechowski’s theorem”, *Physica* **70**, 505 (1973).  
 [5.7] V. Heine, *Group Theory in Quantum Mechanics* (New York: Pergamon Press, 1960).

### Exercises

- 5.1 A spin is in the eigenstate  $\chi_x^+$  and a measurement is made with the  $z'$ -axis oriented along the  $(1, 1, 0)$  direction.
- Find the probability that the measurement result is  $+(1/2)\hbar$ .
  - Find the probability of measuring  $-(1/2)\hbar$ .
  - Show that the sum of the probabilities is unity.
- 5.2 (a) Find the spin eigenstate  $\chi_e^+$  for the  $z'$ -axis along the  $(1, 0, 1)$  direction using Eq. (5.13).  
 (b) Using the IR-matrix,  $D^{(1/2)}$ , rotate  $\chi_z^+$  so that it lies along the  $(1, 0, 1)$  direction.  
 (c) Show that the vectors of (a) and (b) are equal.
- 5.3 Consider the  $d^2$  state,  $|2^+, 1^+\rangle$ .
- Using the operators  $\mathbf{M}_L^2$  and  $\mathbf{M}_S^2$  show that  $L = 3$  and  $S = 1$  (in units of  $\hbar$ ).
  - Use the operator  $L^-$  to generate the remaining  $2L$  states. (Compare your results with those derived in Chapter 4, in Table 4.4.)
  - Show that  ${}^3F(3, 3, 1) = |2^+, 1^+\rangle$  can be separated into the product of an antisymmetric spatial function times a symmetric spinor.
  - Use  $M_S^-$  on the spinor to find the three spin states.
- 5.4 Consider two equivalent  $d$ -electrons.
- Use Table 5.3 to show that the determinantal  $j$ - $j$ -coupled state  $|\Phi(5/2, 5/2) \Phi(3/2, 3/2)\rangle = 1/\sqrt{5}|2^+, 1^+\rangle - 4/\sqrt{5}|2^+2^-\rangle$  in  $L$ - $S$  notation.
  - Show that the state is an eigenstate of  $\mathbf{m}_{j1}^2$ ,  $\mathbf{m}_{j2}^2$ ,  $\mathbf{M}_J$ , and  $\mathbf{M}_J^2$  with eigenvalues  $j_1 = 5/2$ ,  $j_2 = 3/2$ ,  $M_J = 4$ , and  $J = 4$ . Use  $\mathbf{m}_{jk} = \mathbf{m}_{lk} + \mathbf{m}_{sk}$ ,  $\mathbf{M}_J = \sum (\mathbf{m}_{jk})_z$ , and  $\mathbf{M}_J^2 = (\sum \mathbf{m}_{jk})^2$ .
  - What is the spin-orbit energy of this level?
- 5.5 (a) Find one of the eigenstates for the  $J = 7/2$  and  $J = 5/2$  levels for an  $f$ -electron ( $l = 3$ ) in terms of  $L$ - $S$ -coupled states.  
 (b) What is the spin-orbit energy of each level?
- 5.6 (a) For a pair of  $f$ -electrons find the  $J = 5$  and  $J = 6$  eigenstates in the  $j$ - $j$  scheme for the pair  $j_1 = 7/2$  and  $j_2 = 5/2$ .

Hint: Operate on the state  $|\Phi(7/2, 5/2) \Phi(5/2, 5/2)\rangle$  with  $\mathbf{M}_J^2$ .

- (b) What is the spin-orbit energy of these states?
- 5.7 Consider an  $f^3$  outer electron configuration.
  - (a) Show that the  $L$ - $S$  state  $|3^+, 2^+, 1^+\rangle$  is an eigenstate of  $M_L^2$  and  $M_S^2$  and also of  $M_J^2$ .
  - (b) How would this spectroscopic term be written?
- 5.8 (a) Use the direct-product rules to determine the allowed  $J$  values for a  $pd$  electronic configuration.
  - (b) Show that the total number of states is 60.
  - (c) Find the  $J = 4$ ,  $M_J = 3$  state expressed as a linear combination of  $L$ - $S$ -coupled states.
- 5.9 Find the Zeeman level splittings of the  $^1S_{1/2}$ ,  $^2P_{1/2}$ , and  $^2P_{3/2}$  terms of hydrogen (in units of  $\mu_B B$ ).

## 6

### Molecular electronic structure: The LCAO model

Much of what we understand about the chemistry and optical properties of molecules has come from theoretical studies of very simple, empirical models. In most cases the theoretical models employ such drastic approximations that one may wonder why the results have any relevance at all to actual molecular systems. The success of these models may be attributed almost entirely to their use of group-theoretical concepts. In many cases symmetry is the dominant factor determining the electronic structure of a molecule. While the models are crude approximations, the general structure imposed by symmetry is usually exact and often independent of the details of the model employed. As a result many of the features have a much deeper truth than the model from which they are derived.

In this chapter we discuss the use of the LCAO method (linear combinations of atomic orbitals) to analyze the electronic structure of molecules. The term “atomic orbitals” is used loosely to mean one-electron orbitals whose angular functions are the spherical harmonics. The precise specifications of the radial parts of the orbitals are not needed for our discussion.

#### 6.1 *N*-electron systems

It is generally assumed that the electronic states of a molecule or solid can be calculated for fixed positions of the nuclei. The electron’s velocity is very large compared with the speed of vibratory motion, so that in effect the electrons instantly readjust to any motion of the nuclei. This assumption is referred to as the Born–Oppenheimer approximation. With that assumption the Hamiltonian for electrons of the molecule is

$$\mathbb{H}_{\text{mol}} = \sum_i \frac{-\hbar^2}{2m} \nabla_i^2 + \sum_i \sum_{j < i} \frac{e^2}{|\mathbf{r}_i - \mathbf{r}_j|} - \sum_{\mathbf{R}_A} \sum_i \frac{Z_A e^2}{|\mathbf{r}_i - \mathbf{R}_A|}, \quad (6.1)$$

where  $\mathbf{r}_i$  is the position vector of the  $i$ th electron,  $\mathbf{R}_A$  is the position vector of the  $A$ th nucleus, and  $e$  is the magnitude of the electron's charge. We seek solutions of the Schrödinger equation,

$$\mathbb{H}_{\text{mol}} \Psi(\mathbf{r}_1, \mathbf{s}_1, \mathbf{r}_2, \mathbf{s}_2, \dots, \mathbf{r}_N, \mathbf{s}_N) = E \Psi(\mathbf{r}_1, \mathbf{s}_1, \mathbf{r}_2, \mathbf{s}_2, \dots, \mathbf{r}_N, \mathbf{s}_N), \quad (6.2)$$

where  $\Psi$  is an antisymmetrized determinantal wavefunction. For a molecule with  $N > 2$  the solutions of (6.1) are essentially impossible to find analytically. Indeed, even with the use of high-speed computers, numerical solutions of (6.2) without approximations are virtually impossible. To derive useful information it is necessary to make a myriad of approximations. A large number of standard computer programs that employ various approximations and limited basis sets can produce reasonable solutions for the molecular states of small molecules. However, simpler models that employ more drastic approximations are susceptible to theoretical analysis and provide substantial insight into the electronic structure of molecules.

### 6.1.1 Hartree–Fock equations

The Hartree–Fock approach is the simplest method of obtaining approximate solutions for an  $N$ -electron molecule consistent with the Pauli principle. This method replaces the electron–electron interactions with an average or mean-field potential but neglects actual electron–electron correlations. Improved results can be obtained by adding an empirical correlation potential that is based on the local electron density. The wavefunctions are Slater determinantal states constructed from the one-electron orbitals which are determined by the variational principle.

We begin with an orthogonal set of  $N$  (one-electron) wavefunctions  $\psi_k(\tau) = \Phi_k(\mathbf{r}) \chi_k(\mathbf{s})$ ,  $k = 1, 2, \dots, N$ , where  $\tau$  represents  $\mathbf{r}$  and  $\mathbf{s}$ , and  $\chi_k(\mathbf{s})$  is the spinor eigenstate ( $\chi_z^+$  or  $\chi_z^-$ ) for the  $k$ th state. The initial wavefunction is the Slater determinant,

$$\begin{aligned} \Psi &= \frac{1}{\sqrt{N!}} \det\{\psi_1(\tau_1) \psi_2(\tau_2) \psi_3(\tau_3) \dots \psi_N(\tau_N)\} \\ &= |\psi_1(\tau_1) \psi_2(\tau_2) \psi_3(\tau_3) \dots \psi_N(\tau_N)\rangle. \end{aligned} \quad (6.3)$$

The expectation value for the energy of the system is

$$\langle E \rangle = \langle \psi_1(\tau_1) \psi_2(\tau_2) \psi_3(\tau_3) \dots \psi_N(\tau_N) | \mathbb{H} | \psi_1(\tau_1) \psi_2(\tau_2) \psi_3(\tau_3) \dots \psi_N(\tau_N) \rangle. \quad (6.4)$$

According to the variational principle, the best choice of the spin orbitals (the  $\psi_i(\tau_i)$ ) is determined by minimizing  $\langle E \rangle$  with respect to variations in the orbitals. The variations are subject to the constraint that the orbitals remain orthogonal to one another. This constraint is imposed by the use of Lagrange multipliers.

The details of this calculation are available elsewhere [6.1, 6.2, 6.3] and will not be given here. The resulting Hartree–Fock equations for the one-electron orbitals are

$$\left\{ -\frac{\hbar^2}{2m} \nabla^2 + V_N(\mathbf{r}) + V_C(\mathbf{r}) - V_{\text{ex}}(\mathbf{r}) \right\} \Phi_k(\mathbf{r}) = \epsilon_k \Phi_k(\mathbf{r}), \quad (6.5)$$

where

$$V_N(\mathbf{r}) = - \sum_{\mathbf{R}_A} \frac{Z_A e^2}{|\mathbf{r} - \mathbf{R}_A|}, \quad (6.6)$$

$$V_C(\mathbf{r}) = \sum_j \int d\mathbf{r}' \Phi_j^*(\mathbf{r}') \frac{e^2}{|\mathbf{r} - \mathbf{r}'|} \Phi_j(\mathbf{r}'), \quad (6.7)$$

$$V_{\text{ex}}^{(k)}(\mathbf{r}) = \sum_j \int d\mathbf{r}' \Phi_j^*(\mathbf{r}') \frac{e^2}{|\mathbf{r} - \mathbf{r}'|} \frac{\Phi_j(\mathbf{r}')}{\Phi_k(\mathbf{r}')} \Phi_k(\mathbf{r}') \langle \chi(\mathbf{s}_k) | \chi(\mathbf{s}_j) \rangle. \quad (6.8)$$

$V_N(\mathbf{r})$  is the potential due to the nucleus at  $\mathbf{R}_A$  whose charge is  $eZ_A$ ,  $V_C(\mathbf{r})$  is the Coulomb (electrostatic) interaction of the  $k$ th electron with all of the other electrons of the system, and  $V_{\text{ex}}^{(k)}(\mathbf{r})$  is the exchange interaction with all of the other electrons. The exchange interaction between electrons vanishes unless the spins are parallel. That is, the term  $\langle \chi(\mathbf{s}_k) | \chi(\mathbf{s}_j) \rangle$  vanishes unless both electrons are in the same spin state. It should also be noted that the contribution to  $V_C$  for  $j = k$  is exactly canceled out by a contribution to  $V_{\text{ex}}$  for  $j = k$  so that there is no interaction of the electron with itself. Equation (6.5) has the form of a Schrödinger equation for a one-electron system. The eigenvalue,  $\epsilon_k$ , of the Hartree–Fock equation for  $\Phi_k(\mathbf{r})$  plays the role of a one-electron energy. However,  $\epsilon_k$  is not the ionization energy of an electron in the state  $\Phi_k(\mathbf{r})$ ; rather it is the energy difference between an  $N$ -electron determinantal state and an  $(N - 1)$ -electron determinantal state obtained by removing the  $k$ th spin-orbital (Koopman’s theorem). For large  $N$ ,  $\epsilon_k$  approaches the ionization energy, but for small  $N$  the difference between the two can be substantial.

An approximate form of the exchange potential is often employed. One approximation, known as the “ $X\alpha$  approximation”, is based on the Fermi–Thomas model for which the exchange interaction is found to be proportional to the cube root of the charge density. The  $X\alpha$  exchange potential is

$$V_{X\alpha}(\mathbf{r}) = \frac{9}{2} \alpha \left( \frac{3\rho(\mathbf{r})}{8\pi} \right)^{1/3}, \quad (6.9)$$

where  $\rho(\mathbf{r})$  is the charge density at  $\mathbf{r}$ ,

$$\rho(\mathbf{r}) = e \sum_j \phi_j(\mathbf{r})^* \phi_j(\mathbf{r}). \quad (6.10)$$

The empirical parameter,  $\alpha$ , is usually chosen to be in the range between 2/3 and 1.

The Hartree–Fock equations can not be solved directly since the potentials depend on a-priori knowledge of the orbitals being sought. The equations must be solved by use of an iteration scheme. An initial set of orbitals is chosen and used to calculate the potentials. A new set of orbitals can be obtained from the Hartree–Fock equations. These new orbitals can then be used to determine new potentials. The process is iterated until the results are self-consistent, meaning that the input potentials do not differ significantly from the output potentials.

### 6.1.2 The LCAO method

The Hartree–Fock equations are the basis for numerical calculations of molecular and solid-state electronic structures. The LCAO method employs a finite set of atomic or atomic-like orbitals as the starting set of basis states. The advantage of this approach is that it provides a very simple and intuitive interpretation of the electronic structure.

For the LCAO method we assume the orbitals comprising the Slater determinant are linear combinations of hydrogen-like orbitals (states whose angular functions are spherical harmonics),

$$\Phi_k(\mathbf{r}) = \sum_n \sum_{\mu} C_{n\mu}^{(k)} \varphi_{\mu}(\mathbf{r} - \mathbf{R}_n), \quad (6.11)$$

where  $\varphi_{\mu}(\mathbf{r} - \mathbf{R}_n)$  is a hydrogen-like orbital for an atom centered at  $\mathbf{R}_n$ . The index  $\mu$  labels the different angular symmetry types  $\mu = s, p_x, p_y, p_z, d_{xy}, d_{xz}, \dots$ . The coefficients  $C_{n\mu}^{(k)}$  specify the amplitudes of the hydrogen-like orbitals comprising  $\Phi_k$ .

If (6.11) is used in the Hartree–Fock equations (6.5), an eigenvalue equation for the coefficients is obtained, namely

$$\sum_n \sum_{\alpha} \{\mathbb{H}_{m\beta, n\alpha} - \epsilon_k \mathbb{S}_{m\beta, n\alpha}\} C_{n\alpha}^{(k)} = 0, \quad (6.12)$$

where

$$\begin{aligned} \mathbb{H}_{m\beta, n\alpha} = & \int d\mathbf{r} \varphi_{\beta}(\mathbf{r} - \mathbf{R}_m)^* \left\{ \frac{-\hbar^2}{2m} \nabla^2 + V_N(\mathbf{r}) + V_C(\mathbf{r}) - V_{ex}^{(k)}(\mathbf{r}) \right\} \\ & \times \varphi_{\alpha}(\mathbf{r} - \mathbf{R}_n). \end{aligned} \quad (6.13)$$

$\mathbb{H}_{m\beta, n\alpha}$  is the matrix element of the Hartree–Fock Hamiltonian between hydrogenic states centered at  $\mathbf{R}_m$  and  $\mathbf{R}_n$  with symmetries  $\beta$  and  $\alpha$ , respectively, and

$$\mathbb{S}_{m\beta, n\alpha} = \int d\mathbf{r} \varphi_{\beta}(\mathbf{r} - \mathbf{R}_m)^* \varphi_{\alpha}(\mathbf{r} - \mathbf{R}_n) \quad (6.14)$$

is the overlap integral between the states. It should be noted that different hydrogen-like orbitals located on the same site are orthogonal to one another,

$$S_{m\beta, m\alpha} = \delta_{\alpha\beta},$$

but orbitals located on different sites are not. The overlap-matrix elements,  $S_{m\beta, n\alpha}$ , have magnitudes less than or equal to 1. From (6.14) it follows that  $S_{m\beta, n\alpha} = (S_{n\alpha, m\beta})^*$ . Since the overlap matrices are real,  $S_{m\beta, n\alpha} = S_{n\alpha, m\beta}$ .

As mentioned before, the equations must be solved self-consistently. In principle, an infinite set of hydrogen-like orbitals is required. However, in practice the set is finite, and this leads to what are called “truncation” errors.

## 6.2 Empirical LCAO models

Equation (6.12) is the basis for empirical LCAO models that employ a small number of atomic basis states and treat the matrix elements of the Hartree–Fock Hamiltonian and the overlap integrals as adjustable parameters to be determined by experiment or more accurate numerical calculations. Such empirical models provide conceptual understanding of the electronic structures of molecules.

### 6.2.1 LCAO matrix elements

If the Hartree–Fock Hamiltonian is approximated as a sum of spherically symmetric potentials centered on the atomic sites,

$$\mathbb{H}(\mathbf{r}) = \sum_t H_a(\mathbf{r} - \mathbf{R}_t), \quad (6.15)$$

then

$$\mathbb{H}_{n\alpha, m\beta} = \sum_t \int \varphi_\alpha(\mathbf{r} - \mathbf{R}_n)^* H_a(\mathbf{r} - \mathbf{R}_t) \varphi_\beta(\mathbf{r} - \mathbf{R}_m) d\mathbf{r}. \quad (6.16)$$

Equation (6.16) shows that there are several different types of matrix elements.

1. One-center integrals:

$$\int \varphi_\alpha(\mathbf{r} - \mathbf{R}_m)^* H_a(\mathbf{r} - \mathbf{R}_m) \varphi_\alpha(\mathbf{r} - \mathbf{R}_m) d\mathbf{r} \quad (t = m = n).$$

2. Two-center integrals:

$$\int \varphi_\alpha(\mathbf{r} - \mathbf{R}_n)^* H_a(\mathbf{r} - \mathbf{R}_t) \varphi_\beta(\mathbf{r} - \mathbf{R}_m) d\mathbf{r} \quad (t = n \text{ or } t = m).$$

3. Three-center integrals:

$$\int \varphi_\alpha(\mathbf{r} - \mathbf{R}_n)^* H_a(\mathbf{r} - \mathbf{R}_t) \varphi_\beta(\mathbf{r} - \mathbf{R}_m) d\mathbf{r} \quad (n, t, m; \text{all different}).$$

In applying the LCAO method to large molecules or to solids it is necessary to impose some cut-off distance  $R_c$  beyond which interactions and overlaps are



neglected. That is, interactions for which  $|\mathbf{R}_n - \mathbf{R}_m| > R_c$ ,  $|\mathbf{R}_t - \mathbf{R}_m| > R_c$ , or  $|\mathbf{R}_t - \mathbf{R}_n| > R_c$  are neglected.

Since atomic wavefunctions decrease exponentially with distance, it is physically reasonable to expect that the one-center integrals are larger than the two-center integrals and that the two-center integrals are larger than the three-center integrals. For a molecule with  $N$  atoms the numbers of one-center, two-center, and three-center integrals increase approximately as  $N$ ,  $N^2$ , and  $N^3$ , respectively. Therefore, three-center integrals can only be neglected if  $N$  times the magnitude of three-center integrals is small compared with the magnitude of two-center integrals.

### 6.3 Parameterized LCAO models

A simple, but very useful, approach to understanding the electronic structure of molecules is obtained by keeping only the one- and two-center integrals. Consider two atoms,  $A$  and  $B$ , of a molecule separated by the vector  $\mathbf{R}_{AB}$  with hydrogen-like orbitals  $\varphi_\alpha(\mathbf{r} - \mathbf{R}_A)$  and  $\varphi_\beta(\mathbf{r} - \mathbf{R}_B)$ . We define the matrix elements of the Hamiltonian as  $H_{\alpha,\beta}(\mathbf{R}_{AB})$  and the overlap integral as  $S_{\alpha,\beta}(\mathbf{R}_{AB})$ , and regard these matrix elements as parameters. It is further assumed that the potentials are spherically symmetric about each atomic site. This is a rather drastic assumption since the non-spherical charge density between atoms is responsible for molecular bonding. However, the use of this assumption does *not* mean that the resulting wavefunctions will produce a spherical charge density. In fact, the resulting wavefunctions lead to accumulated density between bonded atoms just as one would expect. The way to view this spherical-potential assumption is that it is the first step of a self-consistent procedure. The density computed from the wavefunctions is the second step in a self-consistent procedure.

With these assumptions the two-center matrix elements and overlap integrals vanish unless the two orbitals have the same symmetry about the internuclear axis,  $\mathbf{R}_{AB}$ . As a result matrix elements of the Hamiltonian have the same symmetry properties as the overlap integrals.

The type of overlap between two orbitals centered on different atoms is classified according to the symmetry about the line,  $\mathbf{R}_{AB}$ , joining the centers of the two orbitals. If the overlap is axially symmetric about  $\mathbf{R}_{AB}$  it is referred to as a “sigma” ( $\sigma$ ) overlap. If the overlap has a nodal plane containing  $\mathbf{R}_{AB}$  it is called a “pi” ( $\pi$ ) overlap. If there are two different nodal planes containing  $\mathbf{R}_{AB}$  the overlap is called a “delta” ( $\delta$ ) overlap. We can then define the two-center matrix elements of the Hamiltonian using the same convention as for the overlap integrals. We shall write the overlap integrals as

$$[\alpha\beta\eta]_{AB} = \int d\mathbf{r} \varphi_\alpha(\mathbf{r} - \mathbf{R}_A)^* \varphi_\beta(\mathbf{r} - \mathbf{R}_B), \quad (6.17)$$

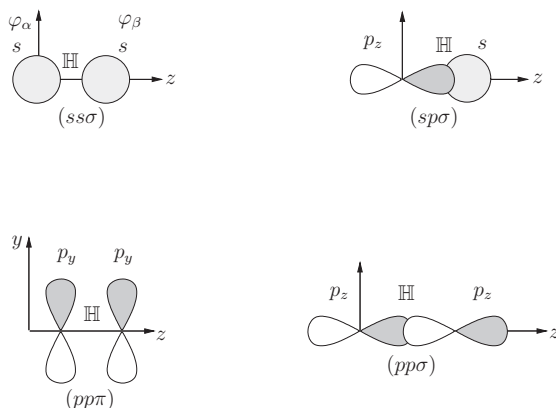


Figure 6.1 Fundamental Hamiltonian matrix elements for  $s$ - and  $p$ -orbitals. The shaded regions have positive phase and the unshaded regions indicate negative phase. The overlap integrals are defined in the same way (without the  $\mathbb{H}$ ).

where  $\eta$  indicates the overlap type, i.e.,  $\sigma$ ,  $\pi$ ,  $\delta$ , ... For the Hamiltonian matrix elements we write

$$(\alpha\beta\eta)_{AB} = \int d\mathbf{r} \varphi_{\alpha}(\mathbf{r} - \mathbf{R}_A)^* \mathbb{H}(\mathbf{r}) \varphi_{\beta}(\mathbf{r} - \mathbf{R}_B). \quad (6.18)$$

With this convention, brackets indicate an overlap integral and parentheses indicate a one- or two-center matrix element of the Hamiltonian. Figure 6.1 defines the fundamental Hamiltonian matrix elements for  $s$ - and  $p$ -orbitals. The same definitions can be used for the two-center overlaps. The phases of the orbitals shown in Fig. 6.1 are part of the definitions. A reversal of the phase of one orbital changes the sign of the overlap or matrix element. For example, if we reverse the  $+$  and  $-$  lobes of  $p_z$ , the  $[sp\sigma]$  overlap becomes  $-[sp\sigma]$ . If we reverse the phase of both functions  $[sp\sigma]$  remains unchanged.

Given  $\varphi_{\alpha}(\mathbf{r} - \mathbf{R}_i)$  and  $\varphi_{\beta}(\mathbf{r} - \mathbf{R}_j)$ , on arbitrary centers the overlap can be expressed in terms of the fundamental overlaps. To accomplish this the orbitals are expressed as linear combinations of orbitals parallel and perpendicular to the internuclear axis. The interactions can then be reduced to the fundamental matrix elements and overlap integrals. The fundamental integrals for the  $s$ - and  $p$ -orbitals are listed in Table 6.1.

Consider two atomic sites for which  $\mathbf{R}_i - \mathbf{R}_j = d(-1, 1, 0)$ . The direction cosines are  $-l = m = 1/\sqrt{2}$ . The interaction between a  $p_x$  orbital at the origin and a  $p_y$  orbital at  $d(-1, 1, 0)$  according to Table 6.1 is  $S_{xy} = -\frac{1}{2}[pp\sigma] + \frac{1}{2}[pp\pi]$  and the Hamiltonian matrix element is  $H_{xy} = -\frac{1}{2}(pp\sigma) + \frac{1}{2}(pp\pi)$ . To distinguish between interactions at different distances we shall affix a subscript on the

Table 6.1 *Overlap and matrix elements of the Hamiltonian between  $\varphi_\alpha(\mathbf{r} - \mathbf{R}_i)$  and  $\varphi_\beta(\mathbf{r} - \mathbf{R}_j)$ . Here  $l$ ,  $m$ , and  $n$  are the direction cosines of the vector  $\mathbf{R}_j - \mathbf{R}_i$ .*

Overlap	Hamiltonian matrix element
$S_{ss} = [ss\sigma]$	$H_{ss} = (ss\sigma)$
$S_{sx} = l[sp\sigma]$	$H_{sx} = l(sp\sigma)$
$S_{sy} = m[sp\sigma]$	$H_{sy} = m(sp\sigma)$
$S_{sz} = n[sp\sigma]$	$H_{sz} = n(sp\sigma)$
$S_{xx} = l^2[pp\sigma] - (1 - l^2)[pp\pi]$	$H_{xx} = l^2(pp\sigma) - (1 - l^2)(pp\pi)$
$S_{xy} = lm[pp\sigma] - lm[pp\pi]$	$H_{xy} = lm(pp\sigma) - lm(pp\pi)$
$S_{xz} = ln[pp\sigma] - ln[pp\pi]$	$H_{xz} = ln(pp\sigma) - ln(pp\pi)$
For $\mathbf{R}_i = \mathbf{R}_j$ :	
$S_{\alpha\beta} = \delta_{\alpha\beta}$	$H_{\alpha\beta} = \epsilon_\alpha \delta_{\alpha\beta}$

parentheses and brackets. For example, a nearest-neighbor interaction is  $[\alpha\beta\eta]_1$  or  $(\alpha\beta\eta)_1$ , and a second-nearest-neighbor interaction is  $[\alpha\beta\eta]_2$  or  $(\alpha\beta\eta)_2$ .

For the  $s$ - and  $p$ -orbital interactions a graphical method is efficient. The  $p$ -orbitals transform as ordinary vectors, and each  $p$ -orbital may be represented as an arrow, with the tip corresponding to positive phase. The  $s$ -orbital of positive phase can be represented by a circle. The fundamental interactions are then graphically represented as  $[ss\sigma] = \bigcirc\bigcirc$ ,  $(ss\sigma) = \bigcirc h \bigcirc$ ,  $[sp\sigma] = \bigcirc \leftarrow$ ,  $(sp\sigma) = \bigcirc h \leftarrow$ ,  $[pp\sigma] = \leftarrow \leftarrow$ ,  $(pp\sigma) = \leftarrow h \leftarrow$ ,  $[pp\pi] = \uparrow \uparrow$ , and  $(pp\pi) = \uparrow h \uparrow$ . From symmetry considerations we see that  $\bigcirc \uparrow = 0$ ,  $\uparrow \rightarrow = 0$ ,  $\bigcirc h \uparrow = 0$ , and  $\uparrow h \rightarrow = 0$ . Figure 6.2 illustrates how to calculate an  $s$ - $p$  and a  $p$ - $p$  overlap when the two atomic sites are on the diagonal of a square. The same resolution applies to the Hamiltonian matrix elements.

### 6.3.1 Orthogonalized basis functions

The matrix equation (6.12) has the same form as the molecular-vibration problem considered in Chapter 1. The group-theoretical methods employed in Chapter 1 can be used to find the eigenvalues and eigenvectors for the electronic states. We can transform the eigenvalue equation to standard form by a similarity transformation. Let  $C^{(k)}$  to be the column vector whose elements are  $C_{n\mu}^{(k)}$ , and define a new vector and Hamiltonian by

$$\mathbb{H}' = \mathbb{S}^{-1/2} \mathbb{H} \mathbb{S}^{-1/2}, \quad (6.19)$$

$$\mathbb{D}^{(k)} = \mathbb{S}^{1/2} C^{(k)}. \quad (6.20)$$

Then the eigenvalue equation becomes

$$\mathbb{H}' \mathbb{D}^{(k)} = \epsilon_k \mathbb{D}^{(k)}. \quad (6.21)$$

$$\begin{aligned}
 & \int \varphi_s(\mathbf{r} - \mathbf{R}_i)^* \varphi_{p_x}(\mathbf{r} - \mathbf{R}_j) d\mathbf{r} \quad \mathbf{R}_i = (0, 0, 0), \mathbf{R}_j = (-1, 1, 0) \\
 & \begin{array}{c} \text{Diagram: A square with a circle at the bottom-left corner and an arrow pointing up and to the right from the top-right corner.} \end{array} = \begin{array}{c} \text{Diagram: A square with a circle at the bottom-left corner and two arrows at the top-right corner, one pointing up and to the right, and one pointing up and to the left, both labeled } \frac{1}{\sqrt{2}}. \end{array} \\
 & = \frac{1}{\sqrt{2}} \text{ (circle)} \leftarrow + \frac{1}{\sqrt{2}} \text{ (circle)} \downarrow \\
 & = \frac{1}{\sqrt{2}} [sp\sigma] \\
 \\
 & \int \varphi_{p_x}(\mathbf{r} - \mathbf{R}_i)^* \varphi_{p_x}(\mathbf{r} - \mathbf{R}_j) d\mathbf{r} \\
 & \begin{array}{c} \text{Diagram: A square with an arrow pointing down from the bottom-left corner and an arrow pointing up and to the right from the top-right corner.} \end{array} = \begin{array}{c} \text{Diagram: A square with two arrows at the bottom-left corner, one pointing down and one pointing left, both labeled } \frac{1}{\sqrt{2}} \frac{1}{\sqrt{2}}, \text{ and two arrows at the top-right corner, one pointing up and to the right, and one pointing up and to the left, both labeled } \frac{1}{\sqrt{2}} \frac{1}{\sqrt{2}}. \end{array} \\
 & = \frac{1}{\sqrt{2}} \frac{1}{\sqrt{2}} \leftarrow \leftarrow + \frac{1}{\sqrt{2}} \frac{1}{\sqrt{2}} \downarrow \downarrow \\
 & = \frac{1}{2} [pp\sigma] + \frac{1}{2} [pp\pi] \\
 \\
 & \int \varphi_{p_x}(\mathbf{r} - \mathbf{R}_i)^* \varphi_{p_y}(\mathbf{r} - \mathbf{R}_j) d\mathbf{r} \\
 & \begin{array}{c} \text{Diagram: A square with an arrow pointing down from the bottom-left corner and an arrow pointing up and to the right from the top-right corner.} \end{array} = \begin{array}{c} \text{Diagram: A square with two arrows at the bottom-left corner, one pointing down and one pointing left, both labeled } \frac{1}{\sqrt{2}} \frac{1}{\sqrt{2}}, \text{ and two arrows at the top-right corner, one pointing up and to the right, and one pointing up and to the left, both labeled } \frac{1}{\sqrt{2}} \frac{1}{\sqrt{2}}. \end{array} \\
 & = \frac{1}{\sqrt{2}} \frac{1}{\sqrt{2}} \leftarrow \rightarrow + \frac{1}{\sqrt{2}} \frac{1}{\sqrt{2}} \downarrow \downarrow \\
 & = -\frac{1}{2} [pp\sigma] + \frac{1}{2} [pp\pi]
 \end{aligned}$$

Figure 6.2 A graphical method for calculating the  $s$ - $p$  overlap and Hamiltonian matrix elements.

The Hamiltonian  $\mathbb{H}'$  is a unitary,  $N \times N$  matrix, where  $N$  is the total number of hydrogen-like orbitals included in the analysis.  $C^{(k)}$  is a column vector with  $N$  components,  $C_{n\mu}^{(k)}$ . Equation (6.21) is in standard eigenvalue form and therefore the eigenvectors  $\mathbb{D}^{(k)}$  ( $k = 1$  to  $N$ ) are orthogonal to one another. The new basis orbitals corresponding to (6.20) are

$$\xi_\mu(\mathbf{r} - \mathbf{R}_n) = \sum_m \sum_v (\mathbb{S}^{-1/2})_{mv, n\mu} \varphi_v(\mathbf{r} - \mathbf{R}_m). \quad (6.22)$$

These functions, known as Löwdin orbitals, are more extended than the hydrogen-like orbitals, but they transform under the operations of the covering group in exactly the same way as do the hydrogen-like orbitals. As a result, the symmetry types of the matrix elements are identical to those of the hydrogen-like orbitals. The advantage of the Löwdin orbitals is that they form an orthogonal set, and the overlaps between *different* sites are zero:

$$\begin{aligned}
 & \int d\mathbf{r} \xi_\mu(\mathbf{r} - \mathbf{R}_n)^* \xi_\nu(\mathbf{r} - \mathbf{R}_m) \\
 & = \sum_j \sum_\alpha \sum_k \sum_\beta \mathbb{S}_{j\alpha, n\mu}^{-1/2} \int d\mathbf{r} \varphi_\alpha(\mathbf{r} - \mathbf{R}_j)^* \varphi_\beta(\mathbf{r} - \mathbf{R}_k) \mathbb{S}_{k\beta, m\nu}^{-1/2}
 \end{aligned}$$

$$\begin{aligned}
&= \sum_j \sum_\alpha \sum_k \sum_\beta \mathbb{S}_{j\alpha, n\mu}^{-1/2} \mathbb{S}_{j\alpha, k\beta} \mathbb{S}_{k\beta, mv}^{-1/2} \\
&= (\mathbb{S}^{-1/2} \mathbb{S} \mathbb{S}^{-1/2})_{n\mu, mv} = \mathbb{I}_{n\mu, mv} = \delta_{nm} \delta_{\mu\nu}.
\end{aligned} \tag{6.23}$$

In arriving at the final result in (6.23) we have used the fact that  $\mathbb{S}_{j\alpha, n\mu}^{-1/2} = \mathbb{S}_{n\mu, j\alpha}^{-1/2}$ .

As a very simple example consider a diatomic molecule,  $AB$ , with a single orbital on each atom. The hydrogen-like orbitals are  $\varphi_\alpha(\mathbf{r} - \mathbf{R}_A)$  and  $\varphi_\beta(\mathbf{r} - \mathbf{R}_B)$ , and the overlap matrix and its inverse are

$$\mathbb{S} = \begin{pmatrix} 1 & S \\ S & 1 \end{pmatrix}, \tag{6.24}$$

$$\mathbb{S}^{-1/2} = \begin{pmatrix} a & b \\ b & a \end{pmatrix}, \tag{6.25}$$

where

$$\begin{aligned}
a &= \frac{1}{2} \left\{ \frac{1}{\sqrt{1+S}} + \frac{1}{\sqrt{1-S}} \right\}, \\
b &= \frac{1}{2} \left\{ \frac{1}{\sqrt{1+S}} - \frac{1}{\sqrt{1-S}} \right\}.
\end{aligned} \tag{6.26}$$

The Löwdin orbitals are then

$$\xi_\alpha(\mathbf{r} - \mathbf{R}_A) = a \varphi_\alpha(\mathbf{r} - \mathbf{R}_A) + b \varphi_\beta(\mathbf{r} - \mathbf{R}_B), \tag{6.27}$$

$$\xi_\beta(\mathbf{r} - \mathbf{R}_B) = a \varphi_\beta(\mathbf{r} - \mathbf{R}_B) + b \varphi_\alpha(\mathbf{r} - \mathbf{R}_A). \tag{6.28}$$

As an illustration, assume an overlap of  $S = 0.2$ , then  $a = 1.015452$  and  $b = -0.102582$ . The Löwdin orbitals  $\xi_\alpha(\mathbf{r} - \mathbf{R}_A)$  and  $\xi_\beta(\mathbf{r} - \mathbf{R}_B)$  are orthogonal to one another since  $(a^2 + b^2)S + 2ab = 0$ . They are also properly normalized since  $a^2 + b^2 + 2abS = 1$ .

Empirical models using Löwdin orbitals are much simpler to deal with because the basis states form an orthogonal set. The absence of overlap integrals reduces the number of parameters by roughly a factor of two. The question of whether the hydrogen-like-orbital model with overlap integrals has more adjustable parameters than an empirical model that is based on the Löwdin orbitals then arises. We could have selected a set of overlap and interaction parameters (e.g., by fitting the results to data) for a hydrogen-like model. If instead we use the Löwdin orbitals the number of apparent empirical parameters is greatly reduced. If we now select the parameters to fit data, the parameters will not be the same as in the previous method because we are identifying the eigenvalues of different basis orbitals with the same physical data.

Often chemists employ what are called hybrid orbitals as the basis functions. These are linear combinations of orbitals that have the same symmetry about the

internuclear axis joining two atomic sites. The  $s$ - $p$  hybrid orbitals, for example, are formed by the sum and difference of  $s$ - and  $p$ -orbitals with the same principal quantum number on the same site. The idea is to form hybrid functions that lead to an accumulation of charge between the atoms that bond in the molecule.

#### 6.4 An example: The electronic structure of squareene

As a tutorial example we shall analyze the electronic structure of the fictitious squareene molecule. Recall that squareene is a square molecule with identical atoms on each corner. For this example let us assume that the outer electrons on the squareene atoms possess  $2s$  and  $2p$  orbitals. The  $1s$  orbitals are tightly bound to their nuclei. These “core states” are far removed in energy from the outer  $2p$  and  $2s$  electrons’ levels and may be omitted since the molecular binding is due principally to the interactions among the  $2s$  and  $2p$  electrons.

In Chapter 1 we restricted our analysis to the plane of the molecule. Here we want to consider all three dimensions, therefore the point group of the covering operations is  $D_{4h}$  ( $D_4 \times i$ ) rather than  $C_{4v}$ . However, as we shall see, we can still derive all of the information we need using the simpler  $C_{4v}$  group. The behavior of the symmetry functions under inversion will be obvious. The coordinates and basis functions to be used in our analysis are shown schematically in Fig. 6.3.

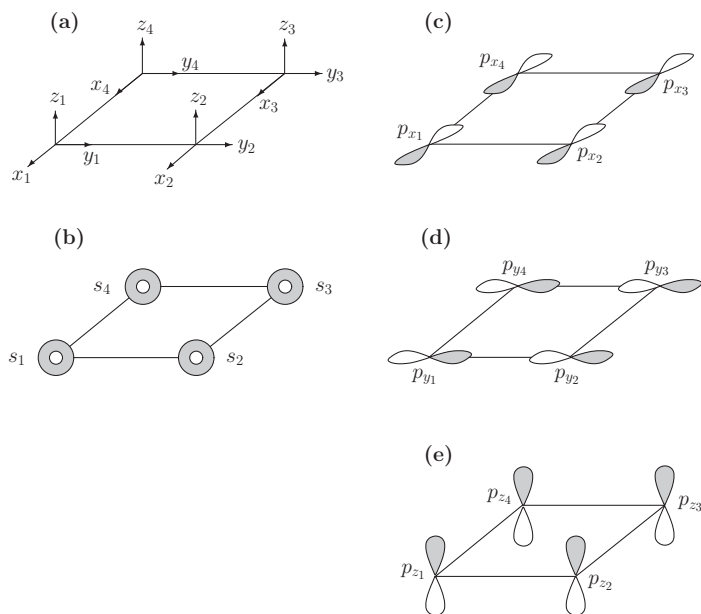


Figure 6.3 The coordinate system and basis functions for squareene: (a) coordinates, (b)  $2s$  orbitals, (c)  $2p_x$  orbitals, (d)  $2p_y$  orbitals, and (e)  $2p_z$  orbitals.

Table 6.2 The action table for the  $2s$  and  $2p$  orbitals of squarene. Here  $s = \varphi_{2s}(\mathbf{r} - \mathbf{R})$  and  $p_\kappa = \varphi_{p\kappa}(\mathbf{r} - \mathbf{R})$ , where  $\kappa = x, y$ , or  $z$ .

	$E$	$C_4$	$C_2$	$C_4^3$	$\sigma_{v1}$	$\sigma_{v2}$	$\sigma_{d1}$	$\sigma_{d2}$
1	1	4	3	2	1	3	2	4
2	2	1	4	3	4	2	1	3
3	3	2	1	4	3	1	4	2
4	4	3	2	1	2	4	3	1
$p_x$	$p_x$	$-p_y$	$-p_x$	$p_y$	$-p_y$	$p_y$	$p_x$	$-p_x$
$p_y$	$p_y$	$p_x$	$-p_y$	$-p_x$	$-p_x$	$p_x$	$-p_y$	$p_y$
$p_z$	$p_z$	$p_z$	$p_z$	$p_z$	$p_z$	$p_z$	$p_z$	$p_z$
$s$	$s$	$s$	$s$	$s$	$s$	$s$	$s$	$s$

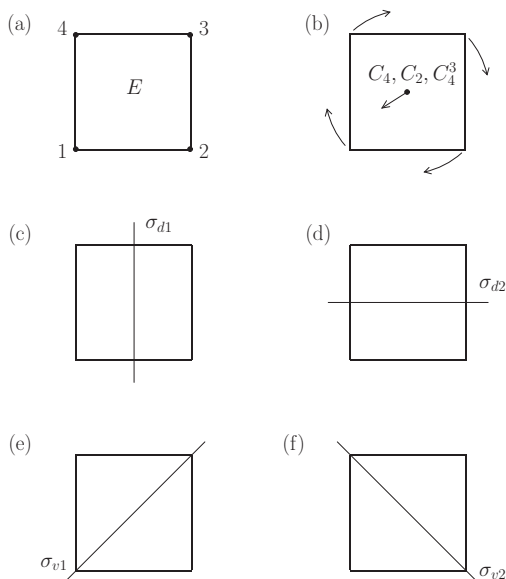


Figure 6.4 Symmetry operations of the  $C_{4v}$  group. (a)  $E$  is the identity. (b) There is a four-fold rotation axis perpendicular to the plane of the molecule. Rotations about this axis include  $C_2$ ,  $C_4$ , and  $C_4^3$ . In (c) and (d) we show  $\sigma_{d1}$  and  $\sigma_{d2}$ : reflections in a line bisecting the sides of the square. In (e) and (f) we show  $\sigma_{v1}$  and  $\sigma_{v2}$ : reflections in a diagonal line passing through diagonally opposite corners of the square.

The operations of the group are to be applied to the basis functions while the coordinate system remains fixed in space. The operations of the  $C_{4v}$  group are given in Chapter 1, but are repeated here for convenience in Fig. 6.4.

The action table for the  $s$ - and  $p$ -orbitals is shown in Table 6.2. This table allows us to determine the effect of any operation on any  $s$  or  $p$  basis function. For example, under the operation  $C_4$ , a  $p_z$  orbital at corner 1 is rotated into a

$p_z$  orbital on corner 4. That is,  $P(C_4) \varphi_{p_z}(\mathbf{r} - \mathbf{R}_1) = \varphi_{p_z}(\mathbf{r} - \mathbf{R}_4)$ . Similarly,  $P(\sigma_{v2}) \varphi_{p_x}(\mathbf{r} - \mathbf{R}_1) = \varphi_{p_y}(\mathbf{r} - \mathbf{R}_3)$ .

Since  $\varphi_{p_x}(\mathbf{r} - \mathbf{R}_i)$ ,  $\varphi_{p_y}(\mathbf{r} - \mathbf{R}_i)$ , and  $\varphi_{p_z}(\mathbf{r} - \mathbf{R}_i)$  transform under the group operations in the same way as the displacement vectors  $r_{x_i}$ ,  $r_{y_i}$ , and  $r_{z_i}$ , the *symmetry* properties of the  $p$ -orbital system are identical to the symmetry properties of the nuclear displacements considered in Chapter 1. The symmetry functions for the  $p$ -orbitals are completely analogous to those of the vibrational problem. However, for the  $p$ -orbital system there are no analogs to the body modes of translation and rotation. As a result the eigenvectors (linear combinations of symmetry functions) will in general be different.

There are in total 16 basis functions for the matrix representations. These are four  $2s$  orbitals, four  $p_z$  orbitals, four  $p_x$  orbitals, and four  $p_y$  orbitals. However, no symmetry element can transform a  $2s$  orbital into a  $p$ -orbital or a  $p_z$  orbital into a  $p_x$  or  $p_y$  orbital. The  $2s$  and also the  $p_z$  orbitals transform only among themselves. However, the  $p_x$  and  $p_y$  orbitals are transformed into one another. As a result of this, the determination of the symmetry functions can be carried out separately for the  $2s$ ,  $p_z$ , and  $(p_x, p_y)$  orbitals.

#### 6.4.1 $s$ - and $p_z$ -orbital symmetry functions

In order to find the orbital symmetry functions, we need the characters for the basis-function representations of the operations. These may be obtained from the action table by simply adding the number of basis functions that are unchanged by an operation minus the number transformed into the negative of themselves. Consider the  $p_z$  orbitals first. From the action table it is clear that only the operations  $E$ ,  $\sigma_{v1}$ , and  $\sigma_{v2}$  leave all or some of orbitals in their original positions. On looking at the column for  $\sigma_{v1}$  we see that  $p_{z1}$  and  $p_{z3}$  are transformed into themselves, and therefore the trace of the representation will be 2. For  $\sigma_{v2}$ ,  $p_{z2}$  and  $p_{z4}$  are transformed into themselves, so the representation character is also 2 (as it must be, since  $\sigma_{v1}$  and  $\sigma_{v2}$  are in the same class). Clearly the character of the matrix representing  $E$  is 4, the number of  $p_z$  orbitals. The same characters are obtained for the  $2s$  orbitals. We designate the representation based on the  $2s$  orbitals as  $\Gamma^{2s}$  and the representation based on the  $p_z$  orbitals as  $\Gamma^z$ . The character table for  $C_{4v}$  is shown in Table 6.3. Characters for the representation matrices of  $\Gamma^z$  and  $\Gamma^{2s}$  are shown on the last two lines of the character table.

The decomposition of a reducible representation,  $\Gamma$ , into the IRs of a group is given by

$$n^\alpha = \frac{1}{h} \sum_R \chi(R)^* \chi^\alpha(R), \quad (6.29)$$



Table 6.3 The character table for  $C_{4v}$  (top) and the characters for the representations  $\Gamma^{xy}$ ,  $\Gamma^z$ , and  $\Gamma^{2s}$ 

$C_{4v}$	$E$	$C_2$	$2C_4$	$2\sigma_{v1}$	$2\sigma_{d1}$
$A_1$	1	1	1	1	1
$A_2$	1	1	1	-1	-1
$B_1$	1	1	-1	1	-1
$B_2$	1	1	-1	-1	1
$\mathcal{E}$	2	-2	0	0	0
$\Gamma^{xy}$	8	0	0	0	0
$\Gamma^z$	4	0	0	2	0
$\Gamma^{2s}$	4	0	0	2	0

where  $h$  is the order of the group ( $h = 8$  in this case),  $\chi(R)$  is the character of the operation for the reducible representation,  $\chi^\alpha(R)$  is the character of the  $\alpha$ th IR of the group ( $C_{4v}$  in this case), and  $n^\alpha$  is the number of times  $\Gamma^\alpha$  is contained in  $\Gamma$ . The index  $R$  runs over the operations of the group. For the  $2s$  and  $p_z$  orbitals the decomposition gives

$$\Gamma^{2s} = a_1 + b_1 + e, \quad (6.30)$$

$$\Gamma^z = a_1 + b_1 + e. \quad (6.31)$$

In (6.30) and (6.31) the labels for the IRs are shown as lower-case letters. In this chapter we shall use lower-case letters for the IRs of one-electron functions and upper-case letters such as  $A_1$  or  $B_1$  to characterize a many-electron molecular state.

To generate the symmetry coordinates for squarene we proceed in the usual way. For the one-dimensional IRs,

$$f^\alpha \propto \sum_R \chi^\alpha(R) P_R f, \quad (6.32)$$

where  $f$  is an arbitrary combination of orbitals. For a representation of higher dimensionality,

$$f_i^\alpha \propto \sum_R D^\alpha(R)_{ii} P_R f, \quad (6.33)$$

where  $D^\alpha(R)_{ii}$  is a diagonal element of the  $\alpha$  IR matrix for the  $R$  operation. For the  $e$  representation the matrix elements were obtained in Chapter 1, in Table 1.7. The non-zero, diagonal matrix elements for row 1 are  $\Gamma^{\mathcal{E}}(E)_{11} = 1$ ,  $\Gamma^{\mathcal{E}}(C_2)_{11} = -1$ ,  $\Gamma^{\mathcal{E}}(\sigma_{d1})_{11} = -1$ , and  $\Gamma^{\mathcal{E}}(\sigma_{d2})_{11} = 1$ . For row 2 the non-zero diagonal matrix elements are  $\Gamma^{\mathcal{E}}(E)_{11} = 1$ ,  $\Gamma^{\mathcal{E}}(C_2)_{11} = -1$ ,  $\Gamma^{\mathcal{E}}(\sigma_{d1})_{11} = 1$ , and  $\Gamma^{\mathcal{E}}(\sigma_{d2})_{11} = -1$ .

(These matrix elements can be deduced from the action table since  $p_x$  and  $p_y$  are basis functions for the  $e$  IR.) Using  $s_1$  as  $f$ , we find (after normalizing the functions) that

$$f^{2s}(a_1) = \frac{1}{2}(s_1 + s_2 + s_3 + s_4), \quad (6.34)$$

$$f^{2s}(b_1) = \frac{1}{2}(s_1 - s_2 + s_3 - s_4), \quad (6.35)$$

$$f^{2s_1}(e) = \frac{1}{2}(s_1 - s_2 - s_3 + s_4) \quad (\text{row 1}), \quad (6.36)$$

$$f^{2s_2}(e) = \frac{1}{2}(s_1 - s_2 + s_3 - s_4) \quad (\text{row 2}). \quad (6.37)$$

Using  $f = p_{z1}$  yields the symmetry coordinates,

$$f^z(a_1) = \frac{1}{2}(p_{z1} + p_{z2} + p_{z3} + p_{z4}), \quad (6.38)$$

$$f^z(b_1) = \frac{1}{2}(p_{z1} - p_{z2} + p_{z3} - p_{z4}), \quad (6.39)$$

$$f_1^z(e) = \frac{1}{2}(p_{z1} - p_{z2} - p_{z3} + p_{z4}) \quad (\text{row 1}), \quad (6.40)$$

$$f_2^z(e) = \frac{1}{2}(p_{z1} + p_{z2} - p_{z3} - p_{z4}) \quad (\text{row 2}). \quad (6.41)$$

The  $2s$  and  $2p_z$  symmetry functions are shown schematically in Fig. 6.5. For the  $2s$  symmetry functions it can be seen that the  $a_1$  and  $b_1$  functions are invariant under inversion and therefore they can be labeled as “ $g$ ” functions. The  $2s$   $e$  functions are antisymmetric under inversion and can be labeled as “ $u$ ” functions. For the  $p_z$  functions the converse is true. The  $a_1$  and  $b_1$  are antisymmetric under inversion, while the  $e$  symmetry functions are symmetric.

Therefore, the decompositions of  $\Gamma^{2s}$  and  $\Gamma^z$  can be written as

$$\Gamma^{2s} = a_{1g} + b_{1g} + e_u, \quad \Gamma^z = a_{1u} + b_{1u} + e_g. \quad (6.42)$$

### 6.4.2 $p_x$ – $p_y$ symmetry functions

The orbitals  $p_x$  and  $p_y$  are transformed into one another by some of the symmetry operations. Therefore they must be considered together. There are four  $p_x$  and four  $p_y$  orbitals, so the representations based on these functions are  $8 \times 8$  matrices. It can be seen from the action table that the only operation with a non-zero trace is the identity, for which  $\chi^{xy}(E) = 8$ .

Therefore the decomposition into the IRs of  $C_{4v}$  is

$$\Gamma^{xy} = a_1 + a_2 + b_1 + b_2 + 2e. \quad (6.43)$$

Table 6.4 Symmetry functions for the  $p_x$  and  $p_y$  basis orbitals. There are two  $e$  representations. The first is labeled “ $a$ ” with partners  $1a$  (row 1) and  $2a$  (row 2); the second is labeled “ $b$ ” with partners  $1b$  and  $2b$ . The “ $g$ ” and “ $u$ ” labels are assigned according the symmetry of the function under inversion.

---

---

$f^{xy}(a_{1g}) = (1/\sqrt{8})(p_{x1} + p_{x2} - p_{x3} - p_{x4} - p_{y1} + p_{y2} + p_{y3} - p_{y4})$
$f^{xy}(a_{2g}) = (1/\sqrt{8})(p_{x1} - p_{x2} - p_{x3} + p_{x4} + p_{y1} + p_{y2} - p_{y3} - p_{y4})$
$f^{xy}(b_{1g}) = (1/\sqrt{8})(p_{x1} - p_{x2} - p_{x3} + p_{x4} - p_{y1} - p_{y2} + p_{y3} + p_{y4})$
$f^{xy}(b_{2g}) = (1/\sqrt{8})(p_{x1} + p_{x2} - p_{x3} - p_{x4} + p_{y1} - p_{y2} - p_{y3} + p_{y4})$
$f_{1a}^{xy}(e_u) = \frac{1}{2}(p_{x1} - p_{x2} + p_{x3} - p_{x4})$
$f_{2a}^{xy}(e_u) = \frac{1}{2}(p_{x1} + p_{x2} + p_{x3} + p_{x4})$
$f_{1b}^{xy}(e_u) = \frac{1}{2}(p_{y1} + p_{y2} + p_{y3} + p_{y4})$
$f_{2b}^{xy}(e_u) = \frac{1}{2}(p_{y1} - p_{y2} + p_{y3} - p_{y4})$

---

---

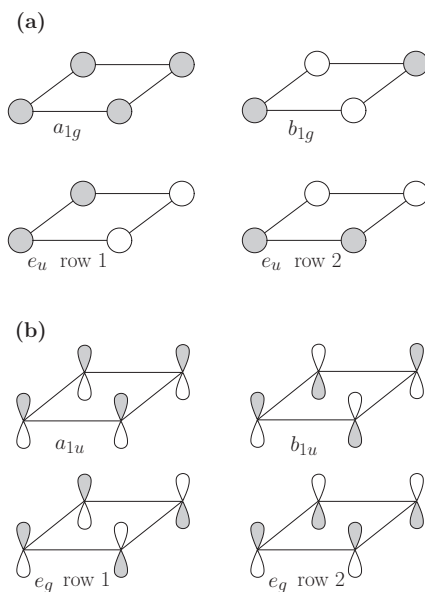


Figure 6.5 Symmetry functions for  $2s$  and  $2p_z$  orbitals. The  $g$  and  $u$  labels have been added to indicate the behavior under the inversion operation.

The  $p_x$ – $p_y$  symmetry functions given in Table 6.4 are shown schematically in Fig. 6.6.

From Fig. 6.6 we can see that the  $a_1$ ,  $a_2$ ,  $b_1$ , and  $b_2$  symmetry functions are symmetric under inversion. The  $e$  symmetry functions are antisymmetric under inversion. Therefore, the decomposition can be written as

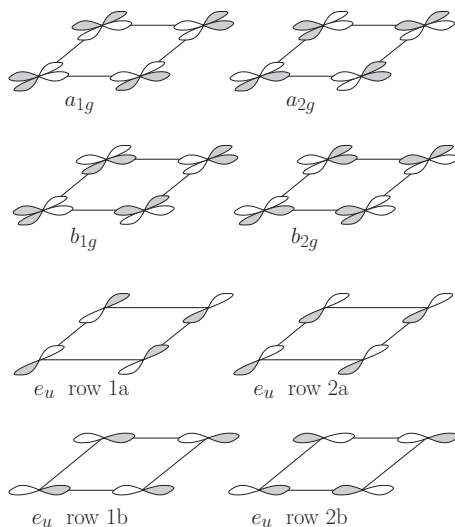


Figure 6.6  $p_x$ - $p_y$  symmetry functions. The labels  $u$  and  $g$  have been added to indicate the behavior of the functions under the inversion operation.

$$\Gamma^{xy} = a_{1g} + a_{2g} + b_{1g} + b_{2g} + 2e_u. \quad (6.44)$$

### 6.4.3 Analysis of the decompositions

The  $16 \times 16$  representation for the molecule,  $\Gamma(\text{molecule})$ , based on all of the orbitals is

$$\begin{aligned} \Gamma(\text{molecule}) &= \Gamma^{2s} + \Gamma^z + \Gamma^{xy} \\ &= 2a_{1g} + a_{2g} + 2b_{1g} + b_{2g} + e_g + a_{1u} + b_{1u} + 3e_u. \end{aligned}$$

We can now determine the blocks of the secular equation (6.12) when it is transformed to symmetry-function coordinates. First we note that  $\Gamma^z$  has no IRs in common with either  $\Gamma^{xy}$  or  $\Gamma^{2s}$ . Therefore the eigenvectors of the  $\Gamma^z$  states will have no mixing with the  $2s$ ,  $p_x$ , or  $p_y$  orbitals. Since the  $p_z$  orbitals interact with each other only by means of the  $\pi$  overlaps and  $\pi$  matrix elements, the  $p_z$  orbitals form pure “ $\pi$  states”. Second, the one-dimensional IRs,  $a_{2g}$ ,  $b_{2g}$ ,  $a_{1u}$ , and  $b_{1u}$ , each occur only once in  $\Gamma(\text{molecule})$ , and therefore the symmetry functions for these representations must also be eigenvectors.

In the symmetry-function representation the secular equation has four  $1 \times 1$  blocks ( $a_{2g}$ ,  $b_{2g}$ ,  $a_{1u}$ , and  $b_{1u}$ ). Furthermore, since the Hamiltonian matrix elements and overlaps between different rows of the same representation vanish, the two partner functions for the  $e_g$  representation are also eigenvectors. That is, the  $2 \times 2$

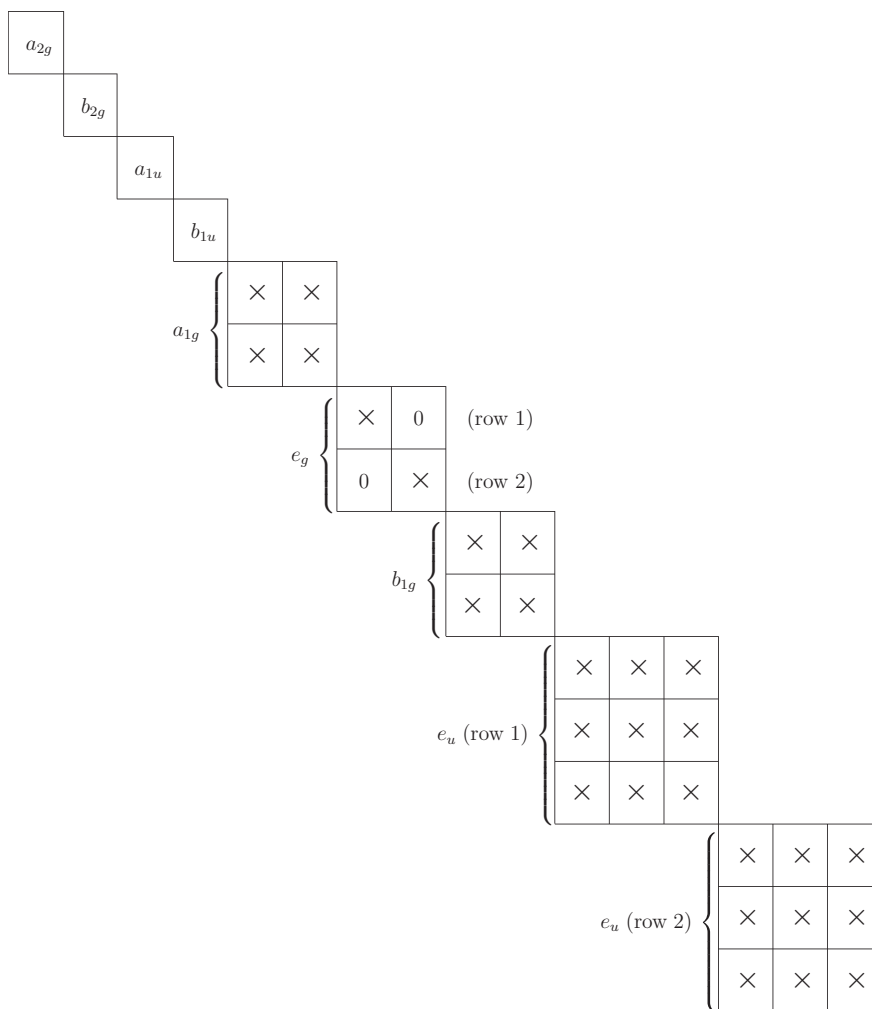


Figure 6.7 The block-diagonal form of the secular matrix when transformed to symmetry-function coordinates.

$e_g$  block must be diagonal. The  $a_{2g}$  and  $b_{2g}$  symmetry functions are unique to  $\Gamma^{xy}$ , and therefore the eigenvectors involve only  $p_x$  and  $p_y$  orbitals. Finally,  $e_u$  occurs three times and that leads to two  $3 \times 3$  blocks; one  $3 \times 3$  block for the first-row functions and one  $3 \times 3$  block for the second-row functions. The eigenfunctions will be admixtures of  $2s$ ,  $2p_x$ , and  $2p_y$  orbitals. The block-diagonal form of the Hamiltonian matrix in the symmetry-function representation is shown in Fig. 6.7.

To find the eigenvalues and eigenvectors of squareene, we can transform the secular matrix from the  $2s$  and  $2p$  representation to the symmetry-function representation. The matrix  $U$  which accomplishes this is constructed from the symmetry

functions. The columns of the  $(16 \times 16)$   $U$  matrix are 16-component column vectors whose components are the coefficients of the symmetry functions. The transformation

$$U^{-1}(\mathbb{H} - \epsilon \mathbb{S})U \quad (6.45)$$

casts the eigenvalue problem into the block-diagonal form shown in Fig. 6.7.

Alternately, we can compute the overlap- and interaction-matrix elements between the symmetry functions belonging to the same IRs. In Chapter 1 we carried out the  $U$  transformation and then solved the secular equations for the smaller blocks. Here we shall use the alternate method of calculating the matrix elements between symmetry functions, a procedure mathematically equivalent to transforming the  $\mathbb{H} - \epsilon \mathbb{S}$  matrix.

Since all of the  $\Gamma^z$  symmetry functions are eigenstates, we need only calculate the diagonal matrix elements and overlap for each  $\Gamma^z$  symmetry function (Table 6.4) to obtain the eigenvalues.

For these functions,

$$\epsilon = \frac{\int f^{z*} \mathbb{H} f^z d\mathbf{r}}{\int f^{z*} f^z d\mathbf{r}}. \quad (6.46)$$

The overlap for  $f^z(a_{1u})$  is

$$\begin{aligned} & \int f^z(a_{1u})^* f^z(a_{1u}) d\mathbf{r} \\ &= \frac{1}{4} \int d\mathbf{r} (p_{z1} + p_{z2} + p_{z3} + p_{z4})^* (p_{z1} + p_{z2} + p_{z3} + p_{z4}) \\ &= \frac{1}{4} \left[ \int d\mathbf{r} (p_{z1}^2 + p_{z2}^2 + p_{z3}^2 + p_{z4}^2) \right. \\ & \quad \left. + 2\{p_{z1}(p_{z2} + p_{z3} + p_{z4}) + p_{z2}(p_{z3} + p_{z4}) + p_{z3}p_{z4}\} \right] \\ &= \int d\mathbf{r} \{(p_{z1}^* p_{z1}) + [p_{z1}^* (p_{z2} + p_{z4})] + (p_{z1}^* p_{z3})\} \\ &= \begin{matrix} 1 + & 2 \uparrow \uparrow_1 & + & \uparrow \uparrow_2 \\ 1 + & 2[pp\pi]_1 & + & [pp\pi]_2, \end{matrix} \quad (6.47) \end{aligned}$$

where  $[pp\pi]_1$  is the overlap between  $p_z$  orbitals on adjacent sites and  $[pp\pi]_2$  is the overlap between  $p_z$  orbitals on diagonally separated sites. For the matrix elements of the Hamiltonian,

$$\int f^z(a_{1u})^* \mathbb{H} f^z(a_{1u}) d\mathbf{r} = \int \frac{p_{z1} + p_{z2} + p_{z3} + p_{z4}}{2} \mathbb{H} \frac{p_{z1} + p_{z2} + p_{z3} + p_{z4}}{2} d\mathbf{r}$$

$$\begin{aligned}
&= 4 \int \frac{1}{4} \{ (p_{z1}^* \mathbb{H} p_{z1}) + [p_{z1}^* \mathbb{H} (p_{z2} + p_{z4})] \\
&\quad + (p_{z1}^* \mathbb{H} p_{z3}) \} d\mathbf{r} \\
&= \epsilon_p + 2(pp\pi)_1 + (pp\pi)_2,
\end{aligned} \tag{6.48}$$

where  $(pp\pi)_1$  is the Hamiltonian matrix element between adjacent  $p_z$  functions on adjacent sites and  $(pp\pi)_2$  is the matrix element between  $p_z$  functions on diagonally separated sites. The diagonal interaction,  $\epsilon_p$ , is roughly the energy of the isolated  $p$ -orbital without any  $2s$  orbital mixing.

From (6.47) and (6.48) we obtain the eigenvalue for the  $a_{1u}$  state,

$$\epsilon(a_{1u}) = \frac{\epsilon_{pz} + 2(pp\pi)_1 + (pp\pi)_2}{1 + 2[pp\pi]_1 + [pp\pi]_2}. \tag{6.49}$$

The result for  $\epsilon(a_{1u})$  involves only  $\pi$ -type overlaps and interactions, and therefore it is sometimes labeled by the symbol  $\pi(a_{1u})$ .

As a second example we consider the  $b_{2g}$  state constructed from  $p_x$  and  $p_y$  orbitals. The analysis is easily carried out using either the graphical method or Table 6.1. To simplify the notation, we use  $x_i$  and  $y_i$  to represent the  $p_{x_i}$  and  $p_{y_i}$  orbitals.

For the  $b_{2g}$  state we need to calculate

$$\frac{\int d\mathbf{r} f^{xy}(b_{2g})^* \mathbb{H} f^{xy}(b_{2g})}{\int d\mathbf{r} |f^{xy}(b_{2g})|^2}$$

with

$$f^{xy}(b_{2g}) = \frac{1}{\sqrt{8}} \{x_1 + x_2 - x_3 - x_4 + y_1 - y_2 - y_3 + y_4\}. \tag{6.50}$$

Consider one of the products,

$$\begin{aligned}
&\int d\mathbf{r} \left( \frac{x_1}{\sqrt{8}} \right)^* \mathbb{H} f^{xy}(b_{2g}) \\
&= \int d\mathbf{r} \frac{1}{8} (x_1)^* \mathbb{H} \{x_1 + x_2 - x_3 - x_4 + y_1 - y_2 - y_3 + y_4\} \\
&= \frac{1}{8} \left[ \epsilon_p + \downarrow\downarrow_1 - \left\{ \frac{1}{2} \downarrow\downarrow_2 + \frac{1}{2} \leftarrow\leftarrow_2 \right\} - \rightarrow\rightarrow_1 \right. \\
&\quad \left. + \downarrow\rightarrow_0 + \downarrow\rightarrow_1 - \left\{ -\frac{1}{2} \rightarrow\rightarrow_2 + \frac{1}{2} \downarrow\downarrow_2 \right\} + \downarrow\rightarrow_1 \right] \\
&= \frac{1}{8} \{ \epsilon_{px} + (pp\pi)_1 - (pp\sigma)_1 - (pp\pi)_2 \}.
\end{aligned} \tag{6.51}$$

It is easily verified that  $\int d\mathbf{r} (\phi/\sqrt{8})^* \mathbb{H} f^{xy}(b_{2g})$  gives the same result, where  $\phi$  is  $-x_2, -x_3, x_4, -y_1, -y_2, y_3$ , or  $y_4$ , so

$$\int d\mathbf{r} f^{xy}(b_{2g})^* \mathbb{H} f^{xy}(b_{2g}) = \{\epsilon_{p_x} + (pp\pi)_1 - (pp\sigma)_1 - (pp\pi)_2\}. \quad (6.52)$$

A similar calculation gives the overlap as

$$\int d\mathbf{r} f^{xy}(b_{2g})^* f^{xy}(b_{2g}) = 1 + [pp\pi]_1 - [pp\sigma]_1 - [pp\pi]_2. \quad (6.53)$$

Therefore, the eigenvalue is

$$\epsilon(b_{2g}) = \frac{\epsilon_{p_x} + (pp\pi)_1 - (pp\sigma)_1 - (pp\pi)_2}{1 + [pp\pi]_1 - [pp\sigma]_1 - [pp\pi]_2}. \quad (6.54)$$

The diagonal parameters  $\epsilon_{p_x}$  and  $\epsilon_{p_y}$  are necessarily equal, since they represent integrals that are symmetrically equivalent; however,  $\epsilon_{p_z}$  will be different because the lobes of the  $p_z$  orbital point into a different environment. For simplicity we have taken all of them to be equal to  $\epsilon_p$ .

As a last example we consider the  $2 \times 2$  block for the  $a_{1g}$  states. These states involve  $f^{xy}(a_{1g})$  and  $f^{2s}(a_{1g})$  symmetry coordinates.

The  $2 \times 2$  secular equation that mixes these two symmetry functions is

$$\begin{vmatrix} M_{11} - \epsilon S_{11} & M_{12} - \epsilon S_{12} \\ M_{12} - \epsilon S_{12} & M_{22} - \epsilon S_{22} \end{vmatrix} = 0, \quad (6.55)$$

where

$$\begin{aligned} M_{11} &= \frac{1}{4} \int d\mathbf{r} (s_1 + s_2 + s_3 + s_4) \mathbb{H} (s_1 + s_2 + s_3 + s_4) \\ &= \epsilon_s + 2(ss\sigma)_1 + (ss\sigma)_2, \end{aligned} \quad (6.56)$$

$$\begin{aligned} M_{12} &= \frac{1}{\sqrt{32}} \int d\mathbf{r} (s_1 + s_2 + s_3 + s_4) \\ &\quad \times \mathbb{H} (x_1 + x_2 - x_3 - x_4 - y_1 + y_2 + y_3 - y_4) \\ &= -\sqrt{2}(ss\sigma)_1 - (ss\sigma)_2, \end{aligned} \quad (6.57)$$

$$\begin{aligned} M_{22} &= \frac{1}{8} \int d\mathbf{r} (x_1 + x_2 - x_3 - x_4 - y_1 + y_2 + y_3 - y_4) \\ &\quad \times \mathbb{H} (x_1 + x_2 - x_3 - x_4 - y_1 + y_2 + y_3 - y_4) \\ &= \epsilon_x + (pp\pi)_1 - (pp\sigma)_1 - (pp\sigma)_2, \end{aligned} \quad (6.58)$$

$$S_{11} = 1 + 2[ss\sigma]_1 + [ss\sigma]_2, \quad (6.59)$$

$$S_{12} = -\sqrt{2}[ss\sigma]_1 - [ss\sigma]_2, \quad (6.60)$$

$$S_{22} = 1 + [pp\pi]_1 - [pp\sigma]_1 - [pp\sigma]_2. \quad (6.61)$$



The eigenvalue equation is of the form  $\epsilon^2 - 2A\epsilon - B = 0$ , where

$$A = \frac{S_{11}M_{22} + S_{22}M_{11} - 2M_{12}S_{12}}{2(1 - S_{12}^2)}, \quad (6.62)$$

$$B = \frac{M_{12}^2 - M_{11}M_{22}}{1 - S_{sp}^2}. \quad (6.63)$$

The eigenvalues and eigenvectors for any matrix of the form of (6.55) are

$$\epsilon^\pm = A \pm \sqrt{A^2 + B}, \quad (6.64)$$

$$f^\pm = \frac{-a^\pm f^1 + b^\pm f^2}{\sqrt{a^{\pm 2} + b^{\pm 2} + 2a^\pm b^\pm S_{12}}}, \quad (6.65)$$

where

$$a^\pm = M_{12} - \epsilon^\pm S_{12}, \quad (6.66)$$

$$b^\pm = M_{11} - \epsilon^\pm S_{11}. \quad (6.67)$$

For our problem here,  $\epsilon^\pm = \epsilon^\pm(a_{1g})$ ,  $f^1 = f^{1s}(a_{1g})$ , and  $f^2 = f^{xy}(a_{1g})$ .

A schematic representation of the eigenvectors is shown in Fig. 6.8. The asymmetrical contours represent the admixtures of  $s$ - and  $p$ -orbitals that make up the eigenfunctions. It can be seen that for the  $f^-(a_{1g})$  state there will be a build up of electron density between the atoms. This internuclear charge enhancement represents the formation of molecular bonds. This state is called a “bonding” state. Conversely, for the  $f^+(a_{1g})$  state the build up of electron density will be pointed away from the internuclear axes. This type of state is called an “antibonding” state. The bonding state is pushed below the atomic  $2s$  level in energy, and the antibonding state is raised above the  $2p$  level.

A correlation diagram showing how all of the molecular states evolve from the  $2s$  and  $2p$  states is presented in Fig. 6.9. The actual ordering of the levels depends on the values of matrix elements and overlap integrals.

For our squareene example let us assume that the outer atomic configuration of each atom of squareene is  $2s^2 2p^2$ . There will be a total of 16 electrons to distribute among the one-electron states of Fig. 6.9. If we assign paired electrons (one spin up and one spin down) to the lowest states ( $1a_{1g}$ ,  $1b_{1g}$ ,  $1e_u$ ,  $b_{2g}$ ,  $a_{2g}$ ,  $2b_{1g}$ , and  $2a_{1g}$ ), each level will be doubly occupied.

The total wavefunction for the molecule is the determinantal state,  $\Psi$ ,

$$\begin{aligned} \Psi = \frac{1}{\sqrt{16!}} \det \Big\{ & (1a_{1g} \uparrow)(1a_{1g} \downarrow)(1b_{1g} \uparrow)(1b_{1g} \downarrow)(1e_u \uparrow)(1e_u \downarrow) \\ & \times (1e_u \uparrow)(1e_u \downarrow)(b_{2g} \uparrow)(b_{2g} \downarrow)(a_{2g} \uparrow)(a_{2g} \downarrow) \\ & \times (2b_{1g} \uparrow)(2b_{1g} \downarrow)(2a_{1g} \uparrow)(2a_{1g} \downarrow) \Big\}, \end{aligned} \quad (6.68)$$

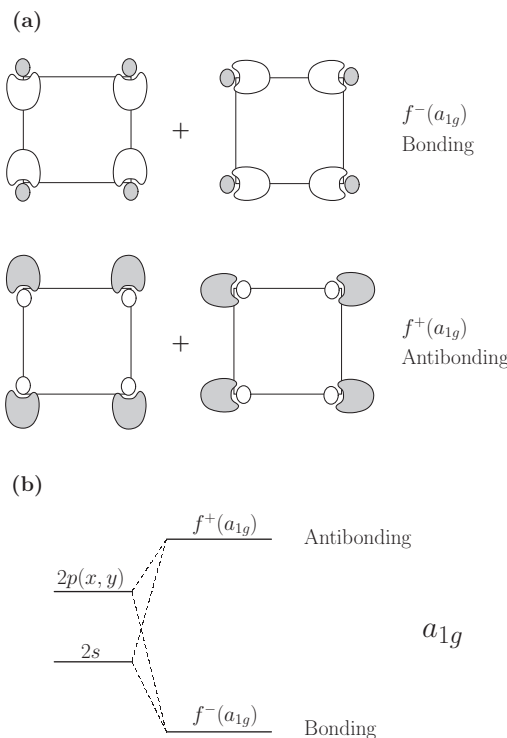


Figure 6.8 One-electron molecular states of squarene. (a) The  $a_{1g}$  eigenstates are a combination of  $s$ - and  $p$ -orbitals.  $f^-(a_{1g})$  is a bonding state with charge accumulating between the atoms.  $f^+(a_{1g})$  is an antibonding state with charge depleted between the atoms. (b) A correlation diagram showing how the  $a_{1g}$  states evolve from  $s$  and  $p$  levels.

or, in abbreviated notation,

$$\Psi = (1a_{1g})^2(1b_{1g})^2(1e_u)^2(1e_u)^2(b_{2g})^2(a_{2g})^2(2b_{1g})^2(2a_{1g})^2.$$

In (6.68) the spin states are indicated by the  $\uparrow$  and  $\downarrow$  arrows.  $\Psi$  is symmetric under inversion since the product of four  $e_u$  functions is a  $g$  function. The total spin is zero, and therefore the molecular state is a singlet. The *total* wavefunction,  $\Psi$ , is labeled by the IR according to which it transforms. To determine the IR of the total molecular state, we must consider the transformation properties of the product of all 16 *occupied* states. This is usually not a difficult thing to do because a doubly occupied one-electron state belonging to a one-dimensional representation will transform as the totally symmetric  $\Gamma^{a_{1g}}$  representation. Furthermore,  $\Gamma^\alpha \times \Gamma^{a_{1g}} = \Gamma^\alpha$ . For our example above, the total molecular state transforms as  $(1e_u \uparrow)(1e_u \downarrow)(1e_u \uparrow)(1e_u \downarrow)$ . These four states consist of two row-1  $e_u$  eigenfunctions and two row-2  $e_u$  eigenfunctions. The product of two row-1 (or

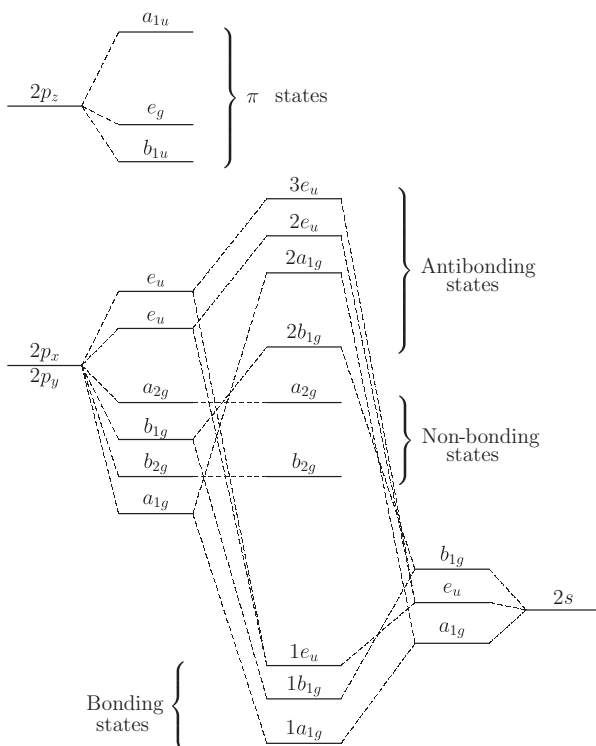


Figure 6.9 A correlation diagram, showing schematically the one-electron energy levels. The  $p_x$  and  $p_y$  states interact to split as shown. The addition of the  $2s$  interactions lead to the formation of the molecular levels shown at the center of the diagram. The bonding states are pushed down in energy (become more stable) compared with the  $2s$  energy. The antibonding states are pushed up in energy (become less stable) compared with the  $2p(x, y)$  energy. The  $b_{2g}$  and  $a_{2g}$  states are non-bonding. The states labeled  $\pi$  states are constructed from  $2p_z$  orbitals perpendicular to the plane of the molecule.

two row-2)  $e_u$  functions transforms as  $\Gamma^{A_{1g}}$ . (This may be verified by applying the symmetry-function-generating machine to the product of two such functions.) As a result of the above reasoning we conclude that the total wavefunction (6.68) is an  $^1A_{1g}$  state. The left-hand superscript indicates the spin multiplicity and the (upper case)  $A$  indicates that it is a many-electron, totally symmetric, molecular state.

A different assignment of the electrons results in a different molecular state. For example, if we place only one electron in the  $2a_{1g}$  and add the remaining electron to the  $2e_u$ , the new molecular state is antisymmetric under inversion. If the  $2a_{1g}$  and  $2e_u$  electrons have opposite spin states then the total molecular spin is still zero,  $S = 0$ . However, if the  $2a_{1g}$  and  $2e_u$  electrons have parallel spins, the total molecular spin is  $S = 1$ . In the first case, with  $S = 0$ , the molecular state is  $^1E_u$  and would be doubly degenerate, since there are two possible degenerate  $e_u$  spatial

functions. In the second case,  $S = 1$ , the molecular state is a triplet, namely  ${}^3\mathcal{E}_u$ , and doubly degenerate.

The determinantal state  $|(1a_{1g})^2(1b_{1g})^2(1e_u)^2(1e_u)^2(b_{2g})^2(a_{2g})^2(2b_{1g})^2(2a_{1g} \uparrow)(2e_u \uparrow)\rangle$  corresponds to  $S = 1$ ,  $M_s = 1$ . In fact, only the  $S = 1$ ,  $M_s = 1$  (or  $M_s = -1$ ) state is described by a single Slater determinant. However, starting with the  $M_s = 1$  state, the  $M_s = 0$  and  $M_s = -1$  can be obtained by applying the spin-lowering operator,  $S^-$ , to the  $M_s = 1$  state. Since  $S^-$  gives a non-zero result only when acting on unpaired spins (singly occupied states), only the one-electron states  $2a_{1g} \uparrow$  and  $2e_u \uparrow$  are affected. Applying the lowering operator to the product of these states gives

$$S^- \Phi(2a_{1g} \uparrow) \Phi(2e_u \uparrow) = \Phi(2a_{1g} \downarrow) \Phi(2e_u \uparrow) + \Phi(2a_{1g} \uparrow) \Phi(2e_u \downarrow), \quad (6.69)$$

and

$$S^- \left\{ \Phi(2a_{1g} \downarrow) \Phi(2e_u \uparrow) + \Phi(2a_{1g} \uparrow) \Phi(2e_u \downarrow) \right\} = 2\Phi(2a_{1g} \downarrow) \Phi(2e_u \downarrow). \quad (6.70)$$

Therefore the normalized, determinantal states are

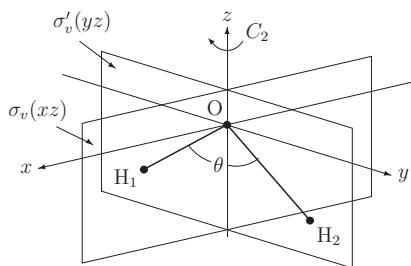
$$\begin{aligned} {}^3\mathcal{E}(M_s = 1) &= \frac{1}{\sqrt{16!}} \det \left\{ (1a_{1g} \uparrow)(1a_{1g} \downarrow) \dots (2a_{1g} \uparrow)(2e_u \uparrow) \right\} \\ &= (1a_{1g})^2(1b_{1g})^2 \dots (2a_{1g} \uparrow)(2e_u \uparrow), \end{aligned} \quad (6.71)$$

$$\begin{aligned} {}^3\mathcal{E}(M_s = 0) &= \frac{1}{\sqrt{16!}} \frac{1}{\sqrt{2}} \left[ \det \left\{ (1a_{1g} \uparrow)(1a_{1g} \downarrow) \dots (2a_{1g} \uparrow)(2e_u \downarrow) \right\} \right. \\ &\quad \left. + \det \left\{ (1a_{1g} \uparrow)(1a_{1g} \downarrow) \dots (2a_{1g} \downarrow)(2e_u \uparrow) \right\} \right] \\ &= \frac{1}{\sqrt{2}} \left\{ (1a_{1g})^2(1b_{1g})^2 \dots (2a_{1g} \uparrow)(2e_u \downarrow) \right. \\ &\quad \left. + (1a_{1g})^2(1b_{1g})^2 \dots (2a_{1g} \downarrow)(2e_u \uparrow) \right\}, \end{aligned} \quad (6.72)$$

$$\begin{aligned} {}^3\mathcal{E}(M_s = -1) &= \frac{1}{\sqrt{16!}} \det \left\{ (1a_{1g} \uparrow)(1a_{1g} \downarrow) \dots (2a_{1g} \downarrow)(2e_u \downarrow) \right\} \\ &= (1a_{1g})^2(1b_{1g})^2 \dots (2a_{1g} \downarrow)(2e_u \downarrow). \end{aligned} \quad (6.73)$$

## 6.5 The electronic structure of H<sub>2</sub>O

As an application to a real molecule, we analyze the electronic structure of H<sub>2</sub>O using molecular-orbital theory. The group for the molecule is  $C_{2v}$ . The coordinate system and symmetry operations are illustrated in Fig. 6.10. We employ the same right-handed coordinate system as we used in Chapter 2. The operations include the identity, a 180° ( $C_2$ ) rotation about the  $z$ -axis, a reflection in the plane of the molecule ( $\sigma'_v(yz)$ ), and a reflection in a plane perpendicular to the plane of the



$C_{2v}(2mm)$			$E$	$C_2$	$\sigma_v(xz)$	$\sigma_v'(yz)$
$x^2, y^2, z^2$	$z$	$A_1$	1	1	1	1
$xy$	$R_z$	$A_2$	1	1	-1	-1
$xz$	$R_y, x$	$B_1$	1	-1	1	-1
$yz$	$R_x, y$	$B_2$	1	-1	-1	1

Figure 6.10 Coordinates and symmetry operations for  $H_2O$ .  $C_2$  is a clockwise rotation about the axis through O in the molecular plane,  $\sigma_v'(yz)$  is a reflection in the plane of the molecule, and  $\sigma_v(xz)$  is a reflection in the plane perpendicular to the molecular plane. The hydrogen atoms are labeled 1 and 2. The symmetry elements operate on the orbitals, not the coordinates.

molecule ( $\sigma_v(xz)$ ). The reader should note that some authors label the reflection in the plane of the molecule as  $\sigma_v$  rather than  $\sigma_v'$ . This interchanges the role of  $x$  and  $y$ , and is not compatible with the character table in Fig. 6.10.

The oxygen and hydrogen atoms have outer electron configurations  $2s^2 2p^4$  and  $1s$ , respectively. As a simple model we shall use as basis functions  $2s(O) = 2s$ ,  $2p_x(O) = x$ ,  $2p_y(O) = y$ ,  $2p_z(O) = z$ ,  $1s(H_1) = s_1$ , and  $1s(H_2) = s_2$  for a total of six orbitals. The representation based on these six functions is denoted by  $\Gamma(\text{molecule})$ .

### 6.5.1 Decomposition of the $\Gamma(\text{molecule})$ representation

The action table, Table 6.5, shows that the basis functions  $(s_1, s_2)$ ,  $2s$ ,  $p_x$ ,  $p_y$ , and  $p_z$  transform respectively only among themselves, and therefore can be considered separately in the symmetry analysis. We can write  $\Gamma(\text{molecule}) = \Gamma^{1s} + \Gamma^{2s} + \Gamma^x + \Gamma^y + \Gamma^z$ .

The characters of the operations can be obtained from the action table. For example, for the two  $1s$  orbitals,  $\chi(E) = \chi(\sigma_v') = 2$ , while  $\chi(C_2) = \chi(\sigma_v) = 0$ . The decomposition is  $\Gamma^{1s} = a_1 + b_2$ . For the other orbitals,  $\Gamma^{2s} = a_1$ ,  $\Gamma^x = b_1$ ,  $\Gamma^y = b_2$ , and  $\Gamma^z = a_1$ . Therefore,

$$\Gamma^{\text{mol}} = 3a_1 + 2b_2 + b_1. \quad (6.74)$$

Table 6.5 The action table for the  $2s$ ,  $2p$ ,  $1s_1$ , and  $1s_2$  orbitals of  $H_2O$ . The  $1s$  orbitals of the two hydrogen atoms are labeled  $s_1$  and  $s_2$ .  $2s$  indicates the oxygen  $2s$  orbital. The  $2p$  orbitals are labeled as  $2p_x = x$ ,  $2p_y = y$ , and  $2p_z = z$ .

$C_{2v}$	$E$	$C_2$	$\sigma_v(xz)$	$\sigma'_v(yz)$
$s_1$	$s_1$	$s_2$	$s_2$	$s_1$
$s_2$	$s_2$	$s_1$	$s_1$	$s_2$
$x$	$x$	$-x$	$x$	$-x$
$y$	$y$	$-y$	$-y$	$y$
$z$	$z$	$z$	$z$	$z$
$2s$	$2s$	$2s$	$2s$	$2s$

The symmetry functions are

$$f^{1s}(a_1) = \frac{1}{\sqrt{2}}[1s_1 + 1s_2], \quad (6.75)$$

$$f^{1s}(b_2) = \frac{1}{\sqrt{2}}[1s_1 - 1s_2], \quad (6.76)$$

$$f^{2s}(a_1) = 2s, \quad (6.77)$$

$$f^x(b_1) = p_x, \quad (6.78)$$

$$f^y(b_2) = p_y, \quad (6.79)$$

$$f^z(a_1) = p_z. \quad (6.80)$$

From the decomposition results it is clear that the secular equation will be block-diagonalized into a  $1 \times 1(b_1)$ , a  $2 \times 2(b_2)$ , and a  $3 \times 3(a_1)$  when transformed to the symmetry-function representation. One immediate result is that  $f^x(b_1)$  is an eigenvector. That is, the oxygen  $2p_x$  (out-of-plane) orbital does not interact with any of the other orbitals. This type of state is called “non-bonding” because it contributes nothing to the hydrogen–oxygen bond. In the ground state the  $b_1$  state is occupied by a pair of electrons called a “lone pair”.<sup>1</sup>

Since  $b_1$  occurs only once,  $p_x$  is an eigenvector with eigenvalue  $\epsilon_p$  (roughly the energy of an isolated  $2p$  oxygen orbital).

The  $b_2$  block involves the interaction between  $f^y(b_2)$  and  $f^{1s}(b_2)$  symmetry functions. The secular-equation matrix for the  $b_2$  states is

$$\begin{vmatrix} M_{11} - \epsilon S_{11} & M_{12} - \epsilon S_{12} \\ M_{12} - \epsilon S_{12} & M_{22} - \epsilon S_{22} \end{vmatrix} = 0, \quad (6.81)$$

<sup>1</sup> Some texts use a different system and have the  $2p_z$  as the non-interacting orbital. Whatever system used, it is the  $2p$  orbital perpendicular to the plane of the molecule which is the non-interacting orbital.

where

$$M_{11} = \epsilon_{1s} - (s_1 s_2 \sigma), \quad (6.82)$$

$$M_{12} = -\frac{1}{\sqrt{2}} \sin\left(\frac{\theta}{2}\right) (1sp\sigma), \quad (6.83)$$

$$M_{22} = \epsilon_p, \quad (6.84)$$

$$S_{11} = 1 - [1sp\sigma], \quad (6.85)$$

$$S_{12} = -\frac{1}{\sqrt{2}} \sin\left(\frac{\theta}{2}\right) [1sp\sigma], \quad (6.86)$$

$$S_{22} = 1, \quad (6.87)$$

where the angle  $\theta$  is the H–O–H angle, about  $105^\circ$ , and  $\epsilon_{p_y} = \epsilon_p$  is the diagonal energy of the  $2p_y$  orbital. It should be noted that  $\epsilon_{p_x}$ ,  $\epsilon_{p_y}$ , and  $\epsilon_{p_z}$  should all be different because no two are in the same symmetry environment. For simplicity we shall take  $\epsilon_{p_x} = \epsilon_{p_y} = \epsilon_{p_z} = \epsilon_p$ . The diagonal (on the same site)  $2s$ – $2p$  interactions vanish by symmetry. The eigenvalues and eigenvectors for the secular equation, (6.81), can be found in the usual manner. As expected, the eigenstates of the  $2 \times 2$  form bonding and antibonding states.

The remaining block is a  $3 \times 3$  for the  $a_1$  molecular states involving mixing of  $f^{1s}(a_1)$ ,  $f^{2s}(a_1)$ , and  $f^z(a_1)$ . The secular-equation matrix elements are

$$\begin{vmatrix} M_{1s,1s} - \epsilon S_{1s,1s} & M_{1s,2s} - \epsilon S_{1s,2s} & M_{1s,z} - \epsilon S_{1s,z} \\ M_{1s,2s} - \epsilon S_{1s,2s} & M_{2s,2s} - \epsilon & 0 \\ M_{1s,z} - \epsilon S_{1s,z} & 0 & M_{z,z} - \epsilon \end{vmatrix} = 0, \quad (6.88)$$

where

$$M_{1s,1s} = \epsilon_{1s} + (s_1 s_2 \sigma), \quad S_{1s,1s} = +[s_1 s_2 \sigma], \quad (6.89)$$

$$M_{1s,2s} = \sqrt{2}(s_1, 2s, \sigma), \quad S_{1s,2s} = \sqrt{2}[s_1, 2s, \sigma], \quad (6.90)$$

$$M_{1s,z} = \sqrt{2} \cos\left(\frac{\theta}{2}\right) (s_1 p\sigma), \quad S_{1s,z} = \sqrt{2} \cos\left(\frac{\theta}{2}\right) [s_1 p\sigma], \quad (6.91)$$

$$M_{2s,2s} = \epsilon_{2s}, \quad (6.92)$$

$$M_{z,z} = \epsilon_{2p}. \quad (6.93)$$

Equation (6.88) leads to a cubic equation in  $\epsilon$  with all roots being real. The eigenvalues can be found from the standard formulas for the roots of a cubic equation, but will not be presented here.

Figure 6.11 shows schematically the molecular levels of  $H_2O$ . For the free atoms, the oxygen  $1s$  energy,  $\epsilon_{1s} = -20.6$  au (1 au = 27.2 eV), is far removed in energy from the  $2s$  and  $2p$  orbital energies, and therefore has little effect on the electronic structure of the valence states. The oxygen  $2s$  energy is  $\epsilon_{2s} = -1.24$  au, the  $2p$  energy is  $\epsilon_p = -0.63$  au, and the energy of the hydrogen  $1s$  is  $-0.50$  au. In

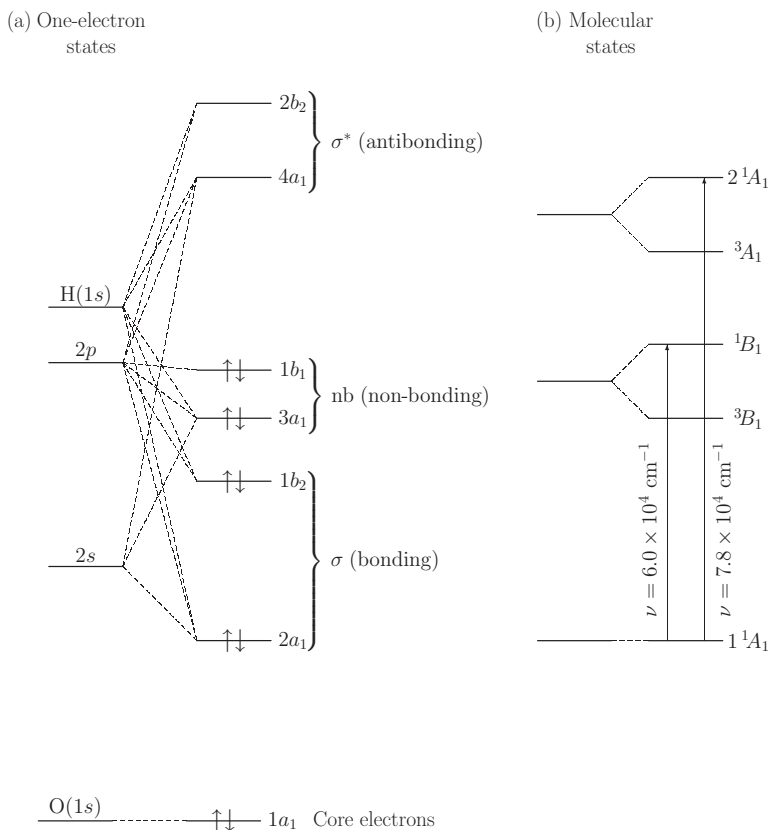


Figure 6.11 The electronic structure of H<sub>2</sub>O. (a) One-electron levels. (b) Electric-dipole transitions between molecular states.

Fig. 6.11 the oxygen 1s state is shown as 1a<sub>1</sub>. The next two levels (2a<sub>1</sub> and 1b<sub>2</sub>) are labeled as “bonding” or “σ” because they are principally responsible for the hydrogen–oxygen molecular bonds. The middle levels (1b<sub>1</sub> and 3a<sub>1</sub>) contribute little or nothing to the molecular bonding, and are labeled “nb” for non-bonding. The upper two levels (4a<sub>1</sub> and 2b<sub>2</sub>) are called “antibonding” or “σ\*” because occupying these levels with electrons reduces the stability of the molecule and because the wavefunctions have depleted rather than enhanced charge between the hydrogen and oxygen atoms.

The configuration of the valence electrons for the oxygen atom is 2s<sup>2</sup>2p<sup>4</sup>, and that for each of the two hydrogen atoms is 1s. Thus there are eight electrons to be distributed among the one-electron valence states (ten including two in the oxygen 1s level). The ground state is constructed by filling the lowest one-electron states with paired electrons as shown in Fig. 6.11. The stability or binding energy of the H<sub>2</sub>O molecule relative to the free atoms is the reduction of the total energy



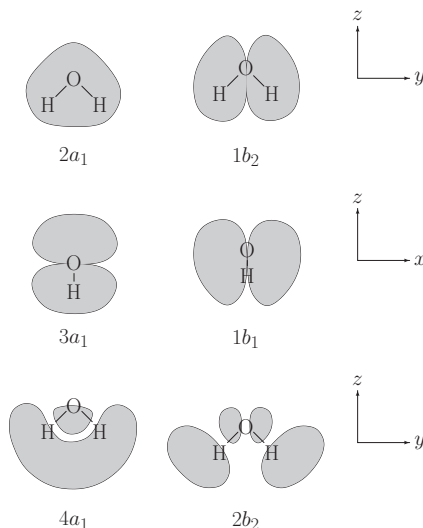


Figure 6.12 Charge distributions for the various one-electron states of  $H_2O$ .

achieved by filling the bonding, one-electron molecular states compared with the total energy of the isolated atoms,

$$E(\text{binding}) = \{2\epsilon_{2s} + 4\epsilon_{2p} + 2\epsilon_{1s}\} - \{2\epsilon(2a_1) + 2\epsilon(1b_2) + 2\epsilon(3a_1) + 2\epsilon(1b_1)\}, \quad (6.94)$$

where  $\epsilon_{2s}$ ,  $\epsilon_{2p}$ , and  $\epsilon_{1s}$  are the free-atom energies. A positive value for  $E(\text{binding})$  means that the molecule is stable. The  $b_1$  energy level is nearly unshifted from the free-atom  $2p$  energy. Clearly the binding energy is positive principally due to the  $2a_1$  and  $1b_2$  bonding states. Sketches of the charge densities of the various one-electron states of  $H_2O$  are shown in Fig. 6.12.

For the one-dimensional representations, we have  $\Gamma \times \Gamma = a_1$  and therefore all of the doubly occupied one-electron states belong to  $a_1$ . The total spin is zero, so the molecular state,  $\Psi$ , is  ${}^1A_1$ . In detail  $\Psi({}^1A_1) = (1/10!)^{1/2} \det\{(1a_1)^2(2a_1)^2(1b_2)^2(3a_1)^2(1b_1)^2\}$  is usually abbreviated as

$$\Psi({}^1A_1) = (1a_1)^2(2a_1)^2(1b_2)^2(3a_1)^2(1b_1)^2,$$

where  $(\Gamma)^2 = \Gamma \uparrow \Gamma \downarrow$  means paired electrons.

From the character table for  $C_{2v}$  we see that  $z$  transforms as  $a_1$ ,  $x$  as  $b_1$ , and  $y$  as  $b_2$ ; therefore, for the electric-dipole operator  $\mu_e$ , the  $z$ -component belongs to  $a_1$ , the  $x$ -component to  $b_1$ , and the  $y$ -component to  $b_2$ . Optical transitions from an initial state  $\Phi(\Gamma^i)$  to a final state  $\Phi(\Gamma^f)$  are not forbidden if  $\Gamma^i \times \Gamma^f$  contains  $a_1$ ,  $b_1$ , or  $b_2$ . However, since the dipole-moment vector lies in the plane of the molecule,

the  $x$ -component (perpendicular to the  $\text{H}_2\text{O}$  plane) of  $\mu_e$  is zero, so the transition  $1b_1 \Rightarrow 4a_1$  observed both in optical and in electron inelastic scattering experiments is not a simple electric-dipole transition. The transition  $3a_1 \Rightarrow 4a_1$  is an allowed electric-dipole transition since  $a_1 \times a_1 = a_1$ . The radiation must be polarized along the  $z$ -axis, in the plane of the molecule.

The excited molecular state created by the transition  $3a_1 \Rightarrow 4a_1$  with no change in spin is a  ${}^1A_1$ . This state is shown on the right-hand side in Fig. 6.11. The molecular transition is  $1{}^1A_1 \Rightarrow 2{}^1A_1$ . The observed peaks in the optical and electron scattering corresponding to this transition occurs near  $\nu = 7.8 \times 10^4 \text{ cm}^{-1}$ . For the  $1b_1 \Rightarrow 4a_1 (1{}^1A_1 \Rightarrow {}^1B_1)$  transition,  $\nu = 6 \times 10^4 \text{ cm}^{-1}$ .

The determinantal wavefunctions for the  ${}^1B_1$  and  $2{}^1A_1$  molecular states are (in abbreviated form)

$$\Psi({}^1B_1) = (1a_1)^2(2a_1)^2(1b_2)^2(3a_1)^2(1b_1\sigma)(4a_1\bar{\sigma}), \quad (6.95)$$

$$\Psi(2{}^1A_1) = (1a_1)^2(2a_1)^2(1b_2)^2(3a_1\sigma)(1b_1)^2(4a_1\bar{\sigma}), \quad (6.96)$$

where  $\sigma = \uparrow$  or  $\downarrow$  and  $\bar{\sigma} = -\sigma$ .

Also shown in Fig. 6.11 are the triplet molecular states. However, these states are not accessible from the ground state by electric-dipole transitions because a change in total spin would be required. Though well studied, the spectra observed for water are complex and as yet not well understood [6.4]. However, there is general agreement that the electronic structure is as outlined here.

## References

- [6.1] R. M. Martin, *Electronic Structure: Basic Theory and Practical Methods*, Vol. 1 (Cambridge: Cambridge University Press, 2008).
- [6.2] T. Wolfram and Ş. Ellialtıoğlu, *Electronic and Optical Properties of d-Band Perovskites* (Cambridge: Cambridge University Press, 2006), pp. 27–39.
- [6.3] M. Tinkham, *Group Theory and Quantum Mechanics* (New York: McGraw-Hill Book Company, 1964).
- [6.4] M. B. Robin, *Higher Excited States of Polyatomic Molecules*, Vol. 1, (New York: Academic Press, 1974).

## Other suggested reading

- C. J. Ballhausen and H. B. Gray, *Molecular Orbital Theory* (New York: W. A. Benjamin, Inc. 1964).
- F. A. Cotton, *Chemical Applications of Group Theory* (New York: Wiley-Interscience, 2nd edn., 1971).
- D. C. Harris and M. D. Bertolucci, *Symmetry and Spectroscopy: An Introduction to Vibrational and Electronic Spectroscopy* (New York: Dover Publications, Inc., 1989).

## Exercises

- 6.1 Consider two sites,  $A$  and  $B$ , with  $\phi(p_x)$ ,  $\phi(p_y)$ , and  $\phi(p_z)$  orbitals on  $A$  and a  $\phi(1s)$  orbital on  $B$  (Fig. 6.13).

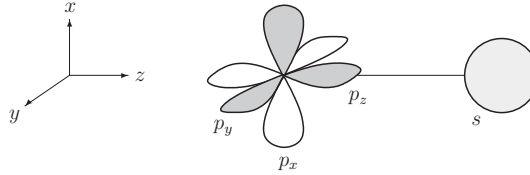


Figure 6.13

- (a) Find the LCAO overlap and Hamiltonian matrices,  $\mathbb{S}$  and  $\mathbb{H}$ . Arrange the rows and columns in the order  $s$ ,  $p_z$ ,  $p_x$ , and  $p_y$ . Use  $\epsilon_s$  and  $\epsilon_p$  for the diagonal Hamiltonian matrix elements and  $S$  for the overlap between the  $s$  and  $p_z$  orbitals.
- (b) Show that the eigenvalues of  $\mathbb{H} - \epsilon \mathbb{S}$  are given by

$$\begin{aligned}\epsilon &= \epsilon_p \text{ (twice),} \\ \epsilon^\pm &= A \pm (A^2 + B)^{1/2}, \\ A &= \frac{\epsilon_s + \epsilon_p - 2S(sp\sigma)}{2(1 - S^2)}, \\ B &= \frac{(sp\sigma)^2 - \epsilon_s \epsilon_p}{1 - S^2}.\end{aligned}$$

- (c) Show that the normalized eigenvectors are  $\phi(p_x)$ ,  $\phi(p_y)$ , and

$$\begin{aligned}\phi^\pm(1s, p_z) \\ = \frac{-(sp\sigma) - \epsilon^\pm S \phi(1s) + (\epsilon_s - \epsilon^\pm) \phi(p_z)}{\sqrt{\{(sp\sigma) - \epsilon^\pm S\}^2 + (\epsilon_s - \epsilon^\pm)^2 - 2S\{(sp\sigma) - \epsilon^\pm S\}(\epsilon_s - \epsilon^\pm)}}.\end{aligned}$$

- 6.2 (a) For the molecule in Exercise 6.1, show that the Löwdin orbitals are  $\xi(p_x) = \phi(p_x)$ ,  $\xi(p_y) = \phi(p_y)$ ,  $\xi^{1s} = a\phi(1s) + b\phi(p_z)$  and  $\xi^{p_z} = a\phi(p_z) + b\phi(1s)$ , where  $a = (1/2)\{(1 + S)^{-1/2} + (1 - S)^{-1/2}\}$  and  $b = (1/2)\{(1 + S)^{-1/2} - (1 - S)^{-1/2}\}$ , where  $S$  is the  $(1s, p_z)$  overlap integral.
- (b) Prove that  $\xi^{1s}$  is orthogonal to  $\xi^{p_z}$ .
- (c) Find the coefficients,  $a$  and  $b$ , for  $S = 0.25$ , and sketch the two Löwdin orbitals,  $\xi^{1s}$  and  $\xi^{p_z}$ .

6.3 (a) For the system in Exercise 6.2, show that

$$\begin{aligned}(sp\sigma)^L &= (a^2 + b^2)(sp\sigma) + ab(\epsilon_{1s} + \epsilon_p) = \frac{(sp\sigma) - S(\epsilon_{1s} + \epsilon_p)/2}{(1 - S^2)}, \\ (\epsilon_{1s})^L &= a^2(\epsilon_{1s}) + b^2(\epsilon_p) + 2(sp\sigma)ab, \\ (\epsilon_p)^L &= b^2(\epsilon_{1s}) + a^2(\epsilon_p) + 2(sp\sigma)ab,\end{aligned}$$

where the superscript “L” means for Löwdin orbitals, and  $a$  and  $b$  are given in Exercise 6.2. The Löwdin parameters are defined by

$$\begin{aligned}(sp\sigma)^L &= \int d\mathbf{r} (\xi^{1s})^* \mathbb{H} \xi^{p_z}, \\ (\epsilon_{1s})^L &= \int d\mathbf{r} (\xi^{1s})^* \mathbb{H} \xi^{1s}, \\ (\epsilon_p)^L &= \int d\mathbf{r} (\xi^{p_z})^* \mathbb{H} \xi^{p_z}.\end{aligned}$$

(b) For  $\epsilon_{1s} = -13$  eV,  $\epsilon_p = -15$  eV,  $S = 0.25$ , and  $(sp\sigma) = 3$  eV, calculate  $(sp\sigma)^L$ ,  $(\epsilon_{1s})^L$ , and  $(\epsilon_p)^L$ .

6.4 Suppose an electron in the  $1b_2$  state of  $\text{H}_2\text{O}$  is removed, leaving an  $\text{H}_2\text{O}^+$  molecule in an excited state.

- Give the two possible determinantal states of the molecule.
- What are the molecular states expressed in the notation  $(2s+1)\Gamma^\alpha$ ?
- What electric-dipole transitions can occur from initial states  $1b_1$  and  $2a_1$  to the final state  $2b_2$  for  $\text{H}_2\text{O}^+$ , and how must light be polarized in order to achieve the transition? Specify the transition between the molecular state labels (i.e.,  $(2s+1)\Gamma^\alpha \rightarrow (2s+1)\Gamma^{\alpha'}$ ).
- What is the frequency of the light required for each transition?

6.5 Consider a  $d_{xy}$  orbital located at the center of a square in the  $x$ - $y$  plane as shown in (a) in Fig. 6.14. Each corner of the square has  $p_x$  and  $p_y$  orbitals. The fundamental definitions of  $(pd\pi)$  and  $[pd\pi]$  are shown in (b) at the bottom left of the figure. The covering group is  $C_{4v}$  and the symmetry elements are shown in (c) at the bottom right of the figure.

- Using the geometry and symmetry elements as shown in Fig. 6.14, construct the action table for the corner numbers,  $p_x$ ,  $p_y$ , and the  $d_{xy}$  orbitals.
- Using the  $C_{4v}$  character table and the action table, find the characters for  $\Gamma(d_{xy}) = \Gamma^d$  and  $\Gamma(p_x, p_y) = \Gamma^{xy}$ , and decompose the representations into the IRs of  $C_{4v}$ .

- (c) Determine the dimensions of the sub-blocks of the secular equation in the symmetry-function representation and label each according to its IR.
- 6.6 For the  $p$ - $d$  system in Exercise 6.5, generate the symmetry functions for each sub-block. For the  $e$  functions use  $p_{x_1}$ ,  $p_{x_2}$ ,  $p_{y_1}$ , and  $p_{y_2}$  as the starting functions for the symmetry-function generator. List the symmetry functions that are also eigenstates and determine their eigenvalues.

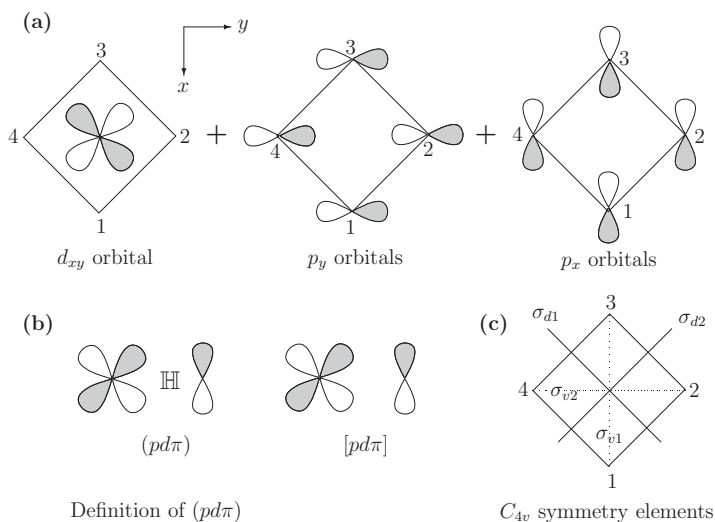


Figure 6.14

- 6.7 For the  $p$ - $d$  system in Exercise 6.5, determine the  $2 \times 2$  secular equation for the  $b_2$  states and find expressions for the eigenvalues and eigenvectors according to the LCAO model including overlap integrals.
- 6.8 (a) For Exercise 6.5 sketch the two row-1  $e$  symmetry functions and the two row-2  $e$  symmetry functions.
- (b) Find the  $2 \times 2$  secular equations for row-1 and row-2 functions.
- (c) Prove that the eigenvalues of the  $2 \times 2$  row-1 secular equation must be the same as those of the  $2 \times 2$  row-2 secular equation.
- 6.9 (a) Calculate the energies of all of the states for Exercise 6.5 using the following parameters (energies in eV, overlaps are dimensionless):

$$\begin{aligned}
 e_d &= -6, & (pd\pi) &= 1, & (pp\sigma)_1 &= 0.5, & (pp\pi)_1 &= 0.2, \\
 & & & & (pp\sigma)_2 &= 0.05, & (pp\pi)_2 &= 0.025, \\
 e_p &= -10, & [pd\pi] &= 0.2, & [pp\sigma]_1 &= 0.1, & [pp\pi]_1 &= 0.1, \\
 & & & & [pp\sigma]_2 &= 0.03, & [pp\pi]_2 &= 0.01.
 \end{aligned}$$

- (b) Make a sketch of the correlation diagram showing how the isolated  $p$  and  $d$  levels correlate with the one-electron molecular levels. Label the states as “ $g$ ” or “ $u$ ”.
- 6.10 Suppose the isolated corner atoms in the system in Exercise 6.5 each have two electrons and the center atom has one.
- (a) Specify the molecular ground-state configuration and its symbol.
  - (b) Which one-electron electric-dipole transitions to the  $1a_{2g}$ ,  $2b_{2g}$ , and  $2e_u$  are forbidden and which are not forbidden? What is the polarization of the light for non-forbidden transitions?
  - (c) Give the configurations and the molecular symbols for the final states that are not forbidden.
  - (d) Using the results from Exercise 6.9, calculate the ground-state molecular binding energy, assuming that  $\epsilon_p$  and  $\epsilon_d$  are the energies of the isolated  $p$ - and  $d$ -orbitals.
  - (e) Using the results of Exercise 6.9, calculate the energies of the photons required for the  $1b_{1g} \rightarrow 2e_u$  and the  $1b_{2g} \rightarrow 2e_u$  transitions.

# 7

## Electronic states of diatomic molecules

### 7.1 Bonding and antibonding states: Symmetry functions

In Chapter 6 we discussed the general approach to molecular-orbital theory for molecules. The methods employed are, of course, equally applicable to diatomic molecules. However, diatomic (or linear) molecules have some special properties that make them worth discussing separately. One special property is the existence of a continuous symmetry operation. For a molecule  $A-A$  or  $A-B$  a rotation by any angle about the internuclear axis is a symmetry element. Thus there is an infinite number of operations. A second feature is the special notation used to specify the molecular states.

There are two types of diatomic molecules: homonuclear  $A-A$  and heteronuclear  $A-B$ . The covering group for homonuclear diatomic molecules is  $D_{\infty h}$ . The “infinity” refers to the infinity of rotations about the internuclear axis. The covering group for  $A-B$  molecules is  $C_{\infty v}$ . The symmetry elements and character tables for these two groups are shown in Table 7.1.

The  $C_{\infty v}$  group has as elements the identity  $E$ , rotation  $C_\phi$  (and  $C_{-\phi}$ ) by any angle  $\phi$  (or  $-\phi$ ) about the internuclear axis (the  $z$ -axis), and a reflection in the  $\sigma_v$  plane. The group  $D_{\infty h}$  is the direct product  $D_{\infty h} = i \times C_{\infty v}$ .<sup>1</sup>

Consider a homonuclear, diatomic molecule with an arbitrary hydrogen-like orbital,  $\phi_\alpha$ , centered on atoms 1 and 2, and denote them as  $\phi_{\alpha 1}$  and  $\phi_{\alpha 2}$ , where  $\alpha$  specifies the orbital symmetry type ( $s, p, d, \dots$ ). The LCAO secular equation for the interaction of these two orbitals is

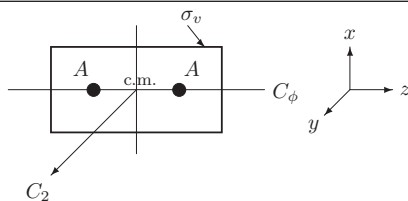
$$\begin{vmatrix} \epsilon - \lambda & H_{12} - \lambda S_{12} \\ H_{12} - \lambda S_{12} & \epsilon - \lambda \end{vmatrix} = 0, \quad (7.1)$$

<sup>1</sup> Other choices of the elements can be made for  $D_{\infty h}$ . For example,  $\sigma_v$  can be omitted and a two-fold rotation added.

Table 7.1 (a) The  $D_{\infty h}$  character table and symmetry elements for a homonuclear, A–A, molecule (c.m. is the center of mass). (b) The  $C_{\infty v}$  character table and symmetry elements for a heteronuclear, A–B, molecule.

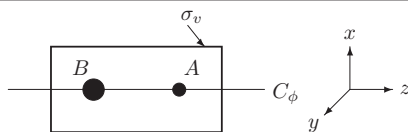
(a)

$D_{\infty h}(\infty/mm)$		$E$	$2C_\phi$	$\sigma_v$	$i$	$2iC_\phi$	$i\sigma_v$
$x^2 + y^2, z^2$	$A_{1g}(\Sigma_g^+)$	1	1	1	1	1	1
	$A_{1u}(\Sigma_u^-)$	1	1	1	-1	-1	-1
	$R_z$	$A_{2g}(\Sigma_g^-)$	1	1	-1	1	-1
	$z$	$A_{2u}(\Sigma_u^+)$	1	1	-1	-1	1
$(xz, yz)$	$(R_x, R_y)$	$E_{1g}(\Pi_g)$	2	$2 \cos \phi$	0	2	$2 \cos \phi$
	$(x, y)$	$E_{1u}(\Pi_u)$	2	$2 \cos \phi$	0	-2	$-2 \cos \phi$
$(x^2 - y^2, xy)$		$E_{2g}(\Delta_g)$	2	$2 \cos 2\phi$	0	2	$2 \cos(2\phi)$
		$E_{2u}(\Delta_u)$	2	$2 \cos 2\phi$	0	-2	$-2 \cos(2\phi)$
...		...	...	...	...	...	...



(b)

$C_{\infty v}(\infty m)$		$E$	$2C_\phi$	$\sigma_v$
$x^2 + y^2, z^2$	$z$	$A_1(\Sigma^+)$	1	1
	$R_z$	$A_2(\Sigma^-)$	1	-1
$(xz, yz)$	$(x, y)$	$E_1(\Pi)$	2	$2 \cos \phi$
$(x^2 - y^2, xy)$	$(R_x, R_y)$	$E_2(\Delta)$	2	$2 \cos(2\phi)$
		...	...	...



where  $\epsilon$  is the diagonal energy,  $H_{11}$ .  $H_{12}$  is the Hamiltonian matrix element, and  $S_{12}$  is the overlap of the two orbitals. The eigenvalues and eigenvectors of (7.1) are

$$\lambda^+(\alpha) = \frac{\epsilon + H_{12}}{1 + S_{12}}, \quad \psi^+(\alpha) = \frac{\phi_{\alpha 1} + \phi_{\alpha 2}}{\sqrt{2(1 + S_{12})}}, \quad (7.2)$$

$$\lambda^-(\alpha) = \frac{\epsilon - H_{12}}{1 - S_{12}}, \quad \psi^-(\alpha) = \frac{\phi_{\alpha 1} - \phi_{\alpha 2}}{\sqrt{2(1 - S_{12})}}. \quad (7.3)$$



Table 7.2 The action table for  $s$ - and  $p_z$  orbitals.

$\psi^b(s) = [\phi_{s1} + \phi_{s2}] / \sqrt{2 + [ss\sigma]}$ ,  $\psi^a(s) = [\phi_{s1} - \phi_{s2}] / \sqrt{2 - [ss\sigma]}$ ,  
 $\psi^b(p_z) = [\phi_{p_{z1}} - \phi_{p_{z2}}] / \sqrt{2 - [sp\sigma]}$ , and  $\psi^a(p_z) = [\phi_{p_{z1}} + \phi_{p_{z2}}] / \sqrt{2 + [sp\sigma]}$ .  
The superscripts “b” and “a” denote bonding and antibonding combinations. An entry in the table of “1” means that the function goes into itself and “−1” means that it goes into the negative of itself.

Atom position	$E$	$C_\phi$	$C'_2$	$i$	$iC_\phi$	$iC'_2$	
1	1	1	1	2	2	2	
2	2	2	2	1	1	1	
Functions							IR basis
$\psi^b(s)$	1	1	1	1	1	1	$\sigma_g^+$
$\psi^a(s)$	1	1	−1	−1	−1	1	$\sigma_u^+$
$\psi^b(p_z)$	1	1	1	1	1	1	$\sigma_g^+$
$\psi^a(p_z)$	1	1	−1	−1	−1	1	$\sigma_u^+$

The bonding/antibonding symmetry of  $\psi^\pm(\alpha)$  depends on  $\alpha$ , the symmetry index. For an  $s$ -state combination  $\psi^+(\alpha)$  is the bonding state and  $\psi^-(\alpha)$  is the antibonding state. The same is true for  $\pi$  orbitals ( $p_x$  or  $p_y$ ). For the  $p_z$ -orbitals combination the opposite is true;  $\psi^-(p_z)$  is the bonding state and  $\psi^+(p_z)$  is the antibonding state. As we shall see later, the states of (7.2) and (7.3) are basis functions for the IRs of  $D_{\infty h}$ .

Let us see how these combinations,  $\psi^\pm$ , transform under the symmetry operations of  $D_{\infty h}$ . The results depend on the symmetry of the orbitals with respect to the internuclear axis. The action table for  $s$ -orbitals and  $p_z$  orbitals is shown in Table 7.2. The superscripts “b” and “a” denote bonding and antibonding combinations.

Comparing the results of Table 7.2 with the character table for  $D_{\infty h}$  shows that  $\psi^b(s)$  and  $\psi^b(p_z)$  transform as  $A_{1g}$  or  $\Sigma_g^+$ . The notation  $\Sigma_g^+$  indicates a function whose symmetry with respect to the internuclear axis is “sigma” (axially symmetric), and is symmetric, “g”, under inversion. The “+” indicates that the function is symmetric under reflection in the  $\sigma_v$  plane. We shall maintain our rule of using lower-case letters for the one-electron states and an upper-case letter for the total molecular state. Therefore we shall use the notation  $\sigma_g^+$  for a one-electron function and  $\Sigma_g^+$  for a multi-electron, molecular state.

According to the character table for  $D_{\infty h}$ , the functions  $\psi^a(s)$  and  $\psi^a(p_z)$  belong to  $\sigma_u^+(A_{2u})$ , meaning that they are “sigma” with respect to the internuclear axis, symmetric under  $\sigma_v$ , and antisymmetric under inversion.

The  $p_\pi$  orbitals perpendicular to the  $A-A$  axis transform into one another under some operations of the group and therefore will form a  $2 \times 2$  representation. Under the operation of  $\sigma_v$ ,  $p_y$  is antisymmetric ( $-$ ) and  $p_x$  is symmetric ( $+$ ). We can form the bonding and antibonding orbitals,

$$\psi^b(p_t) = \frac{p_{t1} + p_{t2}}{\sqrt{2(1 + S_{12})}}, \quad \psi^a(p_t) = \frac{p_{t1} - p_{t2}}{\sqrt{2(1 - S_{12})}} \quad (t = x \text{ and } y),$$

where  $t = x$  and  $y$  indicate  $p_x$  and  $p_y$  orbitals, respectively. Unlike the sigma states,  $\psi^b(p_t)$  is antisymmetric and  $\psi^a(p_t)$  is symmetric under inversion.

If we rotate  $p_x$  by  $\phi$  clockwise  $p_x \rightarrow p_x \cos \phi - p_y \sin \phi$ . The function  $p_y \rightarrow p_x \sin \phi + p_y \cos \phi$ . Therefore, the  $2 \times 2$  representation matrix for the operator  $P_R = P_{C\phi}$  is

$$P_{C\phi} = \begin{pmatrix} \cos \phi & -\sin \phi \\ \sin \phi & \cos \phi \end{pmatrix}. \quad (7.4)$$

For the inversion and  $\sigma_v$  operations,

$$P_i = \begin{pmatrix} -1 & 0 \\ 0 & -1 \end{pmatrix}, \quad (7.5)$$

$$P_{\sigma_v} = \begin{pmatrix} -1 & 0 \\ 0 & 1 \end{pmatrix}. \quad (7.6)$$

From these properties we can calculate the characters for  $\psi^b(p_x)$ ,  $\psi^a(p_x)$ ,  $\psi^b(p_y)$ , and  $\psi^a(p_y)$ . For example,

$$P_{C\phi} \psi^b(p_x) = P_{C\phi} \frac{p_{x1} + p_{x2}}{\sqrt{2(1 + S_{12})}} = \cos \phi \psi^b(p_x) - \sin \phi \psi^b(p_y), \quad (7.7)$$

$$P_{C\phi} \psi^b(p_y) = P_{C\phi} \frac{p_{y1} + p_{y2}}{\sqrt{2(1 + S_{12})}} = \cos \phi \psi^b(p_y) + \sin \phi \psi^b(p_x), \quad (7.8)$$

On the other hand, for the inversion operation,

$$P_i \psi^b(p_x) = P_i \frac{p_{x1} + p_{x2}}{\sqrt{2(1 + S_{12})}} = \frac{-p_{x2} - p_{x1}}{\sqrt{2(1 + S_{12})}} = -\psi^b(p_x), \quad (7.9)$$

$$P_i \psi^a(p_x) = P_i \frac{p_{x1} - p_{x2}}{\sqrt{2(1 - S_{12})}} = \frac{-p_{x2} + p_{x1}}{\sqrt{2(1 - S_{12})}} = +\psi^a(p_x). \quad (7.10)$$

The action table for the  $p$ -orbitals perpendicular to the internuclear axis is given in Table 7.3(a). Using this table one can calculate the characters of the  $2 \times 2$  representations based on the pairs  $\{\psi^b(p_x), \psi^b(p_y)\}$  and  $\{\psi^a(p_x), \psi^a(p_y)\}$ . The character table is shown in Table 7.3(b).

On comparing the results of Table 7.3(b) with the character table of Table 7.1(b) it is seen that the sets  $\{\psi^b(p_x), \psi^b(p_y)\}$  and  $\{\psi^a(p_x), \psi^a(p_y)\}$  are basis functions for the  $\pi_u(\mathcal{E}_{1u})$  and  $\pi_g(\mathcal{E}_{1g})$  IRs, respectively. The  $\pi_u$  and  $\pi_g$  are each doubly

Table 7.3 Symmetry properties of the  $p_x$  and  $p_y$  orbitals. (a) The action table. (b) The character table for the  $2 \times 2$  representations with basis functions  $\{\psi^b(p_x), \psi^b(p_y)\}$  and  $\{\psi^a(p_x), \psi^a(p_y)\}$ . (c) The  $\pi_u(\mathcal{E}_{1u})$  IR matrices for the basis functions  $\{\psi^b(p_x), \psi^b(p_y)\}$ . (d) The  $\pi_g(\mathcal{E}_{1g})$  IR matrices for the basis functions  $\{\psi^a(p_x), \psi^a(p_y)\}$ .

(a)

Atom	$E$	$2C_\phi$	$\sigma_v$	$i$	$2iC_\phi$	$i\sigma_v$
1	1	1	1	2	2	2
2	2	2	2	1	1	1
Orbital						
$p_x$	$p_x$	$p_x \cos \phi$ $- p_y \sin \phi$	$-p_x$	$-p_x$	$-p_x \cos \phi$ $+ p_y \sin \phi$	$p_x$
$p_y$	$p_y$	$p_y \cos \phi$ $+ p_x \sin \phi$	$+p_y$	$-p_y$	$-p_x \cos \phi$ $- p_x \sin \phi$	$-p_y$

(b) Character table for the  $\pi$  states

Functions	IR	$\chi(E)$	$2\chi(C_\phi)$	$\chi(\sigma_v)$	$\chi(i)$	$2\chi(iC_\phi)$	$\chi(i\sigma_v)$
$\{\psi^b(p_x), \psi^b(p_y)\}$	$\pi_u(\mathcal{E}_{1u})$	2	$2 \cos \phi$	0	-2	$-2 \cos \phi$	0
$\{\psi^a(p_x), \psi^a(p_y)\}$	$\pi_g(\mathcal{E}_{1g})$	2	$2 \cos \phi$	0	2	$2 \cos \phi$	0

$$\psi^b(p_t) = \frac{p_{t1} + p_{t2}}{\sqrt{2(1 + S_{12})}} \quad \psi^a(p_t) = \frac{p_{t1} - p_{t2}}{\sqrt{2(1 - S_{12})}} \quad (t = x \text{ and } y)$$

(c)  $\pi_u(\mathcal{E}_{1u})$  IR matrices for the basis functions  $\{\psi^b(p_x), \psi^b(p_y)\}$ 

$$P_E = \begin{pmatrix} 1 & 0 \\ 0 & 1 \end{pmatrix}, \quad P_{C_\phi} = \begin{pmatrix} \cos \phi & -\sin \phi \\ \sin \phi & \cos \phi \end{pmatrix}, \quad P_{\sigma_v} = \begin{pmatrix} -1 & 0 \\ 0 & 1 \end{pmatrix},$$

$$P_i = \begin{pmatrix} -1 & 0 \\ 0 & -1 \end{pmatrix}, \quad P_{iC_\phi} = P_i P_{C_\phi}, \quad P_{i\sigma_v} = P_i P_{\sigma_v}.$$

(d)  $\pi_g(\mathcal{E}_{1g})$  IR matrices for the basis functions  $\{\psi^a(p_x), \psi^a(p_y)\}$ 

$$P_E = \begin{pmatrix} 1 & 0 \\ 0 & 1 \end{pmatrix}, \quad P_{C_\phi} = \begin{pmatrix} \cos \phi & -\sin \phi \\ \sin \phi & \cos \phi \end{pmatrix}, \quad P_{\sigma_v} = \begin{pmatrix} -1 & 0 \\ 0 & 1 \end{pmatrix},$$

$$P_i = \begin{pmatrix} 1 & 0 \\ 0 & 1 \end{pmatrix}, \quad P_{iC_\phi} = P_i P_{C_\phi}, \quad P_{i\sigma_v} = P_i P_{\sigma_v}.$$

degenerate and therefore each can contain two sets of paired electrons. The IR matrices are shown in Tables 7.3(c) and 7.3(d).

The analysis can be continued for  $d$ -,  $f$ -, ... orbitals. For example, the bonding and antibonding combinations of  $d_{xz}$  and  $d_{yz}$  are

$$\psi^a(d_{xz}) = \frac{d_{xz1} + d_{xz2}}{\sqrt{2 + 2[dd\pi]}}, \quad \psi^b(d_{xz}) = \frac{d_{xz1} - d_{xz2}}{\sqrt{2 - 2[dd\pi]}}, \quad (7.11)$$

$$\psi^a(d_{yz}) = \frac{d_{yz1} + d_{yz2}}{\sqrt{2 + 2[dd\pi]}}, \quad \psi^b(d_{yz}) = \frac{d_{yz1} - d_{yz2}}{\sqrt{2 - 2[dd\pi]}}. \quad (7.12)$$

The formation of bonding and antibonding combinations for hydrogen-like functions on the two atoms that have different symmetries with respect to the internuclear axis need not be considered because the Hamiltonian matrix element and the overlap of functions vanish.

What we have accomplished in the above analysis is a simple method for finding the symmetry functions for any type of orbital centered on two atomic sites. Symmetry functions belonging to the same IR will interact, and those belonging to different IRs or different rows of the same IR will not. Thus the block diagonalization of the secular equation can easily be determined.

## 7.2 The “building-up” of molecular orbitals for diatomic molecules

The bonding and antibonding molecular orbitals serve as the first-order approximation to the molecular eigenstates, similar to the manner in which the hydrogen-like orbitals are the first-order approximation to the atomic states. In fact, the labeling of the molecular orbitals,  $\Sigma$ ,  $\Pi$ ,  $\Delta$ , ...,  $\sigma$ ,  $\pi$ ,  $\delta$ , ... is just the Greek-letter equivalent of the  $S$ ,  $P$ ,  $D$ , ... or  $s$ ,  $p$ ,  $d$ , ... for atomic labels. However, the degeneracies are not the same. For example, while  $P$  and  $D$  are three- and five-dimensional, respectively,  $\Pi$  and  $\Delta$  are both two-dimensional.

The bonding and antibonding molecular orbitals are *not* eigenfunctions of the molecular Hamiltonian; they are symmetry functions. The eigenstates are linear combinations of the symmetry functions that transform according to the same row of the same IR of the covering group. Nevertheless, we can specify the molecular electronic configurations in terms of these symmetry functions and deduce qualitative results.

### 7.2.1 Quantum numbers for homonuclear diatomic molecules

Since  $A-A$  diatomic molecules have two centers, the Hamiltonian can not have spherical symmetry. As a result  $L^2$  is not a “good” quantum number. However,  $L_z$ , the angular momentum about the  $z$ -axis, is still appropriate. For  $A-A$  molecules the

notation  $\Lambda$  is customarily used instead of  $\mathbf{L}_z$  to specify the total angular momentum about the  $z$ -axis, where  $\Lambda = |\mathbf{L}_z|$ . The angular momentum for the  $i$ th one-electron molecular state is labeled as  $\lambda_i$ , and  $\Lambda = \sum \lambda_i$ . The spin of the  $i$ th one-electron molecular state is  $s_{iz}$ , and, for the total molecular spin,  $S_z = \sum s_{iz}$ . The values of  $\lambda$  are 0, 1, and 2 for the molecular orbitals  $\sigma$ ,  $\pi$ , and  $\delta$ , or  $\Lambda = 0, 1$ , and 2 for the molecular states  $\Sigma$ ,  $\Pi$ , and  $\Delta$ , respectively.

The one-electron molecular orbitals belonging to a given irreducible representation play a role similar to that of the orbitals of a given atomic shell. A  $\sigma_g^+$  state can be occupied by two electrons of opposite spin, denoted by  $(\sigma_g^+)^2$ . This constitutes a closed shell in the same way that  $(ns)^2$  is a closed shell. Closed shells transform as  $\Sigma_g^+(A_{1g})$ . The same may be said for  $(\sigma_u^+)^2$ ,  $(\sigma_g^-)^2$ , and  $(\sigma_u^-)^2$ , which also transform as  $\Sigma_g^+(A_{1g})$ . However, the pi states are different. They are derived from combinations of  $p_x$  and  $p_y$  orbitals and transform according to the *two-dimensional* IRs of  $D_{\infty h}$  labeled  $\pi_u$  or  $\pi_g$ . Therefore each pi shell can accommodate four electrons, namely two pairs of electrons with oppositely directed spins. As a result  $(\pi_u)^4$  and  $(\pi_g)^4$  are the closed molecular-shell configurations that transform as  $\Sigma_g^+(A_{1g})$ .

In the absence of spin-orbit effects the symbol specifying the total molecular state has the form

$$(2S+1)\Lambda_{(g/u)}^{(\pm)}, \quad (7.13)$$

where  $(2S+1)$  is the spin multiplicity,  $\Lambda$  is the total orbital momentum about the  $z$ -axis,  $+/-$  is the reflection symmetry in a plane containing the  $A-A$  axis, and  $g/u$  is the parity (the inversion symmetry of the spatial part of the function).

To specify the molecular configurations, we need to know the energy ordering of the various bonding and antibonding states. In general the atomic levels are energetically ordered according to  $1s < 2s < 2p$ . For the molecular orbitals,  $\sigma_g^+ < \sigma_u^+$  and  $\pi_u < \pi_g$ . With these rules we can construct two different energy-level arrangements depending upon whether, for the  $2p$  electrons,  $\sigma_g^+ < \pi_u$  or  $\pi_u < \sigma_g^+$ . These two possibilities are shown schematically in Fig. 7.1.

The difference between the orderings in Figs. 7.1(a) and (b) is that for level-ordering 1 (LO1)  $1\pi_u < 3\sigma_g^+$  and in (b) the opposite is true. It is generally believed that LO1 holds for the lightest diatomic molecules,  $H_2$ ,  $He_2$ ,  $Li_2$ ,  $B_2$ ,  $N_2^+$ , and  $C_2$ . For  $O_2$  and  $F_2$ , LO2 is appropriate. The explanation for this switch is that the splitting of the bonding and antibonding levels *decreases* as the nuclear charge ( $Z$ ) increases. Heavier diatoms tend to have greater bond lengths and smaller overlap. Starting from  $F_2$  and moving toward *lighter* molecules the  $\pi_g-\pi_u$  splitting increases faster than the  $\sigma_u^+-\sigma_g^+$  splitting. The  $\pi_u$  level in LO2 drops below the  $\sigma_g^+$  level, resulting in the LO1 scheme. The crossover is shown schematically in Fig. 7.2.

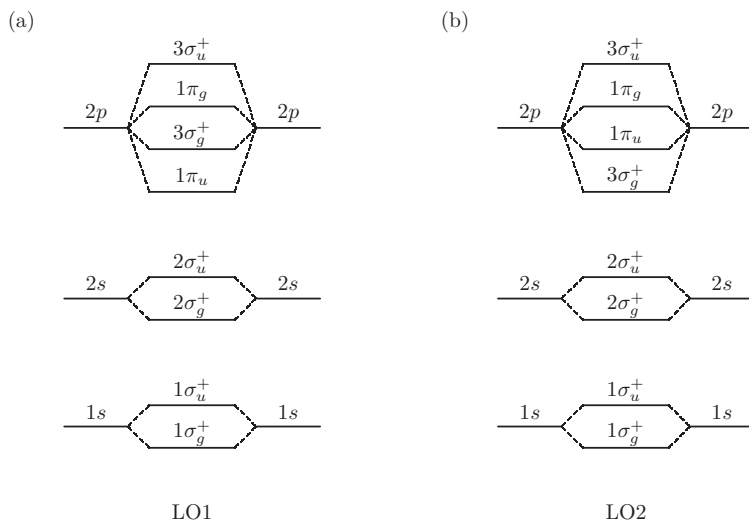


Figure 7.1 A schematic representation of the ordering of the levels for homonuclear, diatomic molecules. (a) Level-ordering 1 (LO1),  $1\pi_u < 3\sigma_g^+$ . (b) Level-ordering 2 (LO2),  $3\sigma_g^+ < 1\pi_u$ .

### 7.2.2 The united-atom concept

A qualitative explanation of the  $\pi_u$ – $\sigma_g^+$  crossover can be obtained from the “united-atom” concept. Consider decreasing the distance between the two atoms of the molecule. When the distance approaches zero we have a single “united atom” with twice the nuclear charge and twice as many electrons. In this limit the orbitals must become the atomic states  $1s$ ,  $2s$ ,  $2p$ ,  $\dots$ . Since the nuclear charge is twice that of a single nucleus, these atomic states must lie at much lower energies than those of a single atom. Increasing the distance between the nuclei eventually produces two non-interacting atoms. Again, in the limit of “separated atoms”, the states must be two identical sets of  $1s$ ,  $2s$ ,  $2p$ ,  $\dots$  states for an atom with a single nuclear charge. These states will be at higher energies than for the corresponding united-atom limit. The internuclear distance changes, but the covering group does not. *Group-theoretical considerations require that a molecular orbital evolving toward the limit of the united atom or the limit of the separated atoms not change its symmetry.* The  $\sigma_g^+$  molecular level arises from the in-phase, linear combination of two  $1s$  states of the separated atoms. As the united-atom limit is approached the two nearly overlapping  $1s$  orbitals have the symmetry of an  $s$ -orbital. Thus  $\sigma_g^+ \Rightarrow 1s$  (united atom). On the other hand,  $\sigma_u^+$ , constructed from two out-of-phase  $1s$  orbitals, has the symmetry of a  $p$ -orbital. Therefore  $\sigma_u^+ \Rightarrow 2p$  (united atom). A  $\pi_g$  state has the same symmetry as a  $d_{xz}$  or  $d_{yz}$  orbital, so  $\phi_1(p_x) - \phi_2(p_x) \Rightarrow \pi_g \Rightarrow d_{xz}$  (united atom), while  $\phi_1(p_x) + \phi_2(p_x) \Rightarrow \pi_u \Rightarrow p_x$  (united atom). These

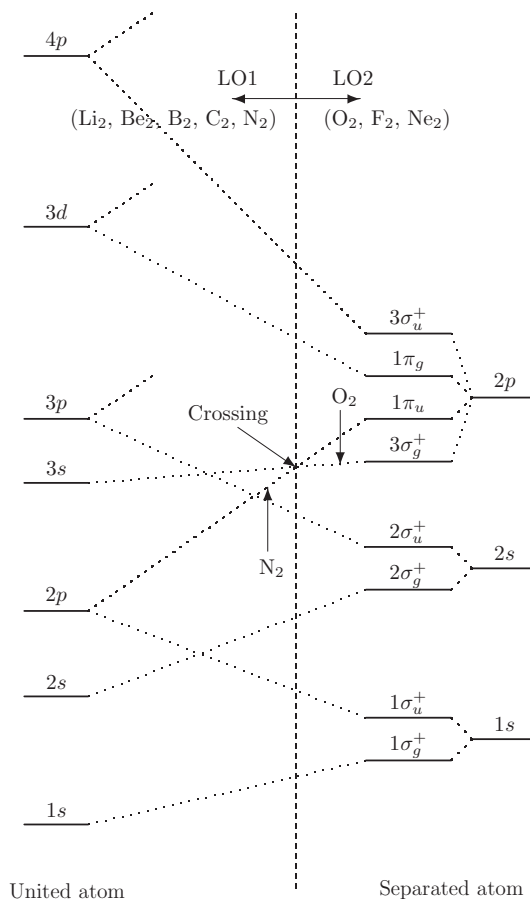


Figure 7.2 A schematic correlation diagram showing the evolution of the states on going from separated atoms to the united atom. The  $1\pi_u$  level drops below the  $3\sigma_g^+$  on going from  $O_2^+$  to  $N_2$  because it correlates with the  $2p$  (united atom), while the  $3\sigma_g^+$  correlates with the  $3s$  (united atom).

rules allow us to construct the qualitative correlation diagram in Fig. 7.2 showing how the molecular states evolve as a function of the internuclear distance.

### 7.2.3 Molecular configurations

We can now build up a picture of the electronic configurations of various diatoms by filling the molecular levels with electrons. For example, for  $N_2$ , each nitrogen atom has 7 electrons, so there are 14 electrons to distribute among the  $N_2$  molecular orbitals. The configuration is  $(1\sigma_g^+)^2(1\sigma_u^+)^2(2\sigma_g^+)^2(2\sigma_u^+)^2(1\pi_u)^4(3\sigma_g^+)^2$  (using the LO1 scheme). The label for the total molecular state is the IR of  $D_{\infty h}$  according to which the product of all of the occupied states transforms. For  $N_2$  the ground state

is  $\Sigma_g^+$ , since all molecular shells are closed. Some typical configurations are shown in Table 7.4 on p. 204.

A more interesting example is that of the  $O_2$  molecule. The electronic configuration is  $(1\sigma_g^+)^2(1\sigma_u^+)^2(2\sigma_g^+)^2(2\sigma_u^+)^2(3\sigma_g^+)^2(1\pi_u)^4(1\pi_g)^2 = (\text{closed shells}) (1\pi_g)^2$ . The total molecule symmetry is determined by the partially filled  $1\pi_g$  shell. There are two electrons in this shell and the possible choices for the spins are  $S = 0$  for  $\uparrow\downarrow$  and  $S = 1$  for  $\uparrow\uparrow$  or  $\downarrow\downarrow$ . The first choice will produce a singlet state and the second a triplet state. There are two choices for the molecular orbitals:  $\psi^a(p_x)$  and  $\psi^a(p_y)$  (see Table 7.3(b)). The product of two  $\pi_g$  states is a “g” state, The orbital symmetries of the possible states are determined by the direct product,  $\pi_g \times \pi_g$ . From Table 7.5 on p. 205 we conclude that the possible total molecular states are  $\Sigma_g^+$ ,  $\Sigma_g^-$ , and  $\Delta_g$ . The spin multiplicity of these states is discussed below.

When a configuration results in several terms, Hund’s rules (discussed in Chapter 3) state that the ground state is the term with the maximum spin and maximum angular momentum. There are exceptions to Hund’s rules but in a large majority of cases they are valid.

It is useful to introduce a simplified notation for the determinantal state. We shall use  $\langle \psi^a(p_x\sigma) \psi^a(p_y\sigma') |$  as an abbreviation for the full determinantal state,

$$\langle \psi^a(p_x\sigma) \psi^a(p_y\sigma') | = \frac{1}{\sqrt{16!}} \det\{(1\sigma_g^+)^2(1\sigma_u^+)^2(2\sigma_g^+)^2(2\sigma_u^+)^2(3\sigma_g^+)^2 \\ (1\pi_u)^4 \psi^a(p_x\sigma) \psi^a(p_y\sigma')\}. \quad (7.14)$$

The determinantal states that can be formed with  $S = 1$  are

$$(1) \quad \langle \psi^a(p_x \uparrow) \psi^a(p_x \uparrow) | = 0 \quad (\text{two states are identical}), \quad (7.15)$$

$$(2) \quad \langle \psi^a(p_x \uparrow) \psi^a(p_y \uparrow) |, \quad (7.16)$$

$$(3) \quad \langle \psi^a(p_y \uparrow) \psi^a(p_y \uparrow) | = 0 \quad (\text{two states are identical}), \quad (7.17)$$

$$(4) \quad \langle \psi^a(p_y \uparrow) \psi^a(p_x \uparrow) | = -\langle \psi^a(p_x \uparrow) \psi^a(p_y \uparrow) |, \quad (7.18)$$

and, for  $S = 0$ ,

$$(5) \quad \langle \psi^a(p_x \uparrow) \psi^a(p_x \downarrow) |, \quad (7.19)$$

$$(6) \quad \langle \psi^a(p_y \downarrow) \psi^a(p_y \uparrow) |, \quad (7.20)$$

$$(7) \quad \langle \psi^a(p_x \uparrow) \psi^a(p_y \downarrow) |, \quad (7.21)$$

$$(8) \quad \langle \psi^a(p_x \downarrow) \psi^a(p_y \uparrow) |. \quad (7.22)$$

There are in total five independent, non-zero, determinantal states. From the direct product we know that the total molecular states are  $\Sigma_g^+ + \Sigma_g^- + \Delta_g$ . There is only one independent  $S = 1$  determinant,  $\langle \psi^a(p_x \uparrow) \psi^a(p_y \uparrow) |$ . This state must belong to a triplet term since  $S = 1$ . Therefore there must be two singlets and one triplet



for a total of five states. To identify which state is the triplet and which states are singlets we must consider how the states transform under the operations of the group.

We first consider the product,  $\psi^a(p_x \uparrow) \psi^a(p_y \uparrow)$ . Making use of equations (7.7) and (7.8) gives

$$\begin{aligned}
 P_{C\phi} \psi^a(p_x(\mathbf{r}) \uparrow) \psi^a(p_y(\mathbf{r}') \uparrow) &= P_{C\phi} \psi^a(p_x(\mathbf{r}) \uparrow) P_{C\phi} \psi^a(p_y(\mathbf{r}') \uparrow) \\
 &= [\cos \phi \psi^a(p_x(\mathbf{r}) \uparrow) - \sin \phi \psi^a(p_y(\mathbf{r}) \uparrow)] \\
 &\quad \times [\cos \phi \psi^a(p_y(\mathbf{r}') \uparrow) + \sin \phi \psi^a(p_x(\mathbf{r}') \uparrow)] \\
 &= \cos^2 \phi [\psi^a(p_x(\mathbf{r}) \uparrow) \psi^a(p_y(\mathbf{r}') \uparrow)] \\
 &\quad - \sin^2 \phi [\psi^a(p_y(\mathbf{r}) \uparrow) \psi^a(p_x(\mathbf{r}') \uparrow)] \\
 &\quad + \cos \phi \sin \phi [\psi^a(p_x(\mathbf{r}) \uparrow) \psi^a(p_x(\mathbf{r}') \uparrow)] \\
 &\quad - \cos \phi \sin \phi [\psi^a(p_y(\mathbf{r}) \uparrow) \psi^a(p_y(\mathbf{r}') \uparrow)].
 \end{aligned} \tag{7.23}$$

We have added the variables  $\mathbf{r}$  and  $\mathbf{r}'$  as a reminder that the states are functions of two different electron coordinates. The determinantal state satisfies the relation

$$\begin{aligned}
 P_{C\phi} \langle \psi^a(p_x \uparrow) \psi^a(p_y \uparrow) | &= \cos^2 \phi \langle \psi^a(p_x \uparrow) \psi^a(p_y \uparrow) | \\
 &\quad - \sin^2 \phi \langle \psi^a(p_y \uparrow) \psi^a(p_x \uparrow) | \\
 &\quad + \cos \phi \sin \phi \langle \psi^a(p_x \uparrow) \psi^a(p_x \uparrow) | \\
 &\quad - \cos \phi \sin \phi \langle \psi^a(p_y \uparrow) \psi^a(p_y \uparrow) |.
 \end{aligned} \tag{7.24}$$

The third and fourth determinants of (7.24) vanish because the last two columns are identical. In addition, the second determinant is the negative of the first determinant, so finally we have

$$P_{C\phi} \langle \psi^a(p_x \uparrow) \psi^a(p_y \uparrow) | = +1 \langle \psi^a(p_x \uparrow) \psi^a(p_y \uparrow) | ; \tag{7.25}$$

that is, the original determinant is invariant under  $P_{C\phi}$ .

It should be noted that the spin is oriented along the  $z$ -axis and therefore it is invariant under  $C_\phi$  and  $\sigma_v$ . It is also invariant under inversion since it is an angular-momentum vector:  $P_i[\mathbf{r} \times d\mathbf{r}/dt] = [-\mathbf{r} \times d(-\mathbf{r})/dt] = [\mathbf{r} \times d\mathbf{r}/dt]$ . Consequently the spin is invariant under all of the operations of the group.

For the reflection  $\sigma_v$ , we have

$$\begin{aligned}
 P_{\sigma_v} \psi^a(p_x \uparrow) \psi^a(p_y \uparrow) &= \frac{P_{\sigma_v}[p_{x1} - p_{x2}][p_{y1} - p_{y2}]}{N_x N_y} \\
 &= \frac{-[p_{x1} - p_{x2}][p_{y1} - p_{y2}]}{N_x N_y} \\
 &= -\psi^a(p_x \uparrow) \psi^a(p_y \uparrow),
 \end{aligned} \tag{7.26}$$

Table 7.4 *Molecular-orbital configurations for some homomolecular diatomic molecules (Mol., molecule)*

Mol. Electronic configuration	# of es	Molecular symbol	Bond order
H <sub>2</sub> <sup>+</sup> (1σ <sub>g</sub> <sup>+</sup> )	1	<sup>2</sup> Σ <sub>g</sub> <sup>+</sup>	1/2
H <sub>2</sub> (1σ <sub>g</sub> <sup>+</sup> ) <sup>2</sup>	2	<sup>1</sup> Σ <sub>g</sub> <sup>+</sup>	1
He <sup>+</sup> (1σ <sub>g</sub> <sup>+</sup> ) <sup>2</sup> (1σ <sub>u</sub> <sup>+</sup> ) <sup>1</sup>	3	<sup>2</sup> Σ <sub>u</sub> <sup>+</sup>	1/2
He <sub>2</sub> (1σ <sub>g</sub> <sup>+</sup> ) <sup>2</sup> (1σ <sub>u</sub> <sup>+</sup> ) <sup>2</sup>	4	<sup>1</sup> Σ <sub>g</sub> <sup>+</sup>	0
Li <sub>2</sub> (1σ <sub>g</sub> <sup>+</sup> ) <sup>2</sup> (1σ <sub>u</sub> <sup>+</sup> ) <sup>2</sup> (2σ <sub>g</sub> <sup>+</sup> ) <sup>2</sup>	6	<sup>1</sup> Σ <sub>g</sub> <sup>+</sup>	1
Be <sub>2</sub> (1σ <sub>g</sub> <sup>+</sup> ) <sup>2</sup> (1σ <sub>u</sub> <sup>+</sup> ) <sup>2</sup> (2σ <sub>g</sub> <sup>+</sup> ) <sup>2</sup> (2σ <sub>u</sub> <sup>+</sup> ) <sup>2</sup>	8	<sup>1</sup> Σ <sub>g</sub> <sup>+</sup>	0
N <sub>2</sub> (1σ <sub>g</sub> <sup>+</sup> ) <sup>2</sup> (1σ <sub>u</sub> <sup>+</sup> ) <sup>2</sup> (2σ <sub>g</sub> <sup>+</sup> ) <sup>2</sup> (2σ <sub>u</sub> <sup>+</sup> ) <sup>2</sup> (1π <sub>u</sub> ) <sup>4</sup> (3σ <sub>g</sub> <sup>+</sup> ) <sup>2</sup>	14	<sup>1</sup> Σ <sub>g</sub> <sup>+</sup>	3
O <sub>2</sub> <sup>+</sup> (1σ <sub>g</sub> <sup>+</sup> ) <sup>2</sup> (1σ <sub>u</sub> <sup>+</sup> ) <sup>2</sup> (2σ <sub>g</sub> <sup>+</sup> ) <sup>2</sup> (2σ <sub>u</sub> <sup>+</sup> ) <sup>2</sup> (3σ <sub>g</sub> <sup>+</sup> ) <sup>2</sup> (1π <sub>u</sub> ) <sup>4</sup> (1π <sub>g</sub> ) <sup>1</sup>	15	<sup>2</sup> A <sub>g</sub>	5/2
O <sub>2</sub> (1σ <sub>g</sub> <sup>+</sup> ) <sup>2</sup> (1σ <sub>u</sub> <sup>+</sup> ) <sup>2</sup> (2σ <sub>g</sub> <sup>+</sup> ) <sup>2</sup> (2σ <sub>u</sub> <sup>+</sup> ) <sup>2</sup> (3σ <sub>g</sub> <sup>+</sup> ) <sup>2</sup> (1π <sub>u</sub> ) <sup>4</sup> (1π <sub>g</sub> ) <sup>2</sup>	16	<sup>1</sup> Σ <sub>g</sub> <sup>+</sup> , <sup>3</sup> Σ <sub>g</sub> <sup>-</sup> , <sup>1</sup> Δ <sub>g</sub>	2
F <sub>2</sub> (1σ <sub>g</sub> <sup>+</sup> ) <sup>2</sup> (1σ <sub>u</sub> <sup>+</sup> ) <sup>2</sup> (2σ <sub>g</sub> <sup>+</sup> ) <sup>2</sup> (2σ <sub>u</sub> <sup>+</sup> ) <sup>2</sup> (3σ <sub>g</sub> <sup>+</sup> ) <sup>2</sup> (1π <sub>u</sub> ) <sup>4</sup> (1π <sub>g</sub> ) <sup>4</sup>	18	<sup>1</sup> Σ <sub>g</sub> <sup>+</sup>	1

where  $N_x$  and  $N_y$  are the normalization factors. Under inversion,

$$P_i \psi^a(p_x \uparrow) \psi^a(p_y \uparrow) = -\psi^a(p_x \uparrow) \times -\psi^a(p_y \uparrow) = +\psi^a(p_x \uparrow) \psi^a(p_y \uparrow). \quad (7.27)$$

From these symmetry properties and Table 7.1(a) we can identify  $\langle \psi^a(p_x \uparrow) \psi^a(p_y \uparrow) |$  as  $^3\Sigma_g^-$  with  $M_s = +1$ . The other two spin states,  $M_s = 0$  and  $M_s = -1$ , can be generated by operating on  $\langle \psi^a(p_x \uparrow) \psi^a(p_y \uparrow) |$  with the spin-lowering operator.

In summary, the O<sub>2</sub> configuration,  $(1\sigma_g^+)^2(1\sigma_u^+)^2(2\sigma_g^+)^2(2\sigma_u^+)^2(3\sigma_g^+)^2(1\pi_u)^4(1\pi_g)^2$ , yields three terms,  $^1\Sigma_g^+$ ,  $^3\Sigma_g^-$ , and  $^1\Delta_g$ . According to Hund's rules,  $^3\Sigma_g^-$  is the ground state. The lowest excited state is  $^1\Delta_g$  and the next higher energy state is  $^1\Sigma_g^+$ . The two excited states are involved in the absorption of light by the atmosphere.

The last column of Table 7.4 specifies the “bond order”. The bond order is defined as the number of electrons occupying bonding states minus the number occupying antibonding states divided by 2. For example, for N<sub>2</sub> the configuration of the ground state includes 10 bonding states and 4 antibonding states, so the bond order is  $6/2 = 3$ . The bond order is a useful qualitative measure of the strength of the bond holding the molecule together. A number of physical properties of a molecule can be correlated with the bond order. The chemical bond enthalpy,  $D_0$ , increases with the bond order. The bond length also correlates with bond order, shorter bond length corresponding to larger bond order for a particular series such as the series B<sub>2</sub>, C<sub>2</sub>, N<sub>2</sub>, O<sub>2</sub>, and F<sub>2</sub> or the series Si<sub>2</sub>, P<sub>2</sub>, S<sub>2</sub>, and Cl<sub>2</sub>. In addition, the vibrational stretching frequency is roughly proportional to the bond

Table 7.5 Direct products for  $C_{\infty v}$  and  $D_{\infty h}$ . For  $D_{\infty h}$  the “g” and “u” labels are omitted. They may be added according to the rule  $g \times g = g$ ,  $g \times u = u$ , and  $u \times u = g$ . The column labeled  $\Lambda$  gives the angular momentum about the interatomic axis.

$C_{\infty v}, D_{\infty h}$ IR	$\Lambda$	$\Sigma^+$	$\Sigma^-$	$\Pi$	$\Delta$	$\Phi$
$\Sigma^+$	0	$\Sigma^+$	$\Sigma^-$	$\Pi$	$\Delta$	$\Phi$
$\Sigma^-$	0	$\Sigma^-$	$\Sigma^+$	$\Pi$	$\Delta$	$\Phi$
$\Pi$	1	$\Pi$	$\Pi$	$\Sigma^+ + \Sigma^- + \Delta$	$\Pi + \Phi$	$\Delta + \Gamma$
$\Delta$	2	$\Delta$	$\Delta$	$\Pi + \Phi$	$\Sigma^+ + \Sigma^- + \Gamma$	$\Pi + H$

order. Molecules with zero bond order (e.g.,  $\text{He}_2$  and  $\text{Be}_2$ ) are considered unstable and to date have not been experimentally detected.

### 7.2.4 Electric-dipole transitions

The electric-dipole transition-matrix element is  $\int d\mathbf{r} \Psi_i^* \mu \Psi_f$ , where  $\mu$  is the electric-dipole moment operator,  $\Psi_i$  is the initial molecular state, and  $\Psi_f$  is the final state. From the character table for  $D_{\infty h}$  we see that the  $z$ -component of the electric-dipole operator belongs to  $\Sigma_u^+(A_{2u})$  and the  $x$ - and  $y$ -components belong to  $\Pi_u(\mathcal{E}_{1u})$ . Therefore the product  $\Psi_i^* \Psi_f$  must transform as  $\Sigma_u^+$  or  $\Pi_u$  or else the transition is forbidden. Alternately we can require that  $\Gamma^\mu \times \Gamma^i$  contains  $\Gamma^f$ , that  $\Gamma^\mu \times \Gamma^f$  contains  $\Gamma^i$ , or that  $\Gamma^i \times \Gamma^f \times \Gamma^\mu$  contains  $\Sigma_g^+$ . In any case,  $\Psi_i$  and  $\Psi_f$  must have different parities since  $\mu$  is odd under inversion. For  $z$ -polarized light selection rules for symmetry-allowed transitions are easily worked out from the direct-product rule that  $\Gamma^i \times \Sigma_u^+$  must contain  $\Gamma^f$ . Using the character table, we find that the allowed transitions are  $\Sigma_u^+ \Leftrightarrow \Sigma_g^+$ ,  $\Sigma_u^- \Leftrightarrow \Sigma_g^-$ , and  $\Pi_u \Leftrightarrow \Pi_g$ .

For light polarized in the  $x$ - $y$  plane (electric dipole belonging to  $\Pi_u$ ) the direct product of two representations of dimensions higher than one can not be obtained from the character table alone. The direct products of some of the IRs are listed in Table 7.5.

If we look at the results in Table 7.5 for  $\Gamma \times \Pi$  we see that the direct product contains the IRs  $\Gamma^{\Lambda+1}$  and  $\Gamma^{\Lambda-1}$  (recall that  $\Lambda$  is the absolute value of the angular momentum about the  $z$ -axis.) For light polarized in the  $x$ - $y$  plane, the electric-dipole operator transforms as  $\Pi_u$ . If  $\Gamma_g^\Lambda$  is the initial state then the final state must be  $\Gamma_u^{\Lambda+1}$  or  $\Gamma_u^{\Lambda-1}$ , or else the transition is forbidden. Conversely, if  $\Gamma_u^\Lambda$  is the initial state then the final state must be  $\Gamma_g^{\Lambda+1}$  or  $\Gamma_g^{\Lambda-1}$ , or else the transition is forbidden. The selection rule requires  $\Delta\Lambda = \pm 1$ . Some of the symmetry-allowed transitions

for radiation polarized in the  $x$ - $y$  plane are  $\Sigma_g^\pm \Leftrightarrow \Pi_u$ ,  $\Sigma_u^\pm \Leftrightarrow \Pi_g$ ,  $\Pi_g \Leftrightarrow \Delta_u$ , and  $\Pi_u \Leftrightarrow \Delta_g$ .

### 7.3 Heteronuclear diatomic molecules

The covering group for  $A$ - $B$  molecules,  $C_{\infty v}$ , is given in Table 7.1(b). It consists of only the operations  $E$ ,  $C_\phi$ , and  $\sigma_v$ , since there is no inversion center. We can proceed with the analysis much as we did with the  $A$ - $A$  molecules, forming bonding and antibonding combinations. Let  $\phi_A(\mathbf{r} - \mathbf{R}_A)$  and  $\phi_B(\mathbf{r} - \mathbf{R}_B)$  be orbitals centered on the atoms  $A$  and  $B$ . For these two orbitals the secular equation is

$$\begin{vmatrix} \epsilon_A - \lambda & H_{AB} - S_{AB}\lambda \\ H_{AB} - S_{AB}\lambda & \epsilon_B - \lambda \end{vmatrix} = 0, \quad (7.28)$$

where  $\epsilon_A$  and  $\epsilon_B$  are the diagonal Hamiltonian matrix elements. The element,  $H_{AB}$  is the matrix element  $\int d\mathbf{r} \phi_A^* \mathbb{H} \phi_B$ , and  $S_{AB}$  is the corresponding overlap between  $\phi_A$  and  $\phi_B$ . We can assume that the two orbitals have the same symmetry with respect to the internuclear axis (if not,  $H_{AB}$  and  $S_{AB}$  vanish). The eigenvalues for (7.28) are

$$\lambda^+ = C - D, \quad (7.29)$$

$$\lambda^- = C + D, \quad (7.30)$$

where

$$C = \frac{\epsilon_A + \epsilon_B - 2H_{AB}S_{AB}}{2(1 - S_{AB}^2)}, \quad (7.31)$$

$$D = \left\{ C^2 - \frac{\epsilon_A \epsilon_B - H_{AB}^2}{1 - S_{AB}^2} \right\}^{1/2}. \quad (7.32)$$

The eigenvectors are

$$\psi^- = \frac{1}{\sqrt{N_A}}(H_{AB} - S_{AB}\lambda^-)\phi_B - (\epsilon_B - \lambda^-)\phi_A, \quad (7.33)$$

$$\psi^+ = \frac{1}{\sqrt{N_B}}(H_{AB} - S_{AB}\lambda^+)\phi_A - (\epsilon_A - \lambda^+)\phi_B, \quad (7.34)$$

$$N_{A/B} = \{(H_{AB} - S_{AB}\lambda^\pm)^2 + (\epsilon_{A/B} - \lambda^\pm)^2 - 2(H_{AB} - S_{AB}\lambda^\pm)(\epsilon_{A/B} - \lambda^\pm)S_{AB}\}^{1/2}. \quad (7.35)$$

The bonding/antibonding combinations depend on the symmetry of the individual orbitals. For example, for  $s_A$  and  $s_B$  orbitals the bonding state corresponds to the plus sign. For  $p_{z1}$  and  $s_2$  orbitals the minus sign gives the bonding state. In general, for the bonding state, the sign is such that the phases of the orbitals are the same in the overlap region between atoms.

Table 7.6 AB molecule bonding and antibonding orbital combinations.

$\psi^{b/a} = A_{b/a}\phi_A + B_{b/a}\phi_B$ , where the coefficients  $A_{b/a}$  and  $B_{b/a}$  are given in Eqs. (7.33) and (7.34).

Function	$\phi_A$	$\phi_B$	$\chi(E)$	$\chi(C_\phi)$	$\chi(\sigma_v)$	IR
$\psi^b(s, s)$	$s$	$s$	1	1	1	$\sigma^+$
$\psi^a(s, s)$	$s$	$s$	1	1	1	$\sigma^+$
$\psi^b(s, p_z)$	$s$	$p_z$	1	1	1	$\sigma^+$
$\psi^a(s, p_z)$	$s$	$p_z$	1	1	1	$\sigma^+$
$\psi^b(p_z, p_z)$	$p_z$	$p_z$	1	1	1	$\sigma^+$
$\psi^a(p_z, p_z)$	$p_z$	$p_z$	1	1	1	$\sigma^+$
$\{\psi^b(p_x, p_x), \psi^b(p_y, p_y)\} (2 \times 2 \text{ IR})$			2	$2 \cos \phi$	0	$\pi$
$\{\psi^a(p_x, p_x), \psi^a(p_y, p_y)\} (2 \times 2 \text{ IR})$			2	$2 \cos \phi$	0	$\pi$
$\psi^{b/a}(p_x, p_x)$	$p_x$	$p_x$				
$\psi^{b/a}(p_y, p_y)$	$p_y$	$p_y$				

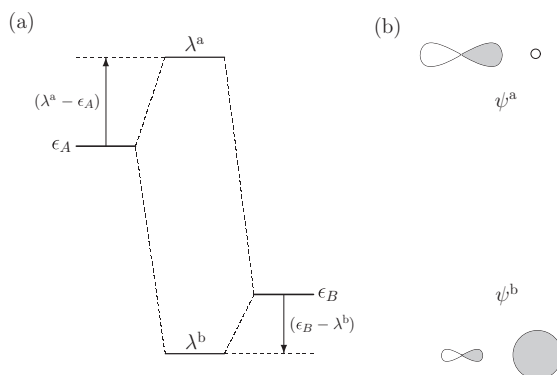


Figure 7.3 (a) A schematic representation of the energy levels for the AB molecule. (b) A schematic representation of the eigenfunctions when  $\phi_A$  is a  $p$ -orbital and  $\phi_B$  is an  $s$ -orbital.

The energy levels resulting from the interaction of  $\phi_A$  and  $\phi_B$  are shown schematically in Fig. 7.3, where  $\lambda^b$  and  $\lambda^a$  are the bonding and antibonding energies, respectively. The lower level,  $\epsilon_B$ , is pushed down by an amount  $(\epsilon_B - \lambda^b)$  and the upper level is pushed up by an amount  $(\lambda^a - \epsilon_A)$ . The eigenvectors are illustrated schematically in Fig. 7.4(b), where  $\phi_A$  is a  $p$ -orbital and  $\phi_B$  is an  $s$ -orbital.

### 7.3.1 Bonding and antibonding combinations for the AB molecule

The action table for the bonding and antibonding combinations is given in Table 7.6. The orbitals are of the form  $A\phi_A + B\phi_B$ . The  $\phi_A$  and  $\phi_B$  orbitals must have the same symmetry about the internuclear axis but *need not be the same type*

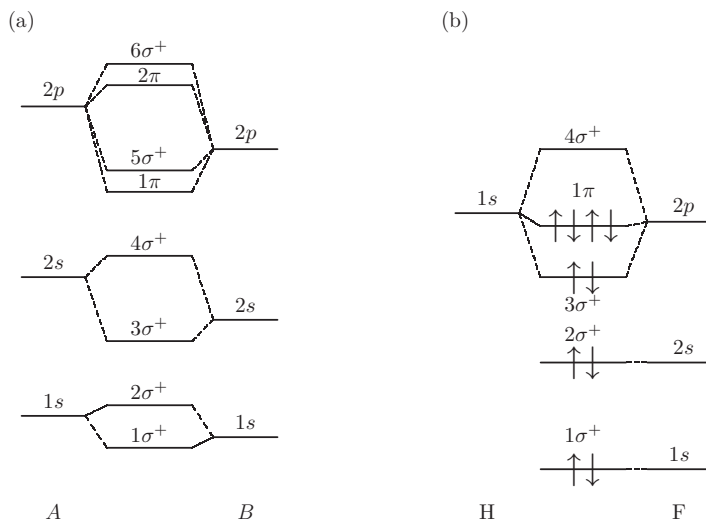


Figure 7.4 Level ordering for  $A-B$  diatomic molecules. (a) Ordering for molecules with not too dissimilar atoms such as CO. (b) Ordering for HF. The H(1s) orbital interacts strongly only with the  $\sigma(2p)$  orbitals. The  $1\pi$  is a two-fold degenerate, non-bonding level that can accommodate up to four electrons (two sets of paired electrons). The HF ground-state configuration is  $(1\sigma^+)^2(2\sigma^+)^2(3\sigma^+)^2(1\pi)^4$ . The occupied states are indicated by the spin arrows.

of orbital. For example, we could use an  $s$ -orbital on atom  $A$  and a  $p_z$  orbital on atom  $B$ . The same is true of the  $A-A$  molecule, but in that case we know that the same orbitals have the same energy and interact most strongly. Therefore, as a first approximation, we can ignore the hybrid combinations such as a  $p_z$  orbital with an  $s$ -orbital. For the  $A-B$  molecule, it is possible that the two orbitals closest in energy are different types of orbitals. This is the case, for example, for HF, where the H(1s) (hydrogen 1s orbital) interacts with the F(2p<sub>z</sub>) (fluorine 2p<sub>z</sub> orbital). The F(1s) and F(2s) are energetically too far removed from the H(1s) to form a bond of any consequence. The level ordering for HF is shown in Fig. 7.4(b). The F( $p_x$ ) and F( $p_y$ ) orbitals do not interact with the H(1s) orbitals. They form the  $1\pi$  level, a two-fold degenerate, non-bonding level that can accommodate up to four electrons (two sets of paired electrons). For  $H-B$  molecules with  $B$  less electronegative than F the  $B(2s)$  may form a sigma bond with the H(1s) if the energy separation is not too large. The possible choices for  $s$ - and  $p$ -orbitals are given in Table 7.6.

The first column of Table 7.6 specifies  $\psi^{b/a}$ , the second and third columns specify the two orbitals used in constructing  $\psi^{b/a}$ . Columns 4, 5, and 6 give the characters under the operations of the group. The functions  $\psi^b(p_x, p_x)$  and  $\psi^b(p_y, p_y)$  are the bases for a two-dimensional representation, as are the functions  $\psi^a(p_x, p_x)$  and  $\psi^a(p_y, p_y)$ . The characters are the sum of the diagonals of the  $2 \times 2$

representation matrices. Each function is a basis function for an IR (or row of an IR) of  $C_{\infty v}$ . The IRs for the functions are given in the last column of Table 7.6.

Figure 7.4(a) shows the level ordering for diatomic molecules with not too dissimilar atoms. On comparing Fig. 7.4(a) with Fig. 7.4(b) it is clear that the actual level ordering depends on the atoms that form the molecule. Experimental data is often required in order to determine the exact ordering. The molecular orbital states we have been discussing are analogous to the  $1s$ ,  $2s$ ,  $2p$ , ... states of the hydrogenic atoms. They provide a starting point for understanding the electronic structure, but are not the molecular eigenstates. Levels having the same symmetry will interact, and the effects of various Hamiltonian perturbations (exchange energy, spin-orbit effects, ...) must be added to the theory in order to find good approximations to the eigenstates. Nevertheless, a great deal of useful information is obtained using this simple, molecular “building-up” principle. Whatever the actual eigenstates are, we can be assured that they possess the same symmetries as those predicted by molecular-orbital theory.

### Exercises

- 7.1 (a) NO and  $O_2^+$  are similar molecules.  $O_2^+$  has an additional proton (and neutron) compared with NO, but they have the same number of electrons. Assume the level ordering (LO2) for the NO molecule is the same as  $O_2^+$ . What is the molecular configuration for NO? (Use Table 7.4. Drop the  $u/g$  designation and renumber the levels.)
- (b) What is the symmetry of the total molecular state of NO?
- (c) What is the bond order of NO?
- (d) Assume the stretching vibration frequency is proportional to the bond order. Calculate the frequencies in  $\text{cm}^{-1}$  for NO and  $O_2$ , given that the frequency for  $N_2$  is  $2,331 \text{ cm}^{-1}$ . (The experimentally observed values are  $1,876 \text{ cm}^{-1}$  and  $1,555 \text{ cm}^{-1}$ .)
- 7.2 Find the  $O_2$  determinantal state for the  $^3\Sigma_g^-$  term with  $S = 1$  and  $M_s = 0$ .
- 7.3 Show that the determinantal state,  $^1\Sigma_g^+$ , for  $O_2$  is

$$\frac{1}{\sqrt{2}} \left[ \langle \psi^a(p_x \uparrow) \psi^a(p_x \downarrow) | + \langle \psi^a(p_y \uparrow) \psi^a(p_y \downarrow) | \right].$$

- 7.4 If  $\Phi = (\Psi_r + \Psi_s)$ , show that

$$\begin{aligned} \det(\Phi, \phi_1, \phi_2, \phi_3, \dots, \phi_N) &= \det(\Psi_r, \phi_1, \phi_2, \phi_3, \dots, \phi_N) \\ &+ \det(\Psi_s, \phi_1, \phi_2, \phi_3, \dots, \phi_N). \end{aligned}$$

- 7.5 Use the results of Exercise 7.3 to derive Eq. (7.24). Start from Eq. (7.23).

- 7.6 For the molecule  $C_2$ , answer the following questions.
- What is the (LO1) molecular configuration and the symmetry?
  - What is the configuration and symmetry of the lowest-lying excited state?
  - What are the possible values of  $S$ ?
  - Is an electronic dipole transition from the ground state to the lowest excited state allowed or forbidden?
- 7.7 The configuration  $(\pi_u)^3$  is equivalent to a  $(\pi_u)$  hole state. A  $(\pi_u)^3$  determinantal state can be formed in two ways. The first is  $\Phi_1 = \langle \psi^b(p_y) \uparrow \psi^b(p_y) \downarrow \psi^b(p_x) \uparrow |$  and the second is  $\Phi_2 = \langle \psi^a(p_x) \uparrow \psi^a(p_x) \downarrow \psi^a(p_y) \uparrow |$ . Show that  $\Phi_1$  and  $\Phi_2$  are basis functions for the IR  $\pi_u$ , and therefore  $(\pi_u)^3$  transforms according to  $\pi_u$  IR.
- 7.8
- Draw a schematic diagram of the molecular levels for the  $(OH)^+$  molecule assuming that the  $H(1s)$  state is nearest in energy to the  $O(2p)$  state.
  - What is the molecular electronic configuration? Indicate the occupied molecular orbitals. (Assume Hund's rule for spin is obeyed.)
  - What are the molecular terms that can be formed from the configuration?
  - Which state would be the ground state according to Hund's rules?



# 8

## Transition-metal complexes

In Chapter 3 we discussed crystal-field theory in which the splitting of the  $d$ -electron levels was attributed to the electrostatic interactions due to the surrounding ligands. In this chapter we extend the theory to include the molecular orbitals representing the ligands.

### 8.1 An octahedral complex

We consider a complex consisting of a transition metal ion,  $M$ , surrounded by an octahedron of ligands ( $L_1$  through  $L_6$ ) as illustrated in Fig. 8.1. The covering group is  $O_h$  and its character table is given in Table 8.1.

As a starting point we assume that each ligand has  $s$ - and  $p$ -electrons outside a closed shell. The metal ion is assumed to have  $s$ -,  $p$ -, and  $d$ -electrons outside its closed shell.

No operation of the group can transform a ligand orbital into a metal orbital (or vice versa), and no operation can transform an  $s$ -orbital into a  $p$ - or  $d$ -orbital. Therefore we can express the representation for the complex as a sum of representations,

$$\Gamma^C = \Gamma^s(M) + \Gamma^p(M) + \Gamma^d(M) + \Gamma^s(L) + \Gamma^p(L), \quad (8.1)$$

where  $\Gamma^C$  is the representation for the total complex,  $\Gamma^\alpha(M)$  is the  $\alpha$ -orbital representation for the metal ion, and  $\Gamma^\beta(L)$  is the  $\beta$ -orbital representation for the ligands.

In Chapter 3 we discussed the  $O_h$  group and its operations. We found that the  $d$ -orbitals  $d_{xy}$ ,  $d_{xz}$ , and  $d_{yz}$  were basis functions for the  $t_{2g}$  IR, and that  $d_{z^2}$  and  $d_{x^2-y^2}$  were basis functions for the  $e_g$  IR of the  $O_h$  group. Therefore we have

$$\Gamma^d(M) = t_{2g} + e_g. \quad (8.2)$$

Table 8.1 The character table for  $O$ .  $O_h = O \times i$ 

$O(432)$	$E$	$8C_3$	$3C_2$	$6\bar{C}_2$	$6C_4$
$A_1$	1	1	1	1	1
$A_2$	1	1	1	-1	-1
$(x^2 - y^2, 3z^2 - r^2)$	$\mathcal{E}$	2	-1	2	0
$(R_x, R_y, R_z)$	$T_1$	3	0	-1	-1
$(x, y, z)$	$T_2$	3	0	-1	1
$(xy, yz, xz)$	$T_2$	3	0	-1	-1

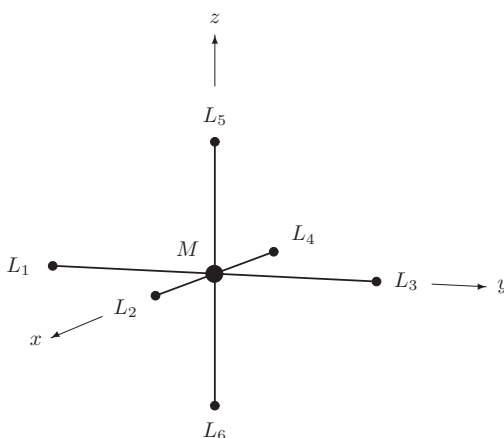


Figure 8.1 A transition metal ion surrounded by an octahedron of ligands. The ligands are numbered  $L_1$  through  $L_6$ . In terms of distance of separation,  $M$  and  $L_i$  are nearest neighbors. Ligands adjacent to one another are second-nearest neighbors. Ligands on opposite sides of the metal ion are third-nearest neighbors.

Without specifying the ligand orbitals, we can already draw a conclusion about the nature of the molecular states. The  $d$ -states are all “ $g$ ” states; hence only ligand “ $g$ ” states can interact with them to form metal–ligand bonds. The “ $u$ ” ligand states will not interact with the  $d$ -states. If only  $d$ -electrons are considered for the metal ion, the “ $u$ ” ligand states will be non-bonding. Now suppose we add an  $s$ -orbital to the collection of metal-ion orbitals. We know that  $\Gamma^s(M)$  belongs to the  $a_{1g}$  IR of  $O_h$  and these states interact only with “ $g$ ” ligand states. However, when we add  $p$ -electrons to the metal orbitals the situation changes. Since  $\Gamma^p(M)$  belongs to  $t_{1u}$ , the  $p$ -orbitals will interact only with the “ $u$ ” ligand states. In summary, the  $s$ - and  $d$ -orbitals of the metal ion form only “ $g$ ” bonds and the  $p$ -orbitals form only “ $u$ ” bonds.

Whatever types of orbitals are used for the ligands’ states, we know that they must be basis functions for a representation of the group and the representation

must decompose into the IRs of the  $O_h$ . For a bond to be formed with the metal ion, the decomposition of the ligand representation must contain  $e_g$  and/or  $t_{2g}$  and/or  $t_{1u}$ . All other IRs in the decomposition are non-bonding with respect to the metal–ligand interactions.<sup>1</sup>

### Representations and symmetry functions

The characters for the representations based on various hydrogen-like atomic orbitals can be deduced from the action table, Table 8.2.

Under the inversion operation the ligand positions change as follows:

$$P_i(L_1) \Rightarrow L_3, \quad (8.3a)$$

$$P_i(L_2) \Rightarrow L_4, \quad (8.3b)$$

$$P_i(L_3) \Rightarrow L_1, \quad (8.3c)$$

$$P_i(L_4) \Rightarrow L_2, \quad (8.3d)$$

$$P_i(L_5) \Rightarrow L_6, \quad (8.3e)$$

$$P_i(L_6) \Rightarrow L_5. \quad (8.3f)$$

Equations (8.3) together with the action table Table 8.2 can be employed to find the characters for the inversion operations. The characters for representations based on the various orbitals are given in Table 8.3.

The decompositions of the representations are

$$\Gamma^s(M) = a_{1g}, \quad (8.4a)$$

$$\Gamma^p(M) = t_{1u}, \quad (8.4b)$$

$$\Gamma^d(M) = e_g + t_{2g}, \quad (8.4c)$$

$$\Gamma^s(L) = a_{1g} + e_g + t_{1u}, \quad (8.4d)$$

$$\Gamma^p(L) = a_{1g} + e_g + t_{1g} + t_{2g} + 2t_{1u} + t_{2u}, \quad (8.4e)$$

$$\Gamma^C = 3a_{1g} + 3e_g + t_{1g} + 2t_{2g} + 4t_{1u} + t_{2u}. \quad (8.4f)$$

From Eq. (8.4f) we see that  $t_{1g}$  and  $t_{2u}$  occur only once in  $\Gamma^C$ . These representations correspond to non-bonding combinations of  $p$ -orbitals. The secular equation,  $\det\{\mathbb{H} - \mathbb{S}\epsilon\} = 0$ , for the molecular states will block-diagonalize as follows.

$a_{1g}$ : One  $3 \times 3$  block involving the  $s(M)$ ,  $s(L)$ , and  $p(L)$  orbitals.

$e_g$ : Two  $3 \times 3$  blocks involving  $d(M)$ ,  $s(L)$ , and  $p(L)$  orbitals.

$t_{1g}$ : Three  $1 \times 1$  blocks involving only  $p(L)$ . These states are non-bonding and the symmetry functions are eigenstates.

<sup>1</sup> The ligand orbitals that do interact with the metal orbitals can in some cases also produce non-bonding states as well as bonding and antibonding states.

Table 8.2 *The action table for the  $O$  group. Functions in bold face go into a multiple of themselves under an operation of the group. A complete discussion of the operations of the group and the irreducible representations is given in Appendix E.*

$E$	$C_3^1$	$C_3^{1^2}$	$C_3^2$	$C_3^{2^2}$	$C_3^3$	$C_3^{3^2}$	$C_3^4$	$C_3^{4^2}$	$C_2^1$	$C_2^2$	$C_2^3$	$\bar{C}_2^1$	$\bar{C}_2^2$	$\bar{C}_2^3$	$\bar{C}_2^4$	$\bar{C}_2^5$	$\bar{C}_2^6$	$C_4^1$	$C_4^{1^3}$	$C_4^2$	$C_4^{2^3}$	$C_4^3$	$C_4^{3^3}$
<b>X</b>	−Y	−Z	−Z	Y	−Y	Z	Z	Y	<b>X</b>	− <b>X</b>	− <b>X</b>	− <b>X</b>	− <b>X</b>	−Z	Z	−Y	Y	<b>X</b>	<b>X</b>	Z	−Z	−Y	Y
<b>Y</b>	Z	−X	X	−Z	−Z	−X	X	Z	− <b>Y</b>	<b>Y</b>	− <b>Y</b>	Z	−Z	−Y	−Y	−X	X	−Z	Z	<b>Y</b>	<b>Y</b>	X	−X
<b>Z</b>	−X	Y	−Y	−X	X	−Y	Y	X	− <b>Z</b>	− <b>Z</b>	<b>Z</b>	Y	−Y	−X	X	− <b>Z</b>	− <b>Z</b>	Y	−Y	−X	X	<b>Z</b>	<b>Z</b>
<b>1</b>	6	2	4	5	5	2	4	6	3	<b>1</b>	3	6	5	3	3	2	4	5	6	<b>1</b>	<b>1</b>	4	2
<b>2</b>	1	6	6	3	1	5	5	3	<b>2</b>	4	4	4	4	6	5	1	3	<b>2</b>	<b>2</b>	5	6	1	3
<b>3</b>	5	4	2	6	6	4	2	5	1	<b>3</b>	1	5	6	1	1	4	2	6	5	<b>3</b>	<b>3</b>	2	4
<b>4</b>	3	5	5	1	3	6	6	1	<b>4</b>	2	2	2	2	5	6	3	1	<b>4</b>	<b>4</b>	6	5	3	1
<b>5</b>	4	3	1	4	2	1	3	2	6	6	<b>5</b>	3	1	4	2	6	6	3	1	4	2	<b>5</b>	<b>5</b>
<b>6</b>	2	1	3	2	4	3	1	4	5	5	<b>6</b>	1	3	2	4	5	5	1	3	2	4	<b>6</b>	<b>6</b>
<b>XY</b>	−YZ	XZ	−XZ	−YZ	YZ	−XZ	XZ	YZ	− <b>XY</b>	− <b>XY</b>	<b>XY</b>	−XZ	XZ	YZ	−YZ	<b>XY</b>	<b>XY</b>	−XZ	XZ	YZ	−YZ	− <b>XY</b>	− <b>XY</b>
<b>XZ</b>	XY	−YZ	YZ	−XY	−XY	−YZ	YZ	XY	− <b>XZ</b>	<b>XZ</b>	− <b>XZ</b>	−XY	XY	<b>XZ</b>	<b>XZ</b>	YZ	−YZ	XY	−XY	− <b>XZ</b>	− <b>XZ</b>	−YZ	YZ
<b>YZ</b>	−XZ	−XY	−XY	XZ	−XZ	XY	XY	XZ	<b>YZ</b>	− <b>YZ</b>	− <b>YZ</b>	<b>YZ</b>	<b>YZ</b>	XY	−XY	XZ	−XZ	− <b>YZ</b>	− <b>YZ</b>	−XY	XY	XZ	−XZ
$\frac{X^2 - Y^2}{2} = a$	$-\frac{1}{2}a - \frac{\sqrt{3}}{2}b$	$-\frac{1}{2}a + \frac{\sqrt{3}}{2}b$	$-\frac{1}{2}a - \frac{\sqrt{3}}{2}b$	$-\frac{1}{2}a + \frac{\sqrt{3}}{2}b$	$-\frac{1}{2}a - \frac{\sqrt{3}}{2}b$	$-\frac{1}{2}a + \frac{\sqrt{3}}{2}b$	$-\frac{1}{2}a - \frac{\sqrt{3}}{2}b$	$-\frac{1}{2}a + \frac{\sqrt{3}}{2}b$	$a$	$a$	$a$	$\frac{1}{2}a - \frac{\sqrt{3}}{2}b$	$\frac{1}{2}a - \frac{\sqrt{3}}{2}b$	$\frac{1}{2}a + \frac{\sqrt{3}}{2}b$	$\frac{1}{2}a + \frac{\sqrt{3}}{2}b$	$-a$	$-a$	$\frac{1}{2}a - \frac{\sqrt{3}}{2}b$	$\frac{1}{2}a - \frac{\sqrt{3}}{2}b$	$\frac{1}{2}a + \frac{\sqrt{3}}{2}b$	$\frac{1}{2}a + \frac{\sqrt{3}}{2}b$	$-a$	$-a$
$\frac{3Z^2 - r^2}{2\sqrt{3}} = b$	$-\frac{1}{2}b + \frac{\sqrt{3}}{2}a$	$-\frac{1}{2}b - \frac{\sqrt{3}}{2}a$	$-\frac{1}{2}b - \frac{\sqrt{3}}{2}a$	$-\frac{1}{2}b + \frac{\sqrt{3}}{2}a$	$-\frac{1}{2}b + \frac{\sqrt{3}}{2}a$	$-\frac{1}{2}b - \frac{\sqrt{3}}{2}a$	$-\frac{1}{2}b - \frac{\sqrt{3}}{2}a$	$-\frac{1}{2}b + \frac{\sqrt{3}}{2}a$	$b$	$b$	$b$	$-\frac{1}{2}b - \frac{\sqrt{3}}{2}a$	$-\frac{1}{2}b - \frac{\sqrt{3}}{2}a$	$-\frac{1}{2}b + \frac{\sqrt{3}}{2}a$	$-\frac{1}{2}b + \frac{\sqrt{3}}{2}a$	$b$	$b$	$-\frac{1}{2}b - \frac{\sqrt{3}}{2}a$	$-\frac{1}{2}b - \frac{\sqrt{3}}{2}a$	$-\frac{1}{2}b + \frac{\sqrt{3}}{2}a$	$-\frac{1}{2}b + \frac{\sqrt{3}}{2}a$	$b$	$b$

Table 8.3 The character table for the different types of orbital representations

Orbital	$E$	$8C_3$	$3C_2$	$6\bar{C}_2$	$6\bar{C}_4$	$i$	$8iC_3$	$3iC_2$	$6\bar{C}_2$	$6\bar{C}_4$
$\Gamma^s(M)$	1	1	1	1	1	1	1	1	1	1
$\Gamma^p(M)$	3	-1	1	1	-1	5	-1	1	1	-1
$\Gamma^d(M)$	5	0	-1	-1	1	-3	0	1	1	-1
$\Gamma^s(L)$	6	0	2	0	2	0	0	4	2	0
$\Gamma^p(L)$	18	0	-2	0	2	0	0	4	2	0
$\Gamma^C$	33	0	1	1	5	3	0	11	7	-1

$t_{2g}$ : Three  $2 \times 2$  blocks involving  $d(M)$  and  $p(L)$  orbitals.

$t_{1u}$ : Three  $4 \times 4$  blocks involving  $p(M)$ ,  $s(L)$ , and  $p(L)$  orbitals.

$t_{2u}$ : Three  $1 \times 1$  blocks involving only  $p(L)$ . These states are non-bonding and the symmetry functions are eigenstates.

The symmetry functions for the representations can be found using the symmetry-function-generating machine,

$$f_i^\alpha \propto \sum_R D_{ii}^\alpha(R)^* P_R f, \quad (8.5)$$

where  $f_i^\alpha$  is a symmetry function that transforms according to the  $i$ th row of the  $\Gamma^\alpha$  IR,  $D_{ii}^\alpha(R)$  is the diagonal element of the IR matrix for the  $R$  operation of the group, and  $f$  is an arbitrary linear combination of orbitals. The matrix elements for the different IRs of  $O_h$  are given in Appendix E, in Section E.4. The results for the symmetry functions are listed in Table 8.4.

### 8.1.1 Energy levels of an octahedral complex

The eigenvectors and eigenvalues of an octahedral complex can be calculated in terms of the LCAO overlap and interaction integrals. It is instructive to begin with the model for which the metal  $s$ -,  $p$ -, and  $d$ -orbitals interact only with the ligand  $p$ -orbitals. In many cases the ligand  $s$ -orbitals are far removed in energy from the metal-ion orbitals. For example, for F the  $2s$  ionization energy is 46.4 eV and the  $2p$  ionization energy is 18.7 eV, while the ionization energy for a  $d$ -electron ( $3d^{n-1}4s \Rightarrow 3d^{n-2}4s$ ) is 5.6 and 7.2 eV for Ti and Cr, respectively. Therefore, omission of the  $2s$  ligand orbitals is not a severe approximation.

The ligand  $p$ -orbitals divide into two classes. The first class consists of  $p$ -orbitals that can form a sigma interaction with the metal ion. These “ $p$ -sigma” orbitals are aligned along the  $x$ -,  $y$ -, and  $z$ -axes. They are labeled  $y_1$ ,  $x_2$ ,  $y_3$ ,  $x_4$ ,  $z_5$ , and  $z_6$ , where  $x_i$ ,  $y_i$ , and  $z_i$  represent the  $p$ -orbitals,  $p_x$ ,  $p_y$ , and  $p_z$ , respectively.

Table 8.4 Symmetry functions for the octahedral complex. The first column lists the IR of  $O_h$ . The second column lists the row of the IR for multidimensional IRs. The third column lists the orbital type: (L) indicates ligand and (M) indicates central metal ion. The fourth column lists the symmetry functions for each row of the IR. Notation:  $s_i$  and  $x_i$ ,  $y_i$ , and  $z_i$  ( $i = 1, 2, \dots, 6$ ) indicate the ligand  $s$ - and  $p$ -orbitals, respectively. The last column lists the type of interaction the metal orbitals have with the ligand orbitals of the same symmetry type, where “NB” indicates non-bonding with the metal orbitals.

IR	Row	Orbital type	Symmetry function	Type
$a_{1g}$		$s(M)$	$s(M)$	
		$s(L)$	$(s_1 + s_2 + s_3 + s_4 + s_5 + s_6)/\sqrt{6}$	Sigma
		$p(L)$	$(y_1 - x_2 - y_3 + x_4 - z_5 + z_6)/\sqrt{6}$	Sigma
$e_g$	1	$d(M)$	$d_{x^2}(M)$	
	2		$d_{z^2}(M)$	
	1	$s(L)$	$(s_1 - s_2 + s_3 - s_4)/2$	Sigma
	2		$(s_1 + s_2 + s_3 + s_4 - 2s_5 - 2s_6)/\sqrt{12}$	Sigma
	1	$p(L)$	$(y_1 + x_2 - y_3 - x_4)/2$	Sigma
	2		$(y_1 - x_2 - y_3 + x_4 + 2z_5 - 2z_6)/\sqrt{12}$	Sigma
$t_{1g}$	1	$p(L)$	$(z_1 - z_3 + y_5 - y_6)/2$	NB pi
	2		$(x_5 - x_6 + z_4 - z_2)/2$	NB pi
	3		$(x_1 - x_3 + y_2 - y_4)/2$	NB pi
$t_{2g}$	1	$d(M)$	$d_{xy}(M)$	
	2		$d_{xz}(M)$	
	3		$d_{yz}(M)$	
	1	$p(L)$	$(x_1 - y_2 - x_3 + y_4)/2$	Pi
	2		$(z_2 - z_4 - x_6 + x_5)/2$	Pi
	3		$(z_1 - z_3 + y_6 - y_5)/2$	Pi
$t_{1u}$	1	$p(M)$	$x(M)$	
	2		$y(M)$	
	3		$z(M)$	
	1	$s(L)$	$(s_2 - s_4)/\sqrt{2}$	Sigma
	2		$(s_1 - s_3)/\sqrt{2}$	Sigma
	3		$(s_5 - s_6)/\sqrt{2}$	Sigma
	1	$p(L)$	$(x_1 + x_3 + x_5 + x_6)/2$	Pi
	2		$(y_2 + y_4 + y_5 + y_6)/2$	Pi
	3		$(z_1 + z_2 + z_3 + z_4)/2$	Pi
	1	$p(L)$	$(x_2 + x_4)/\sqrt{2}$	Sigma
	2		$(y_1 + y_3)/\sqrt{2}$	Sigma
	3		$(z_5 + z_6)/\sqrt{2}$	Sigma
$t_{2u}$	1	$p(L)$	$(z_1 + z_3 - z_2 - z_4)/2$	NB pi
	2		$(y_2 + y_4 - y_5 - y_6)/2$	NB pi
	3		$(x_1 + x_3 - x_5 - x_6)/2$	NB pi

The second class of ligand  $p$ -orbitals consists of those that can form pi bonds with the metal orbitals, the “ $p$ -pi” orbitals. The  $p$ -pi orbitals are oriented perpendicular to the  $x$ -,  $y$ -, and  $z$ -axes. They include  $x_1, z_1, y_2, z_2, x_3, z_3, y_4, z_4, x_5, y_5, x_6$ , and  $y_6$ . The class of  $p$ -orbitals involved in an eigenstate is indicated in the last column in Table 8.4. All of the eigenstates involving ligand– $d$ -orbital interactions are either pi or sigma. The  $t_{1u}$  states are different. They involve ligand orbitals and metal  $p$ -orbitals, and have both sigma and pi ligand–metal interactions.

In many chemistry texts  $s$ – $p$  hybrid orbitals are used for the ligand sigma orbitals. The use of hybrid orbitals is not necessary if both the  $s$  and the  $p$  ligand orbitals are included in the set of basis functions. The formation of  $s$ – $p$  hybrid-like bonds and anti-bonds occurs automatically. The use of the  $s$ – $p$  hybrid orbitals has no effect on the group-theoretical analysis. The hybrid orbitals transform under the group operations exactly as the  $p$ -sigma orbitals.

The orbitals for the  $e_g$  and  $t_{2g}$  symmetries are given in Table 8.4. The secular equation for the  $t_{2g}$  states consists of three symmetry-equivalent  $2 \times 2$  matrices. For simplicity we shall assume the orbitals are orthogonal Löwdin functions so that we do not have to deal with overlap integrals. The LCAO interactions for  $s$ -,  $p$ -, and  $d$ -orbitals are given in Table 8.5 [8.1].

The secular equation for the interaction of the two row-1  $t_{2g}$  symmetry functions is then

$$\begin{vmatrix} \epsilon_d - \epsilon & -2(pd\pi)_1 \\ -2(pd\pi)_1 & \epsilon'_p - \epsilon \end{vmatrix} = 0, \quad (8.6)$$

where

$$\begin{aligned} \epsilon_d &= \int d_{xy}^* \mathbb{H} d_{xy} dr, \\ \epsilon'_p &= \int \frac{1}{2}(p_{x_1} - p_{y_2} - p_{x_3} + p_{y_4})^* \mathbb{H} \frac{1}{2}(p_{x_1} - p_{y_2} - p_{x_3} + p_{y_4}) dr \\ &= \epsilon_p + (p_L p_L \pi)_2 - (p_L p_L \sigma)_2 - (p_L p_L \pi)_3, \\ \epsilon_p &= \int p_{\alpha j}^* \mathbb{H} p_{\alpha j} dr \quad (\alpha = x, y, \text{ or } z, \text{ and } i = 1, 2, \dots, 6), \end{aligned}$$

and

$$\int d_{xy}^* \mathbb{H} \frac{1}{2}(p_{x_1} - p_{y_2} - p_{x_3} + p_{y_4}) dr = -2(pd\pi).$$

Table 8.5 *LCAO two-center integrals [8.1] for orbitals centered at  $\vec{R}_i$  and  $\vec{R}_j$ . The variables  $\ell$ ,  $m$ , and  $n$  are the direction cosines of the vector  $(\vec{R}_j - \vec{R}_i)$ .*

$E_{s,s}$	$(ss\sigma)$
$E_{s,x}$	$\ell(sp\sigma)$
$E_{x,x}$	$\ell^2(pp\sigma) + (1 - \ell^2)(pp\pi)$
$E_{x,y}$	$\ell m(pp\sigma) - \ell m(pp\pi)$
$E_{x,z}$	$\ell n(pp\sigma) - \ell n(pp\pi)$
$E_{s,xy}$	$\sqrt{3}\ell m(sd\sigma)$
$E_{s,x^2-y^2}$	$\frac{1}{2}\sqrt{3}(\ell^2 - m^2)(sd\sigma)$
$E_{s,3z^2-r^2}$	$[n^2 - \frac{1}{2}(\ell^2 + m^2)](sd\sigma)$
$E_{x,xy}$	$\sqrt{3}\ell^2 m(pd\sigma) + m(1 - 2\ell^2)(pd\pi)$
$E_{x,yz}$	$\sqrt{3}\ell mn(pd\sigma) - 2\ell mn(pd\pi)$
$E_{x,zx}$	$\sqrt{3}\ell^2 n(pd\sigma) + n(1 - 2\ell^2)(pd\pi)$
$E_{x,x^2-y^2}$	$\frac{1}{2}\sqrt{3}\ell(\ell^2 - m^2)(pd\sigma) + \ell(1 - \ell^2 + m^2)(pd\pi)$
$E_{y,x^2-y^2}$	$\frac{1}{2}\sqrt{3}m(\ell^2 - m^2)(pd\sigma) - m(1 + \ell^2 - m^2)(pd\pi)$
$E_{z,x^2-y^2}$	$\frac{1}{2}\sqrt{3}n(\ell^2 - m^2)(pd\sigma) - n(\ell^2 - m^2)(pd\pi)$
$E_{x,3z^2-r^2}$	$\ell[n^2 - \frac{1}{2}(\ell^2 + m^2)](pd\sigma) - \sqrt{3}\ell n^2(pd\pi)$
$E_{y,3z^2-r^2}$	$m[n^2 - \frac{1}{2}(\ell^2 + m^2)](pd\sigma) - \sqrt{3}mn^2(pd\pi)$
$E_{z,3z^2-r^2}$	$n[n^2 - \frac{1}{2}(\ell^2 + m^2)](pd\sigma) + \sqrt{3}n(\ell^2 + m^2)(pd\pi)$
$E_{xy,xy}$	$3\ell^2 m^2(dd\sigma) + (\ell^2 + m^2 - 4\ell^2 m^2)(dd\pi) + (n^2 + \ell^2 m^2)(dd\delta)$
$E_{xy,yz}$	$3\ell m^2 n(dd\sigma) + \ell n(1 - 4m^2)(dd\pi) + \ell n(m^2 - 1)(dd\delta)$
$E_{xy,xz}$	$3\ell^2 mn(dd\sigma) + mn(1 - 4\ell^2)(dd\pi) + mn(\ell^2 - 1)(dd\delta)$
$E_{xy,x^2-y^2}$	$\frac{3}{2}\ell m(\ell^2 - m^2)(dd\sigma) + 2\ell m(m^2 - \ell^2)(dd\pi) + \frac{1}{2}\ell m(\ell^2 - m^2)(dd\delta)$
$E_{yz,x^2-y^2}$	$\frac{3}{2}mn(\ell^2 - m^2)(dd\sigma) - mn[1 + 2(\ell^2 - m^2)](dd\pi) + mn[1 + \frac{1}{2}(\ell^2 - m^2)](dd\delta)$
$E_{zx,x^2-y^2}$	$\frac{3}{2}n\ell(\ell^2 - m^2)(dd\sigma) + n\ell[1 - 2(\ell^2 - m^2)](dd\pi) - n\ell[1 - \frac{1}{2}(\ell^2 - m^2)](dd\delta)$
$E_{xy,3z^2-r^2}$	$\sqrt{3}\ell m[n^2 - \frac{1}{2}(\ell^2 + m^2)](dd\sigma) - 2\sqrt{3}\ell mn^2(dd\pi) + \frac{1}{2}\sqrt{3}\ell m(1 + n^2)(dd\delta)$
$E_{yz,3z^2-r^2}$	$\sqrt{3}mn[n^2 - \frac{1}{2}(\ell^2 + m^2)](dd\sigma) + \sqrt{3}mn(\ell^2 + m^2 - n^2)(dd\pi) - \frac{1}{2}\sqrt{3}mn(\ell^2 + m^2)(dd\delta)$
$E_{zx,3z^2-r^2}$	$\sqrt{3}\ell n[n^2 - \frac{1}{2}(\ell^2 + m^2)](dd\sigma) - 2\sqrt{3}\ell n(\ell^2 + m^2 - n^2)(dd\pi) + \frac{1}{2}\sqrt{3}\ell n(\ell^2 + m^2)(dd\delta)$
$E_{x^2-y^2,x^2-y^2}$	$\frac{3}{4}(\ell^2 - m^2)^2(dd\sigma) + [\ell^2 + m^2 - (\ell^2 - m^2)^2](dd\pi) + [n^2 + \frac{1}{4}(\ell^2 - m^2)^2](dd\delta)$
$E_{x^2-y^2,3z^2-r^2}$	$\frac{1}{2}\sqrt{3}(\ell^2 - m^2)[n^2 - \frac{1}{2}(\ell^2 + m^2)](dd\sigma) + \sqrt{3}n^2(m^2 - \ell^2)(dd\pi) + \frac{1}{4}\sqrt{3}(1 + n^2)(\ell^2 - m^2)(dd\delta)$
$E_{3z^2-r^2,3z^2-r^2}$	$[n^2 - \frac{1}{2}(\ell^2 + m^2)](dd\sigma) + 3n^2(\ell^2 + m^2)(dd\pi) + \frac{3}{4}(\ell^2 + m^2)^2(dd\delta)$



The subscripts 2 and 3 on the  $(p_L\pi p_L\pi)$  parameters indicate interactions between orbitals that are second-nearest and third-nearest neighbors as indicated in the caption of Fig. 8.1. The eigenvalues are

$$\epsilon^\pm(t_{2g}) = \frac{1}{2}(\epsilon_d + \epsilon'_p) \pm \sqrt{\left[\frac{1}{2}(\epsilon_d - \epsilon'_p)\right]^2 + 4(pd\pi)^2}. \quad (8.7)$$

The plus sign in (8.7) corresponds to an antibonding level,  $2t_{2g}$ , and the minus sign gives the  $1t_{2g}$  bonding level. The other two rows of the  $t_{2g}$  symmetry functions yield the same result, therefore the eigenvalues are three-fold degenerate. For the  $e_g$  states we have that the secular equation (ignoring the ligand  $s$ -orbitals) is

$$\begin{vmatrix} \epsilon_d - \epsilon & -\sqrt{3}(pd\sigma)_1 \\ -\sqrt{3}(pd\sigma)_1 & \epsilon''_p - \epsilon \end{vmatrix} = 0. \quad (8.8)$$

The eigenvalues are

$$\epsilon^\pm(e_g) = \frac{1}{2}(\epsilon_d + \epsilon''_p) \pm \sqrt{\left[\frac{1}{2}(\epsilon_d - \epsilon''_p)\right]^2 + 3(pd\sigma)^2}, \quad (8.9)$$

$$\epsilon''_p = \epsilon_p + (p_L p_L \sigma)_2 - (p_L p_L \pi)_2 - (p_L p_L \sigma)_3. \quad (8.10)$$

The plus sign gives the energy of the antibonding state,  $2e_g$ , and the minus sign gives the energy of the  $1e_g$  bonding state. The row-2  $e_g$ -symmetry functions give the same result, so the  $e_g$  states are each two-fold degenerate. The splitting of the  $d$ -orbital antibonding levels is

$$\begin{aligned} \Delta &= \epsilon^+(e_g) - \epsilon^+(t_{2g}) \\ &= (p_L p_L \pi)_2 + (p_L p_L \sigma)_2 - \frac{1}{2}(p_L p_L \sigma)_3 - (p_L p_L \pi)_3 \\ &\quad + \sqrt{\left[\frac{1}{2}(\epsilon_d - \epsilon''_p)\right]^2 + 3(p_L d_M \sigma)_1^2} \\ &\quad - \sqrt{\left[\frac{1}{2}(\epsilon_d - \epsilon'_p)\right]^2 + 4(p_L d_M \pi)_1^2}, \end{aligned} \quad (8.11)$$

where the subscripts  $L$  and  $M$  indicate ligand and metal, respectively.

The energy difference  $\Delta$  is the molecular-orbital equivalent of “ $10Dq$ ” in crystal-field theory (Chapter 3). Here, however, the splitting derives from covalent mixing of the  $d$ -ion orbitals with the ligand orbitals, whereas in crystal-field theory the splitting is due to the electrostatic field of the ligands. The covalent mixing of the  $e_g$  states is larger than that of  $t_{2g}$  states, so  $\Delta$  is positive. With this type of simple model the interaction parameters are usually determined by fitting the

results to experimental data or more accurate numerical calculations. The electric-dipole transition  $t_{2g} \Rightarrow e_g$  is forbidden unless accompanied by “ $u$ ” excitation (e.g., a molecular vibration transition). A weak absorption band observed for  $[\text{TiF}_6]^{3-}$  indicates that  $\Delta$  is about  $17,000 \text{ cm}^{-1}$  (2.11 eV).

Usually  $|(pd\sigma)|$  is in the range of 2–5 eV in magnitude. It is two to five times larger than  $|(pd\pi)|$ . The  $p_L - p_L$  interactions  $|(p_L p_L \sigma)_2|$  and  $|(p_L p_L \pi)_2|$  are roughly a factor of 10 smaller than  $|(pd\sigma)|$ . The two quantities  $|(p_L p_L \sigma)_3|$  and  $|(p_L p_L \pi)_3|$  are often small enough to neglect.

The empirical LCAO model can not be used to carry out accurate calculations of the energies or the wavefunctions. However, the symmetries of the molecular states derived from the LCAO model are correct. The principal value of the model is conceptual. It provides a scheme for understanding the physics, chemistry, and optical properties of transition metal complexes.

The energies of the secular equations for the various molecular levels are summarized in Table 8.6.

Figure 8.2 is a schematic representation of the molecular levels resulting from  $M-L$  and  $L-L$  interactions and overlaps.

As examples, we consider the electronic structures of two complexes,  $[\text{TiF}_6]^{3-}$  and  $[\text{CrF}_6]^{3-}$ . The electronic configurations of the atoms are  $\text{Ti} = [\text{Ar}]3d^24s^2$ ,  $\text{Cr} = [\text{Ar}]3d^54s$ , and  $\text{F} = [\text{He}]2s^22p^5$ . The number of electrons outside the closed  $[\text{Ar}]$  shell is four for Ti, and for F the number of electrons outside the  $[\text{He}]2s^2$  closed shells is five. The total number of electrons to be assigned to the molecular orbitals for the  $[\text{TiF}_6]^{3-}$  complex is therefore  $4 + 6(5) + 3 = 37$ , where the last number of 3 is due to the charge on the complex. For  $[\text{CrF}_6]^{3-}$  the number of electrons to be assigned is  $6 + 6(5) + 3 = 39$ .

If we fill the lowest energy levels in Fig. 8.2, then the configuration for  $[\text{TiF}_6]^{3-}$  is

$$(1a_{1g})^2(1e_g)^4(1t_{2g})^6(1t_{1u})^6(2t_{1u})^6(1t_{2g})^6(1t_{1g})^6(2t_{2g})^1. \quad (8.12)$$

Since there is a single  $2t_{2g}$  electron outside of closed molecular shells, the total molecular state is  $T_{2g}$ ; and since there is a single unpaired spin, the state is a spin doublet,  $^2T_{2g}$ . For  $[\text{CrF}_6]^{3-}$  we must assign two more electrons to the  $2t_{2g}$  level, so the molecular configuration is

$$(1a_{1g})^2(1e_g)^4(1t_{2g})^6(1t_{1u})^6(2t_{1u})^6(1t_{2g})^6(1t_{1g})^6(2t_{2g})^3. \quad (8.13)$$

The three electrons in the  $2t_{2g}$  molecular orbitals produce several terms. In Table 8.4 there are two  $t_{2g}$  symmetry functions for each of the three rows, giving a total of six symmetry functions. The eigenstates will be linear combinations of the functions from the same rows. Three of the six eigenstates correspond to the  $1t_{2g}$  bonding states, while the other three are the  $2t_{2g}$  antibonding states. We have

Table 8.6 LCAO molecular energy levels for an octahedral complex using orthogonal Löwdin orbitals. Included are  $s$ ,  $p$ , and  $d$  metal orbitals and six ligand  $p$ -orbitals. Here  $(p_L d_M \sigma)_1 = (pd\sigma)$  and  $(p_L d_M \pi)_1 = (pd\pi)$ , with subscripts  $L$  for ligand and  $M$  for metal. “NB” denotes non-bonding. The last column gives the degeneracy ( $D$ ) of the molecular levels

IR	Energy	Type	$D$
$a_{1g}$	$\epsilon^\pm(a_{1g}) = \frac{1}{2}(\epsilon_s(M) - \epsilon'_p) \pm \sqrt{\left[\frac{1}{2}(\epsilon_s(M) - \epsilon'_p)\right]^2 + 6(s_M p_L \sigma)_1^2}$ $\epsilon'_p = \epsilon_p + 2[(p_L p_L \pi)_2 - (p_L p_L \sigma)_2] - (p_L p_L \sigma)_3$	Sigma	1
$e_g$	$\epsilon^\pm(e_g) = \frac{1}{2}(\epsilon_d + \epsilon''_p) \pm \sqrt{\left[\frac{1}{2}(\epsilon_d - \epsilon''_p)\right]^2 + 3(pd\sigma)^2}$ $\epsilon''_p = \epsilon_p + (p_L p_L \sigma)_2 - (p_L p_L \pi)_2 + (p_L p_L \sigma)_3$	Sigma	2
$t_{1g}$	$\epsilon(t_{1g}) = \epsilon_p + (p_L p_L \sigma)_2 - (p_L p_L \pi)_2 - (p_L p_L \sigma)_3$	NB	3
$t_{2g}$	$\epsilon^\pm(t_{2g}) = \frac{1}{2}(\epsilon_d + \epsilon'_p) \pm \sqrt{\left[\frac{1}{2}(\epsilon_d - \epsilon'_p)\right]^2 + 4(pd\pi)^2}$ $\epsilon'_p = \epsilon_p + (p_L p_L \pi)_2 - (p_L p_L \sigma)_2 - (p_L p_L \pi)_3$	Pi	3
$t_{1u}$	$\begin{vmatrix} \epsilon_d - \epsilon & \sqrt{2}(p_M p_L \pi)_1 & \sqrt{2}(p_M p_L \sigma)_1 \\ \sqrt{2}(p_M p_L \pi)_1 & \epsilon'_p - \epsilon & [(\sigma)_2 + (\pi)_2]/\sqrt{2} \\ \sqrt{2}(p_M p_L \sigma)_1 & [(\sigma)_2 + (\pi)_2]/\sqrt{2} & \epsilon''_p - \epsilon \end{vmatrix} = 0$ $\epsilon'_p = \epsilon_p + 2(p_L p_L \pi)_2 + (p_L p_L \pi)_3$ $\epsilon''_p = \epsilon_p + (p_L p_L \sigma)_3$ $[(\sigma)_2 + (\pi)_2] = (p_M p_L \sigma)_2 + (p_M p_L \pi)_2$	Pi and sigma	3
$t_{2u}$	$\epsilon(t_{2u}) = \epsilon_p - 2(p_L p_L \pi)_2 + (p_L p_L \pi)_3$	NB	3

three electrons outside of the closed molecular shells to be distributed among the three  $2t_{2g}$  states.

Let us label the three  $2t_{2g}$  molecular eigenstates as “ $a$ ”, “ $b$ ”, and “ $c$ ”, where “ $a$ ” is the row-1 eigenstate, “ $b$ ” is the row-2 eigenstate, and “ $c$ ” is the row-3 eigenstate. There are 10 independent spatial determinantal states that can be formed with three electrons distributed among the three eigenstates. They are

$$(\text{group I}) \quad \langle abc|, \quad (8.14)$$

$$(\text{group II}) \quad \langle aaa|, \langle bbb|, \langle ccc|, \quad (8.15)$$

$$(\text{group III}) \quad \langle aab|, \langle aac|, \langle bba|, \langle bbc|, \langle cca|, \langle ccb|. \quad (8.16)$$

(Permutations of  $a$ ,  $b$ , and  $c$  do not produce a new state; they simply produce the same or the negative of the same determinant.) The group II states are forbidden by the Pauli exclusion principle. Therefore we are left with seven independent

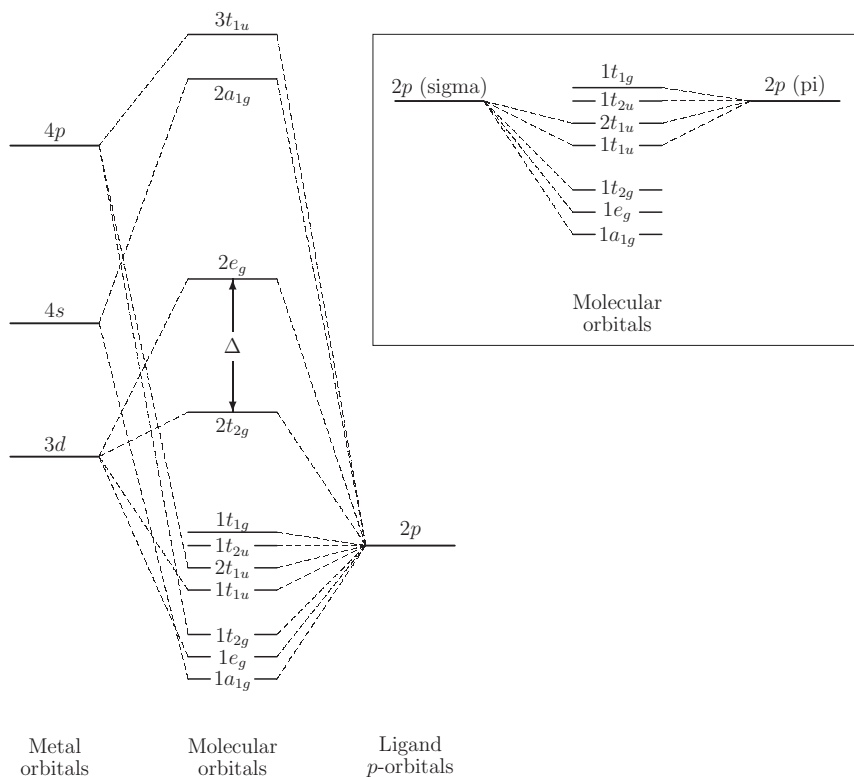


Figure 8.2 Molecular-orbital energy levels. Typical ordering of molecular levels for a transition metal ion surrounded by an octahedron of ligands such as  $[\text{CrF}_6]^{3-}$  or  $[\text{TiF}_6]^{3-}$ . The energy difference between the  $2t_{2g}$  and  $2e_g$  levels (labeled  $\Delta$ ) is the molecular-orbital equivalent of  $10Dq$  in crystal-field theory. The inset shows how the ligand  $p$ -sigma and  $p$ -pi orbitals are correlated with the molecular bonding levels. Note that the  $t_{1u}$  levels include both the sigma and the pi ligand orbitals.

determinantal states. Our task is to find the linear combinations of these states that are basis functions for the IRs of the  $O_h$  group.

The molecular state “a” must transform under the group operations exactly as the function  $d_{xy}$ . Similarly, “b” must transform as  $d_{xz}$  and “c” as  $d_{yz}$ .

The group I state is the only determinant that allows all of the spins to be parallel. The lowest energy state, according to Hund’s rules, is the determinantal state,  $\langle a \uparrow b \uparrow c \uparrow | = \langle abc | \alpha_1 \alpha_2 \alpha_3$ . This state has  $S = 3/2$  (also  $S_z = 3/2$ ), and is therefore a spin quartet. Using the action table, we can determine the characters of the product  $abc$ . Since  $abc$  must transform as  $(xy)(xz)(yz)$ , we have

$$P(E) abc \Rightarrow P(E) (xy)(xz)(yz) = (xy)(xz)(yz) \Rightarrow abc, \quad (8.17)$$

$$P(C_3^1) abc \Rightarrow P(C_3^1) (xy)(xz)(yz) = (-yz)(xy)(-xz) \Rightarrow abc, \quad (8.18)$$

$$P(C_2^1) abc \Rightarrow P(C_2^1) (xy)(xz)(yz) = (-xy)(-xz)(yz) \Rightarrow abc, \quad (8.19)$$

$$P(\bar{C}_2^1) abc \Rightarrow P(\bar{C}_2^1) (xy)(xz)(yz) = (-xz)(-xy)(yz) \Rightarrow abc, \quad (8.20)$$

$$P(\bar{C}_4^1) abc \Rightarrow P(\bar{C}_4^1) (xy)(xz)(yz) = (-xz)(xy)(-yz) \Rightarrow abc, \quad (8.21)$$

and  $\chi(E) = \chi(C_3) = \chi(C_2) = \chi(\bar{C}_2) = \chi(\bar{C}_4) = 1$ .

The arrows in Eqs. (8.17)–(8.21) indicate symmetry-equivalent functions. From the characters we conclude that  $abc$  belongs to the  $a_{1g}$  representation. From the above information we see that the ground state of  $[\text{CrF}_6]^{3-}$  is, according to Hund's rules,  $^4A_{1g}$ . The other spin states,  $S_z = 1/2, -1/2$ , and  $-3/2$ , can be obtained in the usual way by operating with the spin-lowering operator. For example,

$$\begin{aligned} S^- \langle abc | \alpha_1 \alpha_2 \alpha_3 \\ = \langle abc | \frac{1}{\sqrt{3}} \{ \beta_1 \alpha_2 \alpha_3 + \beta_2 \alpha_1 \alpha_3 + \beta_3 \alpha_1 \alpha_2 \} \quad \left( S_z = \frac{1}{2} \right), \end{aligned} \quad (8.22)$$

$$\begin{aligned} S^- \langle abc | \{ \beta_1 \alpha_2 \alpha_3 + \beta_2 \alpha_1 \alpha_3 + \beta_3 \alpha_1 \alpha_2 \} \\ = \langle abc | \frac{1}{\sqrt{3}} \{ \alpha_1 \beta_2 \beta_3 + \alpha_2 \beta_1 \beta_3 + \alpha_3 \beta_1 \beta_3 \} \quad \left( S_z = -\frac{1}{2} \right), \end{aligned} \quad (8.23)$$

$$S^- \langle abc | \frac{1}{\sqrt{3}} \{ \alpha_1 \beta_2 \beta_3 + \alpha_2 \beta_1 \beta_3 + \alpha_3 \beta_1 \beta_3 \} = \langle abc | \{ \beta_1 \beta_2 \beta_3 \} \quad \left( S_z = -\frac{3}{2} \right). \quad (8.24)$$

The molecular-orbital states of the other IRs (terms) can be obtained using the symmetry-function-generating machine. These calculations are simple, but can be tedious.

Let us consider the functions from group III. The six symmetry-equivalent functions  $\langle aab|$ ,  $\langle ccb|$ ,  $\langle bba|$ ,  $\langle bbc|$ ,  $\langle cca|$ , and  $\langle ccb|$  are all “g” functions. Under the operations of the group,  $aab$  must transform as  $(xy)(xy)(xz)$ ,  $ccb$  must transform as  $(yz)(yz)(xz)$ , and so forth. From the action table we find, for example,

$$P(C_3^1) |aab\rangle \Rightarrow P(C_3^1) (xy)(xy)(xz) = (-yz)(-yz)(xy) \Rightarrow \langle cca|,$$

where the arrows indicate symmetry-equivalent functions. Table 8.7 summarizes the results for all of the operations of the group acting on  $\langle aab|$ .

If we apply the symmetry-function-generating machine, (8.5), to the results in Table 8.7, using the matrix elements for  $T_1$  in Appendix E, we find that

$$f_1^{(t_1)} \propto \sum_R D_{11}^{t_1}(R)^* P_R \langle aab| = 0, \quad (8.25)$$

$$f_2^{(t_1)} \propto \sum_R D_{22}^{t_1}(R)^* P_R \langle aab| = 4\langle aab| - 4\langle ccb|, \quad (8.26)$$

$$f_3^{(t_1)} \propto \sum_R D_{33}^{t_1}(R)^* P_R \langle aab| = 0. \quad (8.27)$$

Table 8.7 Results of operating on  $\langle aab|$  with the operations of the  $O_h$  group

$E$ $\langle aab $	$C_3^{(1)}$ $\langle cca $	$C_3^{(1)^2}$ $-\langle bbc $	$C_3^{(2)}$ $\langle bbc $	$C_3^{(2)^2}$ $-\langle cca $	$C_3^{(3)}$ $-\langle cca $	$C_3^{(3)^2}$ $-\langle bbc $	$C_3^{(4)}$ $\langle bbc $
$C_3^{(4)^2}$ $\langle cca $	$C_2^{(1)}$ $-\langle abb $	$C_2^{(2)}$ $\langle abb $	$C_2^{(3)}$ $-\langle aab $	$\bar{C}_2^{(1)}$ $-\langle bba $	$\bar{C}_2^{(2)}$ $\langle bba $	$C_2^{(3)}$ $\langle ccb $	$C_2^{(4)}$ $\langle ccb $
$\bar{C}_2^{(5)}$ $\langle aac $	$\bar{C}_2^{(6)}$ $-\langle aac $	$C_4^{(1)}$ $\langle bba $	$C_4^{(1)^3}$ $-\langle bba $	$C_4^{(2)}$ $-\langle ccb $	$C_4^{(2)^3}$ $-\langle ccb $	$C_4^{(3)}$ $-\langle aac $	$C_4^{(3)^3}$ $\langle aac $

Thus, we can conclude that the function  $[\langle aab| - \langle ccb|]$  transforms according to the second row of the  $t_{1g}$  IR of  $O_h$ . Similar calculations show that the three  $t_{1g}$  (normalized) functions are

$$t_{1g}(\text{row 1}) = \frac{1}{\sqrt{2}} [\langle aac| - \langle bbc|], \quad (8.28)$$

$$t_{1g}(\text{row 2}) = \frac{1}{\sqrt{2}} [\langle aab| - \langle ccb|], \quad (8.29)$$

$$t_{1g}(\text{row 3}) = \frac{1}{\sqrt{2}} [\langle bba| - \langle cca|]. \quad (8.30)$$

Since each of the functions has one doubly occupied orbital, it follows that  $S = 1/2$ . Thus we see that the molecular state is  $^2T_{1g}$ . Including spin, the determinantal states are

$$t_{1g}(\text{row 1}) = \frac{1}{\sqrt{2}} [\langle (a\alpha)(a\beta)(c\alpha)| - \langle (b\alpha)(b\beta)(c\alpha)|], \quad (8.31)$$

$$t_{1g}(\text{row 2}) = \frac{1}{\sqrt{2}} [\langle (a\alpha)(a\beta)(b\alpha)| - \langle (c\alpha)(c\beta)(b\alpha)|], \quad (8.32)$$

$$t_{1g}(\text{row 3}) = \frac{1}{\sqrt{2}} [\langle (b\alpha)(b\beta)(a\alpha)| - \langle (c\alpha)(c\beta)(a\alpha)|]. \quad (8.33)$$

A similar calculation using the diagonal matrix elements of the  $T_{2g}$  IR gives the determinantal states

$$t_{2g}(\text{row 1}) = \frac{1}{\sqrt{2}} [\langle (b\alpha)(b\beta)(a\alpha)| + \langle (c\alpha)(c\beta)(a\alpha)|], \quad (8.34)$$

$$t_{2g}(\text{row 2}) = \frac{1}{\sqrt{2}} [\langle (a\alpha)(a\beta)(b\alpha)| + \langle (c\alpha)(c\beta)(b\alpha)|], \quad (8.35)$$

$$t_{2g}(\text{row 3}) = \frac{1}{\sqrt{2}} [\langle (a\alpha)(a\beta)(c\alpha)| + \langle (b\alpha)(b\beta)(c\alpha)|]. \quad (8.36)$$

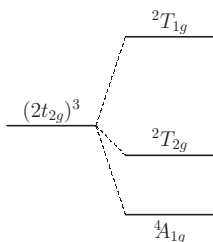


Figure 8.3 Molecular terms for three electrons in  $2t_{2g}$  orbitals. The ground state is  $^4A_{1g}$  according to Hund's rules.

Figure 8.3 shows schematically the (total) molecular states arising from three electrons in the three  $2t_{2g}$  level. The ordering of the states is not determined by group theory.

There are many ways to form excited states. For example, we could assign two electrons to the  $2t_{2g}$  and one to the  $2e_g$ . States of this type, considering only the metal orbitals, were discussed in Chapter 3.

The molecular eigenstates are linear combinations of metal and ligand orbitals, and, for Löwdin orbitals, are of the form

$$\Psi = \frac{1}{\sqrt{N}} \left\{ \sum_i a_i(M) \phi_i(M) + \sum_j b_j(L) \phi_j(L) \right\}, \quad (8.37)$$

$$N = \sum_i a_i^2 + \sum_j b_j^2, \quad (8.38)$$

where  $a_i$  and  $b_j$  are the amplitudes for the metal and ligand orbitals, respectively, and  $\sqrt{N}$  is the normalization factor. In a very approximate way,  $\Psi$  distributes the electron's charge between the metal and ligand ions,

$$q(M) = \frac{e}{N} \sum_i a_i^2, \quad (8.39)$$

$$q(L) = \frac{e}{N} \sum_j b_j^2, \quad (8.40)$$

where  $q(M)$  is the charge residing in metal orbitals and  $q(L)$  is the charge residing on ligand orbitals. Generally, the bonding and non-bonding eigenstates have more charge in the ligand orbitals than in the metal orbitals,  $q(L) > q(M)$ . For the antibonding eigenstates the converse is true,  $q(M) > q(L)$ .

Therefore, an electronic transition from a bonding or non-bonding eigenstate to an antibonding eigenstate has the effect of moving some charge from the ligands to the metal ion. It is also possible for transitions to transfer charge from the metal ion to the ligands. These types of transitions are called “charge-transfer” transitions.

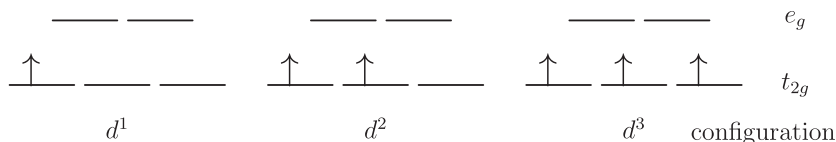
An example of an  $L \Rightarrow M$  charge transfer is  $1t_{1g} \Rightarrow 2t_{2g} + \text{"}u\text{" vibration}$  (see Fig. 8.2). The  $1t_{1g}$  states are non-bonding, so for the initial state there is little charge residing in the metal orbitals. The final state is an antibonding state, and therefore most of the charge resides in metal orbitals.

### 8.1.2 High- and low-spin states

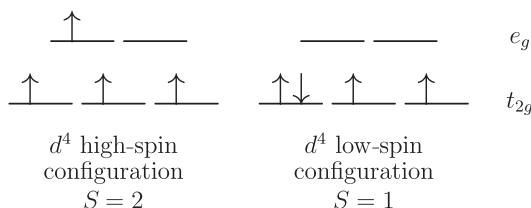
For transition metal molecules or complexes the highest occupied levels are usually partially filled  $t_{2g}$  and/or  $e_g$   $d$ -electron antibonding levels. The magnetic properties of a complex are dependent upon the electron occupation of these  $d$ -electron states. If the net spin is non-zero, the complex is paramagnetic, whereas if the net spin is zero it is diamagnetic.

In the simple model that neglects spin-orbit interactions there are two principal energies to be considered. The first is the "pairing energy",  $P$ . The repulsion between two electrons is less for parallel spins than for antiparallel spins due to the exchange energy. Also the repulsion between electrons occupying the same orbital is greater than the repulsion between electrons occupying different orbitals. The pairing energy is a measure of the extra energy required for electrons with paired spins ( $\uparrow\downarrow$ ) compared with the case of electrons with unpaired spins ( $\uparrow\uparrow$ ) or ( $\downarrow\downarrow$ ). The second important energy,  $\Delta$ , is the splitting of the  $e_g$  and  $t_{2g}$  levels.

For complexes with three or fewer electrons in  $d$ -levels, Hund's rules require that the electron be assigned to the  $t_2$  states with parallel spins. These configurations are indicated below:



For four  $d$ -electrons the lowest energy state depends upon whether  $\Delta$  is greater than  $P$  or less than  $P$ . If  $P > \Delta$ , it is energetically favorable to place the fourth electron in the  $e_g$  level with its spin up. However, if  $P < \Delta$ , the fourth electron will occupy one of the three  $t_{2g}$  levels with spin down. These two cases are shown below:





The “high-spin configuration” results when the pairing energy is greater than the  $e_g - t_{2g}$  splitting. When the number of  $d$ -electrons lies between four and seven there will be a high- or low-spin configuration for  $P > \Delta$  or  $P < \Delta$ , respectively. For five  $d$ -electrons the high-spin configuration has  $S = 5/2$ , and the low-spin configuration has  $S = 1/2$ . For six  $d$ -electrons,  $S = 2$  and  $S = 0$ ; and for seven  $d$ -electrons,  $S = 3/2$  and  $S = 1/2$ . For 8, 9, and 10  $d$ -electrons the spin of the lowest energy state is the same for  $P > \Delta$  and  $P < \Delta$ , since the  $t_{2g}$  levels are fully occupied by electron pairs.

The pairing energy is in the range 12,000–25,000  $\text{cm}^{-1}$ , and  $\Delta$  is in the range 6,000–30,000  $\text{cm}^{-1}$ . Therefore, these two energies are comparable, and which is larger depends upon the transition metal ion and the ligands of the complex. As an example,  $\text{Fe}^{3+}$  has five  $d$ -electrons. The complex  $[\text{Fe}(\text{NO}_2)]^{3-}$  has  $\Delta > P$ , and exists as a low-spin complex with  $S = 1/2$ . However,  $\text{Fe}^{3+}$  in  $[\text{Fe}(\text{Br})]^{3-}$  is in a high-spin configuration with  $S = 5/2$ .

Some examples of transition metal ions with high/low-spin states are given below:

Configuration	Ion	$S$ high spin	$S$ low spin
$d^4$	$\text{Cr}^{2+}$	2	1
$d^5$	$\text{Fe}^{3+}$	$\frac{5}{2}$	$\frac{1}{2}$
$d^6$	$\text{Fe}^{2+}$	2	0
$d^7$	$\text{Co}^{2+}$	$\frac{3}{2}$	$\frac{1}{2}$
$d^8$	$\text{Ni}^{2+}$	1	—

## 8.2 A tetrahedral complex

The geometry and coordinate system for a tetrahedral molecular complex is shown in Fig. 8.4 for the molecular complex  $ML_4$  (inscribed in a cube), where  $M$  is the metal ion and  $L$  is a ligand. The metal ion is at the center surrounded by four ligands. The group of covering operations is  $T_d$ . The tetrahedron does not have a center of inversion, and therefore the “ $g$ ” and “ $u$ ” designations are inapplicable.

### 8.2.1 Elements of $T_d$

The  $T_d$  group and its IRs are discussed in detail in Appendix F. It consists of the 24 operations, namely rotations and reflections, that leave a tetrahedron unchanged. For visual purposes it is useful to show the tetrahedron inscribed within a cube as shown in Fig. 8.4. The symmetry elements in addition to the identity are listed below.

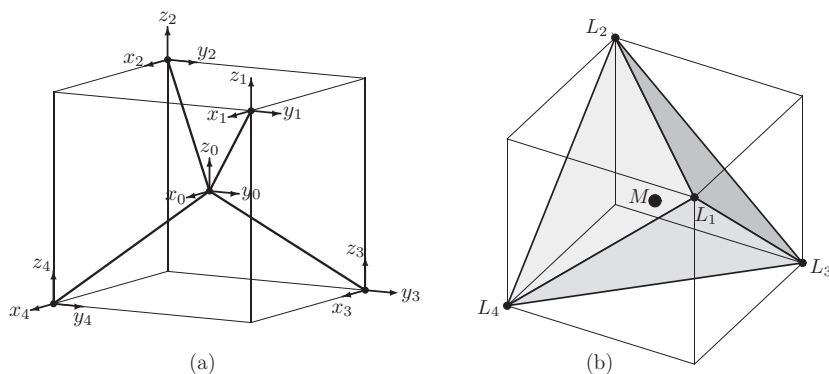


Figure 8.4 A tetrahedral molecular complex consisting of five atoms. (a) The coordinate system. (b) The tetrahedron for  $ML_4$ , where  $M$  is the metal ion and  $L$  represents a ligand. The ligands are labeled 1 through 4, and the  $M$  ion is at the center of the tetrahedron.

- (1)  $C_3$ . Four three-fold axes: 120- and 240-degree, clockwise rotations about the cube body diagonals.
- (2)  $C_2$ . Three two-fold axes: 180-degree, clockwise rotations about the  $x$ -,  $y$ -, and  $z$ -axes.
- (3)  $\sigma_d$ . Six reflections. The reflection planes are defined by a pair of parallel face diagonals on opposite sides of the circumscribed cube.
- (4)  $S_4$ . Six improper rotations: Clockwise rotations by 90 degrees and 270 degrees about one of the three  $C_2$  axes ( $x$ -,  $y$ -, and  $z$ -axes through the center atom), followed by a reflection in the plane perpendicular to the axis of rotation.

The symmetry axes and reflection planes are shown in Appendix F, in Fig. F.1.

### 8.2.2 Symmetry functions for the $ML_4$ complex

We consider a complex,  $ML_4$ , that has  $s$ -,  $p$ -, and  $d$ -orbitals on the metal ( $M$ ) ion, and  $s$ - and  $p$ -orbitals on each of the four equivalent ligands ( $L_4$ ). We have in mind here a transition metal ion with  $3d$ ,  $4p$ , and  $4s$  orbitals interacting with ligands that have  $2s$  and  $2p$  or  $3s$  and  $3p$  valence orbitals. To analyze the electronic states of the  $ML_4$  complex, our first task is to determine the number and types of IRs contained in the orbital representation. To do this we make use of the character table, Table 8.8, and the action table, Table 8.9. The representation for the tetrahedral complex,  $\Gamma^C$ , using the  $s(M)$ ,  $p(M)$ ,  $d(M)$ ,  $s(L)$ , and  $p(L)$  orbitals, may be written as

$$\Gamma^C = \Gamma^{d(M)} + \Gamma^{s(M)} + \Gamma^{s(L)} + \Gamma^{p(M)} + \Gamma^{p(L)}. \quad (8.41)$$

Table 8.8 *The character table for the  $T_d$  group. Basis functions are listed in order of rows. Note the order for  $T_2$ .*

	$A_1$	1	1	1	1	1
	$A_2$	1	1	1	-1	-1
$(x^2 - y^2, 3z^2 - r^2)$	$\mathcal{E}$	2	-1	2	0	0
$[x(z^2 - y^2), y(z^2 - x^2), z(x^2 - y^2)]$	$T_1$	3	0	-1	-1	1
$(x, y, z); (yz, xz, xy)$	$T_2$	3	0	-1	1	-1
$s$ -orbitals on metal ion	$\Gamma^{s(M)}$	1	1	1	1	1
$s$ -orbitals on ligands	$\Gamma^{s(L)}$	4	1	0	2	0
$p$ -orbitals on metal ion	$\Gamma^{p(M)}$	3	0	-1	1	-1
$p$ -orbitals on ligands	$\Gamma^{p(L)}$	12	0	0	2	0
$d$ -orbitals on metal ion	$\Gamma^{d(M)}$	5	-1	1	1	-1
all orbitals on molecule	$\Gamma^C$	25	1	1	7	-1

We can find the characters for each of the orbital representations on the right-hand side of (8.41). The representations may then be decomposed into the IRs of  $T_d$  using the character table (Table 8.8). We find

$$\Gamma^{d(M)} = e + t_2, \quad (8.42)$$

$$\Gamma^{s(M)} = a_1, \quad (8.43)$$

$$\Gamma^{s(L)} = a_1 + t_2, \quad (8.44)$$

$$\Gamma^{p(M)} = t_2, \quad (8.45)$$

$$\Gamma^{p(L)} = a_1 + e + t_1 + 2t_2, \quad (8.46)$$

$$\Gamma^C = 3a_1 + 2e + t_1 + 5t_2. \quad (8.47)$$

Analysis of (8.47) yields some useful information. The  $d(M)$  orbitals belong to the  $e$  and  $t_2$  IRs. Therefore we can conclude that there are in total five triply degenerate  $t_2$  states (15 states) and two doubly degenerate  $e$  states (4 states) that could possibly form bonding and antibonding states with metal  $d$ -orbitals. The three states derived from the  $a_1$  IRs form bonding and antibonding states with the metal  $s$ -orbital. The  $t_1$  states are non-bonding, and, since  $t_1$  occurs only once in (8.47), the three  $t_1$  symmetry functions are also the eigenstates. The secular equation for the complex is a  $25 \times 25$  matrix that will block-diagonalize into

- one  $3 \times 3$  matrix for the  $a_1$  states,
- two  $2 \times 2$  matrices for the  $e$  states,
- three  $1 \times 1$  matrices for the  $t_1$  states,
- three  $5 \times 5$  matrices for the  $t_2$  states.

Table 8.9 The action table for an  $ML_4$  complex with  $T_d$  symmetry. The first row gives the symmetry elements. The first column lists the functions and ligand numbers. The other rows give the result of operating on the function with the symmetry operation at the top of the column.

$E$	$C_3^1$	$C_3^{1^2}$	$C_2^3$	$C_2^{2^2}$	$C_3^3$	$C_3^{3^2}$	$C_4^3$	$C_4^{3^2}$	$C_2^1$	$C_2^2$	$C_2^3$	$\sigma_d^1$	$\sigma_d^2$	$\sigma_d^3$	$\sigma_d^4$	$\sigma_d^5$	$\sigma_d^6$	$S_4^1$	$S_4^{1^3}$	$S_4^2$	$S_4^{2^3}$	$S_4^3$	$S_4^{3^3}$
$X$	$Z$	$Y$	$-Z$	$Y$	$Z$	$-Y$	$-Z$	$-Y$	$X$	$-X$	$-X$	$X$	$X$	$-Z$	$Z$	$Y$	$-Y$	$-X$	$-X$	$Z$	$-Z$	$-Y$	$Y$
$Y$	$X$	$Z$	$X$	$-Z$	$-X$	$-Z$	$-X$	$Z$	$-Y$	$Y$	$-Y$	$Z$	$-Z$	$Y$	$Y$	$X$	$-X$	$-Z$	$Z$	$-Y$	$-Y$	$X$	$-X$
$Z$	$Y$	$X$	$-Y$	$-X$	$-Y$	$X$	$Y$	$-X$	$-Z$	$-Z$	$Z$	$Y$	$-Y$	$-X$	$X$	$Z$	$Z$	$Y$	$-Y$	$-X$	$X$	$-Z$	$-Z$
1	1	1	4	3	2	4	3	2	4	3	2	1	4	3	1	1	2	3	2	2	4	4	3
2	3	4	2	2	4	1	1	3	3	4	1	3	2	2	4	2	1	1	4	3	1	3	4
3	4	2	1	4	3	3	2	1	2	1	4	2	3	1	3	4	3	4	1	4	2	1	2
4	2	3	3	1	1	2	4	4	1	2	3	4	1	4	2	3	4	2	3	1	3	2	1
$XY$	$XZ$	$YZ$	$-XZ$	$-YZ$	$-XZ$	$YZ$	$XZ$	$YZ$	$-XY$	$-XY$	$XY$	$XZ$	$-XZ$	$-YZ$	$YZ$	$XY$	$XY$	$XZ$	$-XZ$	$-YZ$	$YZ$	$-XY$	$-XY$
$XZ$	$YZ$	$XY$	$YZ$	$-XY$	$-YZ$	$-XY$	$YZ$	$XY$	$-XZ$	$XZ$	$-XZ$	$XY$	$-XY$	$XZ$	$XZ$	$YZ$	$-YZ$	$-XY$	$XY$	$-XZ$	$-XZ$	$YZ$	$-YZ$
$YZ$	$XY$	$XZ$	$-XY$	$XZ$	$XY$	$-XZ$	$-XY$	$-XZ$	$YZ$	$-YZ$	$-YZ$	$YZ$	$YZ$	$-XY$	$XY$	$XZ$	$-XZ$	$-YZ$	$-YZ$	$XY$	$-XY$	$-XZ$	$XZ$
$\frac{X^2-Y^2}{2} = a$	$-\frac{1}{2}a - \frac{\sqrt{3}}{2}b$	$-\frac{1}{2}a + \frac{\sqrt{3}}{2}b$	$-\frac{1}{2}a + \frac{\sqrt{3}}{2}b$	$-\frac{1}{2}a - \frac{\sqrt{3}}{2}b$	$-\frac{1}{2}a + \frac{\sqrt{3}}{2}b$	$-\frac{1}{2}a - \frac{\sqrt{3}}{2}b$	$-\frac{1}{2}a + \frac{\sqrt{3}}{2}b$	$-\frac{1}{2}a - \frac{\sqrt{3}}{2}b$	$a$	$a$	$a$	$\frac{1}{2}a - \frac{\sqrt{3}}{2}b$	$\frac{1}{2}a - \frac{\sqrt{3}}{2}b$	$\frac{1}{2}a + \frac{\sqrt{3}}{2}b$	$\frac{1}{2}a + \frac{\sqrt{3}}{2}b$	$-a$	$-a$	$\frac{1}{2}a - \frac{\sqrt{3}}{2}b$	$\frac{1}{2}a - \frac{\sqrt{3}}{2}b$	$\frac{1}{2}a + \frac{\sqrt{3}}{2}b$	$\frac{1}{2}a + \frac{\sqrt{3}}{2}b$	$-a$	$-a$
$\frac{3Z^2-Y^2}{2\sqrt{3}} = b$	$-\frac{1}{2}b + \frac{\sqrt{3}}{2}a$	$-\frac{1}{2}b - \frac{\sqrt{3}}{2}a$	$-\frac{1}{2}b - \frac{\sqrt{3}}{2}a$	$-\frac{1}{2}b + \frac{\sqrt{3}}{2}a$	$-\frac{1}{2}b - \frac{\sqrt{3}}{2}a$	$-\frac{1}{2}b + \frac{\sqrt{3}}{2}a$	$-\frac{1}{2}b - \frac{\sqrt{3}}{2}a$	$-\frac{1}{2}b + \frac{\sqrt{3}}{2}a$	$b$	$b$	$b$	$-\frac{1}{2}b - \frac{\sqrt{3}}{2}a$	$-\frac{1}{2}b - \frac{\sqrt{3}}{2}a$	$-\frac{1}{2}b + \frac{\sqrt{3}}{2}a$	$-\frac{1}{2}b + \frac{\sqrt{3}}{2}a$	$b$	$b$	$-\frac{1}{2}b - \frac{\sqrt{3}}{2}a$	$-\frac{1}{2}b - \frac{\sqrt{3}}{2}a$	$-\frac{1}{2}b + \frac{\sqrt{3}}{2}a$	$-\frac{1}{2}b + \frac{\sqrt{3}}{2}a$	$b$	$b$

Table 8.10 Symmetry functions for the tetrahedral complex  $ML_4$ . Here  $x_i$ ,  $y_i$ , and  $z_i$  are  $p_x$ ,  $p_y$ , and  $p_z$  orbitals centered on the  $i$ th ligand site. Metal ( $M$ ) orbitals are centered at the origin.

IR	Row	Orbital	Symmetry function	Bonding
$a_1$		$s(M)$	$s(M)$	Sigma
		$s(L)$	$(s_1 + s_2 + s_3 + s_4)/2$	
		$p(L)$	$(x_1 + y_1 + z_1 - x_2 - y_2 + z_2 - x_3 + y_3 - z_3 + x_4 - y_4 - z_4)/\sqrt{12}$	
$e$	1	$d(M)$	$d_{x^2}(M)$	Pi
	2		$d_{z^2}(M)$	
	1	$p(L)$	$(x_1 - y_1 - x_2 + y_2 - x_3 - y_3 + x_4 + y_4)/\sqrt{8}$	
	2		$(x_1 + y_1 - 2z_1 - x_2 - y_2 - 2z_2 - x_3 + y_3 - 2z_3 + x_4 - y_4 + 2z_4)/\sqrt{24}$	
$t_1$	1	$p(L)$	$(x_1 - z_1 + x_2 + z_2 - x_3 + z_3 - x_4 - z_4)/\sqrt{8}$	NB
	2		$(y_1 - z_1 + y_2 + z_2 - y_3 - z_3 - y_4 + z_4)/\sqrt{8}$	
	3		$(x_1 - y_1 - x_2 + y_2 + x_3 + y_3 - x_4 - y_4)/\sqrt{8}$	
$t_2$	1	$p(M)$	$p_x(M)$	Sigma   Pi + Sigma   Pi + Sigma
	2		$p_y(M)$	
	3		$p_z(M)$	
	1	$d(M)$	$d_{yz}(M)$	
	2		$d_{xz}(M)$	
	3		$d_{xy}(M)$	
	1	$s(L)_1$	$(s_1 - s_2 - s_3 + s_4)/2$	
	2	$s(L)_2$	$(s_1 - s_2 + s_3 - s_4)/2$	
	3	$s(L)_3$	$(s_1 + s_2 - s_3 - s_4)/2$	
	1	$p(L)_{1a}$	$(x_1 + x_2 + x_3 + x_4)/2$	
	2	$p(L)_{2a}$	$(y_1 + y_2 + y_3 + y_4)/2$	
	3	$p(L)_{3a}$	$(z_1 + z_2 + z_3 + z_4)/2$	
	1	$p(L)_{1b}$	$(y_1 + z_1 + y_2 - z_2 - y_3 + z_3 - y_4 - z_4)/\sqrt{8}$	
	2	$p(L)_{2b}$	$(x_1 + z_1 + x_2 - z_2 - x_3 - z_3 - x_4 + z_4)/\sqrt{8}$	
	3	$p(L)_{3b}$	$(x_1 + y_1 - x_2 - y_2 + x_3 - y_3 - x_4 + y_4)/\sqrt{8}$	

Equation (8.5) can be used to find the required symmetry functions. The results are given in Table 8.10.

### 8.2.3 $t_2$ symmetry functions

The symmetry functions listed in Table 8.10 are not unique when a representation is contained more than once in the decomposition. The symmetry function generated by the generating machine depends upon the choice of the “arbitrary” function.

Consider the  $a_1$  ligand functions generated by the arbitrarily chosen functions  $x_1(p_{x1}(L))$  and  $s_1(L)$ , respectively. If we had chosen  $s_1(L) \pm x_1$  as the generating function, we would have obtained the symmetry functions  $f^+(a_1)$  and  $f^-(a_1)$ ,

$$f^\pm(a_1) = (s_1 + s_2 + s_3 + s_4) \pm (x_1 + y_1 + z_1 - x_2 - y_2 + z_2 - x_3 + y_3 - z_3 + x_4 - y_4 - z_4). \quad (8.48)$$

The combinations of the  $p$ -orbitals of  $f^\pm(a_1)$  are aligned parallel or antiparallel to the metal–ligand intra-atomic axes. When these are combined with the  $s$ -orbitals, “ $sp^3$ ” hybrid orbitals are obtained, as shown schematically in Fig. 8.5.

Functions oriented along the internuclear axes are often called sigma symmetry functions. For the tetrahedron these functions do have sigma overlap with the  $t_2$  metal  $s$ -orbitals but not with the  $t_2$  metal  $p$  and  $d$  symmetry functions. The LCAO interactions between the  $p$  (or  $sp^3$ ) functions and the  $p$  and  $d$  metal functions of  $t_2$  involve both sigma and pi bonding. Regardless of what linear combinations are taken for the symmetry functions, the eigenvectors and eigenvalues obtained from the secular equations are the same. The hybrid orbitals are conceptually useful, but there is no particular mathematical advantage to choosing axes aligned along and perpendicular to the internuclear axes. The formation of hybrid orbital combinations occurs automatically when the secular equation is diagonalized. That is, the eigenvectors will contain the appropriate linear combinations of symmetry functions.

### 8.2.4 Eigenvalues for a tetrahedral complex

The LCAO interactions for the tetrahedral complex are different from those of the octahedral complex. For example, in the octahedral case the metal orbitals  $d_{xy}$ ,  $d_{xz}$ , and  $d_{yz}$  form pi bonds, while the metal orbitals  $d_{x^2}$  and  $d_{z^2}$  form sigma bonds

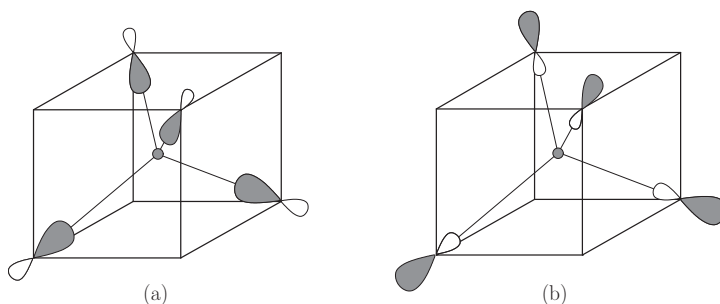


Figure 8.5 The  $sp^3$  hybrid orbitals. (a)  $f^-(a_1)$ , bonding hybrid orbitals. (b)  $f^+(a_1)$ , antibonding hybrid orbitals.

with the  $p$ -orbitals of the ligands. For the tetrahedral complex  $d_{xy}$ ,  $d_{xz}$ , and  $d_{yz}$  form both sigma and pi metal–ligand bonds, while the  $d_{z^2}$  and  $d_{x^2}$  orbitals form only pi metal–ligand bonds. Also, if we choose  $x$ ,  $y$ , and  $z$  as the basis functions for the first, second, and third rows of the  $t_2$  IR, then the  $d_{yz}$  orbital is a first-row function. The  $d$ -orbitals  $d_{xz}$  and  $d_{xy}$  are second- and third-row symmetry functions, respectively. The  $d$ -orbitals split into the  $e$  and  $t_2$  groups as in the octahedral case; however, for the tetrahedron the  $e$  level lies lower in energy than the  $t_2$  level. This is explained by noting that the lobes of the  $d_{xy}$ ,  $d_{xz}$ , and  $d_{yz}$  are directed more toward the ligands than the lobes of  $d_{x^2}$  and  $d_{z^2}$ , resulting in greater electrostatic repulsion.

The eigenvalues and eigenvectors for the various molecular levels can be found in terms of the LCAO two-center interactions and overlap integrals. The  $t_1$  and  $e$  eigenvalues can easily be obtained; however, the remaining levels require solution of  $3 \times 3$  and  $5 \times 5$  secular equations.

As an example we shall find the LCAO eigenvalues for the  $e$  states using Löwdin orbitals. We need only find the energy for the row-1 functions. The eigenvalues of the row-2 functions are the same. The following definitions are used:

$$\epsilon_d = \int dr d_{x^2}^* \mathbb{H} d_{x^2} = \int dr d_{z^2}^* \mathbb{H} d_{z^2}, \quad (8.49)$$

$$\epsilon_p = \int dr p_k^* \mathbb{H} p_k \quad (k = x, y, \text{ and } z), \quad (8.50)$$

$$\begin{aligned} \epsilon_{p_L} = \int dr \frac{1}{\sqrt{8}} (x_1 - y_1 - x_2 + y_2 - x_3 - y_3 + x_4 + y_4)^* \\ \times \mathbb{H} \frac{1}{\sqrt{8}} (x_1 - y_1 - x_2 + y_2 - x_3 - y_3 + x_4 + y_4), \end{aligned} \quad (8.51)$$

$$M_{12} = \int dr d_{x^2}^* \mathbb{H} \frac{1}{\sqrt{8}} (x_1 - y_1 - x_2 + y_2 - x_3 - y_3 + x_4 + y_4) = M_{21}. \quad (8.52)$$

We can evaluate  $\epsilon_{p_L}$  and  $M_{12}$  in terms of the LCAO parameters. Consider the first term of (8.51),

$$\begin{aligned} & \frac{1}{8} \int dr x_1 \mathbb{H} (x_1 - y_1 - x_2 + y_2 - x_3 - y_3 + x_4 + y_4) \\ &= \frac{1}{8} \left[ \epsilon_p - H_{x_1, x_2} - H_{x_1, x_3} + H_{x_1, x_4} - H_{x_1, y_1} + H_{x_1, y_2} - H_{x_1, y_3} + H_{x_1, y_4} \right]. \end{aligned} \quad (8.53)$$

From Table 8.5 we have

$$H_{x,x} = l^2(pp\sigma) + (1 - l^2)(pp\pi) \quad (8.54)$$

and

$$H_{x,y} = lm(pp\sigma) - lm(pp\pi), \quad (8.55)$$

where  $l$  and  $m$  are the direction cosines for the vector joining the two ligand sites. For our tetrahedron,

	$l^2$	$m^2$	$lm$
$\mathbf{R}_{12}$	1/2	1/2	1/2
$\mathbf{R}_{13}$	1/2	0	0
$\mathbf{R}_{14}$	0	1/2	0

where  $\mathbf{R}_{ij}$  is the vector joining ligand sites  $i$  and  $j$ . Using these results in (8.49) and (8.50) gives

$$H_{x_1,x_2} = H_{x_1,x_3} = \frac{1}{2}[(pp\sigma) + (pp\pi)], \quad (8.56)$$

$$H_{x_1,x_4} = (pp\pi), \quad (8.57)$$

$$H_{x_1,y_1} = H_{x_1,y_3} = H_{x_1,y_4} = 0, \quad (8.58)$$

$$H_{x_1,y_2} = \frac{1}{2}[(pp\sigma) - (pp\pi)], \quad (8.59)$$

$$\begin{aligned} & \frac{1}{8}[\epsilon_p - H_{x_1,x_2} - H_{x_1,x_3} + H_{x_1,x_4} + H_{x_1,y_1} + H_{x_1,y_2} - H_{x_1,y_3} + H_{x_1,y_4}] \\ &= \frac{1}{8} \left\{ \epsilon_p - \frac{1}{2}[(pp\sigma) + (pp\pi)] \right\}. \end{aligned} \quad (8.60)$$

All of the other terms of the product in (8.51) yield the same result, so

$$\epsilon_{pL} = \epsilon_p - \frac{1}{2}[(pp\sigma) + (pp\pi)]. \quad (8.61)$$

For  $M_{12}$  we have

$$\begin{aligned} & \int dr d_{x_2}^* \mathbb{H} \frac{1}{\sqrt{8}}(x_1 - y_1 - x_2 + y_2 - x_3 - y_3 + x_4 + y_4) \\ &= H_{x^2,x_1} - H_{x^2,y_1} - H_{x^2,x_2} + H_{x^2,y_2} - H_{x^2,x_3} - H_{x^2,y_3} + H_{x^2,x_4} + H_{x^2,y_4}. \end{aligned} \quad (8.62)$$

The direction cosines for the vectors from the metal ion to the ligands are

	$l$	$m$	$n$
$\mathbf{R}_{01}$	$1/\sqrt{3}$	$1/\sqrt{3}$	$1/\sqrt{3}$
$\mathbf{R}_{02}$	$-1/\sqrt{3}$	$-1/\sqrt{3}$	$1/\sqrt{3}$
$\mathbf{R}_{03}$	$-1/\sqrt{3}$	$1/\sqrt{3}$	$-1/\sqrt{3}$
$\mathbf{R}_{04}$	$1/\sqrt{3}$	$-1/\sqrt{3}$	$-1/\sqrt{3}$



where  $\mathbf{R}_{0i}$  is the vector from the metal ion to the  $i$ th  $p$ -ligand site.

From Table 8.5 we have

$$H_{x^2, x} = \frac{\sqrt{3}}{2} l(l^2 - m^2)(pd\sigma) + l(1 - l^2 + m^2)(pd\pi) = l(pd\pi), \quad (8.63)$$

$$H_{x^2, y} = \frac{\sqrt{3}}{2} l(l^2 - m^2)(pd\sigma) - m(1 + l^2 - m^2)(pd\pi) = -m(pd\pi), \quad (8.64)$$

$$H_{x^2, x_1} = H_{x^2, y_2} = H_{x^2, y_4} = H_{x^2, x_4} = \frac{1}{\sqrt{3}}(pd\pi), \quad (8.65)$$

$$H_{x^2, x_2} = H_{x^2, x_3} = H_{x^2, y_3} = H_{x^2, y_1} = -\frac{1}{\sqrt{3}}(pd\pi). \quad (8.66)$$

Using these results we find that

$$M_{12} = \sqrt{\frac{8}{3}}(pd\pi). \quad (8.67)$$

The eigenvalues of the  $e$  states are determined by the condition that

$$\det \begin{pmatrix} \epsilon_d - \epsilon & \sqrt{\frac{8}{3}}(pd\pi) \\ \sqrt{\frac{8}{3}}(pd\pi) & \epsilon_{pL} - \epsilon \end{pmatrix} = 0, \quad (8.68)$$

where  $\epsilon_{pL} = \epsilon_p - \frac{1}{2}[(pp\sigma) + (pp\pi)]$ .

The eigenvalues are

$$\epsilon(e)^\pm = \frac{1}{2}(\epsilon_d + \epsilon_{pL}) \pm \sqrt{\left[\frac{1}{2}(\epsilon_d - \epsilon_{pL})\right]^2 + \frac{8}{3}(pd\pi)^2}. \quad (8.69)$$

The “+” sign goes with the antibonding  $e$  state and the “−” sign with the bonding  $e$  state.

Figure 8.6 shows a schematic representation of the molecular energy levels for the tetrahedral complex. The ordering of the levels depends upon the particular  $ML_4$  complex. The ordering shown is approximately what is expected for the first transition series with oxygen or chlorine ligands. For tetrahedral oxide anions such as  $\text{TiO}_4^-$ ,  $\text{VO}_4^{3-}$ ,  $\text{CrO}_4^{2-}$ ,  $\text{MnO}_4^-$ , and  $\text{FeO}_4$  the ordering of the lower levels has been suggested to be [8.2]  $1a_1$ ,  $1t_2$ ,  $1e$ ,  $2t_2$ ,  $1t_1$ ,  $3t_2$ ,  $2e$ ,  $4t_2$ ,  $2a_1$ .

### 8.2.5 High- and low-spin states for a tetrahedral complex

As in the case of the octahedral complex high- and low-spin configurations are possible. Assuming that the antibonding  $t_2$  and  $e$  molecular orbitals are partially occupied, the spin configuration depends on the size of the pairing energy,  $P$ , compared with the  $e-t_2$  splitting,  $\Delta_{\text{tet}}$ . The spin configurations appropriate for the tetragonal complex are different from those of the octahedral complex because



For more than six  $d$ -electrons, the spin configuration for the lowest energy states does not depend on the magnitude of  $P$  compared with  $\Delta_{\text{tet}}$ .

### References

- [8.1] J. C. Slater and G. F. Koster, "Simplified LCAO method for the periodic potential problem", *Phys. Rev.* **94**, 1498–1524 (1954).
- [8.2] G. V. Ionova and M. E. Dyatkina, "Molecular orbitals of tetrahedral oxide anions of transition metals communication IV.  $\text{FeO}_4$  molecule", *J. Struct. Chem.* **6**, 764–765 (1966).

### Exercises

- 8.1 Make schematic sketches of the symmetry functions for the  $a_{1g}$ ,  $e_g$ , and  $t_{2g}$  states of an octahedral complex.
- 8.2 Calculate the LCAO matrix elements for the secular equation,  $\det(\mathbb{H} - \epsilon \mathbb{S}) = 0$ , for the  $a_{1g}$  levels for an octahedral complex. Include all three atomic orbitals,  $s(M)$ ,  $s(L)$ , and  $p(L)$ , and overlap integrals. Table 8.5 can also be used to determine the overlap integrals. Take  $H_{s_M s_M} = \epsilon_s(M)$ ,  $H_{s_L s_L} = \epsilon_s(L)$ , and  $H_{xx} = H_{yy} = H_{zz} = \epsilon_p(L)$ .
- 8.3 (a) Calculate the row-1  $t_{1g}$  energy for hydrogen-like orbitals in terms of LCAO parameters including the overlap.  
(b) Show that the energy calculated using Löwdin orbitals is equal to the energy calculated using hydrogen-like orbitals.
- 8.4 Consider an octahedral complex with 38 electrons. Assign the electrons to the levels in Fig. 8.2.  
(a) What is the configuration for the lowest energy state according to Hund's rules?  
(b) What is the symmetry symbol for the total molecular ground state?
- 8.5 (a) For the molecular state in Exercise 8.4, what is the lowest-energy electric-dipole transition where the final state is  $2t_{2g}$  (according to Fig. 8.2)?  
(b) Would it be correct to call the transition in (a) a charge-transfer transition?  
(c) Show that the excited molecular state with  $S = 3/2$  is  ${}^4T_{2u}$ .
- 8.6 (a) For an octahedral complex with 8, 9, or 10  $d$ -electrons Hund's ground-state spin configuration (high spin/low spin) does not depend on the ratio  $P/\Delta_{\text{oct}}$ . Explain why.  
(b) For a tetrahedral complex with more than six  $d$ -electrons, Hund's ground-state spin configuration does not depend on the ratio of  $P/\Delta_{\text{tet}}$ . Why do the tetrahedral and octahedral cases differ?

- 8.7 Methane,  $\text{CH}_4$ , is a tetrahedral molecule. Using  $2s$  and  $2p$  orbitals for the C atom and  $1s$  orbitals for the H atoms, do the following:
- Find the IRs of  $T_d$  contained in the orbital representations.
  - Describe the block-diagonalized secular equation: the symmetry, the dimensions of the secular equations, and what orbitals are involved.
  - Find the symmetry functions.
  - What is the electronic configuration of the ground state in terms of the one-electron molecular states? What is the symmetry label for the total molecule ground state?
- 8.8
- Calculate the energies of the molecular levels in terms of the LCAO parameters for the methane molecule in Exercise 8.7, including overlap integrals.
  - Construct a schematic representation of the molecular levels and label them according to their IRs. Assume  $\epsilon_{2s} < \epsilon_{1s} < \epsilon_{2p}$  and that  $\text{CH}_4$  is diamagnetic.
  - What is the symmetry symbol for the ground state of the molecule?
  - Photoelectron spectroscopy shows ionization of electrons corresponding to 14 eV and 23 eV. How would you interpret these results?
- 8.9 Using the action table and the matrix elements of the  $t_2$  IR for the  $T_d$ , show that  $d_{yz}$  (not  $d_{xy}$ ) is a row-1 basis function for the  $t_2$  IR.
- 8.10 For an octahedral complex, Hund's ground state for  $(t_2)^3$  has  $S = 3/2$  and each of the  $t_2$   $d$ -orbitals is singly occupied. The determinantal state is  $\langle d_{xy}\uparrow d_{xz}\uparrow d_{yz}\uparrow |$ . Show that the product  $d_{xy}d_{xz}d_{yz}$  transforms as  $a_1$  (i.e., is invariant under all of the operations of the group).

## 9

# Space groups and crystalline solids

### 9.1 Definitions

A **crystal** or **crystalline solid** is an ordered array of atoms, molecules, or ions whose pattern or lattice is repeated periodically. A “single crystal” is perfectly ordered. Most crystalline solids are polycrystalline, meaning that they are composed of many small single crystals with defective, bounding surfaces between them. Large single crystals occur in nature, but often it is necessary to prepare them by special crystal-growth methods in laboratories. Single crystals are the preferred form for studying the intrinsic properties of a crystalline material.

Theoretical analysis of single-crystal properties usually assumes the crystalline structure is infinite or imposes periodic boundary conditions requiring the wavefunction to repeat itself after a sufficiently large number of chemical units. This is a reasonable approximation, since a cubic-centimeter crystal contains on the order of  $10^{22}$  to  $10^{24}$  repeated units.

To sharpen our description of a lattice some definitions are useful.

- **Bravais lattice.** A Bravais lattice is a space-filling array of points generated by three *primitive* lattice vectors, **a**, **b**, and **c**. The vectors of the infinite set of vectors  $\{\mathbf{R}(l, m, n)\}$  terminate on the Bravais lattice points. These vectors are  $\mathbf{R}(l, m, n) = l\mathbf{a} + m\mathbf{b} + n\mathbf{c}$ , where  $l$ ,  $m$ , and  $n$  are positive or negative integers or zero. Instead of the vectors **a**, **b**, and **c**, a Bravais lattice can be specified by the magnitudes of the primitive vectors,  $a = |\mathbf{a}|$ ,  $b = |\mathbf{b}|$ , and  $c = |\mathbf{c}|$ , and the angles between them,  $\alpha$ ,  $\beta$ , and  $\gamma$ . Here  $\alpha$  is the angle between **a** and **c**,  $\beta$  is the angle between **b** and **c**, and  $\gamma$  is the angle between **a** and **b**. The numbers  $a$ ,  $b$ , and  $c$  are called the lattice constants. The 14 distinct Bravais lattices are shown in Fig. 9.1.
- **Unit cell.** The parallelepiped defined by the vectors **a**, **b**, and **c** containing a formula unit (basis) of the material is called the unit cell. The volume of the unit cell is  $V = \mathbf{a} \cdot (\mathbf{b} \times \mathbf{c})$ . The atoms or molecules of a crystal may be located

Crystal systems

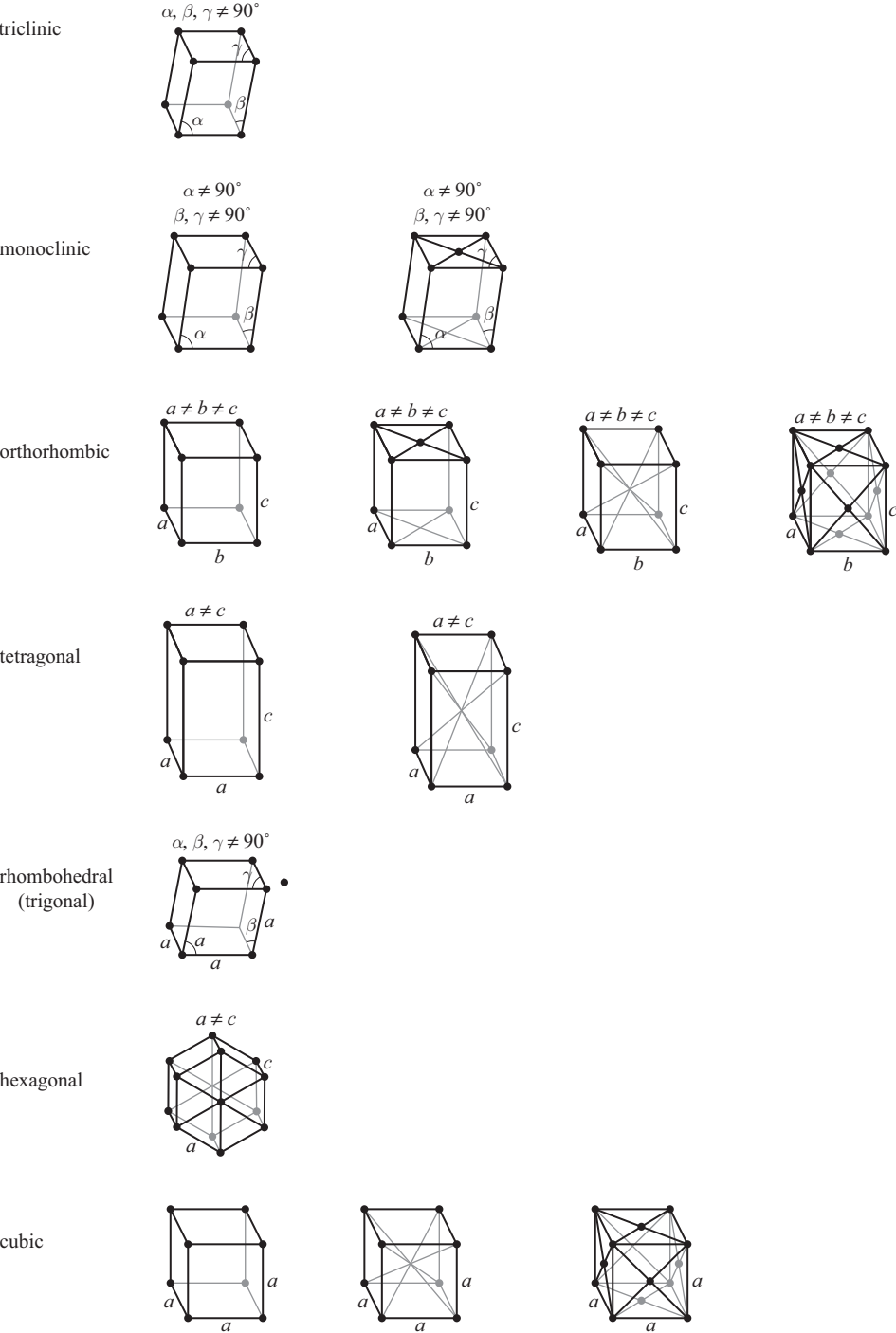


Figure 9.1 The 14 distinct Bravais lattices.

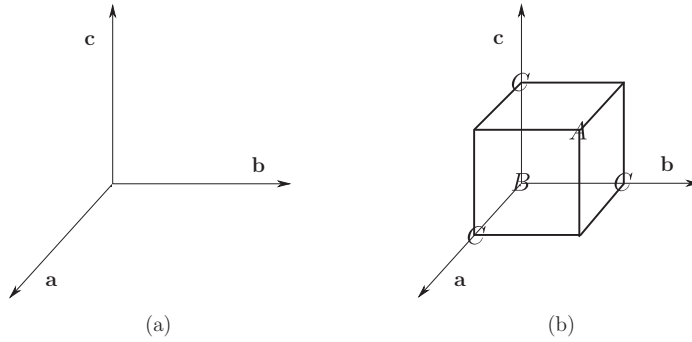


Figure 9.2 (a) Cubic Bravais-lattice primitive vectors.  $a = b = c$ ;  $\alpha = \beta = \gamma = 90$  degrees. (b) The unit cell with ions for the  $ABC_3$  cubic perovskite structure. The  $B$  ion is at  $(0, 0, 0)$ , the  $C$  ions are located at  $(a/2, 0, 0)$ ,  $(0, a/2, 0)$ ,  $(0, 0, a/2)$ , and the  $A$  ion is at  $(a/2, a/2, a/2)$ , where  $a$  is the lattice spacing. Translation of the unit cell by the set of vectors  $\{\mathbf{R}(l, m, n)\}$  leads to the perovskite structure with  $B$  atoms at  $a(l, m, n)$ ,  $C$  atoms at  $a(l + 1/2, m, n)$ ,  $a(l, m + 1/2, n)$ , and  $a(l, m, n + 1/2)$ , and  $A$  atoms at  $a(l + 1/2, m + 1/2, n + 1/2)$ .

anywhere on or within the unit cell, but are located at the same relative positions in every unit cell of the crystal. The chemical composition of the material is represented by the atoms belonging to a unit cell. For example, the unit cell of an  $ABC_3$  crystal ( $\text{SrTiO}_3$  for example) contains one  $A$  atom, one  $B$  atom, and three  $C$  atoms as shown in Fig. 9.2.

- **Translational invariance.** A Bravais lattice is invariant under a translation by any of the vectors  $\{\mathbf{R}(l, m, n)\}$ . The smallest non-zero translations under which the lattice is invariant are the primitive vectors  $\mathbf{a}$ ,  $\mathbf{b}$ , and  $\mathbf{c}$ . The infinite, single-crystalline solid is invariant under the same set of translations as its Bravais lattice.

Before launching into a formal discussion of space groups it is worthwhile to look at a couple of very simple examples of wave solutions in a crystal. We consider a two-dimensional square lattice with orthogonal Löwdin  $s$ -orbitals,  $\Phi[\mathbf{r} - \mathbf{R}(m, n)]$ , on the Bravais lattice points with lattice vectors  $a\mathbf{e}_x$  and  $a\mathbf{e}_y$ , as shown in Fig. 9.3. The LCAO wavefunction for the electron states is

$$\psi(r) = \sum_{m,n} A_{mn} \Phi[\mathbf{r} - \mathbf{R}(m, n)], \quad (9.1)$$

with

$$\int \Phi[\mathbf{r} - \mathbf{R}(m, n)]^* \Phi[\mathbf{r} - \mathbf{R}(m', n')] d\mathbf{r} = \delta_{mm'} \delta_{nn'}, \quad (9.2)$$

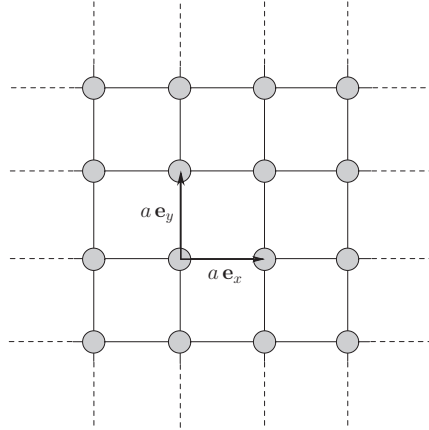


Figure 9.3 The square Bravais lattice with  $s$ -orbitals on each lattice point. The nearest-neighbor LCAO interaction parameter is  $(ss\sigma)$ .

where  $\Phi[\mathbf{r} - \mathbf{R}(m, n)]$  is a Löwdin  $s$ -orbital located at the lattice point  $\mathbf{R}(m, n) = a(m\mathbf{e}_x + n\mathbf{e}_y)$  and  $A_{mn}$  is the amplitude of the orbital at that site. We want to find the solutions to the eigenvalue equation

$$\mathbb{H} \psi(\mathbf{r}) = E \psi(\mathbf{r}). \quad (9.3)$$

For simplicity assume only nearest-neighbor atoms interact. Substitute (9.1) into (9.3), multiply both sides of the equation by  $\Phi[\mathbf{r} - \mathbf{R}(m', n')]^*$ , and integrate over  $\mathbf{r}$ . This procedure leads to an eigenvalue matrix equation,

$$\sum_{m', n'} \{(\epsilon - E)\delta_{mm'} \delta_{nn'} + (ss\sigma)\delta_{m\pm 1, m'}\delta_{nn'} + (ss\sigma)\delta_{mm'}\delta_{m, n\pm 1}\} A_{m'n'} = 0, \quad (9.4)$$

where

$$\epsilon = \int \Phi[\mathbf{r} - \mathbf{R}(m, n)]^* \mathbb{H} \Phi[\mathbf{r} - \mathbf{R}(m, n)] d\mathbf{r}, \quad (9.5)$$

$$\begin{aligned} (ss\sigma) &= \int \Phi[\mathbf{r} - \mathbf{R}(m, n)]^* \mathbb{H} \Phi[\mathbf{r} - \mathbf{R}(m \pm 1, n)] d\mathbf{r} \\ &= \int \Phi[\mathbf{r} - \mathbf{R}(m, n)]^* \mathbb{H} \Phi[\mathbf{r} - \mathbf{R}(m, n \pm 1)] d\mathbf{r}. \end{aligned} \quad (9.6)$$

To obtain solutions to (9.4), we write

$$A_{mn} = A(\mathbf{k})e^{i\mathbf{k} \cdot \mathbf{R}(m, n)}, \quad (9.7)$$



where  $\mathbf{k} = k_x \mathbf{e}_x + k_y \mathbf{e}_y$  and  $A(\mathbf{k})$  is a constant for fixed  $\mathbf{k}$ . Substitution of (9.7) into (9.4) gives

$$\left\{ (\epsilon - E_{\mathbf{k}}) + 2(ss\sigma)[\cos(k_x a) + \cos(k_y a)] \right\} A(\mathbf{k}) = 0. \quad (9.8)$$

If  $A(\mathbf{k})$  is not zero, the eigenenergy is

$$E_{\mathbf{k}} = \epsilon + 2(ss\sigma)[\cos(k_x a) + \cos(k_y a)]. \quad (9.9)$$

As the  $\mathbf{k}$ -vector varies,  $E_{\mathbf{k}}$  describes a band of energies that lie between  $\epsilon - 4(ss\sigma)$  and  $\epsilon + 4(ss\sigma)$ . For this reason, a graph of  $E_{\mathbf{k}}$  versus  $\mathbf{k}$  is called an *energy band*.

The energy of a particular state is determined by the  $\mathbf{k}$ -vector. Therefore we shall write the solutions of (9.3) as  $\psi_{\mathbf{k}}(\mathbf{r})$ .

Since  $\cos(k_x a)$  and  $\cos(k_y a)$  are periodic functions, the energy of  $\psi_{\mathbf{k}}(\mathbf{r})$  is the same as the energies of the states  $\psi_{(\mathbf{k}+\mathbf{K})}(\mathbf{r})$ , where

$$\mathbf{K}a = 2\pi(s\mathbf{e}_x + t\mathbf{e}_y) \quad (s, t = 0, \text{ or any positive or negative integer}). \quad (9.10)$$

Therefore we can restrict  $k_x a$  and  $k_y a$  to the ranges

$$0 \leq k_x \leq \frac{2\pi}{a} \quad \text{and} \quad 0 \leq k_y \leq \frac{2\pi}{a}. \quad (9.11)$$

A different, but equivalent, choice is

$$-\pi \leq k_x a \leq \pi \quad \text{and} \quad -\pi \leq k_y a \leq \pi. \quad (9.12)$$

For our two-dimensional square Bravais lattice, the area described by (9.12) is the *first Brillouin zone* and the  $\mathbf{K}$ -vectors of (9.10) are *reciprocal-lattice vectors*. A general description of the reciprocal-lattice vectors and the first Brillouin zone for any Bravais lattice is given later in this chapter.

There are some features of  $E_{\mathbf{k}}$  worth mentioning. If  $\alpha$  is an operation that leaves the Bravais lattice invariant, then  $E_{\mathbf{k}} = E_{\alpha\mathbf{k}}$ . For our example above, a counter-clockwise rotation  $\alpha = \pi/2$  applied to the  $\mathbf{k}$ -vector takes  $k_x \rightarrow k_y$  and  $k_y \rightarrow -k_x$ , so that  $E_{\alpha\mathbf{k}} = \epsilon + 2(ss\sigma)[\cos(k_y a) + \cos(-k_x a)] = E_{\mathbf{k}}$ . Similarly, a reflection,  $\sigma$ , through the  $x$ -axis takes  $k_x \rightarrow k_x$  and  $k_y \rightarrow -k_y$ , and  $E_{\sigma\mathbf{k}} = E_{\mathbf{k}}$ . In general, every operation,  $R$ , that leaves the Bravais lattice invariant produces a new wavevector,  $\mathbf{k}' = R\mathbf{k}$ , such that  $E_{R\mathbf{k}} = E_{\mathbf{k}}$ . In addition, because of the periodic nature of  $\psi_{\mathbf{k}}$ ,  $E_{\mathbf{k}} = E_{\mathbf{k}+\mathbf{K}}$ , where  $\mathbf{K}$  is any reciprocal-lattice vector.

In the case that there are  $n$  different atomic orbitals associated with each lattice point, there will be  $n$  different energy bands. When there are several atoms in the unit cell, the number of energy bands that result is equal to the total number of atomic orbitals associated with all of the atoms of the unit cell. If we denote these energy bands as  $E_{n\mathbf{k}}$ , where  $n$  indexes the various bands, then each  $E_{n\mathbf{k}}$  possesses the properties discussed in the previous paragraph:  $E_{n\mathbf{k}} = E_{n\alpha\mathbf{k}}$  and

$E_{n(\mathbf{k}+\mathbf{K})} = E_{n\mathbf{k}}$ . To illuminate this feature, for the model just discussed, let us assign two orbitals to each lattice point. For simplicity, suppose there is a  $1s$  and a  $2s$  orbital on each site, and again assume nearest-neighbor interactions. In this case the LCAO wavefunction is a linear combination of both  $1s$  and  $2s$  orbitals,

$$\psi(\mathbf{r}) = \sum_{m,n} \{A_{mn} \Phi_{1s}[\mathbf{r} - \mathbf{R}(m, n)] + B_{mn} \Phi_{2s}[\mathbf{r} - \mathbf{R}(m, n)]\}, \quad (9.13)$$

where  $A_{mn}$  is the amplitude of the  $1s$  orbital and  $B_{mn}$  is the amplitude of the  $2s$  orbital at  $\mathbf{R}(m, n)$ . The LCAO parameters involved are  $\epsilon_1, \epsilon_2, (s_1s_1\sigma), (s_1s_2\sigma)$ , and  $(s_2s_2\sigma)$ . The subscripts “1” and “2” refer to the  $1s$  and  $2s$  orbitals, respectively. Proceeding as before, we take

$$A_{mn} = A(\mathbf{k})e^{i\mathbf{k}\cdot\mathbf{R}(m,n)}, \quad (9.14)$$

$$B_{mn} = B(\mathbf{k})e^{i\mathbf{k}\cdot\mathbf{R}(m,n)}, \quad (9.15)$$

and obtain a  $2 \times 2$  matrix eigenvalue equation,

$$\begin{pmatrix} \epsilon_1 + 2(s_1s_1\sigma)C(\mathbf{k}) - E_{\mathbf{k}} & 2(s_1s_2\sigma)C(\mathbf{k}) \\ 2(s_1s_2\sigma)C(\mathbf{k}) & \epsilon_2 + 2(s_2s_2\sigma)C(\mathbf{k}) - E_{\mathbf{k}} \end{pmatrix} \begin{pmatrix} A(\mathbf{k}) \\ B(\mathbf{k}) \end{pmatrix} = 0, \quad (9.16)$$

where  $C(\mathbf{k}) = \cos(k_x a) + \cos(k_y a)$ , and  $\epsilon_1$  and  $\epsilon_2$  are the diagonal matrix elements of the Hamiltonian for the  $1s$  and  $2s$  orbitals, respectively.

There are two orbitals per unit cell and two energy bands,

$$E_{\mathbf{k}}^{\pm} = \frac{1}{2} \{ \epsilon_1 + \epsilon_2 + 2[(s_1s_1\sigma) + (s_2s_2\sigma)]C(\mathbf{k}) \} \pm \sqrt{\left\{ \frac{1}{2} [\epsilon_1 - \epsilon_2 + 2[(s_1s_1\sigma) - (s_2s_2\sigma)]C(\mathbf{k})] \right\}^2 + 4(s_1s_2\sigma)^2 C(\mathbf{k})^2}. \quad (9.17)$$

Each of these energy bands satisfies the conditions that  $E_{\mathbf{k}}^{\pm} = E_{\mathbf{k}+\mathbf{K}}^{\pm}$  and  $E_{\mathbf{k}}^{\pm} = E_{\alpha\mathbf{k}}^{\pm}$ , where  $\mathbf{K}$  is a reciprocal-lattice vector and  $\alpha\mathbf{k} = P_{\alpha-1}\mathbf{k}$ .

The properties of the eigenfunctions and eigenvalues derived above for the square lattice with nearest-neighbor interactions are true in general for any lattice and any Hamiltonian with a periodic potential, irrespective of the range of the interactions. The proof lies in the mathematics of space groups.

## 9.2 Space groups

An infinite single crystal is an array of repeated unit cells. The covering group of the Bravais lattice is a space group,  $G$ . The elements of  $G$  consist of combinations

of point-group elements (rotations, reflections, inversions) and translations under which an infinite, single-crystal structure is invariant. Alternately, we can consider a finite crystal subject to periodic boundary conditions that require the physical functions to repeat after a significantly large number of translations. After the analysis is complete we may then let the large number of translations tend to infinity. In either case the electronic Hamiltonian of a crystal must also be invariant under any of the operations of the space group.

The convention is to write a space-group symmetry element in the form

$$\{\alpha|\mathbf{T}\}, \quad (9.18)$$

where  $\alpha$  is a point-group element (rotation, reflection, or inversion) performed on the coordinate system with one point (the origin) fixed and  $\mathbf{T}$  is a translation vector. A point-group element is  $\{\alpha|0\}$  and a pure translation is  $\{E|\mathbf{T}\}$ , where  $E$  is the identity. A space-group operation applied to a vector  $\mathbf{r}$  is a rotation, reflection, or inversion followed by a translation,

$$\{\alpha|\mathbf{T}\}\mathbf{r} = \alpha\mathbf{r} + \mathbf{T}, \quad (9.19)$$

where on the right-hand side of (9.19)  $\alpha\mathbf{r}$  represents a rotation of the coordinate system and  $\mathbf{T}$  is a translation of the origin of coordinates. In some instances,  $\mathbf{T}$  *need not* be a translation by a lattice vector, as will be explained shortly. Group multiplication of elements is defined as

$$\{\alpha|\mathbf{T}_1\}\{\beta|\mathbf{T}_2\} = \{\alpha\beta|\alpha\mathbf{T}_2 + \mathbf{T}_1\}. \quad (9.20)$$

To constitute a space group the elements must meet the same requirements as those imposed on point groups, namely the following.

- The product of any two elements in the space group is an element of the space group.
- There is an identity element,  $\{E|0\}$ , in the space group.
- Every element,  $\{\alpha|\mathbf{T}_1\}$ , in the space group has an inverse,  $\{\alpha|\mathbf{T}_1\}^{-1}$ , such that  $\{\alpha|\mathbf{T}_1\}\{\alpha|\mathbf{T}_1\}^{-1} = \{\alpha|\mathbf{T}_1\}^{-1}\{\alpha|\mathbf{T}_1\} = \{E|0\}$ .

From the definition of multiplication (9.20) it follows that

$$\{\alpha|\mathbf{T}\}^{-1} = \{\alpha^{-1}|\alpha^{-1}\mathbf{T}\}, \quad (9.21)$$

since

$$\{\alpha|\mathbf{T}\}^{-1}\{\alpha|\mathbf{T}\} = \{\alpha^{-1}|\alpha^{-1}\mathbf{T}\}\{\alpha|\mathbf{T}\} = \{\alpha^{-1}\alpha|\alpha^{-1}\mathbf{T} - \alpha^{-1}\mathbf{T}\} = \{E|0\} \quad (9.22)$$

and

$$\{\alpha|\mathbf{T}\}\{\alpha|\mathbf{T}\}^{-1} = \{\alpha|\mathbf{T}\}\{\alpha^{-1}| - \alpha^{-1}\mathbf{T}\} = \{\alpha\alpha^{-1}| - \alpha\alpha^{-1}\mathbf{T} + \mathbf{T}\} = \{E|0\}. \quad (9.23)$$

Pure translation elements commute and therefore every element of the translation subgroup is in a class by itself. However, in general space-group operations do not commute. For example,

$$\{\alpha|\mathbf{T}_1\}\{\beta|\mathbf{T}_2\} = \{\alpha\beta|\alpha\mathbf{T}_2 + \mathbf{T}_1\}, \quad (9.24)$$

but

$$\{\beta|\mathbf{T}_2\}\{\alpha|\mathbf{T}_1\} = \{\beta\alpha|\beta\mathbf{T}_1 + \mathbf{T}_2\}. \quad (9.25)$$

For these two products to be the same one requires that  $\{\alpha\beta|\alpha\mathbf{T}_2 + \mathbf{T}_1\} = \{\beta\alpha|\beta\mathbf{T}_1 + \mathbf{T}_2\}$ , a condition that is generally not true.

The space group  $G_s$  contains operations of the form  $\{E|\mathbf{T}\}$ . One might suppose that the translation,  $\mathbf{T}$ , in (9.18) must be one of the Bravais lattice vectors,  $\mathbf{R}(l, m, n)$ ; however, this is not the case. Some crystal space groups possess *compound symmetry elements* that require both a point-group operation and a non-primitive translation. Such elements are not of the form  $\{\alpha|\mathbf{R}(l, m, n)\}$ , where  $\mathbf{R}(l, m, n)$  is a lattice vector. There are two types of such compound symmetry elements, *screw axes* and *glide planes*. As the name implies, a screw axis consists of a rotation about an axis accompanied by non-primitive translation along the same axis. A glide-plane operation consists of a translation parallel to a given plane plus a reflection in the same plane.

We can express a general space-group operation as

$$\{\alpha|\mathbf{T}\} = \{\alpha|\mathbf{R}(l, m, n) + \mathbf{t}_\alpha\}, \quad (9.26)$$

where  $\mathbf{R}(l, m, n)$  is a lattice vector and  $\mathbf{t}_\alpha$  is a translation vector whose magnitude is less than that of a primitive lattice vector. If all of the elements of  $G$  have  $\mathbf{t}_\alpha = 0$ , the space group is *symmorphic* and the set  $\{\alpha|\mathbf{T}\}$  is equal to the set  $\{\alpha|\mathbf{T}\}_{T=0}$ . If any  $\mathbf{t}_\alpha$  is unequal to zero,  $G$  is *non-symmorphic* and the set  $\{\alpha|0\}$  is not the same as  $\{\alpha|\mathbf{T}\}_{T=0}$  (distinct elements obtained by setting  $T = 0$ ). In three dimensions there are 230 distinct space groups, of which 73 are symmorphic.

### 9.3 The reciprocal lattice

The primitive vectors that define the Bravais (direct) lattice, namely  $\mathbf{a}$ ,  $\mathbf{b}$ , and  $\mathbf{c}$ , can be used to construct what is called the *reciprocal* lattice. The primitive vectors for the reciprocal lattice, denoted as  $a^*$ ,  $b^*$ , and  $c^*$ , are defined by

$$\mathbf{a}^* = \frac{2\pi}{V}(\mathbf{b} \times \mathbf{c}), \quad \mathbf{b}^* = \frac{2\pi}{V}(\mathbf{c} \times \mathbf{a}), \quad \mathbf{c}^* = \frac{2\pi}{V}(\mathbf{a} \times \mathbf{b}), \quad (9.27)$$

where  $V = \mathbf{a} \cdot (\mathbf{b} \times \mathbf{c})$  is the volume of the unit cell. The reciprocal lattice is generated from the primitive reciprocal-lattice vectors in the same way as a Bravais lattice is generated from direct-lattice vectors. The vectors in the set of vectors  $\mathbf{K}(s, t, u) = s\mathbf{a}^* + t\mathbf{b}^* + u\mathbf{c}^*$ , where  $s$ ,  $t$ , and  $u$  are zero, positive or negative integers, terminate on the points of the reciprocal lattice. The reciprocal-lattice vectors have the important property that

$$e^{i\mathbf{K}(s,t,u) \cdot \mathbf{R}(l,m,n)} = 1 \quad \text{for all } r, s, t \text{ and all } l, m, n.$$

Thus

$$\begin{aligned} \mathbf{K}(s, t, u) \cdot \mathbf{R}(l, m, n) &= \mathbf{a}^* \cdot \mathbf{a}(sl) + \mathbf{b}^* \cdot \mathbf{b}(tm) + \mathbf{c}^* \cdot \mathbf{c}(un) \\ &= \frac{2\pi}{V}[\mathbf{a} \cdot (\mathbf{b} \times \mathbf{c})](sl + tm + un) \\ &= 2\pi(\text{integer}), \end{aligned} \quad (9.28)$$

and hence

$$e^{i\mathbf{K}(s,t,u) \cdot \mathbf{R}(l,m,n)} = e^{2\pi i(\text{integer})} = 1. \quad (9.29)$$

The reciprocal lattice for a simple-cubic Bravais lattice is also a simple-cubic Bravais lattice. The reciprocal lattice for a face-centered cubic lattice is a body-centered cubic lattice. The reciprocal lattice for a body-centered cubic lattice is a face-centered cubic lattice. Finally, the reciprocal lattice for a simple hexagonal lattice is a simple hexagonal lattice as well, but with a rotation of  $30^\circ$ .

## 9.4 Brillouin zones

Consider a reciprocal lattice and select any lattice point to be the origin. The Brillouin zones are constructed by erecting perpendicular planes<sup>1</sup> that bisect the reciprocal-lattice vectors from the origin to any of the other reciprocal-lattice points. The collection of points that can be connected to the origin without crossing any of the erected planes comprises a volume called the first Brillouin zone. The second Brillouin zone is the volume whose points can be connected to the origin by a line that crosses one and only one of the erected planes. The  $n$ th Brillouin zone is the volume whose points can be connected to the origin by a line that crosses  $n - 1$  and only  $n - 1$  erected planes. The volume in reciprocal-lattice space of each of the Brillouin zones is the same. The construction of the first Brillouin zone for a two-dimensional hexagonal lattice is shown in Fig. 9.4.

<sup>1</sup> Each of these planes is a Bragg plane.

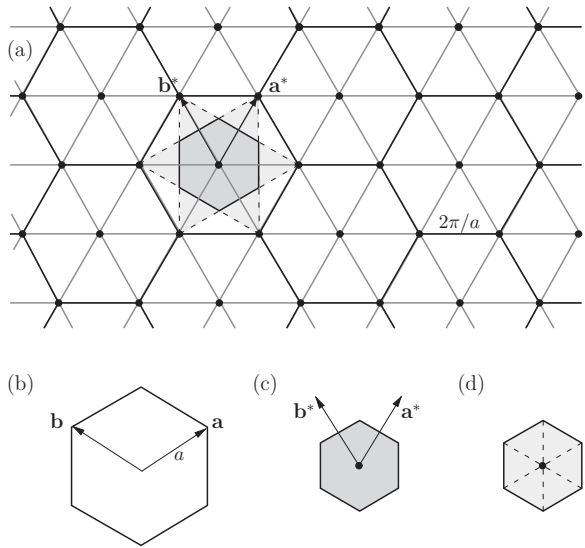


Figure 9.4 (a) A two-dimensional, hexagonal reciprocal lattice. The center hexagon shows the construction of the first Brillouin zone. The dashed lines are the bisectors of the nearest-neighbor reciprocal vectors and the darker shaded area is the first Brillouin zone. The area outside the first Brillouin zone within the six-pointed star formed by the bisectors is the second Brillouin zone (pale shaded). (b) The primitive lattice vectors,  $\mathbf{a}$  and  $\mathbf{b}$ , in direct space. (c) The first Brillouin zone, showing the primitive reciprocal-lattice vectors,  $\mathbf{a}^*$  and  $\mathbf{b}^*$ . (d) Folded second Brillouin zone.

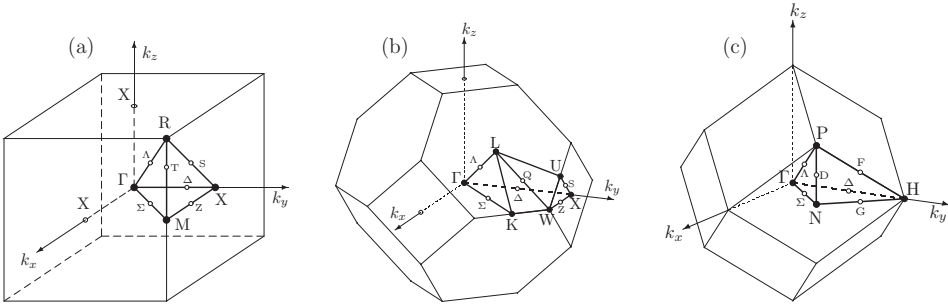


Figure 9.5 Brillouin zones for the (a) simple-cubic, (b) face-centered cubic, and (c) body-centered cubic Bravais lattices. The heavy lines define the irreducible zones (1/48th of the whole), and letters label special symmetry features.

The first Brillouin zones for the simple-cubic, face-centered cubic, and body-centered cubic lattices are illustrated in Fig. 9.5. The letters label special high-symmetry lines and points. A point on the interior of the Brillouin zone with no special symmetry properties is referred to as a *general* point. The primitive direct-lattice and reciprocal-lattice vectors are given in Table 9.1.

Table 9.1 *Direct- and reciprocal-lattice vectors for the simple-cubic, face-centered cubic, body-centered cubic, and hexagonal lattices*

Lattice type	Primitive direct-lattice vectors	Primitive reciprocal-lattice vectors
Simple cubic	$\mathbf{a} = a\mathbf{e}_x$ $\mathbf{b} = a\mathbf{e}_y$ $\mathbf{c} = a\mathbf{e}_z$	$\mathbf{a}^* = (2\pi/a)\mathbf{e}_x$ $\mathbf{b}^* = (2\pi/a)\mathbf{e}_y$ $\mathbf{c}^* = (2\pi/a)\mathbf{e}_z$
Face-centered cubic	$\mathbf{a} = (a/2)(\mathbf{e}_y + \mathbf{e}_z)$ $\mathbf{b} = (a/2)(\mathbf{e}_x + \mathbf{e}_z)$ $\mathbf{c} = (a/2)(\mathbf{e}_x + \mathbf{e}_y)$	$\mathbf{a}^* = (2\pi/a)(-\mathbf{e}_x + \mathbf{e}_y + \mathbf{e}_z)$ $\mathbf{b}^* = (2\pi/a)(\mathbf{e}_x - \mathbf{e}_y + \mathbf{e}_z)$ $\mathbf{c}^* = (2\pi/a)(\mathbf{e}_x + \mathbf{e}_y - \mathbf{e}_z)$
Body-centered cubic	$\mathbf{a} = (a/2)(-\mathbf{e}_x + \mathbf{e}_y + \mathbf{e}_z)$ $\mathbf{b} = (a/2)(\mathbf{e}_x - \mathbf{e}_y + \mathbf{e}_z)$ $\mathbf{c} = (a/2)(\mathbf{e}_x + \mathbf{e}_y - \mathbf{e}_z)$	$\mathbf{a}^* = (2\pi/a)(\mathbf{e}_y + \mathbf{e}_z)$ $\mathbf{b}^* = (2\pi/a)(\mathbf{e}_x + \mathbf{e}_z)$ $\mathbf{c}^* = (2\pi/a)(\mathbf{e}_x + \mathbf{e}_y)$
Hexagonal	$\mathbf{a} = a((\sqrt{3}/2)\mathbf{e}_x + \frac{1}{2}\mathbf{e}_y)$ $\mathbf{b} = a(-(\sqrt{3}/2)\mathbf{e}_x + \frac{1}{2}\mathbf{e}_y)$ $\mathbf{c} = c\mathbf{e}_z$	$\mathbf{a}^* = (2\pi/a)((1/\sqrt{3})\mathbf{e}_x + \mathbf{e}_y)$ $\mathbf{b}^* = (2\pi/a)(-(1/\sqrt{3})\mathbf{e}_x + \mathbf{e}_y)$ $\mathbf{c}^* = (2\pi/c)\mathbf{e}_z$

### 9.5 Bloch waves and symmorphic groups

Until stated otherwise, we shall limit our discussion to symmorphic space groups. For these groups the allowed translations,  $\mathbf{R}(l, m, n)$ , are Bravais-lattice vectors.

The Hamiltonian,  $\mathbb{H}(\mathbf{r})$ , describing electrons or phonons or any wave-like excitation in a crystalline solid must be invariant under a translation  $\mathbf{R}(l, m, n)$ . The quantum eigenvalue equation for a wave excitation is of the form

$$\mathbb{H}(\mathbf{r}) \psi(\mathbf{r}) = \lambda \psi(\mathbf{r}), \quad (9.30)$$

where  $\psi(\mathbf{r})$  is the wavefunction and  $\lambda$  is the eigenvalue. According to Bloch's theorem, Theorem 9.1, the wavefunction is of the form  $\psi_{n\mathbf{k}}(\mathbf{r}) = \exp(i\mathbf{k} \cdot \mathbf{r})u_{n\mathbf{k}}(\mathbf{r})$ , where  $\mathbf{k}$  belongs to the first Brillouin zone. The function  $u_{n\mathbf{k}}(\mathbf{r})$  is periodic,  $u_{n\mathbf{k}}(\mathbf{r} + \mathbf{R}(l, m, n)) = u_{n\mathbf{k}}(\mathbf{r})$ , with  $\mathbf{R}$  any lattice vector. The subscripts  $n$  and  $\mathbf{k}$  characterize the solutions of wavefunctions (label the IRs) for a periodic structure. The meaning of  $n$ , the band index, will be made clear later in this chapter.

**Theorem 9.1** (Bloch waves) *The eigenfunctions of the equation*

$$\mathbb{H}(\mathbf{r}) \psi(\mathbf{r}) = \lambda \psi(\mathbf{r}),$$

where  $\mathbb{H}(\mathbf{r})$  is invariant under translation by any lattice vector, are of the form

$$\psi_{n\mathbf{k}}(\mathbf{r}) = e^{i\mathbf{k} \cdot \mathbf{r}} u_{n\mathbf{k}}(\mathbf{r}), \quad (\text{GT9.1})$$

where  $n$  labels the different bands,  $\mathbf{k}$  is a vector belonging to the first Brillouin zone, and  $u_{n\mathbf{k}}(\mathbf{r})$  is a function with the same translation symmetry (periodicity) as  $\mathbb{H}(\mathbf{r})$  so that  $u_{n\mathbf{k}}(\mathbf{r} + \mathbf{R}(l, m, n)) = u_{n\mathbf{k}}(\mathbf{r})$ , where  $\mathbf{R}$  is any lattice vector.

Bloch's theorem holds for the wave-like eigenfunctions of a Hamiltonian with a periodic potential, including, but not limited to, electrons, phonons, magnons, and electromagnetic waves inside a periodic crystal.

Let  $P_{\{\alpha|\mathbf{R}\}}$  be the operator for the point-group element,  $\alpha$ , and translation,  $\mathbf{R}$ . (For a symmorphic group,  $\mathbf{R}$  is a lattice vector.) Consistently with our convention that  $P$  operates on a function, rather than on the coordinate system, we have that

$$P_{\{\alpha|\mathbf{R}\}}f(\mathbf{r}) = f[\{\alpha|\mathbf{R}\}^{-1}\mathbf{r}] = f(\alpha^{-1}\mathbf{r} - \alpha^{-1}\mathbf{R}) = f[\alpha^{-1}(\mathbf{r} - \mathbf{R})], \quad (9.31)$$

so that for the pure point-group elements

$$P_{\{\alpha|0\}}f(\mathbf{r}) = f(\alpha^{-1}\mathbf{r}), \quad (9.32)$$

a result that is consistent with our definition of the action of the operator for a point-group operation  $\alpha$  as defined in Chapter 3, in Eq. (3.2). For a pure translation, (9.31) gives

$$P_{\{E|\mathbf{R}\}}f(\mathbf{r}) = f(\mathbf{r} - \mathbf{R}). \quad (9.33)$$

However, some texts [9.1] define  $P_{\{E|\mathbf{R}\}}f(\mathbf{r}) = f(\mathbf{r} + \mathbf{R})$ .

We can establish that the Bloch functions,

$$\psi_{n\mathbf{k}}(\mathbf{r}) = \exp(i\mathbf{k} \cdot \mathbf{r})u_{n\mathbf{k}}(\mathbf{r}), \quad (9.34)$$

are basis functions for a diagonal representation of the translation subgroup:

$$\begin{aligned} P_{\{E|\mathbf{R}(l,m,n)\}}\psi_{n\mathbf{k}}(\mathbf{r}) &= e^{i\mathbf{k} \cdot (\mathbf{r} - \mathbf{R}(l,m,n))}u_{n\mathbf{k}}(\mathbf{r} - \mathbf{R}(l,m,n)) \\ &= e^{-i\mathbf{k} \cdot \mathbf{R}(l,m,n)}\psi_{n\mathbf{k}}(\mathbf{r}). \end{aligned} \quad (9.35)$$

Equation (9.35) shows that the operator  $P_{\{E|\mathbf{R}(l,m,n)\}}$  transforms  $\psi_{n\mathbf{k}}(\mathbf{r})$  into a multiple of itself. Therefore the representation matrix is one-dimensional and the character for the operator  $P_{\{E|\mathbf{R}(l,m,n)\}}$  is  $\exp(-i\mathbf{k} \cdot \mathbf{R}(l,m,n))$ .

To understand why the  $\mathbf{k}$ -vector in Bloch's theorem is restricted to the first Brillouin zone, consider a finite cubic crystal with  $N$  unit cells in the three primitive lattice directions. The operator for any lattice translation can be written as the product of three translation operators:

$$P_{\{E|\mathbf{R}(l,m,n)\}} = P_{\{E|\mathbf{R}(l,0,0)\}}P_{\{E|\mathbf{R}(0,m,0)\}}P_{\{E|\mathbf{R}(0,0,n)\}}. \quad (9.36)$$

The set of translations along the  $\mathbf{a}$ -direction,  $\mathbf{R}(l, 0, 0)$  ( $l = 1, 2, 3, \dots, N$ ), forms a subgroup of translations. So do the sets  $\mathbf{R}(0, m, 0)$  ( $m = 1, 2, 3, \dots, N$ ) and



$\mathbf{R}(0, 0, n)$  ( $n = 1, 2, 3, \dots, N$ ). We impose periodic boundary conditions on the system and require that

$$P_{\{E|\mathbf{R}(N,0,0)\}} = P_{\{E|\mathbf{R}(1,0,0)\}}^N = P_{\{E|0\}}, \quad (9.37)$$

$$P_{\{E|\mathbf{R}(0,N,0)\}} = P_{\{E|\mathbf{R}(0,1,0)\}}^N = P_{\{E|0\}}, \quad (9.38)$$

$$P_{\{E|\mathbf{R}(0,0,N)\}} = P_{\{E|\mathbf{R}(0,0,1)\}}^N = P_{\{E|0\}}. \quad (9.39)$$

With these periodic boundary conditions it may be seen that the subgroup with operators  $P_{\{E|\mathbf{R}(l,0,0)\}}$  ( $l = 1, 2, 3, \dots, N$ ) is a cyclic group with period  $N$ , since  $P_{\{E|\mathbf{R}(l,0,0)\}} P_{\{E|\mathbf{R}(l',0,0)\}} = P_{\{E|\mathbf{R}(l+l',0,0)\}}$  and  $P_{\{E|\mathbf{R}(1,0,0)\}}^N = P_{\{E|0\}}$ . The group is also an Abelian group because the translation operations commute with one another. The same is true for the subgroups for translations along the **b**- and **c**-directions.

**Theorem 9.2** (Cyclic groups) *A group, all of whose elements can be generated from a single element,  $g$ , as powers of  $g$  is a cyclic group. A cyclic group of period  $N$  consists of the elements  $(g, g^2, g^3, \dots, g^N)$  with  $g^N = E$ . The element  $g$  is called the generator. Cyclic groups are Abelian, meaning that the elements commute with one another. Because the elements commute, each element is in a class by itself. Therefore there are  $N$  elements,  $N$  classes, and  $N$  irreducible representations.*

*The characters of  $g$  for the IRs of a cyclic group of elements of period  $N$  are the  $N$  roots of unity,  $\exp(iq2\pi/N)$ ,  $q = 1, 2, 3, \dots, N$ . The character of the element,  $g^m$ , for the  $q$ th IR is  $[\exp(2\pi iq/N)]^m$ . There is an IR for each value of  $q$ , so the values of  $q$  can be used as unique labels for the IRs of a cyclic group.*

According to Theorem 9.2 the character of the generating element,  $g = \{E|\mathbf{R}(1, 0, 0)\}$ , for the  $q$ th IR of the subgroup associated with translation along the **a**-direction is  $\exp(2\pi iq_a/N)$ . For the operator,  $P_g = P_{\{E|\mathbf{R}(1,0,0)\}}$ , the character is

$$\chi_q(P_g) = e^{-2\pi iq_a/N}. \quad (9.40)$$

According to (9.35) (with  $l = 1$ ,  $m = 0$ , and  $n = 0$ ) the character for a Bloch wave is

$$\chi_q(P_g) = e^{-i\mathbf{k} \cdot \mathbf{R}(l,0,0)} = e^{-i\mathbf{k} \cdot \mathbf{R}(1,0,0)} = e^{-ik_a a}, \quad (9.41)$$

since  $u_{n\mathbf{k}}(\mathbf{r}) = u_{n\mathbf{k}}(\mathbf{r} - \mathbf{R})$ . In (9.41),  $a$  is the length of the primitive lattice vector **a** and  $k_a$  is the component of the **k**-vector along the **a**-direction.

Equating the characters from (9.35) and (9.41) defines  $k_a$  for the  $q_a$  IR:

$$e^{-ik_a a} = e^{-2\pi iq_a/N}, \quad (9.42)$$

$$k_a = \frac{2\pi q_a}{Na}, \quad (9.43)$$

$$q_a = 1, 2, 3, \dots, N. \quad (9.44)$$

Each value of  $q_a$  specifies one of the  $N$  IRs of the cyclic group. We can also consider  $q_a > N$  or  $q_a < 0$ . In these cases  $q_a$  can be written as  $q' + nN$ , where  $n$  is an appropriate positive or negative integer and  $0 \leq q' \leq N$ . The character of such a  $q_a$  is

$$e^{2\pi i q_a / N} = e^{2\pi i q' / N} e^{i 2n\pi} = e^{2\pi i q' / N}. \quad (9.45)$$

In other words, any  $q_a > N$  is equivalent to some IR with  $0 < q_a < N$ .

From (9.36) it follows that a  $\mathbf{k}$ -vector can be defined to uniquely specify the IRs of the three-dimensional subgroup of translation operators,

$$\mathbf{k}(\mathbf{q}) = \frac{2\pi}{N} \left[ \left( \frac{q_a}{a} \right) \mathbf{e}_a^* + \left( \frac{q_b}{b} \right) \mathbf{e}_b^* + \left( \frac{q_c}{c} \right) \mathbf{e}_c^* \right], \quad (9.46)$$

where  $\mathbf{e}_a^*$ ,  $\mathbf{e}_b^*$ , and  $\mathbf{e}_c^*$  are unit vectors along the  $\mathbf{a}^*$ -,  $\mathbf{b}^*$ -, and  $\mathbf{c}^*$ -directions, and  $a$ ,  $b$ , and  $c$  are the magnitudes of  $\mathbf{a}$ ,  $\mathbf{b}$ , and  $\mathbf{c}$ , respectively. Each component of  $\mathbf{k}(\mathbf{q})$  takes on the values between  $2\pi/(Nd)$  and  $2\pi/d$ , where  $d = a, b$ , or  $c$  depending on the component chosen. As  $N \rightarrow \infty$ ,  $\mathbf{k}(\mathbf{q})$  approaches a continuous variable with each component restricted to the reciprocal-lattice space from 0 to  $2\pi/d$ . An alternate but equivalent scheme is to restrict each component to be in the range from  $-\pi/d$  to  $+\pi/d$ . For this choice, the  $\mathbf{k}$ -vector is restricted to the first Brillouin zone. A vector  $\mathbf{k}$  that is outside of the first Brillouin zone can be written as  $\mathbf{k} = \mathbf{k}' + \mathbf{K}(s, t, u)$ , where  $\mathbf{k}'$  is in the first Brillouin zone, and  $s$ ,  $t$ , and  $u$  are appropriate integers. Adding a reciprocal-lattice vector to  $\mathbf{k}'$  is analogous to adding multiples of  $N$  to  $q_a$ ,  $q_b$ , or  $q_c$ . Thus  $\mathbf{k} = \mathbf{k}' + \mathbf{K}$  belongs to the same IR as  $\mathbf{k}'$ .

## 9.6 Point-group symmetry of Bloch waves

We confine our discussion to symmorphic space groups for which  $\{\alpha|\mathbf{R}\}$  can be factored into the product of a point-group element and a pure translation element  $\{\alpha|\mathbf{R}\} = \{E|\mathbf{R}\}\{\alpha|0\}$ . Note that  $\{\alpha|0\}$  and  $\{E|\mathbf{R}\}$  do not commute, and neither do the operators  $P_{\{\alpha|0\}}$  and  $P_{\{E|\mathbf{R}\}}$ . On the other hand, the set  $\{\mathbf{g}\}$  consisting of all of the operations of the space group of the form  $P_{\{\alpha|0\}}$  and the set  $\{\mathbf{g}_\mathbf{R}\}$  consisting of all of the operations of the space group of the form  $P_{\{E|\mathbf{R}\}}$  do commute. That is,  $\{\mathbf{g}\}\{\mathbf{g}_\mathbf{R}\}$  contains the same set of operators as  $\{\mathbf{g}_\mathbf{R}\}\{\mathbf{g}\}$  (but the order in which the operators appear is different). The entire symmorphic group,  $G$ , can be obtained from the direct product of the two subgroups:  $G = \mathbf{g} \times \mathbf{g}_\mathbf{R}$ . This suggests that the IRs of  $G$  are the direct products of the IRs of  $\mathbf{g}$  with those of  $\mathbf{g}_\mathbf{R}$ . This conjecture is true, but the proof will not be presented here.

It is clear from the form of the Bloch wave,  $\psi_\mathbf{k}(\mathbf{r}) = \exp(i\mathbf{k} \cdot \mathbf{r})u_{n\mathbf{k}}(\mathbf{r})$ , that it does not have the same periodic nature as the crystal (excluding the cases  $\mathbf{k} = 0$  or  $\mathbf{K}$ ). However, since  $u_{n\mathbf{k}}(\mathbf{r})$  is periodic, the symmetry properties of a Bloch wave

are determined by the modulating exponential factor. The  $\mathbf{k}$ -vector appears in the exponential only as the scalar product,  $\mathbf{k} \cdot \mathbf{r}$ . Let us consider the effect of a point-group operation on the scalar product,

$$(\mathbf{k} \cdot P_{\{\alpha|0\}} \mathbf{r}) = \mathbf{k} \cdot [(\alpha^{-1} \mathbf{r})]. \quad (9.47)$$

The scalar product on the right-hand side of (9.47) must be unchanged if both  $\mathbf{k}$  and  $\alpha^{-1} \mathbf{r}$  are rotated through the same angle. Therefore, if we apply  $P_{\{\alpha|0\}}^{-1}$  to both vectors, the scalar product must be unchanged:

$$\begin{aligned} [P_{\{\alpha|0\}}^{-1} \mathbf{k}] \cdot [P_{\{\alpha|0\}}^{-1} (\alpha^{-1} \mathbf{r})] &= (\alpha \mathbf{k}) \cdot (\alpha \alpha^{-1} \mathbf{r}) = (\alpha \mathbf{k}) \cdot \mathbf{r} \\ &= (P_{\{\alpha|0\}}^{-1} \mathbf{k}) \cdot \mathbf{r} = (\mathbf{k} \cdot P_{\{\alpha|0\}} \mathbf{r}). \end{aligned} \quad (9.48)$$

Equation (9.48) states that the effect of  $P_{\{\alpha|0\}}$  operating on  $\mathbf{r}$  in the scalar product is the same as applying  $P_{\{\alpha|0\}}^{-1}$  to  $\mathbf{k}$ .

From (9.48) it also follows that, for a Bloch wave,

$$P_{\{\alpha|0\}} \psi_{n\mathbf{k}}(\mathbf{r}) = \psi_{n\mathbf{k}}(\alpha^{-1} \mathbf{r}) = e^{i\mathbf{k} \cdot \alpha^{-1} \mathbf{r}} u_{n\mathbf{k}}(\alpha^{-1} \mathbf{r}) = e^{i(\alpha \mathbf{k}) \cdot \mathbf{r}} u'_{n(\alpha \mathbf{k})}(\mathbf{r}). \quad (9.49)$$

The function  $u'_{n(\alpha \mathbf{k})}(\mathbf{r})$  need not be equal to  $u_{n(\alpha \mathbf{k})}(\mathbf{r})$ , but it must have the same periodicity. If the energy associated with the Bloch wave,  $E_{n\mathbf{k}}$ , is non-degenerate, the two functions can differ at most by a phase factor,  $e^{i\phi(\alpha)}$ . However, if  $E_{n\mathbf{k}}$  is degenerate,  $u'_{n(\alpha \mathbf{k})}(\mathbf{r})$  may be a linear combination of the  $u$ -functions of the degenerate states.

### 9.6.1 The group of the $\mathbf{k}$ -vector

If  $\mathbf{R}$  is a lattice vector, then  $P_{\{\alpha|0\}} \mathbf{R} = \mathbf{R}'$  is also a lattice vector. Similarly, if  $\mathbf{K}$  is a reciprocal-lattice vector, then  $P_{\{\alpha|0\}} \mathbf{K} = \mathbf{K}'$  is also a reciprocal-lattice vector. A Bravais lattice and its reciprocal lattice are invariant under the point-group operations of the same space group.

If  $\mathbf{k}$  and  $\mathbf{k}'$  differ by a reciprocal-lattice vector ( $\mathbf{k} = \mathbf{k}' + \mathbf{K}$ ), they are symmetry-equivalent or simply “equivalent”, and the two Bloch waves,  $\psi_{n\mathbf{k}}$  and  $\psi_{n\mathbf{k}'}$ , belong to the same IR. Here,  $\mathbf{K}$  is a reciprocal-lattice vector and  $\mathbf{k}$  and  $\mathbf{k}'$  are vectors in the first Brillouin zone.

The collection of all the point-group operations that transform  $\mathbf{k}$  into itself or an equivalent vector forms a subgroup of the space group called the group of the  $\mathbf{k}$ -vector or the group of the wavevector. We shall denote this group by the symbol  $g_{\mathbf{k}}$ .

We can demonstrate that  $g_{\mathbf{k}}$  is, in fact, a group. Let  $P_{\{\alpha|0\}}$  and  $P_{\{\beta|0\}}$  be point-group operations in  $g_{\mathbf{k}}$  so that

$$P_{\{\alpha|0\}} \mathbf{k} = \mathbf{k} + \mathbf{K}, \quad (9.50)$$

$$P_{\{\beta|0\}} \mathbf{k} = \mathbf{k} + \mathbf{K}'. \quad (9.51)$$

Then,

$$P_{\{\beta|0\}} P_{\{\alpha|0\}} \mathbf{k} = P_{\{\beta|0\}} [\mathbf{k} + \mathbf{K}] = \mathbf{k} + \mathbf{K}' + P_{\{\beta|0\}} \mathbf{K}. \quad (9.52)$$

$P_{\{\beta|0\}} \mathbf{K}$  is a reciprocal-lattice vector. Since  $\mathbf{K}' + P_{\{\beta|0\}} \mathbf{K}$  is the sum of two reciprocal-lattice vectors, it also is a reciprocal-lattice vector,

$$\mathbf{K}' + P_{\{\beta|0\}} \mathbf{K} = \mathbf{K}''. \quad (9.53)$$

Therefore,

$$P_{\{\beta|0\}} P_{\{\alpha|0\}} \mathbf{k} = P_{\{\beta\alpha|0\}} \mathbf{k} = \mathbf{k} + \mathbf{K}''. \quad (9.54)$$

Equation (9.54) shows that, if  $P_{\{\beta|0\}}$  and  $P_{\{\alpha|0\}}$  belong to  $\mathbf{g}_{\mathbf{k}}$ , then  $P_{\{\beta\alpha|0\}}$  also belongs to  $\mathbf{g}_{\mathbf{k}}$ . The set of operators  $\mathbf{g}_{\mathbf{k}}$  always has the identity  $P_{\{E|0\}}$ , therefore all that remains is to show that every operator in  $\mathbf{g}_{\mathbf{k}}$  has an inverse that is also in  $\mathbf{g}_{\mathbf{k}}$ .

$P_{\{\alpha|0\}} = \{\alpha^{-1}|0\}$  and its inverse  $P_{\{\alpha^{-1}|0\}} = \{\alpha|0\}$ . We need to show that, if  $\alpha^{-1}\mathbf{k}$  is equivalent to  $\mathbf{k}$ , then so is  $\alpha\mathbf{k}$ . We have that

$$\alpha^{-1}\mathbf{k} = \mathbf{k} + \mathbf{K}. \quad (9.55)$$

Multiplying both sides of (9.55) by  $\alpha$  gives

$$\alpha\alpha^{-1}\mathbf{k} = \mathbf{k} = \alpha(\mathbf{k} + \mathbf{K}) = \alpha\mathbf{k} + \mathbf{K}', \quad (9.56)$$

where  $\mathbf{K}'$  is a reciprocal-lattice vector. From (9.56) we obtain

$$\alpha\mathbf{k} = \mathbf{k} + (-\mathbf{K}'), \quad (9.57)$$

showing that  $\alpha\mathbf{k}$  is equivalent to  $\mathbf{k}$ . Thus the operators of  $\mathbf{g}_{\mathbf{k}}$  satisfy the requirements of a group.

All of the set of Bloch waves

$$\psi_{n(\alpha\mathbf{k})}(\mathbf{r}) = e^{i\alpha\mathbf{k}\cdot\mathbf{r}} u_{n(\alpha\mathbf{k})}(\mathbf{r}) \quad (\text{for all } \alpha \text{ in } \mathbf{g}_{\mathbf{k}} \text{ including } E) \quad (9.58)$$

have the same energies (are degenerate),  $E_{n\mathbf{k}} = E_{n\alpha\mathbf{k}}$ , since the wavefunctions are related to one another by a symmetry operation. More than one of the operations of  $\mathbf{g}_{\mathbf{k}}$  may produce the same (identical, not just equivalent)  $\mathbf{k}$ -vector. The proper set of degenerate states consists of those that are distinct. We know that the distinct, degenerate eigenstates of a Hamiltonian form the basis for a representation of the group, hence the (distinct) degenerate Bloch waves of (9.58) form a basis for a representation of the subgroup  $\mathbf{g}_{\mathbf{k}}$ .

It is useful to distinguish two different types of degeneracies. The first occurs as a result of symmetry requirements. The second, called “accidental” degeneracy, is not a symmetry requirement but rather a fortuitous result dependent upon the details of the Hamiltonian. For energy bands we can distinguish degeneracies of the form  $E_{n\mathbf{k}} = E_{n(\alpha\mathbf{k})}$  and  $E_{n\mathbf{k}} = E_{n'\mathbf{k}}$ . For the latter case the energies of two

Bloch waves from different bands,  $n$  and  $n'$ , coincide for the same  $\mathbf{k}$ -vector. The first condition,  $E_{n\mathbf{k}} = E_{n(\alpha\mathbf{k})}$ , is a result of symmetry and therefore is an essential degeneracy. The condition  $E_{n\mathbf{k}} = E_{n'\mathbf{k}}$  can be a result of symmetry or an accidental degeneracy.

*Basis functions for representations (symmorphic space groups)*

The periodic parts of the Bloch-wave functions,  $u_{n(\alpha\mathbf{k})}(\mathbf{r})$  (where  $\alpha$  is in  $\mathbf{g}_{\mathbf{k}}$ ), are basis functions for a representation of  $\mathbf{g}_{\mathbf{k}}$ :

$$P_{\{\alpha|0\}} u_{n\mathbf{k}}(\mathbf{r}) = \sum_{\mathbf{k}'} D(\alpha)_{\mathbf{k}'\mathbf{k}} u_{\mathbf{k}'}(\mathbf{r}), \quad (9.59)$$

where  $\mathbf{k}'$  runs over the distinct, equivalent  $\mathbf{k}$ -vectors generated by the operators in  $\mathbf{g}_{\mathbf{k}}$ , and  $D(\alpha)_{\mathbf{k}'\mathbf{k}}$  are the representation-matrix elements. It should be noted that  $D$  may be reducible.

The exponential functions,  $e^{i\mathbf{k}\cdot\mathbf{r}}$ , are basis functions for the translation subgroup,  $\mathbf{g}_{\mathbf{R}}$ , whose operators are  $P_{\{E|\mathbf{R}\}}$ , where  $\mathbf{R} = \mathbf{R}(l, m, n)$  is any lattice vector. The matrix representation is diagonal:

$$P_{\{E|\mathbf{R}\}} e^{i\mathbf{k}\cdot\mathbf{r}} = e^{-i\mathbf{k}\cdot\mathbf{R}} e^{i\mathbf{k}\cdot\mathbf{r}}. \quad (9.60)$$

Since this representation is one-dimensional, it is irreducible.

### 9.6.2 Subgroups and $\mathbf{k}$ -vectors

The notation to be used for the various operators and groups is summarized in Box 9.1.

**Box 9.1 Notation for groups and subgroups of a symmorphic space group**

Symbol	Definition
$G$	Space group with operators $P_{\{\alpha \mathbf{R}\}}$ .
$\mathbf{g}$	Subgroup of $G$ consisting of all pure point-group operators, $P_{\{\alpha 0\}}$ . (Sometimes called the big group.)
$h(\mathbf{g})$	Number of operators in $\mathbf{g}$ .
$P_{\alpha}$	Operator belonging to $\mathbf{g}$ . $P_{\alpha} = P_{\{\alpha 0\}}$ .
$\mathbf{g}_{\mathbf{k}}$	Group of the wavevector. Subgroup of $G$ and $\mathbf{g}$ consisting of all pure point-group operators of $G$ for which $P_{\{\alpha 0\}}\mathbf{k} = \mathbf{k} + \mathbf{K}$ . (Sometimes called the little group.)
$h(\mathbf{k})$	Number of operators in $\mathbf{g}_{\mathbf{k}}$ .
$P(\mathbf{k})_{\alpha}$	Operator in the group $\mathbf{g}_{\mathbf{k}}$ .
$\mathbf{g}_{\mathbf{R}}$	Translation subgroup. Subgroup of $G$ consisting of pure translation operators, $P_{\{E \mathbf{R}\}}$ .
$P_{\mathbf{R}}$	Operator in $\mathbf{g}_{\mathbf{R}}$ .

$g_{\mathbf{k}}$	The space group of the $\mathbf{k}$ -vector (or wavevector), $g_{\mathbf{k}} \times g_{\mathbf{R}}$ .
$s(\mathbf{k})$	The star of $\mathbf{k}$ . The set of distinct, mutually inequivalent wavevectors produced by the operators of $g$ acting on $\mathbf{k}$ .
$h(\text{star})$	Number of distinct wavevectors in $s(\mathbf{k})$ .
Array of $\mathbf{k}$	The set of wavevectors produced by the operators of $g$ acting on $\mathbf{k}$ .

The pure point-group operations form a subgroup of the space group,  $G$ . We denote this subgroup by the symbol,  $g$ , and its operations by  $P_{\alpha}$ , and use  $h(g)$  for the number of operators in  $g$ .

Given a wavevector,  $\mathbf{k}$ , we can form  $h(g)$  wavevectors by applying the operators of  $g$  to  $\mathbf{k}$ ,

$$P_{\alpha}\mathbf{k} = \alpha^{-1}\mathbf{k}, \quad (9.61)$$

where  $\alpha$  runs over all  $h(g)$  operations of  $g$ . We shall refer to the collection of these vectors as the *array of the  $\mathbf{k}$ -vector*. The  $h(g)$  wavevectors of the array are not necessarily distinct. For a general point  $\mathbf{k}$  in the first Brillouin zone, all the vectors are distinct, but when  $\mathbf{k} = 0$  or  $\mathbf{k}$  corresponds to a point or line of high symmetry or to the surface of the Brillouin zone the number of distinct  $\mathbf{k}$ -vectors produced will usually be less than  $h(g)$ .

The array of  $\mathbf{k}$ -vectors can be separated into two sets: (a) those vectors  $P_{\alpha}\mathbf{k}$  that are equivalent to  $\mathbf{k}$  and (b) those that are inequivalent to  $\mathbf{k}$ . The set of *operations* of  $g$  that produces the mutually equivalent vectors forms the *group of the  $\mathbf{k}$ -vector* or the *group of the wavevector*,  $g_{\mathbf{k}}$ . We represent the number of elements in  $g_{\mathbf{k}}$  by  $h(\mathbf{k})$ . The set of distinct, mutually inequivalent vectors forms what is called the *star of the wavevector*.

The star, denoted as  $s(\mathbf{k})$ , is defined to include the original  $\mathbf{k}$ . For a  $\mathbf{k}$  having no special symmetry properties (general point),  $s(\mathbf{k})$  contains *all* of the distinct  $\mathbf{k}$ -vectors generated by all of the  $P_{\alpha}\mathbf{k}$ . In this case,  $g_{\mathbf{k}}$  has only the identity operation. If, however, the  $\mathbf{k}$ -vector is a special symmetry point, the number of  $\mathbf{k}$ -vectors in the star will be smaller than in the case of the general point and the operators belonging to  $g_{\mathbf{k}}$  form a larger group.

If we select any of the vectors of the star of  $\mathbf{k}$ , say  $\mathbf{k}'$ , and apply the operations of  $g$  to it, the same array of  $\mathbf{k}$ -vectors is produced again. The operators that produce equivalent  $\mathbf{k}'$ -vectors need not be the same as those that produce equivalent  $\mathbf{k}$ -vectors, but they form a group that is isomorphic to  $g_{\mathbf{k}}$ . In general, if the number of operators of  $g_{\mathbf{k}}$  is  $h(\mathbf{k})$  and the number of distinct vectors of the star is  $h(\text{star})$ , then

$$h(g) = h(\mathbf{k})h(\text{star}). \quad (9.62)$$

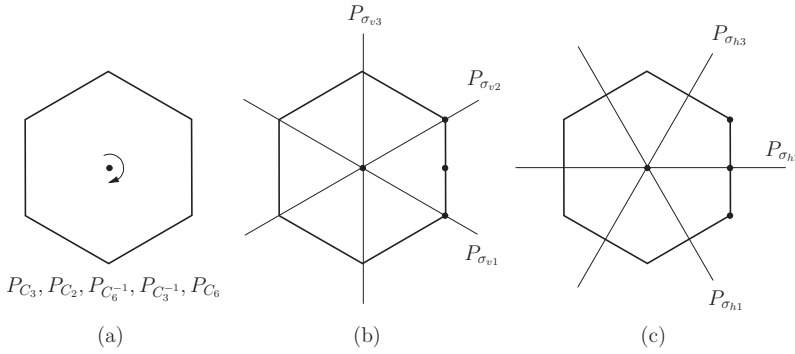


Figure 9.6 Symmetry operations for  $C_{6v}$ : (a) six-fold axis, (b) three  $\sigma_v$  reflection lines, and (c) three  $\sigma_h$  reflection lines.

As examples of the star and the group of the wavevector, consider a simple hexagonal reciprocal lattice in two dimensions. The lattice is formed by the primitive reciprocal-lattice vectors  $\mathbf{a}^*$  and  $\mathbf{b}^*$  (given in Table 9.1). As shown in Fig. 9.4, the reciprocal lattice is hexagonal and so is the first Brillouin zone.

The elements consist of the identity, rotations about a six-fold axis, and six mirror planes perpendicular to the plane of the paper. By class, the rotations include (a)  $E$ , (b)  $2C_6$  ( $\pm 60^\circ$  rotations), (c)  $2C_3$  ( $\pm 120^\circ$  rotations), and (d)  $C_2$  ( $180^\circ$  rotation). By class the reflection planes are  $3\sigma_v$  (planes passing through the corners of the hexagon) and  $3\sigma_h$  (planes bisecting the edges of the hexagon). The symmetry operations are shown in Fig. 9.6.

For  $\mathbf{k} = 0$  ( $\Gamma$  in the Brillouin zone) all of the vectors  $P_{\alpha}\mathbf{k} = 0$ , and therefore  $\mathbf{g}_{\mathbf{k}} = \mathbf{g} = C_{6v}$ . The star of the  $\mathbf{k}$ -vector is just  $\mathbf{k}$ . Now consider a non-zero  $\mathbf{k}$ -vector from the origin ( $\Gamma$ ) to an arbitrary, general point within the first Brillouin zone. For the two-dimensional hexagon the point-group operations of the space group applied to the  $\mathbf{k}$ -vector produces 12 inequivalent  $\mathbf{k}$ -vectors as illustrated in Fig. 9.7(b). The mutually *inequivalent*  $\mathbf{k}$ -vectors form *the star of the  $\mathbf{k}$ -vector*. The only operation that transforms  $\mathbf{k}$  into itself or into  $(\mathbf{k} + \mathbf{K})$  is the identity operation. Therefore the group of the  $\mathbf{k}$ -vector,  $\mathbf{g}_{\mathbf{k}}$ , is just the identity. The star of the  $\mathbf{k}$ -vector has 12 inequivalent vectors. Next consider a  $\mathbf{k}$ -vector extending from  $\Gamma$  to some point on the  $\Sigma$  line, but not extending to  $\mathbf{M}$ , as shown in Fig. 9.7(c). The point-group operations that transform  $\mathbf{k}$  into itself or  $(\mathbf{k} + \mathbf{K})$  are  $P_E$  and  $P_{\sigma_{h2}}$ . In this case these two operations form  $\mathbf{g}_{\mathbf{k}}$ , the group of the  $\mathbf{k}$ -vector. The six vectors shown are the star of the  $\mathbf{k}$ -vector. Figure 9.7(d) shows a  $\mathbf{k}$ -vector extending from  $\Gamma$  to  $\mathbf{M}$ . In this case there are four operations in  $\mathbf{g}_{\mathbf{k}}$ , namely  $E$ ,  $P_{C2}$ ,  $P_{\sigma_{v3}}$ , and  $P_{\sigma_{h2}}$ .  $P_{C2}$  and  $P_{\sigma_{v3}}$  transform  $\mathbf{k}$  into  $\mathbf{k} + \mathbf{K}$ , where  $\mathbf{K} = \mathbf{a}^* + \mathbf{b}^*$ . The star of the  $\mathbf{k}$ -vector consists of  $\mathbf{k}$  and the two dashed vectors in Fig. 9.7(d). Finally, Fig. 9.7(f) shows the vector extending from  $\Gamma$  to  $\mathbf{K}$ . In this instance all of the point-group operations

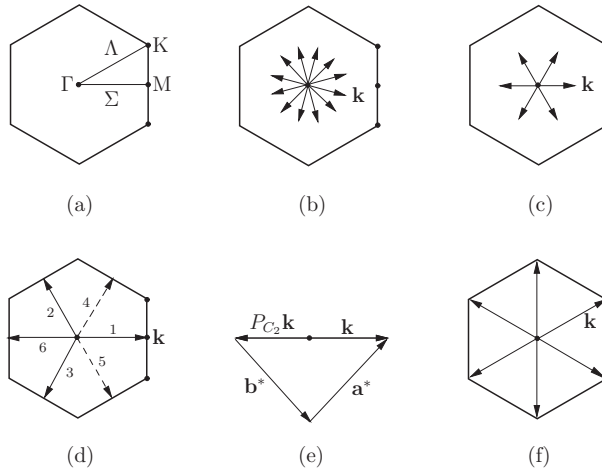


Figure 9.7 (a) The first Brillouin zone, showing the high-symmetry points and lines. (b) An arbitrary, general  $\mathbf{k}$ -vector within the first Brillouin zone. Only the identity transforms  $\mathbf{k}$  into an equivalent vector. The 12 operations of  $C_{6v}$  applied to  $\mathbf{k}$  produce 12 inequivalent  $\mathbf{k}$ -vectors that form the star of the wavevector. (c)  $\mathbf{k}$  along the line  $\Sigma$  in the first Brillouin zone. The operations  $E$  and  $\sigma_{h2}$  form  $g_{\mathbf{k}}$  in this case. The star of the wavevector has six mutually inequivalent vectors. (d)  $\mathbf{k}$  extends from  $\Gamma$  to the point  $M$  on the edge of the Brillouin zone. The  $g_{\mathbf{k}}$  group consists of  $P_E$ ,  $P_{\sigma_{h2}}$ ,  $P_{C_2}$  and  $P_{\sigma_{v3}}$ . The last two operations transform  $\mathbf{k}$  into  $\mathbf{k} + \mathbf{K}$ , where  $\mathbf{K}$  is a reciprocal-lattice vector  $\mathbf{a}^* + \mathbf{b}^*$  as illustrated in (e). The star consists of the three, distinct, non-equivalent vectors labeled 1, 2, and 3. The dashed vector labeled 4 is equivalent to 3 ( $\mathbf{k}_4 = \mathbf{k}_3 + \mathbf{a}^*$ ), and the dashed vector 5 is equivalent to 2 ( $\mathbf{k}_5 = \mathbf{k}_2 + \mathbf{b}^*$ ). (f)  $\mathbf{k}$  extends from  $\Gamma$  to  $K$ . All six vectors (each generated twice) are equivalent, so the star has only the vector  $\mathbf{k}$ . The group of the wavevector is  $g(C_{6v})$ . For  $\mathbf{k} = 0$ ,  $g_{\mathbf{k}}$  is also  $C_{6v}$ .

of the space group transform  $\mathbf{k}$  into  $\mathbf{k}$  or a  $(\mathbf{k} + \mathbf{K})$ -vector, and  $g_{\mathbf{k}} = g$  is the full point group,  $C_{6v}$ . The star consists of  $\mathbf{k}$  alone.

### 9.7 The space group of the $\mathbf{k}$ -vector, $g_{\mathbf{k}}^s$

To simplify the notation we shall denote a pure point-group operation,  $P_{\{\alpha|0\}}$ , by  $P_{\alpha}$ , and a pure translation,  $P_{\{E|\mathbf{R}\}}$ , by  $P_{\mathbf{R}}$ . Also we shall use  $g_{\mathbf{R}}$  to represent the subgroup of pure lattice-vector translations.

The group of the wavevector,  $g_{\mathbf{k}}$ , consists of operators,  $P_{\alpha}$ , for which  $\mathbf{k}$  and  $P_{\alpha}\mathbf{k}$  are equivalent. To denote when  $P_{\alpha}$  is an operation belonging to  $g_{\mathbf{k}}$  we shall use the notation  $P(\mathbf{k})_{\alpha}$ . Thus  $P_{\alpha}$  is a member of the space group for any  $\alpha$ , but  $P(\mathbf{k})_{\alpha}$  includes only the  $P_{\alpha}$  that belong to  $g_{\mathbf{k}}$ .

The *space group of the  $\mathbf{k}$ -vector*,  $g_{\mathbf{k}}^s$ , includes both point-group operations and translations. For a symmorphic group the operators of  $g_{\mathbf{k}}^s$  are of the type  $P(\mathbf{k})_{\alpha} P_{\mathbf{R}}$ , where  $\mathbf{R}$  is any lattice vector. The space group  $g_{\mathbf{k}}^s$  consists of products of  $P(\mathbf{k})_{\alpha}$



and  $P_R$ . The operators  $P(\mathbf{k})_\alpha$  and  $P_R$  do not commute, but the set of all pure translations,  $\{P_R\}$ , and the set of all pure point-group operations,  $\{P(\mathbf{k})_\alpha\}$ , do commute (see Appendix B for a discussion of a factor group). The space group  $g_k^s$  is the direct product of  $g_k$  and  $g_R$ ,

$$g_k^s = g_k \times g_R. \quad (9.63)$$

$g_k^s$  is a group of importance when analyzing the energy bands or wave-like phenomena of crystals.

### 9.8 Irreducible representations of $g_k^s$

The IRs of  $g_k^s$  are the direct products of the IRs of  $g_k$  and  $g_R$ . We have already shown that the Bloch waves  $\psi_{n\mathbf{k}}(\mathbf{r})$  are basis functions for the IRs of  $g_R$ . Since  $P_R \psi_{n\mathbf{k}}(\mathbf{r}) = \exp(-i\mathbf{k} \cdot \mathbf{R}) \psi_{n\mathbf{k}}(\mathbf{r})$  the IRs are diagonal matrices,

$$D(P_R)_{\mathbf{k}'\mathbf{k}} = e^{-i\mathbf{k} \cdot \mathbf{R}} \delta_{\mathbf{k}'\mathbf{k}}. \quad (9.64)$$

The group  $g_k$  is a set of point-group operations, isomorphic to one of the 32 crystallographic point groups described in Appendix B. As mentioned above, the distinct functions produced by  $P(\mathbf{k})_\alpha u_{n(\mathbf{k})} = u_{n(\alpha\mathbf{k})}$  are basis functions for a representation of  $g_k$ . If there are, in number,  $n(g_k)$  distinct  $u_{n(\alpha\mathbf{k})}$  functions they form the basis for an  $n(g_k)$ -dimensional representation of  $g_k$ . For notational simplicity, let us designate these distinct  $u$ -functions as  $u_{n\mathbf{k}}^i$ , where  $i = 1, 2, 3, \dots, n(g_k)$ . Since the  $u$ -functions are a basis for a representation, we have that

$$P(\mathbf{k})_\alpha u_{n\mathbf{k}}^i = \sum_v [D(\alpha)^\Gamma]_{vi} u_{n\mathbf{k}}^v, \quad (9.65)$$

where  $\Gamma$  is the representation based on the  $u_{n\mathbf{k}}$  functions and  $[D(\alpha)^\Gamma]_{vi}$  is the  $vi$  matrix element. The representation is usually reducible and can be decomposed into the IRs of  $g_k$  by the usual methods. The group  $g_k$  is sometimes called the *little group*, and an IR of  $g_k$  is called a *small representation*. The above discussion of representations may seem a bit confusing at first. However, an example may serve to clarify the situation.

As noted in Section 9.5.1, for the two-dimensional hexagonal lattice,  $g$  is  $C_{6v}$  and  $g_k$  is  $C_{6v}$  or a subgroup of  $C_{6v}$  depending on  $\mathbf{k}$ . For a simple cubic Bravais lattice,  $g$  will be  $O_h$  and  $g_k$  will be  $O_h$  or a subgroup of the  $O_h$ . As a result, the IRs of  $g_k$  can be obtained in the same way as for point groups. Let  $[D^j(\alpha)^k]_{\kappa\nu}$  be the matrix element of the  $j$ th IR of  $g_k$ ; then the matrix elements of the IR for  $g_k^s$  are

$$D^j(\alpha, \mathbf{R})_{\kappa\nu} = e^{-i\mathbf{k} \cdot \mathbf{R}} [D^j(\alpha)]_{\kappa\nu}. \quad (9.66)$$

Thus, for symmorphic space groups, the IRs for a given  $\mathbf{k}$  are determined by the point-group IRs of  $g_k$  and a phase factor corresponding to the translation,  $\mathbf{R}$ .

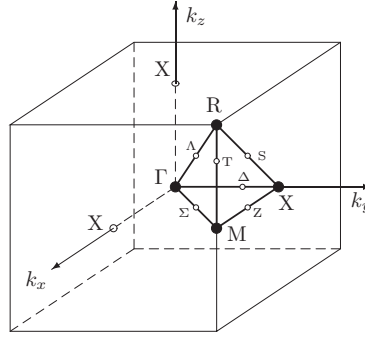


Figure 9.8 The Brillouin zone for a simple cubic Bravais lattice. The reduced Brillouin zone is the tetrahedron bounded by the lines  $\Gamma$ -X, X-M, M- $\Gamma$ ,  $\Gamma$ -R, R-X, and R-M, which represents 1/48 of the total Brillouin zone.

### 9.9 Compatibility of the irreducible representations of $g_{\mathbf{k}}$

At  $\Gamma(\mathbf{k} = 0)$  the group of the  $\mathbf{k}$ -vector,  $g_{\mathbf{k}}$ , is the full point group of the Bravais lattice,  $g$ . The matrix elements of the IRs are the same as those for the point group. As  $\mathbf{k}$  is extended away from  $\Gamma$  to  $\mathbf{k}'$  the symmetry is usually reduced and  $g_{\mathbf{k}'}$  corresponds to a subgroup of  $g$ . At a general point in the Brillouin zone, the symmetry may be reduced to a group containing only the identity. As a result, in most cases the number of *degenerate* Bloch-wave solutions will be reduced, and therefore the dimensions of the IRs will diminish. In general, the IRs of  $g_{\mathbf{k}}$  can be decomposed into the IRs of the lower symmetry group,  $g_{\mathbf{k}'}$ . The process is analogous to the splitting of degenerate atomic wavefunctions by a crystal field. However, in this instance the symmetry-lowering factor is the  $\mathbf{k}$ -vector of the Bloch wave. If  $\Gamma_{\mathbf{k}}$  is an IR of  $g_{\mathbf{k}}$ , and  $\Gamma_{\mathbf{k}'}$  is an IR of  $g_{\mathbf{k}'}$ , the two IRs are said to be *compatible* if and only if  $\Gamma_{\mathbf{k}'}$  is contained in the decomposition of  $\Gamma_{\mathbf{k}}$ . The concept of compatible IRs provides a method of connecting energy bands as the wave-vector traverses some circuit in the Brillouin zone. We shall now present a few examples for a cubic lattice to illustrate the principles outlined above.

The first Brillouin zone and special  $\mathbf{k}$ -vector points for a simple cubic solid are illustrated in Fig. 9.8. (A discussion of the  $O_h$  group may be found in Appendix E.) The volume bounded by the lines  $\Gamma$ -X, X-M, M- $\Gamma$ ,  $\Gamma$ -R, R-X, and R-M is 1/48 of the total volume. If this volume is subjected to all 48 operations of  $O_h$ , the entire volume of the first Brillouin zone is mapped out.<sup>2</sup> Therefore, all of the possible energies,  $E_{n\mathbf{k}}$ , and the IRs of  $g_{\mathbf{k}}$  can be obtained from this segment of the first Brillouin zone. The segment is called the *irreducible Brillouin zone*, the *reduced Brillouin zone*, or just the *reduced zone*. Any  $\mathbf{k}$  in the first Brillouin zone

<sup>2</sup> The statistical weights of points on the bounding surface of the reduced zone are  $1/n_s$ , where  $n_s$  is the number of segments that share the point.

Table 9.2 The character table for  $\mathbf{g}_{\mathbf{k}} = O_h$  at  $\Gamma$  ( $\mathbf{k} = 0$ ). The labels for the IRs are listed in the first three columns. The first column is the label used in point-group theory. The second and third columns are labels used in solid-state physics; in the second the  $\pm$  superscripts indicate the parity of a basis function corresponding to the IR

IR			$E$	$8C_3$	$3C_4^3$	$6C_4$	$6\bar{C}_2$	$i$	$8iC_3$	$3iC_4^3$	$6iC_4$	$6i\bar{C}_2$
$A_{1g}$	$\Gamma_1(\Gamma_1^+)$	$\Gamma_{1g}$	1	1	1	1	1	1	1	1	1	1
$A_{2g}$	$\Gamma_2(\Gamma_2^+)$	$\Gamma_{2g}$	1	1	1	-1	-1	1	1	1	-1	-1
$\mathcal{E}_g$	$\Gamma_{12}(\Gamma_{12}^+)$	$\Gamma_{3g}$	2	-1	2	0	0	2	-1	2	0	0
$T_{1u}$	$\Gamma_{15}(\Gamma_{15}^-)$	$\Gamma_{4u}$	3	0	-1	1	-1	-3	0	1	-1	1
$T_{2u}$	$\Gamma_{25}(\Gamma_{25}^-)$	$\Gamma_{5u}$	3	0	-1	-1	1	-3	0	1	1	-1
$A_{1u}$	$\Gamma'_1(\Gamma_1^-)$	$\Gamma_{1u}$	1	1	1	1	1	-1	-1	-1	-1	-1
$A_{2u}$	$\Gamma'_2(\Gamma_2^-)$	$\Gamma_{2u}$	1	1	1	-1	-1	-1	-1	-1	1	1
$\mathcal{E}_u$	$\Gamma'_{12}(\Gamma_{12}^-)$	$\Gamma_{3u}$	2	-1	2	0	0	-2	1	-2	0	0
$T_{1g}$	$\Gamma'_{15}(\Gamma_{15}^+)$	$\Gamma_{4g}$	3	0	-1	1	-1	3	0	-1	1	-1
$T_{2g}$	$\Gamma'_{25}(\Gamma_{25}^+)$	$\Gamma_{5g}$	3	0	-1	-1	1	3	0	-1	-1	1

that does not belong to the reduced zone can be obtained from some  $\mathbf{k}_1$  that *does* belong to the reduced zone by the relation  $P_\alpha \mathbf{k}_1 = \mathbf{k}$ , and therefore  $E_{\mathbf{k}1} = E_{\mathbf{k}}$ . Although the star of  $\mathbf{k}$  and that of  $\mathbf{k}_1$  may have different vectors, the group of  $\mathbf{g}_{\mathbf{k}1}$  is isomorphic to the group of  $\mathbf{g}_{\mathbf{k}}$ , and hence they have the same IRs. The character table and IRs for  $\mathbf{g}_{\mathbf{k}} = O_h$  are given in Table 9.2. For any model, an energy band state must belong to one of these IRs of  $\mathbf{g}_{\mathbf{k}}$ . *Different* bands (different  $n$  values of the  $u_{n\mathbf{k}}(\mathbf{r})$  functions) may belong to different IRs or may serve as different rows of the same IR. The question of what band belongs to which IR depends on the basis functions selected for the energy band model.

Consider a  $\mathbf{k}$ -vector extending from  $\Gamma$  to some point on the  $\Lambda$ -line but short of  $R$ . The operations of  $\mathbf{g}$  which transform  $\mathbf{k}$  into an equivalent vector are  $E$ ,  $2C_3$ , and  $3iC_2$ . (The precise elements can be determined from the operations discussed in Appendix E. They are  $E$ ,  $C_3$  about axis 4,  $C_3^2$  about axis 4,  $i\bar{C}_2$  about axis 2,  $i\bar{C}_2$  about axis 3, and  $i\bar{C}_2$  about axis 5.) These operations form a group that is isomorphic to  $C_{3v}$ . Therefore, for a  $\mathbf{k}$ -vector along the  $\Lambda$ -line,  $\mathbf{g}_{\mathbf{k}}$  abruptly changes from  $O_h$  for  $\mathbf{k} = 0$  to  $C_{3v}$ . However, if  $\mathbf{k}$  extends to the  $R$ -point,  $\mathbf{g}_{\mathbf{k}}$  becomes  $O_h$  again. The character tables for  $C_{3v}$  and  $C_{4v}$  are given in Table 9.3 and Table 9.4, respectively. The labels of the IRs are given for the atomic and solid-state conventions. The IRs at  $\Gamma$  must decompose into IRs of  $C_{3v}$  for  $\mathbf{k}$  along the  $\Lambda$ -line. It may be seen that the dimensions of the IRs for  $C_{3v}$  are 1 for  $\Lambda_1(A_1)$ , 1 for  $\Lambda_2(A_2)$ , and 2 for  $\Lambda_3(\mathcal{E})$ . Therefore any three-dimensional IR at  $\Gamma$  must split into at least two

Table 9.3 The character table for  $C_{3v}$ . The operator classes shown are those from Appendix E. The specific operations within the classes are also indicated.

$C_{3v}$		$2C_3$	$3i\bar{C}_2$
IRs	$E$	$C_3^{(4)}, (C_3^{(4)})^2$	$i\bar{C}_2^{(2)}, i\bar{C}_2^{(3)}, i\bar{C}_2^{(5)}$
$\Delta_1(A_1)$	1	1	1
$\Delta_2(A_2)$	1	1	-1
$\Delta_3(\mathcal{E})$	2	-1	0

Table 9.4 The character table for  $C_{4v}$ . The operations are those from Appendix E. The equivalent reflections,  $\sigma_d$  and  $\sigma_v$  for  $C_{4v}$ , are also indicated.

$C_{4v}$		$2C_4$	$C_2$	$2iC_2 = 2\sigma_v$	$2i\bar{C}_2 = 2\sigma_d$
IRs	$E$	$C_4^{(1)}, (C_4^{(1)})^3$	$C_2^{(1)}$	$iC_2^{(2)}, iC_2^{(3)}$	$i\bar{C}_2^{(1)}, i\bar{C}_2^{(2)}$
$\Delta_1(A_1)$	1	1	1	1	1
$\Delta_{1'}(A_2)$	1	1	1	-1	-1
$\Delta_2(B_1)$	1	-1	1	1	-1
$\Delta_{2'}(B_2)$	1	-1	1	-1	1
$\Delta_5(\mathcal{E})$	2	0	-2	0	0

IRs of  $C_{3v}$  for  $\mathbf{k}$  along the  $\Lambda$ -line (excluding  $R$ ). Table 9.5 shows how the  $O_h$  IRs decompose into those of  $C_{3v}$ .

Similarly, for  $\mathbf{k}$  along the  $y$ -axis, the  $\Delta$ -line,  $g_{\mathbf{k}}$  is isomorphic to  $C_{4v}$ . The decompositions of the IRs of  $O_h$  into those of  $C_{4v}$  are also shown in Table 9.5.

As an example, consider the energy bands for a simple-cubic lattice with  $p$ -orbitals on each site, with on-site and nearest-neighbor interactions. There are three orbitals in each unit cell, so there will be three energy bands. For simplicity we can use orthogonal Löwdin orbitals and assume solutions of the form

$$\psi_{\mathbf{k}}(\mathbf{r}) = \sum_{\mathbf{R}} \sum_{\alpha} A_{\alpha}(\mathbf{R}) p_{\alpha}(\mathbf{r} - \mathbf{R}), \quad (9.67)$$

where the sum over  $\mathbf{R}$  is over all lattice vectors. Owing to the translational symmetry we may take  $A_{\alpha}(\mathbf{R}) = \exp(i\mathbf{k} \cdot \mathbf{R}) A_{\alpha}(0)$ , with  $\alpha = x, y$ , or  $z$ . Consequently,

$$\psi_{n\mathbf{k}}(\mathbf{r}) = \sum_{\mathbf{R}} \sum_{\alpha} A_{\alpha}(0) e^{i\mathbf{k} \cdot \mathbf{R}} p_{\alpha}(\mathbf{r} - \mathbf{R}) \quad (\alpha = x, y, \text{ or } z). \quad (9.68)$$

Table 9.5 *Decomposition of the IRs of  $O_h$  into the IRs of  $C_{3v}$  and  $C_{4v}$ . The first column is the IR of  $O_h$ . The second column is the decomposition into the IRs of  $C_{3v}$ . The numbers in parentheses are the dimensions of the representations. The third column is the decomposition into the IRs of  $C_{4v}$ .*

$\Gamma(l)$	IRs of $C_{3v}$	IRs of $C_{4v}$
$\Gamma_1(1)$	$\Lambda_1(1)$	$\Delta_1(1)$
$\Gamma_2(1)$	$\Lambda_2(1)$	$\Delta_2(1)$
$\Gamma_{12}(2)$	$\Lambda_3(2)$	$\Delta_1(1) + \Delta_2(1)$
$\Gamma_{15}(3)$	$\Lambda_1(1) + \Lambda_3(2)$	$\Delta_1(1) + \Delta_5(2)$
$\Gamma_{25}(3)$	$\Lambda_2(1) + \Lambda_3(2)$	$\Delta_2(1) + \Delta_5$
$\Gamma'_1(1)$	$\Lambda_1(2)$	$\Delta'_1(1)$
$\Gamma'_2(1)$	$\Lambda_1(1)$	$\Delta'_2(1)$
$\Gamma'_{12}(2)$	$\Lambda_3(2)$	$\Delta'_1(1) + \Delta'_2(1)$
$\Gamma'_{15}(3)$	$\Lambda_2(1) + \Lambda_3(2)$	$\Delta'_1(1) + \Delta_5(2)$
$\Gamma'_{25}(3)$	$\Lambda_1(1) + \Lambda_3(2)$	$\Delta'_2(1) + \Delta_5(2)$

Note that the wavefunction of (9.68) can be cast in the Bloch-wave form,  $\psi_{\mathbf{k}}(\mathbf{r}) = u_{\mathbf{k}}(\mathbf{r}) \exp(i\mathbf{k} \cdot \mathbf{r})$ , where  $u_{\mathbf{k}}(\mathbf{r}) = \sum_{\mathbf{R}} \sum_{\alpha} A_{\alpha}(0) e^{-i\mathbf{k} \cdot (\mathbf{r} - \mathbf{R})} p_{\alpha}(\mathbf{r} - \mathbf{R})$  is clearly invariant under any lattice-vector translation,  $\mathbf{r} \rightarrow \mathbf{r} + \mathbf{R}'$ .

The energies of the three bands are given by

$$E^{\alpha\beta\gamma}(\mathbf{k}) = \epsilon_p + 2(pp\sigma) \cos(k_{\alpha}a) + 2(pp\pi)[\cos(k_{\beta}a) + \cos(k_{\gamma}a)], \quad (9.69)$$

where  $\alpha, \beta$ , and  $\gamma$  are any of the three combinations  $k_x, k_y, k_z$ ;  $k_y, k_x, k_z$ ; or  $k_z, k_x, k_y$ , respectively. At  $\Gamma$ ,  $\mathbf{g}_{\mathbf{k}}$  is  $O_h$ . The three bands are degenerate, with  $E^{\alpha\beta\gamma}(\Gamma) = \epsilon_p + 2(pp\sigma) + 4(pp\pi)$ , and belong to the  $\Gamma_{15}(T_{1u})$  IR.

For  $\mathbf{k} = (k_x, 0, 0)$ ,  $\mathbf{k} = (0, k_y, 0)$ , or  $\mathbf{k} = (0, 0, k_z)$ ,  $\mathbf{g}_{\mathbf{k}}$  is isomorphic to the group  $C_{4v}$ , and the energies are

$$E^{xyz}(\Delta_1) = \epsilon_p + 2(pp\sigma) \cos(k_x a) + 4(pp\pi), \quad (9.70)$$

$$E^{yxz}(\Delta_5) = E^{zxy}(\Delta_5) = \epsilon_p + 2(pp\sigma) + 2(pp\pi)[\cos(k_x a) + 1]. \quad (9.71)$$

Along the  $\Delta$ -line, the three-fold degeneracy present at  $\Gamma$  evolves into a non-degenerate  $\Delta_1$  energy band and a two-fold degenerate  $\Delta_5$  energy band as indicated in Table 9.5. The wavefunctions are

$$\psi_{\Delta_1}(\mathbf{r}) = \frac{1}{N^{3/2}} \sum_{\mathbf{R}} e^{ik_x R_x} p_x(\mathbf{r} - \mathbf{R}), \quad (9.72)$$

$$\psi_{\Delta_5}^{(1)}(\mathbf{r}) = \frac{1}{N^{3/2}} \sum_{\mathbf{R}} e^{ik_x R_x} p_y(\mathbf{r} - \mathbf{R}), \quad (9.73)$$

$$\psi_{\Delta_5}^{(2)}(\mathbf{r}) = \frac{1}{N^{3/2}} \sum_{\mathbf{R}} e^{ik_x R_x} p_z(\mathbf{r} - \mathbf{R}), \quad (9.74)$$

where we assume periodic boundary conditions of order  $N$  along the  $x$ -,  $y$ -, and  $z$ -axes. The superscripts (1) and (2) indicate row-1 and row-2 partner functions for the  $\Delta_5$  IR, respectively.

Along the  $\Lambda$ -line  $k = k_x = k_y = k_z$ . The eigenvectors transform as  $\Lambda_1(A_1)$  and  $\Lambda_3(\mathcal{E})$ . The energies of the  $\Lambda_1$  and  $\Lambda_3$  bands are accidentally degenerate, with

$$E = \epsilon_p + [2(pp\sigma) + 4(pp\pi)] \cos(ka). \quad (9.75)$$

The wavefunctions can be generated using the symmetry-function-generating machine. We find that

$$\psi_{\Lambda_1}(\mathbf{r}) = \frac{1}{\sqrt{N^3}} \sum_{\mathbf{R}} e^{i(k_x R_x + k_y R_y + k_z R_z)} \frac{1}{\sqrt{3}} \sum_{\alpha} p_{\alpha}(\mathbf{r} - \mathbf{R}), \quad (9.76)$$

$$\psi_{\Lambda_5}^{(1)}(\mathbf{r}) = \frac{1}{\sqrt{N^3}} \sum_{\mathbf{R}} e^{i(k_x R_x + k_y R_y + k_z R_z)} \frac{1}{\sqrt{2}} [p_x(\mathbf{r} - \mathbf{R}) - p_y(\mathbf{r} - \mathbf{R})], \quad (9.77)$$

$$\begin{aligned} \psi_{\Lambda_5}^{(2)}(\mathbf{r}) = & \frac{1}{\sqrt{N^3}} \sum_{\mathbf{R}} e^{i(k_x R_x + k_y R_y + k_z R_z)} \\ & \times \frac{1}{\sqrt{6}} [p_x(\mathbf{r} - \mathbf{R}) + p_y(\mathbf{r} - \mathbf{R}) - 2p_z(\mathbf{r} - \mathbf{R})]. \end{aligned} \quad (9.78)$$

### 9.9.1 Representations of non-symmorphic space groups

A non-symmorphic space group,  $G$ , contains operations  $\{\alpha|\mathbf{R} + \mathbf{t}\}$ , where  $\mathbf{t}$  is not a lattice vector. Such an element can not be separated into a product of operators of  $G$  of the form  $\{E|\mathbf{R} + \mathbf{t}\}|\alpha|0\rangle$ , since  $\{E|\mathbf{R} + \mathbf{t}\}$  is not an operation of  $G$ . This feature does not change the procedure for obtaining the IRs of the group of the wavevector provided that  $\mathbf{k}$  does not lie on the boundary of the Brillouin zone. When  $\mathbf{k}$  lies on the zone boundary, special theoretical methods involving “multiplier groups” are required in order to effectively separate the representations of point-group operations from the translation representations. These methods will not be discussed here, but may be found in the literature [9.2, 9.3].

In any case, we note that the Bloch waves still form the basis for the representations and the space-group IRs are still derived from the usual point-group representations for the group of the  $\mathbf{k}$ -vector. However, the characters for operations involving  $\mathbf{t}$ , a non-lattice vector, may acquire an additional phase factor of the form  $\exp(i\mathbf{k} \cdot \mathbf{t})$ .

### 9.10 Energy bands in the plane-wave approximation

We consider the wavefunctions for a single electron in a crystal with a periodic potential  $V(\mathbf{r})$  that satisfy the Schrödinger eigenvalue equation,

$$\mathbb{H} \psi_{n\mathbf{k}} = \left[ -\frac{\hbar^2}{2m} \nabla^2 + V(\mathbf{r}) \right] \psi_{n\mathbf{k}} = E_{n\mathbf{k}} \psi_{n\mathbf{k}}, \quad (9.79)$$

where  $\psi_{n\mathbf{k}}$  is a normalized Bloch wave,

$$\psi_{n\mathbf{k}} = \frac{1}{\sqrt{\Omega}} e^{i\mathbf{k} \cdot \mathbf{r}} u_{n\mathbf{k}}(\mathbf{r}), \quad (9.80)$$

with  $\Omega$ , the normalization factor, equal to the volume of the crystal.

Substitution of (9.80) into Schrödinger's equation yields an equation for  $u_{n\mathbf{k}}$ ,

$$-\frac{\hbar^2}{2m} \left[ \nabla^2 - k^2 + 2i\mathbf{k} \cdot \nabla \right] u_{n\mathbf{k}} + V(\mathbf{r}) u_{n\mathbf{k}} = E_{n\mathbf{k}} u_{n\mathbf{k}}, \quad (9.81)$$

or

$$-\frac{\hbar^2}{2m} \nabla^2 u_{n\mathbf{k}} + \left[ V(\mathbf{r}) + \frac{\hbar^2}{m} i\mathbf{k} \cdot \nabla + \frac{\hbar^2 k^2}{2m} \right] u_{n\mathbf{k}} = E_{n\mathbf{k}} u_{n\mathbf{k}}. \quad (9.82)$$

The function  $u_{n\mathbf{k}}(\mathbf{r})$  can be expressed as a Fourier series in reciprocal-lattice space,

$$u_{n\mathbf{k}}(\mathbf{r}) = \sum_{\mathbf{K}} A_{n\mathbf{k}}(\mathbf{K}) e^{i\mathbf{K} \cdot \mathbf{r}}, \quad (9.83)$$

where  $A_{n\mathbf{k}}(\mathbf{K})$  are the expansion coefficients and  $\mathbf{K}$  runs over all of the reciprocal-lattice vectors. We see that the functions of (9.83) have the proper periodicity, since

$$u_{n\mathbf{k}}[\mathbf{r} + \mathbf{R}(l, m, n)] = \sum_{\mathbf{K}} A_{n\mathbf{k}}(\mathbf{K}) e^{i\mathbf{K} \cdot \mathbf{r}} e^{i\mathbf{K} \cdot \mathbf{R}(l, m, n)} = u_{n\mathbf{k}}(\mathbf{r}), \quad (9.84)$$

where we have used the fact that  $\exp[i\mathbf{K} \cdot \mathbf{R}(l, m, n)] = 1$ .

Using (9.83) in (9.82) gives

$$\sum_{\mathbf{K}} \left\{ \frac{\hbar^2}{2m} [\mathbf{K}^2 + \mathbf{k}^2 + 2\mathbf{k} \cdot \mathbf{K}] + V(\mathbf{r}) - E_{n\mathbf{k}} \right\} A_{n\mathbf{k}}(\mathbf{K}) e^{i\mathbf{K} \cdot \mathbf{r}} = 0. \quad (9.85)$$

Multiply (9.85) by  $(1/\Omega)^{1/2} \exp(-i\mathbf{K}' \cdot \mathbf{r})$  and integrate over all space to get

$$\left[ \frac{\hbar^2}{2m} (\mathbf{K}' + \mathbf{k})^2 - E_{n\mathbf{k}} \right] A_{n\mathbf{k}}(\mathbf{K}') = - \sum_{\mathbf{K}} V_{\mathbf{K}\mathbf{K}'} A_{n\mathbf{k}}(\mathbf{K}), \quad (9.86)$$

where

$$V_{\mathbf{K}\mathbf{K}'} = \frac{1}{\Omega} \int d\mathbf{r} V(\mathbf{r}) e^{i(\mathbf{K}-\mathbf{K}') \cdot \mathbf{r}}. \quad (9.87)$$

In obtaining (9.86) we have used the orthogonality of the plane waves, namely

$$\frac{1}{\Omega} \int d\mathbf{r} e^{i(\mathbf{K}-\mathbf{K}')\cdot\mathbf{r}} = \delta(\mathbf{K} - \mathbf{K}'). \quad (9.88)$$

From (9.87) it can be seen that  $V_{\mathbf{K}\mathbf{K}'}$  depends only on the vector difference  $\mathbf{K} - \mathbf{K}'$  and the diagonal matrix element, when  $\mathbf{K} = \mathbf{K}'$ , is a constant, and does not depend upon  $\mathbf{K}$  or  $\mathbf{K}'$ .  $V_{\mathbf{K}\mathbf{K}}$  is the integral of  $V(\mathbf{r})$  over the entire crystal divided by the crystal volume. Therefore  $V_{\mathbf{K}\mathbf{K}}$  is the average of  $V(\mathbf{r})$  over a unit cell. Since  $V_{\mathbf{K}\mathbf{K}}$  is independent of  $\mathbf{K}$ , we shall denote it by the symbol  $V_0$ .

The off-diagonal term,  $V_{\mathbf{K}\mathbf{K}'} = V_{(\mathbf{K}-\mathbf{K}')} = V_{\mathbf{K}''}$ , is the Fourier transform of  $V(\mathbf{r})$  for the component  $\mathbf{K}'' = \mathbf{K} - \mathbf{K}'$ . Thus increasing values of  $|\mathbf{K}''|$  measure increasingly rapid spatial variations of  $V(\mathbf{r})$  within the unit cell.

Equation (9.86) defines a matrix eigenvalue problem for the determination of the energy eigenvalues,  $E_{n\mathbf{k}}$ , and the Fourier expansion coefficients (eigenvectors),  $A_{n\mathbf{k}}(\mathbf{K})$ . The matrix equation is of degree  $N$  (of the order of the number of atoms in the crystal) and therefore actual solutions of (9.86) are not possible. In practice approximate solutions are found by truncating the equations for  $|\mathbf{K}''| > K_0$ , where  $K_0$  is an arbitrarily chosen number.

### 9.10.1 Constant potential

It is useful to investigate the energy bands for a constant potential,  $V(\mathbf{r}) = V_0$ . For this case the eigenvalue equation (9.86) reduces to

$$\left[ \frac{\hbar^2}{2m} (\mathbf{K}_n + \mathbf{k})^2 + V_0 - E_{n\mathbf{k}} \right] A_{n\mathbf{k}} = 0. \quad (9.89)$$

$\mathbf{K}_n$  is uncoupled to any other reciprocal-lattice vector. That is, the eigenvalue matrix is diagonal and the eigenvalues are

$$E_{n\mathbf{k}} = \frac{\hbar^2}{2m} (\mathbf{K}_n + \mathbf{k})^2 + V_0. \quad (9.90)$$

Each reciprocal-lattice vector  $\mathbf{K}_n$  has associated with it an energy band whose energy as a function of  $\mathbf{k}$  is given by (9.90). Here  $\mathbf{k}$  is a wavevector restricted to the first Brillouin zone. From (9.90) we can see that the energy bands for a non-zero  $V_0$  and for  $V = 0$  (called the empty-lattice model) are the same except for a constant shift in the zero of energy.

As an example, consider the energy bands for a simple cubic lattice and write

$$\mathbf{K}_n = \frac{2\pi}{a} (n_x, n_y, n_z), \quad (9.91)$$

$$\mathbf{k} = \frac{2\pi}{a} (\kappa_x, \kappa_y, \kappa_z), \quad (9.92)$$



where the components of  $\mathbf{n} = (n_x, n_y, n_z)$  are integers that specify the reciprocal-lattice vector,  $\mathbf{K}_n$ . The energy bands (9.90) can then be written in dimensionless form,

$$\begin{aligned}\epsilon_{n\kappa} &= \left(\frac{a}{2\pi}\right)^2 \left(\frac{2m}{\hbar^2}\right) (E_{n\kappa} - V_0) \\ &= (n_x + \kappa_x)^2 + (n_y + \kappa_y)^2 + (n_z + \kappa_z)^2.\end{aligned}\quad (9.93)$$

For the first energy band,  $\mathbf{n} = (0, 0, 0)$  and  $\epsilon_{(0,0,0)\kappa} = \kappa^2$ . For the next six lowest bands, having  $\mathbf{n} = (\pm 1, 0, 0)$ ,  $(0, \pm 1, 0)$ , and  $(0, 0, \pm 1)$ , the energies are given by

$$\epsilon_{(\pm 1, 0, 0)\kappa} = (1 \pm \kappa_x)^2 + \kappa_y^2 + \kappa_z^2, \quad (9.94)$$

$$\epsilon_{(0, \pm 1, 0)\kappa} = \kappa_x^2 + (\kappa_y \pm 1)^2 + \kappa_z^2, \quad (9.95)$$

$$\epsilon_{(0, 0, \pm 1)\kappa} = \kappa_x^2 + \kappa_y^2 + (\kappa_z \pm 1)^2. \quad (9.96)$$

The  $\mathbf{k}$ -vector is restricted to the first Brillouin zone, so for the simple cubic system  $-1/2 \leq \kappa_x, \kappa_y, \kappa_z \leq 1/2$ . The next 12 lowest bands are for  $\mathbf{n} = (\pm 1, \pm 1, 0)$ ,  $(\pm 1, 0, \pm 1)$ , and  $(0, \pm 1, \pm 1)$  (the plus and minus signs on the components may be chosen independently), and the energies are

$$\epsilon_{(\pm 1, \pm 1, 0)\kappa} = (1 \pm \kappa_x)^2 + (1 \pm \kappa_y)^2 + \kappa_z^2, \quad (9.97)$$

$$\epsilon_{(\pm 1, 0, \pm 1)\kappa} = (1 \pm \kappa_x)^2 + \kappa_y^2 + (1 \pm \kappa_z)^2, \quad (9.98)$$

$$\epsilon_{(0, \pm 1, \pm 1)\kappa} = \kappa_x^2 + (1 \pm \kappa_y)^2 + (1 \pm \kappa_z)^2. \quad (9.99)$$

For the cases of  $\kappa = (t, 0, 0)$  and  $\kappa = (t, t, 0)$  with  $t$  varying from 0 to 1/2 (i.e.,  $\mathbf{k}$  varies from  $\Gamma$  to  $X$  and  $\Gamma$  to  $M$ ) the lowest 19 energy bands are given in Table 9.6 and graphs are shown in Fig. 9.9.

*The statement  $E_{n\mathbf{k}} = E_{n(\mathbf{k}+\mathbf{K})}$  can lead to some confusion, particularly when dealing with the plane-wave approximation. Clearly the energy expressed in (9.90),  $E_{n\mathbf{k}} = (\hbar^2/(2m))(\mathbf{K}_n + \mathbf{k})^2 + V_0$ , is not equal to  $E_{n(\mathbf{k}+\mathbf{K})} = (\hbar^2/(2m))(\mathbf{K}_n + (\mathbf{k} + \mathbf{K}))^2 + V_0$ , unless  $\mathbf{K} = 0$ . The problem is that the expressions for the energies hold only for  $\mathbf{k}$  restricted to the first Brillouin zone and for the same band (same  $\mathbf{K}_n$ ). The energy given above for  $E_{n(\mathbf{k}+\mathbf{K})}$  is actually the energy for the band  $E_{n'\mathbf{k}}$ , where  $n'$  corresponds to the band whose reciprocal-lattice vector is  $\mathbf{K}_n + \mathbf{K}$ , that is, the energy for a different band. If we let  $\mathbf{k}$  go beyond the first Brillouin zone, then the energy bands simply repeat themselves, as shown in Fig. 9.10 for two bands along the  $\Gamma$ - $X$  direction.*

### 9.10.2 Reciprocal-lattice-vector and plane-wave representations of $g_{\mathbf{k}}$

The Bravais-lattice vectors and also the reciprocal-lattice vectors are bases for representations of the space group,  $G$ . The group of the  $\mathbf{k}$ -vector is a subgroup

Table 9.6 *Dimensionless energies and irreducible representations (a) for  $\kappa = (t, 0, 0)$ , with  $\mathbf{k}$  along the  $[100]$  direction, and (b) for  $\kappa = (t, t, 0)$ , with  $\mathbf{k}$  along the  $[110]$  direction. The degeneracy ( $D$ ) of a particular band is shown in column 4. The numerical band label (arbitrary) given in column 5 (BL) is used as identification in Fig. 9.9.*

(a) $\kappa = (t, 0, 0)$	$\epsilon_{\mathbf{n}\kappa}$	$\kappa + \mathbf{n} = (t + l, m, n)$	$D$	BL
$\Delta_1(A_1)$	$t^2$	$(t, 0, 0)$	1	1
$\Delta_1(A_1)$	$(t + 1)^2$	$(t + 1, 0, 0)$	1	4
$\Delta_1(A_1)$	$(t - 1)^2$	$(t - 1, 0, 0)$	1	2
$\Delta_1 + \Delta_2 + \Delta_5$	$t^2 + 1$	$(t, 1, 0), (t, 0, 1),$ $(t, -1, 0), (t, 0, -1)$	4	3
$\Delta_1 + \Delta_2 + \Delta_5$	$(t + 1)^2 + 1$	$(t + 1, 1, 0), (t + 1, -1, 0),$ $(t + 1, 0, 1), (t + 1, 0, -1)$	4	7
$\Delta_1 + \Delta_2 + \Delta_5$	$(t - 1)^2 + 1$	$(t - 1, 0, 1), (t - 1, 1, 0),$ $(t - 1, -1, 0), (t - 1, 0, -1)$	4	5
$\Delta_1 + \Delta_2 + \Delta_5$	$t^2 + 2$	$(t, 1, 1), (t, -1, 1),$ $(t, 1, -1), (t, -1, -1)$	4	6
(b) $\kappa = (t, t, 0)$	$\epsilon_{\mathbf{n}\kappa}$	$\kappa + \mathbf{n} = (t + l, t + m, n)$	$D$	BL
$\Sigma_1(A_1)$	$2t^2$	$(t, t, 0)$	1	1
$\Sigma_1(A_1) + \Sigma_2(A_2)$	$(t + 1)^2 + t^2$	$(t + 1, t, 0), (t, t + 1, 0)$	2	4
$\Sigma_1(A_1) + \Sigma_2(A_2)$	$(t - 1)^2 + t^2$	$(t - 1, t, 0), (t - 1, 0, t)$	2	2
$\Sigma_1(A_1) + \Sigma_3(B_1)$	$2t^2 + 1$	$(t, t, 1), (t, t, -1)$	2	3
$\Sigma_1(A_1)$	$2(t + 1)^2$	$(t + 1, t + 1, 0)$	1	9
$\Sigma_1(A_1)$	$2(t - 1)^2$	$(t - 1, t - 1, 0)$	1	5
$\Sigma_1(A_1) + \Sigma_3(B_1)$	$2(t^2 + 1)$	$(t + 1, t - 1, 0), (t - 1, t + 1, 0)$	2	7
$\Sigma_1 + \Sigma_2 + \Sigma_3 + \Sigma_4$	$(t + 1)^2 + t^2 + 1$	$(t, t + 1, \pm 1), (t + 1, t, \pm 1)$	4	8
$\Sigma_1 + \Sigma_2 + \Sigma_3 + \Sigma_4$	$(t - 1)^2 + t^2 + 1$	$(t, t - 1, \pm 1), (t - 1, t, \pm 1)$	4	6

of  $G$ , and therefore the dimensionless reciprocal-lattice vectors,  $\mathbf{n}$ , are also bases for representations of  $g_{\mathbf{k}}$ . The dimensionless reciprocal-lattice vectors  $\mathbf{n} + \kappa$  also are bases for representations of  $g_{\mathbf{k}}$ . Finally, of course, the Bloch waves are basis functions for a representation of the space group  $g_{\mathbf{k}}^s$ . In general, however, these representations are reducible. The energy bands are labeled by the IRs of the group of the  $\mathbf{k}$ -vector. We can find which energy bands are labeled by which IRs by decomposing the reducible representations into the IRs of  $g_{\mathbf{k}}$ . Since no point-group operation of  $g_{\mathbf{k}}$  changes the length of a vector, a representation of  $g_{\mathbf{k}}$  in terms of reciprocal-lattice vectors will involve only vectors having the same length. For example, the set of six vectors  $(\pm 1, 0, 0)$ ,  $(0, \pm 1, 0)$ ,  $(0, 0, \pm 1)$  provides bases for a six-dimensional reducible representation. However, if, instead,

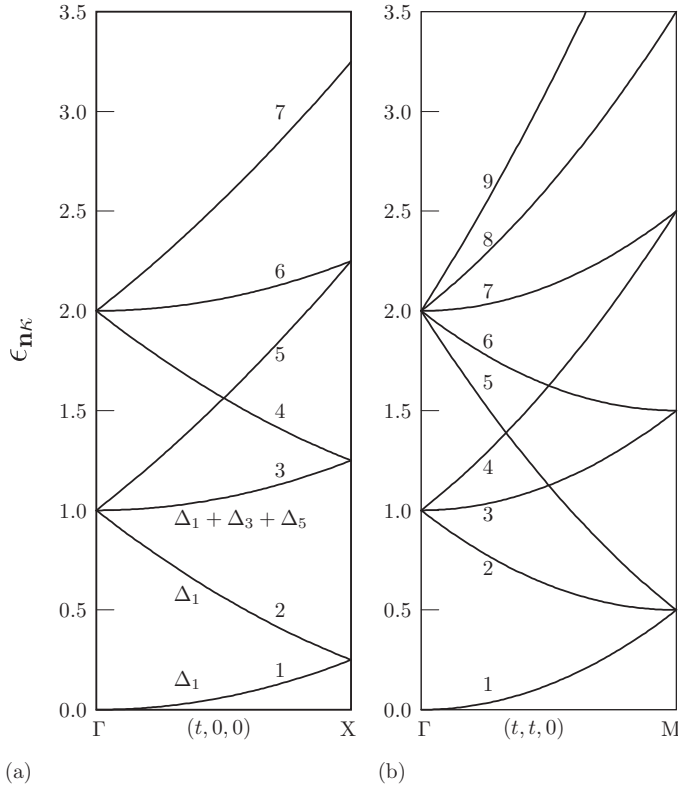


Figure 9.9 Energy bands for the simple-cubic lattice. The IRs and associated reciprocal-lattice-vector degeneracies for each band are shown in Table 9.6. (a) Energy bands  $\Gamma$ -X for  $\kappa = (t, 0, 0)$ . (b) Energy bands  $\Gamma$ -M for  $\kappa = (t, t, 0)$ .

we use the  $(\mathbf{K} + \mathbf{k})$ -vectors, we see that along the  $\Gamma$ -X line there are two different lengths,  $|(\kappa_x + 1, 0, 0)|$  and  $|(\kappa_x - 1, 0, 0)|$ , and four equal lengths  $|(\kappa_x, \pm 1, 0)|$  and  $|(\kappa_x, 0, \pm 1)|$ . Therefore, the  $(\mathbf{K} + \mathbf{k})$ -based representation is useful because it is already partially decomposed. The two representations based on  $(\kappa_x + 1, 0, 0)$  and  $(\kappa_x - 1, 0, 0)$  are one-dimensional, so they must be irreducible. The remaining four vectors are bases for a four-dimensional (reducible) representation. The Bloch waves  $\exp[i(\mathbf{K} + \mathbf{k}) \cdot \mathbf{r}]$  form a reducible representation that is the same as that associated with the  $(\mathbf{K} + \mathbf{k})$ -vectors. This follows because, if  $P_\alpha(\mathbf{K} + \mathbf{k}) = \alpha(\mathbf{K} + \mathbf{k})$ , then  $P_\alpha \exp[i(\mathbf{K} + \mathbf{k}) \cdot \mathbf{r}] = \exp\{i\alpha(\mathbf{K} + \mathbf{k}) \cdot \mathbf{r}\}$ . The decomposition of a reducible representation is accomplished in the usual manner by calculating the trace of the matrices or by using the symmetry-function-generating machine to find the linear combinations of the vectors which belong to a particular row of an IR of  $\mathbf{g}_k$ .

As an example let us find the IRs corresponding to the energy bands of Table 9.5 shown in Fig. 9.9. We start with the energy band corresponding to  $\kappa = (\kappa_x, 0, 0)$

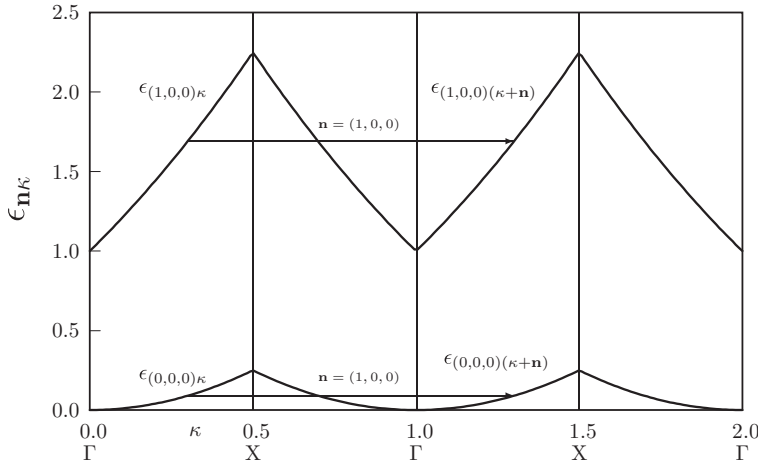


Figure 9.10 The extended Brillouin zone showing  $\epsilon_{n\kappa} = \epsilon_{n(\kappa+n)}$  (for band 1 and band 4 of Fig. 9.9) for a simple-cubic crystal along the  $\Gamma$ -X direction.

along the line  $\Gamma$ -X. The group of the  $\mathbf{k}$ -vector is  $C_{4v}$  and its operations are given in Table 9.2. The vector  $\mathbf{k} = (k_x, 0, 0)$  is invariant under all of the operations of  $\mathbf{g}_k$ . The vectors  $\mathbf{K} + \mathbf{k} = (2\pi/a)(1 \pm n_x, 0, 0)$  are also invariant under all of the operations of  $\mathbf{g}_k$  and therefore these IRs must belong to the totally symmetric IR,  $\Delta_1(A_1)$ . Each of the corresponding Bloch waves,  $\exp[i(2\pi/a)n_x x]$  and  $\exp[i(2\pi/a)(1 \pm n_x)x]$ , is a symmetry function for a  $\Delta_1$  IR.

The next set of vectors,  $(\kappa, \pm 1, 0)$  and  $(\kappa, 0, \pm 1)$ , is associated with degenerate states, and therefore these vectors are bases for a four-dimensional representation. To decompose the representation based on these vectors we need to find their behavior under the operations of  $C_{4v}$ . This can be conveniently accomplished using the action table in Appendix E, Table E.1. To employ the table we need to recognize that a reciprocal-lattice vector,  $(n_x, n_y, n_z)$ , transforms as  $(x, y, z)$  under the operations of the group. To simplify the notation, define  $(\kappa, 1, 0) = \mathbf{A}$ ,  $(\kappa, -1, 0) = \mathbf{B}$ ,  $(\kappa, 0, 1) = \mathbf{C}$ , and  $(\kappa, 0, -1) = \mathbf{D}$ . The action of  $P(i\tilde{C}_2^{(1)})$  on  $\mathbf{A}$ , for example, is, according to Table E.1,  $x \rightarrow x$ ,  $y \rightarrow -z$ , and  $z \rightarrow -y$ . Therefore  $(1, 1, 0) \rightarrow (1, 0, -1)$ , that is,  $\mathbf{A} \rightarrow \mathbf{D}$ . Table 9.7 shows the results of operating with the elements of  $C_{4v}$  on the four basis functions.

The characters shown in the last row of Table 9.7 are the sums of the number of functions that transform into themselves less the number going into the negative of themselves. The decomposition into the IRs of  $C_{4v}$  is  $\Gamma(\Delta) = \Delta_1 + \Delta_2 + \Delta_5$ . This result is also shown in Table 9.6 in the first column.

We can also determine the symmetry functions for the IRs of the decomposition by employing the symmetry-function-generating machine and Table 9.7. The (un-normalized) symmetry function for  $\Delta_1$  is  $f(\Delta_1) \propto (\mathbf{A} + \mathbf{B} + \mathbf{C} + \mathbf{D})$ . For the

Table 9.7 *The action table and characters of the four-dimensional representation of  $C_{4v}$  based on the vectors **A**, **B**, **C**, and **D**:  $(\kappa, 1, 0) = \mathbf{A}$ ,  $(\kappa, -1, 0) = \mathbf{B}$ ,  $(\kappa, 0, +1) = \mathbf{C}$ , and  $(\kappa, 0, -1) = \mathbf{D}$ . The characters for the four-dimensional representation are listed in the last row.*

$\Gamma(\Delta)$	$E$	$C_2^{(1)}$	$C_4^{(1)}$	$(C_4^{(1)})^3$	$iC_2^{(2)}$	$iC_2^{(3)}$	$i\bar{C}_2^{(1)}$	$\bar{C}_2^{(2)}$
<b>A</b>	<b>A</b>	<b>B</b>	<b>D</b>	<b>C</b>	<b>B</b>	<b>A</b>	<b>D</b>	<b>C</b>
<b>B</b>	<b>B</b>	<b>A</b>	<b>C</b>	<b>D</b>	<b>A</b>	<b>B</b>	<b>C</b>	<b>D</b>
<b>C</b>	<b>C</b>	<b>D</b>	<b>A</b>	<b>B</b>	<b>C</b>	<b>D</b>	<b>B</b>	<b>A</b>
<b>D</b>	<b>D</b>	<b>C</b>	<b>B</b>	<b>A</b>	<b>D</b>	<b>C</b>	<b>A</b>	<b>B</b>
$\chi$	4	0	0	0	2	2	0	0

$\Delta_2$  symmetry function,  $f(\Delta_2) \propto (\mathbf{A} + \mathbf{B} - \mathbf{C} - \mathbf{D})$ . To obtain the symmetry functions for  $\Delta_5$  we must use the matrix elements of the  $\mathcal{E}$  IR. These matrix elements are given in Appendix E, in Section E.4. Using the diagonal matrix elements of  $\mathcal{E}$  gives the row-1 function as  $f_1(\Delta_5) \propto (2\mathbf{A} + 2\mathbf{B} + \mathbf{C} + \mathbf{D})$ . The row-2 function is  $f_2(\Delta_5) \propto (2\mathbf{A} + 2\mathbf{B} - \mathbf{C} - \mathbf{D})$ . *These results should not be interpreted as a simple vector sum*, since, for example, the vector sum of  $\mathbf{A} + \mathbf{B} + \mathbf{C} + \mathbf{D} = (4\kappa, 0, 0)$ . To use the results, we note that the Bloch wavefunctions of the set  $\exp[i(2\pi/a)\mathbf{A} \cdot \mathbf{r}]$ ,  $\exp[i(2\pi/a)\mathbf{B} \cdot \mathbf{r}]$ ,  $\exp[i(2\pi/a)\mathbf{C} \cdot \mathbf{r}]$ , and  $\exp[i(2\pi/a)\mathbf{D} \cdot \mathbf{r}]$  transform under the operations of  $\mathbf{g}_{\mathbf{k}}$  in exactly the same way as **A**, **B**, **C**, and **D**. The utility of a result such as  $f(\Delta_1) \propto (\mathbf{A} + \mathbf{B} + \mathbf{C} + \mathbf{D})$  is that  $\psi_{\mathbf{k}}^{\Delta_1}(\mathbf{r}) \propto \{\exp[i(2\pi/a)\mathbf{A} \cdot \mathbf{r}] + \exp[i(2\pi/a)\mathbf{B} \cdot \mathbf{r}] + \exp[i(2\pi/a)\mathbf{C} \cdot \mathbf{r}] + \exp[i(2\pi/a)\mathbf{D} \cdot \mathbf{r}]\}$  is a symmetry function belonging to the  $\Delta_1$  IR of  $\mathbf{g}_{\mathbf{k}}$ . The sum of Bloch waves,  $\psi_{\mathbf{k}}^{\Delta_1}(\mathbf{r})$ , can be taken in a literal mathematical sense:

$$\begin{aligned} \psi_{\mathbf{k}}^{\Delta_1}(\mathbf{r}) &\propto \left[ e^{i(2\pi/a)\mathbf{A} \cdot \mathbf{r}} + e^{i(2\pi/a)\mathbf{B} \cdot \mathbf{r}} + e^{i(2\pi/a)\mathbf{C} \cdot \mathbf{r}} + e^{i(2\pi/a)\mathbf{D} \cdot \mathbf{r}} \right] \\ &= e^{ik_x x} \left[ \cos\left(\frac{2\pi y}{a}\right) + \cos\left(\frac{2\pi z}{a}\right) \right], \end{aligned} \quad (9.100)$$

where  $k_x$  is the  $x$ -component of the  $\mathbf{k}$ -vector,  $(2\pi\kappa/a)$ . Similarly,

$$\begin{aligned} \psi_{\mathbf{k}}^{\Delta_2}(\mathbf{r}) &\propto \left[ e^{i(2\pi/a)\mathbf{A} \cdot \mathbf{r}} + e^{i(2\pi/a)\mathbf{B} \cdot \mathbf{r}} - e^{i(2\pi/a)\mathbf{C} \cdot \mathbf{r}} - e^{i(2\pi/a)\mathbf{D} \cdot \mathbf{r}} \right] \\ &= e^{ik_x x} \left[ \cos\left(\frac{2\pi y}{a}\right) - \cos\left(\frac{2\pi z}{a}\right) \right], \end{aligned} \quad (9.101)$$

is a Bloch wave belonging to the  $\Delta_2$  IR of  $\mathbf{g}_{\mathbf{k}}$ . Since the Bloch waves are of the form  $\exp(i\mathbf{k} \cdot \mathbf{r}) u_{n\mathbf{k}}(\mathbf{r})$ , for the previous example  $u_{n\mathbf{k}}(\mathbf{r}) = [\cos(2\pi y/a) - \cos(2\pi z/a)]$ . The degeneracies evident in Table 9.6 hold for  $-1/2 < \kappa < 1/2$ , but change at the Brillouin-zone center and boundaries,  $\kappa = 0$  and  $\kappa = \pm 1/2$ . At  $\Gamma$

( $\mathbf{k} = \kappa = 0$ ), the degree of degeneracy is maximal, since all bands associated with  $\mathbf{K}$ -vectors of the same length are degenerate,  $\epsilon_{(0,0,0)0} = 0$ ,  $\epsilon_{(\pm 1,0,0)0} = \epsilon_{(\pm 1,0,0)0} = \epsilon_{(0,\pm 1,0)0} = 1$ , and  $\epsilon_{(\pm 1,\pm 1,0)0} = \epsilon_{(\pm 1,0,\pm 1)0} = \epsilon_{(0,\pm 1,\pm 1)0} = 2$ . At  $\Gamma$ ,  $\mathbf{g}_{\mathbf{k}} = O_h$  and the reducible representation,  $\Gamma^1$ , associated with the set of reciprocal vectors  $\{(\pm 1, 0, 0), (\pm 1, 0, 0), (0, \pm 1, 0)\}$  is six-dimensional. The decomposition is  $\Gamma^1 = \Gamma_{1g}(A_{1g}) + \Gamma_{3g}(\mathcal{E}_g) + \Gamma_{4u}(T_{1u})$ . As  $\mathbf{k}$  moves away from  $\kappa = 0$  along the  $[100]$  direction, the IRs of  $O_h$  evolve as determined by decomposing them into the IRs of  $C_{4v}$ :  $\Gamma_{1g}(A_1) \rightarrow \Delta_1(A_1)$ ,  $\Gamma_{3g}(\mathcal{E}_g) \rightarrow \Delta_1(A_1) + \Delta_2(B_1)$ , and  $\Gamma_{4u}(T_{1u}) \rightarrow \Delta_1(A_1) + \Delta_5(\mathcal{E})$ .

At  $\mathbf{k} = X = (\pi/a, 0, 0)$ ,  $\kappa = (1/2, 0, 0)$ . The group of the  $\mathbf{k}$ -vector increases in size because  $+\kappa$  and  $-\kappa$  are equivalent,  $\kappa = -\kappa + (1, 0, 0)$ , and the inversion operation is now a member of the group. As a result, the group of the  $\mathbf{k}$ -vector changes from  $C_{4v}$  (along  $\Delta$ ) to  $D_{4h}$  (at  $X$ ). To find the appropriate operations for  $\mathbf{g}_{\mathbf{k}}$  use Table E.1 and identify any operation that takes  $x$  into  $x$  or  $-x$ . There are eight such operations, namely  $E$ ,  $C_2^{(1)}$ ,  $C_2^{(2)}$ ,  $C_2^{(3)}$ ,  $C_4^{(1)}$ ,  $(C_4^{(1)})^3$ ,  $\bar{C}_2^{(1)}$ , and  $\bar{C}_2^{(2)}$ . Together with inversion, there are in total 16 operations in  $\mathbf{g}_{\mathbf{k}}$ . The character table for  $D_{4h}$  is shown in Table 9.8.

At  $X$  the energies are given by

$$\epsilon_{(l,m,n)\kappa} = \left(l + \frac{1}{2}\right)^2 + m^2 + n^2, \quad (9.102)$$

with  $\kappa = 1/2$ . The energies for the first 19 bands are

$$\epsilon_{(0,0,0)} = \epsilon_{(-1,0,0)} = \frac{1}{4}, \quad (9.103)$$

$$\epsilon_{(-1,\pm 1,0)} = \epsilon_{(-1,0,\pm 1)} = \epsilon_{(0,0,\pm 1)} = \epsilon_{(0,\pm 1,0)} = \frac{5}{4}, \quad (9.104)$$

$$\epsilon_{(1,0,0)} = \epsilon_{(-1,\pm 1,\pm 1)} = \epsilon_{(0,\pm 1,\pm 1)} = \frac{9}{4}. \quad (9.105)$$

The states at  $X$  associated with  $\mathbf{n} = (0, 0, 0)$  and  $(-1, 0, 0)$  having respectively  $\mathbf{n} + \kappa = (1/2, 0, 0)$  and  $\mathbf{n} + \kappa = (-1/2, 0, 0)$  are degenerate and correspond to Bloch waves  $\exp(+i\pi x/a)$  and  $\exp(-i\pi x/a)$ . These two waves are basis functions for  $\Gamma_a$ , a two-dimensional representation of  $\mathbf{g}_{\mathbf{k}}$ . Using Table E.1, we find the characters of the representation as shown in Table 9.8 for  $\Gamma_a$ .

Decomposition of  $\Gamma_a$  into the IRs of  $D_{4h}$  yields

$$\Gamma_a = X_{1g}(A_{1g}) + X_{4u}(A_{2u}). \quad (9.106)$$

The symmetry functions can be obtained by using the symmetry-function-generating machine operating on  $e^{i(\pi x/a)}$ . The results are  $f(X_{1g}) \propto \cos(\pi x/a)$  and  $f(X_{4u}) \propto \sin(\pi x/a)$ .

Table 9.8 The character table for  $D_{4h}$ . The operations of  $O_h$  corresponding to those of  $D_4$  are  $C_2^{(1)}$ ,  $C_4^{(1)}$ ,  $(C_4^{(1)})^3$ ,  $C_2^{(2)}$ ,  $C_2^{(3)}$ ,  $\bar{C}_2^{(1)}$ , and  $\bar{C}_2^{(2)}$ . At  $X$ ,  $\Gamma_a$  is the two-dimensional representation based on  $\mathbf{n} + \kappa = (1/2, 0, 0)$  and  $(-1/2, 0, 0)$ . At  $X$ ,  $\Gamma_b$  is the eight-dimensional representation based on  $\mathbf{n} + \kappa = (-1/2, \pm 1, 0)$ ,  $(-1/2, 0, \pm 1)$ ,  $(1/2, 0, \pm 1)$ , and  $(1/2, \pm 1, 0)$ . The last three rows show how  $x$ ,  $y$ , and  $z$  transform under the operations of  $D_{4h}$ . The matrices for the  $\mathcal{E}$  representation of  $D_{4h}$  are given at the bottom of the table.

$D_{4h}$	$E$	$C_2^{(1)}$	$C_4^{(1)}$	$(C_4^{(1)})^3$	$C_2^{(2)}$	$C_2^{(3)}$	$\bar{C}_2^{(1)}$	$\bar{C}_2^{(2)}$	$i$	$iC_2^{(1)}$	$iC_4^{(1)}$	$(iC_4^{(1)})^3$	$iC_2^{(2)}$	$iC_2^{(3)}$	$i\bar{C}_2^{(1)}$	$i\bar{C}_2^{(2)}$
$X_{1g}(A_{1g})$	1	1	1	1	1	1	1	1	1	1	1	1	1	1	1	1
$X_{4g}(A_{2g})$	1	1	1	1	-1	-1	-1	-1	1	1	1	1	-1	-1	-1	-1
$X_{2g}(B_{1g})$	1	1	-1	-1	1	1	-1	-1	1	1	-1	-1	1	1	-1	-1
$X_{3g}(B_{2g})$	1	1	-1	-1	-1	-1	1	1	1	1	-1	-1	-1	-1	1	1
$X_{5g}(\mathcal{E}_g)$	2	-2	0	0	0	0	0	0	2	-2	0	0	0	0	0	0
$X_{1u}(A_{1u})$	1	1	1	1	1	1	1	1	-1	-1	-1	-1	-1	-1	-1	-1
$X_{4u}(A_{2u})$	1	1	1	1	-1	-1	-1	-1	-1	-1	-1	-1	1	1	1	1
$X_{2u}(B_{1u})$	1	1	-1	-1	1	1	-1	-1	-1	-1	1	1	-1	-1	1	1
$X_{3u}(B_{2u})$	1	1	-1	-1	-1	-1	1	1	-1	-1	1	1	1	1	-1	-1
$X_{5u}(\mathcal{E}_u)$	2	-2	0	0	0	0	0	0	-2	2	0	0	0	0	0	0
$\Gamma_a$	2	2	2	2	0	0	0	0	0	0	0	0	2	2	2	2
$\Gamma_b$	8	0	0	0	0	0	0	0	0	0	0	0	4	4	0	0
$x$	$x$	$x$	$x$	$x$	$-x$	$-x$	$-x$	$-x$	$-x$	$-x$	$-x$	$-x$	$x$	$x$	$x$	$x$
$y$	$y$	$-y$	$-z$	$z$	$y$	$-y$	$z$	$-z$	$-y$	$y$	$z$	$-z$	$-y$	$y$	$-z$	$z$
$z$	$z$	$-z$	$y$	$-y$	$-z$	$z$	$y$	$-y$	$-z$	$z$	$-y$	$y$	$z$	$-z$	$-y$	$y$

$\mathcal{E}$  matrices. Basis functions are  $y$  and  $z$ .

$$\mathcal{E} = \begin{pmatrix} 1 & 0 \\ 0 & 1 \end{pmatrix}, C_2^{(1)} = \begin{pmatrix} -1 & 0 \\ 0 & -1 \end{pmatrix}, C_4^{(1)} = \begin{pmatrix} 0 & -1 \\ 1 & 0 \end{pmatrix}, (C_2^{(1)})^3 = \begin{pmatrix} 0 & 1 \\ -1 & 0 \end{pmatrix},$$

$$C_2^{(2)} = \begin{pmatrix} 1 & 0 \\ 0 & -1 \end{pmatrix}, C_2^{(3)} = \begin{pmatrix} -1 & 0 \\ 0 & 1 \end{pmatrix}, \bar{C}_2^{(1)} = \begin{pmatrix} 0 & 1 \\ 1 & 0 \end{pmatrix}, \bar{C}_2^{(2)} = \begin{pmatrix} 0 & -1 \\ -1 & 0 \end{pmatrix}.$$

The states at X for  $\mathbf{n} = (-1, \pm 1, 0)$ ,  $(-1, 0, \pm 1)$ ,  $(0, 0, \pm 1)$ , and  $(0, \pm 1, 0)$  with  $\kappa = (1/2, 0, 0)$  are also degenerate and correspond to the eight Bloch waves

$$e^{i\left(\frac{2\pi}{a}\right)\left[\frac{x}{2} \pm y\right]}, \quad (9.107)$$

$$e^{i\left(\frac{2\pi}{a}\right)\left[\frac{x}{2} \pm z\right]}, \quad (9.108)$$

$$e^{i\left(\frac{2\pi}{a}\right)\left[-\frac{x}{2} \pm y\right]}, \quad (9.109)$$

$$e^{i\left(\frac{2\pi}{a}\right)\left[-\frac{x}{2} \pm z\right]}. \quad (9.110)$$

These Bloch waves form an eight-dimensional reducible representation,  $\Gamma_b$ , of  $g_k$ . The characters of  $\Gamma_b$  can be determined using the transformation properties of  $x$ ,  $y$ , and  $z$  as shown in Table 9.8.

For example,  $P(iC_2^{(2)})(x, y, z) \rightarrow P_i(-x, y, -z) = (x, -y, z)$ , therefore

$$P(iC_2^{(2)})e^{i\left(\frac{2\pi}{a}\right)\left[\frac{x}{2} \pm y\right]} \rightarrow e^{i\left(\frac{2\pi}{a}\right)\left[\frac{x}{2} \mp y\right]}, \quad (9.111)$$

$$P(iC_2^{(2)})e^{i\left(\frac{2\pi}{a}\right)\left[\frac{x}{2} \pm z\right]} \rightarrow e^{i\left(\frac{2\pi}{a}\right)\left[\frac{x}{2} \pm z\right]}, \quad (9.112)$$

$$P(iC_2^{(2)})e^{i\left(\frac{2\pi}{a}\right)\left[-\frac{x}{2} \pm y\right]} \rightarrow e^{i\left(\frac{2\pi}{a}\right)\left[-\frac{x}{2} \mp y\right]}, \quad (9.113)$$

$$P(iC_2^{(2)})e^{i\left(\frac{2\pi}{a}\right)\left[-\frac{x}{2} \pm z\right]} \rightarrow e^{i\left(\frac{2\pi}{a}\right)\left[-\frac{x}{2} \pm z\right]}. \quad (9.114)$$

Only the functions in (9.112) and (9.114) are transformed into themselves, so the character of  $P(iC_2^{(2)}) = 4$ . Proceeding in this way, we find the characters listed for  $\Gamma_b$  in Table 9.8. The decomposition of  $\Gamma_b$  into the IRs of  $D_{4h}$  is

$$\Gamma_b = X_{1g}(A_{1g}) + X_{4u}(A_{2u}) + X_{2g}(B_{1g}) + X_{3u}(B_{2u}) + X_{5g}(\mathcal{E}_g) + X_{5u}(\mathcal{E}_u). \quad (9.115)$$

Some texts use the notation “+” and “−” instead of “ $g$ ” and “ $u$ ”, for example  $X_1^+$  and  $X_5^-$  instead of  $X_{1g}$  and  $X_{5u}$ . The symmetry functions for these representations can be generated from the function  $\exp\{i(2\pi/a)[x/2 + y]\}$ . The results are

$$f(X_{1g}) \propto \cos\left(\frac{\pi x}{a}\right) \left[ \cos\left(\frac{2\pi y}{a}\right) + \cos\left(\frac{2\pi z}{a}\right) \right], \quad (9.116)$$

$$f(X_{4u}) \propto \sin\left(\frac{\pi x}{a}\right) \left[ \cos\left(\frac{2\pi y}{a}\right) + \cos\left(\frac{2\pi z}{a}\right) \right], \quad (9.117)$$

$$f(X_{2g}) \propto \cos\left(\frac{\pi x}{a}\right) \left[ \cos\left(\frac{2\pi y}{a}\right) - \cos\left(\frac{2\pi z}{a}\right) \right], \quad (9.118)$$

$$f(X_{3u}) \propto \sin\left(\frac{\pi x}{a}\right) \left[ \cos\left(\frac{2\pi y}{a}\right) - \cos\left(\frac{2\pi z}{a}\right) \right], \quad (9.119)$$



$$f(X_{5g}) \text{ row-1} \propto \sin\left(\frac{\pi x}{a}\right) \sin\left(\frac{2\pi z}{a}\right), \quad (9.120)$$

$$f(X_{5g}) \text{ row-2} \propto \sin\left(\frac{\pi x}{a}\right) \sin\left(\frac{2\pi y}{a}\right), \quad (9.121)$$

$$f(X_{5u}) \text{ row-1} \propto \cos\left(\frac{\pi x}{a}\right) \sin\left(\frac{2\pi y}{a}\right), \quad (9.122)$$

$$f(X_{5u}) \text{ row-2} \propto \cos\left(\frac{\pi x}{a}\right) \sin\left(\frac{2\pi z}{a}\right). \quad (9.123)$$

The symmetry functions for the  $\mathcal{E}$  IR are found from the matrix elements given in Table 9.8 using the functions  $\exp\{i(2\pi/a)[x/2 + y]\}$  and  $\exp\{i(2\pi/a)[x/2 + z]\}$  as initial generating functions. The symmetry functions are the zeroth-order (constant-potential) wavefunctions for the energy band states. Since they are constructed from degenerate functions, the energies of the symmetry functions are also degenerate. Degeneracy associated with functions belonging to different IRs is “accidental” degeneracy. If we now allow  $V(\mathbf{r})$  to be non-constant so that at least some matrix elements,  $V_{\mathbf{K}\mathbf{K}'}$ , other than  $\mathbf{K} = \mathbf{K}'$  are non-zero then these matrix elements will alter the energies and lift the accidental degeneracies. We know that there can be no non-zero matrix elements between states that belong to different IRs. Therefore bands of different IRs may cross. Two bands with the same IR (and same row) may, and usually will, have non-zero interactions (matrix elements between them). As a result, we expect degenerate bands of the same IRs to repel one another near intersection. This leads to energy gaps, particularly at points of high symmetry. For example, in Fig. 9.9(a), bands 1 and 2 belong to the  $\Delta_1$  IR. These bands become degenerate at the X point. Hence one expects that, to first order, the secular equation would be of the form

$$\det \begin{vmatrix} E_0 - \epsilon & M_{12} \\ M_{12}^* & E_0 - \epsilon \end{vmatrix} \begin{pmatrix} f_1 \\ f_2 \end{pmatrix} = 0, \quad (9.124)$$

where  $f_1$  and  $f_2$  are the zeroth-order wavefunctions,  $M_{12}$  is the matrix element between them, and  $E_0$  is the degenerate energy at X for  $M_{12} = 0$ . The wavefunctions are then  $\psi^\pm \propto f_1 \pm f_2$  and the energies are  $\epsilon = E_0 \pm |M_{12}|$ . Thus an energy gap of  $2|M_{12}|$  develops at X. According to (9.106) the degenerate states split into  $X_{1g}(A_{1g}) + X_{4u}(A_{2u})$ , where  $X_{1g} \propto f_1 + f_2$  and  $X_{4u} \propto f_1 - f_2$ . Figure 9.11 is a schematic diagram of energy bands showing the gaps that develop when there are non-zero matrix elements between bands with the same IR.

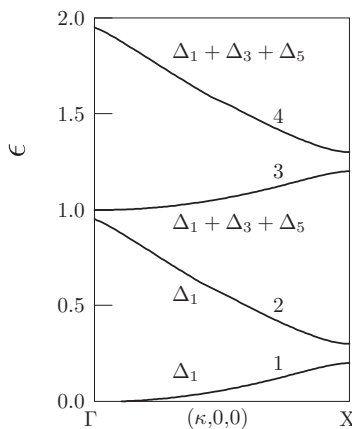


Figure 9.11 Gap formation. Two bands belonging to the same IR interact and repel one another, forming an energy gap. Shown is a schematic diagram of  $\Delta_1$  bands forming gaps at  $\Gamma$  and X.

### References

- [9.1] M. S. Dresselhaus, G. Dresselhaus, and A. Jorio, *Group Theory Application to the Physics of Condensed Matter* (Berlin: Springer-Verlag, 2008).
- [9.2] M. Lax, *Symmetry Principles in Solid-State and Molecular Physics* (New York: Wiley, 1974).
- [9.3] P. Jacobs, *Group Theory with Applications in Chemical Physics* (Cambridge: Cambridge University Press, 2005).

### Exercises

- 9.1 Consider a lattice vector,  $\mathbf{V} = r\mathbf{a} + s\mathbf{b} + t\mathbf{c}$ , and the reciprocal-lattice vector,  $\mathbf{V}^* = h\mathbf{a}^* + k\mathbf{b}^* + l\mathbf{c}^*$ , and show that  $\mathbf{V} \cdot \mathbf{V}^* = 2\pi(hr + ks + lt)$ .
- 9.2 (a) For face-centered cubic crystals each primitive cube has atoms on each of its eight corners and atoms at the center of each of the six faces. How many atoms are there per unit cell?  
 (b) Give a set of coordinates for basis atoms of the unit cell.  
 (c) The primitive direct-lattice vectors for the body-centered cubic lattice are given in Table 9.1. Using the equations in (9.27), calculate the primitive reciprocal-lattice vectors.
- 9.3 (a) The important energy bands for perovskite crystals such as  $\text{SrTiO}_3$  and  $\text{KTaO}_3$  are derived from the  $d$ -orbitals of the transition metal ions and the  $p$ -orbitals of the oxygen ions. How many  $p$ - $d$  energy bands are associated with these orbitals?  
 (b) Consider an electron in a simple-cubic crystal having lattice constant  $a = 3.5 \text{ \AA}$  with  $V(\mathbf{r}) = 0$  (empty lattice). What energy bands

(reciprocal-lattice vectors) are included in the range  $0 \leq E_{\mathbf{K}\mathbf{k}} \leq 100$  eV at  $\Gamma$  in the first Brillouin zone?

- 9.4 A plane may be defined by its intercepts with the axes of the primitive vectors  $\mathbf{a}$ ,  $\mathbf{b}$ , and  $\mathbf{c}$ . Denote these intercepts as  $i_{\mathbf{a}}$ ,  $i_{\mathbf{b}}$ , and  $i_{\mathbf{c}}$ . The *Miller indices*,  $(hkl)$ , for the set of parallel planes are obtained from the reciprocals of the intercepts:  $h = (\alpha a/i_{\mathbf{a}})$ ,  $k = (\alpha b/i_{\mathbf{b}})$ , and  $l = (\alpha c/i_{\mathbf{c}})$ , where  $a$ ,  $b$ , and  $c$  are the lattice constants, and  $\alpha$  is an integer chosen so that  $h$ ,  $k$ , and  $l$  are the smallest integers having the same ratios as the reciprocal intercepts. For example, a plane,  $P$ , with intercepts  $\mathbf{a}$ ,  $2\mathbf{b}$ , and  $3\mathbf{c}$  has reciprocal intercepts  $a$ ,  $b/2$ , and  $c/3$ , so  $\alpha = 6$  and  $(hkl) = (632)$ . The Miller indices are the same for all planes parallel to  $P$  (not containing the origin), and therefore specify a **set** of parallel planes.
- Find the Miller indices for the sets of planes whose intercepts  $i_{\mathbf{a}}$ ,  $i_{\mathbf{b}}$ , and  $i_{\mathbf{c}}$  are respectively  $2a$ ,  $3b$ ,  $5c$ ;  $2a$ ,  $2b$ ,  $0c$ ; and  $a$ ,  $b$ ,  $2c$ .
  - Show that the reciprocal-lattice vector  $\mathbf{K}(hkl) = h\mathbf{a}^* + k\mathbf{b}^* + l\mathbf{c}^*$  is perpendicular to the set of parallel planes designated by the Miller indices  $(hkl)$ .
  - Using the general equation  $\mathbf{K}(p_1, p_2, p_3) \cdot \mathbf{R}(m_1, m_2, m_3) = 2\pi n$ , where  $p_i$ ,  $m_i$ , and  $n$  are integers, show that the distance from the origin to the closest  $(hkl)$  plane is given by  $2\pi/|\mathbf{K}(hkl)|$ .
  - Show that the spacing between consecutive  $(hkl)$  planes is uniform.
  - What is the spacing between  $(123)$  planes for a cubic lattice with lattice constant  $a$ ?
- 9.5 X-rays incident on a crystal scatter from the electrons of the atoms causing interference patterns. The electron charge density,  $\rho(\mathbf{r})$ , must be a periodic function, and therefore can be represented as a Fourier series in reciprocal-lattice vectors,

$$\rho(\mathbf{r}) = \sum_{\mathbf{K}} \rho(\mathbf{K}) e^{i\mathbf{K} \cdot \mathbf{r}}.$$

- Show that the probability,  $P_{\mathbf{k}\mathbf{k}'}$ , that an initial X-ray with wavefunction  $(1/V)^{1/2} \exp(i\mathbf{k} \cdot \mathbf{r})$  is scattered by  $\rho(\mathbf{r})$  into the final state  $(1/V)^{1/2} \exp(i\mathbf{k}' \cdot \mathbf{r})$  is proportional to

$$P_{\mathbf{k}\mathbf{k}'} = \sum_{\mathbf{K}} \rho(\mathbf{K}) \delta(\mathbf{k}' - \mathbf{k} - \mathbf{K}),$$

where  $\delta(\mathbf{k}' - \mathbf{k} - \mathbf{K}) = 1$  for  $\mathbf{k}' - \mathbf{k} = \mathbf{K}$  and 0 otherwise.

- From (a) we see that the maxima for  $P_{\mathbf{k}\mathbf{k}'}$  occur for  $\mathbf{k}' - \mathbf{k} = \mathbf{K}$  (if  $\rho(\mathbf{K})$  is not zero). If the energy of the X-ray is conserved (elastic scattering),

show that the maxima occur according to Bragg's interference equation,  $2d \sin \theta = \lambda$ . Here,  $\theta$  is the angle between  $\mathbf{k}$  and the lattice plane,  $P$ , whose normal is  $\mathbf{K}$ , and  $d$  is the spacing between planes parallel to  $P$ .

- 9.6 Prove that the reciprocal lattice of the body-centered cubic Bravais lattice is the face-centered cubic lattice using the primitive lattice vectors and the definitions of  $\mathbf{a}^*$ ,  $\mathbf{b}^*$ , and  $\mathbf{c}^*$ .
- 9.7 For a cubic Bravais lattice consider the plane-wave approximation (Table 9.6) for constant  $V$  for energy bands along the  $\Lambda$ -line.
- (a) Show that the (dimensionless) energy is

$$\epsilon_{\mathbf{n}\kappa} = 3\kappa^2 + 2\kappa(n_x + n_y + n_z) + n_x^2 + n_y^2 + n_z^2.$$

- (b) Calculate  $\epsilon_{\mathbf{n}\kappa}$  for the eight reciprocal-lattice vectors  $\mathbf{K}(a/(2\pi)) = \mathbf{n} = (n_x, n_y, n_z) = (\pm 1, \pm 1, \pm 1)$ , and construct a table similar to Table 9.6 showing the energy and which bands are degenerate.
- (c) Identify the IRs for each group of degenerate states.
- 9.8 For the representation based on the functions  $A = \exp[i(2\pi/a)(\kappa + 1, \kappa + 1, \kappa - 1) \cdot \mathbf{r}]$ ,  $B = \exp[i(2\pi/a)(\kappa + 1, \kappa - 1, \kappa + 1) \cdot \mathbf{r}]$ , and  $C = \exp[i(2\pi/a)(\kappa - 1, \kappa + 1, \kappa + 1) \cdot \mathbf{r}]$ , do the following.
- (a) Find the symmetry functions for the  $\Lambda_1(A_1)$  and  $\Lambda_3(\mathcal{E})$  IRs.
- (b) Identify the  $u_{\mathbf{n}\kappa}(\mathbf{r})$  functions of the Bloch waves.
- (c) Plot a graph of the dimensionless energy  $\epsilon_{\mathbf{n}\kappa}$  versus  $\kappa$  for these energy bands.
- 9.9 (a) For a body-centered cubic lattice with constant lattice potential show that the band energies are given by

$$\begin{aligned} \epsilon_{\mathbf{n}\kappa} &= \left(\frac{a}{2\pi}\right)^2 \left(\frac{2m}{\hbar^2}\right) [E_{\mathbf{n}\kappa} - V_0] \\ &= (\kappa_x + n_b + n_c)^2 + (\kappa_y + n_a + n_c)^2 + (\kappa_z + n_a + n_b)^2, \end{aligned}$$

where  $\kappa = (a/2\pi)(k_x, k_y, k_z)$  and  $\mathbf{K}_n(a/(2\pi)) = (a/(2\pi))[n_a\mathbf{a}^* + n_b\mathbf{b}^* + n_c\mathbf{c}^*]$ .

- (b) What is the group of the wavevector for  $\mathbf{k}$  along the  $\Sigma$ -line (excluding  $\Gamma$  and  $N$ ), that is, for  $\kappa = (t, t, 0)$ ?
- (c) Along the  $\Sigma$ -line,  $\mathbf{k} = (2\pi/a)(t, t, 0)$  ( $\kappa = (t, t, 0)$ ,  $0 < t < 1/2$ ). Find the energy,  $\epsilon_{\mathbf{n}\kappa}$ , for the smallest and second-smallest vectors of the form  $\mathbf{K} + \mathbf{k}$ .
- (d) Show that each of these vectors is a basis vector for the  $\Sigma_1$  IR, and determine the Bloch waves for the IRs of (c).

- (e) Find the third-smallest vectors of the form  $\mathbf{K} + \mathbf{k}$  and decompose the representation based on these vectors into the IRs of  $\mathbf{g}_{\mathbf{k}}$  and determine  $\epsilon_{n\kappa}$ .
- (f) Determine the Bloch waves for each IR in (e).
- (g) Plot a graph of  $\epsilon_{n\kappa}$  for the states in (c) and (e) for  $t = 0$  to  $1/2$  ( $\mathbf{k}$  from  $\Gamma$  to  $N$ ).

# 10

## Application of space-group theory: Energy bands for the perovskite structure

In Chapter 9 nearly free-electron energy bands were discussed. In this chapter we discuss the energy bands of a crystal for which the electronic states are derived from atomic-like orbitals. For molecules this approach is the LCAO model. Applied to crystalline solids, it is referred to as the *tight-binding model*. In either case the wavefunctions are linear combinations of atomic-like orbitals. We shall analyze the energy bands of a class of perovskite oxides known as the *d*-band perovskites.<sup>1</sup>

### 10.1 The structure of the $ABO_3$ perovskites

We consider the cubic  $ABO_3$  oxides having the perovskite structure with the *transition metal*  $B$  ions. Examples include insulators, such as  $SrTiO_3$ ,  $BaTiO_3$ , and  $KTaO_3$ , and metals, such as  $NaWO_3$  and  $ReO_3$  (a perovskite without an  $A$  ion). The structure of these oxides is shown in Fig. 10.1. Many oxides (e.g.,  $BaTiO_3$  and  $SrTiO_3$ ) undergo structural phase transitions at lower temperatures, leading to non-cubic lattices and ferroelectric and piezoelectric properties. Here we are concerned with the cubic phase.

As illustrated in Fig. 10.1, the  $B$  ions are at the center of a cube, the oxygen ions are on the faces of a cube, and the  $A$  ions are on the corners of a cube.

The five ions of the unit cell are labeled  $A$ ,  $B$ , 2, 3, and 5 in Fig. 10.1. The origin is taken at the  $B$  site and the oxygen ions are located at  $a(1, 0, 0)$ ,  $a(0, 1, 0)$ , and  $a(0, 0, 1)$ . The  $A$  ion is located at  $a(1, 1, 1)$ , where  $2a$  is the lattice constant. For the crystal as a whole, the  $B$  ions are on a cubic lattice whose sites are at  $a(2n_x, 2n_y, 2n_z)$ , the oxygen ions are located at  $a(2n_x + 1, 2n_y, 2n_z)$ ,  $a(2n_x, 2n_y + 1, 2n_z)$ , and  $a(2n_x, 2n_y, 2n_z + 1)$ , and the  $A$  ions are at  $a(2n_x + 1, 2n_y + 1, 2n_z + 1)$ , where  $n_x$ ,  $n_y$ , and  $n_z$  are positive or negative integers or zero.

<sup>1</sup> Perovskites for which electron–electron correlation is strong can not be described by band theory. This includes many of the insulating and magnetic perovskites.

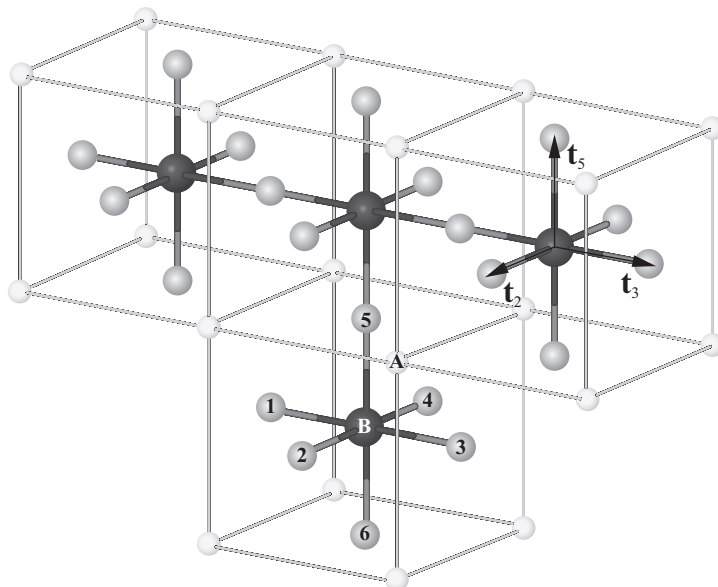


Figure 10.1 The  $ABO_3$  perovskite structure. The  $B$  ions are at the centers of the cubes. The  $O$  ions are on the faces of the cubes. The  $A$  ions are at the corners of the cubes. The five ions comprising the unit cell are labeled  $B$ ,  $A$ , and 2, 3, and 5 (oxygen ions). The numbering of the oxygen ions is chosen so that the action table in Appendix E may be used. The vectors  $\mathbf{t}_2 = a\mathbf{e}_x$ ,  $\mathbf{t}_3 = a\mathbf{e}_y$ , and  $\mathbf{t}_5 = a\mathbf{e}_z$  join the  $B$  ion to the oxygen ions in a unit cell.

The electronic binding of the  $d$ -band perovskites includes both ionic and covalent contributions. The chemically important energy bands are derived from the  $d$ -orbitals of the transition metal ion ( $B$  ion) and the  $p$ -orbitals of the oxygen ions. The energy bands associated with the  $A$  ions, usually derived from their  $s$ -orbitals, are at higher energies. Typically, the  $A$ -ion energy bands are unoccupied by electrons and do not contribute strongly to the electronic or chemical properties. That is not to say that the  $A$  ions are unimportant. The ionic charge of the  $A$  ion plays a central role in determining the relative energies of the  $d$ - and  $p$ -orbitals, and its ionic radius has a strong influence on the stability of the structure. For a more complete discussion of the  $d$ -band perovskites the reader is directed to the literature [10.1].

The Bravais lattice is simple cubic. The  $B$  ions are surrounded by 6 oxygen ions, and the  $A$  ions are surrounded by 12 oxygens. Both the  $B$  ions and the  $A$  ions are at sites of cubic ( $O_h$ ) symmetry. The oxygen ions, however, are at sites with  $D_{4h}$  symmetry. As a result, the  $p$ -orbitals divide into two groups. Those whose lobes are parallel to the  $B$ – $O$  axis form  $\sigma$ -bonds with the  $d$ -orbitals, and those whose lobes are perpendicular to the  $B$ – $O$  axis form  $\pi$ -bonds with the  $d$ -orbitals. Since the environment (symmetry) of the sigma  $p$ -orbitals differs from

that of the pi  $p$ -orbitals the LCAO diagonal energies will be different. The  $d$ -ion orbitals separate into the  $t_{2g}$  and  $e_g$  types due to the octahedral arrangement of the oxygen ions.

## 10.2 Tight-binding wavefunctions

The LCAO method discussed in connection with molecular wavefunctions in previous chapters can be applied to crystals. The method is most useful for compounds whose properties strongly reflect the character of the atomic structure of its constituents, that is, when the energy bands can be associated with the atomic states of the ions of the crystal.

Neglecting the  $A$  ion, the perovskite unit cell includes the five  $d$ -orbitals of the  $B$  ion and nine  $p$ -orbitals (three for each of the three oxygen ions). This makes a total of 14 orbitals, so there will be 14 energy bands for the crystal.

The one-electron Hamiltonian is of the form

$$\mathbb{H}(\mathbf{r}) = \sum_m \left\{ \mathbb{H}_B(\mathbf{r} - \mathbf{R}_m) + \sum_i \mathbb{H}_O(\mathbf{r} - \mathbf{R}_m - \mathbf{t}_i) \right\} + V_{\text{int}}(\mathbf{r}), \quad (10.1)$$

where  $\mathbb{H}_B(\mathbf{r} - \mathbf{R}_m)$  is the atomic Hamiltonian for an isolated  $B$  ion located at  $\mathbf{R}_m$ ,  $\mathbb{H}_O(\mathbf{r} - \mathbf{R}_m - \mathbf{t}_i)$  is the atomic Hamiltonian for an isolated oxygen ion located at  $\mathbf{R}_m + \mathbf{t}_i$ , and  $V_{\text{int}}(\mathbf{r})$  is the effective potential due to interactions between the ions. The vectors  $\mathbf{t}_i$ ,  $i = 2, 3$ , and  $5$ , are vectors from the origin to the O ions labeled 2, 3, and 5 in Fig. 10.1.

Because of translational invariance, the crystalline wavefunctions are characterized by a wavevector,  $\mathbf{k}$ , just as in the case of the nearly free electrons in the previous chapter. The amplitudes of the orbitals in different unit cells can differ at most by a phase factor. From the space-group results of Chapter 9, we know that the phase factor for translation by a lattice vector  $\mathbf{R}$  is  $\exp(i\mathbf{k} \cdot \mathbf{R})$ .

The LCAO or tight-binding wavefunction has the form

$$\psi_{\mathbf{k}}(\mathbf{r}) = \sum_{\mathbf{R}_m} e^{i\mathbf{k} \cdot \mathbf{R}_m} \left\{ \sum_{\alpha} A_{\mathbf{k}\alpha} \phi_{d\alpha}(\mathbf{r} - \mathbf{R}_m) + \sum_i \sum_{\beta} B_{\mathbf{k}\beta i} \phi_{p\beta}[\mathbf{r} - (\mathbf{R}_m + \mathbf{t}_i)] \right\}. \quad (10.2)$$

In (10.2),  $\mathbf{R}_m$  is a lattice vector from the origin to a  $B$  ion and  $\mathbf{t}_i$  is a vector from the  $B$  ion to an oxygen ion. For the unit cell at  $\mathbf{R}_m$ , the three oxygen sites are at  $\mathbf{R}_m + \mathbf{t}_i$  with  $i = 2, 3$ , or  $5$ . The terms  $A_{\mathbf{k}\alpha} \exp(i\mathbf{k} \cdot \mathbf{R}_m)$  and  $B_{\mathbf{k}\beta i} \exp(i\mathbf{k} \cdot \mathbf{R}_m)$  are the amplitudes of the  $d_{\alpha}$  and  $p_{\beta}$  orbitals located at  $\mathbf{R}_m$  and  $\mathbf{R}_m + \mathbf{t}_i$ , respectively. In this case,  $\alpha$  denotes one of the five  $d$ -orbitals,  $d_{xy}$ ,  $d_{xz}$ ,  $d_{yz}$ ,  $d_{z^2}$ , or  $d_{x^2}$ ,  $\beta$  indicates one of the three  $p$ -orbitals,  $p_x$ ,  $p_y$ , or  $p_z$ , and  $i$  specifies the  $i$ th oxygen-site vector,  $\mathbf{t}_i$ .



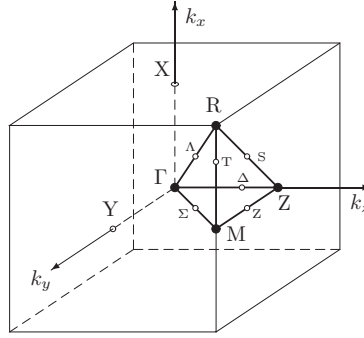


Figure 10.2 The Brillouin zone for the simple-cubic lattice. The high-symmetry lines and points are labeled.

Equation (10.2) can also be written in the Bloch-wave form,  $u_{\mathbf{k}}(\mathbf{r}) \exp(i\mathbf{k} \cdot \mathbf{r})$ , where  $u_{\mathbf{k}}(\mathbf{r}) = \sum_m \exp[-i\mathbf{k} \cdot (\mathbf{r} - \mathbf{R}_m)] \{ \sum_{\alpha} A_{\mathbf{k}\alpha} \phi_{d\alpha}(\mathbf{r} - \mathbf{R}_m) + \sum_{\beta} B_{\mathbf{k}\beta} \phi_{d\beta}[\mathbf{r} - (\mathbf{R}_m + \mathbf{t}_j)] \}$ . It is clear from its form that  $u_{\mathbf{k}}(\mathbf{r})$  has the periodicity of the lattice.

### 10.3 The group of the wavevector, $g_k$

The space group for these perovskites is symmorphic, and therefore it may be considered as the direct product of the group of the wavevector,  $g_k$ , and the translation subgroup. The matrix elements of the IRs are then  $\Gamma_{\mathbf{k}}^{\lambda}(A)_{rs} = \exp(i\mathbf{k} \cdot \mathbf{R}) \Gamma^{\lambda}(A)_{rs}$ , where  $\Gamma^{\lambda}(A)_{rs}$  is the  $rs$  matrix element of the  $\lambda$ th IR of  $g_k$  for the operation  $A$ , and  $\mathbf{R}$  is the translation lattice vector.

The Brillouin zone for the simple cubic lattice is shown in Fig. 10.2.

The group of the wavevector,  $g_k$ , for any  $\mathbf{k}$  in the zone can be found from Table E.2 in Appendix E, by selecting the operations that leave the  $\mathbf{k}$ -vector unchanged or transformed to an equivalent vector,  $\mathbf{k} + \mathbf{K}$ . For example, for  $\mathbf{k} = (0, 0, k)$  (along a line equivalent to the  $\Delta$ -line shown in Fig. 10.2) with  $0 < k < \pi/a$ , the operations in Table E.2 under which  $\mathbf{k}$  is invariant are just those that leave  $z$  invariant. If an operation,  $A$ , listed in Table E.2 carries  $z$  into  $-z$ , then the operation  $iA$  carries  $z$  into  $z$ .

The operations under which  $\mathbf{k} = (0, 0, k)$  remains invariant are  $E, iC_2^{(1)}, iC_2^{(2)}, C_2^{(3)}, i\bar{C}_2^{(5)}, i\bar{C}_2^{(6)}, C_4^{(3)}$ , and  $(C_4^{(3)})^3$ . These eight operations form  $g_k$ , a group that is isomorphic to the group  $C_{4v}$ . The correspondence to the usual  $C_{4v}$  elements is shown in Table 10.1.

For the point X,  $\mathbf{k} = (0, 0, \pi/a)$ , and  $\mathbf{k}$  and  $-\mathbf{k}$  are equivalent, since they are related by a reciprocal-lattice vector:  $-\mathbf{k} + (0, 0, 2\pi/a) = +\mathbf{k}$ . Using Table E.2 we find the operations that carry  $\mathbf{k}$  into  $\mathbf{k}$  or  $-\mathbf{k}$  ( $z$  into  $z$  or  $-z$ ) to be  $i, E, C_2^{(1)}, C_2^{(2)}, C_2^{(3)}, iC_2^{(1)}, iC_2^{(2)}, iC_2^{(3)}, \bar{C}_2^{(5)}, \bar{C}_2^{(6)}, i\bar{C}_2^{(5)}, i\bar{C}_2^{(6)}, C_4^{(3)}, (C_4^{(3)})^3, iC_4^{(3)}$ , and  $i(C_4^{(3)})^3$ . This set of 16 operators forms a group isomorphic to  $D_{4h}$ . By identifying

Table 10.1 Operations of  $O_h$  forming a  $C_{4v}$  group

$g_{\mathbf{k}}$ operator	Usual element of $C_{4v}$
$E$	$E$
$C_2^{(3)}$	$C_2$
$C_4^{(3)}$ and $(C_4^{(3)})^3$	$2C_4$
$iC_2^{(1)}$ and $iC_2^{(2)}$	$2\sigma_v$
$i\bar{C}_2^{(5)}$ and $i\bar{C}_2^{(6)}$	$2\sigma_d$

Table 10.2 Group of the wavevector for lines and points of high symmetry in the Brillouin zone

$\mathbf{k}$	Symmetry		$g_{\mathbf{k}}$ group of the wavevector	Operation in Table E.2
	Point	Line		
(0, 0, 0)	$\Gamma$		$O_h$	All
(0, 0, $k$ )		$\Delta$	$C_{4v}$	$z \rightarrow z$
(0, 0, $\pi/a$ )	X		$D_{4h}$	$z \rightarrow z, z \rightarrow -z$
( $k$ , $k$ , 0)		$\Sigma$	$C_{2v}$	$x \rightarrow x, y \rightarrow y$ and $x \rightarrow y, y \rightarrow x$
( $\pi/a$ , $\pi/a$ , 0)	M		$D_{4h}$	$x \rightarrow \pm x, y \rightarrow \pm y$ and $x \rightarrow \pm y, y \rightarrow \pm x$
( $k$ , $k$ , $k$ )		$\Lambda$	$C_{3v}$	$+x, +y, +z \rightarrow$ any ordering of $+x, +y,$ or $+z$ (all positive)
( $\pi/a$ , $\pi/a$ , $\pi/a$ )	R		$O_h$	all

the operations under which  $\mathbf{k}$  is invariant or carried into an equivalent  $\mathbf{k}$  we can find the group of the wavevector for the various points and lines of symmetry. Some selected results are summarized in Table 10.2. For Table 10.2,  $0 < k < \pi/a$ .

#### 10.4 Irreducible representations for the perovskite energy bands

We choose the origin at one of the  $B$ -ion sites, and refer to this unit cell as the *central cell*. Since no symmetry operation can transform a  $d$ -orbital into a  $p$ -orbital, each set of orbitals separately forms a basis for a representation of  $g_{\mathbf{k}}$ . The  $B$  site of the central unit cell is invariant under the operations of  $g_{\mathbf{k}}$ , and therefore the  $d$ -orbitals of the central cell transform among themselves. The  $d$ -orbitals are at a site of cubic symmetry and therefore are basis functions for three-dimensional  $T_{2g}$  and two-dimensional  $E_g$  representations.

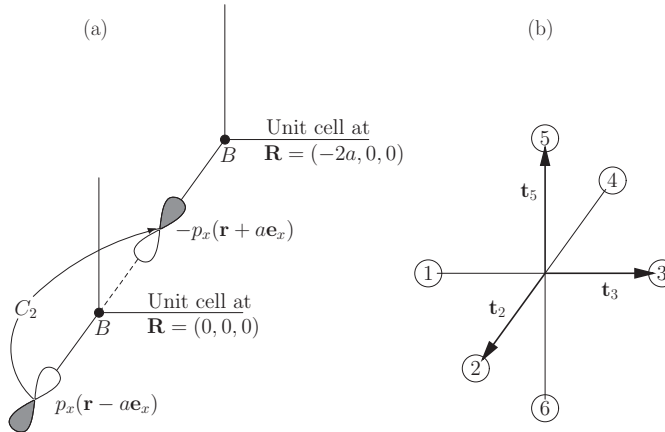


Figure 10.3 (a) A  $P(C_2)$  operation on  $p_x(\mathbf{r} - a\mathbf{e}_x)$  transforms the orbital to the negative of an equivalent orbital,  $p_x(\mathbf{r} + a\mathbf{e}_x)$ . The operation acting on the sites is equivalent to a translation by the lattice vector  $\mathbf{R} = -2a(1, 0, 0)$  that carries site 2 into site 4. As a result, the contribution of  $p_x(\mathbf{r} - a\mathbf{e}_x)$  to the character of the  $P(C_2)$  operation is  $-\exp(2ik_x a)$ , where  $2a$  is the lattice constant. (b) Atoms labeled 2, 3, and 5 are in the central cells. Atoms 4, 1, and 6 are (respectively) the equivalent sites in neighboring cells. The numbering of the oxygen sites is chosen to match the numbering used in the action table, Table E.2, of Appendix E.

The O sites behave differently. Under the operations of  $\mathbf{g}_{\mathbf{k}}$  the O sites in the central unit cell are transformed among themselves, but also into O sites in adjacent unit cells. If an atomic site in the central unit cell is transformed into an *equivalent* site in a neighboring cell, the operation is equivalent to a lattice translation. In determining the character of a point-group operation that transforms an atomic site into an equivalent site, *the equivalent site is regarded as being the same as the original site*. However, the character of the operation must also be multiplied by the character for the translation. If the original site and the transformed site are separated by the lattice vector  $\mathbf{R}$ , then the phase factor to be assigned is  $\exp(i\mathbf{k} \cdot \mathbf{R})$ . This situation is illustrated in Fig. 10.3, which shows a  $p_x$  orbital in the central cell rotated into a  $-p_x$  orbital in the neighboring cell. The contribution to the character for the operation is therefore  $(-1)\exp(i\mathbf{k} \cdot \mathbf{R})$ . For the case shown in Fig. 10.3,  $\mathbf{k} \cdot \mathbf{R} = -2k_x a$ .

The nine  $p$ -orbitals of the central cell are basis functions for a nine-dimensional representation. However, the representation can be immediately reduced. The  $p$ -orbitals can be distinguished as  $\sigma$  and  $\pi$  orbitals with respect to the axis between the B ion and the oxygen ion. Those  $p$ -orbitals in the unit cell with lobes parallel to the B–O axes are  $\sigma$  and those perpendicular to the B–O axis are  $\pi$  orbitals. Since no symmetry operation can transform a sigma orbital into a pi orbital (or vice

versa), the  $p$ -orbital representation can be divided into a three-dimensional (sigma) and a six-dimensional (pi) representation.

The IRs of the energy bands for  $\mathbf{k}$  corresponding to the various points and lines of high symmetry can be determined by decomposing the representations based on the  $p$ - and  $d$ -orbitals. As mentioned earlier, the  $d$ -orbital representation decomposes into  $T_{2g} + E_g$ . For the  $p$ -orbitals we have to consider which orbitals remain on the same site or are moved to an equivalent site in a neighboring unit cell. Only orbitals that remain unmoved or are moved to an equivalent site contribute to the character of an operation.

#### 10.4.1 The $\sigma$ and $\pi$ $p$ -orbitals

The sigma orbitals in the central cell are  $p_x(\mathbf{r} - a\mathbf{e}_x)$ ,  $p_y(\mathbf{r} - a\mathbf{e}_y)$ , and  $p_z(\mathbf{r} - a\mathbf{e}_z)$ , and the equivalent orbitals in adjacent unit cells are  $p_x(\mathbf{r} + a\mathbf{e}_x)$ ,  $p_y(\mathbf{r} + a\mathbf{e}_y)$ , and  $p_z(\mathbf{r} + a\mathbf{e}_z)$ , respectively. In Fig. 10.3(b) the atomic sites for these orbitals are labeled 1 through 6. The central cell oxygens are at sites numbered 2, 3, and 5, and the equivalent sites in neighboring cells are labeled 4, 1, and 6, respectively. The numbering is chosen to agree with the action table, Table E.2, of Appendix E. With this assignment we can simplify the notation a bit. We write  $p_x(\mathbf{r} - a\mathbf{e}_x) = p_x(2)$ ,  $p_y(\mathbf{r} - a\mathbf{e}_y) = p_y(3)$ , and  $p_z(\mathbf{r} - a\mathbf{e}_z) = p_z(5)$ . The equivalent orbitals are  $p_x(4)$ ,  $p_y(1)$ , and  $p_z(6)$ , respectively. To obtain the character for an operation of  $\mathbf{g}_k$  we use the action table, Table E.2, paying attention to the equivalent orbitals and their phase factors.

#### 10.4.2 Irreducible representations at $\Gamma(\mathbf{k} = 0)$

At  $\Gamma(\mathbf{k} = 0)$  the equivalent-site phase factors are all unity and the group of the wavevector is  $O_h$ . The contribution of each sigma orbital to the character of an operation can easily be found. For example, the contribution to the character of  $P(C_2^{(1)})$  is obtained by applying  $P(C_2^{(1)})$  to the three sigma orbitals. The  $p$ -orbitals transform as  $x$ ,  $y$ , and  $z$ . According to Table E.2, under the  $P(C_2^{(1)})$  operation,  $x \rightarrow x$  and  $2 \rightarrow 2$ ; therefore the contribution to the character of the operation applied to  $p_x(2)$  is +1. For  $P(C_2^{(1)})$  applied to  $p_y(3)$ , we have  $y \rightarrow -y$  and  $3 \rightarrow 1$ . Since site 1 is equivalent to site 3, the contribution from this orbital to the character of the operation is  $-1$ . For  $P(C_2^{(1)})$  applied to  $p_z(5)$ ,  $z \rightarrow -z$  and  $5 \rightarrow 6$ . Since site 6 is equivalent to site 5 the orbital makes a contribution of  $-1$  to the character of  $P(C_2^{(1)})$ . The sum of the contributions gives the three-dimensional,  $p$ -orbital representation a character of  $-1$  for  $P(C_2^{(1)})$ . Since  $P(C_2^{(2)})$  and  $P(C_2^{(3)})$  are in the same class as  $P(C_2^{(1)})$ , they have the same character. By proceeding in this manner we can find the characters of all of the operations. The character table for  $O_h$  and the  $p$ -orbitals is given in Table 10.3.

Table 10.3 Characters for the IRs of  $O_h$  and the characters of the representations based on the  $p$ - and  $d$ -orbitals at  $\Gamma$ . The names of the IRs are given for several conventions. Those in parentheses are the labels commonly used in solid-state physics.

IRs	$E$	$8C_3$	$3C_2$	$6\bar{C}_2$	$6C_4$	$i$	$6iC_3$	$3iC_2$	$6i\bar{C}_2$	$6iC_4$
$A_{1g}(\Gamma_1, \Gamma_1^+, \Gamma_{1g})$	1	1	1	1	1	1	1	1	1	1
$A_{2g}(\Gamma_2, \Gamma_2^+, \Gamma_{2g})$	1	1	1	-1	-1	1	1	1	-1	-1
$\mathcal{E}_g(\Gamma_{12}, \Gamma_{12}^+, \Gamma_{3g})$	2	-1	2	0	0	2	-1	2	0	0
$T_{1g}(\Gamma'_{15}, \Gamma_{15}^+, \Gamma_{4g})$	3	0	-1	-1	1	3	0	-1	-1	1
$T_{2g}(\Gamma'_{25}, \Gamma_{25}^+, \Gamma_{5g})$	3	0	-1	1	-1	3	0	-1	1	-1
$A_{1u}(\Gamma'_1, \Gamma_1^-, \Gamma_{1u})$	1	1	1	1	1	-1	-1	-1	-1	-1
$A_{2u}(\Gamma'_2, \Gamma_2^-, \Gamma_{2u})$	1	1	1	-1	-1	-1	-1	-1	1	1
$\mathcal{E}_u(\Gamma'_{12}, \Gamma_{12}^-, \Gamma_{3u})$	2	-1	2	0	0	-2	1	-2	0	0
$T_{1u}(\Gamma'_{15}, \Gamma_{15}^-, \Gamma_{4u})$	3	0	-1	-1	1	-3	0	1	1	-1
$T_{2u}(\Gamma'_{25}, \Gamma_{25}^-, \Gamma_{5u})$	3	0	-1	1	-1	-3	0	1	-1	1
IR decompositions										
$\Gamma^{p\sigma} = T_{1u}(\Gamma_{15})$	3	0	-1	-1	1	-3	0	1	1	-1
$\Gamma^{p\pi} = T_{1u}(\Gamma_{15}) + T_{2u}(\Gamma_{25})$	6	0	-2	0	0	-6	0	2	0	0
$\Gamma^d = T_{2g}(\Gamma'_{25}) + \mathcal{E}_g(\Gamma_{12})$	5	-1	1	1	-1	5	-1	1	1	-1

The same process can be applied to the oxygen  $\pi$  orbitals. There are six  $\pi$  orbitals:  $p_y(\mathbf{r} - a\mathbf{e}_x)$ ,  $p_z(\mathbf{r} - a\mathbf{e}_x)$ ,  $p_x(\mathbf{r} - a\mathbf{e}_y)$ ,  $p_z(\mathbf{r} - a\mathbf{e}_y)$ ,  $p_x(\mathbf{r} - a\mathbf{e}_z)$ , and  $p_y(\mathbf{r} - a\mathbf{e}_z)$ . We label these orbitals as  $p_y(2)$ ,  $p_z(2)$ ,  $p_x(3)$ ,  $p_z(3)$ ,  $p_x(5)$ , and  $p_y(5)$ , respectively. The equivalent sites are 4, 1, and 6, respectively, and the corresponding equivalent orbitals are  $p_y(4)$ ,  $p_z(4)$ ,  $p_x(1)$ ,  $p_z(1)$ ,  $p_x(6)$ , and  $p_y(6)$ . Using Table E.2, we can find the characters for the operations. For example, according to Table E.2,  $P(C_2^{(1)})$  transforms  $x \rightarrow x$ ,  $y \rightarrow -y$ , and  $z \rightarrow -z$ , and  $2 \rightarrow 2$ ,  $3 \rightarrow 1$ , and  $5 \rightarrow 6$ . It follows that the contribution of  $p_y(2)$  and  $p_z(2)$  orbitals to the character of  $P(C_2^{(1)})$  is  $-2$ . For the pairs,  $p_x(2)$  and  $p_z(2)$ , and  $p_x(5)$  and  $p_y(5)$  the contributions sum to zero. On adding all of the contributions we find that the character of  $P(C_2^{(1)})$  for the pi orbitals is  $-2$ . The characters of the operations of the  $O_h$  group are listed in Table 10.3.

Some important conclusions can be extracted from the decomposition of the  $p$ - and  $d$ -orbital representations shown at the bottom of Table 10.3. First, we note that the  $p$ - and  $d$ -orbitals have no IRs in common. As a result, the eigenstates are composed of either  $d$ -orbital or  $p$ -orbital functions. That is, there are no interactions between, or mixing of, the  $p$ - and  $d$ -orbitals at  $\Gamma$ . Second, the  $p$ -sigma and  $p$ -pi orbitals both contain the  $\Gamma_{15}(T_{1u})$  IR. Therefore the  $\Gamma_{15}$  eigenstates may be admixtures of both types of  $p$ -orbitals. Third, we see that the  $p$ -pi orbital representation

contains the  $\Gamma_{25}(T_{2u})$  IR once and that no other representation contains  $\Gamma_{25}$ . This means that the three  $\Gamma_{25}$  symmetry functions are eigenstates and are composed exclusively of  $p$ -pi orbitals. Finally, we can characterize the 14 energy-band states at  $\Gamma$  as follows.

- (a)  $\Gamma(\text{perovskite}) = 2\Gamma_{15}(T_{1u}) + \Gamma_{25}(T_{2u}) + \Gamma'_{25}(T_{2g}) + \Gamma_{12}(\mathcal{E}_g)$ .
- (b) The block-diagonal secular equation consists of
  - a. Three  $2 \times 2$ ,  $\Gamma_{15}$  blocks that have the same eigenvalues.  
That is, two triply degenerate energies,  $\mathcal{E}_a(15)$  and  $\mathcal{E}_b(15)$ .
  - b. Three  $1 \times 1$  blocks yielding a triply degenerate energy,  $\mathcal{E}(25) = \mathcal{E}(T_{2u})$ .
  - c. Three  $1 \times 1$  blocks yielding a triply degenerate energy,  $\mathcal{E}(25') = \mathcal{E}(T_{2g})$ .
  - d. Two  $1 \times 1$  blocks yielding a doubly degenerate energy,  $\mathcal{E}(12) = \mathcal{E}(\mathcal{E}_g)$ .
- (c) For the 14 band energies at  $\Gamma$ , there are at most five independent eigenvalues.
- (d) For  $\Gamma_{15}$  and  $\Gamma_{25}$  the wavefunctions are purely of  $p$ -orbital composition. For  $\Gamma'_{25}$  and  $\Gamma_{12}$  the wavefunctions are purely of  $d$ -orbital composition.

### 10.4.3 Symmetry functions at $\Gamma$

The symmetry functions for the central cell can be generated by means of the symmetry-function-generating machine. As an example, let us find the eigenstates corresponding to the  $\Gamma_{25}$  IR. We know from the decompositions that they are composed of  $p$ -pi orbitals, so we choose the function  $p_z(2)$  as the “arbitrary” function from which we will generate  $\Gamma_{25}$  symmetry functions. We shall need the diagonal matrix elements of the  $\Gamma_{25}(T_{2u})$  IR. These elements are given in Section E.4 of Appendix E and are summarized in Table 10.4.

A function,  $f^i(\Gamma_j)$ , transforming according to the  $i$ th row of the  $\Gamma_j$  IR is given by

$$f^i(\Gamma_j) \propto \sum_A D_{ii}^{\Gamma_j}(A) P_A f(\mathbf{r}), \quad (10.3)$$

where  $A$  denotes an element of  $\mathbf{g}_k$ ,  $P_A$  is the operator,  $D_{ii}^{\Gamma_j}(A)$  is a diagonal matrix element of the  $\Gamma_j$  IR, and  $f(\mathbf{r})$  is an arbitrary function of the orbitals.

Applying (10.3) to the function  $f(\mathbf{r}) = p_z(2)$  gives the following results:

$$\begin{aligned} f^1(\Gamma_{25}) &= \sum_{\mathbf{R}} D_{11}^{\Gamma_{25}}(\mathbf{R}) P_{\mathbf{R}} p_z(2) \\ &\propto p_z(2) + p_z(2) + p_z(4) + p_z(4) + p_y(4) - p_y(4) \\ &\quad - p_x(6) + p_x(6) - p_z(1) - p_z(3) + p_y(2) \\ &\quad - p_y(2) - p_x(6) + p_x(6) - p_z(1) - p_z(3) \\ &= 2p_z(2) + 2p_z(4) - 2p_z(1) - 2p_z(3) \\ &= 4p_z(2) - 4p_z(3). \end{aligned} \quad (10.4)$$

Table 10.4 Diagonal matrix elements of the  $T_2$  IR for the  $O$  group. The diagonal elements for all eight of the  $C_3$  operations are zero and therefore omitted from the table. The character for the operation  $iA$  is the same or the negative of that for the operation  $A$  for a  $g$  or  $u$  representation, respectively.

	$E$	$C_2^1$	$C_2^2$	$C_2^3$	$\bar{C}_2^1$	$\bar{C}_2^2$	$\bar{C}_2^3$	$\bar{C}_2^4$	$\bar{C}_2^5$	$\bar{C}_2^6$
Row 1	1	-1	-1	1	0	0	0	0	1	1
Row 2	1	-1	1	-1	0	0	1	1	0	0
Row 3	1	1	-1	-1	1	1	0	0	0	0
					$C_4^1$	$(C_4^1)^3$	$C_4^2$	$(C_4^2)^3$	$C_4^3$	$(C_4^3)^3$
Row 1					0	0	0	0	-1	-1
Row 2					0	0	-1	-1	0	0
Row 3					-1	-1	0	0	0	0

The last line of (10.4) results since sites 2 and 4, and sites 1 and 3, are equivalent. The normalized function is

$$f^1(\Gamma_{25}) = \frac{p_z(2) - p_z(3)}{\sqrt{2(1 - S_{23})}}, \quad (10.5)$$

where  $S_{23}$  is the overlap integral  $\int p_z(2)^* p_z(3) d\mathbf{r}$ .

Using the row-2 and row-3 diagonal matrix elements with  $p_y(2)$  and  $p_x(5)$  as the generators gives the partner wavefunctions

$$f^2(\Gamma_{25}) = \frac{p_y(2) - p_y(5)}{\sqrt{2(1 - S_{23})}}, \quad (10.6)$$

$$f^3(\Gamma_{25}) = \frac{p_x(3) - p_x(5)}{\sqrt{2(1 - S_{23})}}. \quad (10.7)$$

These functions are repeated in each unit cell, so the total eigenfunctions are

$$\psi^1(\Gamma_{25}) = \frac{1}{\sqrt{N}} \sum_{\mathbf{R}_n} \frac{p_z(\mathbf{r} - \mathbf{R}_n - \mathbf{t}_2) - p_z(\mathbf{r} - \mathbf{R}_n - \mathbf{t}_3)}{\sqrt{2(1 - S_{23})}}, \quad (10.8)$$

$$\psi^2(\Gamma_{25}) = \frac{1}{\sqrt{N}} \sum_{\mathbf{R}_n} \frac{p_y(\mathbf{r} - \mathbf{R}_n - \mathbf{t}_2) - p_y(\mathbf{r} - \mathbf{R}_n - \mathbf{t}_5)}{\sqrt{2(1 - S_{23})}}, \quad (10.9)$$

$$\psi^3(\Gamma_{25}) = \frac{1}{\sqrt{N}} \sum_{\mathbf{R}_n} \frac{p_x(\mathbf{r} - \mathbf{R}_n - \mathbf{t}_3) - p_x(\mathbf{r} - \mathbf{R}_n - \mathbf{t}_5)}{\sqrt{2(1 - S_{23})}}, \quad (10.10)$$

where  $N$  is the number of unit cells in the crystal, and the vectors  $\mathbf{t}_2$ ,  $\mathbf{t}_3$ , and  $\mathbf{t}_5$  are shown in Fig. 10.3(b).

We also know the cell eigenfunctions for the  $d$ -orbitals. They are just the  $\Gamma'_{25}(t_{2g})$  and  $\Gamma_{12}(e_g)$   $d$ -electron states, namely the  $d_{xy}$ ,  $d_{xz}$ , and  $d_{yz}$ , and  $d_{x^2}$  and  $d_{z^2}$  orbitals, respectively. The total LCAO wavefunctions for the  $\Gamma'_{25}$  and  $\Gamma_{12}$  band states are

$$\psi^1(\Gamma'_{25}) = \frac{1}{\sqrt{N}} \sum_{\mathbf{R}_n} d_{xy}(\mathbf{r} - \mathbf{R}_n), \quad (10.11)$$

$$\psi^2(\Gamma'_{25}) = \frac{1}{\sqrt{N}} \sum_{\mathbf{R}_n} d_{xz}(\mathbf{r} - \mathbf{R}_n), \quad (10.12)$$

$$\psi^3(\Gamma'_{25}) = \frac{1}{\sqrt{N}} \sum_{\mathbf{R}_n} d_{yz}(\mathbf{r} - \mathbf{R}_n), \quad (10.13)$$

and

$$\psi^1(\Gamma_{12}) = \frac{1}{\sqrt{N}} \sum_{\mathbf{R}_n} d_{z^2}(\mathbf{r} - \mathbf{R}_n), \quad (10.14)$$

$$\psi^2(\Gamma_{12}) = \frac{1}{\sqrt{N}} \sum_{\mathbf{R}_n} d_{x^2}(\mathbf{r} - \mathbf{R}_n). \quad (10.15)$$

For the  $\Gamma_{15}(T_{1u})$  wavefunction at  $\mathbf{k} = 0$  the wavefunction is a mixture of sigma and pi  $p$ -orbitals. The  $T_{1u}$  diagonal matrix elements are given in Section E.4 of Appendix E. The symmetry functions can be generated using (10.3). The results are given in Table 10.5. The wavefunctions and energies can be calculated using the LCAO method. For simplicity we use the orthogonal Löwdin orbitals discussed in Chapter 6. The  $\Gamma_{15}$  states are admixtures of  $\pi$  and  $\sigma$  orbitals belonging to the same row of the  $T_{1u}$  IR. For row 1, we have a secular equation involving the functions  $p_x(\mathbf{r} - \mathbf{R}_n - \mathbf{t}_2)$  and  $[p_x(\mathbf{r} - \mathbf{R}_n - \mathbf{t}_3) + p_x(\mathbf{r} - \mathbf{R}_n - \mathbf{t}_5)]/\sqrt{2}$ . If we include only nearest-neighbor (nn)  $p$ - $d$  interactions, the secular matrix eigenvalue equation is diagonal because the  $p$ - $p$  interactions are second-nearest-neighbor interactions (which we are ignoring).

Figure 10.4(a) shows schematically the cell functions and the corresponding energies. Figure 10.4(b) shows the  $\Gamma_{25}$  functions in the central cell and neighboring unit cells.

#### 10.4.4 Irreducible representations along the $\Delta$ -line

Along the symmetry line  $\Delta$  in the Brillouin zone the group of the wavevector,  $\mathbf{g}_\mathbf{k}$ , is  $C_{4v}$ . The phase factor for equivalent oxygen sites in neighboring cells along the  $\Delta$ -line is  $\exp(i\mathbf{k} \cdot \mathbf{R}) = \exp(ik_z R_z)$ , where  $R_z$  is the component of a lattice vector,  $\mathbf{R}$ , along the  $z$ -axis. The phase factor for translation along the  $x$ - and  $y$ -directions is  $+1$ , since  $k_x = k_y = 0$ .



Table 10.5 Symmetry functions for the central cell for the  $p$ - and  $d$ -orbitals of a perovskite. The notation is  $p_\alpha(j) = p_\alpha(\mathbf{r} - \mathbf{t}_j)$ . See Fig. 10.3 for definitions of the  $\mathbf{t}_j$  vectors. LCAO energies are given in the last column. Using only nearest-neighbor (nn) interactions, the  $T_{1u}(\Gamma_{15})$   $\pi$  states and  $T_{2u}(\Gamma_{15})$  energies are accidentally degenerate. The Löwdin orbitals discussed in Chapter 6 are assumed, so that the overlap integrals between different orbitals vanish.

IR	Row	$d$ -Orbital type	Unit-cell symmetry function	LCAO energy (Löwdin orbitals, nn interactions)
$T_{2g}$	1	$t$	$d_{xy}(0)$	$E_t = \int d_{xy}(0)^* \mathbb{H} d_{xy}(0) d\mathbf{r}$
	2	$t$	$d_{xz}(0)$	$E_t$
	3	$t$	$d_{yz}(0)$	$E_t$
$\mathcal{E}_g$	1	$e$	$d_{x^2}(0)$	$E_e = \int d_{x^2}(0)^* \mathbb{H} d_{x^2}(0) d\mathbf{r}$
	2	$e$	$d_{z^2}(0)$	$E_e$
<hr/>				
$p$ -Orbital type				
$T_{2u}$	1	$\pi$	$[p_x(3) - p_x(5)]/\sqrt{2}$	$E_\pi = \int p_x(3)^* \mathbb{H} p_x(3) d\mathbf{r}$
	2	$\pi$	$[p_y(2) - p_y(5)]/\sqrt{2}$	$E_\pi$
	3	$\pi$	$[p_z(2) - p_z(3)]/\sqrt{2}$	$E_\pi$
$T_{1u}$	1	$\sigma$	$p_x(2)$	$E_\sigma = \int p_x(2)^* \mathbb{H} p_x(2) d\mathbf{r}$
	1	$\pi$	$[p_x(3) + p_x(5)]/\sqrt{2}$	$E_\pi$
	2	$\sigma$	$p_y(3)$	$E_\sigma$
	2	$\pi$	$[p_y(2) + p_y(5)]/\sqrt{2}$	$E_\pi$
	3	$\sigma$	$p_z(5)$	$E_\sigma$
	3	$\pi$	$[p_z(2) + p_z(3)]/\sqrt{2}$	$E_\pi$

The operations of  $\mathbf{g}_k$  are summarized in Table 10.6, and the characters for these operations are listed for the IRs for  $C_{4v}$ . The characters based on the  $d$ - and  $p$ -orbital representations are given at the bottom of the table, together with the decompositions into the IRs of  $C_{4v}$ .

Using the symmetry functions, the secular equation for the  $\Delta$ -band states will block-diagonalize as follows.

1. One  $3 \times 3$   $\Delta_1$  block associated with  $p$ -sigma,  $p$ -pi, and  $d$ - $\mathcal{E}_g$  orbitals.
2. One  $2 \times 2$   $\Delta_3$  block associated with  $p$ -pi and  $d$ - $\mathcal{E}_g$  orbitals.
3. One  $1 \times 1$   $\Delta_4$  block associated with  $T_{2g}$  orbitals.
4. Two  $4 \times 4$   $\Delta_5$  blocks associated with  $p$ -sigma,  $p$ -pi, and  $d$ - $T_{2g}$  orbitals.

Some conclusions can be drawn from the decompositions. There is only one  $\Delta_4$  symmetry function, and therefore it must be an eigenstate. The  $p$ - and  $d$ -orbitals

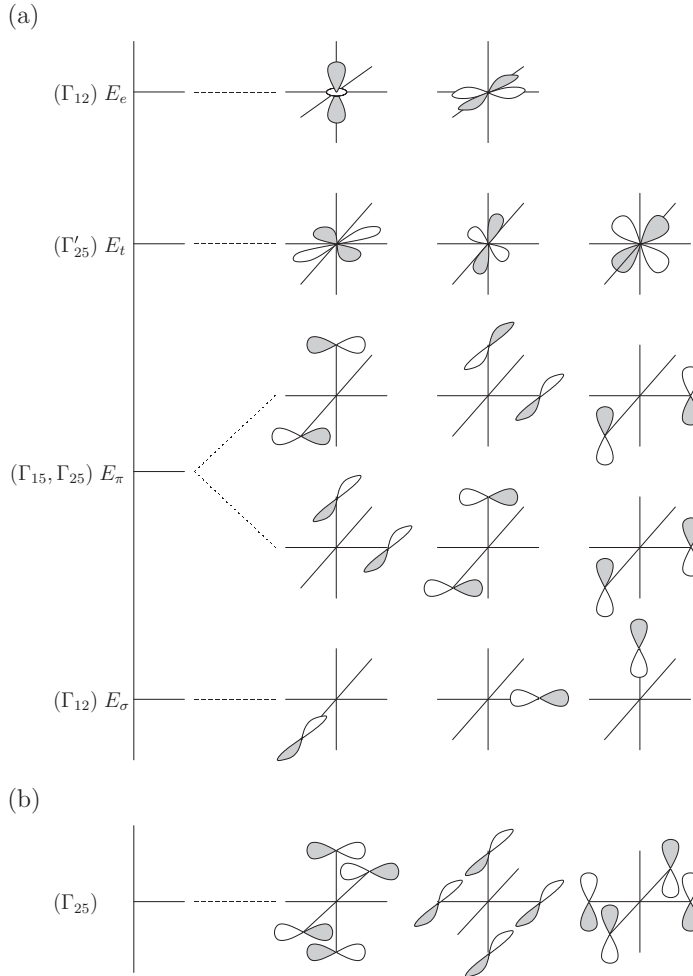


Figure 10.4 (a) LCAO energies at  $\Gamma$  using Löwdin orbitals and nearest-neighbor interactions. The central cell symmetry functions are shown schematically for each row of the IR. These functions are repeated in each unit-cell of the crystal. (b) The central unit-cell and neighboring unit-cell functions for the  $\Gamma'_{25}$  band.

are mixed in forming the  $\Delta_1$ ,  $\Delta_3$ ,  $\Delta_4$ , and  $\Delta_5$  band wavefunctions. However, we note that the  $T_{2g}$  and  $E_g$   $d$ -orbitals are never mixed together in any wavefunction, since they belong to different IRs of  $O_h$ .

#### 10.4.5 Symmetry functions for $\mathbf{k}$ on the $\Delta$ -line

The wavevector,  $\mathbf{k}$ , is  $(0, 0, k_z)$ , with  $0 < k_z < \pi/(2a)$ ; that is,  $\mathbf{k}$  is along a  $\Delta$ -line. We use the symmetry-function-generating machine to find the symmetry functions. For example, let us find the  $\Delta_4$  eigenstate. Since the IR is one-dimensional, we need

Table 10.6 The character table for  $C_{4v}$ . The last four rows give the characters for the  $p$ - and  $d$ -orbital representations and their decompositions.  $\Gamma^t$  is the  $3 \times 3$  representation based on the  $T_{2g}$   $d$ -orbitals and  $\Gamma^e$  is the  $2 \times 2$  representation based on the  $\mathcal{E}_g$   $d$ -orbitals.

$C_{4v}$	$E$	$C_2^{(3)}$	$C_4^{(3)}$	$(C_4^{(3)})^3$	$iC_2^{(1)}$	$iC_2^{(2)}$	$i\bar{C}_2^{(5)}$	$i\bar{C}_2^{(6)}$
$\Delta_1(A_1)$	1	1	1	1	1	1	1	1
$\Delta_2(A_2)$	1	1	1	1	-1	-1	-1	-1
$\Delta_3(B_1)$	1	1	-1	-1	1	1	-1	-1
$\Delta_4(B_2)$	1	1	-1	-1	-1	-1	1	1
$\Delta_5(\mathcal{E})$	2	-2	0	0	0	0	0	0
$\Gamma^\pi = \Delta_1(A_1) + \Delta_3(B_1) + 2\Delta_5(\mathcal{E})$	6	-2	0	0	2	2	0	0
$\Gamma^\sigma = \Delta_1(A_1) + \Delta_5(\mathcal{E})$	3	-1	1	1	1	1	1	1
$\Gamma^t = \Delta_5(\mathcal{E}) + \Delta_4(B_2)$	3	-1	-1	-1	-1	-1	1	1
$\Gamma^e = \Delta_1(A_1) + \Delta_3(B_1)$	2	2	0	0	2	2	0	0

only the characters. This state is derived from the  $T_{2g}$   $d$ -orbitals, and therefore we can use  $d_{xy}$  as the generating function.

Application of (10.3) to  $d_{xy}$  gives

$$\begin{aligned}
 f(\Delta_4) &\propto \sum_A \chi^{\Delta_4}(A) P_A d_{xy} \\
 &= +1(d_{xy}) + 1(d_{xy}) - 1(-d_{xy}) - 1(-d_{xy}) \\
 &\quad - 1(-d_{xy}) - 1(-d_{xy}) + 1(d_{xy}) + 1(d_{xy}) \\
 &= 8d_{xy}.
 \end{aligned} \tag{10.16}$$

Thus, for the model that uses only the  $p$ - and  $d$ -orbitals, the normalized eigenfunction is just  $d_{xy}$ . The LCAO energy of this eigenstate is  $E_t$  (see Table 10.5). From this result we can conclude that the  $\Delta_4(d_{xy})$  band extending from  $\Gamma$  along the  $(0, 0, k_z)$  direction (the  $\Delta$  symmetry line) is “flat”. That is, it has no dispersion.

A more complex example is the symmetry functions for the  $\Delta_1$  bands. These involve the  $p$ -sigma,  $p$ -pi, and  $\mathcal{E}_g$   $d$ -orbitals. Each orbital type can be used to generate a  $\Delta_1$  symmetry function. For the  $p$ -sigma functions we have

$$\begin{aligned}
 f_z(\Delta_1) &\propto \sum_A \chi^{\Delta_1}(A) P_A p_z(5) = 8p_z(5), \\
 f_x(\Delta_1) &\propto \sum_A \chi^{\Delta_1}(A) P_A p_x(2) = 2p_x(2) - 2p_x(4) + 2p_y(3) - 2p_y(1) \\
 &\rightarrow 0 \text{ (equivalent orbitals cancel out),}
 \end{aligned}$$

Table 10.7 Symmetry functions and energies for  $\mathbf{k}$  along the  $\Delta$ -line of symmetry,  $\mathbf{k} = (0, 0, k_z)$ 

$C_{4v}$ IR	Row	Orbital type	Symmetry function	LCAO energy (Löwdin orbitals, nn interactions)
$\Delta_1(A_1)$	1a	$p_\sigma$	$p_z(5)$	$E_{me} \pm \sqrt{(E_{ge}/2)^2 + 2(pd\sigma)^2 S_z^2}$
	1b	$d_{z^2}$	$d_{z^2}$	$E_{ab}^\pm(\Delta_1) = \text{mixture of 1a and 1b}$
	1c	$p_\pi$	$[p_z(2) + p_z(3)]/\sqrt{2}$	$E_c(\Delta_1) = E_\pi$
$\Delta_3(B_1)$	1a	$p_\pi$	$[p_z(2) - p_z(3)]/\sqrt{2}$	$E_a(\Delta_3) = E_\pi$
	1b	$d_{x^2}$	$d_{x^2}(0)$	$E_b(\Delta_3) = E_e$
$\Delta_4(B_2)$	1	$d_{xy}$	$d_{xy}$	$E(\Delta_4) = E_t$
$\Delta_5(\mathcal{E})$	1a, 2a	$p_\sigma$	$p_x(2), p_y(2)$	$E_a(\Delta_5) = E_\sigma$ doubly degenerate
	1b, 2b	$p_\pi$	$p_x(3), p_y(3)$	$E_b(\Delta_5) = E_\pi$ doubly degenerate
				$E_c^\pm(\Delta_5) = E_m$
	1c, 2c	$p_\pi$	$p_x(5), p_y(5)$	$\pm \sqrt{(E_g/2)^2 + 4(pd\pi)^2 S_z^2}$
	1d, 2d	$d_{xz}$	$d_{xz}(0), d_{yz}(0)$	Mixture of 1c and 1d or 2c and 2d, doubly degenerate

$$E_{me} = (E_e + E_\sigma)/2, \\ E_{ge} = E_e - E_\sigma,$$

$$E_m = (E_t + E_\pi)/2, \\ E_g = E_t - E_\pi,$$

$$2a \text{ is the lattice spacing,} \\ S_z = \sin(k_z a).$$

$$f_y(\Delta_1) \propto \sum_A \chi^{\Delta_1}(A) P_A p_y(3) = 2p_y(3) - 2p_y(1) - 2p_x(4) + 2p_x(2) \\ \rightarrow 0 \text{ (equivalent orbitals cancel out).}$$

(Note that the phase factors are  $\exp(ik_z \Delta R_z) = 1$  for all of the equivalent  $p$ -orbitals, since  $\Delta R_z = 0$  for the operations of  $C_{4v}$ .) The symmetry function derived from the  $p$ -sigma orbitals is therefore  $p_z(5)$ . By proceeding in the same way we find that for the  $p$ -pi orbitals the normalized  $\Delta_1$  symmetry function is  $[p_z(2) + p_z(3)]/\sqrt{2}$ . Table 10.7 gives the symmetry functions and LCAO energies for all of the band states for  $\mathbf{k}$  along the  $\Delta$ -line of symmetry.

The calculation of the LCAO-model energy from the symmetry functions is discussed in Chapter 6. For example, for the  $\Delta_1$  band energies, we have a  $3 \times 3$  matrix secular equation corresponding to the three symmetry functions. The matrix elements are

$$M_{11} = \int p_z(5)^* \mathbb{H} p_z(5) d\mathbf{r} = E_\sigma, \quad (10.17)$$

$$M_{12} = \int p_z(5)^* \mathbb{H} \frac{1}{\sqrt{2}} [p_z(2) + p_z(3)] d\mathbf{r} \\ = 0 \text{ (nn approximation),} \quad (10.18)$$

$$\begin{aligned}
M_{13} &= \int p_z(5)^* \mathbb{H}[d_{z^2}(\mathbf{r}) + d_{z^2}(\mathbf{r} - 2a\mathbf{e}_z)]d\mathbf{r} \\
&= 2i(pd\sigma)e^{ik_z a} \sin(k_z a), \tag{10.19}
\end{aligned}$$

$$M_{22} = \frac{1}{2} \int [p_z(2) + p_z(3)]^* \mathbb{H}[p_z(2) + p_z(3)]d\mathbf{r} = E_\pi, \tag{10.20}$$

$$\begin{aligned}
M_{23} &= \int \frac{1}{\sqrt{2}} [p_z(2) + p_z(3)]^* \mathbb{H} d_{z^2} d\mathbf{r} \\
&= 0 \text{ (nn approximation)}, \tag{10.21}
\end{aligned}$$

$$M_{33} = \int d_{z^2}^* \mathbb{H} d_{z^2} d\mathbf{r} = E_e, \tag{10.22}$$

$$M_{ij} = M_{ji}^*. \tag{10.23}$$

The eigenvalues are determined from  $\det(\mathbb{M} - E) = 0$ . The resulting three  $\Delta_1(A_1)$  energies are shown in Table 10.7. The unit-cell eigenvectors are

$$\Phi_\pm(\mathbf{r}) = \frac{[E_\sigma - E_{k_z}^\pm(\Delta_1)]p_z(5) - 2i(pd\sigma)\exp(ik_z a)S_z d_{z^2}(\mathbf{r})}{\sqrt{[E_\sigma - E_{k_z}^\pm(\Delta_1)]^2 + 4(pd\sigma)^2 S_z^2}}, \tag{10.24}$$

$$\Phi_\pi(\mathbf{r}) = \frac{1}{2}[p_z(2) + p_z(3)]. \tag{10.25}$$

The total  $\Delta_1$  crystal wavefunctions are

$$\Psi_\pm(\mathbf{r}) = \frac{1}{\sqrt{N}} \sum_{\mathbf{R}} \Phi_\pm(\mathbf{r} - \mathbf{R})e^{ik_z R_z}, \tag{10.26}$$

$$\Psi_\pi(\mathbf{r}) = \frac{1}{\sqrt{N}} \sum_{\mathbf{R}} \Phi_\pi(\mathbf{r} - \mathbf{R})e^{ik_z R_z}, \tag{10.27}$$

where  $\mathbf{R}$  is a lattice vector and  $N$  is the total number of unit cells.

For the  $\Delta_5$  bands we have two  $4 \times 4$  matrix secular equations that yield the same eigenvalues. To obtain the symmetry functions we need the diagonal matrix elements of the  $\mathcal{E}$  IR for  $C_{4v}$ . *Note that this  $\mathcal{E}$  representation is not the same as the  $\mathcal{E}$  of the  $O_h$  group.* Since  $x$  and  $y$  are bases for the  $\mathcal{E}$  IR of  $C_{4v}$ , we can generate the matrices from Table E.2. The results for the diagonal elements are shown in Table 10.8.

Table 10.8 *Diagonal elements for the  $\mathcal{E}$  IR of  $C_{4v}$*

	$E$	$C_2^{(3)}$	$C_4^{(1)}$	$(C_4^{(1)})^3$	$iC_2^{(1)}$	$iC_2^{(2)}$	$i\bar{C}_2^{(5)}$	$i\bar{C}_2^{(6)}$
Row 1	1	-1	0	0	-1	1	0	0
Row 2	1	-1	1	-1	0	0	1	1

The symmetry functions generated and the LCAO energies are shown in Table 10.7. For our nn interaction model the  $4 \times 4$  matrix is block-diagonal, consisting of two  $1 \times 1$  blocks and a  $2 \times 2$  block.  $p_x(2)$  and  $p_x(3)$  have zero for the  $p$ - $d$  matrix elements, and are therefore eigenstates with energies  $E_\sigma$  and  $E_\pi$ , respectively. The  $p_x(5)$  orbital interacts with the  $d_{xz}$  orbitals and the  $2 \times 2$  matrix elements are

$$M_{11} = E_\pi, \quad (10.28)$$

$$M_{12} = 2i(pd\pi)e^{ik_z a} S_z = M_{21}^*, \quad (10.29)$$

$$M_{22} = E_t. \quad (10.30)$$

The eigenvalues of  $\det(\mathbb{M} - E) = 0$  are

$$E^\pm(\Delta_5) = E_m \pm \sqrt{(E_g/2)^2 + 4(pd\pi)^2 S_z^2}, \quad (10.31)$$

$$E_m = \frac{1}{2}(E_t + E_\pi), \quad (10.32)$$

$$E_g = E_t - E_\pi. \quad (10.33)$$

The unit-cell eigenfunctions are

$$\Phi_\pm = \frac{1}{\sqrt{N}} \{ [E_\pi - E^\pm(\Delta_5)] p_x(5) - 2i(pd\sigma)e^{ik_z a} S_z d_{xz}(\mathbf{r}) \}, \quad (10.34)$$

where

$$N = [E_\pi - E^\pm(\Delta_5)]^2 + 4(pd\sigma)^2 S_z^2. \quad (10.35)$$

The row-2 functions produce the same eigenvalues, and the cell wavefunctions can be obtained from (10.34) by substituting  $p_y(5)$  for  $p_x(5)$  and  $d_{yz}(\mathbf{r})$  for  $d_{xz}(\mathbf{r})$ . For  $\mathbf{k}$  along the  $\Delta$ -line, the 14 energy bands are shown in Fig. 10.5.

#### 10.4.6 Irreducible representations along the $\Sigma$ -line

Along the  $\Sigma$ -line  $\mathbf{k} = (t, t, 0)$  and the translation phase factor is  $\exp(i\mathbf{k} \cdot \mathbf{R}) = \exp(itR_x + itR_y) = \exp[2ita(n_x + n_y)]$ . The group of the wavevector,  $\mathbf{g}_\mathbf{k}$ , is  $C_{2v}$ , as indicated in Table 10.1. The elements of  $O_h$  which leave  $(t, t, 0)$  invariant are shown in Table 10.9.

The  $p$ -sigma orbitals are bases for a three-dimensional representation of  $C_{2v}$ . The  $p$ -pi are bases for a six-dimensional representation, and the  $d$ -orbitals are bases for a five-dimensional representation. The characters of these representations can be found in the usual manner, namely by applying the operations of  $\mathbf{g}_\mathbf{k}$  to the orbitals and determining the number of orbitals that are transformed into a multiple of themselves or a multiple of equivalent orbitals. The results are summarized in

Table 10.9 The character table for  $C_{2v}$ . The characters and decompositions of  $p$ - and  $d$ -orbital representations are given in the last three rows.

$C_{2v}$ usual symbols	$E$	$C_2$	$\sigma_v$	$\sigma'_v$	$\mathbf{k} = (t, t, 0)$
$O_h$ elements in $\mathbf{g_k}$	$E$	$\bar{C}_2^{(6)}$	$i\bar{C}_2^{(5)}$	$iC_2^{(3)}$	Basis functions
$\Sigma_1(A_1)$	1	1	1	1	$z$
$\Sigma_2(A_2)$	1	1	-1	-1	Rotation about the (1, 1, 0) symmetry axis, $[p_z(2) - p_z(3)]/\sqrt{2}$
$\Sigma_3(B_1)$	1	-1	1	-1	$x$
$\Sigma_4(B_2)$	1	-1	-1	1	$y$
$\Gamma^\sigma = \Sigma_1 + \Sigma_3 + \Sigma_4$	3	-1	1	1	$x(2), y(3), z(5)$
$\Gamma^\pi = 2\Sigma_1 + \Sigma_2 + \Sigma_3 + 2\Sigma_4$	6	0	0	2	$x(3), x(5), y(2), y(5),$ $z(2), z(3)$
$\Gamma^d = 2\Sigma_1 + \Sigma_2 + \Sigma_3 + \Sigma_4$	5	1	1	1	$d_{xy}, d_{xz}, d_{yz}, d_{z^2}, d_{x^2}$

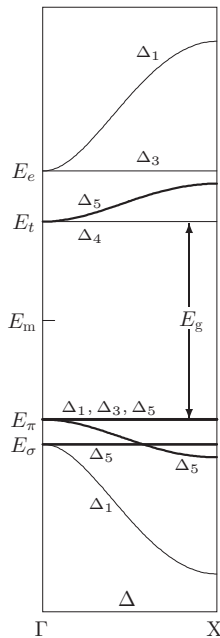


Figure 10.5 Energy bands along the symmetry line,  $\Delta$ .

Table 10.9. In the nearest-neighbor approximation there is additional block-diagonalization among the symmetry functions belonging to the same row of the same IR. For example, for the  $\Sigma_1$  states, the  $5 \times 5$  secular equation block-diagonalizes into two  $2 \times 2$  blocks (1a and 1b, and 1c and 1d,

Table 10.10 *Symmetry functions and LCAO energies for  $\mathbf{k}$  along  $\Sigma$ ,  $\mathbf{k} = (t, t, 0)$* 

$C_{2v}$ IR	Row	Orbital type	Unit-cell symmetry function	LCAO energy (Löwdin orbitals, nn interactions)
$\Sigma_1(A_1)$	1a	$p_\sigma$	$[p_x(2) + p_y(3)]/\sqrt{2}$	$E(\Sigma_1)^\pm = \text{mixture 1a and 1b}$
	1b	$d_{z^2}$	$d_{z^2}(0)$	$= E_{me} \pm \sqrt{(E_{ge}/2)^2 + 2(pd\sigma)^2 s^2}$
	1c	$p_\pi$	$[p_x(3) + p_y(2)]/\sqrt{2}$	$E(\Sigma_1)^\pm = \text{mixture of 1c and 1d}$
	1d	$d_{xy}$	$d_{xy}(0)$	$= E_m \pm \sqrt{(E_g/2)^2 + 8(pd\pi)^2 s^2}$
	1e	$p_\pi$	$[p_x(5) + p_y(5)]/\sqrt{2}$	$E(\Sigma_1) = E_\pi$
$\Sigma_2(A_2)$	1a	$p_\pi$	$[p_z(2) - p_z(3)]/\sqrt{2}$	$E(\Sigma_2)^\pm = \text{mixture of 1a and 1b}$
	1b	$d_{xz}, d_{yz}$	$[d_{xz}(0) - d_{yz}(0)]/\sqrt{2}$	$= E_m \pm \sqrt{(E_g/2)^2 + 4(pd\pi)^2 s^2}$
$\Sigma_3(B_1)$	1a	$p_\sigma$	$p_z(5)$	$E(\Sigma_3) = E_\sigma$
	1b	$p_\pi$	$[p_z(2) + p_z(3)]/\sqrt{2}$	$E(\Sigma_3)^\pm = \text{mixture of 1b and 1c}$
	1c	$d_{xz}, d_{yz}$	$[d_{xz}(0) + d_{yz}(0)]/\sqrt{2}$	$= E_m \pm \sqrt{(E_g/2)^2 + 4(pd\pi)^2 s^2}$
$\Sigma_4(B_2)$	1a	$p_\sigma$	$[p_x(2) - p_y(3)]/\sqrt{2}$	$E(\Sigma_4)^\pm = \text{mixture of 1a and 1b}$
	1b	$d_{x^2}$	$d_{x^2}(0)$	$= E_{me} \pm \sqrt{(E_{ge}/2)^2 + 6(pd\sigma)^2 s^2}$
	1c	$p_\pi$	$[p_x(3) - p_y(2)]/\sqrt{2}$	$E(\Sigma_4) = E_\pi$
	1d	$p_\pi$	$[p_x(5) - p_y(5)]/\sqrt{2}$	$E(\Sigma_4) = E_\pi$

$$E_{me} = (E_e + E_\sigma)/2, \quad E_m = (E_t + E_\pi)/2, \quad 2a \text{ is the lattice spacing,}$$

$$E_{ge} = E_e - E_\sigma, \quad E_g = E_t - E_\pi, \quad s = \sin(ta), \quad t = k_x = k_y, \quad k_z = 0.$$

respectively) and a  $1 \times 1$  block for 1e. The additional block-diagonalization is indicated in Table 10.10 by the mixtures of the orbitals shown in the last column.

The symmetry functions and energies for  $\mathbf{k}$  along  $\Sigma$  are given in Table 10.10.

### 10.5 LCAO energies for arbitrary $\mathbf{k}$

The nearest-neighbor LCAO model we have been using to determine the approximate energies for the perovskite bands can be solved analytically for an arbitrary  $\mathbf{k}$ -vector [10.1]. For this model only the nearest-neighbor  $p$ - $d$  interactions are retained, and orthogonal Löwdin orbitals are used. The resulting energies for the 14 bands are

$$E_\pi \quad (\text{triply degenerate}), \quad (10.36)$$

$$E_\pi^\pm(\alpha\beta) = E_m \pm \sqrt{(E_g/2)^2 + 4(pd\pi)^2(S_\alpha^2 + S_\beta^2)}, \quad \alpha\beta = xy, xz, yz$$

$$(\text{six bands}), \quad (10.37)$$

$$E_\sigma \quad (\text{one band}), \quad (10.38)$$



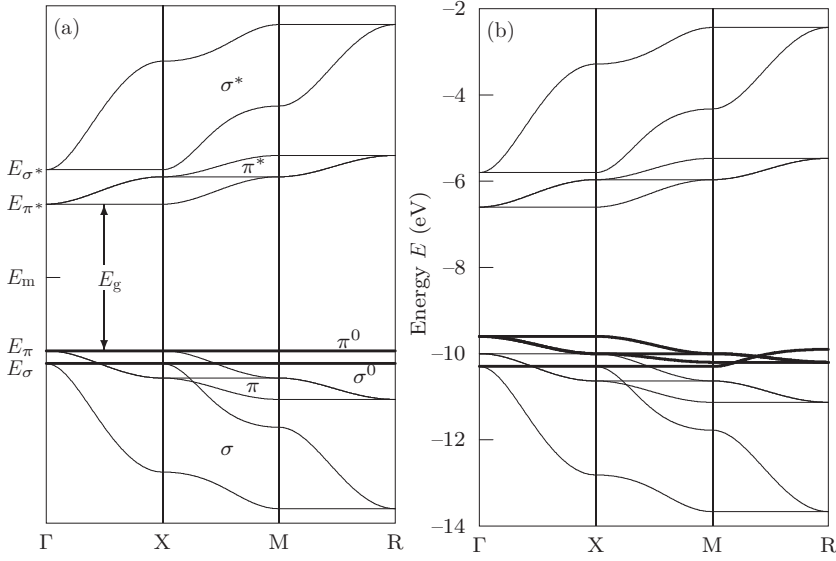


Figure 10.6 The 14 energy bands for  $d$ -band perovskite oxides. (a) The LCAO model with nearest-neighbor interactions, and (b) bands including next-nearest-neighbor oxygen–oxygen interactions. The  $\pi^*$  and the  $\sigma^*$  bands are the “conduction bands”, whereas the  $\pi$ ,  $\pi_0$ ,  $\sigma$ , and  $\sigma_0$  are the “valence bands”. The valence bands are separated from the conduction bands by an energy gap,  $E_g$ .

$$E_{\sigma}^{\pm}(\pm) = E_{me} \pm \sqrt{(E_{ge}/2)^2 + 2(pd\sigma)^2(S_x^2 + S_y^2 + S_z^2 \pm S^2)},$$

(four bands),

(10.39)

where

$$S_{\alpha} = \sin(k_{\alpha}a), \quad (10.40)$$

$$S^2 \equiv \sqrt{S_x^4 + S_y^4 + S_z^4 - S_x^2 S_z^2 - S_y^2 S_z^2 - S_x^2 S_y^2}, \quad (10.41)$$

$$E_m = \frac{1}{2}(E_t + E_{\pi}), \quad E_{me} = \frac{1}{2}(E_e + E_{\sigma}), \quad (10.42)$$

$$E_g = E_t - E_{\pi}, \quad E_{ge} = E_e - E_{\sigma}. \quad (10.43)$$

For this model there are four flat bands (i.e., bands with no dispersion), including one  $E_{\sigma}$  band and a triply degenerate  $E_{\pi}$  band. The next-nearest-neighbor interactions are the oxygen–oxygen interactions. These interactions are much weaker but serve to add dispersion to the flat bands. Figure 10.6 shows the energy bands with and without the  $p$ – $p$  interactions. It can be seen that the addition of the  $p$ – $p$  interactions makes significant changes only in the flat bands.

Figure 10.7 shows a comparison of the LCAO-model results with the bands calculated numerically using the local-density approximation (LDA) [10.2]. The

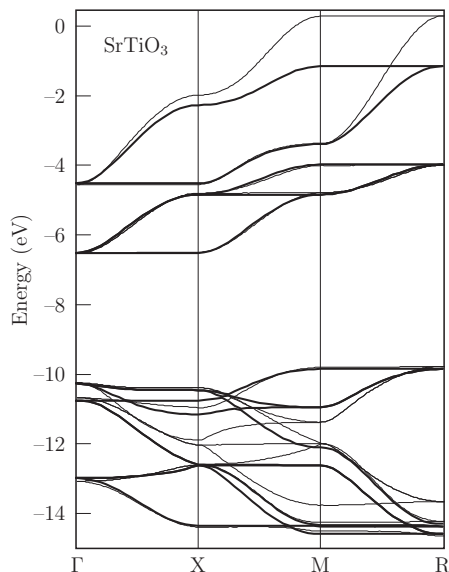


Figure 10.7 A comparison of the LCAO model including  $p$ - $p$  interactions (heavy lines) with calculations using the local-density approximation (LDA) for  $\text{SrTiO}_3$  [10.2] (thin lines). The LCAO parameters employed (in units of eV) are  $E_e = -4.52$ ,  $E_t = -6.52$ ,  $E_\pi = -10.95$ ,  $E_\sigma = -12.10$ ,  $(pd\sigma) = 2.35$ ,  $(pd\pi) = 1.60$ ,  $(pp\pi) = 0.50$ , and  $(pp\sigma) = -0.05$ . Note that the calculated LDA bands give an energy gap between the conduction and valence bands that is too small compared with experiment. To correct this, the conduction bands have been shifted up about 1.5 eV at every  $k$ -point.

general features of the two models are in reasonable agreement. The  $\pi^*$  (conduction bands) are the most important bands in determining the electronic, chemical, and optical properties of a  $d$ -band perovskite. These bands are nearly identical for the LCAO and LDA models, and therefore the LCAO model is quite useful for understanding the nature of the  $d$ -band perovskites.

### 10.6 Characteristics of the perovskite bands

The general properties of a  $d$ -band perovskite can be understood from the nature of the energy bands shown in Fig. 10.5. Consider, for example,  $\text{SrTiO}_3$ . A simple ionic description of the crystal has one  $\text{Ti}^{4+}$ , one  $\text{Sr}^{2+}$ , and three  $\text{O}^{2-}$  ions. The  $\text{Ti}^{4+}$  ion has a closed-shell [Ar] core, and  $\text{Sr}^{2+}$  has a closed-shell [Kr] core. Each  $\text{O}^{2-}$  ion has a [Ne] closed-shell configuration. The crystal is therefore an ionic insulator held together by Coulomb forces (Madelung potentials).

According to the band description, the oxygen  $p$ -orbitals and Ti  $d$ -orbitals overlap and form the energy bands we have been discussing. The number of electrons

to be distributed among the energy bands is 18; 4 from Ti, 2 from Sr, and 4 from each of the three oxygen atoms. Each energy band accommodates two electrons (per unit cell), one with spin up and one with spin down. The 18 electrons will occupy the lowest-lying energy bands. Referring to Fig. 10.6(a), we see that the electrons occupy the following bands:

$$\begin{array}{rcl}
 2 \text{ electrons in each of the two } \sigma \text{ bands} & = & 4 \\
 2 \text{ electrons in each of the three } \pi \text{ bands} & = & 6 \\
 2 \text{ electrons in each of the three } \pi_0 \text{ bands} & = & 6 \\
 2 \text{ electrons in the non-degenerate } \sigma_0 \text{ band} & = & \underline{2} \\
 \text{Total number of electrons} & = & 18
 \end{array}$$

Therefore, all of the valence bands are occupied, and there are no occupied states in the conduction bands. The occupied bands are separated from the unoccupied bands by a sizable energy gap,  $E_g$ , which is a few electron volts for most perovskites. The crystal is an insulator because there are no available empty states in the lower (valence) bands.

Next, consider the perovskite oxide  $\text{NaWO}_3$ . For this material the metal ions contribute 7 electrons and the oxygen ions 12, for a total of 19 electrons to be assigned to the energy bands. The additional electron (compared with the case of  $\text{SrTiO}_3$ ) will occupy the  $\pi^*$  bands. The  $\pi^*$  bands can accommodate  $3 \times 2 = 6$  electrons, and therefore are only partially occupied. As a result  $\text{NaWO}_3$  is a metal.

Insulating perovskites can be made semiconducting or metallic by doping or by making the composition deficient in one of the ions. In addition, n-type  $\text{SrTiO}_3$  and  $\text{Na}_x\text{WO}_3$  ( $0.24 < x < 0.49$ ) and several other perovskites are superconductors.

The  $\pi$ -band energies,  $E_\pi^\pm(xy)$ ,  $E_\pi^\pm(xz)$ , and  $E_\pi^\pm(yz)$ , each depend only on two components of the wavevector,  $\mathbf{k}$ . As a result each is mathematically equivalent to a two-dimensional band. This feature has important physical consequences. For example, the density of electronic states has a jump discontinuity at the conduction-band edges (at  $E_t$  and  $E_m + [(E_g/2)^2 + 8(pd\pi)^2]^{1/2}$ ) and a logarithmic infinity at  $E = E_m \pm [(E_g/2)^2 + 4(pd\pi)^2]^{1/2}$ . The effects of these “*Van Hove*” singularities are clearly evident in the optical properties of the  $d$ -band perovskites [10.1, 10.3].

## References

- [10.1] T. Wolfram and Ş. Ellialtıoğlu, *Electronic and Optical Properties of d-Band Perovskites* (Cambridge: Cambridge University Press, 2006).
- [10.2] E. Mete, R. Shaltaf, and Ş. Ellialtıoğlu, “Electronic and structural properties of a 4d-perovskite: Cubic phase of  $\text{SrZrO}_3$ ”, *Phys. Rev. B* **68**, 035119 (2003) (4 pages).
- [10.3] T. Wolfram, “Two-dimensional character of the conduction bands of d-band perovskites”, *Phys. Rev. Lett.* **29**, 1383–1387 (1972).

## Exercises

(All problems refer to the perovskite structure.)

- 10.1 At  $R$  ( $\mathbf{k} = (\pi/(2a))(1, 1, 1)$ ) in the Brillouin zone, answer the following.
  - (a) What group is  $g_{\mathbf{k}}$ ?
  - (b) What is the phase factor for translation by a lattice vector  $\mathbf{R}_n = 2a(n_x, n_y, n_z)$ ?
  - (c) What is the phase factor for translation from the origin to a nearest-neighbor unit cell?
- 10.2
  - (a) Find the characters of the  $p$ - and  $d$ -orbital representations at  $R$ .
  - (b) Decompose the  $p$ - and  $d$ -orbital representations into the IRs of  $g_{\mathbf{k}}$  at  $R$ . (Note that the  $p$ -orbitals are “ $g$ ” under inversion because of the phase factor of  $-1$  between adjacent unit cells.)
- 10.3
  - (a) For Exercise 10.2, describe the form of the block-diagonalized secular equation and the degeneracies at  $R$ . Label the blocks as IRs of  $O_h$ .
  - (b) What symmetry functions will also be eigenfunctions?
- 10.4 For Exercise 10.3 use the symmetry-function-generating machine to find the 14 symmetry functions at  $R$ . Label them as IRs of  $O_h$ .
- 10.5 Use the nearest-neighbor, tight-binding model to find the energies of the 14 bands at  $R$  found in Exercise 10.4.
- 10.6
  - (a) According to symmetry-derived selection rules what electric-dipole transitions are allowed for insulating  $\text{SrTiO}_3$  at  $\Gamma$  ( $\mathbf{k} = 0$ ) in the Brillouin zone?
  - (b) Find the transition energies of the allowed optical transitions using the results in Table 10.5.
  - (c) Repeat (a) and (b) for  $\mathbf{k}$  at  $R$  in the Brillouin zone using the results from Exercises 10.4 and 10.5.
- 10.7 Calculate the tight-binding energies of the  $T_{2u}$  states at  $\Gamma$  ( $\mathbf{k} = 0$ ) in the Brillouin zone including the second-nearest-neighbor interactions (i.e., including the  $p$ - $p$  interactions).
- 10.8 What energy bands are occupied in the cubic perovskite  $\text{ReO}_3$ ? Is this compound an insulator or a metal?
- 10.9 If a cubic  $ABO_3$  perovskite undergoes a transition to a tetragonal structure with  $D_{4h}$  symmetry, what additional energy splitting would be expected at  $\Gamma$  ( $\mathbf{k} = 0$ ) in the Brillouin zone?
- 10.10 Assuming the structure is elongated along the  $z$ -axis, which  $p$ - $d$  interactions would be reduced? Make a sketch of how  $\mathcal{E}_g$  and  $T_{2g}$  states split and label the levels according to the IRs of  $D_{4h}$ .  
(Hint: Make use of the basis functions for the IRs of  $D_{4h}$ .)

- 10.11 The density of electronic states of the  $j$ th energy band,  $\rho_j(E)$ , can be calculated from the expression

$$\rho_j(E) = -\frac{1}{\pi} \Im \left\{ \frac{1}{\Omega} \int \frac{d\mathbf{k}}{E - E_{j\mathbf{k}} + i\epsilon} \right\},$$

where  $\Omega$  is the volume of the Brillouin zone,  $E_{j\mathbf{k}}$  is the  $j$ th band energy as a function of  $\mathbf{k}$ ,  $\epsilon$  is a positive infinitesimal, and  $\Im\{\dots\}$  means the imaginary part of the enclosed expression. Consider one of the  $\pi^*$  bands (whose energy is given by (10.36) with the  $+$  sign), and show that  $\rho_\pi(E)$  has a jump discontinuity at  $E = E_t$  of the form

$$\rho(E) = \begin{cases} 0 & \text{for } E = E_t - \epsilon, \\ E_g / [4\pi(p d \pi)^2] & \text{for } E = E_t + \epsilon, \end{cases}$$

in the limit as  $\epsilon \rightarrow 0$ . Hint: Make use of the result that

$$-\frac{1}{\pi} \lim_{\epsilon \rightarrow 0} \Im \left\{ \frac{1}{x - s + i\epsilon} \right\} = \delta(x - s).$$

# 11

## Applications of space-group theory: Lattice vibrations

The atoms of a crystal execute small, oscillatory motions about their equilibrium positions called lattice vibrations. These vibrations are stimulated by thermal energy or by external agents such as electromagnetic and mechanical forces. As with molecular vibrations, the atomic motions of the lattice can be expressed as linear combinations of the normal modes of motion. Classically, the energy contained in a given normal mode is unrestricted. In quantum theory the energy in a normal mode is quantized in discrete units of  $\hbar\omega$ . A quantum ( $\hbar\omega$ ) of energy in a normal mode of vibration is called a phonon. More loosely, the lattice vibration wave in a crystal is also called a phonon.

Because of the translation symmetry of an (infinite) crystal the normal modes are characterized by a wavevector,  $\mathbf{k}$ . In the case of lattice vibrations we associate a vector with the physical displacement of each atom from its equilibrium position. The Cartesian components of displacements transform in the same way as the  $p$ -orbitals and therefore the application of space-group theory to lattice vibrations is analogous to finding the tight-binding energy bands of a crystal with only  $p$ -orbitals on each atom.<sup>1</sup> The method of analysis of lattice vibrations is the same as that employed in Chapter 10 for tight-binding energy bands. Instead of energy bands we obtain “phonon branches”.

There are, however, a couple of major differences between the treatment of lattice vibration and that of tight-binding energy bands. In the case of lattice vibrations there is a requirement that three of the branches have a zero eigenvalue at  $\Gamma$  ( $\mathbf{k} = 0$ ) in the Brillouin zone (for the translation modes). In addition, in forming eigenvectors, a vibrational symmetry function does not mix with the translation symmetry function even if these two functions belong to the same row of the same IR.

<sup>1</sup> If the unit cell contains more than one atom the analogous energy-band problem would have two or more inequivalent  $p$ -orbitals at each atomic site.

### 11.1 Eigenvalue equations for lattice vibrations

To describe the motions of the atoms of a crystal with more than one atom per unit cell we need several indices. The first index locates the unit cell, the second index specifies the various atoms in the unit cell, and the third index specifies the Cartesian components of the vector from the origin (in the central cell) to the atom. For example, the displacement vector of  $\xi(\mathbf{R}_i^\lambda)$  specifies the displacement vector of the  $\lambda$ -atom in the unit cell located at  $\mathbf{R}_i$ . Its Cartesian components are  $\xi_\alpha(\mathbf{R}_i^\lambda)$ . For clarity, in the discussion we shall use the following notation:

#### Atoms within the unit cell

$\lambda, \mu$ , or  $\nu$  (superscript)

#### Unit-cell locations

$\mathbf{R}_i, \mathbf{R}_j, \mathbf{R}_k$  or  $\mathbf{R}_n$

( $i, j, k$ , or  $n$  subscript)

#### Equilibrium atomic positions

$\mathbf{R}_i^\lambda = \mathbf{R}_i + \mathbf{d}^\lambda$

( $\mathbf{d}^\lambda$  locates the  $\lambda$ -atom within a unit cell)

$\mathbf{R}_{ij}^{\lambda\nu} \equiv \mathbf{R}_i^\lambda - \mathbf{R}_j^\nu$

#### Cartesian coordinate indices

$\alpha, \beta$ , or  $\gamma$  (subscript)

#### Displacements from equilibrium

$\xi_i^\lambda \equiv \xi(\mathbf{R}_i^\lambda)$

bra  $\langle a_1, a_2, \dots, a_n |$

$n$ -component row vector

ket  $|a_1, a_2, \dots, a_n\rangle$

$n$ -component column vector

#### Cartesian components of vectors

$\xi_{\alpha i}^\lambda \equiv \xi_\alpha(\mathbf{R}_i^\lambda); \mathbf{R}_{\alpha ij}^{\lambda\nu} \equiv \mathbf{R}_{\alpha i}^\lambda - \mathbf{R}_{\alpha j}^\nu$

The instantaneous position of the  $\nu$ -atom in the  $n$ th unit cell is  $\mathbf{R}_n^\nu + \xi(\mathbf{R}_n^\nu, t)$ , where  $\xi(\mathbf{R}_n^\nu, t)$  is the vector displacement from equilibrium of the  $\nu$ -atom in the cell at  $\mathbf{R}_n$  at the atomic position  $\mathbf{R}_n^\nu = \mathbf{R}_n + \mathbf{d}^\nu$  and  $t$  denotes time.

For the harmonic approximation the potential energy due to the vibratory motion of the atoms is assumed to be quadratic in the displacements,

$$U = \frac{1}{2} \sum_{\lambda\alpha i} \sum_{\nu\beta j} f_{\alpha\beta}(\mathbf{R}_{ij}^{\lambda\nu}) \xi_{\alpha i}^\lambda \xi_{\beta j}^\nu, \quad (11.1)$$

where  $f_{\alpha\beta}(\mathbf{R}_{ij}^{\lambda\nu})$  are force constants. Specifying the unit-cell vectors,  $\mathbf{R}_i$  and  $\mathbf{R}_j$ , the atoms,  $\lambda$  and  $\nu$ , and the components  $\alpha$  and  $\beta$  uniquely specifies which interaction force constant is involved. The force constant for the interaction between  $\lambda$  and  $\nu$  atoms depends only on the difference  $\mathbf{R}_\alpha^\lambda - \mathbf{R}_\beta^\nu$  and the components  $\alpha$  and  $\beta$ . The force constants  $f_{\alpha\beta}(\mathbf{R}_{ij}^{\lambda\nu})$  (in units of dynes/cm) give the restoring force on the atom at  $\mathbf{R}_i^\lambda$  in the  $\alpha$ -direction due to the motion of the atom at  $\mathbf{R}_j^\nu$  in the  $\beta$ -direction.

To simplify the notation we define  $f_{\alpha\beta ij}^{\lambda\nu} \equiv f_{\alpha\beta}(\mathbf{R}_{ij}^{\lambda\nu})$ , keeping in mind that the dependence on  $i$  and  $j$  is only through the difference  $|\mathbf{R}_i^\lambda - \mathbf{R}_j^\nu|$ .

The force on the  $\lambda$ -atom in the unit cell at  $\mathbf{R}_i$  in the  $\alpha$ -direction due to all of the atoms in motion is

$$F_\alpha(\mathbf{R}_i^\lambda) = -\frac{\partial U}{\partial \xi_{\alpha i}^\lambda} = -\sum_{\nu\gamma j} f_{\alpha\gamma ij}^{\lambda\nu} \xi_{\gamma j}^\nu. \quad (11.2)$$

The equations of motion are

$$-\sum_{\nu\gamma j} f_{\alpha\gamma ij}^{\lambda\nu} \xi_{\gamma j}^\nu = m^\lambda \frac{\partial^2}{\partial t^2} \xi_{\alpha i}^\lambda(t), \quad (11.3)$$

where  $m^\lambda$  is the mass of the  $\lambda$ -atom. We can simplify (11.3) by taking

$$\xi_{\alpha j}^\lambda = \xi_\alpha^\lambda(\mathbf{0}) e^{i\mathbf{k}\cdot\mathbf{R}_j} e^{i\omega t}, \quad (11.4)$$

where  $\xi_\alpha^\lambda(\mathbf{0})$  is the  $\alpha$ -component of the displacement of the  $\lambda$ -atom in the central unit cell. Using (11.4) in (11.2) gives

$$\sum_{\nu\gamma j} f_{\alpha\gamma ij}^{\lambda\nu} [\xi_\gamma^\nu(\mathbf{0}) e^{i\mathbf{k}\cdot\mathbf{R}_j}] = m^\lambda \omega^2 \xi_\alpha^\lambda(\mathbf{0}) e^{i\mathbf{k}\cdot\mathbf{R}_i}. \quad (11.5)$$

Multiplying both sides of (11.5) by  $\exp(-i\mathbf{k}\cdot\mathbf{R}_i)$  yields

$$\sum_{\nu\gamma j} f_{\alpha\gamma ij}^{\lambda\nu} \xi_\gamma^\nu(\mathbf{0}) e^{i\mathbf{k}\cdot(\mathbf{R}_j-\mathbf{R}_i)} = m^\lambda \omega^2 \xi_\alpha^\lambda(\mathbf{0}). \quad (11.6)$$

Now define  $\mathbf{R}_p = \mathbf{R}_j - \mathbf{R}_i$  to obtain

$$\sum_{\nu\gamma p} f_{\alpha\gamma p}^{\lambda\nu} \xi_\gamma^\nu(\mathbf{0}) e^{i\mathbf{k}\cdot\mathbf{R}_p} = m^\lambda \omega^2 \xi_\alpha^\lambda(\mathbf{0}), \quad (11.7)$$

since the sum over  $j$  in (11.6) is the same as the sum over  $p$  in (11.7) except for rearrangement of the terms. Equation (11.7) involves only the displacements within the central unit cell. It can be written as a  $3n \times 3n$  matrix equation, where  $n$  is the number of atoms per unit cell. In matrix form we have

$$[\mathbb{F}(\mathbf{k}) - \mathbb{M}\omega^2]\xi = 0, \quad (11.8)$$

where  $\xi$  is a  $3n$ -vector whose components are  $\xi_\alpha^\lambda(\mathbf{0})$ , and the matrix elements of  $\mathbb{F}(\mathbf{k})$  are

$$\begin{aligned} \mathbb{F}(\mathbf{k})_{\alpha\gamma}^{\lambda\nu} &= \sum_p f_{\alpha\gamma p}^{\lambda\nu} e^{i\mathbf{k}\cdot\mathbf{R}_p}, \\ \mathbb{M}_{\alpha\beta}^{\lambda\mu} &= \delta_{\lambda\mu} \delta_{\alpha\beta} m^\lambda. \end{aligned} \quad (11.9)$$

Equation (11.9) can be put into standard eigenvalue form,

$$[\mathbb{D}(\mathbf{k}) - \omega^2 \mathbb{I}]\eta = 0, \quad (11.10)$$



with

$$\begin{aligned}\mathbb{D}(\mathbf{k}) &= \mathbb{M}^{-1/2} \mathbb{F}(\mathbf{k}) \mathbb{M}^{-1/2} \\ \eta &= \mathbb{M}^{1/2} \xi.\end{aligned}$$

The  $\mathbb{D}$  matrix of (11.10) is called the *dynamic matrix*. The eigenvectors are Bloch lattice waves described by  $\eta(\mathbf{k}, \zeta)$ , where  $\zeta$  denotes the various eigenvectors and  $\eta(\mathbf{k}, \zeta)$  is a  $3n$ -vector whose components are  $\eta_\alpha^\lambda(\mathbf{k}, \zeta)$  with  $\alpha = x, y, \text{ or } z$  ( $\zeta = 1, 2, \dots, 3n$ ) and the eigenvalues are  $\omega^2(\mathbf{k}, \zeta)$ . The atomic displacements in the unit cell at  $\mathbf{R}_p$  associated with a particular normal mode ( $\zeta$ ) are given by

$$\xi_\alpha^\lambda(\mathbf{R}_p, \zeta) = [\mathbb{M}^{-1/2} \eta(\mathbf{k}, \zeta)]_\alpha^\lambda e^{i\mathbf{k} \cdot \mathbf{R}_p}. \quad (11.11)$$

### The axially symmetric lattice-dynamics model

In principle it is possible to calculate the force constants,  $f_{\alpha\gamma p}^{\lambda\nu}$ , numerically from a model for the electron energy as a function of the atomic positions, but more often an empirical force-constant model that has a limited range of interactions between the atoms is employed. The parameters are then determined using some experimental data. Usually the force constants are neglected beyond the  $p$ th-nearest neighbors, where  $p$  is typically from 2 to 4. There are several different lattice-dynamics models. Here, we shall discuss only one, the *axially symmetric model* [11.1].

The basis for the axially symmetric (AS) model is the assumption that the vibrational potential energy can be taken as a sum of pair-wise atomic interactions. Consider an atom of type  $\lambda$  at  $\mathbf{R}_i^\lambda$  interacting with an atom of type  $\nu$  at  $\mathbf{R}_j^\nu$ , and write the vibrational potential energy of the pair as

$$\begin{aligned}U_{ij}^{\lambda\nu} &= \frac{C_{ij}^{\lambda\nu}}{(R_{ij}^{\lambda\nu})^2} \{[\xi(\mathbf{R}_i^\lambda) - \xi(\mathbf{R}_j^\nu)] \cdot \mathbf{R}_{ij}^{\lambda\nu}\}^2 \\ &\quad + \frac{K_{ij}^{\lambda\nu}}{(R_{ij}^{\lambda\nu})^2} \{[\xi(\mathbf{R}_i^\lambda) - \xi(\mathbf{R}_j^\nu)] \times \mathbf{R}_{ij}^{\lambda\nu}\}^2, \quad (11.12)\end{aligned}$$

where  $C_{ij}^{\lambda\nu} = C_{ij}(\mathbf{R}_{ij}^{\lambda\nu})$ ,  $K_{ij}^{\lambda\nu} = K_{ij}(\mathbf{R}_{ij}^{\lambda\nu})$ , and  $R_{ij}^{\lambda\nu} = |\mathbf{R}_i^\lambda - \mathbf{R}_j^\nu|$ . The first term of (11.12) is the energy associated with stretching of the distance between the two atoms and  $C_{ij}^{\lambda\nu}$  is a *stretching* force constant. The second term is the energy associated with relative motion normal to the line joining the two atoms and  $K_{ij}^{\lambda\nu}$  is a *bending* force constant. (For molecules,  $C$  and  $K$  are called the *bond-stretching* and *bond-bending* force constants, respectively.) The bending force constant is the same for any direction of motion normal to the line between the two atoms (at rest), and hence the interaction is axially symmetric for the pair of atoms.

The cross-product term in (11.12) can be simplified as follows. Consider vectors  $\mathbf{v}$  and  $\mathbf{w}$ . We may write

$$\mathbf{v}^2 = \frac{[\mathbf{v} \cdot \mathbf{w}]^2}{|\mathbf{w}|^2} + \frac{[\mathbf{v} \times \mathbf{w}]^2}{|\mathbf{w}|^2}$$

or

$$\frac{[\mathbf{v} \times \mathbf{w}]^2}{|\mathbf{w}|^2} = \mathbf{v}^2 - \frac{[\mathbf{v} \cdot \mathbf{w}]^2}{|\mathbf{w}|^2}.$$

Using this result in (11.12) gives

$$\begin{aligned} U_{ij}^{\lambda\nu} &= \frac{J_{ij}^{\lambda\nu}}{|\mathbf{R}_{ij}^{\lambda\nu}|^2} [(\xi_i^\lambda - \xi_j^\nu) \cdot \mathbf{R}_{ij}^{\lambda\nu}]^2 + K_{ij}^{\lambda\nu} (\xi_i^\lambda - \xi_j^\nu)^2 \\ &= \sum_{\alpha\beta} \left\{ \frac{J_{ij}^{\lambda\nu}}{|\mathbf{R}_{ij}^{\lambda\nu}|^2} R_{\alpha ij}^{\lambda\nu} R_{\beta ij}^{\lambda\nu} + \delta_{\alpha\beta} K_{ij}^{\lambda\nu} \right\} (\xi_{\alpha i}^\lambda - \xi_{\alpha j}^\nu)(\xi_{\beta i}^\lambda - \xi_{\beta j}^\nu), \quad (11.13) \end{aligned}$$

where  $J_{ij}^{\lambda\nu} = [C_{ij}^{\lambda\nu} - K_{ij}^{\lambda\nu}]$ . The vibrational potential energy for the entire crystal is then

$$U = \frac{1}{4} \sum_{\lambda\nu ij} U_{ij}^{\lambda\nu}. \quad (11.14)$$

The force in the  $\gamma$ -direction acting on the  $\mu$ -atom located at  $\mathbf{R}_n^\mu$  is

$$\begin{aligned} F_\gamma(\mathbf{R}_n^\mu) &= -\frac{\partial U}{\partial \xi_{\gamma n}^\mu} = -\sum_{\nu\beta j} \left[ J_{nj}^{\mu\nu} \frac{R_{\beta nj}^{\mu\nu} R_{\gamma nj}^{\mu\nu}}{|\mathbf{R}_{nj}^{\mu\nu}|^2} + \delta_{\gamma\beta} K_{nj}^{\mu\nu} \right] (\xi_{\beta n}^\mu - \xi_{\beta j}^\nu) \\ &= -m^\mu \omega^2 \xi_{\gamma n}^\mu. \quad (11.15) \end{aligned}$$

We take  $\xi_i^\lambda = \xi(\mathbf{R}_i^\lambda) = \xi^\lambda(\mathbf{0}) \exp(i\mathbf{k} \cdot \mathbf{R}_i^\lambda)$ , where  $\xi^\lambda(\mathbf{0})$  is the displacement vector for the  $\lambda$ -atom in the central unit cell. (This procedure is slightly different than that in Section 11.1, where we took  $\xi_i^\lambda = \xi^\lambda(\mathbf{0}) \exp(i\mathbf{k} \cdot \mathbf{R}_i)$ . Either assumption is permissible. The eigenvectors in Section 11.1 will contain the intra-cell phase factors. In the present case, the intra-cell phase is already assumed. For example,  $\xi^\lambda(\mathbf{0}) \exp(i\mathbf{k} \cdot \mathbf{R}_i^\lambda) = \xi^\lambda(\mathbf{0}) \exp(i\mathbf{k} \cdot [\mathbf{R}_i + \mathbf{d}^\lambda]) = \xi^\lambda(\mathbf{0})' \exp(i\mathbf{k} \cdot \mathbf{R}_i)$ , where  $\xi^\lambda(\mathbf{0})' = \xi^\lambda(\mathbf{0}) \exp(i\mathbf{k} \cdot \mathbf{d}^\lambda)$  and  $\mathbf{d}^\lambda$  is the vector from the origin of the unit cell to the  $\lambda$ -atom.) We may choose  $\mathbf{R}_n$  as the origin of the central unit cell so that the equation of motion is

$$\sum_{\nu\beta j} \left[ J_j^{\mu\nu} \frac{R_{\beta j}^{\mu\nu} R_{\gamma j}^{\mu\nu}}{|\mathbf{R}_j^{\mu\nu}|^2} + \delta_{\gamma\beta} K_j^{\mu\nu} \right] [\xi_\beta^\mu(0) - \xi_\beta^\nu(0) \exp(i\mathbf{k} \cdot \mathbf{R}_i^\nu)] = m^\mu \omega^2 \xi_\gamma^\mu(0). \quad (11.16)$$

The  $3n \times 3n$  dynamic matrix may be expressed as [11.2]

$$D_{\alpha\beta}^{\lambda\nu}(\mathbf{k}) = \frac{1}{\sqrt{m^\lambda m^\nu}} \left\{ \left[ \sum_{\mu} A_{\alpha\beta}^{\lambda\mu}(0^+) \right] \delta_{\lambda\nu} - A_{\alpha\beta}^{\lambda\nu}(\mathbf{k}) \right\}, \quad (11.17)$$

where  $0^+$  indicates the limit as  $\mathbf{k} \rightarrow 0$  and  $\mathbb{A}$  is a  $3n \times 3n$  matrix whose elements are

$$A_{\alpha\beta}^{\lambda\nu} = \sum_s \left\{ -\frac{J(R_s^{\lambda\nu})}{(R_s^{\lambda\nu})^2} \frac{\partial^2}{\partial k_\alpha \partial k_\beta} + K(R_s^{\lambda\nu}) \delta_{\alpha\beta} \right\} G_s^{\lambda\nu}, \quad (11.18)$$

where

$$G_s^{\lambda\nu} = \sum_{n(s)} e^{i\mathbf{k} \cdot \mathbf{R}_{n(s)}^{\lambda\nu}}. \quad (11.19)$$

In (11.18) and (11.19), the index  $s$  denotes a *shell* of  $\nu$ -neighbors that are equidistant (at the distance  $|\mathbf{R}_s^{\lambda\nu}| = R_s^{\lambda\nu}$ ) from the  $\lambda$ -atom in the central cell. The sum over  $s$  is over all of the different shells. The sum over  $n(s)$  is over all of the atoms in the  $s$ th shell. The notation  $\mathbf{R}_{n(s)}^{\lambda\nu}$  means a vector from the  $\lambda$ -atom in the central cell to the  $\nu$ -atom in the  $s$ th shell (with both atoms at their equilibrium positions). Thus the sum over all the atomic sites is expressed as a sum over  $s$  and  $n(s)$ . In applications of the model, the sum over  $s$  is truncated for  $s$  greater than some selected cut off (e.g., the third-nearest neighbors). The function  $G$  in (11.19) serves as a generator from which the matrix elements of  $\mathbb{D}$  can be generated by differentiation. For example, for a cubic crystal with one atom per unit cell the nearest neighbors are located at  $(\pm a, 0, 0)$ ,  $(0, \pm a, 0)$ , and  $(0, 0, \pm a)$ , so  $G^{11}(1) = \{\exp(ik_x a) + \exp(-ik_x a) + \exp(ik_y a) + \exp(-ik_y a) + \exp(ik_z a) + \exp(-ik_z a)\} = 2\{\cos(k_x a) + \cos(k_y a) + \cos(k_z a)\}$ . For the second-nearest neighbors,  $G^{11}(2) = 4\{\cos(k_x a) \cos(k_y a) + \cos(k_x a) \cos(k_z a) + \cos(k_y a) \cos(k_z a)\}$ .

Some properties of the dynamic matrix are evident from (11.16) through (11.19). In particular, it can be seen that  $D_{\alpha\beta}^{\lambda\nu}(\mathbf{k}) = D_{\beta\alpha}^{\lambda\nu}(\mathbf{k}) = D_{\beta\alpha}^{\nu\lambda}(\mathbf{k})^*$  and that  $D_{\alpha\beta}^{\lambda\nu}(\mathbf{0}) = D_{\beta\alpha}^{\lambda\nu}(\mathbf{0}) = D_{\beta\alpha}^{\nu\lambda}(\mathbf{0})$ , so the dynamic matrix is Hermitian and at  $\mathbf{k} = 0$  it is symmetric.

## 11.2 Acoustic-phonon branches

As a simple, tutorial example consider a simple-cubic lattice with one atom per unit cell. Since there is only one type of atom, we may omit the upper superscripts. The dynamic matrix is a  $3 \times 3$  and the eigenvalue equation, (11.10), is a  $3 \times 3$  with  $M_{\alpha\beta} = m\delta_{\alpha\beta}$ . For this simple case the  $\eta$ -vectors are proportional to the  $\xi$ -vectors, so the normalized eigenvectors are the same in either system. The three displacement components,  $\xi_\alpha$  (or the three mass-weighted components,

$\eta_\alpha = \sqrt{m}\xi_\alpha$ ), are basis functions for a three-dimensional representation of the group of the wavevector,  $g_k$ .

### 11.2.1 $\mathbf{k} = 0$ irreducible representations

At  $\Gamma$  in the Brillouin zone ( $\mathbf{k} = 0$ ) the group of the wavevector is  $O_h$ . The displacement components,  $\xi_\alpha$  ( $\alpha = x, y$ , and  $z$ ), are basis functions for a three-dimensional representation of  $O_h$ . They transform under the operations of the group as  $x, y$ , and  $z$ . From the character table for  $O$  (Table E.1 in Appendix E) it is evident that  $x, y$ , and  $z$  are the basis functions for the three rows of the  $T_1$  representation. Since  $x, y$ , and  $z$  are “ungerade” (odd under inversion) functions, they are the basis functions for the  $T_{1u}$  IR of the  $O_h$  group. Therefore there are three degenerate phonon normal modes whose eigenvectors are  $\xi_\alpha$  ( $\alpha = x, y$ , and  $z$ ) or, in ket form,  $|1, 0, 0\rangle$ ,  $|0, 1, 0\rangle$ , and  $|0, 0, 1\rangle$ . At  $\Gamma$  the phase factor  $\exp(i\mathbf{k} \cdot \mathbf{R}_m) = 1$ , and the atoms have the same displacement vector in every unit cell. Clearly these modes correspond to translation in the  $x$ -,  $y$ -, and  $z$ -directions. For a crystal undergoing translation as a unit there are no restoring forces exerted on any atom, and therefore  $\omega = 0$  for all three modes for  $\mathbf{k} = 0$ . (This places restrictions on the force constants discussed below.)

### 11.2.2 $\mathbf{k}$ along the $\Delta$ -line

The group of the wavevector,  $g_k$ , for  $\mathbf{k}$  along various symmetry lines of a simple cubic lattice was discussed in Chapter 9. The same results apply to lattice vibrations or any other excitations of the crystal characterized by a wavevector. In Chapter 9, we found that, along the  $\Delta$ -line,  $\mathbf{k} = (0, 0, t)$ ,  $g_k$  is the group  $C_{4v}$ . The character table for  $C_{4v}$  (Table 1.6 in Chapter 1) shows that  $z$  is the basis function for the  $\Delta_1(A_1)$  IR, and  $x$  and  $y$  are the basis functions for the two-dimensional  $\Delta_5(\mathcal{E})$  IR. Therefore the representation based on  $\xi_\alpha$  decomposes into  $\Delta_1(A_1) + \Delta_5(\mathcal{E})$ . The secular equation (11.10) is diagonal. The diagonal elements are the mass-weighted squares of the frequencies corresponding to the  $\Delta_1(A_1)$  normal mode and two (degenerate)  $\Delta_5(\mathcal{E})$  normal modes. The cell eigenvectors are  $|0, 0, 1\rangle$  for  $\Delta_1(A_1)$ , and  $|1, 0, 0\rangle$  and  $|0, 1, 0\rangle$  for  $\Delta_5(\mathcal{E})$ . The displacement  $\xi_z$  is parallel (or antiparallel) to  $\mathbf{k}$  for the  $\Delta_1(A_1)$  phonon branch. This branch is therefore called the *longitudinal acoustic branch*. The  $\Delta_5(\mathcal{E})$  modes have displacements perpendicular to  $\mathbf{k}$ . These two branches are called the *transverse acoustic branches*.

The translation phase factor is  $\exp(ik_z R_{mz})$ , so there is wave-like motion along the  $z$ -axis, but the displacements are uniform in any  $x$ - $y$  plane in lattice space. At X in the Brillouin zone,  $\mathbf{k} = (\pi/c)(0, 0, 1)$ . Consider any lattice vector,  $R_{mz} = c(0, 0, m)$ , where  $c$  is the lattice constant and  $m$  is any integer. The phase factor

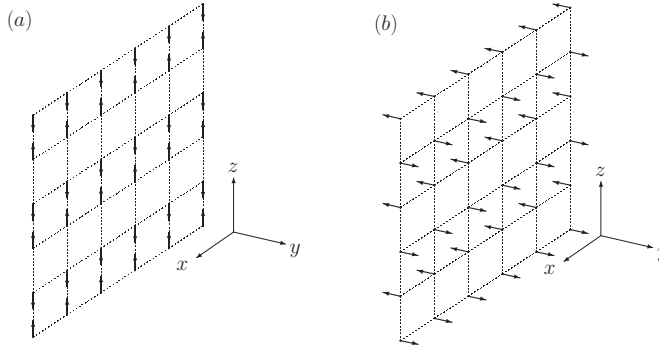


Figure 11.1 Displacements for the acoustic modes at X in the Brillouin zone. The group of the wavevector is  $D_{4h}$ . The phase of the displacements varies by  $180^\circ$  from unit cell to unit cell along the  $z$ -axis. The displacements in an  $x$ - $y$  plane are uniform. (a) Longitudinal mode. Compression and dilation between adjacent  $x$ - $y$  planes. (b) Transverse mode. Shear between adjacent  $x$ - $y$  planes. The two transverse modes are degenerate.

is  $\exp(ik_z R_{zm}) = \exp(im\pi) = (-1)^m$ . Thus, at X, the displacements in alternate  $x$ - $y$  planes are  $180^\circ$  out of phase with one another. The displacement vectors at X are shown schematically in Fig. 11.1.

### 11.2.3 $\mathbf{k}$ along the $\Sigma$ -line

For  $\mathbf{k}$  along the  $\Sigma$ -line of symmetry ( $\mathbf{k} = (t, t, 0)$ ), the group of the wavevector is  $C_{2v}$ . The character table for the group for  $C_{2v}$  (Table 10.8) assumes that the two-fold axis is in the  $z$ -direction. If we take the coordinate  $z$ -axis along the  $[110]$  direction and the  $x$ - and  $y$ -axes perpendicular to the  $\Sigma$ -line, the decomposition of the representation based on the components of  $\xi$  is evident from the character table.  $\xi_z$  is the basis function for the  $\Sigma_1(A_1)$  IR (longitudinal branch),  $\xi_y$  is the basis for the  $\Sigma_4(B_2)$  IR (transverse branch), and  $\xi_x$  is the basis for the  $\Sigma_3(B_1)$  IR (transverse branch). With this choice of the coordinate axes the vibrational displacement eigenvectors in ket notation are  $|0, 0, 1\rangle$ ,  $|0, 1, 0\rangle$ , and  $|1, 0, 0\rangle$  for the  $\Sigma_1(A_1)$ ,  $\Sigma_4(B_2)$ , and  $\Sigma_3(B_1)$  modes, respectively. If we use our original coordinate system, where the  $\Sigma$ -line is along the  $[110]$  direction (as shown in Fig. 10.2), then  $\mathbf{k} = (t, t, 0)$ . In this system the eigenvectors are  $2^{-1/2}|1, 1, 0\rangle$  for the  $\Sigma_1(A_1)$  branch,  $2^{-1/2}|-1, 1, 0\rangle$  for the  $\Sigma_3(B_1)$  branch, and  $|0, 0, 1\rangle$  for the  $\Sigma_4(B_2)$  branch. The translation phase factor is  $\exp(i\mathbf{k} \cdot \mathbf{R}_m) = \exp[ict(m_x + m_y)]$ , where  $m_x$  and  $m_y$  are integers, and  $c$  is the lattice constant. At M the group of the wavevector changes to  $D_{4h}$ . The longitudinal acoustic branch is  $M'_2(A_{2u})$ . The two transverse acoustic branches are  $M'_5(\mathcal{E}_u)$ . The two modes are shown in Fig. 11.2. Figure 11.2(a)

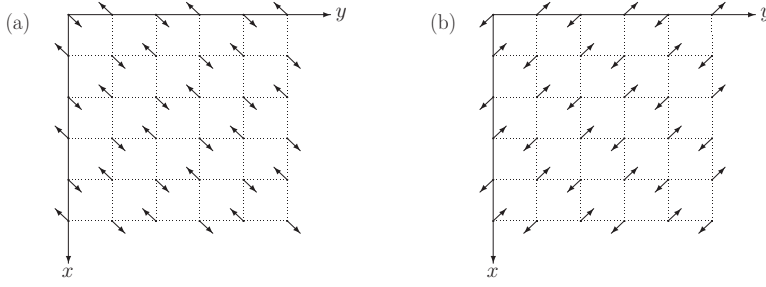


Figure 11.2 Atomic displacements for the acoustic modes at M in the Brillouin zone. The group of the wavevector is  $D_{4h}$ . The displacements are in phase along the line  $m_x = m_y + 2n$ . However adjacent lines,  $m_x = m_y + n$  and  $m_x = m_y + n + 1$ , have opposite phases. The phase is constant in the  $z$ -direction. (a)  $M'_2(A_{2u})$  (longitudinal acoustic) and (b) one of the  $M'_5(E_u)$  modes (transverse acoustic).

shows the  $M'_2(A_{2u})$  (longitudinal acoustic) mode, and Fig. 11.2(b) shows one of the  $M'_5(E_u)$  modes (transverse acoustic). At M,  $\mathbf{k} = (\pi/c)(1, 1, 0)$  and the phase factor is  $\exp[i\pi(m_x + m_y)] = (-1)^{m_x + m_y}$ . Along the line  $x = y$  in the  $x$ - $y$  plane in lattice space,  $m_x = m_y$ , so the phase factor is  $(-1)^{2n} = 1$ . For adjacent lines  $m_x = m_y + n$  and  $m_x = m_y + n + 1$  the relative displacements are  $180^\circ$  out of phase as shown in Fig. 11.2.

### Phonon energies

Group theory provides the IRs of the phonon branches from which important information such as the symmetry functions, degeneracies, and optical selection rules can be obtained. In many cases it also provides the eigenvectors for the lattice modes. However, group theory alone can not give the energies of the phonons. A force-constant model in which the force constants are treated as parameters chosen to fit experimental data may be employed. Data may be obtained from neutron inelastic scattering, X-ray diffuse scattering, or optical measurements. The measured elastic constants can also be used to help determine the parameters [11.1].

The frequencies of the acoustic branches can be expressed in terms of the matrix elements of the dynamic matrix,  $\mathbb{D}$ . For the simple-cubic lattice with one atom per unit cell,

$$\omega^2(\zeta) = \langle \eta^\zeta | \mathbb{D}(\mathbf{k}) | \eta^\zeta \rangle,$$

where  $\eta^\zeta$  is any eigenvector. For example, For  $\mathbf{k} = (0, 0, t)$ , the eigenvalues are

$$\begin{aligned} \omega^2(\Delta_1) &= \langle 0, 0, 1 | \mathbb{D}(\mathbf{k}) | 0, 0, 1 \rangle = D_{zz}(\mathbf{k}), \\ \omega^2(\Delta_5) &= \langle 1, 0, 0 | \mathbb{D}(\mathbf{k}) | 1, 0, 0 \rangle = D_{xx}(\mathbf{k}) = D_{yy}(\mathbf{k}). \end{aligned}$$

For  $\mathbf{k} = (t, t, 0)$  the eigenvalues are

$$\begin{aligned}\omega^2(\Sigma_4) &= \langle 0, 0, 1 | \mathbb{D}(\mathbf{k}) | 0, 0, 1 \rangle = D_{zz}(\mathbf{k}), \\ \omega^2(\Sigma_1) &= \frac{1}{2} \langle 1, 1, 0 | \mathbb{D}(\mathbf{k}) | 1, 1, 0 \rangle = \frac{1}{2} \{ D_{xx}(\mathbf{k}) + D_{yy}(\mathbf{k}) + D_{xy}(\mathbf{k}) + D_{yz}(\mathbf{k}) \} \\ &= D_{xx}(\mathbf{k}) + D_{xy}(\mathbf{k}), \\ \omega^2(\Sigma_3) &= \frac{1}{2} \langle -1, 1, 0 | \mathbb{D}(\mathbf{k}) | -1, 1, 0 \rangle = D_{xx}(\mathbf{k}) - D_{xy}(\mathbf{k}).\end{aligned}$$

Figure 11.3 shows the results for the axially symmetric model compared with experimental results for the acoustic modes of copper [11.3]. The upper curve is the longitudinal acoustic branch, and the lower two curves are the two transverse acoustic branches. All of the acoustic branches have  $\omega = 2\pi\nu$  proportional to  $|\mathbf{k}|$  as  $\mathbf{k} \rightarrow 0$ . The proportionality constant depends on the direction of  $\mathbf{k}$  and the branch (as is evident in Fig. 11.3). The linearity of the acoustic dispersion curves in the long-wavelength limit is a general property of phonons and elastic waves. The slope of the dispersion curve as  $\mathbf{k} \rightarrow 0$  determines the velocity of sound for the branch.

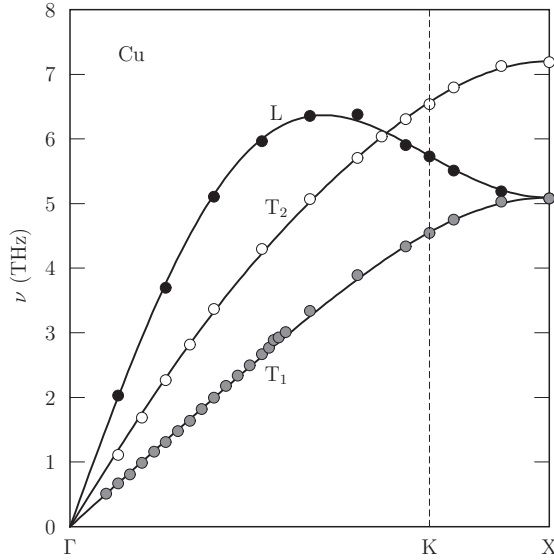


Figure 11.3 Dispersion curves for face-centered cubic copper along the [110] directions  $\Gamma K$  and  $KX$  in the Brillouin zone. The solid lines are for the axially symmetric lattice-dynamics model [11.1] with parameters  $k_1(1) = 30.0$ ,  $k_1(2) = 0.25$ ,  $k_1(3) = 1.50$ ,  $C_B(1) = -2.06$ ,  $C_B(2) = -0.38$ , and  $C_B(3) = 0.03$  in the notation used in [11.1]. The circles are inelastic-neutron-scattering data [11.3]. The upper curve is the longitudinal acoustic branch, and the lower two curves are transverse acoustic branches. The frequency  $\nu = \omega/(2\pi)$ , and  $k_{\max} = \sqrt{2}\pi/c = K$ , where  $c$  is the lattice constant for copper.

### 11.3 Optical branches: Two atoms per unit cell

When a crystal's unit cell contains more than one atom, additional vibration branches occur. If the unit cell contains  $n$  atoms, there will be  $3n$  branches. Three of the branches are always acoustic branches because there are three translation modes in the limit as  $\mathbf{k} \rightarrow 0$ . The remaining  $3n - 3$  branches are called *optical branches*. The frequencies of the optical branches are non-zero at  $\mathbf{k} = 0$ . In fact, in many cases the frequencies lie in the infrared and can be excited optically, which explains the name “optical branches”.

To explore the nature of these optical branches we shall analyze the lattice vibrations of a simple-cubic structure with two atoms per cell. Atom “ $a$ ” with mass  $m$  is at the center of the unit cell cube, and atom “ $b$ ” with mass  $M$  is at the corner of the cube, as shown in Fig. 11.4. With two atoms per unit cell, the secular equation, (11.10), is a  $6 \times 6$  matrix equation. The  $\eta$ -vector is a six-component vector,  $\eta_\alpha^\lambda = \sqrt{m^\lambda} \xi_\alpha^\lambda$ , where  $m^\lambda = m$  for  $\lambda = a$  and  $m^\lambda = M$  for  $\lambda = b$ ; and  $\alpha = x, y$ , or  $z$ . The lattice constant is  $2c$ . The vector joining atoms  $a$  and  $b$  in the unit cell is  $\mathbf{t} = c(1, 1, 1)$ , as shown in Fig. 11.4.

#### 11.3.1 Vibration modes at $\Gamma$ ( $\mathbf{k} = 0$ )

At  $\mathbf{k} = 0$ ,  $g_{\mathbf{k}}$  is the  $O_h$  group. If we choose the  $a$ -atom site as the origin then the  $a$ -site is invariant under all the operations of the group. The  $b$ -atom site transforms into itself or one of the seven other equivalent sites in adjacent unit cells. The translation phase factor is 1 at  $\mathbf{k} = 0$ . The  $a$  and  $b$  atoms are never transformed into one another, so each of the sets of displacements  $\{\xi_x^a, \xi_y^a, \xi_z^a\}$  and  $\{\xi_x^b, \xi_y^b, \xi_z^b\}$

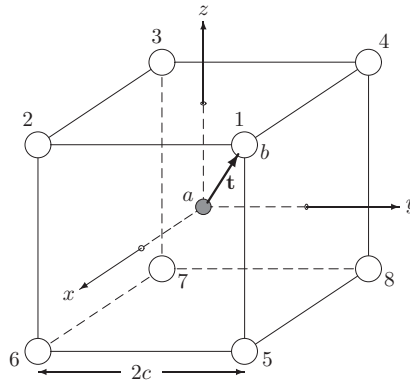


Figure 11.4 A unit cell with two atoms. Atom  $a$  is at  $c(0, 0, 0)$  and atom  $b$  is at  $c(1, 1, 1)$ , where  $2c$  is the lattice constant for the simple-cubic Bravais lattice. The open circles labeled 1 through 8 indicate equivalent atom- $b$  sites in adjacent unit cells. The vector  $\mathbf{t} = c(1, 1, 1)$ .



is a basis function for a three-dimensional representation of  $O_h$ . Since the displacements transform as  $x$ ,  $y$ , and  $z$ , each set is the basis for the  $T_{1u}$  irreducible representation. That is, the decomposition of the six-dimensional representation based on displacements is  $2T_{1u}$ . The set  $\{\xi_x^a, \xi_y^a, \xi_z^a\}$  is the basis for one  $T_{1u}$ , and the set  $\{\xi_x^b, \xi_y^b, \xi_z^b\}$  is the basis for the other  $T_{1u}$ . These two sets of symmetry functions belong to the same IR. Therefore the eigenvectors for the normal vibration modes are of the form  $A\xi_\alpha^a + B\xi_\alpha^b$ . At  $\mathbf{k} = 0$ , three of the modes correspond to translation along the  $x$ -,  $y$ -, and  $z$ -axes with normalized ket eigenvectors,

displacement eigenvectors	mass-weighted eigenvectors
$\xi_x^{(\text{trans})} = (1/\sqrt{2}) 1, 0, 0, 1, 0, 0\rangle,$	$\eta_x^{(\text{trans})} = (1/\sqrt{m+M}) \sqrt{m}, 0, 0, \sqrt{M}, 0, 0\rangle,$
$\xi_y^{(\text{trans})} = (1/\sqrt{2}) 0, 1, 0, 0, 1, 0\rangle,$	$\eta_y^{(\text{trans})} = (1/\sqrt{m+M}) 0, \sqrt{m}, 0, 0, \sqrt{M}, 0\rangle,$
$\xi_z^{(\text{trans})} = (1/\sqrt{2}) 0, 0, 1, 0, 0, 1\rangle,$	$\eta_z^{(\text{trans})} = (1/\sqrt{m+M}) 0, 0, \sqrt{m}, 0, 0, \sqrt{M}\rangle.$

The remaining three (vibrational) eigenvectors must be orthogonal to one another and to the translation eigenvectors. The orthogonality requirements are sufficient to determine the remaining three eigenvectors,

vibrational eigenvectors

$$\begin{aligned}\eta_x^{\text{opt}} &= (1/\sqrt{m+M})|\sqrt{M}, 0, 0, -\sqrt{m}, 0, 0\rangle, \\ \eta_y^{\text{opt}} &= (1/\sqrt{m+M})|0, \sqrt{M}, 0, 0, -\sqrt{m}, 0\rangle, \\ \eta_z^{\text{opt}} &= (1/\sqrt{m+M})|0, 0, \sqrt{M}, 0, 0, -\sqrt{m}\rangle.\end{aligned}$$

At  $\mathbf{k} = 0$  the frequencies of the translation modes are zero, but the vibration eigenstates are optical modes and they have non-zero  $\omega$ . At  $\mathbf{k} = 0$  the optical modes are characterized by the motions of the two atoms being 180 degrees out of phase. A schematic representation of the symmetry functions is shown in Fig. 11.5.

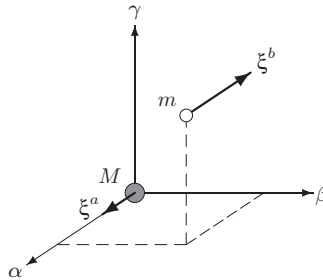


Figure 11.5 A schematic representation of the unit-cell optical-mode displacements at  $\mathbf{k} = 0$  for  $M > m$ . The vectors  $\xi^a$  and  $\xi^b$  are the physical displacement vectors,  $\xi^b = -(M/m)\xi^a$ . For the vibration modes the center of mass is at rest.

### 11.3.2 Matrix elements of $\mathbb{D}(\mathbf{k} = 0)$

Since we were able to find the eigenvectors at  $\mathbf{k} = 0$ , the dynamic matrix  $\mathbb{D}(0)$  is completely specified in terms of the three optical frequencies. For the simple-cubic structure we are considering, these optical frequencies are degenerate. Therefore the dynamic matrix is completely specified in terms of a single frequency that we shall call  $\omega^0$ .

The method of finding the elements of  $\mathbb{D}(0)$  is the same as that employed in Chapter 1. The matrix of eigenvectors expressed as kets (column vectors) can be used to diagonalize  $\mathbb{D}(0)$ . Let  $\mathbb{S}$  be the matrix of eigenvectors,

$$\begin{aligned} \mathbb{S} &= (\eta_x^{\text{opt}}, \eta_y^{\text{opt}}, \eta_z^{\text{opt}}, \eta_x^{\text{T}}, \eta_y^{\text{T}}, \eta_z^{\text{T}}) \\ &= \frac{1}{\sqrt{M+m}} \begin{pmatrix} \sqrt{M} & 0 & 0 & \sqrt{m} & 0 & 0 \\ 0 & \sqrt{M} & 0 & 0 & \sqrt{m} & 0 \\ 0 & 0 & \sqrt{M} & 0 & 0 & \sqrt{m} \\ -\sqrt{m} & 0 & 0 & \sqrt{M} & 0 & 0 \\ 0 & -\sqrt{m} & 0 & 0 & \sqrt{M} & 0 \\ 0 & 0 & -\sqrt{m} & 0 & 0 & \sqrt{M} \end{pmatrix}. \end{aligned} \quad (11.20)$$

The inverse matrix,  $\mathbb{S}^{-1}$ , is the transpose of  $\mathbb{S}$ . The similarity transformation  $\mathbb{S}^{-1} \mathbb{D}(0) \mathbb{S}$  diagonalizes  $\mathbb{D}(0)$ ,

$$\mathbb{S}^{-1} \mathbb{D}(0) \mathbb{S} = \begin{pmatrix} (\omega^0)^2 & 0 & 0 & 0 & 0 & 0 \\ 0 & (\omega^0)^2 & 0 & 0 & 0 & 0 \\ 0 & 0 & (\omega^0)^2 & 0 & 0 & 0 \\ 0 & 0 & 0 & 0 & 0 & 0 \\ 0 & 0 & 0 & 0 & 0 & 0 \\ 0 & 0 & 0 & 0 & 0 & 0 \end{pmatrix}. \quad (11.21)$$

It then follows that

$$\begin{aligned} \mathbb{D}(0) &= \mathbb{S}[\mathbb{S}^{-1} \mathbb{D}(0) \mathbb{S}] \mathbb{S}^{-1} = \frac{1}{M+m} \times \\ &\begin{pmatrix} M(\omega^0)^2 & 0 & 0 & -\sqrt{Mm}(\omega^0)^2 & 0 & 0 \\ 0 & M(\omega^0)^2 & 0 & 0 & -\sqrt{Mm}(\omega^0)^2 & 0 \\ 0 & 0 & M(\omega^0)^2 & 0 & 0 & -\sqrt{Mm}(\omega^0)^2 \\ -\sqrt{Mm}(\omega^0)^2 & 0 & 0 & m(\omega^0)^2 & 0 & 0 \\ 0 & -\sqrt{Mm}(\omega^0)^2 & 0 & 0 & m(\omega^0)^2 & 0 \\ 0 & 0 & -\sqrt{Mm}(\omega^0)^2 & 0 & 0 & m(\omega^0)^2 \end{pmatrix}. \end{aligned} \quad (11.22)$$

If we rearrange the rows and columns of  $\mathbb{D}(\mathbf{0})$  it takes the block-diagonal form

$$\frac{1}{M+m} \begin{vmatrix} \begin{bmatrix} M(\omega^0)^2 & -\sqrt{Mm}(\omega^0)^2 \\ -\sqrt{Mm}(\omega^0)^2 & m(\omega^0)^2 \end{bmatrix} & \begin{bmatrix} M(\omega^0)^2 & -\sqrt{Mm}(\omega^0)^2 \\ -\sqrt{Mm}(\omega^0)^2 & m(\omega^0)^2 \end{bmatrix} \\ \begin{bmatrix} M(\omega^0)^2 & -\sqrt{Mm}(\omega^0)^2 \\ -\sqrt{Mm}(\omega^0)^2 & m(\omega^0)^2 \end{bmatrix} & \begin{bmatrix} M(\omega^0)^2 & -\sqrt{Mm}(\omega^0)^2 \\ -\sqrt{Mm}(\omega^0)^2 & m(\omega^0)^2 \end{bmatrix} \end{vmatrix}. \quad (11.23)$$

Therefore the dynamic matrix  $\mathbb{D}(\mathbf{0})$  is completely determined if the frequency of the optical mode is known. Often,  $\omega^0$  can be measured by optical or neutron-scattering experiments. Conversely, the optical frequency can be expressed in terms of the dynamic matrix.

From the matrix elements of the dynamic matrix in (11.22) it is clear that

$$(\omega^0)^2 = \frac{m+M}{M} D_{\alpha\alpha}^{aa}. \quad (11.24)$$

Other relationships that can be deduced from (11.22) include

$$\begin{aligned} D_{\alpha\alpha}^{aa}(\mathbf{0}) &= \frac{M}{m} D_{\alpha\alpha}^{bb}(\mathbf{0}), \\ D_{\alpha\alpha}^{ab}(\mathbf{0}) &= D_{\alpha\alpha}^{ba}(\mathbf{0}), \\ D_{\alpha\alpha}^{ba}(\mathbf{0}) &= -\sqrt{\frac{M}{m}} D_{\alpha\alpha}^{aa}(\mathbf{0}), \\ D_{\alpha\beta}^{\lambda\nu}(\mathbf{0}) &= 0 \text{ for } \alpha \neq \beta. \end{aligned} \quad (11.25)$$

As a result of these relationships the dynamic matrix has only one independent matrix element.

As mentioned before, the “longitudinal” and “transverse” designations are fuzzy for  $\mathbf{k} = 0$ , since the direction of the wavevector is indeterminate. However, we can define the  $\mathbf{k} = 0$  branches as the limit as  $\mathbf{k} \rightarrow 0$ . For this to make sense, the limiting frequency must be independent of the direction of the wavevector. This presents no problem here because the three optical frequencies are degenerate at  $\mathbf{k} = 0$  (see the discussion in the box below).

*The dynamic matrix presented in Section 11.1 accounts only for the short-range forces assuming the ions are “rigid”. This model works well for metals and non-ionic crystals. For ionic crystals such as CsCl the long-range forces due to the charges on the ions and the polarizability of the ions cause the longitudinal and transverse optical modes to have different frequencies even for very small values of the wavevector. The lattice vibrations for these ionic crystals are usually analyzed using what is called a lattice “shell model”. The shell model allows the ion cores to move relative to their outer shell of electrons and includes the subsequent polarization of*

the ions caused by such movements [11.4]. For a cubic crystal with the CsCl structure the three optical modes must be degenerate if the wavevector is **identically** zero. However, an applied electromagnetic field will establish a preferred direction so that the symmetry is no longer cubic. In the case of optical absorption the electric field of the light wave establishes a preferred direction and conservation of momentum means that the stimulated lattice wave has  $\mathbf{k}$  unequal to zero. The same is true for inelastic scattering of neutrons. In order to distinguish a transverse mode from a longitudinal mode, there must be a preferred direction. Generally any probe of the lattice modes will establish a preferred direction, and therefore the  $\mathbf{k} = 0$  point is not accessible to experiment. Mathematically,  $\mathbf{k} = 0$  is a singular point. The results of the shell model should be interpreted as the limit as  $\mathbf{k} \rightarrow 0$ .

### 11.3.3 $\mathbf{k}$ along the $\Delta$ -line

Along the  $\Delta$ -line,  $\mathbf{k} = (0, 0, t)$ , the group of the wavevector is  $C_{4v}$ . Again, the sets of displacements  $\{\xi_x^a, \xi_y^a, \xi_z^a\}$  and  $\{\xi_x^b, \xi_y^b, \xi_z^b\}$  provide bases for two reducible representations of  $C_{4v}$ . According to the character table  $z$  is the basis function for the  $\Delta_1(A_1)$ , while  $x$  and  $y$  are bases for the  $\Delta_5(\mathcal{E})$  IR. Therefore the representation based on  $\{\xi_x^a, \xi_y^a, \xi_z^a\}$  decomposes into  $\Delta_1(A_1) + \Delta_5(\mathcal{E})$ .

Under the operations of  $\mathbf{g}_\mathbf{k}$  the  $b$ -atoms transform into themselves, but also into  $b$ -atoms on equivalent sites. We must consider the translation phase factors,  $\exp(ik_z \delta R_z)$ , where  $\delta R_z$  is the  $z$ -component of the change in the position of an atom due to the symmetry operation. However, these factors are always unity for  $\mathbf{k}$  along the  $\Delta$ -line because an operation that leaves  $k_z$  unchanged has  $\delta R_z = 0$ . By definition, the operations of  $\mathbf{g}_\mathbf{k}$  for  $\mathbf{k} = (0, 0, t)$  do not change the  $z$ -components of the position vectors. For example, consider the  $C_2$  rotation about the  $z$ -axis. This operation carries the  $b$ -atom at site 1 into site 3. The translation of site 1 into site 3 is a translation by  $2c(1, 1, 0)$ , so the phase factor  $\exp(i\mathbf{k} \cdot \mathbf{R}) = \exp[i(0, 0, t) \cdot 2c(1, 1, 0)] = \exp(0) = 1$ . Since all the phase factors are unity, the representation based on  $\{\xi_x^b, \xi_y^b, \xi_z^b\}$  also decomposes into  $\Delta(A_1) + \Delta_5(\mathcal{E})$ . At the X point in the Brillouin zone, where new operations that transform  $\mathbf{k}$  into  $\mathbf{k} + \mathbf{K}$  are included,  $\mathbf{g}_\mathbf{k}$  changes from  $C_{4v}$  to  $D_{4h}$ .

As a result of the above consideration, we see that the dynamic matrix has the block-diagonal form: a  $2 \times 2$   $\Delta_1(A_1)$  block whose symmetry functions are  $\xi_z^a$  and  $\xi_z^b$ ; a  $2 \times 2$ , row-1,  $\Delta_5(\mathcal{E})$  block whose symmetry functions are  $\xi_x^a$  and  $\xi_x^b$ ; and a  $2 \times 2$ , row-2,  $\Delta_5(\mathcal{E})$  block whose symmetry functions are  $\xi_y^a$  and  $\xi_y^b$ . The normalized  $\eta$ -symmetry functions and the normalized  $\xi$ -symmetry functions are the same in this case,

Table 11.1 *Phonon eigenvalues for  $\mathbf{k} = (0, 0, t)$ , for the simple-cubic structure, with two atoms per unit cell*

Mode	Eigenvalue ( $\omega^2$ )	Degeneracy
LA $\Delta_1$	$\frac{1}{2}(D_{zz}^{aa} + D_{zz}^{bb}) - \sqrt{[\frac{1}{2}(D_{zz}^{aa} - D_{zz}^{bb})]^2 +  D_{zz}^{ab} ^2}$	1
LO $\Delta_1$	$\frac{1}{2}(D_{zz}^{aa} + D_{zz}^{bb}) + \sqrt{[\frac{1}{2}(D_{zz}^{aa} - D_{zz}^{bb})]^2 +  D_{zz}^{ab} ^2}$	1
TA $\Delta_5$	$\frac{1}{2}(D_{xx}^{aa} + D_{xx}^{bb}) - \sqrt{[\frac{1}{2}(D_{xx}^{aa} - D_{xx}^{bb})]^2 +  D_{xx}^{ab} ^2}$	2
TO $\Delta_5$	$\frac{1}{2}(D_{xx}^{aa} + D_{xx}^{bb}) + \sqrt{[\frac{1}{2}(D_{xx}^{aa} - D_{xx}^{bb})]^2 +  D_{xx}^{ab} ^2}$	2

$$D_{\alpha\beta}^{\lambda\nu} = D_{\alpha\beta}^{\lambda\nu}(\mathbf{k}), \mathbf{k} = (0, 0, t).$$

LA (TA), longitudinal (transverse) acoustic; LO (TO), longitudinal (transverse) optical.

IR	Symmetry functions
$\Delta_1(A_1)$	$\eta_1 =  0, 0, 1, 0, 0, 0\rangle$ $\eta_2 =  0, 0, 0, 0, 0, 1\rangle$
$\Delta_5(\mathcal{E})$ row 1	$\eta_3 =  1, 0, 0, 0, 0, 0\rangle$ $\eta_4 =  0, 0, 0, 1, 0, 0\rangle$
$\Delta_5(\mathcal{E})$ row 2	$\eta_5 =  0, 1, 0, 0, 0, 0\rangle$ $\eta_6 =  0, 0, 0, 0, 1, 0\rangle$

The eigenfunctions are linear combinations of the symmetry functions that transform according to the same row of the same IR. The two  $\Delta_1(A_1)$  symmetry functions have displacements parallel to the wavevector, and therefore will mix to form the longitudinal modes, one acoustic and one optical. The four  $\Delta_5(\mathcal{E})$  modes are transverse modes, two acoustic and two optical. The secular equation for the normal modes is of the form

$$\begin{vmatrix} \langle \eta_i | \mathbb{D} | \eta_i \rangle - \omega^2 & \langle \eta_i | \mathbb{D} | \eta_j \rangle \\ \langle \eta_j | \mathbb{D} | \eta_i \rangle & \langle \eta_j | \mathbb{D} | \eta_j \rangle - \omega^2 \end{vmatrix} = 0, \quad (11.26)$$

where  $i = 1$  and  $j = 2$  for the  $\Delta_1(A_1)$  modes, and  $i = 3$  and  $j = 4$  (or  $i = 5$  and  $j = 6$ ) for the  $\Delta_5(\mathcal{E})$  modes. Table 11.1 lists the eigenvalues in terms of the dynamic matrix elements.

### 11.3.4 $\mathbf{k}$ along the $\Sigma$ -line

Along the  $\Sigma$ -line of symmetry, the group of the wavevector is  $C_{2v}$ , and  $\mathbf{k} = (t, t, 0)$ . The translation phase factor,  $\exp[ik(\delta R_x + \delta R_y)]$ , is unity for all of the

operations of  $C_{2v}$ . A couple of examples show why this is so. Consider the phase factor for the  $b$ -atom under the operation  $P(\bar{C}_2^{(6)})$ . (The equivalence of the “barred” symbols to the usual  $C_{2v}$  symbols is given in Table 10.9.) Site 1 is translated into site 5. The translation vector is  $\delta\mathbf{R} = 2c(0, 0, -1)$  and  $k_x \delta R_x = k_y \delta R_y = 0$ . Next consider the effect of  $P(i\bar{C}_2^{(5)})$  on site 1.  $P(\bar{C}_2^{(5)})$  translates site 1 into site 7, and  $P(i)$  carries site 7 back to site 1. Therefore site 1 is invariant, and the phase factor is again unity.

Since the phase factors are all unity, we can identify the IRs for the vibrational modes directly from the point-group character table for  $C_{2v}$ . It should be noted that the character table uses the  $z$ -axis as the principal axis. So in the  $C_{2v}$  character table the  $z$ -axis is along the  $[110]$  direction. Consider coordinates in which the  $z$ -axis is parallel to the  $\Sigma$ -line and the  $x$ - and  $y$ -axes are perpendicular to the  $\Sigma$ -line. Table 10.9 shows that  $z$  is the basis for the  $\Sigma_1(A_1)$  IR,  $x$  is the basis for the  $\Sigma_3(B_1)$  IR, and  $y$  is the basis for the  $\Sigma_4(B_2)$ . The normalized symmetry functions for  $z$  along the  $\Sigma$ -line and for the original  $x$ -,  $y$ -, and  $z$ -axes are shown below. The normalized symmetry functions for  $\eta$ -vectors and  $\xi$ -vectors are the same.

$C_{2v}$ IR	Symmetry functions $z$ along $[110]$	Symmetry functions $z$ along $[001]$
$\Sigma_1(A_1)$	$ 0, 0, 1, 0, 0, 0\rangle$ $ 0, 0, 0, 0, 0, 1\rangle$	$\eta_1 = (1/\sqrt{2}) 1, 1, 0, 0, 0, 0\rangle$ $\eta_2 = (1/\sqrt{2}) 0, 0, 0, 1, 1, 0\rangle$
$\Sigma_3(B_1)$	$ 1, 0, 0, 0, 0, 0\rangle$ $ 0, 0, 0, 1, 0, 0\rangle$	$\eta_3 = (1/\sqrt{2}) -1, 1, 0, 0, 0, 0\rangle$ $\eta_4 = (1/\sqrt{2}) 0, 0, 0, -1, 1, 0\rangle$
$\Sigma_4(B_2)$	$ 0, 1, 0, 0, 0, 0\rangle$ $ 0, 0, 0, 0, 1, 0\rangle$	$\eta_5 =  0, 0, 1, 0, 0, 0\rangle$ $\eta_6 =  0, 0, 0, 0, 0, 1\rangle$

Since there are two symmetry functions for each IR, the block-diagonal form of the secular equation is three  $2 \times 2$  blocks. Each block of the secular equation takes the form of (11.26). For the  $\Sigma_1(B_1)$  IR modes,  $i = 1$  and  $j = 2$ . For the  $\Sigma_3(B_1)$  modes,  $i = 3$  and  $j = 4$ . For the  $\Sigma_4(B_2)$  modes,  $i = 5$  and  $j = 6$ . The eigenvalues are shown in Table 11.2.

#### 11.4 Lattice vibrations for the perovskite structure

The tight-binding or LCAO energy bands of the simple-cubic, perovskite structure were discussed in Chapter 10. Here we are concerned with the lattice vibrations. The perovskite unit cell contains one  $A$ , one  $B$ , and three  $O$  atoms (here  $O$  does not necessarily indicate oxygen) as shown in Fig. 11.6(a). A fixed  $x, y, z$  coordinate system is erected at each of the sites in the central unit cell (see Fig. 11.6(b)). Various atomic displacements are denoted by

Table 11.2 Phonon eigenvalues for  $\mathbf{k} = (0, t, t)$ , for the simple-cubic structure, with two atoms per unit cell. All have degeneracies equal to 1.

Mode	Eigenvalue ( $\omega^2$ ) $z$ along [001]
LA $\Sigma_1$	$\frac{1}{2}(D_{xx}^{aa} + D_{xy}^{aa} + D_{xx}^{bb} + D_{xy}^{bb})$ $-\sqrt{\left[\frac{1}{2}(D_{xx}^{aa} + D_{xy}^{aa} - D_{xx}^{bb} - D_{xy}^{bb})\right]^2 +  D_{xx}^{ab} + D_{xy}^{ab} ^2}$
LO $\Sigma_1$	$\frac{1}{2}(D_{xx}^{aa} + D_{xy}^{aa} + D_{xx}^{bb} + D_{xy}^{bb})$ $+\sqrt{\left[\frac{1}{2}(D_{xx}^{aa} + D_{xy}^{aa} - D_{xx}^{bb} - D_{xy}^{bb})\right]^2 +  D_{xx}^{ab} + D_{xy}^{ab} ^2}$
TA $\Sigma_3$	$\frac{1}{2}(D_{xx}^{aa} - D_{xy}^{aa} + D_{xx}^{bb} - D_{xy}^{bb})$ $-\sqrt{\left[\frac{1}{2}(D_{xx}^{aa} - D_{xy}^{aa} - D_{xx}^{bb} + D_{xy}^{bb})\right]^2 +  D_{xx}^{ab} - D_{xy}^{ab} ^2}$
TO $\Sigma_3$	$\frac{1}{2}(D_{xx}^{aa} - D_{xy}^{aa} + D_{xx}^{bb} - D_{xy}^{bb})$ $+\sqrt{\left[\frac{1}{2}(D_{xx}^{aa} - D_{xy}^{aa} - D_{xx}^{bb} + D_{xy}^{bb})\right]^2 +  D_{xx}^{ab} - D_{xy}^{ab} ^2}$
TA $\Sigma_4$	$\frac{1}{2}(D_{zz}^{aa} + D_{zz}^{bb}) - \sqrt{\left[\frac{1}{2}(D_{zz}^{aa} - D_{zz}^{bb})\right]^2 -  D_{zz}^{ab} ^2}$
TO $\Sigma_4$	$\frac{1}{2}(D_{zz}^{aa} + D_{zz}^{bb}) + \sqrt{\left[\frac{1}{2}(D_{zz}^{aa} - D_{zz}^{bb})\right]^2 -  D_{zz}^{ab} ^2}$

$$D_{\alpha\beta}^{\lambda\nu} = D_{\alpha\beta}^{\lambda\nu}(\mathbf{k}), \quad \mathbf{k} = (t, t, 0); \quad D_{xx}^{\lambda\lambda} = D_{yy}^{\lambda\lambda}, \quad D_{xy}^{\lambda\nu} = D_{yx}^{\lambda\nu} = D_{xy}^{\nu\lambda}.$$

LA, longitudinal acoustic, LO, longitudinal optical,

TA, transverse acoustic, TO, transverse optical.

$\xi^B$  for the  $B$  atom,

$\xi^A$  for the  $A$  atom,

$\xi^{(2)}, \xi^{(3)}, \xi^{(5)}$ , for the three O atoms.

#### 11.4.1 $\mathbf{k} = 0$ irreducible representations

At  $\Gamma$  ( $\mathbf{k} = 0$ ) the group of the wavevector is  $O_h$ . The sets of displacement components for the  $A$  and  $B$  atoms,  $\{\xi_x^A, \xi_y^A, \xi_z^A\}$  and  $\{\xi_x^B, \xi_y^B, \xi_z^B\}$ , are each bases for the  $\Gamma_{15}(T_{1u})$  IR of  $O_h$ . For the O-atom displacements we note that the set  $\xi_x^{(2)}, \xi_y^{(3)}, \xi_z^{(5)}$  may be classified as  $\sigma$ -type displacements since they are along the  $B$ -O internuclear axis of the unit cell. By contrast, the set  $\xi_y^{(2)}, \xi_z^{(2)}, \xi_x^{(3)}, \xi_z^{(3)}, \xi_x^{(5)}, \xi_y^{(5)}$  are  $\pi$ -type displacements since they are displacements perpendicular to the  $B$ -O internuclear axis of the unit cell. No operation of  $O_h$  can transform a  $\sigma$ -displacement into a  $\pi$ -displacement and vice versa. Therefore, the sets of  $\sigma$ - and  $\pi$ -displacements form separate representations. The displacements transform

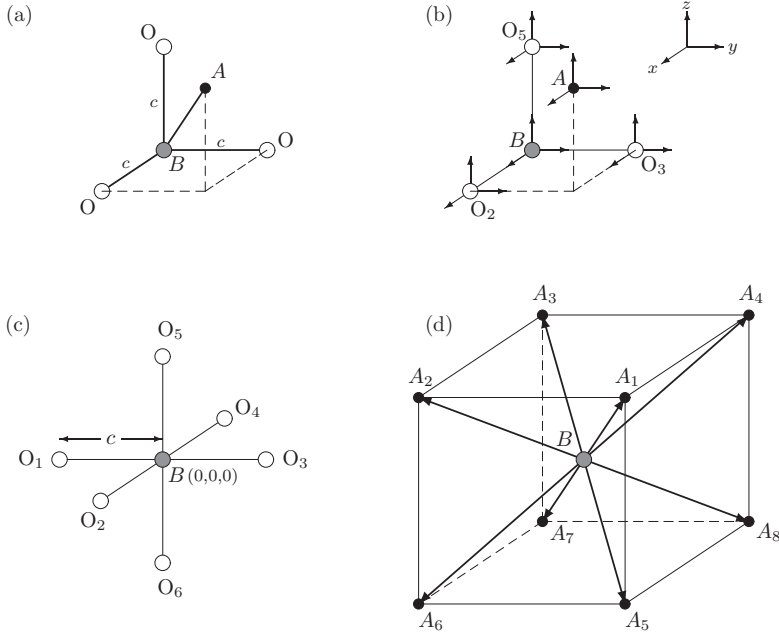


Figure 11.6 (a) The unit cell containing one  $B$ , one  $A$ , and three  $O$  atoms. The  $B$ - $O$  distance is  $c$ . (b) The coordinate system for the atoms of the unit cell. (c) The six equivalent  $O$  atoms surrounding the  $B$  atom. The pairs of equivalent  $O$ -atom sites are 2 and 4, 1 and 3, and 5 and 6. (d) The eight equivalent sites for the  $A$  atom. The lattice spacing is  $2c$  and the origin is at the  $B$  site.

in the same way as  $p$ -orbitals. We may use the results of Table 10.3 in Chapter 10 to obtain the decompositions based on the displacements. They are

$$\begin{aligned}
 \Gamma(A) &= \Gamma_{15}(T_{1u}), \\
 \Gamma(B) &= \Gamma_{15}(T_{1u}), \\
 \Gamma^\sigma(O) &= \Gamma_{15}(T_{1u}), \\
 \Gamma^\pi(O) &= \Gamma_{15}(T_{1u}) + \Gamma_{25}(T_{2u}), \\
 \Gamma(ABO_3) &= 4\Gamma_{15}(T_{1u}) + \Gamma_{25}(T_{2u}).
 \end{aligned}$$

The above decomposition indicates that the secular equation will block-diagonalize into three degenerate  $1 \times 1$  blocks for the  $\Gamma_{25}(T_{2u})$  modes and three  $4 \times 4$  blocks for the  $\Gamma_{15}(T_{1u})$  modes.

#### 11.4.2 Symmetry functions for the perovskites at $\Gamma$

The symmetry functions for the  $O$ -atom displacements are analogous to those for the  $p$ -orbitals. Therefore, the  $\pi$  and  $\sigma$  symmetry functions may be taken directly



from Table 10.5 by substituting  $\xi_\alpha^{(j)}$  for  $p_\alpha(\mathbf{r}-\mathbf{R}_j)$ . The symmetry functions for the  $A$  and  $B$  atoms are just the displacement components,  $\xi_x^A, \xi_y^A, \xi_z^A$  and  $\xi_x^B, \xi_y^B, \xi_z^B$ .

The IR  $\Gamma_{25}(T_{2u})$  occurs only once in the decomposition, and hence the symmetry functions are eigenstates (normal modes). The frequency is triply degenerate.

For the remaining vibrational modes it is necessary to combine four symmetry functions belonging to a specific row of  $\Gamma_{15}(T_{1u})$  to form an eigenvector. The four frequencies of the  $\Gamma_{15} 4 \times 4$  block are triply degenerate. That is, each of the three  $4 \times 4$  blocks yields the same four frequencies. Before transformation by the matrix of symmetry functions, the dynamic matrix is a  $15 \times 15$  matrix. After transformation by the symmetry functions, it consists of three uncoupled  $5 \times 5$  blocks, each of which consists of a  $1 \times 1 \Gamma_{25}(T_{2u})$  block and a  $4 \times 4 \Gamma_{15}(T_{1u})$  block. Furthermore, each  $4 \times 4$  block must yield a translation mode with zero frequency. Therefore if we use the translation mode as one of the symmetry functions, each  $4 \times 4$  block is further block-diagonalized into a  $1 \times 1$  block and a  $3 \times 3$  block.

We shall represent a five-column vector as the ket whose entries correspond to the amplitudes of displacement of the  $A$ ,  $B$ , O(2), O(3), and O(5) atoms in the  $\alpha$ -direction. With this choice, a ket such as  $\mathbf{v}_\alpha = |\alpha; 1, 0, 0, 0, 1\rangle$  represents a vector whose displacement amplitudes are unity for  $\xi_\alpha^A$ , zero for  $\xi_\alpha^B, \xi_\alpha^{(2)},$  and  $\xi_\alpha^{(3)}$ , and unity for  $\xi_\alpha^{(5)}$ . Expanded into a 15-component vector such as  $\mathbf{v}_y = |y; 1, 0, 0, 0, 1\rangle$ , this is  $|0, 0, 0, 0, 0, 1, 0, 0, 0, 1, 0, 0, 0, 0, 0\rangle$ . In the mass-weighted  $\eta$ -system the normalized ket  $\mathbf{v}_y = (m_A + m)^{-1/2}|y; \sqrt{m_A}, 0, 0, 0, \sqrt{m}\rangle$ . Note that a normalized ket involving only one type of atom is the same in the  $\xi$ - and  $\eta$ -systems, but when two or more different atom types are involved the kets in the  $\xi$ - and  $\eta$ -systems are not the same. Table 11.3 summarizes the results.

Table 11.3 *IRs and vibration symmetry functions at  $\mathbf{k} = 0$  for the cubic perovskites.  $m_A$  is the mass of the  $A$  atom,  $m_B$  is the mass of the  $B$  atom, and  $m$  is the mass of each  $O$  atom. The kets' entries are ordered as  $|\alpha; \xi_\alpha^A, \xi_\alpha^B, \xi_\alpha^{(2)}, \xi_\alpha^{(3)}, \xi_\alpha^{(5)}\rangle$ .*

Atom	IR	Normalized symmetry functions $\alpha = x, y, z/\text{row } 1, 2, 3$
$A$	$\Gamma_{15}(T_{1u})$	$\eta_\alpha^A(\Gamma_{25}) =  \alpha; 1, 0, 0, 0, 0\rangle$
$B$	$\Gamma_{15}(T_{1u})$	$\eta_\alpha^B(\Gamma_{15}) =  \alpha; 0, 1, 0, 0, 0\rangle$
O- $\sigma$	$\Gamma_{15}(T_{1u})$	$\eta_\alpha^\sigma(\Gamma_{15}) =  \alpha; 0, 0, 1, 0, 0\rangle$
O- $\pi$	$\Gamma_{15}(T_{1u})$	$\eta_x^\pi(\Gamma_{15}) = 2^{-1/2} x; 0, 0, 0, 1, 1\rangle$ row 1 $\eta_y^\pi(\Gamma_{15}) = 2^{-1/2} y; 0, 0, 1, 0, 1\rangle$ row 2 $\eta_z^\pi(\Gamma_{15}) = 2^{-1/2} z; 0, 0, 1, 1, 0\rangle$ row 3
O- $\pi$	$\Gamma_{25}(T_{2u})$	$\eta_x^\pi(\Gamma_{25}) = 2^{-1/2} x; 0, 0, 0, 1, -1\rangle$ row 1 $\eta_y^\pi(\Gamma_{25}) = 2^{-1/2} y; 0, 0, 1, 0, -1\rangle$ row 2 $\eta_z^\pi(\Gamma_{25}) = 2^{-1/2} z; 0, 0, 1, -1, 0\rangle$ row 3

### 11.4.3 Eigenfrequencies of the optical modes at $\mathbf{k} = 0$

Without any further analysis, we already have 6 of the 15 normal modes at  $\Gamma$ . The three translation eigenvectors are known and, since  $\Gamma_{25}(T_{2u})$  occurs only once in the decomposition, we know that the three symmetry functions,  $\eta_\alpha(\Gamma_{25}) = 2^{-1/2}|\alpha; 0, 0, 0, 1, -1\rangle$  with  $\alpha = x, y$ , and  $z$ , are also eigenvectors. The  $\Gamma_{25}$  eigenvalue expressed in terms of these dynamic matrix elements is

$$\begin{aligned}\omega^2(\Gamma_{25}) &= \langle \eta_\alpha^\pi(\Gamma_{25}) | \mathbb{D}(\mathbf{0}) | \eta_\alpha^\pi(\Gamma_{25}) \rangle \quad (\alpha = x, y, z) \\ &= \frac{1}{2} \langle \alpha; 0, 0, 0, 1, -1 | \mathbb{D}(\mathbf{0}) | \alpha; 0, 0, 0, 1, -1 \rangle \\ &= \frac{1}{2} [D_{\alpha\alpha}^{33}(\mathbf{0}) + D_{\alpha\alpha}^{55}(\mathbf{0}) - D_{\alpha\alpha}^{35}(\mathbf{0}) - D_{\alpha\alpha}^{53}(\mathbf{0})].\end{aligned}\quad (11.27)$$

The eigenvalue is the same for each  $\alpha$ , so  $\omega^2(\Gamma_{25})$  is triply degenerate.

#### Constraints on the dynamic matrix

The requirement that the translation frequency vanish ( $\omega^2(t_\alpha) = 0$ ) places constraints on the general dynamic matrix defined by (11.9) and (11.10). In particular, if  $\eta_t$  is a translation in any direction, it requires that  $\mathbb{D}\eta_t = 0$ . For a translation in an arbitrary direction,  $(t_x, t_y, t_z)$ , one requires

$$\sum_{v\beta} D_{\alpha\beta}^{\lambda v}(0) t_\beta \sqrt{m_v} = 0 \quad (\eta_\beta^v = t_\beta \sqrt{m_v}).$$

Since  $t_\beta$  is arbitrary it follows that each term ( $\beta = x, y, z$ ) must vanish separately, so

$$\sum_v D_{\alpha\beta}^{\lambda v}(0) \sqrt{m_v} = 0.$$

For the axially symmetric model these constraints are automatically satisfied. (In (11.16) set  $\mathbf{k} = 0$  and note that  $\xi_\beta^\mu = \xi_\beta^v$  for any translation.)

The eigenvectors for the translation modes are

$$\xi_{t\alpha} = \frac{1}{\sqrt{5}} |\alpha; 1, 1, 1, 1, 1\rangle \quad (\alpha = x, y, z), \quad (11.28)$$

$$\eta_{t\alpha} = \frac{1}{\sqrt{m_T}} |\alpha; \sqrt{m_A}, \sqrt{m_B}, \sqrt{m}, \sqrt{m}, \sqrt{m}\rangle, \quad (11.29)$$

where  $m_A$ ,  $m_B$ , and  $m$  are the masses of the  $A$ ,  $B$ , and  $O$  atoms, respectively, and  $m_T$  is the total mass of the unit cell,  $m_T = m_A + m_B + 3m$ . The translation eigenvalue is  $\omega^2(t_\alpha) = 0$ .

*Symmetry functions orthogonal to translations*

It is useful to construct symmetry functions that are orthogonal to the translation eigenfunctions. Since the symmetry functions do not mix different rows of the representations, we now limit our discussion to the row-1 functions. We already have two of the five row-1 eigenvectors. The remaining three eigenvectors must be constructed as linear combinations of the  $\Gamma_{15}$  row-1 symmetry functions. They must be mutually orthogonal and orthogonal to  $\eta_x(\Gamma_{25})$  and  $\eta_{tx}$ . The vectors  $\eta_x(\Gamma_{25})$  and  $\eta_{tx}$  are already orthogonal to each other. We can not determine the remaining eigenvectors from group theory alone. Knowledge of the dynamic matrix is required. However, we can form new symmetry functions that are mutually orthogonal and orthogonal to  $\eta_x(\Gamma_{25})$  and  $\eta_{tx}$ . To accomplish this, we may employ the Gram–Schmidt process.

**The Gram–Schmidt orthogonalization process**

Suppose we have  $n$  vectors,  $\mathbf{v}_1, \mathbf{v}_2, \dots, \mathbf{v}_n$ , and wish to form  $n$  mutually orthogonal vectors,  $\mathbf{u}_1, \mathbf{u}_2, \dots, \mathbf{u}_n$ . The Gram–Schmidt process gives a recipe for the  $\mathbf{u}$ -vectors in terms of the original  $\mathbf{v}$ -vectors:

$$\begin{aligned}\mathbf{u}_1 &= \mathbf{v}_1, \\ \mathbf{u}_2 &= \mathbf{v}_2 - \frac{(\mathbf{u}_1 \cdot \mathbf{v}_2)}{(\mathbf{u}_1 \cdot \mathbf{u}_1)} \mathbf{u}_1, \\ \mathbf{u}_3 &= \mathbf{v}_3 - \frac{(\mathbf{u}_1 \cdot \mathbf{v}_3)}{(\mathbf{u}_1 \cdot \mathbf{u}_1)} \mathbf{u}_1 - \frac{(\mathbf{u}_2 \cdot \mathbf{v}_3)}{(\mathbf{u}_2 \cdot \mathbf{u}_2)} \mathbf{u}_2, \\ \mathbf{u}_n &= \mathbf{v}_n - \sum_{i=1}^{n-1} \frac{(\mathbf{u}_i \cdot \mathbf{v}_n)}{(\mathbf{u}_i \cdot \mathbf{u}_i)} \mathbf{u}_i.\end{aligned}$$

The  $\mathbf{u}_i$  vectors are mutually orthogonal but not normalized.

For our analysis we take the original vectors to be

$$\eta_{t_a} = \frac{1}{\sqrt{m_T}} |x; \sqrt{m_A}, \sqrt{m_B}, \sqrt{m}, \sqrt{m}, \sqrt{m}\rangle, \quad (11.30)$$

$$\eta_x^B(\Gamma_{15}) = |x; 0, 1, 0, 0, 0\rangle, \quad (11.31)$$

$$\eta_x^\sigma(\Gamma_{15}) = |x; 0, 0, 1, 0, 0\rangle, \quad (11.32)$$

$$\eta_x^\pi(\Gamma_{15}) = \frac{1}{\sqrt{2}} |x; 0, 0, 0, 1, 1\rangle, \quad (11.33)$$

and apply the Gram–Schmidt process to obtain four mutually orthogonal, normalized symmetry functions:

$$\eta_{t_x} = \frac{1}{\sqrt{m_T}} \mathbb{M}^{1/2} |x; 1, 1, 1, 1, 1\rangle, \quad (11.34)$$

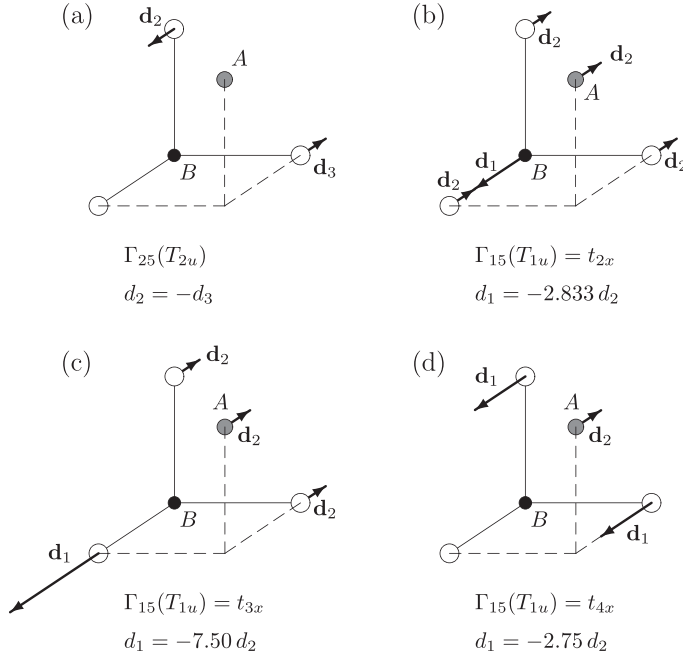


Figure 11.7 Symmetry functions for the  $\mathbf{k} = 0$  vibration modes of the  $ABO_3$  perovskites. The center of mass remains stationary for all of the vibration symmetry functions. (a) Relative physical displacements for the  $\Gamma_{25}(T_{2u})$  symmetry functions. The  $B$  atom and one of the three  $O$  atoms are stationary. (b) Relative physical displacements for the  $\Gamma_{15}(T_{1u})$  symmetry functions,  $\mathbb{M}^{-1/2} \eta_{2x}$ . (c) Relative physical displacements for the  $\Gamma_{15}(T_{1u})$  symmetry functions,  $\mathbb{M}^{-1/2} \eta_{3x}$ . (d) Relative physical displacements for the  $\Gamma_{15}(T_{1u})$  symmetry function,  $\mathbb{M}^{-1/2} \eta_{4x}$ . The  $B$  atom and one of the three  $O$  atoms are stationary. The numerical ratios of the displacements shown are for  $\text{SrTiO}_3$  with  $m_A = 88$ ,  $m_B = 48$ , and  $m = 16$  in atomic units.

$$\eta_{2x} = \frac{1}{\sqrt{N_2}} \mathbb{M}^{1/2} |x; 1, -c_2, 1, 1, 1\rangle, \quad (11.35)$$

$$\eta_{3x} = \frac{1}{\sqrt{N_3}} \mathbb{M}^{1/2} |x; 1, 0, -c_3, 1, 1\rangle, \quad (11.36)$$

$$\eta_{4x} = \frac{1}{\sqrt{N_4}} \mathbb{M}^{1/2} |x; -c_1, 0, 0, 1, 1\rangle, \quad (11.37)$$

where

$$m_T = m_A + m_B + 3m, \quad c_1 = \frac{2m}{m_A}, \quad c_2 = \frac{m_T - m_B}{m_B}, \quad c_3 = \frac{m_A + 2m}{m},$$

$$N_2 = m_A + c_2^2 m_B + 3m, \quad N_3 = m_A + (c_3^2 + 2)m, \quad N_4 = c_1^2 m_A + 2m.$$

The symmetry functions in (11.34)–(11.37) are the mass-weighted displacements of the atoms of the unit cell. The physical displacement vectors are obtained from these equations by omitting multiplication by the square root of the mass matrix,  $\mathbb{M}^{1/2}$ . The relative displacements of the atoms are shown in Fig. 11.7 for the masses of  $\text{SrTiO}_3$ . The center of mass is stationary for all of the vibration symmetry functions. That is,  $\sum_{\nu} m^{\nu} \mathbf{d}^{\nu} = 0$ , where  $\mathbf{d}^{\nu}$  is the displacement vector for the  $\nu$ -atom of the unit cell. The symmetry functions  $\eta_{t_x}$  (translation) and  $\eta_{2x}$  ( $\Gamma_{25}$ ) are eigenfunctions. The remaining three symmetry functions are not eigenvectors. The linear combination of  $\eta_{2x}$ ,  $\eta_{3x}$ , and  $\eta_{4x}$  required in order to construct the eigenvectors is determined by the dynamic matrix,  $\mathbb{D}$ . The secular equation is

$$\det \begin{bmatrix} \langle \eta_{2x} | \mathbb{D}(0) | \eta_{2x} \rangle - \omega^2 & \langle \eta_{2x} | \mathbb{D}(0) | \eta_{3x} \rangle & \langle \eta_{2x} | \mathbb{D}(0) | \eta_{4x} \rangle \\ \langle \eta_{3x} | \mathbb{D}(0) | \eta_{2x} \rangle & \langle \eta_{3x} | \mathbb{D}(0) | \eta_{3x} \rangle - \omega^2 & \langle \eta_{3x} | \mathbb{D}(0) | \eta_{4x} \rangle \\ \langle \eta_{4x} | \mathbb{D}(0) | \eta_{2x} \rangle & \langle \eta_{4x} | \mathbb{D}(0) | \eta_{3x} \rangle & \langle \eta_{4x} | \mathbb{D}(0) | \eta_{4x} \rangle - \omega^2 \end{bmatrix} = 0. \quad (11.38)$$

The solutions of (11.38) are  $\mathbf{k} = 0$  optical modes. The eigenvalues and eigenvectors can be obtained in terms of the dynamic-matrix elements by employing the formulas for the roots of a cubic equation. We shall not reproduce the results here.

## 11.5 Localized vibrations

Impurities in a lattice can produce vibrational modes that are highly localized in the neighborhood of the impurity. These modes can have frequencies that lie above the top of the acoustic branches, in gaps between branches, or above the optical branches of the pure crystal. In this section we illustrate the nature of these localized modes, starting with the simplest model possible. The extension to more complex models is then outlined.

We consider a simple-cubic crystal with one atom per unit cell, with restoring forces due to nearest-neighbor atoms only. The host-crystal atoms have mass  $m$  and the impurity atoms are isotopes with mass  $m'$ . If the concentration of impurities is small, we can approximate the system by a single impurity in an otherwise perfect crystal. For the isotope of the host crystal the force constants would be expected to be essentially the same as the force constants for the regular atoms. Therefore the entire perturbation is the difference in mass,  $\Delta M = m' - m$ . The problem of determining the localized vibrational modes is analogous to the case of isotopically substituted molecules discussed in Chapter 2. However, in the molecular case the number of vibrational modes of the host molecule is small. For a crystal, the number of vibrational modes is essentially infinite. Nevertheless, the same approach is applicable.

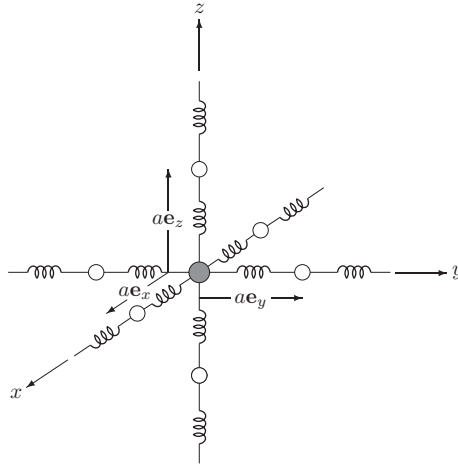


Figure 11.8 A model for the simple-cubic crystal with nearest-neighbor “springs”. The nearest-neighbor vectors are  $a\mathbf{e}_x$ ,  $a\mathbf{e}_y$ , and  $a\mathbf{e}_z$ . The white circles represent normal atoms, and the gray circle indicates the isotopic atom. The spring constant is  $f$  and the lattice constant is  $a$ . The masses of the atoms throughout the crystal are  $m$ , except at  $\mathbf{R}_i = 0$ , where the mass is  $m'$ .

Assume the impurity is located at  $\mathbf{R}_0$ . The equations of motion for the atomic displacement from equilibrium at  $\mathbf{R}_i$ ,  $\mathbf{d}(\mathbf{R}_i)$ , are

$$\begin{aligned}
 -f \sum_{\alpha} \{ [\mathbf{d}_{\alpha}(\mathbf{R}_i, t) - \mathbf{d}_{\alpha}(\mathbf{R}_i + a\mathbf{e}_{\alpha}, t)] + [\mathbf{d}_{\alpha}(\mathbf{R}_i, t) - \mathbf{d}_{\alpha}(\mathbf{R}_i - a\mathbf{e}_{\alpha}, t)] \} \\
 = m\omega^2 [1 + \epsilon \delta_{\mathbf{R}_i, \mathbf{R}_0}] \frac{\partial^2}{\partial t^2} \mathbf{d}_{\alpha}(\mathbf{R}_i, t) \quad (\alpha = x, y, \text{ and } z), \quad (11.39)
 \end{aligned}$$

where  $f$  is the effective “spring constant” (force/cm) between nearest-neighbor atoms (see Fig. 11.8). For our simple-cubic crystal the nearest neighbors in the  $\alpha$ -direction are located at  $\pm a\mathbf{e}_{\alpha}$ , where  $a$  is the lattice spacing and  $\epsilon = (m' - m)/m$ .

For the simple spring model we are considering, the motion of an ion in the  $\alpha$ -direction does not produce a force on the neighboring ion in a perpendicular direction. As a consequence the displacements in the  $x$ -,  $y$ -, and  $z$ -directions are uncoupled, but each obeys equivalent equations of motion. Consequently we may drop the subscript  $\alpha$ .

Therefore the model is essentially three, uncoupled, infinite, one-dimensional lines of atoms with an isotopic mass at the origin. Each line has the same set of normal modes. Because of the isotope, the crystal no longer possesses translation symmetry, and the eigenstates are *not* characterized by a wavevector.

For simplicity, let us consider a line of  $2N + 1$  atoms extending from  $-Na$  to  $+Na$ , where  $a$  is the lattice constant, and with the isotopic mass located at the

origin. Later we shall take the limit as  $N$  tends to infinity. The notation  $d(n, t)$  represents the displacement of the atom located at  $na$ , where  $n$  is a positive or negative integer, or zero, and  $t$  is time. For harmonic motion we can take  $d(n, t) = d(n) \exp(-i\omega t)$ , so Eq. (11.39) reduces to

$$\{[d(n) - d(n+1)] + [d(n) - d(n-1)]\} - \frac{\omega^2}{\gamma}[1 + \epsilon\delta_{n0}]d(n) = 0, \quad (11.40)$$

where  $\gamma = f/m$ .

Let the  $(2N+1)$ -column vector  $\mathbf{d}$  represent the  $2N+1$  displacements,

$$\mathbf{d} = \begin{pmatrix} d(N) \\ d(N-1) \\ \vdots \\ d(0) \\ \vdots \\ d(-N+1) \\ d(-N) \end{pmatrix}. \quad (11.41)$$

Each entry is a displacement at a lattice site, so the secular equation is a  $(2N+1) \times (2N+1)$  matrix equation,

$$\left[ \mathbb{K} - \frac{\omega^2}{\gamma} \mathbb{I} - \frac{\omega^2}{\gamma} \Delta \right] \mathbf{d} = 0, \quad (11.42)$$

where  $\mathbb{K}$  is a matrix with elements

$$K_{nn'} = [2\delta_{nn'} - \delta_{n+1,n'} - \delta_{n-1,n'}], \quad (11.43)$$

$\mathbb{I}$  is the unit matrix, and the elements of  $\Delta$  are

$$\Delta_{nn'} = \epsilon\delta_{nn'}\delta_{n0}. \quad (11.44)$$

In Eq. (11.42) we can factor out the matrix representing the perfect crystal and obtain

$$\left[ \mathbb{K} - \frac{\omega^2}{\gamma} \mathbb{I} \right] \left[ \mathbb{I} - \frac{\omega^2}{\gamma} \mathbb{G}(\omega^2) \Delta \right] \mathbf{d} = 0, \quad (11.45)$$

where  $\mathbb{G}(\omega^2) = [\mathbb{K} - (\omega^2/\gamma) \mathbb{I}]^{-1}$ . The eigenvalues are determined by

$$\det \left\{ \left[ \mathbb{K} - \frac{\omega^2}{\gamma} \mathbb{I} \right] \left[ \mathbb{I} - \frac{\omega^2}{\gamma} \mathbb{G}(\omega^2) \Delta \right] \right\} = \det \left[ \mathbb{K} - \frac{\omega^2}{\gamma} \mathbb{I} \right] \times \det \left[ \mathbb{I} - \frac{\omega^2}{\gamma} \mathbb{G}(\omega^2) \Delta \right] = 0. \quad (11.46)$$

The eigenvalues of the first determinant are those of the perfect crystal. The eigenvalues of the second factor are those associated with the isotopic mass. Therefore the solutions we seek are given by the condition

$$\det \left[ \mathbb{I} - \frac{\omega^2}{\gamma} \mathbb{G}(\omega^2) \Delta \right] = 1 - \epsilon \frac{\omega^2}{\gamma} G_{00}(\omega^2) = 0, \quad (11.47)$$

and the displacements satisfy the equation

$$\left[ \mathbb{I} - \frac{\omega^2}{\gamma} \mathbb{G}(\omega_{\text{iso}}^2) \Delta \right] \mathbf{d} = 0, \quad (11.48)$$

where  $\omega$  is evaluated at the eigenvalue of (11.47),  $\omega_{\text{iso}}$ . Equation (11.48) yields

$$\mathbf{d}(n) = \frac{\omega_{\text{iso}}^2}{\gamma} \epsilon G_{n0}(\omega_{\text{iso}}^2) \mathbf{d}(0). \quad (11.49)$$

To find  $\omega_{\text{iso}}^2$  we need to obtain expressions for the lattice Green's function,  $G_{00}(\omega^2)$ . The eigenvectors of the matrix  $[\mathbb{K} - (\omega^2/\gamma) \mathbb{I}]$  are the column vectors,  $\mathbf{d}^0(\mathbf{k}_p)$ , where

$$\mathbf{d}^0(k_p) = \frac{1}{\sqrt{2N+1}} \begin{bmatrix} e^{Nk_p a} \\ e^{(N-1)k_p a} \\ e^{(N-2)k_p a} \\ \vdots \\ e^{k_p a} \\ e^0 \\ e^{-k_p a} \\ \vdots \\ e^{(-N+1)k_p a} \\ e^{-Nk_p a} \end{bmatrix}, \quad (11.50)$$

and

$$\left[ \mathbb{K} - \frac{\omega^2}{\gamma} \mathbb{I} \right] \mathbf{d}^0(k_p) = \left[ [2 - 2 \cos(k_p a)] - \frac{\omega^2}{\gamma} \right] \mathbf{d}^0(k_p), \quad (11.51)$$

where  $k_p a = p\pi/(2N+1)$ ,  $p = -N, -N+1, \dots, 0, \dots, N-1, N$ . We form the  $(2N+1) \times (2N+1)$  unitary matrix  $\mathbb{U}$  and its transpose complex conjugate,  $\mathbb{U}^\dagger$ , from the eigenvectors  $\mathbf{d}^0(k_p)$ ,

$$U_{pm} = d^0(k_p)_m = \frac{1}{\sqrt{2N+1}} e^{ik_p m a}, \quad (11.52)$$

$$U_{ns}^\dagger = U_{sn}^* = \frac{1}{\sqrt{2N+1}} e^{-ik_s n a}, \quad (11.53)$$



and  $\mathbb{U}^\dagger \mathbb{U} = \mathbb{I}$ . The transformed matrix  $\mathbb{U}^\dagger [\mathbb{K} - \omega^2 \mathbb{I}] \mathbb{U} = \Lambda(\omega^2)$  is a diagonal matrix of the eigenvalues,

$$\Lambda_{pp'} = \{[2 - 2 \cos(k_p a)] - \omega^2/\gamma\} \delta_{pp'}. \quad (11.54)$$

The inverse of  $\Lambda(\omega^2)$  is

$$\Lambda_{pp'}^{-1} = \frac{\delta_{pp'}}{[2 - 2 \cos(k_p a)] - \omega^2/\gamma}, \quad (11.55)$$

and, since  $\mathbb{U} \Lambda^{-1} \mathbb{U}^\dagger = [\mathbb{K} - (\omega^2/\gamma) \mathbb{I}]^{-1} = \mathbb{G}(\omega^2)$ , we have a prescription for the lattice Green's-function matrix. In detail, we have

$$\begin{aligned} G(\omega^2)_{mn} &= \frac{1}{\sqrt{2N+1}} \sum_p \sum_s \frac{e^{ik_p m a} \delta_{ps} e^{-ik_s n a}}{[2 - 2 \cos(k_p a)] - \omega^2/\gamma} \\ &= \frac{1}{\sqrt{2N+1}} \sum_p \frac{e^{ik_p(m-n)a}}{[2 - 2 \cos(k_p a)] - \omega^2/\gamma}. \end{aligned} \quad (11.56)$$

In the limit of large  $N$ , the sum in (11.56) may be converted into an integral,

$$G(\omega^2)_{mn} = \frac{a}{2\pi} \int_{-\pi/a}^{\pi/a} dk \frac{e^{ik_p(m-n)a}}{[2 - 2 \cos(k_p a)] - \omega^2/\gamma}. \quad (11.57)$$

To determine the isotope eigenvalue we need only  $G(\omega^2)_{00}$ , which is given by

$$\begin{aligned} G(\omega^2)_{00} &= \frac{a}{2\pi} \int_{-\pi/a}^{\pi/a} \frac{dk}{[2 - 2 \cos(ka)] - \omega^2/\gamma} \\ &= \frac{a}{2\pi} \int_{-\pi/a}^{\pi/a} \frac{dk}{4 \sin^2(ka/2) - \omega^2/\gamma} \\ &= \frac{1}{2\pi} \int_0^{\pi/2} \frac{dx}{\sin^2 x - \omega^2/(4\gamma)} \\ &= \frac{-1/4}{\sqrt{(\omega^2/(4\gamma))[\omega^2/(4\gamma) - 1]}}. \end{aligned} \quad (11.58)$$

Substituting (11.58) into (11.47) gives the condition for an isotopic, local-mode, eigenvalue,

$$1 + \frac{\epsilon \lambda}{\sqrt{\lambda(\lambda - 1)}} = 0, \quad (11.59)$$

where  $\lambda = \omega^2/(4\gamma)$ .

### 11.5.1 Eigenvalues and eigenvectors for isotopic local modes

From (11.59) we see that there is a singularity at  $\lambda = 1$  or at  $\omega^2 = 4\gamma$ . The perfect crystal has an acoustic branch described by  $\omega^2 = [2 - 2\cos(ka)] = 4\sin^2(ka/2)$ . As  $ka/2$  varies from 0 to  $\pi/2$ ,  $\omega^2$  varies from 0 to  $4\gamma$ , and therefore  $\omega^2 = 4\gamma$  occurs at the maximum frequency of the acoustic branch. It is clear from (11.59) that there are no real solutions to the local-mode equation for  $\lambda$  less than 1 ( $\omega^2$  less than  $4\gamma$ ) because the square-root denominator becomes purely imaginary. Thus, a local mode can exist only above the top of the acoustic branch. Second, we also note that there are no solutions for positive values of  $\epsilon = (m' - m)/m$ . Negative values of  $\epsilon$  occur when the isotopic mass is less than the mass of the normal atom. However, physically  $\epsilon$  must be greater than  $-1$ , since the isotope mass must be positive. Equation (11.59) can be solved for  $\lambda$ :

$$\lambda = \frac{1}{1 - \epsilon^2} \quad (-1 < \epsilon < 0). \quad (11.60)$$

The frequency,  $\omega_{\text{iso}}$ , satisfying the above condition for  $\lambda$  must be greater than  $4\gamma$ , and therefore lies above the top of the pure-crystal vibration band. As  $\epsilon$  tends to  $-1^+$ , the frequency tends to infinity, because the isotopic mass is approaching zero. As  $\epsilon$  tends to  $0^-$ , the frequency approaches that of the top of the acoustic band, since the mass is approaching the normal mass.

To examine the eigenvector for the isotope mode, we may employ (11.49), to obtain

$$\frac{d(n)}{d(0)} = \frac{\omega_{\text{iso}}^2}{\gamma} \epsilon G_{n0}(\omega_{\text{iso}}^2).$$

Since  $G_{n0}(\omega^2)$  is real for  $\lambda = \omega^2/(4\gamma) > 1$ , it follows that  $G_{n0} = G_{0n}^* = G_{0n}$ . Therefore, the displacements for the isotopic mode are symmetrical about the origin:  $d(n) = d(-n)$ . From (11.57) we have

$$G_{n0}(\omega^2) = -\frac{1}{2\pi} \int_0^{\pi/2} \frac{dx \cos(2nx)}{\lambda - \sin^2(x)} \quad (\lambda > 1). \quad (11.61)$$

In particular,

$$G_{10}(\omega^2) = (1 - 2\lambda)G_{00}(\omega^2) - \frac{1}{2} = \frac{(-1/4)(1 - 2\lambda)}{\sqrt{\lambda(\lambda - 1)}} - \frac{1}{2}. \quad (11.62)$$

Using (11.60) gives

$$\frac{d(\pm 1)}{d(0)} = \frac{\omega_{\text{iso}}^2}{\gamma} \epsilon G_{10}(\omega_{\text{iso}}^2) = \frac{-(1 + \epsilon)}{1 - \epsilon}, \quad -1 < \epsilon < 0. \quad (11.63)$$

Since  $-1 < \epsilon < 0$ , (11.63) shows that the displacements for the neighbors are opposite to that of the isotopic atom. The displacements of adjacent atoms are  $180^\circ$

out of phase. The mode is similar to an optical mode except that the amplitudes of the displacements decrease with distance from the isotope site. For example, for  $\epsilon = -0.5$ ,  $d(n)/d(0) = (-1/3)^{|n|}$ . This corresponds to exponential decay of the amplitude,  $|d(n)/d(0)| = \exp(-|n\theta|)$  with  $\theta = 1.098\,612\,3$  (see Exercise 11.9). For very small negative values of  $\epsilon$  the amplitudes of the displacements are significant over a long distance, but, as  $\epsilon$  approaches  $-1$ , significant displacements occur only at the isotope site. That is, the mode becomes highly localized.

The simple model discussed above serves as an introduction to the general local-mode problem. For more realistic force-constant models the determination of the eigenvalues and eigenvectors usually requires numerical calculations. Nevertheless, the analytic approach to finding solutions is essentially the same.

In the most general case we are faced with solving the matrix equation

$$[\mathbb{F} + \Delta\mathbb{F} - \omega^2 \mathbb{M} - \omega^2 \Delta\mathbb{M}]\mathbf{d} = 0, \quad (11.64)$$

where now  $\mathbb{F}$  includes all of the forces that one atom can exert on another when they are in motion. In addition, there may be several atoms per unit cell. The impurity may be a foreign atom rather than an isotope, and therefore changes in the force constants,  $\Delta\mathbb{F}$ , also occur. The vector  $\mathbf{d}$  will be a column vector with  $3nN$  entries, where  $n$  is the number of atoms per unit cell and  $N$  is the total number of unit cells in the crystal. The eigenvalue equation is a  $3nN \times 3nN$  equation. However, assuming that the perturbations in force constants and mass are localized at and near the impurity ion, and that the concentration of impurities is small, the Green's-function approach is still useful in reducing the problem to a more manageable size.

Writing the matrix equation as

$$\{(\mathbb{D} - \omega^2) - \mathbb{M}^{-1/2}[\omega^2 \Delta\mathbb{M} - \Delta\mathbb{F}]\mathbb{M}^{-1/2}\}\mathbf{q} = 0 \quad (11.65)$$

leads to the eigenvalue equation

$$\det\{\mathbb{I} - \mathbb{G}(\omega^2)[\omega^2 \epsilon - \Delta\mathbf{f}]\} = 0, \quad (11.66)$$

where  $\epsilon \equiv \mathbb{M}^{-1/2} \Delta\mathbb{M} \mathbb{M}^{-1/2}$ ,  $\Delta\mathbf{f} \equiv \mathbb{M}^{-1/2} \Delta\mathbb{F} \mathbb{M}^{-1/2}$  and  $\mathbb{G}(\omega^2) = (\mathbb{D} - \omega^2)^{-1}$ . If the range of the perturbations affects  $m$  neighboring cells, then (11.66) will be a  $3nm \times 3nm$  determinant. However, it should be kept in mind that the number of solutions with real values of  $\omega^2$  may be less than  $3nm$ , or there may be none at all. In general the Green's function,  $\mathbb{G}(\omega^2)$ , is complex when  $\omega^2$  lies within a band of frequencies of the host crystal. When a solution of (11.66) is a complex number,  $\omega = \omega(\text{real}) + i\Gamma$ , the local mode is not a stationary state. Rather, it is interpreted as a mode with a finite lifetime that is proportional to  $1/\Gamma$ . Such finite-lived modes are called continuum resonances.

The lattice Green's function has the full space-group symmetry of the host crystal, but the introduction of an impurity removes the translation operations, so that

the solutions of (11.66) will be characterized by the point-group symmetry of the perturbations,  $\Delta\mathbb{F}$  or  $\Delta\mathbb{M}$ , depending on which has the lower symmetry.

### References

- [11.1] G. W. Lehman, T. Wolfram, and R. E. De Wames, “Axially symmetric model for lattice dynamics of metals with application to Cu, Al, and  $\text{ZrH}_2$ ”, *Phys. Rev.* **128**, 1593–1599 (1962).
- [11.2] C. B. Walker, “X-ray study of lattice vibrations in aluminum”, *Phys. Rev.* **103**, 547–557 (1956).
- [11.3] E. C. Svensson, B. N. Brockhouse, and J. M. Rowe, “Crystal dynamics of copper”, *Phys. Rev.* **155**, 619–632 (1967).
- [11.4] B. G. Dick, Jr. and A. W. Overhauser, “Theory of the dielectric constants of alkali halide crystals”, *Phys. Rev.* **112**, 90–103 (1958).  
A. D. B. Woods, W. Cochran, and B. N. Brockhouse, “Lattice dynamics of alkali halide crystals”, *Phys. Rev.* **119**, 980–999 (1960).

### Exercises

- 11.1 Consider the perovskite structure with  $\mathbf{k} = (0, 0, t)$ ,  $0 \leq t \leq \pi/c$ .
- (a) What is the group of the wavevector,  $\mathbf{g}_{\mathbf{k}}$ ?
  - (b) Identify the operations of  $\mathbf{g}_{\mathbf{k}}$  in terms of the operations listed in Table E.2 of Appendix E.
  - (c) Construct a table showing how the 2, 3, and 5 O sites of the central unit cell transform under the operations of  $\mathbf{g}_{\mathbf{k}}$ . Mark the sites that transform into themselves or an equivalent site. Include in the table rows showing how  $x$ ,  $y$ , and  $z$  transform among themselves.
  - (d) Use the table to find the character of each of the operations of  $\mathbf{g}_{\mathbf{k}}$  for the  $9 \times 9$  representation based on the nine displacement vectors of the three O atoms.
  - (e) What are the translation phase factors?
  - (f) Decompose the  $9 \times 9$  representation into the IRs of  $\mathbf{g}_{\mathbf{k}}$ .
  - (g) Decompose the two  $3 \times 3$  representations based on the displacement vectors for the  $A$  and  $B$  atoms.
  - (h) Discuss the form of the block-diagonal dynamic matrix.
- 11.2 Consider the perovskite structure with  $\mathbf{k} = (0, 0, t)$ ,  $0 \leq t \leq \pi/c$ .
- (a) Use the information in Exercise 11.1 to find 15 symmetry functions.
  - (b) Make a sketch of the displacements associated with the symmetry functions.
  - (c) Identify the transverse and longitudinal symmetry functions.
  - (d) Which symmetry functions are eigenfunctions?

(e) Show that

$$\omega^2(B_1) = \frac{1}{2}[D_{zz}^{22} + D_{zz}^{33} - D_{zz}^{23} - D_{zz}^{32}],$$

where, for  $D_{zz}^{nn'}$ ,  $n$  and  $n'$  indicate the O-atom site numbers.

11.3 For the perovskite structure (in the phonon ground state) answer the following.

- (a) What vibration modes at  $\mathbf{k} = 0$  are infrared active?
- (b) Which modes are Raman active?
- (c) Absorption of a photon requires conservation of wavevector as well as conservation of energy. Therefore absorption of a photon resulting in the creation of a phonon is not a vertical transition. That is, if the initial state has  $\mathbf{k} = 0$ , the final phonon state can not have  $\mathbf{k} = 0$ . Calculate the ratio of the wavevector of a  $1,000\text{-cm}^{-1}$  infrared photon to the smallest reciprocal-lattice vector for a cubic crystal with lattice constant  $a = 4 \text{ \AA}$ . What can be concluded about the neglect of the conservation of momentum?

11.4 For the CsCl structure with  $\mathbf{k}$  along the  $\Lambda$  line of symmetry ( $\mathbf{k} = (t, t, t)$ , with  $0 \leq t \leq \pi/c$ ):

- (a) Find  $\mathbf{g}_{\mathbf{k}}$  and its elements in terms of the operators in Table E.1.
- (b) Find the IRs of the vibrations.
- (c) Find the six symmetry functions, and identify the transverse and longitudinal functions.
- (d) Find expressions for the longitudinal acoustic and optical modes in terms of the matrix elements of the dynamic matrix,  $\mathbb{D}$ .

11.5 For the axially symmetric model, translations automatically give zero frequencies. However, for the general model, Eqs. (11.2)–(11.10), the requirement that a translation have zero frequency places constraints on its dynamic matrix. For the CsCl structure,  $|1, 1, 1, 1, 1, 1\rangle$  represents a translation in  $\xi$ -space. Show that this requires

$$\begin{aligned} \sum_{\beta} D_{\alpha\beta}^{aa} &= -\sqrt{\frac{m_B}{m_A}} \sum_{\beta} D_{\alpha\beta}^{ab}, \\ \sum_{\beta} D_{\alpha\beta}^{bb} &= -\sqrt{\frac{m_A}{m_B}} \sum_{\beta} D_{\alpha\beta}^{ba}, \\ m_A \sum_{\beta} D_{\alpha\beta}^{aa} &= m_B \sum_{\beta} D_{\alpha\beta}^{bb}. \end{aligned}$$

- 11.6 According to the theory of elastic media, the velocity of sound,  $v$ , for a cubic crystal is given by the solutions of

$$\det\{\mathbb{E} - \rho v^2 \mathbb{I}\} = 0,$$

where  $\mathbb{E}$  is the  $3 \times 3$  elastic-constant matrix,  $\rho$  is the mass density,  $v$  is the velocity of sound for a given direction of the wavevector  $\mathbf{k}$ , and  $\mathbb{I}$  is the unit matrix. The matrix elements of  $\mathbb{E}$  are given by

$$E_{11} = c_{11} l^2 + c_{44}(m^2 + n^2),$$

$$E_{22} = c_{11} m^2 + c_{44}(l^2 + n^2),$$

$$E_{33} = c_{11} n^2 + c_{44}(l^2 + m^2),$$

$$E_{12} = E_{21} = (c_{12} + c_{44})lm,$$

$$E_{13} = E_{31} = (c_{12} + c_{44})ln,$$

$$E_{23} = E_{32} = (c_{12} + c_{44})mn,$$

where  $l$ ,  $m$ , and  $n$  are the direction cosines of the wavevector  $\mathbf{k}$ , and  $c_{ij}$  are the elastic constants for the crystal.

Find the sound velocities for propagation along the [100], [110], and [111] directions in terms of the elastic constants. (Hint: For the [111] direction, use symmetry functions to diagonalize the  $\mathbb{E}$  matrix.)

- 11.7 For the perovskite  $\text{SrTiO}_3$ , the elastic constants are  $c_{11} = 3.162$ ,  $c_{12} = 1.035$ , and  $c_{44} = 1.212$ , all in units of  $10^{12}$  dynes/cm<sup>2</sup>. Calculate the sound velocities in cm/s for  $\mathbf{k}$  in the three directions [100], [110], and [111]. In calculating the density  $\rho$ , assume the lattice constant is 4 Å.
- 11.8 (a) Using the axially symmetric model (Eqs. (11.17)–(11.19)) for a cubic crystal with one atom per unit cell, find the dynamic-matrix elements,  $D_{\alpha\beta}(\mathbf{k})$  including nearest- and next-nearest-neighbor interactions.
- (b) Find the longitudinal and transverse frequencies in terms of the elements of the dynamic matrix for  $\mathbf{k} = (t, 0, 0)$ .
- (c) Repeat part (b) for  $\mathbf{k} = (t, t, 0)$ .
- 11.9 For the localized vibration modes discussed in the chapter, do the following.
- (a) Show that, for  $|n| > 1$ ,

$$\left| \frac{d(|n|)}{d(0)} \right| = (-1)^{|n|} e^{-|n|\theta},$$

where  $e^{-\theta} = (1 + \epsilon)/(1 - \epsilon)$  and  $\theta$  is a real positive number.

- (b) Show that, for  $\epsilon = -0.5$ ,  $\theta = 1.098\,612\,3$ .

# 12

## Time reversal and magnetic groups

### 12.1 Time reversal in quantum mechanics

In this chapter we investigate the effects of time-reversal symmetry on quantum operators and systems. For Newton's classical equations the force on an object is related to the second time derivative,  $\partial^2 \mathbf{r} / \partial t^2$ , of the spatial variable,  $\mathbf{r}$ . Substitution of  $-t$  for  $t$  does not change the equations of motion. Therefore, if  $\mathbf{r}(t)$  is a solution of the equations of motion, so is  $\mathbf{r}(-t)$ . On the other hand, the velocity or momentum is reversed (flows backward), meaning that  $\mathbf{p}(t) = -\mathbf{p}(-t)$  under time reversal. The oddness of the momentum under time inversion applies not only to linear momentum but also to angular momentum.

In quantum mechanics we are concerned with Schrödinger's equation and the effect of time reversal on the quantum operators and wavefunctions. The time evolution of the wavefunction,  $\Psi(\mathbf{r}, t)$ , is determined by the unitary operator,  $\exp(-iHt)$ , where  $\mathbb{H}$  is the system Hamiltonian. The evolution of  $\Psi$  from 0 to  $t$  is given by  $\Psi(t) = \exp[-iHt] \Psi(0)$ . If  $\mathbb{H}$  itself is time-independent and  $t$  is reversed, the wavefunction evolves backward in time according to  $\Psi(-t) = \exp[+iHt] \Psi(0)$ .

#### 12.1.1 Properties of the time-reversal operator, $\mathbb{T}$

An appropriate time-reversal operator,  $\mathbb{T}$ , when applied to a system must accomplish a number of things. If we denote space coordinates by  $\mathbf{r}$ , velocity by  $\mathbf{v}$ , linear momentum by  $\mathbf{p}$ , angular momentum by  $\mathbf{J}$ , current by  $I$ , charge density by  $\rho$ , electric field by  $\mathbf{E}$ , magnetic field by  $\mathbf{H}_f$ , and the spin by  $\mathbf{S}$ , then

$$\mathbb{T} f(\mathbf{r}) \rightarrow f(\mathbf{r}),$$

$$\mathbb{T} \mathbf{E} \rightarrow \mathbf{E},$$

$$\mathbb{T} \rho \rightarrow \rho,$$

$$\mathbb{T}(\mathbf{v}, \mathbf{J}, I) \rightarrow -(\mathbf{v}, \mathbf{J}, I),$$

$$\mathbb{T}(\mathbf{H}_f, \mathbf{S}) \rightarrow -(\mathbf{H}_f, \mathbf{S}).$$

The appropriate time-reversal operator depends on the Hamiltonian. If  $\mathbb{H}$  includes no spin operators or external magnetic field,  $\mathbb{T}$  may be chosen as the complex-conjugation operator,  $\mathbb{K}_0$ , since  $\mathbb{K}_0[\exp(-iHt)] = [\exp(-iHt)]^* = [\exp(iHt)] = [\exp(-iH(-t))]$ . When spin-dependent terms are present in  $\mathbb{H}$ ,  $\mathbb{T}$  must also reverse the spins, since they are angular-momentum operators. Finally, if an external magnetic field is also present,  $\mathbb{T}$  must also reverse the direction of the field. For stationary states of Schrödinger's equation,  $\Psi(\mathbf{r}, t) = \exp(-iEt) \psi(\mathbf{r})$  and  $\mathbb{T} \Psi(\mathbf{r}, t) = \exp(iEt) \mathbb{T} \psi(\mathbf{r}, 0)$ . We can define the time-reversal operator by the requirement that it commutes with coordinates and functions of coordinates, but anticommutes with momentum operators,

$$\mathbb{T} \mathbf{r} = \mathbf{r} \mathbb{T}, \quad (12.1)$$

$$\mathbb{T} V(r) = V(r) \mathbb{T}, \quad (12.2)$$

$$\mathbb{T} \mathbf{p} = \mathbb{T} (-i\hbar \nabla) = i\hbar \nabla \mathbb{T} = -\mathbf{p} \mathbb{T}, \quad (12.3)$$

$$\mathbb{T} \mathbf{J} = \mathbb{T} (\mathbf{r} \times \mathbf{p}) = -(\mathbf{r} \times \mathbf{p}) \mathbb{T} = -\mathbf{J} \mathbb{T}, \quad (12.4)$$

$$\mathbb{T} \mathbf{S} = -\mathbf{S} \mathbb{T}, \quad (12.5)$$

where  $\mathbf{J}$  is any angular-momentum operator, and  $\mathbf{S}$  is the total spin vector operator.

If a one-electron Hamiltonian is of the form

$$\mathbb{H} = \frac{p^2}{2m} + V(r), \quad (12.6)$$

without spin operators, then (12.1)–(12.5) are satisfied by  $\mathbb{T} = \mathbb{K}_0$ , the complex-conjugate operator.<sup>1</sup> Since the Hamiltonian of (12.6) is real,  $\mathbb{K}_0$  commutes with  $\mathbb{H}$ . However, if  $\mathbb{H}$  contains spin operators, as it does in the case when spin-orbit interactions are included,  $\mathbb{K}_0$  is not adequate, because it does not reverse the spin angular momentum as required by (12.5). A Hamiltonian with spin-orbit interactions is of the form

$$\mathbb{H} = \frac{p^2}{2m} + V(r) + \frac{\hbar}{4m^2c^2} [\nabla V(r) \times \mathbf{p} \cdot \boldsymbol{\sigma}]. \quad (12.7)$$

In this instance the time-reversal operator can be taken as a product of operators,<sup>2</sup>

$$\mathbb{T} = \sigma_y \mathbb{K}_0, \quad (12.8)$$

<sup>1</sup> Representing the time-reversal operator by complex conjugation is valid only in a spatial-coordinate representation such as Schrödinger's equation.

<sup>2</sup>  $\mathbb{T}$  could also be chosen as  $\sigma_y \mathbb{K}_0$  or  $e^{i\theta} \sigma_y \mathbb{K}_0$ , where  $\theta$  is an arbitrary, but fixed, real number. In particular,  $\mathbb{T}$  could be taken as  $i\sigma_y \mathbb{K}_0$ .



where  $\sigma_y$  is the Pauli spin matrix,

$$\sigma_y = \begin{pmatrix} 0 & -i \\ i & 0 \end{pmatrix}. \quad (12.9)$$

We can demonstrate that  $\mathbb{T} = \sigma_y \mathbb{K}_0$  satisfies (12.1)–(12.5). Since  $\sigma_y$  operates only on the spin, we need only show that  $\sigma_y \mathbb{K}_0$  anticommutes with the spin vector operator  $\sigma$  and commutes with the spin–orbit term of the Hamiltonian of (12.7). First consider a one-electron Hamiltonian with spin–orbit interaction, with  $\sigma = \mathbf{e}_x \sigma_x + \mathbf{e}_y \sigma_y + \mathbf{e}_z \sigma_z$ , where  $\mathbf{e}_x$ ,  $\mathbf{e}_y$ , and  $\mathbf{e}_z$  are unit vectors along the  $x$ -,  $y$ -, and  $z$ -directions, respectively. We have

$$\begin{aligned} \sigma_y \mathbb{K}_0(\mathbf{e}_x \sigma_x) &= \mathbf{e}_x \sigma_y \sigma_x^* \mathbb{K}_0 = \mathbf{e}_x \begin{pmatrix} 0 & -i \\ i & 0 \end{pmatrix} \begin{pmatrix} 0 & 1 \\ 1 & 0 \end{pmatrix} \mathbb{K}_0 \\ &= \mathbf{e}_x \begin{pmatrix} -i & 0 \\ 0 & i \end{pmatrix} \mathbb{K}_0 = -(\mathbf{e}_x \sigma_x) \sigma_y \mathbb{K}_0, \end{aligned} \quad (12.10)$$

$$\begin{aligned} \sigma_y \mathbb{K}_0(\mathbf{e}_y \sigma_y) &= \mathbf{e}_y \sigma_y \sigma_y^* \mathbb{K}_0 = \mathbf{e}_y \begin{pmatrix} 0 & -i \\ i & 0 \end{pmatrix} \begin{pmatrix} 0 & i \\ -i & 0 \end{pmatrix} \mathbb{K}_0 \\ &= -\mathbf{e}_y \begin{pmatrix} 1 & 0 \\ 0 & 1 \end{pmatrix} \mathbb{K}_0 = -(\mathbf{e}_y \sigma_y) \sigma_y \mathbb{K}_0, \end{aligned} \quad (12.11)$$

$$\begin{aligned} \sigma_y \mathbb{K}_0(\mathbf{e}_z \sigma_z) &= \mathbf{e}_z \sigma_y \sigma_z^* \mathbb{K}_0 = \mathbf{e}_z \begin{pmatrix} 0 & -i \\ i & 0 \end{pmatrix} \begin{pmatrix} 1 & 0 \\ 0 & -1 \end{pmatrix} \mathbb{K}_0 \\ &= \mathbf{e}_z \begin{pmatrix} 0 & i \\ i & 0 \end{pmatrix} \mathbb{K}_0 = -(\mathbf{e}_z \sigma_z) \sigma_y \mathbb{K}_0. \end{aligned} \quad (12.12)$$

On collecting the components together, we have

$$\mathbb{T} \sigma = -\sigma \mathbb{T}. \quad (12.13)$$

$\mathbb{T}$  also commutes with the spin–orbit term for real  $V(r)$ ,

$$\begin{aligned} \sigma_y \mathbb{K}_0[\nabla V(r) \times \mathbf{p} \cdot \sigma] &= \sigma_y[\nabla V(r) \times (-\mathbf{p}) \cdot \sigma] \mathbb{K}_0 \\ &= [\nabla V(r) \times (-\mathbf{p}) \cdot (-\sigma)] \sigma_y \mathbb{K}_0 \\ &= [\nabla V(r) \times \mathbf{p} \cdot \sigma] \sigma_y \mathbb{K}_0, \end{aligned} \quad (12.14)$$

and therefore commutes with the Hamiltonian.

The above proof establishes a valid time-reversal operator for a single electron. The form of the many-electron Hamiltonian is

$$\mathbb{H} = \sum_i \left\{ \frac{p_i^2}{2m} + \frac{\hbar}{4m^2 c^2} [\nabla_i V(r_1, r_2, \dots, r_N) \times \mathbf{p}_i \cdot \sigma_i] \right\} + V(r_1, r_2, \dots, r_N). \quad (12.15)$$

For the  $N$ -electron system we may take the time-reversal operator as

$$\mathbb{T} = \Theta \mathbb{K}_0, \quad \Theta = \prod_{n=1}^N \sigma_{ny}, \quad (12.16)$$

where  $\sigma_{ny}$  is the  $y$ -component of the spin operator which operates only on the  $n$ th electron's spinor.

## 12.2 The effect of $\mathbb{T}$ on an electron wavefunction

Let  $\Psi(r_1, r_2, \dots, r_N; \sigma_{1z}, \sigma_{2z}, \dots, \sigma_{Nz}) = \Psi(r_i, \sigma_{iz})$  be an antisymmetrized stationary state of an  $N$ -electron system, where  $r_i$  is a space coordinate and  $\sigma_{iz}$  is the spin state of the  $i$ th electron. The spin,  $\sigma_{iz}$ , may be either  $\alpha$  (spin up) or  $\beta$  (spin down). For the Hamiltonian of (12.15),  $\mathbb{T} = \Theta \mathbb{K}_0 = \Pi_i \sigma_{iy} \mathbb{K}_0$  is a symmetry operation. Since

$$\mathbb{T} \alpha = i \beta \quad \text{and} \quad \mathbb{T} \beta = -i \alpha, \quad (12.17)$$

it follows that

$$\mathbb{T} \Psi(r_i, \sigma_{iz}) = i^{n(\alpha)} (-i)^{n(\beta)} \Psi(r_i, -\sigma_{iz})^*, \quad (12.18)$$

where  $n(\alpha)$  is the number of  $\sigma_{iz}$  that are equal to  $\alpha$ ,  $n(\beta)$  is the number of  $\sigma_{iz}$  that are equal to  $\beta$  in  $\Psi(r_i, \sigma_{iz})$ , and  $-\sigma_{iz}$  is the opposite spin state of  $\sigma_{iz}$  (that is, if  $\sigma_{iz} = \alpha$  then  $-\sigma_{iz} = \beta$  and vice versa). Note that, for  $\Psi(r_i, -\sigma_{iz})$ ,  $n(\alpha)$  is the number of  $\beta$  spins and  $n(\beta)$  is the number of  $\alpha$  spins. As a result,

$$\mathbb{T}^2 \Psi = [i^{n(\alpha)} (-i)^{n(\beta)}]^* [i^{n(\beta)} (-i)^{n(\alpha)}] \Psi = i^{2N} \Psi = (-1)^N \Psi, \quad (12.19)$$

where  $N = n(\alpha) + n(\beta)$ . The final result is

$$\mathbb{T}^2 \Psi = \pm \Psi \quad (+ \text{ for } N \text{ even, } - \text{ for } N \text{ odd}). \quad (12.20)$$

Since (12.20) holds for every  $N$ -electron wavefunction, we can infer that the  $\mathbb{T}$  operator satisfies the condition

$$\mathbb{T}^2 = \pm 1. \quad (12.21)$$

If  $\Psi$  is an eigenstate with eigenvalue  $\lambda$ , and  $\mathbb{T}$  commutes with the Hamiltonian, then  $\mathbb{T} \Psi$  is also an eigenstate with the same eigenvalue. The question is whether  $\mathbb{T} \Psi$  is a linearly independent state or simply  $\Psi$  multiplied by a phase factor,  $e^{i\theta}$ . If  $\mathbb{T} \Psi = e^{i\theta} \Psi$  then  $\Psi$  and  $\mathbb{T} \Psi$  are equivalent, and time reversal does not require additional degeneracy. It turns out (as we show below) that if the number of electrons is odd then  $\mathbb{T} \Psi$  is orthogonal to  $\Psi$  and therefore is an independent state. In this case, at least two different states have the same eigenvalue,  $\lambda$ . For atoms and molecules this means that the energy level is at least doubly degenerate (Kramers' theorem [12.1]).

**Kramers' theorem [12.1]**

If the Hamiltonian commutes with the time-reversal operator, the eigenvalues of a system with an odd number of electrons are at least doubly degenerate. In general the degeneracy is even; that is, the degeneracy of the eigenvalue is  $2n$ , where  $n$  is a positive integer greater than zero. The degeneracy is not lifted by an electric field or a crystal field, but may be lifted by application of an external magnetic field.

To show that  $\mathbb{T}\Psi$  is orthogonal to  $\Psi$ , we show that the (Hermitian) scalar product  $\langle \Psi | \mathbb{T}\Psi \rangle = 0$  if the number of electrons is odd. Consider two arbitrary functions,  $f$  and  $g$ . We have that

$$\langle \mathbb{T}g | \mathbb{T}f \rangle = \langle \Theta \mathbb{K}_0 g | \Theta \mathbb{K}_0 f \rangle = \langle \mathbb{K}_0 g | \mathbb{K}_0 f \rangle = \langle g | f \rangle^* = \langle f | g \rangle. \quad (12.22)$$

The second equality results because  $\Theta$  is a unitary operator, and applying a unitary operator to both functions does not change the scalar product. If we choose  $f = \Psi$  and  $g = \mathbb{T}\Psi$ , then (12.22) yields

$$\langle \mathbb{T}g | \mathbb{T}f \rangle = \langle \mathbb{T}(\mathbb{T}\Psi) | \mathbb{T}\Psi \rangle = \langle \mathbb{T}^2 \Psi | \mathbb{T}\Psi \rangle = -\langle \Psi | \mathbb{T}\Psi \rangle = -\langle f | g \rangle, \quad (12.23)$$

since  $\mathbb{T}^2 = -1$  when  $N$  is odd. Both (12.22) and (12.23) can be true if and only if

$$\langle \Psi | \mathbb{T}\Psi \rangle = 0. \quad (12.24)$$

Equation (12.24) shows that  $\Psi$  and  $\mathbb{T}\Psi$  are orthogonal states when  $N$  is odd. If  $N$  is even, the same proof yields only the tautology  $\langle \Psi | \mathbb{T}\Psi \rangle = \langle \Psi | \mathbb{T}\Psi \rangle$ . It should be noted that (12.24) depends only on having time reversal as a symmetry operator.

**12.3 Time reversal with an external field**

In the presence of an external electric field the Hamiltonian will contain a potential-energy term,  $e\mathbf{E}$ , where  $\mathbf{E}$  is the electric field. The time-reversal operator commutes with this term. In general, however, electromagnetic fields are accommodated in quantum systems by the replacement of  $\mathbf{p}$  with  $(\mathbf{p} - e\mathbf{A}/c)$ , where  $\mathbf{A}$  is a vector potential,  $c$  is the velocity of light, and  $e$  is the magnitude of the electron charge. If the fields are time-varying, the requirements of the time-reversal operator are

$$\mathbb{T}\mathbf{E}(\mathbf{r}, t) = \mathbf{E}(\mathbf{r}, -t) \quad (\mathbf{E} \text{ is the electric field}), \quad (12.25)$$

$$\mathbb{T}\mathbf{A}(\mathbf{r}, t) = -\mathbf{A}(\mathbf{r}, -t) \quad (\mathbf{A} \text{ is the magnetic vector potential}), \quad (12.26)$$

$$\mathbb{T}\mathbf{H}_f(\mathbf{r}, t) = -\mathbf{H}_f(\mathbf{r}, -t) \quad (\mathbf{H}_f \text{ is the magnetic field strength}). \quad (12.27)$$

If  $\mathbb{T}$  satisfies Eqs. (12.25)–(12.27) and commutes with the Hamiltonian, and  $\Psi(\mathbf{r}, \mathbf{H}_f, t)$  is an eigenstate of the Hamiltonian, then  $\mathbb{T}\Psi(\mathbf{r}, \mathbf{H}_f, t) = \Psi(\mathbf{r}, -\mathbf{H}_f, -t)$  is also an eigenstate with the same eigenvalue. If a  $180^\circ$  rotation,  $\delta$ ,

about an axis perpendicular to the direction of  $\mathbf{H}_f$  commutes with the Hamiltonian in the absence of the magnetic field, then the time-reversal operator may be taken as  $\delta \Theta \mathbb{K}_0$ .

### Unitary and antiunitary operators

An operator  $\mathbb{U}$  is unitary if  $\mathbb{U}^{-1}$  is the transpose, complex conjugate of  $\mathbb{U}$ .  $\mathbb{U}$  is a linear operator that satisfies  $\mathbb{U}(c \psi(\mathbf{r}) + d \phi(\mathbf{r})) = c \mathbb{U} \psi(\mathbf{r}) + d \mathbb{U} \phi(\mathbf{r})$  ( $c$  and  $d$  constants) and  $\langle \mathbb{U} \psi(\mathbf{r}) | \mathbb{U} \phi(\mathbf{r}) \rangle = \langle \psi | \phi \rangle$ .

An operator  $\mathbb{A}$  is an antiunitary operator that satisfies  $\mathbb{A}[c \psi(\mathbf{r}) + d \phi(\mathbf{r})] = c^* \mathbb{A} \psi(\mathbf{r}) + d^* \mathbb{A} \phi(\mathbf{r})$  and  $\langle \mathbb{A} \psi(\mathbf{r}) | \mathbb{A} \phi(\mathbf{r}) \rangle = \langle \psi(\mathbf{r}) | \phi(\mathbf{r}) \rangle^*$ .

The time-reversal operator,  $\mathbb{T}$ , is an antiunitary operator.  $\mathbb{T} = \Theta \mathbb{K}_0$  is a product of a unitary operator,  $\Theta$ , and an antiunitary operator,  $\mathbb{K}_0$ .

The product of two unitary or two antiunitary operators is unitary. The product of a unitary operator with an antiunitary operator is antiunitary.

## 12.4 Time-reversal degeneracy and energy bands

For crystalline solids the symmetry elements belong to a space group. The wavefunctions for the energy bands are one-electron Bloch waves characterized by a wavevector  $\mathbf{k}$ , as discussed in Chapter 9. Let  $\psi_{\mathbf{k},\alpha}$  and  $\psi_{\mathbf{k},\beta}$  represent the Bloch waves for spin-up and spin-down states. The two states are degenerate in the absence of spin-dependent terms in the Hamiltonian and an external magnetic field.

Applying  $\mathbb{T} = \sigma_y \mathbb{K}_0$  to the Bloch wavefunctions gives

$$\sigma_y \mathbb{K}_0 \psi_{\mathbf{k},\alpha}(\mathbf{r}) = \sigma_y [e^{-i\mathbf{k}\cdot\mathbf{r}} u_{\mathbf{k},\alpha}^*(\mathbf{r})] \alpha = e^{-i\mathbf{k}\cdot\mathbf{r}} u_{\mathbf{k},\alpha}^*(\mathbf{r}) (i\beta), \quad (12.28)$$

$$\sigma_y \mathbb{K}_0 \psi_{\mathbf{k},\beta}(\mathbf{r}) = \sigma_y [e^{-i\mathbf{k}\cdot\mathbf{r}} u_{\mathbf{k},\beta}^*(\mathbf{r})] \beta = e^{-i\mathbf{k}\cdot\mathbf{r}} u_{\mathbf{k},\beta}^*(\mathbf{r}) (-i\alpha). \quad (12.29)$$

We define

$$i u_{\mathbf{k},\alpha}^*(\mathbf{r}) = u_{-\mathbf{k},\beta}(\mathbf{r}), \quad (12.30)$$

$$-i u_{\mathbf{k},\beta}^*(\mathbf{r}) = u_{-\mathbf{k},\alpha}(\mathbf{r}), \quad (12.31)$$

so that

$$\mathbb{T} \psi_{\mathbf{k},\alpha} = \psi_{-\mathbf{k},\beta}, \quad (12.32)$$

$$\mathbb{T} \psi_{\mathbf{k},\beta} = \psi_{-\mathbf{k},\alpha}. \quad (12.33)$$

If  $\psi_{\mathbf{k},s}$  is an eigenfunction of a Hamiltonian,  $\mathbb{T} \psi_{\mathbf{k},s} = \psi_{-\mathbf{k},-s}$  is also an eigenstate with the same eigenvalue. It follows that every one-electron eigenvalue is at least doubly degenerate (Kramers' theorem). To distinguish Bloch waves of different energy bands we can add the index  $n$  so that  $\psi_{n,\mathbf{k},s}$  is a wavefunction for the  $n$ th band with wavevector  $\mathbf{k}$  and spin state  $s$ .

If  $\mathbb{T}$  is a symmetry operator of the space group, the states  $\psi_{n,\mathbf{k},s}$  and  $\psi_{n,-\mathbf{k},-s}$  have the same energy, so

$$E(n, \mathbf{k}, s) = E(n, -\mathbf{k}, -s). \quad (12.34)$$

If the space group also contains spatial inversion, then

$$E(n, \mathbf{k}, s) = E(n, -\mathbf{k}, s). \quad (12.35)$$

In this case the states  $\psi_{n,\mathbf{k},s}$  and  $\psi_{n,-\mathbf{k},s}$  and their time-reversed partners  $\psi_{n,-\mathbf{k},-s}$  and  $\psi_{n,\mathbf{k},-s}$  all have the same energy. The energy as a function of  $\mathbf{k}$  is shown in Figs. 12.1(a) and (b). If the group of the Hamiltonian does not have spatial inversion, then only (12.34) holds. In this case only the time-reversed pairs have equal energy, as illustrated in Figs. 12.1(c) and (d). For a “spinless” Hamiltonian, the energy will display inversion in  $\mathbf{k}$ -space even if inversion is not a symmetry operator, since in this case  $\Psi_{n,\mathbf{k}}$  and  $\Psi_{n,-\mathbf{k}}$  are time-reversed partners. In general, if  $\mathbf{k}$  is not a point of high symmetry, and there are no spin-dependent terms in the Hamiltonian,  $\Psi_{n,\mathbf{k},s}$  and  $\Psi_{n,-\mathbf{k},-s}$  have the same energy. In addition,  $E(n, -\mathbf{k}, s) = E(n, \mathbf{k}, s)$ , so the *energy eigenvalue* is four-fold degenerate with  $E(n, \pm\mathbf{k}, s) = E(n, \mathbf{k}, \pm s)$  (Figs. 12.1(a) and (b)).

If the Hamiltonian does not contain spin-dependent terms but does contain the time reversal and spatial inversion, then the gradient of the energy  $\nabla_{\mathbf{k}} E(n, \mathbf{k}, s)$  must vanish at  $\mathbf{k} = \mathbf{K}/2$ , where  $\mathbf{K}$  is any reciprocal-lattice vector (including  $\mathbf{K} = 0$ ). To see this, note that the  $i$ th Cartesian component of the gradient is

$$\frac{\partial E(n, \frac{1}{2}\mathbf{K}, s)}{\partial k_i} = \lim_{+\Delta\mathbf{k}_i \rightarrow 0} \left\{ \frac{E(n, (\frac{1}{2}\mathbf{K} + \Delta\mathbf{k}_i), s) - E(n, (\frac{1}{2}\mathbf{K} - \Delta\mathbf{k}_i), s)}{+2\Delta k_i} \right\}. \quad (12.36)$$

Under spatial inversion,

$$E(n, \mathbf{k}, s) = E(n, -\mathbf{k}, s). \quad (12.37)$$

This yields

$$E\left(n, \left(\frac{1}{2}\mathbf{K} - \Delta\mathbf{k}_i\right), s\right) = E\left(n, \left(-\frac{1}{2}\mathbf{K} + \Delta\mathbf{k}_i\right), s\right). \quad (12.38)$$

We also have

$$E(n, \mathbf{k}, s) = E(n, (\mathbf{k} + \mathbf{K}), s), \quad (12.39)$$

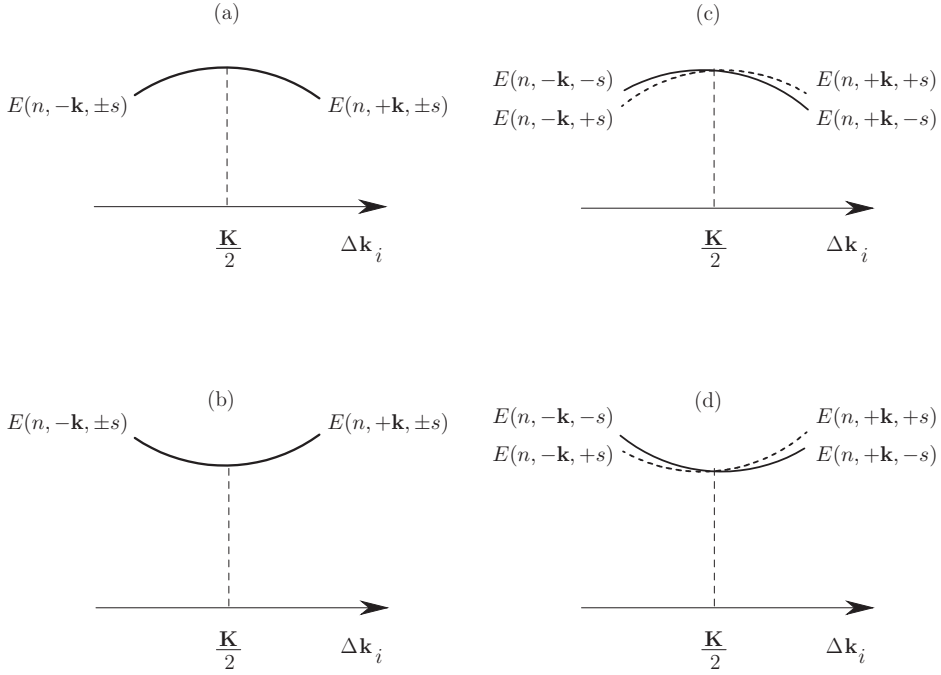


Figure 12.1 A schematic representation of energy bands near  $\mathbf{k} = \mathbf{K}/2$ : (a) and (b), time reversal and inversion symmetry for convex and concave bands,  $\nabla_{\mathbf{k}} E(n, \mathbf{k}, s) = 0$  at  $\mathbf{k} = \mathbf{K}/2$ ; (c) and (d), time reversal but no inversion symmetry for convex and concave bands,  $\nabla_{\mathbf{k}} E(n, \mathbf{k}, s) \neq 0$  at  $\mathbf{k} = \mathbf{K}/2$ .

so (12.38) becomes

$$\begin{aligned}
 E\left(n, \left(\frac{\mathbf{K}}{2} - \Delta \mathbf{k}_i\right), s\right) &= E\left(n, \left(-\frac{\mathbf{K}}{2} + \mathbf{K} + \Delta \mathbf{k}_i\right), s\right) \\
 &= E\left(n, \left(\frac{\mathbf{K}}{2} + \Delta \mathbf{k}_i\right), s\right), \quad (12.40)
 \end{aligned}$$

and therefore the numerator of (12.36) vanishes. This proves that in the absence of spin-dependent terms in the Hamiltonian the gradient vanishes at  $\mathbf{k} = \mathbf{K}/2$ , where  $\mathbf{K}$  is any reciprocal-lattice vector.

If the Hamiltonian has spin-dependent terms,  $\nabla_{\mathbf{k}} E$  is not required to vanish because of symmetry. The time-reversed pairs still have the same energy, ( $E(n, \mathbf{k}, s) = E(n, -\mathbf{k}, -s)$  and  $E(n, \mathbf{k}, -s) = E(n, -\mathbf{k}, s)$ ), but  $E(n, -\mathbf{k}, -s) \neq E(n, \mathbf{k}, -s)$ . This situation is illustrated in Figs. 12.1(c) and (d).

A test for “additional” degeneracy (resulting from time reversal) that employs only the characters of the point group  $\mathbf{g}_{\mathbf{k}}$  (group of the wavevector) of the space group has been developed by Herring [12.2]. Denote an operator that carries the wavevector,  $\mathbf{k}$ , into  $-\mathbf{k}$  or its equivalent by the symbol  $\mathbb{Q}_i$ , and denote the set of

such operators as  $\{\mathbb{Q}\}$ . It follows that  $\mathbb{Q}_i^2$  carries  $\mathbf{k}$  into itself or an equivalent vector and therefore must be an operator in  $\mathbf{g}_{\mathbf{k}}$ . The Herring test involves the sum of the characters of the squares of the operators,  $\sum_i \chi(\mathbb{Q}_i^2)$ . The sum has three possible values, namely  $h_{\mathbb{Q}}$ , 0, and  $-h_{\mathbb{Q}}$ , where  $h_{\mathbb{Q}}$  is the number of operators in  $\{\mathbb{Q}\}$ . The additional degeneracy of the energy levels belonging to  $\Gamma^\alpha$  due to the addition of the time-reversal symmetry depends upon the value of  $\sum_i \chi^\alpha(\mathbb{Q}_i^2)$ .

**Theorem 12.1** (Herring rules for additional degeneracy of energy bands) *Let  $\Gamma^\alpha$  be an IR of a point group,  $\mathbf{g}_{\mathbf{k}}$ , and  $\mathbb{Q}_i$  an operator that transforms  $\mathbf{k}$  into  $-\mathbf{k}$  or  $-\mathbf{k} + \mathbf{K}$  (where  $\mathbf{K}$  is a reciprocal-lattice vector). The sum of the characters,  $\sum_i \chi^\alpha(\mathbb{Q}_i^2)$ , has three possible values, namely  $h_{\mathbb{Q}}$ , 0, and  $-h_{\mathbb{Q}}$ , where  $h_{\mathbb{Q}}$  is the number of  $\mathbb{Q}_i$  operators. The additional degeneracy of the levels belonging to  $\Gamma^\alpha$  due to the addition of the time-reversal operator is determined by the value of  $\sum_i \chi^\alpha(\mathbb{Q}_i^2)$ .*

(a)  $\sum_i \chi^\alpha(\mathbb{Q}_i^2) = h_{\mathbb{Q}}$ .

*Time reversal leads to no additional degeneracy for integral spin, but doubles the degeneracy for half-integral spin.*

(b)  $\sum_i \chi^\alpha(\mathbb{Q}_i^2) = 0$ .

*Time reversal leads to a doubling of the degeneracy both for integral and for half-integral spin.*

(c)  $\sum_i \chi^\alpha(\mathbb{Q}_i^2) = -h_{\mathbb{Q}}$ .

*Time reversal leads to a doubling of the degeneracy for integral spin but no additional degeneracy for half-integral spin.*

To employ the Herring test, we need to find the  $\mathbb{Q}$  operators. The group  $\mathbf{g}_{\mathbf{k}}$  contains all of the point-group operations that transform  $\mathbf{k}$  into  $\mathbf{k}$  or  $\mathbf{k} + \mathbf{K}$ , where  $\mathbf{K}$  is a reciprocal-lattice vector. Denote the set of operators in  $\mathbf{g}_{\mathbf{k}}$  by  $\{O_j\}$ ,  $j = 1, 2, \dots, h(\mathbf{g}_{\mathbf{k}})$ . We consider two cases.

Case (1) The group of the wavevector,  $\mathbf{g}_{\mathbf{k}}$ , contains the inversion operator,  $P_{\text{inv}}$ .

We note that  $P_{\text{inv}}\mathbf{k} = -\mathbf{k}$ , and therefore  $P_{\text{inv}}$  can be a member of  $\mathbf{g}_{\mathbf{k}}$  only if  $\mathbf{k} = 0$  or  $\mathbf{K}/2$ , where  $\mathbf{K}$  is a reciprocal-lattice vector. If  $\mathbf{k} = 0$  or  $\mathbf{K}/2$ , then any  $O_j$  in  $\mathbf{g}_{\mathbf{k}}$  satisfies the condition that  $O_j\mathbf{k} = -\mathbf{k}$  or its equivalent. In this case the set  $\{\mathbb{Q}_i\} = \{O_j\} = \mathbf{g}_{\mathbf{k}}$ , so  $\sum_i \chi(\mathbb{Q}_i^2) = \sum_j \chi(O_j^2)$ .

Case (2) The group of the wavevector,  $\mathbf{g}_{\mathbf{k}}$ , does not contain the inversion operator. For this case  $P_{\text{inv}}$  is not a member of  $\mathbf{g}_{\mathbf{k}}$ ; however, if  $\mathbf{k} \neq 0$  or  $\mathbf{K}/2$ , then  $(P_{\text{inv}}O_j)\mathbf{k} = P_{\text{inv}}(\mathbf{k} + \mathbf{K}) = -\mathbf{k} + \mathbf{K}'$ . Therefore the set of operators  $\{P_{\text{inv}}O_j\} = P_{\text{inv}}\mathbf{g}_{\mathbf{k}} = \{\mathbb{Q}_i\}$ . When an operator in  $P_{\text{inv}}\mathbf{g}_{\mathbf{k}}$  is squared, usually (but not always) the inversion operator drops out. If  $P_{\text{inv}}$  commutes with the operators of  $\mathbf{g}_{\mathbf{k}}$ , then  $(P_{\text{inv}}O_j)^2 = P_{\text{inv}}^2 O_j^2 = O_j^2$ . In this instance we have again that  $\sum_i \chi(\mathbb{Q}_i^2) = \sum_j \chi(O_j^2)$ .

Table 12.1 *The character table for the double group  $C_3$ . The last column lists the type of IR when time-reversal symmetry is added.*

$C_3$	$E$	$C_3^2$	$C_3$	IR type
$A$	1	1	1	a
$\mathcal{E}$	1	$\omega$	$\omega^2$	b
$\mathcal{E}$	1	$\omega^2$	$\omega$	b

$$\omega = e^{2\pi i/3}$$

In summary, if  $P_{\text{inv}}$  commutes with the operators of  $\mathbf{g}_{\mathbf{k}}$ , then  $\sum_i \chi(Q_i^2) = \sum_j \chi(O_j^2)$  regardless of the  $\mathbf{k}$ -vector.

As an example of the Herring rules we consider  $\mathbf{g}_{\mathbf{k}} = C_3$ . The character table is given in Table 12.1.

The group  $C_3$  does not contain the inversion operator, hence  $\{Q\} = \{P_{\text{inv}}(g_{\mathbf{k}})\}$ , where  $P_{\text{inv}}$  is the inversion operator. The set  $\{P_{\text{inv}}(g_{\mathbf{k}})\} = \{i, iC_3, iC_3^2\}$ . The square of the operators is the set  $\{E, C_3^2, C_3\}$ , which is just the operators of the group  $C_3$ .

For the squares of the various operators of  $C_3$  we have  $\chi(E^2) = \chi(E)$ ,  $\chi([C_3]^2) = \chi(C_3)$ , and  $\chi([C_3^2]^2) = \chi(C_3)$ .

$\sum_i Q_i^2 = 3$  for  $\Gamma^A$ , and therefore this IR is of type (a) according to the Herring rules. For this IR time reversal leads to no additional degeneracy for integral spin, but doubles the degeneracy for half-integral spin. For the two  $\mathcal{E}$  IRs,  $\sum_i Q_i^2 = 1 + e^{i\pi/3} + e^{2i\pi/3} = 0$ , so they are IRs of type (b). For these two IRs, time reversal leads to a doubling of the degeneracy both for integral and for half-integral spin.

## 12.5 Magnetic crystal groups

Crystals with magnetic (ferromagnetic, ferrimagnetic, or antiferromagnetic) order are not invariant under the time-reversal operator,  $\mathbb{T}$ , since this operation reverses the direction of the spins. However, in some cases (e.g., antiferromagnets) the crystal may be invariant under a space-group operation  $\{\mathbb{T}|\tau\}$ , that is, time reversal plus a translation. Also, even when  $\mathbb{T}$  itself is not in the point symmetry group, product operators such as  $\mathbb{T}\mathbb{U}$ , where  $\mathbb{U}$  represents an ordinary (unitary) operation, may be. The aim of the discussion here is to express the magnetic point groups in terms of the 32 ordinary point groups (type I groups) and certain invariant subgroups.

### *Invariant subgroups*

Before beginning our discussion of magnetic crystal groups, we need to introduce the concept of an invariant subgroup or normal divisor. Theorem 12.2 provides a definition.



**Theorem 12.2** (Invariant subgroups)

1. A collection of elements of  $G_0$  that themselves form a smaller group is a subgroup of  $G_0$ . There may be several distinct subgroups. A subgroup  $G_u$  is an invariant subgroup if it consists of complete classes of  $G_0$ .
2. Let  $G_u$  be an invariant subgroup of  $G_0$ . Suppose  $G_0$  has  $h_0$  elements and  $G_u$  has  $h_u$  elements, then  $h_0/h_u$  is the index of  $G_u$  relative to  $G_0$ . The index is a positive integer. That is,  $h_u$  is a divisor of  $h_0$ ; hence  $G_u$  is called a normal divisor of  $G$ .
3. An invariant subgroup has the property that  $\{X G_u\} = \{G_u X\}$ , where  $X$  is any element of  $G_0$ . If we consider the ordering of the elements in the sets to be irrelevant, we may write  $X G_u = G_u X$ . This property follows from the fact that  $G_u$  consists of complete classes.
4. If  $G_u$  is an invariant subgroup of  $G_0$ , and  $X$  is a member of  $G_0$  but not of  $G_u$ , then  $X G_u = \{G_0 - G_u\}$  (the order of elements is irrelevant).
5. Any subgroup of index 2 is an invariant subgroup.

As an example of an invariant subgroup, consider the group  $C_{4v}$ . The multiplication table is shown in Table 12.2. The classes for this group are  $\{E\}$ ,  $\{C_4, C_4^3\}$ ,  $\{C_2\}$ ,  $\{\sigma_{v1}, \sigma_{v2}\}$ , and  $\{\sigma_{d1}, \sigma_{d2}\}$ . (For a detailed description of the operations, see Table 1.1 in Chapter 1.) Inspection of Table 12.2 shows that  $\{E, C_2\}$  is an invariant subgroup (index 4) since it consists of entire classes. Another invariant subgroup is  $\{E, C_4, C_4^3, C_2\}$  (index 2).

For the purpose here we shall be concerned only with invariant subgroups of index 2. For the  $C_{4v}$  group there are several index-2, invariant subgroups:  $\{E, C_2, C_4, C_4^3\}$ ,  $\{E, C_2, \sigma_{v1}, \sigma_{v2}\}$ , and  $\{E, C_2, \sigma_{d1}, \sigma_{d2}\}$ . The second subgroup is isomorphic (equivalent) to the third.

### 12.5.1 Types of magnetic crystal groups

#### Type II magnetic groups

For diamagnetic or paramagnetic crystals the time-averaged magnetic moment vanishes. The time-reversal operator,  $\mathbb{T}$ , is an element of the magnetic point group,  $\underline{G}$ . For these systems,  $\underline{G}$  is the combination of the unitary operations  $\{\mathbb{U}\}$  of  $G_0$  and antiunitary operations  $\{\mathbb{T}\mathbb{U}\}$ , where “ $\{\dots\}$ ” denotes a set of operators. These groups, called type II magnetic groups, have

$$\underline{G} = \{\mathbb{U}\} + \{\mathbb{T}\mathbb{U}\} = G_0 + \mathbb{T} G_0 \quad (\text{type II}). \quad (12.41)$$

For type II groups,  $G_0$  is the invariant subgroup of  $\underline{G}$  of index 2. For each of the 32 ordinary point groups we can form a type II magnetic group,  $G_0 + \mathbb{T} G_0$ , and therefore there are 32 such magnetic groups.

Table 12.2 The multiplication table for the group  $C_{4v}$ 

$C_4$	$E$	$C_4$	$C_2$	$C_4^3$	$\sigma_{v1}$	$\sigma_{v2}$	$\sigma_{d1}$	$\sigma_{d2}$
$E$	$E$	$C_4$	$C_2$	$C_4^3$	$\sigma_{v1}$	$\sigma_{v2}$	$\sigma_{d1}$	$\sigma_{d2}$
$C_4$	$C_4$	$C_2$	$C_4^3$	$E$	$\sigma_{d1}$	$\sigma_{d2}$	$\sigma_{v2}$	$\sigma_{v1}$
$C_2$	$C_2$	$C_4^3$	$E$	$C_4$	$\sigma_{v2}$	$\sigma_{v1}$	$\sigma_{d2}$	$\sigma_{d1}$
$C_4^3$	$C_4^3$	$E$	$C_4$	$C_2$	$\sigma_{d2}$	$\sigma_{d1}$	$\sigma_{v1}$	$\sigma_{v2}$
$\sigma_{v1}$	$\sigma_{v1}$	$\sigma_{d2}$	$\sigma_{v2}$	$\sigma_{d1}$	$E$	$C_2$	$C_4^3$	$C_4$
$\sigma_{v2}$	$\sigma_{v2}$	$\sigma_{d1}$	$\sigma_{v1}$	$\sigma_{d2}$	$C_2$	$E$	$C_4$	$C_4^3$
$\sigma_{d1}$	$\sigma_{d1}$	$\sigma_{v1}$	$\sigma_{d2}$	$\sigma_{v2}$	$C_4$	$C_4^3$	$E$	$C_2$
$\sigma_{d2}$	$\sigma_{d2}$	$\sigma_{v2}$	$\sigma_{d1}$	$\sigma_{v1}$	$C_4^3$	$C_4$	$C_2$	$E$

### Type III magnetic groups

For magnetic crystals with a net magnetic moment the time-reversal operator  $\mathbb{T}$  is *not* in the point group  $\underline{G}$ , but operators such as  $\mathbb{T}\mathbb{U}$  can be. For example, if a ferromagnet has a  $C_2$  symmetry axis perpendicular to the magnetic direction, then  $\mathbb{T}C_2$  leaves the magnetic moments unchanged. In this case  $\mathbb{T}$  is not a symmetry operation, but  $\mathbb{T}C_2$  is.

Let  $G_0$  be one of the 32 ordinary point groups. We may write  $G_0 = G_u + \{G_0 - G_u\}$ , where  $G_u$  is an invariant subgroup of  $G_0$  of index 2 and  $\{G_0 - G_u\}$  is the set of operators not in  $G_u$ . (Note that  $\{G_0 - G_u\}$  is not a group, since it does not contain the identity operator.) A type III magnetic point group,  $\underline{G}$ , can be formed from the group of unitary operators,  $G_u$ , and the set of antiunitary operators  $\mathbb{T}\{G_0 - G_u\}$ :

$$\underline{G} = G_0 + \mathbb{T}\{G_0 - G_u\} \quad (\text{type III}). \quad (12.42)$$

Magnetic, type II and type III, point groups can also be constructed as

$$\underline{G} = G_u + \mathbb{A}G_u, \quad (12.43)$$

where  $\mathbb{A}$  is any antiunitary operator in  $\underline{G}$ . If  $\underline{G}$  contains  $\mathbb{T}$  then we may choose  $\mathbb{A} = \mathbb{T}$ . In this instance  $\underline{G} = G_u + \mathbb{T}G_u$ , which is a type II magnetic point group with  $G_u$  an invariant subgroup of  $\underline{G}$  of index 2. If  $\mathbb{T}$  itself is not in  $\underline{G}$  we may choose  $\mathbb{A} = \mathbb{T}\mathbb{U}_i$ , where  $\mathbb{U}_i$  is any member of  $\{G_0 - G_u\}$ . In this case  $\underline{G} = G_u + \mathbb{T}\mathbb{U}_iG_u$ . However, for an invariant subgroup of index 2,  $\mathbb{U}_iG_u = \{G_0 - G_u\}$  (see Theorem 12.2). Therefore we arrive at the same construction as (12.42).

In summary, the three types of groups are

$$\text{type I, } G = G_0 \quad (32 \text{ ordinary point groups}), \quad (12.44)$$

$$\text{type II, } G = G_0 + \mathbb{T}G_0 \quad (\text{paramagnetic, diamagnetic}), \quad (12.45)$$

$$\text{type III, } G = G_u + \mathbb{T}(G_0 - G_u) \quad (\text{ferromagnetic, ferrimagnetic, antiferromagnetic}), \quad (12.46)$$

$$\text{type III, } G = G_u + \mathbb{A} G_u \quad (\mathbb{A} \text{ any member of } \mathbb{T}\{G_0 - G_u\}). \quad (12.47)$$

There are 32 type I (ordinary point groups), 32 type II magnetic point groups, and 58 (distinct) type III magnetic point groups. The type II and type III groups are shown in Table 12.3 for different crystal systems. Also indicated are the magnetic orderings corresponding to the magnetic point groups.

The magnetic point groups are called Shubnikov [12.3] point groups or color groups. For type II and type III, the magnetic point groups contain antiunitary operators, and the representations do *not* obey the usual matrix-multiplication rules. This aspect of magnetic groups is discussed in Section 12.6.

As an example of the construction of a type III magnetic group, consider the squares shown in Fig. 12.2. In Fig. 12.2(a) we have a square with identical atoms (with no magnetic moments) on each of the four corners. In Fig. 12.2(b) we have atoms with their magnetic vectors alternating in direction. For Fig. 12.2(a), the simple square of non-magnetic atoms, the two-dimensional covering group is  $G_0 = C_{4v}$ . The operations of the group for Fig. 12.2(a) shown in Fig. 12.2(c) include the eight operators  $E, C_2, C_4, C_4^3, \sigma_{d1}, \sigma_{d2}, \sigma_{v1},$  and  $\sigma_{v2}$ . The set of symmetry elements  $\{E, C_2, \sigma_{v1}, \sigma_{v2}\} = G_u$  forms an invariant subgroup of  $C_{4v}$  of index 2, and the square in Fig. 12.2(b) remains invariant under these operations. For the square in Fig. 12.2(b) time reversal is not a symmetry operation since it reverses the magnetic vectors. In addition, the operators of the set  $\{C_4, C_4^3, \sigma_{d1}, \sigma_{d2}\} = \{G_0 - G_u\}$  are also *not* symmetry operations for the square in Fig. 12.2(b). However, the operators for the set  $\mathbb{T}\{C_4, C_4^3, \sigma_{d1}, \sigma_{d2}\} = \mathbb{T}\{G_0 - G_u\}$  are symmetry operations for the square

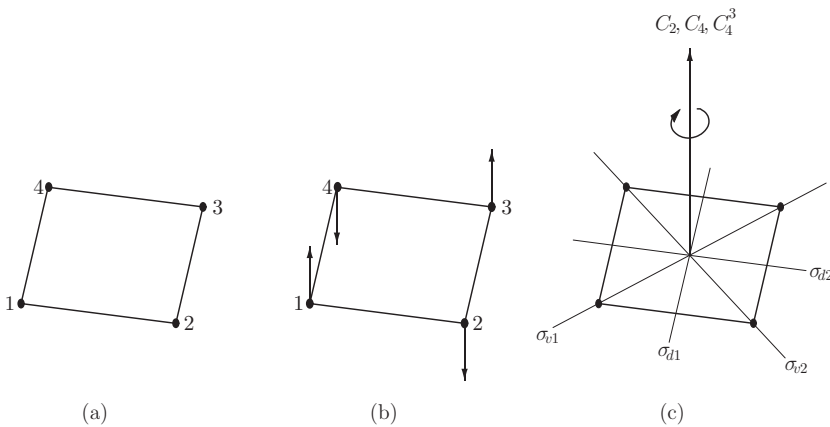


Figure 12.2 (a) A square with  $C_{4v}$  symmetry. (b) Symmetry reduced by magnetic vectors. (c) Rotation and reflection operations of  $C_{4v}$ .

in Fig. 12.2(b). In this case  $G_0 = G_u + (G_0 - G_u)$  is a point group for Fig. 12.2(a), and  $\underline{G} = G_u + \mathbb{T}(G_0 - G_u)$  is a magnetic point group for Fig. 12.2(b). The alternate construction of  $\underline{G}$  for  $C_{4v}$  (Eq. (12.43)) gives the same results. Note that we could have formed a type III magnetic point group with  $G_u = \{E, C_2, \sigma_{d1}, \sigma_{d2}\}$  and  $\{G_0 - G_u\} = \{C_4, C_4^3, \sigma_{v1}, \sigma_{v2}\}$ . This magnetic group is isomorphic to the previous one, and corresponds to simply rotating the square in Fig. 12.2(b) by  $90^\circ$ .

In general, a magnetic point group can also be specified in Schönflies notation as  $G_0(G_u)$ . For example,  $D_{6h}(C_{6v})$  is the type III group for which  $G_0 = D_{6h}$ ,  $G_u = C_{6v}$ , and  $\underline{G} = C_{6v} + \mathbb{T}(D_{6h} - C_{6v})$ . The type II and type III magnetic point groups for different crystal systems are shown in Table 12.3 using the Hermann–Mauguin/international notation.

### Hermann–Mauguin/international notation

International notation specifies some of the symmetry elements of a group, but gives only the information necessary to deduce the entire group of symmetry elements.

The first integer,  $n$ , specifies the principal  $n$ -fold symmetry axis. Subsequent integers indicate lesser rotation axes (in descending order).

Inversion through a point followed by a rotation is indicated as “ $\bar{n}$ ”. Mirror planes that contain a rotation axis or that are perpendicular to an  $n$ -fold axis are indicated by the symbol “ $m$ ”. If the mirror plane is perpendicular to a rotation axis, then a slash is placed between the axis number and the “ $m$ ”. For example, “ $m/n$ ” indicates an  $n$ -fold rotation axis with a mirror plane perpendicular to it.

For magnetic groups, underlined characters indicate complementary operations, that is, operations of the type  $\mathbb{T}\mathbb{O}$ , where  $\mathbb{O}$  is a rotation or mirror operation.

Indications of screw axes and glide planes can be added. These are shown by adding an integer subscript to the notation. The integer indicates the fraction of the translation along the axis. For example,  $2_1$  is a  $180^\circ$  rotation about the two-fold axis and translation by half of the lattice constant along the axis, whereas  $6_2$  indicates a  $60^\circ$  rotation about a six-fold axis and translation by  $2/6 = 1/3$  of a lattice constant along the axis.

The possible screw axes are  $2_1, 3_1, 3_2, 4_2, 6_1, 6_2$ , and  $6_3$ . The symbols  $a, b$ , and  $c$  indicate glide-plane axes along the  $a, b$ , and  $c$  crystal axes, respectively.

## 12.6 Co-representations for groups with time-reversal operators

For a group that contains antiunitary operators the usual representation matrices are inadequate. Instead, a different type of representation called a co-representation must be employed. The algebra of co-representations was initially worked out by Wigner [12.4]. For a different discussion see Lax [12.5]. Here we shall give brief summary of co-representations and a few examples.

Table 12.3 *Type II and type III ( $32 + 58 = 90$ ) magnetic point groups. Each group is designated by specifying the ordinary point group,  $G_0$ , and the unitary, invariant subgroup (index 2),  $G_u$ . The international notation for each group and the type of magnetic ordering are given in the last two columns. The 32 type I groups (ordinary groups not involving the time-reversal operator) are not included. F, ferromagnetic; AF, antiferromagnetic.*

Crystal system	Group $G_0$	Subgroup $G_u$	Number of elements	International notation	Magnetic order
Triclinic	$C_1$ $S_2(C_i)$	$C_1$	1	$1$	F
		$S_2$	2	$\bar{1}$	F
		$C_i$		$\bar{1}$	AF
Monoclinic	$C_{1h}$	$C_{1h}$	2	$m$	F
		$C_1$		$\underline{m}$	F
	$C_2$	$C_2$	2	$2$	F
		$C_1$		$\underline{2}$	F
	$C_{2h}$	$C_{2h}$	4	$2/m$	F
		$C_i$		$\underline{2/m}$	AF
		$C_2$		$\underline{2/m}$	AF
		$C_{1h}$		$\underline{2/m}$	AF
Rhombic	$C_{2v}$	$C_{2v}$	4	$2mm$	AF
		$C_{1h}$		$\underline{2mm}$	F
		$C_2$		$\underline{2mm}$	F
	$D_2$	$D_2$	4	$222$	AF
		$C_2$		$\underline{222}$	F
	$D_{2h}$	$D_{2h}$	8	$mmm$	AF
		$C_{2h}$		$\underline{mmm}$	F
		$C_{2v}$		$\underline{mmm}$	AF
		$D_2$		$\underline{mmm}$	AF
		$C_4$	4	$4$	F
Tetragonal	$C_4$	$C_4$	4	$4$	F
		$C_2$		$\underline{4}$	AF
		$S_4$	4	$\underline{4}$	F
	$C_{4h}$	$C_2$		$\underline{4}$	AF
		$C_{4h}$	8	$4/m$	F
		$C_{2h}$		$\underline{4/m}$	AF
		$C_4$		$\underline{4/m}$	AF
		$S_4$		$\underline{4/m}$	AF
	$D_{2d}$	$D_{2d}$	8	$\bar{4}2m$	AF
		$C_{2v}$		$\bar{4}2m$	AF
		$D_2$		$\bar{4}2m$	AF
		$S_4$		$\bar{4}2m$	F
		$C_{4v}$	8	$4mm$	AF
	$C_{4v}$	$C_{2v}$		$\underline{4mm}$	AF
		$C_4$		$\underline{4mm}$	F
		$D_4$	8	$42(422)$	AF
		$D_2$		$\underline{42}$	AF
		$C_4$		$\underline{42}$	F
	$D_{4h}$	$D_{4h}$	16	$4/mmm$	AF
		$D_{2h}$		$\underline{4/mmm}$	AF
		$C_{4h}$		$\underline{4/mmm}$	F

Table 12.3 (cont.)

Rhombohedral		$D_{2d}$		$\underline{4/mmm}$	AF
		$C_{4v}$		$4/\underline{mmm}$	AF
		$D_4$		$4/\underline{mmm}$	AF
	$C_3$	$C_3$	3	$\underline{3}$	F
	$S_6$	$S_6$	6	$\underline{\bar{3}}$	F
		$C_3$		$\underline{\bar{3}}$	AF
	$C_{3v}$	$C_{3v}$	6	$\underline{3m}$	AF
		$C_3$		$\underline{3m}$	F
	$D_3$	$D_3$	6	$\underline{32}$	AF
		$C_3$		$\underline{32}$	F
	$D_{3d}$	$D_{3d}$	12	$\underline{\bar{3}m}$	AF
		$S_6$		$\underline{\bar{3}m}$	F
		$C_{3v}$		$\underline{\bar{3}m}$	AF
		$D_3$		$\underline{\bar{3}m}$	AF
Hexagonal	$C_{3h}$	$C_{3h}$	6	$\underline{6}$	F
		$C_3$		$\underline{\bar{6}}$	AF
	$C_6$	$C_6$	6	$\underline{6}$	F
		$C_3$		$\underline{6}$	AF
	$C_{6h}$	$C_{6h}$	12	$\underline{6/m}$	F
		$S_6$		$\underline{6/m}$	AF
		$C_{3h}$		$\underline{6/m}$	AF
		$C_6$		$\underline{6/m}$	AF
	$D_{3h}$	$D_{3h}$	12	$\underline{\bar{6}m2}$	AF
		$C_{3v}$		$\underline{\bar{6}m2}$	AF
		$D_3$		$\underline{\bar{6}m2}$	AF
		$C_{3h}$		$\underline{\bar{6}m2}$	F
	$C_{6v}$	$C_{6v}$	12	$\underline{6mm}$	AF
		$C_{3v}$		$\underline{6mm}$	AF
		$C_6$		$\underline{6mm}$	F
	$D_6$	$D_6$	12	$\underline{62(622)}$	AF
		$D_3$		$\underline{62}$	AF
		$C_6$		$\underline{62}$	F
	$D_{6h}$	$D_{6h}$	24	$\underline{6/mmm}$	AF
		$D_{3d}$		$\underline{6/mmm}$	AF
		$C_{6h}$		$\underline{6/mmm}$	F
		$D_{3h}$		$\underline{6/mmm}$	AF
		$C_{6v}$		$\underline{6/mmm}$	AF
		$D_6$		$\underline{6/mmm}$	AF
Cubic	$T$	$T$	12	$\underline{23}$	AF
	$T_h$	$T_h$	24	$\underline{m3}$	AF
		$T$		$\underline{m3}$	AF
	$T_d$	$T_d$	24	$\underline{43m}$	AF
		$T$		$\underline{43m}$	AF
	$O$	$O$	24	$\underline{43(432)}$	AF
		$T$		$\underline{43}$	AF
	$O_h$	$O_h$	48	$\underline{m3m}$	AF
		$T_h$		$\underline{m3m}$	AF
		$T_d$		$\underline{m3m}$	AF
		$O$		$\underline{m3m}$	AF
				$\underline{m3m}$	AF

In the discussion here we will, for simplicity, use  $\mathbb{U}_i$  for  $\mathbb{P}_{\mathbb{U}_i}$ , a unitary operator, and  $\mathbb{A}_i$  for  $\mathbb{P}_{\mathbb{A}_i}$ , an antiunitary operator. We shall consider magnetic point groups of type II and type III that have the form  $\underline{G} = G_u + \mathbb{A}_0 G_u$ , where  $\mathbb{A}_0$  is any antiunitary operator belonging to  $\mathbb{T}(G_0 - G_u)$ . The notation to be used is summarized below.

- $G_s$  A space group.
- $G_0$  A unitary point group obtained from  $G_s$  by setting all translations to zero, or any type I, ordinary point group.
- $\underline{G}$  A magnetic point group.
- $G_u$  An invariant subgroup of  $G_0$  (or  $\underline{G}$  for type II) of index 2.
- $\mathbb{A}_i$  Antiunitary operators of  $\underline{G}$  (or of the set  $\{\mathbb{A}_0 G_u\}$ ).
- $\mathbb{U}_i$  Unitary operators of  $\underline{G}$  (or  $G_u$ ).
- $\Gamma$  An IR of an ordinary point group or subgroup.
- $\underline{\Gamma}$  A representation of a magnetic point group.
- $\underline{D}$  An IR of a magnetic group.

### 12.6.1 Basis functions for co-representations

We consider a magnetic group  $\underline{G} = G_u + \mathbb{A}_0 G_u$ . The rules for the operators are as follows. (1) The product of two unitary operators or two antiunitary operators is unitary and is a member of  $G_u$  and  $\underline{G}$ . (2) The product of a unitary operator and an antiunitary operator is an antiunitary operator that is a member of  $\mathbb{A}_0 G_u$  and  $\underline{G}$ . (3) The product of any two operators in  $\underline{G}$  is a member of  $\underline{G}$ . (4) Since the number of operators in  $G_u$  (index 2) is equal to the number in  $\mathbb{A}_0 G_u$ , we can label the operators as  $\mathbb{U}_i$  and  $\mathbb{A}_i = \mathbb{A}_0 \mathbb{U}_i$ ,  $i = 1, 2, \dots, h_u$ , where  $h_u$  is the number of operators belonging to  $G_u$  (half the number belonging to  $\underline{G}$ ).

Let  $f_\lambda$  ( $\lambda = 1, 2, \dots, l$ ) be a set of basis functions for  $\Gamma$ , an  $l$ -dimensional IR of the unitary group,  $G_u$ . Define a second set of the functions as  $\{\mathbb{A}_0 f_\lambda\} = \{g_\lambda\}$ . For the discussion in this section, assume that the functions of  $f_\lambda$  are orthogonal to those of  $\mathbb{A}_0 f_\lambda$ .

Since  $\Gamma$  is an  $l$ -dimensional IR of  $G_u$  based on the functions of  $f_\lambda$  ( $\lambda = 1, 2, \dots, l$ ),

$$\mathbb{U}_i f_\lambda = \sum_{\mu} f_{\mu} \Gamma(\mathbb{U}_i)_{\mu\lambda}. \quad (12.48)$$

It follows that

$$\begin{aligned} \mathbb{U}_i g_\lambda &= \mathbb{U}_i \mathbb{A}_0 f_\lambda = \mathbb{A}_0 \mathbb{A}_0^{-1} \mathbb{U}_i \mathbb{A}_0 f_\lambda = \mathbb{A}_0 \sum_{\mu} \Gamma(\mathbb{A}_0^{-1} \mathbb{U}_i \mathbb{A}_0)_{\mu\lambda} f_{\mu} \\ &= \sum_{\mu} \Gamma^{\mathbb{A}_0}(\mathbb{U}_i)_{\mu\lambda} \mathbb{A}_0 f_{\mu} = \sum_{\mu} \Gamma^{\mathbb{A}_0}(\mathbb{U}_i)_{\mu\lambda} g_{\mu}, \end{aligned} \quad (12.49)$$

where

$$\Gamma^{\mathbb{A}_0}(\mathbb{U}_i) \equiv \Gamma(\mathbb{A}_0^{-1} \mathbb{U}_i \mathbb{A}_0)^*. \quad (12.50)$$

Since  $\mathbb{A}_0^{-1} \mathbb{U}_i \mathbb{A}_0$  is a unitary operator, it is a member of  $G_u$ . If  $\Gamma$  is irreducible then  $\Gamma^{\mathbb{A}_0}$  is also irreducible. To prove this, assume that  $\Gamma$  is irreducible, but  $\Gamma^{\mathbb{A}_0}$  can be reduced by the unitary transformation matrix  $\mathbb{V}$ . In that case,  $\mathbb{V} \Gamma^{\mathbb{A}_0}(\mathbb{U}_i) \mathbb{V}^{-1} = [\mathbb{V}^* \Gamma(\mathbb{A}_0^{-1} \mathbb{U}_i \mathbb{A}_0)_{\mu\lambda} (\mathbb{V}^*)^{-1}]^*$ , which implies that  $\Gamma(\mathbb{A}_0^{-1} \mathbb{U}_i \mathbb{A}_0)$  is reduced by the unitary transformation  $\mathbb{V}^*$  for all  $\mathbb{U}_i$  in  $G_u$ . But  $(\mathbb{A}_0^{-1} \mathbb{U}_i \mathbb{A}_0)$  is a unitary operator belonging to  $G_u$  and the set,  $\{\mathbb{A}_0^{-1} \mathbb{U}_i \mathbb{A}_0\} = G_u$ . Therefore,  $\Gamma$  is reducible by  $\mathbb{V}^*$ . That conclusion contradicts the assumption that  $\Gamma$  is irreducible. Therefore, if  $\Gamma$  is irreducible, so is  $\Gamma^{\mathbb{A}_0}$ .

For the antiunitary operators,

$$\begin{aligned} \mathbb{A}_i f_\lambda &= \mathbb{A}_0 \mathbb{U}_i f_\lambda = \mathbb{A}_0 \sum_{\mu} \Gamma(U_i)_{\mu\lambda} f_\mu = \sum_{\mu} \Gamma(\mathbb{U}_i)^*_{\mu\lambda} \mathbb{A}_0 f_\mu \\ &= \sum_{\mu} \Gamma(U_i)^*_{\mu\lambda} g_\mu, \end{aligned} \quad (12.51)$$

$$\begin{aligned} \mathbb{A}_i g_\lambda &= (\mathbb{A}_0 \mathbb{U}_i)(\mathbb{A}_0 f_\lambda) = (\mathbb{A}_0 \mathbb{U}_i \mathbb{A}_0) f_\lambda \\ &= \sum_{\mu} \Gamma(\mathbb{A}_0 \mathbb{U}_i \mathbb{A}_0)_{\mu\lambda} f_\mu. \end{aligned} \quad (12.52)$$

Define the row vector (bra) by

$$\langle f, g | = \langle f_1, f_2, \dots, f_l, g_1, g_2, \dots, g_l |. \quad (12.53)$$

Then we can express (12.48) to (12.52) by the  $2 \times 2$  supermatrix form,

$$\begin{aligned} \langle f, g | \mathbb{U}_i &= \langle f, g | \underline{D}(\mathbb{U}_i), \\ \langle f, g | \mathbb{A}_i &= \langle f, g |^* \underline{D}(\mathbb{A}_i), \end{aligned} \quad (12.54)$$

where  $\underline{D}(\mathbb{U}_i)$  is a  $2l \times 2l$  supermatrix ( $l$  is the dimensionality of  $\Gamma$ ) given by

$$\underline{D}(\mathbb{U}_i) = \begin{pmatrix} \Gamma(\mathbb{U}_i) & 0 \\ 0 & \Gamma^{\mathbb{A}_0}(\mathbb{U}_i) \end{pmatrix} \quad (\text{type b}) \quad (12.55)$$

and

$$\underline{D}(\mathbb{A}_i) = \begin{pmatrix} 0 & \Gamma(\mathbb{A}_0 \mathbb{U}_i \mathbb{A}_0) \\ \Gamma(\mathbb{U}_i)^* & 0 \end{pmatrix} \quad (\text{type b}). \quad (12.56)$$

Noting that  $\mathbb{A}_0 \mathbb{U}_i = \mathbb{A}_i$  and that  $\mathbb{U}_i = \mathbb{A}_0^{-1} \mathbb{A}_i$ , the matrix in (12.56) can also be written as

$$\underline{D}(\mathbb{A}_i) = \begin{pmatrix} 0 & \Gamma(\mathbb{A}_i \mathbb{A}_0) \\ \Gamma(\mathbb{A}_0^{-1} \mathbb{A}_i)^* & 0 \end{pmatrix} \quad (\text{type b}). \quad (12.57)$$



The notation “(type b)” is explained below. All of the operator products in (12.56) and (12.57) are unitary elements of  $G_u$ . The co-representation matrices are unitary, since they consist of unitary matrices, all of which belong to an IR of  $G_u$ . For a type II group where  $\mathbb{T}$  itself is in  $G$  we may choose  $\mathbb{A}_0 = \mathbb{T}$ , and, since  $\mathbb{T}$  commutes with  $\mathbb{U}_i$ , (12.55) and (12.56) reduce to

$$\underline{D}(\mathbb{U}_i) = \begin{pmatrix} \Gamma(\mathbb{U}_i) & 0 \\ 0 & \Gamma(\mathbb{U}_i)^* \end{pmatrix} \quad (\text{type b})$$

and

$$\underline{D}(\mathbb{A}_i) = \begin{pmatrix} 0 & \Gamma(\mathbb{U}_i) \\ \Gamma(\mathbb{U}_i)^* & 0 \end{pmatrix} \quad (\text{type b}).$$

The matrices  $\underline{D}(\mathbb{U}_i)$  and  $\underline{D}(\mathbb{A}_i)$  above do not form an ordinary matrix representation because they do not obey the group product rules. For example,

$$\begin{aligned} \underline{D}(\mathbb{A}) \underline{D}(\mathbb{U}) &= \begin{pmatrix} 0 & \Gamma(\mathbb{A} \mathbb{A}_0) \Gamma(\mathbb{A}_0^{-1} \mathbb{U} \mathbb{A}_0)^* \\ \Gamma(\mathbb{A}_0^{-1} \mathbb{A})^* \Gamma(\mathbb{U}) & 0 \end{pmatrix} \\ &= \begin{pmatrix} 0 & \Gamma(\mathbb{A} \mathbb{U} \mathbb{A}_0)^* \\ \Gamma(\mathbb{A}_0^{-1} \mathbb{A})^* \Gamma(\mathbb{U}) & 0 \end{pmatrix}, \end{aligned} \quad (12.58)$$

but

$$\underline{D}(\mathbb{A} \mathbb{U}) = \begin{pmatrix} 0 & \Gamma(\mathbb{A} \mathbb{U} \mathbb{A}_0) \\ \Gamma(\mathbb{A}_0^{-1} \mathbb{A} \mathbb{U})^* & 0 \end{pmatrix} \neq \underline{D}(\mathbb{A}) \underline{D}(\mathbb{U}). \quad (12.59)$$

In order to have a consistent multiplication system, the co-representations obey the rules

$$\underline{D}(\mathbb{U}_1) \underline{D}(\mathbb{U}_2) = \underline{D}(\mathbb{U}_1 \mathbb{U}_2), \quad (12.60a)$$

$$\underline{D}(\mathbb{U}) \underline{D}(\mathbb{A}) = \underline{D}(\mathbb{U} \mathbb{A}), \quad (12.60b)$$

$$\underline{D}(\mathbb{A}) \underline{D}(\mathbb{U})^* = \underline{D}(\mathbb{A} \mathbb{U}), \quad (12.60c)$$

$$\underline{D}(\mathbb{A}_1) \underline{D}(\mathbb{A}_2)^* = \underline{D}(\mathbb{A}_1 \mathbb{A}_2). \quad (12.60d)$$

For example,

$$\begin{aligned} \underline{D}(\mathbb{A}) \underline{D}(\mathbb{U})^* &= \begin{pmatrix} 0 & \Gamma(\mathbb{A} \mathbb{A}_0) \Gamma(\mathbb{A}_0^{-1} \mathbb{U} \mathbb{A}_0) \\ \Gamma(\mathbb{A}_0^{-1} \mathbb{A})^* \Gamma(\mathbb{U})^* & 0 \end{pmatrix} \\ &= \begin{pmatrix} 0 & \Gamma(\mathbb{A} \mathbb{U} \mathbb{A}_0) \\ \Gamma(\mathbb{A}_0^{-1} \mathbb{A} \mathbb{U})^* & 0 \end{pmatrix} = \underline{D}(\mathbb{A} \mathbb{U}). \end{aligned} \quad (12.61)$$

**The multiplication rule for the product of two co-representation matrices**

If the first matrix represents an antiunitary operator, the complex conjugate of the second representation matrix is used in the matrix product; otherwise, ordinary matrix multiplication is used.

Given the product rules of (12.60a)–(12.60d), the problem of constructing irreducible corepresentations revolves around the question of whether or not  $\Gamma$  is equivalent to  $\Gamma^{\mathbb{A}_0}$ .  $\Gamma$  and  $\Gamma^{\mathbb{A}_0}$  are equivalent if there is a fixed unitary matrix  $Z$  such that  $\Gamma(\mathbb{U}) = Z \Gamma(\mathbb{A}_0^{-1} \mathbb{U} \mathbb{A}_0)^* Z^{-1}$  for all  $\mathbb{U}$  in  $G_u$ . If  $\Gamma$  is an IR of  $G_u$  and is *inequivalent* to  $\Gamma^{\mathbb{A}_0}$ , then the IRs, namely  $\underline{D}(\mathbb{U})$  and  $\underline{D}(\mathbb{A})$ , are given by (12.55) and (12.57).

In general, the forms of the IRs of the magnetic point groups can be expressed in terms of the IRs of the invariant subgroups of  $G_u$ . There are three possibilities: (a)  $\Gamma$  and  $\Gamma^{\mathbb{A}_0}$  are equivalent to the same real representation; (b)  $\Gamma$  and  $\Gamma^{\mathbb{A}_0}$  are inequivalent; and (c)  $\Gamma$  and  $\Gamma^{\mathbb{A}_0}$  are equivalent, but both can not be expressed as real representations. For details see [12.4, 12.6].

Equations (12.55) and (12.57) refer to a type (b) IR of the magnetic point group. The IRs for type (a) and type (c), for which  $\Gamma$  and  $\Gamma^{\mathbb{A}_0}$  are equivalent, are

$$\underline{D}(\mathbb{U}) = \Gamma(\mathbb{U}) \quad (\text{type a}), \quad (12.62)$$

$$\underline{D}(\mathbb{A}) = \pm \Gamma(\mathbb{A} \mathbb{A}_0^{-1}) Z \quad (\text{type a}), \quad (12.63)$$

$$\Gamma(\mathbb{U}) = Z \Gamma(\mathbb{A}_0^{-1} \mathbb{U} \mathbb{A}_0)^* Z^{-1}, \quad (12.64)$$

$$ZZ^* = \Gamma(\mathbb{A}_0^2). \quad (12.65)$$

Note that in this case  $\underline{D}$  consists of single,  $l \times l$  matrices, rather than  $2l \times 2l$  supermatrices. The “+” sign holds for integer-spin systems and the “−” for half-integer-spin systems.

For type (c),

$$\underline{D}(\mathbb{U}) = \begin{pmatrix} \Gamma(\mathbb{U}) & 0 \\ 0 & \Gamma(\mathbb{U}) \end{pmatrix} \quad (\text{type c}), \quad (12.66)$$

$$\underline{D}(\mathbb{A}) = \begin{pmatrix} 0 & -\Gamma(\mathbb{A} \mathbb{A}_0) Z \\ \Gamma(\mathbb{A} \mathbb{A}_0^{-1}) Z & 0 \end{pmatrix} \quad (\text{type c}), \quad (12.67)$$

$$\Gamma(\mathbb{U}) = Z \Gamma(\mathbb{A}_0^{-1} \mathbb{U} \mathbb{A}_0)^* Z^{-1} \quad \text{and} \quad ZZ^* = -\Gamma(\mathbb{A}_0^2). \quad (12.68)$$

The group properties of these co-representations can be verified by multiplying matrices and using the rules of (12.60a)–(12.60d). However, one must employ the equivalence of  $\Gamma$  and  $\Gamma^{\mathbb{A}_0}$  and the equation  $ZZ^* = \Gamma(\mathbb{A}_0^2)$  for type (a) or  $ZZ^* = -\Gamma(\mathbb{A}_0^2)$  for type (c). For example, for the type (a) matrices,

$$\underline{D}(\mathbb{A}) \underline{D}(\mathbb{U})^* = \pm \Gamma(\mathbb{A} \mathbb{A}_0^{-1}) Z \Gamma(\mathbb{U})^*. \quad (12.69)$$

From (12.64) we have  $\Gamma(\mathbb{U})^* = Z^* \Gamma(\mathbb{A} \mathbb{A}_0^2) Z Z^{-1*}$ , and, from (12.65),  $Z^{-1*} = \Gamma(\mathbb{A}_0^{-2}) Z$  and  $Z = \Gamma(\mathbb{A}_0^2) Z^{*-1}$ . Substitution of these relations into (12.69) gives

$$\begin{aligned} \underline{D}(\mathbb{A}) \underline{D}(\mathbb{U})^* &= \pm \Gamma(\mathbb{A} \mathbb{A}_0^{-1} \mathbb{A}_0^2 \mathbb{A}_0^{-1} \mathbb{U} \mathbb{A}_0) Z \\ &= \pm \Gamma(\mathbb{A} \mathbb{U} \mathbb{A}_0^{-1}) = \underline{D}(\mathbb{A} \mathbb{U}) \quad (\text{type a}). \end{aligned} \quad (12.70)$$

As a second example, consider the type (b) matrices. We have that

$$\begin{aligned} \underline{D}(\mathbb{A}_1) \underline{D}(\mathbb{A}_2)^* &= \begin{pmatrix} 0 & \Gamma(\mathbb{U}_1) \\ \Gamma(\mathbb{U}_1)^* & 0 \end{pmatrix} \begin{pmatrix} 0 & \Gamma(\mathbb{U}_2)^* \\ \Gamma(\mathbb{U}_2) & 0 \end{pmatrix} \\ &= \begin{pmatrix} \Gamma(\mathbb{U}_1) \Gamma(\mathbb{U}_2) & 0 \\ 0 & \Gamma(\mathbb{U}_1)^* \Gamma(\mathbb{U}_2)^* \end{pmatrix} \\ &= \begin{pmatrix} \Gamma(\mathbb{U}_1 \mathbb{U}_2) & 0 \\ 0 & \Gamma(\mathbb{U}_1 \mathbb{U}_2)^* \end{pmatrix} \\ &= \underline{D}(\mathbb{A}_1 \mathbb{A}_2) \quad (\text{type b}). \end{aligned} \quad (12.71)$$

### 12.7 Degeneracies due to time-reversal symmetry

A method to determine the relationship of  $\Gamma$  and  $\Gamma^{\mathbb{A}_0}$  that uses only the characters of the squares of operations of  $\{\mathbb{A}_0 G_u\}$  is the Frobenius–Schur test described in Theorem 12.3 below.

**Theorem 12.3** (Frobenius–Schur test for magnetic point groups) *Let  $\Gamma^\alpha$  be an IR of the invariant subgroup  $G_u$ , and let  $\mathbb{A}_i = \mathbb{A}_0 \mathbb{U}_i$  be an operator belonging to the set  $\{\mathbb{A}_0 G_u\}$ , where  $\mathbb{A}_0$  is an arbitrary, but fixed, antiunitary operator of the magnetic point group,  $\underline{G}$ . The sum of the characters,  $\sum_i \chi^\alpha(\mathbb{A}_i^2)$ , has three possible values, namely  $h_u$ , 0, and  $-h_u$ , where  $h_u$  is the number of operators in  $G_u$ . The additional degeneracies of the levels belonging to  $\Gamma^\alpha$  due to the addition of the time-reversal operator is determined by the value of  $\sum_i \chi^\alpha(\mathbb{A}_i^2)$ .*

(a)  $\sum_i \chi^\alpha(\mathbb{A}_i^2) = h_u$ .

*Time reversal leads to no additional degeneracy for integral spin, but doubles the degeneracy for half-integral spin.*

(b)  $\sum_i \chi^\alpha(\mathbb{A}_i^2) = 0$ .

*Time reversal leads to a doubling of the degeneracy both for integral and for half-integral spin.*

(c)  $\sum_i \chi^\alpha(\mathbb{A}_i^2) = -h_u$ .

*Time reversal leads to a doubling of degeneracy for integral spin, but no additional degeneracy for half-integral spin.*

Tinkham [12.7] has given an informative discussion of the magnetic group for antiferromagnets such as  $\text{MnF}_2$ ,  $\text{FeF}_2$ , and  $\text{CoF}_2$  (rutile structure). The crystal

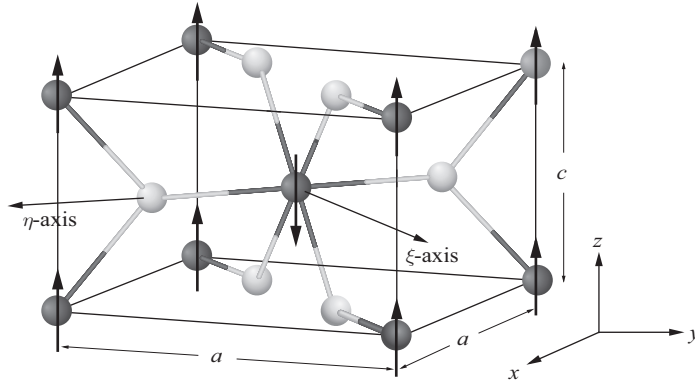
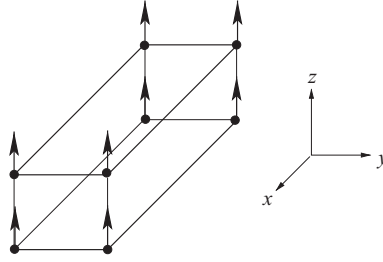


Figure 12.3 The magnetic unit cell for  $\text{MnF}_2$ . The dark gray circles represent the Mn ions and the light gray circles represent the F ions. The unit cell contains two magnetic metal ions; the central shaded ion and the corner metal ions (each shared by eight other cells). The crystal is tetragonal, with lattice constants  $a = b$  unequal to  $c$ . The F ions lie in an  $x$ - $y$  plane along diagonals in the planes. The Mn-F nearest-neighbor spacing in all  $x$ - $y$  planes is the same. (Note that the width of the figure has been elongated for improved presentation. The width and depth are both  $a$ .)

structure is illustrated in Fig. 12.3. In the non-magnetic state (above the Néel temperature) there are symmetry operations involving a non-primitive translation,  $\tau_0 = (1/2)(a, a, c)$ . The space-group operations include

- |                             |                                     |
|-----------------------------|-------------------------------------|
| 1. $\{E 0\}$                | 9. $\{i 0\}$                        |
| 2. $\{C_{2z} 0\}$           | 10. $\{C_{2z} 0\}\{i 0\}$           |
| 3. $\{C_{2\xi} 0\}$         | 11. $\{C_{2\xi} 0\}\{i 0\}$         |
| 4. $\{C_{2\eta} 0\}$        | 12. $\{C_{2\eta} 0\}\{i 0\}$        |
| 5. $\{C_{4z} \tau_0\}$      | 13. $\{C_{4z} \tau_0\}\{i 0\}$      |
| 6. $\{C_{4z}^{-1} \tau_0\}$ | 14. $\{C_{4z}^{-1} \tau_0\}\{i 0\}$ |
| 7. $\{C_{2x} \tau_0\}$      | 15. $\{C_{2x} \tau_0\}\{i 0\}$      |
| 8. $\{C_{2y} \tau_0\}$      | 16. $\{C_{2y} \tau_0\}\{i 0\}$ .    |

The subscripts  $x$ ,  $y$ ,  $z$ ,  $\xi$ , and  $\eta$  indicate the axis of rotation, with  $\xi$  and  $\eta$  being rotations about axes parallel to the  $(110)$  and  $(1\bar{1}0)$  directions, respectively. If we now set  $\tau_0 = 0$ , the first eight operations are those of the group  $D_4$ . Operations 9–16 are the products of the first eight operations times the inversion operator. Therefore the point group is  $G_0 = D_4 \times \mathbf{i} = D_{4h}$ . The time-reversal operator itself is not a symmetry operator, so the magnetic group  $\underline{G}$  is of type III. The appropriate invariant subgroup is  $D_{2h} = G_u$ , and the magnetic group is  $\underline{G} = D_{4h}(D_{2h}) = D_{2h} + \mathbb{T}(D_{4h} - D_{2h})$ .

 $C_2$  character table

IR	$E$	$C_{2z}$
$A$	1	1
$B$	1	-1

Figure 12.4 A ferromagnet with  $\underline{G} = D_2(C_2)$ , and the character table for  $C_2$ .

In detail,

$$\begin{aligned} \underline{G} = & (E, C_{2z}, C_{2x}, C_{2y}, i, iC_{2z}, iC_{2x}, iC_{2y}) \\ & + \mathbb{T}(C_{2\xi}, C_{2\eta}, C_{4z}, C_{4z}^{-1}, iC_{2\xi}, iC_{2\eta}, iC_{4z}, iC_{4z}^{-1}), \end{aligned}$$

where  $\mathbb{T} = \Theta \mathbf{K}_0$ . We could also use the form  $\underline{G} = G_u + \mathbb{A}_0 G_u$ . In this case  $A_0$  is any of the operators in  $\mathbb{T}(G_0 - G_u)$ . For the discussion here we choose  $\mathbb{A}_0 = \mathbb{T} C_{4z}$ .

The Frobenius–Schur test of Theorem 12.3 gives  $\sum_i \chi^\Gamma(A_i^2) = \pm[4\chi(E) + 4\chi(C_2)] = \pm 8$  for the  $A_{1g}$ ,  $A_{1u}$ ,  $A_{2g}$ , and  $A_{2u}$  IRs of  $G_u(D_{2h})$ , and therefore these IRs are of type (a) for integer spin and type (c) for half-integer spin.  $E_g$  and  $E_u$  IRs have  $\sum_i \chi^\Gamma(A_i^2) = 0$  and are IRs of type (b).

As a simple example of a co-representation consider the magnetic group  $D_2(C_2)$ . The group  $\underline{G} = C_2 + \mathbb{T}(D_2 - C_2)$  is applicable to a ferromagnet of the type shown in Fig. 12.4. This group has been discussed in connection with the ferromagnetic superconductor UGe<sub>2</sub> [12.8]. The operators of  $\underline{G}$  are  $E$ ,  $C_{2z}$ ,  $\mathbb{T} C_{2y}$ , and  $\mathbb{T} C_{2x}$ . For integral spin we take  $\mathbb{T}^2 = +1$ . The operator rules are  $C_{2i}C_{2j} = C_{2k}$ , where  $i$ ,  $j$ , and  $k$  can take the values  $x$ ,  $y$ , or  $z$  but no two may be the same. For example  $C_{2x}C_{2y} = C_{2y}C_{2x} = C_{2z}$ . The type of co-representations may be determined using the Frobenius–Schur test. We have that  $(\mathbb{T} C_{2y})^2 = \mathbb{T}^2 C_{2y}^2 = E$ , and  $(\mathbb{T} C_{2x})^2 = E$ , so that  $\sum_i \chi(A_i^2) = 2\chi(E) = h_u$ . Therefore the co-representations are of type (a). The co-representation  $\mathbf{D}(\mathbf{U}) = \Gamma(\mathbf{U})$ , and  $\mathbf{D}(\mathbb{A}) = \Gamma(\mathbb{A} \mathbb{A}_0^{-1})Z$ , where  $\mathbb{A}$  is  $\mathbb{T} C_{2y}$  or  $\mathbb{T} C_{2x}$  and  $\mathbb{A}_0$  is an arbitrary operator from the set  $\mathbb{T}(D_2 - C_2)$  ( $\mathbb{T} C_{2y}$  or  $\mathbb{T} C_{2x}$  in this case). We arbitrarily choose  $\mathbb{A}_0 = \mathbb{T} C_{2x}$ .

We must also have  $ZZ^* = \Gamma(\mathbb{A}_0^2)$  and  $\Gamma(\mathbf{U}) = Z\Gamma(A_0^{-1}UA)^*Z^{-1}$ , where  $\mathbf{U}$  is  $E$  or  $C_{2z}$ . The quantity  $\Gamma(\mathbb{A}_0^2) = \Gamma(\mathbf{K}C_{2x}\mathbf{K}C_{2x})^* = \Gamma(E) = 1$ . It follows that  $|Z|^2 = 1$ , so  $Z = \exp(i\phi)$ , where  $\phi$  is a real, positive number. To test this

choice we ask whether  $\Gamma(\mathbf{U}) = Z\Gamma(\mathbf{A}_0^{-1}\mathbf{U}\mathbf{A})^*Z^{-1}$  for the  $\mathbf{U}$  operators of  $C_2$ . Since the IRs of  $C_2$  are one-dimensional, real numbers,  $Z\Gamma(\mathbf{A}_0^{-1}\mathbf{U}\mathbf{A})^*Z^{-1}$  reduces to  $\Gamma(C_{2x}\mathbb{T}^{-1}\mathbf{U}\mathbb{T}C_{2x})$ . For  $\mathbf{U} = E$ , we obtain  $\Gamma(C_{2x}\mathbb{T}^{-1}E\mathbb{T}C_{2x}) = \Gamma(E)$ . For  $\mathbf{U} = C_{2z}$ , we obtain  $\Gamma(C_{2x}\mathbb{T}^{-1}C_{2z}\mathbb{T}C_{2x}) = \Gamma(C_{2x}C_{2z}C_{2x}) = \Gamma(C_{2x}C_{2y}) = \Gamma(C_{2z})$ . Therefore (12.64) is satisfied.

For the  $A$  irreducible representation of the invariant subgroup  $C_2$ :

$$\begin{aligned} \mathbf{D}(E) &= \Gamma(E) = 1, \\ \mathbf{D}(C_{2z}) &= \Gamma(C_{2z}) = 1, \\ \mathbf{D}(\mathbb{T}C_{2y}) &= \Gamma(\mathbb{T}C_{2y}\mathbf{A}^{-1})Z = \Gamma(\mathbb{T}C_{2y}C_{2x}\mathbb{T})Z = \Gamma(C_{2z})Z = e^{i\phi}, \\ \mathbf{D}(\mathbb{T}C_{2x}) &= \Gamma(\mathbb{T}C_{2x}\mathbf{A}^{-1})Z = \Gamma(\mathbb{T}C_{2x}C_{2x}\mathbb{T})Z = \Gamma(E)Z = e^{i\phi}. \end{aligned}$$

For the  $B$  irreducible representation of the invariant subgroup  $C_2$ :

$$\begin{aligned} \mathbf{D}(E) &= \Gamma(E) = 1, \\ \mathbf{D}(C_{2z}) &= \Gamma(C_{2z})Z = -1, \\ \mathbf{D}(\mathbb{T}C_{2y}) &= \Gamma(\mathbb{T}C_{2y}\mathbf{A}^{-1})Z = \Gamma(\mathbb{T}C_{2y}C_{2x}\mathbb{T})Z = \Gamma(C_{2z})Z = -e^{i\phi}, \\ \mathbf{D}(\mathbb{T}C_{2x}) &= \Gamma(\mathbb{T}C_{2x}\mathbf{A}^{-1})Z = \Gamma(\mathbb{T}C_{2x}C_{2x}\mathbb{T})Z = \Gamma(E)Z = e^{i\phi}. \end{aligned}$$

The character table for  $\underline{G} = D_2(C_2)$  with  $\mathbb{T}^2 = +1$  is then

IR	$E$	$C_{2z}$	$\mathbb{T}C_{2x}$	$\mathbb{T}C_{2y}$	
$A$	1	1	$w$	$w$	$w = e^{i\phi}$
$B$	1	-1	$w$	$-w$	

Since the IRs are one-dimensional, the  $D(\mathbb{U})$  and  $D(\mathbb{A})$  matrices are the same as the characters in the table. These two representations obey the multiplication rules given by Eqs. (12.60a)–(12.60d).

For the case  $\mathbb{T}^2 = -1$ ,  $\sum_x (\mathbb{A}_i^2) = -2$ , so the IRs are of type (c). The matrix elements are

$$D(\mathbb{U}) = \begin{pmatrix} \Gamma(\mathbb{U}) & 0 \\ 0 & \Gamma(\mathbb{U}) \end{pmatrix}, \quad D(\mathbb{A}) = \begin{pmatrix} 0 & -\Gamma(\mathbb{A}\mathbb{A}_0^{-1})Z \\ \Gamma(\mathbb{A}\mathbb{A}_0^{-1})Z & 0 \end{pmatrix}$$

and  $ZZ^* = -\Gamma(\mathbb{A}_0^2) = -\Gamma(\mathbb{T}C_{2x}\mathbb{T}C_{2x}) = +\Gamma(E) = 1$ , so again  $Z = e^{i\phi}$ .

We have that

$$\Gamma(\mathbb{T}C_{2x}\mathbb{A}_0^{-1})Z = \Gamma(\mathbb{T}C_{2x}C_{2x}\mathbb{T}^{-1})e^{i\phi} = \Gamma(E)e^{i\phi} = e^{i\phi}, \quad (12.72)$$

$$\Gamma(\mathbb{T}C_{2y}\mathbb{A}_0^{-1})Z = \Gamma(\mathbb{T}C_{2y}C_{2x}\mathbb{T}^{-1})e^{i\phi} = \Gamma(C_{2z})e^{i\phi} = -e^{i\phi}. \quad (12.73)$$

The co-representation matrices are

$$D(E) = \begin{pmatrix} 1 & 0 \\ 0 & 1 \end{pmatrix}, \quad D(\mathbb{T} C_{2x}) = \begin{pmatrix} 0 & -e^{i\phi} \\ e^{i\phi} & 0 \end{pmatrix},$$

$$D(C_2) = \begin{pmatrix} 1 & 0 \\ 0 & 1 \end{pmatrix}, \quad D(\mathbb{T} C_{2y}) = \begin{pmatrix} 0 & e^{i\phi} \\ -e^{i\phi} & 0 \end{pmatrix}$$

for the  $A$  IR, and

$$D(E) = \begin{pmatrix} 1 & 0 \\ 0 & 1 \end{pmatrix}, \quad D(\mathbb{T} C_{2x}) = \begin{pmatrix} 0 & -e^{i\phi} \\ e^{i\phi} & 0 \end{pmatrix},$$

$$D(C_2) = \begin{pmatrix} -1 & 0 \\ 0 & -1 \end{pmatrix}, \quad D(\mathbb{T} C_{2y}) = \begin{pmatrix} 0 & e^{i\phi} \\ -e^{i\phi} & 0 \end{pmatrix}$$

for the  $B$  IR.

### References

- [12.1] H. A. Kramers, “Théorie générale de la rotation paramagnétique dans les cristaux”, *Koninkl. Ned. Akad. Wetenschap.* **33**, 959–972 (1930).
- [12.2] C. Herring, “Effect of time-reversal symmetry on energy bands of crystals”, *Phys. Rev.* **52**, 361–365 (1937).
- [12.3] S. V. Shubnikov and N. V. Belov, *Colored Symmetry* (Oxford: Pergamon Press, 1964).
- [12.4] E. P. Wigner, *Group Theory and Its Application to the Quantum Mechanics of Atomic Spectra* (New York: Academic Press, 1959), Chapter 26.
- [12.5] M. Lax, *Symmetry Principles in Solid State and Molecular Physics* (New York: Wiley, 1974).
- [12.6] P. Jacobs, *Group Theory with Applications in Chemical Physics* (Cambridge: Cambridge University Press, 2005).
- [12.7] M. Tinkham, *Group Theory and Quantum Mechanics* (New York: McGraw-Hill, 1964).
- [12.8] I. A. Fomin and P. L. Kapitza, “Gap nodes in the superconducting phase of the itinerant ferromagnet UGe<sub>2</sub>”, arXiv:cond-mat/0207152v1 (2002) (7 pages).

### Exercises

- 12.1 If the set of operators  $\{\mathbb{R}_1, \mathbb{R}_2, \dots, \mathbb{R}_m\}$  forms a class of the group  $G$ , prove that  $\chi(\mathbb{R}_i^2)$  is the same for all operators of the class.
- 12.2 Consider the type II magnetic group  $\underline{G} = O + \mathbb{T} O$ , where  $O$  is the octahedral group. Using the Frobenius–Schur test, classify the IRs of  $\underline{G}$  as types (a), (b), or (c). Show that there are no additional degeneracies due to time reversal for either integer or half-integer spin.

- 12.3 Consider the type III magnetic group  $O_h(O)$  for which  $\underline{G} = O + \mathbb{T}(O_h - O)$ , where  $O$  is the octahedral group and  $O_h = O \times i$ . Using the Frobenius–Schur test, classify the IRs of  $\underline{G}$  as types (a), (b), or (c). Show that there are no additional degeneracies due to time reversal for either integer or half-integer spin.
- 12.4 For  $\underline{G} = C_{4v}(C_{2v})$ , what is the magnetic point-group type (a, b, or c)? Find the  $B_1$  irreducible representation for the magnetic point group for  $\mathbb{T}^2 = 1$  (integral or no spin).
- 12.5 For an antiferromagnet with the rutile structure (e.g.,  $\text{MnF}_2$ ) what is the difference between the group  $G_0$  and the pure point-group operations of the space group?
- 12.6 Consider the energy bands of a simple cubic crystal along the  $\Delta$  symmetry line.
- What is the group of the wavevector,  $\mathbf{g}_k$ ?
  - What are  $\mathbb{Q}$  operators?
  - Classify the IRs using the Herring rules (Theorem 12.1).
  - What additional degeneracies result from time reversal?
- 12.7 Given a group,  $G$ , with an invariant subgroup,  $G_u$ , of index 2, prove that the set  $\{XG_u\} = \{(G - G_u)\}$ , where  $X$  is any member of  $G$  not in  $G_u$ .
- 12.8 The orthogonality theorem of group theory states that, if  $\Gamma^\alpha$  and  $\Gamma^\beta$  are IRs of the same group,  $\sum_j \Gamma^\alpha(\mathbb{U}_j)_{pq}^* \Gamma^\beta(\mathbb{U}_j)_{rs} = \delta_{\alpha\beta} \delta_{pr} \delta_{qs} (h/l_\alpha)$ , where the sum over  $j$  is over all the operators,  $\mathbb{U}_j$ , of the group,  $h$  is the order of the group, and  $l_\alpha$  is the dimensionality of  $\Gamma^\alpha$ . For the magnetic group  $\underline{G} = G_u + \mathbb{A}_0 G_u$ , use the orthogonality theorem to show that  $\sum_i \chi(\mathbb{A}_i^2) = 0$  if  $\Gamma$  is *inequivalent* to  $\Gamma^{\mathbb{A}_0}$ .
- 12.9 For  $\underline{G} = G_u + \mathbb{A}_0 G_u$ , assume that  $\Gamma$  is *equivalent* to  $\Gamma^{\mathbb{A}_0}$ , then there exists a unitary matrix  $Z$ , such that  $Z \Gamma^{\mathbb{A}_0} Z^{-1} = \Gamma$ . Show that in this case  $\sum_i \chi(\mathbb{A}_i^2) = \pm h_u$  for  $ZZ^* = \pm(\Gamma^{\mathbb{A}_0})^2$ .



# 13

## Graphene

### 13.1 Graphene structure and energy bands

Graphene is a two-dimensional monolayer of carbon atoms. It is the basic building block for several carbon allotropes such as graphite, carbon nanotubes, and fullerenes. The atoms are arranged in a hexagonal array as shown schematically in Fig. 13.1(a). With the origin of coordinates chosen at the center of the hexagon, the primitive translation vectors of the Bravais lattice and the reciprocal lattice are

$$\begin{aligned}\mathbf{a} &= \frac{a}{2}(\sqrt{3}\mathbf{e}_x + \mathbf{e}_y), & \mathbf{b} &= \frac{a}{2}(-\sqrt{3}\mathbf{e}_x + \mathbf{e}_y), \\ \mathbf{a}^* &= \frac{2\pi}{a} \left( \frac{1}{\sqrt{3}}\mathbf{e}_x + \mathbf{e}_y \right), & \mathbf{b}^* &= \frac{2\pi}{a} \left( -\frac{1}{\sqrt{3}}\mathbf{e}_x + \mathbf{e}_y \right),\end{aligned}$$

where  $a$  is the spacing between the adjacent hexagon centers, and  $\mathbf{e}_x$  and  $\mathbf{e}_y$  are unit vectors along the  $x$ - and  $y$ -axes.

There are two carbon atoms per unit cell (A and B carbons). The A and B carbons are located at  $\mathbf{R}_A(m, n) = m\mathbf{a} + n\mathbf{b} + \tau_A$  and  $\mathbf{R}_B(m, n) = m\mathbf{a} + n\mathbf{b} + \tau_B$ , respectively, where  $m$  and  $n$  are positive or negative integers including 0,  $\tau_A = (a/2)(\mathbf{e}_x/\sqrt{3} + \mathbf{e}_y)$ , and  $\tau_B = (a/\sqrt{3})\mathbf{e}_x$ .

Each A carbon has three B carbons as nearest neighbors, and each B carbon has three A carbons as nearest neighbors, as shown in Fig. 13.1(a) by the heavy lines. The vectors from an A carbon to its neighboring B carbons are  $-(a/\sqrt{3})\mathbf{e}_x$ ,  $(a/2)(\mathbf{e}_x/\sqrt{3} + \mathbf{e}_y)$ , and  $(a/2)(\mathbf{e}_x/\sqrt{3} - \mathbf{e}_y)$ . The vectors from B to A carbons are the negatives of the vectors from A to B carbons.

The outer configuration of carbon is  $2s^2 2p^2$ . In the honeycomb lattice the  $s^2 p^2$  configuration becomes  $sp^2 + p_z$  configuration for the interacting carbon atoms, i.e., the  $s$ - and  $p$ -sigma orbitals ( $p_x$  and  $p_y$ ) hybridize to form low-lying, bonding bands and high-lying, antibonding bands. The carbon  $p_z$  orbitals form the  $\pi$  and  $\pi^*$  bands situated in energy above the three lowest hybrid bands and below the three highest hybrid bands. There are two atoms per unit cell and eight outer electrons

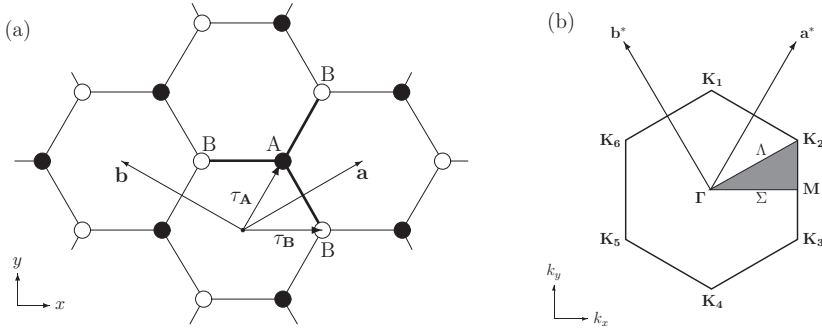


Figure 13.1 (a) The two-dimensional graphene lattice showing the primitive lattice vectors  $\mathbf{a}$  and  $\mathbf{b}$ . The two inequivalent atoms of the unit cell are shown as (A) solid and (B) open circles. The heavy lines indicate the three nearest neighbors of an A carbon. (b) The reciprocal lattice and the Brillouin zone, showing the vectors  $\mathbf{a}^*$  and  $\mathbf{b}^*$ . The corners of the zone are labeled  $\mathbf{K}_i$  ( $i = 1$  to 6). There are two inequivalent corners. Even-numbered  $\mathbf{K}_i$  are equivalent and odd-numbered  $\mathbf{K}_i$  are equivalent. Odd-odd and even-even pairs of  $\mathbf{K}_i$  are related by a reciprocal-lattice vector.

including spin. Six of the electrons occupy the  $2s-2p$  hybrid valence bands. The remaining two occupy the  $p_z$   $\pi$  valence bands. Consequently the  $\pi$  valence bands are filled and the  $\pi^*$  antibonding, conduction bands are empty. The core states,  $1s$ , lie at much lower energies, and have only a small effect on the  $\pi$  bands.

The simplest model for the  $\pi$  bands is an LCAO-like “tight-binding” model involving only the  $p_z$  orbitals and only interactions between the nearest-neighbor orbitals. The Bloch wavefunction is of the form

$$\Psi_{\mathbf{k}}(\mathbf{r}) = \Phi_{\mathbf{A}\mathbf{k}}(\mathbf{r}) + \Phi_{\mathbf{B}\mathbf{k}}(\mathbf{r}), \quad (13.1)$$

$$\Phi_{\mathbf{A}\mathbf{k}}(\mathbf{r}) = \frac{C_{\mathbf{A}\mathbf{k}}}{\sqrt{N}} \sum_{m,n} e^{i\mathbf{k} \cdot [\mathbf{R}(m,n) + \boldsymbol{\tau}_{\mathbf{A}}]} p_z(\mathbf{r} - [\mathbf{R}(m,n) + \boldsymbol{\tau}_{\mathbf{A}}]), \quad (13.2)$$

$$\Phi_{\mathbf{B}\mathbf{k}}(\mathbf{r}) = \frac{C_{\mathbf{B}\mathbf{k}}}{\sqrt{N}} \sum_{m,n} e^{i\mathbf{k} \cdot [\mathbf{R}(m,n) + \boldsymbol{\tau}_{\mathbf{B}}]} p_z(\mathbf{r} - [\mathbf{R}(m,n) + \boldsymbol{\tau}_{\mathbf{B}}]), \quad (13.3)$$

where  $N$  is the number of carbon atoms,  $\mathbf{k}$  is the wavevector, and  $p_z(\mathbf{r} - \mathbf{R})$  is a  $p$ -orbital oriented along the  $z$ -axis at  $\mathbf{R}$ . The coefficients  $C_{\mathbf{A}\mathbf{k}}$  and  $C_{\mathbf{B}\mathbf{k}}$  are the amplitudes of the  $p_z$  orbitals at the A and B sites in the unit cell.

Using orthogonalized Löwdin orbitals, the LCAO secular equation is

$$\begin{pmatrix} \epsilon_p - E_{\mathbf{k}} & H_{\mathbf{AB}}(\mathbf{k}) \\ H_{\mathbf{AB}}^*(\mathbf{k}) & \epsilon_p - E_{\mathbf{k}} \end{pmatrix} \begin{pmatrix} C_{\mathbf{A}\mathbf{k}}(\mathbf{r}) \\ C_{\mathbf{B}\mathbf{k}}(\mathbf{r}) \end{pmatrix} = 0, \quad (13.4)$$

where

$$\epsilon_p = \int p_z(\mathbf{R}_A)^* \mathbb{H} p_z(\mathbf{R}_A) d\mathbf{r}, \quad (13.5)$$

$$\begin{aligned}
H_{AB}(\mathbf{k}) &= \int \Phi_{A\mathbf{k}}(\mathbf{r})^* \mathbb{H} \Phi_{B\mathbf{k}}(\mathbf{r}) d\mathbf{r} \\
&= (pp\pi) \left\{ e^{-ik_x a/\sqrt{3}} + e^{i[k_x/\sqrt{3}+k_y]a/2} + e^{i[k_x/\sqrt{3}-k_y]a/2} \right\}, \quad (13.6)
\end{aligned}$$

$$(pp\pi) \equiv \int p_z(\mathbf{R}_A)^* \mathbb{H} p_z(\mathbf{R}_B) d\mathbf{r}, \quad (13.7)$$

and in (13.6) and (13.7) only nearest-neighbor interactions are retained.

We may write

$$H_{AB}(\mathbf{k}) = h(\mathbf{k})e^{i\theta}, \quad (13.8)$$

with  $h(\mathbf{k}) = |H_{AB}(\mathbf{k})|$  and  $\theta = \tan^{-1}(\Im H_{AB}/\Re H_{AB})$ , where  $\Im$  and  $\Re$  denote the imaginary and real parts, respectively. The secular equation then takes the form

$$\begin{pmatrix} \epsilon_p - E_{\mathbf{k}} & h(\mathbf{k})e^{i\theta} \\ h(\mathbf{k})e^{-i\theta} & \epsilon_p - E_{\mathbf{k}} \end{pmatrix} \begin{pmatrix} C_{A\mathbf{k}}(\mathbf{r}) \\ C_{B\mathbf{k}}(\mathbf{r}) \end{pmatrix} = 0. \quad (13.9)$$

Solution of the eigenvalue equation (13.9) gives

$$\begin{aligned}
\Omega_{\mathbf{k}}^{\pm} &= \frac{\epsilon_p - E_{\mathbf{k}}}{|(pp\pi)|} = \pm \frac{h(\mathbf{k})}{|(pp\pi)|} \\
&= \pm \left[ 1 + 4 \cos^2\left(\frac{k_y a}{2}\right) + 4 \cos\left(\frac{\sqrt{3}k_x a}{2}\right) \cos\left(\frac{k_y a}{2}\right) \right]^{1/2}, \quad (13.10)
\end{aligned}$$

and the eigenvectors are

$$V^+(\mathbf{k}) = \frac{1}{\sqrt{2}} \begin{pmatrix} e^{i\theta/2} \\ -e^{-i\theta/2} \end{pmatrix}, \quad (13.11)$$

$$V^-(\mathbf{k}) = \frac{1}{\sqrt{2}} \begin{pmatrix} e^{i\theta/2} \\ e^{-i\theta/2} \end{pmatrix}. \quad (13.12)$$

The energy surface and dispersion curves for  $\Omega_{\mathbf{k}}^{\pm}$  versus  $\mathbf{k}$ , and the corresponding density of states, are shown in Figs. 13.2(a), (b), and (c), respectively.

The density-of-states expression for graphene from [13.1] is

$$\rho(\Omega) = \begin{cases} [\sqrt{|\Omega|}/(2\pi^2)]K(m), & 1 \leq |\Omega| \leq 3, \\ [\sqrt{|\Omega|}/(2\pi^2)](1/m)K(1/m), & |\Omega| \leq 1, \end{cases}$$

where

$$m^2 = \frac{(1 + |\Omega|^2)^2 - (\Omega^2 - 1)^2/4}{4|\Omega|}$$

and  $K(m)$  is the complete elliptic function of the first kind.

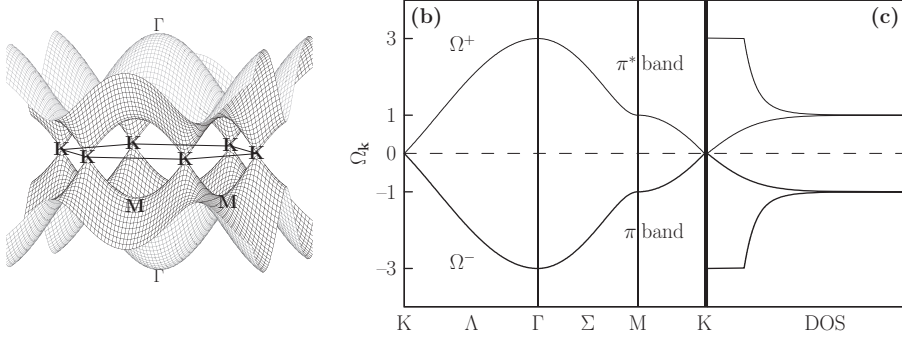


Figure 13.2 (a) The energy surface generated by  $\Omega$  for  $\mathbf{k}$  ranging over the entire first Brillouin zone. (b)  $\Omega_{\mathbf{k}}^{\pm}$  versus  $\mathbf{k}$  along symmetry lines. (c) The corresponding density of states.

As can be seen from Fig. 13.2,  $\Omega_{\mathbf{k}}^{\pm}$  vanishes at the  $\mathbf{K}$ -points in the first Brillouin zone. This is not immediately obvious from the dispersion formula (13.10), but can be seen from the expression for  $H_{AB}$  in (13.6) as follows. The  $\mathbf{K}$ -points are

$$\mathbf{K}_1 = -\mathbf{K}_4 = \frac{4\pi}{3a} \mathbf{e}_y, \quad (13.13a)$$

$$\mathbf{K}_2 = -\mathbf{K}_5 = \frac{2\pi}{3a} (\sqrt{3}\mathbf{e}_x + \mathbf{e}_y), \quad (13.13b)$$

$$\mathbf{K}_3 = -\mathbf{K}_6 = \frac{2\pi}{3a} (\sqrt{3}\mathbf{e}_x - \mathbf{e}_y). \quad (13.13c)$$

At  $\mathbf{k} = \mathbf{K}_i$  the three exponential factors of  $H_{AB}$  become the three roots of unity ( $1, \exp(i2\pi/3)$ , and  $\exp(-i2\pi/3)$ ), and the sum of the three roots is zero. When  $H_{AB}$  vanishes,  $\Omega_{\mathbf{k}}^{\pm}$  vanishes. The lower band (labeled  $\Omega_{\mathbf{k}}^-$ ) is the valence band, and the upper band (labeled  $\Omega_{\mathbf{k}}^+$ ) is the conduction band. For the model considered here the two bands are mirror reflections of one another.<sup>1</sup> For an infinite sheet of graphene the valence band is completely occupied and the conduction band is empty. The Fermi level bisects the two bands at  $\Omega_{\mathbf{k}}^{\pm} = 0$ . At absolute zero there are no electrons in the conduction ( $\pi^*$ ) band, but also there is no gap between the filled and empty states. At finite temperatures electrons will be thermally excited into the bottom of the conduction band and there will be holes in the top of the valence band. As a result graphene is a semi-metal.

It is of some interest to explore the behavior of the energy bands near a  $\mathbf{K}$ -point because the energy surfaces consist of six cones, each centered at one of the

<sup>1</sup> If atomic-like orbitals are employed, the overlap causes the valence band to be narrower than the conduction band.

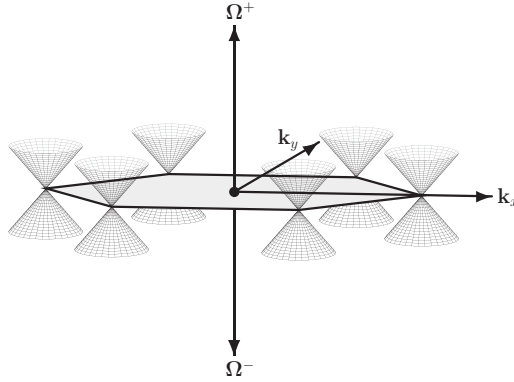


Figure 13.3 A schematic representation of  $\Omega^\pm$  near the  $\mathbf{K}$ -symmetry points. The surfaces are cones near each  $\mathbf{K}$ -point.  $\Omega^\pm$  is proportional to  $\pm|\delta\mathbf{k}|$  as  $|\delta\mathbf{k}| \rightarrow 0$ .

$\mathbf{K}$ -points in graphene. Let  $\mathbf{k} = \mathbf{K}_1 + \delta\mathbf{k} = (4\pi/(3a))\mathbf{e}_y + \delta k_x \mathbf{e}_x + \delta k_y \mathbf{e}_y$ ; then

$$\begin{aligned} H_{AB}(\mathbf{k}) &\rightarrow -\frac{\sqrt{3}a}{2}(pp\pi)(i\delta k_x - \delta k_y) \\ &= \frac{\sqrt{3}a}{2}(pp\pi)|\delta\mathbf{k}|e^{-i(\pi/2+\eta)}, \end{aligned} \quad (13.14)$$

where  $\eta$  is  $\tan^{-1}(\delta k_y/\delta k_x)$ . The dimensionless energy,

$$\Omega_{\mathbf{K}_1+\delta\mathbf{k}}^\pm = \pm \frac{\hbar(\mathbf{K}_1 + \delta\mathbf{k})}{(pp\pi)} \rightarrow \pm \frac{\sqrt{3}a}{2}|\delta\mathbf{k}|, \quad (13.15)$$

depends linearly on the magnitude of  $\delta\mathbf{k}$ . Therefore, near a  $\mathbf{K}$ -point the  $\Omega^\pm$  versus  $\mathbf{k}$  surfaces are cones, as illustrated schematically in Fig. 13.3. The cell wavefunctions near  $\mathbf{K}_1$  are

$$V^+(\mathbf{K}_1 + \delta\mathbf{k}) = \frac{1}{\sqrt{2}} \begin{pmatrix} e^{-i\eta/2} \\ -ie^{i\eta/2} \end{pmatrix}, \quad (13.16)$$

$$V^-(\mathbf{K}_1 + \delta\mathbf{k}) = \frac{1}{\sqrt{2}} \begin{pmatrix} e^{-i\eta/2} \\ ie^{i\eta/2} \end{pmatrix}. \quad (13.17)$$

The above results obtained for  $\mathbf{k}$  near  $\mathbf{K}_1$  hold for each of the six  $\mathbf{K}$ -points in the first Brillouin zone. Because of the phase factor,  $\exp(\pm i\eta/2)$ , the cell wavefunction changes sign when  $\eta$  changes by  $2\pi$ . Therefore, if  $\mathbf{k}$  adiabatically follows a path in  $\mathbf{k}$ -space that circles a  $\mathbf{K}$ -point, the wavefunction goes into the negative of itself (acquires a Berry phase of  $-1$ ) [13.2, 13.3]. The  $\mathbf{k}$ -vector must circle a  $\mathbf{K}$ -point twice for the wavefunction to return to its original state. In a magnetic field this feature leads to half-integer quantization of the Landau levels. If atomic orbitals

are used instead of Löwdin orbitals to calculate the energy bands, the overlap of the  $p_z$  orbitals causes the valence band to be narrower than the conduction band. However, the essential features of the bands near the  $\mathbf{K}$ -points, including linear dispersion, are preserved.

Near the  $\mathbf{K}$ -points,  $E(\mathbf{K} + \delta\mathbf{k}) \propto \xi r$ , where  $r = (\delta k_x^2 + \delta k_y^2)^{1/2}$  and  $\xi = (\sqrt{3}a/2)(pp\pi)$ . The radial effective mass,  $m_r^*$ , is given by

$$\frac{\hbar^2}{m_r^*} = \frac{\partial^2 E}{\partial r^2} + \frac{1}{r} \frac{\partial E}{\partial r} \propto \frac{1}{r}, \quad (13.18)$$

$$m_r^* \propto r. \quad (13.19)$$

The radial effective mass is independent of the angle on the energy cone. An electron (or hole) near  $\mathbf{K}$  behaves as a massless particle as  $r \rightarrow 0$  ( $\mathbf{k} \rightarrow \mathbf{K}$ , a Dirac point). The radial group velocity of an electron or a hole near a  $\mathbf{K}$ -point is

$$v_g = \frac{1}{\hbar} \frac{\partial E_{\mathbf{k}}}{\partial (|\delta\mathbf{k}|)} = \pm \frac{\sqrt{3}a}{2} \frac{1}{\hbar} |(pp\pi)|. \quad (13.20)$$

For graphene  $|(pp\pi)|$  is approximately 3 eV and  $a = 2.46 \text{ \AA}$ , so  $v_g = 9.74 \times 10^7 \text{ cm/s}$ . This velocity far exceeds the group velocity in typical semiconductors.

### 13.2 The analogy with the Dirac relativistic theory for massless particles

For electrons or holes with a  $\mathbf{k}$ -vector near any of the  $\mathbf{K}$ -points, the energy dispersion is linear, the group velocity is constant, and the effective mass is zero. The description of the electrons (holes) is similar to the massless particles described by the relativistic Dirac equation [13.4]. Near a  $\mathbf{K}$ -point the secular equation can be written as

$$-i v_g \hbar \begin{pmatrix} 0 & \partial/\partial x - i \partial/\partial y \\ \partial/\partial x + i \partial/\partial y & 0 \end{pmatrix} \begin{pmatrix} \Phi_{A\mathbf{k}}(\mathbf{r}) \\ \Phi_{B\mathbf{k}}(\mathbf{r}) \end{pmatrix} = E_{\mathbf{k}} \begin{pmatrix} \Phi_{A\mathbf{k}}(\mathbf{r}) \\ \Phi_{B\mathbf{k}}(\mathbf{r}) \end{pmatrix}, \quad (13.21)$$

where  $\Phi_{A\mathbf{k}}(\mathbf{r})$  and  $\Phi_{B\mathbf{k}}(\mathbf{r})$  are the sublattice Bloch waves (Eqs. (13.1)–(13.3)). This is the same equation as that satisfied by massless Dirac particles, except that  $v_g = c$ , the velocity of light, for the Dirac particles.

The two-dimensional states near a  $\mathbf{K}$ -point are often referred to as Dirac states and the  $\mathbf{K}$ -points are called Dirac points.

There are two inequivalent  $\mathbf{K}$ -points, and the others are related to these two by reciprocal-lattice vectors.  $\mathbf{K}_1$  is equivalent to  $\mathbf{K}_3$  and  $\mathbf{K}_5$ , while  $\mathbf{K}_2$  is equivalent to  $\mathbf{K}_4$  and  $\mathbf{K}_6$ . For example,  $\mathbf{K}_1 = \mathbf{a}^* - \mathbf{K}_3$ . The Dirac states at  $\mathbf{K}_1$  and  $-\mathbf{K}_1 = \mathbf{K}_4$  are inequivalent, but their energies are degenerate. The Dirac form can be extended to a four-component matrix equation describing the energy bands of electrons near  $\mathbf{K}$  and  $-\mathbf{K}$ . In this case the equations are analogous to those of the Dirac–Weyl equations for massless neutrinos [13.5].

### 13.3 Graphene lattice vibrations

The group of the wavevector,  $g_{\mathbf{k}}$ , for an infinite monolayer of graphene at various high-symmetry points is given in Table 13.1.

At  $\Gamma$ ,  $g_{\mathbf{k}}$  is  $D_{6h}$ . The  $D_{6h}$  group is the direct product of  $D_6$  with inversion. The action table for  $D_6$  is shown in Table 13.2.

The action tables for various symmetry points in the Brillouin zone can be obtained by selecting the operations in Table 13.2 that leave  $\mathbf{k}$  invariant or carry it into an equivalent  $\mathbf{k}$ -vector. The operators for the group of the wavevector at the  $\mathbf{M}$ - and  $\mathbf{K}$ -points and on the  $\Sigma$ -line are given in Table 13.3.

Table 13.1 *The group of the wavevector,  $g_{\mathbf{k}}$ , for an infinite monolayer of graphene. For a  $\mathbf{k}$ -vector at a general point in the Brillouin zone  $g_{\mathbf{k}} = C_{1h}$ .*

Space group	$\Gamma$	$\mathbf{K}$	$\mathbf{M}$	$\Lambda$	$\Sigma$
$P6/mmm$	$D_{6h}$	$D_{3h}$	$D_{2h}$	$C_{2v}$	$C_{2v}$

Table 13.2 *The action table for  $D_6$ .  $D_{6h} = D_6 \times \mathbf{i}$ . The coordinate system and numbering of the sites are shown below the table, where the operations are defined. The left-hand system of rotation is used, so the result is that of  $P_R$  rather than rotation of the axes.*

	$E$	$C_2$	$C_3$	$C_3^{-1}$	$C_6$	$C_6^{-1}$	$C_2^{(1)'} $	$C_2^{(2)'} $	$C_2^{(3)'} $	$C_2^{(1)''}$	$C_2^{(2)''}$	$C_2^{(3)''}$
$x$	$x$	$-x$	$\xi_{--}$	$\xi_{-+}$	$\xi_{+-}$	$\xi_{++}$	$-x$	$\xi_{+-}$	$\xi_{++}$	$\xi_{-+}$	$x$	$\xi_{--}$
$y$	$y$	$-y$	$\zeta_{+-}$	$\zeta_{--}$	$\zeta_{++}$	$\zeta_{-+}$	$y$	$\zeta_{--}$	$\zeta_{+-}$	$\zeta_{++}$	$-y$	$\zeta_{-+}$
$z$	$z$	$z$	$z$	$z$	$z$	$z$	$-z$	$-z$	$-z$	$-z$	$-z$	$-z$
1	1	4	3	5	2	6	6	4	2	1	3	5
2	2	5	4	6	3	1	5	3	1	6	2	4
3	3	6	5	1	4	2	4	2	6	5	1	3
4	4	1	6	2	5	3	3	1	5	4	6	2
5	5	2	1	3	6	4	2	6	4	3	5	1
6	6	3	2	4	1	5	1	5	3	2	4	6

$$\xi_{ss'} \equiv s \frac{1}{2}x + s' \frac{\sqrt{3}}{2}y \text{ and } \zeta_{ss'} \equiv s \frac{\sqrt{3}}{2}x + s' \frac{1}{2}y \text{ with } s, s' = \{+, -\}$$

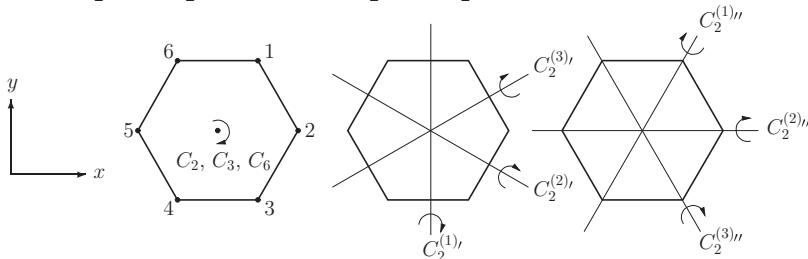


Table 13.3  $g_{\mathbf{k}}$  operations for  $\mathbf{M}$ ,  $\mathbf{K}$ , and  $\Sigma$ .  $D_{2h} = D_2 \times \mathbf{i}$  and  $D_{3h} = D_3 \times \mathbf{i}$ . Additional operations (not shown) for  $D_{2h}$  and  $D_{3h}$  include the operations listed times the inversion operator. (See Appendix E for  $D_n$  operator symbols.)

$\mathbf{M}(D_{2h})$	$E$	$C_2$	$C_2^{(1)'}$	$C_2^{(2)''}$		
$\mathbf{K}(D_{3h})$	$E$	$C_3$	$C_3^{-1}$	$C_2^{(1)''}$	$C_2^{(2)''}$	$C_2^{(3)''}$
$\Sigma(C_{2v})$	$E$	$C_2^{(2)'}$	$iC_2$	$iC_2^{(1)''}$		

Table 13.4 The character table for  $D_6$ .  $D_{6h} = D_6 \times \mathbf{i}$

	$D_6(622)$		$E$	$C_2$	$2C_3$	$2C_6$	$3C'_2$	$3C''_2$
$x^2 + y^2, z^2$		$A_1$	1	1	1	1	1	1
	$R_z, z$	$A_2$	1	1	1	1	-1	-1
		$B_1$	1	-1	1	-1	1	-1
		$B_2$	1	-1	1	-1	-1	1
$(xz, yz)$	$(x, y), (R_x, R_y)$	$E_1$	2	-2	-1	1	0	0
$(x^2 - y^2, xy)$		$E_2$	2	2	-1	-1	0	0

Even though graphene is a two-dimensional sheet, we must include the  $z$ -coordinate in order to account for the “out-of-plane” normal modes of vibration.

### 13.3.1 Out-of-plane normal modes at $\Gamma$

We begin by examining the out-of-plane vibrations of graphene. At  $\mathbf{k} = 0$  the group of the wavevector,  $g_{\mathbf{k}}$ , is  $D_{6h}$ . We make use of the action table (Table 13.2) and the equivalences of sites 2, 4, and 6 to find the symmetry functions based on the transformation properties of the displacements. We see that the  $x_1, y_1, x_2$ , and  $y_2$  transform among themselves and are therefore basis functions for a  $4 \times 4$  representation. At the  $\Gamma$ -point all the phase factors are unity. For the  $2 \times 2$  representation based on  $z_1$  and  $z_2$  we find that

$$\begin{aligned} \chi(E) &= 2, & \chi(C_2) &= 0, & \chi(C_3) &= 2, \\ \chi(C_6) &= 0, & \chi(C'_2) &= 0, & \chi(C''_2) &= -2. \end{aligned} \quad (13.22)$$

Using the character table, Table 13.4, we find that the decomposition into IRs of  $D_6$  is  $A_2 + B_1$ . If we include the inversion operations of  $D_{6h}$ , the decomposition is  $A_{2u} + B_{1g}$ . We can use the symmetry-function-generating machine to find the out-of-plane modes, starting with  $z_1$  as the trial function.



Table 13.5 The characters for the  $\Gamma(x, y)$  representation

$\Gamma(x, y)$	$E$	$C_2$	$2C_3$	$2C_6$	$3C'_2$	$C_2^{(1)''}$	$C_2^{(2)''}$	$C_2^{(3)''}$
$x_1$	1	0	$-\frac{1}{2}$	0	0	$-\frac{1}{2}$	1	$-\frac{1}{2}$
$x_2$	1	0	$-\frac{1}{2}$	0	0	$-\frac{1}{2}$	1	$-\frac{1}{2}$
$y_1$	1	0	$-\frac{1}{2}$	0	0	$\frac{1}{2}$	-1	$\frac{1}{2}$
$y_2$	1	0	$-\frac{1}{2}$	0	0	$\frac{1}{2}$	-1	$\frac{1}{2}$
Trace	4	0	-2	0	0	0	0	0

We have that  $f_z(A_2) \propto \sum_R \chi^{A_2}(P_R) P_R z_1 = 2z_1 + 2z_2 + 2z_3 + 2z_4 + 2z_5 + 2z_6$ . Using the equivalence of  $z_1, z_3$ , and  $z_5$ , and the equivalence of  $z_2, z_4$ , and  $z_6$ , gives  $f_z(A_2) \propto (z_1 + z_2)$ . If we include the inversion operations, the *normalized* symmetry function for the unit cell is  $f_z(A_{2u}) = (z_1 + z_2)/\sqrt{2}$ . Similar calculations give  $f_z(B_{1g}) = (z_1 - z_2)/\sqrt{2}$ . Clearly  $f_z(A_{2u})$  corresponds to translation in the  $z$ -direction. It is an acoustic mode at  $\Gamma$ . The function  $f_z(B_{1g})$  is an optical vibration at  $\Gamma$ . Both symmetry functions must also be normal modes, since  $A_{2u}$  and  $B_{1g}$  occur only once in the decomposition.

### 13.3.2 In-plane normal modes at $\Gamma$

Consider the matrix representation based on the functions  $x_1, x_2, y_1$ , and  $y_2$ . The traces of the  $4 \times 4$  representation matrices can be found from the action table. Using the equivalence of carbons 1, 3, and 5, and that of carbons 2, 4, and 6, we find the results in Table 13.5.

The decomposition of  $\Gamma(x, y)$  into the IRs of  $D_6$  yields

$$\Gamma(x, y) = \mathcal{E}_1 + \mathcal{E}_2. \quad (13.23)$$

The coordinates  $x$  and  $y$  are basis functions for the  $\mathcal{E}_1$  IR. The matrix elements can be read directly from the action table,

$$\begin{aligned}
 E &= \begin{pmatrix} 1 & 0 \\ 0 & 1 \end{pmatrix}, & C_2 &= \begin{pmatrix} -1 & 0 \\ 0 & -1 \end{pmatrix}, & C_3 &= \begin{pmatrix} -\frac{1}{2} & -\sqrt{3}/2 \\ \sqrt{3}/2 & -\frac{1}{2} \end{pmatrix}, \\
 C_3^{-1} &= \begin{pmatrix} -\frac{1}{2} & \sqrt{3}/2 \\ -\sqrt{3}/2 & -\frac{1}{2} \end{pmatrix}, & C_6 &= \begin{pmatrix} \frac{1}{2} & -\sqrt{3}/2 \\ \sqrt{3}/2 & \frac{1}{2} \end{pmatrix}, \\
 C_6^{-1} &= \begin{pmatrix} \frac{1}{2} & \sqrt{3}/2 \\ -\sqrt{3}/2 & \frac{1}{2} \end{pmatrix}, & C_2^{(1)'} &= \begin{pmatrix} -1 & 0 \\ 0 & 1 \end{pmatrix}, \\
 C_2^{(2)'} &= \begin{pmatrix} \frac{1}{2} & -\sqrt{3}/2 \\ -\sqrt{3}/2 & -\frac{1}{2} \end{pmatrix}, & C_2^{(3)'} &= \begin{pmatrix} \frac{1}{2} & \sqrt{3}/2 \\ \sqrt{3}/2 & -\frac{1}{2} \end{pmatrix},
 \end{aligned}$$

$$\begin{aligned}
C_2^{(1)''} &= \begin{pmatrix} -\frac{1}{2} & \sqrt{3}/2 \\ -\sqrt{3}/2 & \frac{1}{2} \end{pmatrix}, & C_2^{(2)''} &= \begin{pmatrix} 1 & 0 \\ 0 & -1 \end{pmatrix}, \\
C_2^{(3)''} &= \begin{pmatrix} -\frac{1}{2} & -\sqrt{3}/2 \\ -\sqrt{3}/2 & \frac{1}{2} \end{pmatrix}.
\end{aligned} \tag{13.24}$$

Note that  $x_1$  and  $y_1$  *do not* form bases for a representation of  $\mathcal{E}_1$  because some operations of the group transform carbon 1 into carbon 2 or its equivalent and vice versa. Instead, the basis functions for one representation of  $\mathcal{E}_1$  are  $(x_1 + x_2)/\sqrt{2}$  and  $(y_1 + y_2)/\sqrt{2}$ . The functions  $(x_1 - x_2)/\sqrt{2}$  and  $(y_1 - y_2)/\sqrt{2}$  are basis functions for the representation of  $\mathcal{E}_2$ . The first set clearly corresponds to translation in the  $x$ - and  $y$ -directions (acoustic branches at  $\Gamma$ ). The second set of basis functions corresponds to vibration modes (optical branches at  $\Gamma$ ). If we include the inversion operations, the normal modes are

$$\mathcal{E}_{1u}(\Gamma_5^-) = \frac{x_1 + x_2}{\sqrt{2}} \quad (\text{row 1}), \tag{13.25a}$$

$$\mathcal{E}_{1u}(\Gamma_5^-) = \frac{y_1 + y_2}{\sqrt{2}} \quad (\text{row 2}), \tag{13.25b}$$

$$\mathcal{E}_{2g}(\Gamma_6^+) = \frac{x_1 - x_2}{\sqrt{2}} \quad (\text{row 1}), \tag{13.25c}$$

$$\mathcal{E}_{2g}(\Gamma_6^+) = \frac{y_1 - y_2}{\sqrt{2}} \quad (\text{row 2}), \tag{13.25d}$$

$$A_{2u}(\Gamma_2^-) = \frac{z_1 + z_2}{\sqrt{2}}, \tag{13.25e}$$

$$B_{1g}(\Gamma_4^+) = \frac{z_1 - z_2}{\sqrt{2}}. \tag{13.25f}$$

The commonly used  $\Gamma$ -labels are shown in parentheses. That these functions are symmetry functions can be verified by using the symmetry-function-generating machine and the atomic-site equivalences.

At  $\Gamma$  all of the symmetry functions are also eigenvectors, since no two symmetry functions transform according to the same row of the same IR. The normal modes are shown schematically in Fig. 13.4.

### 13.3.3 Lattice vibrations of graphene at $M$

From the action table we can find the operations that leave  $\mathbf{k}(\mathbf{M}) = (2\pi/a)(3^{-1/2}, 0, 0)$  invariant or carry  $\mathbf{k}(\mathbf{M})$  into an equivalent wavevector ( $-\mathbf{k}(\mathbf{M})$  is equivalent to  $\mathbf{k}(\mathbf{M})$ ). The group consists of  $E$ ,  $C_2$ ,  $C_2^{(2)''}$ ,  $C_2^{(1)''}$ , and  $\mathbf{i}$  times these operators. Noting that  $C_2 = C_2^z$ ,  $C_2^{(2)''} = C_2^x$ , and  $C_2^{(1)''}$  is equivalent to  $C_2^y$ , we can identify the group of the wavevector as  $D_{2h}$ . The *phase factors* between carbon atoms are given in Table 13.6.

Table 13.6 Phase angles and phase factors between carbon atoms for  $\mathbf{k}(\mathbf{M})$ 

$\mathbf{R}_j - \mathbf{R}_i$	$\mathbf{k}(\mathbf{M}) \cdot (\mathbf{R}_j - \mathbf{R}_i)$	$\exp[i\mathbf{k}(\mathbf{M}) \cdot (\mathbf{R}_j - \mathbf{R}_i)]$
$\mathbf{R}_2 - \mathbf{R}_1$	$\phi$	$e^{i\phi}$
$\mathbf{R}_3 - \mathbf{R}_1$	0	1
$\mathbf{R}_4 - \mathbf{R}_1$	$-2\phi$	$-e^{i\phi}$
$\mathbf{R}_5 - \mathbf{R}_1$	$-3\phi$	-1
$\mathbf{R}_6 - \mathbf{R}_1$	$-2\phi$	$-e^{i\phi}$
$\mathbf{R}_3 - \mathbf{R}_2$	$-\phi$	$e^{-i\phi}$
$\mathbf{R}_4 - \mathbf{R}_2$	$-3\phi$	-1
$\mathbf{R}_5 - \mathbf{R}_2$	$-4\phi$	$-e^{-i\phi}$
$\mathbf{R}_6 - \mathbf{R}_2$	$-3\phi$	-1

$\phi = \pi/3$ ,  $n - m$  phase angle is negative of  $m - n$ .

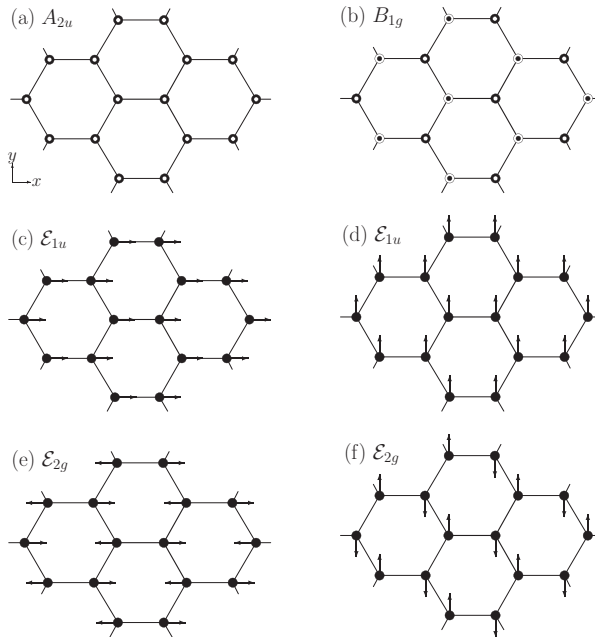


Figure 13.4 Normal modes of graphene at  $\Gamma$  ( $\mathbf{k} = 0$ ). Black circles with white centers represent displacements along the  $+z$ -direction (perpendicular to the plane of the paper); the white circles with black centers represent displacements along the  $-z$ -direction: (a) the acoustic mode,  $A_{2u}$ , in the  $z$ -direction; (b) the out-of-plane, optical mode,  $B_{1g}$ ; (c) and (d) in-plane, acoustic normal modes,  $E_{1u}$ ; and (e) and (f) in-plane, optical normal modes,  $E_{2g}$ . The  $E_{2g}$  modes produce the “G-band” observed in spectroscopic experiments.

Table 13.7 The character table for  $D_2$ .  $D_{2h} = \mathbf{i} \times D_2$ 

$D_2(222)$			$E$	$C_2^z$	$C_2^y$	$C_2^x$
$x^2, y^2, z^2$		$A_1$	1	1	1	1
$xy$	$R_z, z$	$B_1$	1	1	-1	-1
$xz$	$R_y, y$	$B_2$	1	-1	1	-1
$yz$	$R_x, x$	$B_3$	1	-1	-1	1

A representation of  $D_2$ ,  $\Gamma(\mathbf{M})$ , with bases  $x_1, x_2, y_1, y_2, z_1$ , and  $z_2$ , has the following characters (note that all of the phase factors involved in calculating the traces are +1):

$$\begin{aligned}
 \chi(E) &= 6, & \chi(i) &= 0, \\
 \chi(C_2) &= \chi(C_2^Z) = 0 & \chi(iC_2^Z) &= 2, \\
 \chi(C_2^{(1)'}) &= \chi(C_2^Y) = 0, & \chi(iC_2^Y) &= 2, \\
 \chi(C_2^{(2)'}) &= \chi(C_2^X) = -2, & \chi(iC_2^X) &= 0.
 \end{aligned}$$

From Table 13.7 we find that the decomposition into the IRs of  $D_{2h}$  gives

$$\Gamma(\mathbf{M}) = [B_{1u} + B_{2g}] + A_{1g} + B_{1g} + B_{2u} + B_{3u}, \quad (13.26)$$

where the two IRs in brackets correspond to the out-of-plane vibrations involving only  $z_1$  and  $z_2$ . Since no IR occurs more than once, all of the symmetry functions will also be normal modes (eigenvectors). Using the symmetry-function-generating machine and the appropriate phase factors, we find

$$B_{1u}(\mathbf{M}_2^-) = \frac{1}{\sqrt{2}}(z_1 - z_2 e^{i\phi}) \quad (\text{TA}), \quad (13.27a)$$

$$B_{2g}(\mathbf{M}_4^+) = \frac{1}{\sqrt{2}}(z_1 + z_2 e^{i\phi}) \quad (\text{TO}), \quad (13.27b)$$

$$A_{1g}(\mathbf{M}_1^+) = \frac{1}{\sqrt{2}}(x_1 + x_2 e^{i\phi}) \quad (\text{LO}), \quad (13.27c)$$

$$B_{2g}(\mathbf{M}_3^+) = \frac{1}{\sqrt{2}}(x_1 - x_2 e^{i\phi}) \quad (\text{LA}), \quad (13.27d)$$

$$B_{3u}(\mathbf{M}_4^-) = \frac{1}{\sqrt{2}}(y_1 - y_2 e^{i\phi}) \quad (\text{TA}), \quad (13.27e)$$

$$B_{1g}(\mathbf{M}_2^+) = \frac{1}{\sqrt{2}}(y_1 + y_2 e^{i\phi}) \quad (\text{TO}), \quad (13.27f)$$

where TA indicates a transverse acoustic mode, TO indicates a transverse optical mode, LA indicates a longitudinal acoustic mode, and LO indicates a longitudinal optical mode. (The  $\mathbf{M}$  labels commonly used for the IRs are shown in parentheses.)

### Notes on the symmetry functions

The symmetry functions displayed in Eqs. (13.27a)–(13.27f) specify the amplitudes of displacements for carbon atoms labeled 1 and 2 in the central unit cell (shown in Fig. 13.1). The symmetry function can also be considered as a two-component vector,  $\mathbf{V}_i$ . For example, for the  $A_{1g}$  mode the displacements in the unit cell centered at  $\mathbf{R}(m, n)$  are

$$\mathbf{V}_k(A_{1g})_{mn} = \frac{1}{\sqrt{2}} \begin{bmatrix} \mathbf{e}_x \\ -\mathbf{e}_x e^{i\phi} \end{bmatrix} e^{i\mathbf{k}(\mathbf{M}) \cdot \mathbf{R}(m,n)}.$$

The total normalized  $A_{1g}$  normal mode is

$$\frac{1}{\sqrt{N}} \sum_{m,n} \mathbf{V}_k(A_{1g})_{mn},$$

where  $N$  is the total number of carbon atoms in the graphene sheet.

Had we considered the equivalent  $\mathbf{M}$  point,  $-\mathbf{k}(\mathbf{M})$ , the symmetry functions' phase factor  $e^{-i\phi}$  would instead be  $e^{i\phi}$ . Since  $\mathbf{k}(\mathbf{M})$  and  $-\mathbf{k}(\mathbf{M})$  are equivalent, the modes are degenerate. In fact, the Bloch waves for these two states are time-reversed partners since the time-reversal operator is the complex-conjugate operator. Therefore, one can take combinations of the two Bloch waves to form atomic displacements that are real. For example, the Bloch waves for  $\mathbf{k}(\mathbf{M})$  and  $-\mathbf{k}(\mathbf{M})$  are  $N^{-1/2} \zeta(\mathbf{k}) \exp(i\mathbf{k} \cdot \mathbf{R})$  and  $N^{-1/2} \zeta(-\mathbf{k}) \exp(-i\mathbf{k} \cdot \mathbf{R})$ , where  $\zeta(\mathbf{k})$  is the unit-cell eigenvector and  $\mathbf{R}$  is a vector from the origin to any of the hexagon centers. The sum of the two waves gives the stationary state (standing wave),

$$\begin{aligned} \zeta(\mathbf{k}) e^{i\mathbf{k} \cdot \mathbf{R}} + \zeta(-\mathbf{k}) e^{-i\mathbf{k} \cdot \mathbf{R}} &= \zeta(\mathbf{k}) e^{i\mathbf{k} \cdot \mathbf{R}} + \zeta(\mathbf{k})^* e^{-i\mathbf{k} \cdot \mathbf{R}} \\ &= 2 \Re\{\zeta(\mathbf{k})\} \cos(\mathbf{k} \cdot \mathbf{R}) - 2 \Im\{\zeta(\mathbf{k})\} \sin(\mathbf{k} \cdot \mathbf{R}), \end{aligned} \quad (13.28)$$

where  $\Re\{\zeta(\mathbf{k})\}$  and  $\Im\{\zeta(\mathbf{k})\}$  are the real and imaginary parts of  $\zeta(\mathbf{k})$ , respectively. The difference of the two waves gives the vector (not normalized),

$$-2 \Re\{\zeta(\mathbf{k})\} \sin(\mathbf{k} \cdot \mathbf{R}) + 2 \Im\{\zeta(\mathbf{k})\} \cos(\mathbf{k} \cdot \mathbf{R}). \quad (13.29)$$

For  $\mathbf{k} = \mathbf{k}(\mathbf{M})$  the phase factor  $\sin(\mathbf{k} \cdot \mathbf{R}) = 0$  for all  $\mathbf{R}$ , so the sum of the Bloch waves is proportional to  $\Re\{\zeta(\mathbf{k})\} \cos(\mathbf{k} \cdot \mathbf{R})$ . Consider a line of hexagon centers in the  $y$ -direction with one of the centers as the origin. The phase factor  $\mathbf{k}(\mathbf{M}) \cdot \mathbf{R} = 0$  for this line since  $R_x = 0$  and  $\mathbf{k}(\mathbf{M})$  is parallel to the  $x$ -axis. The adjacent centers on a line to the right, also oriented along the  $y$ -axis, will have  $R_x = +\sqrt{3}a/2$ ,

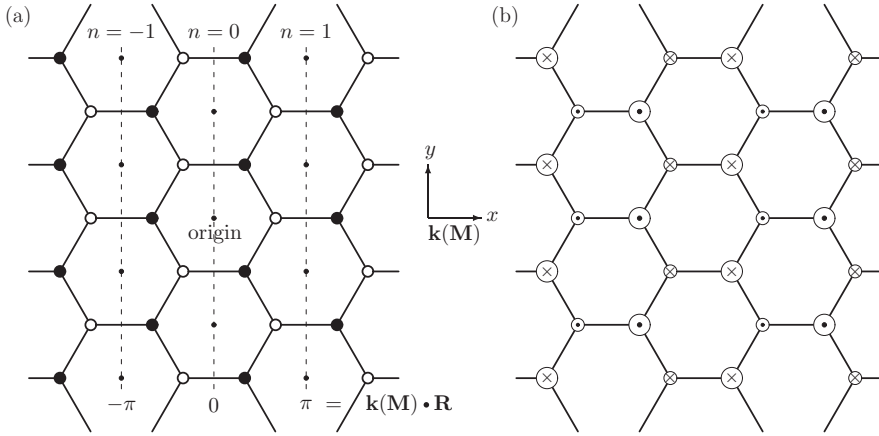


Figure 13.5 (a) Stacks of hexagons along the  $y$ -axis. The factor  $\mathbf{k}(\mathbf{M}) \cdot \mathbf{R}$  is constant for cells in a given stack, where  $\mathbf{R}$  is a lattice vector of the cell (vector from the origin to the center of a hexagon) and  $\mathbf{k}(\mathbf{M})$  is oriented along the  $x$ -axis. (b) Displacements for the  $B_{1u}$  stationary state constructed from the symmetry functions for  $\mathbf{k}(\mathbf{M})$  and  $-\mathbf{k}(\mathbf{M})$ . The large circles indicate a displacement twice as large as that for the small circles. The circles with the dot in the center represent positive displacement perpendicular to the plane of the paper and the circles with “ $\times$ ” in the center represent negative displacement perpendicular to the surface.

giving  $\mathbf{k}(\mathbf{M}) \cdot \mathbf{R} = \pi$ . The line to the left has  $\mathbf{k}(\mathbf{M}) \cdot \mathbf{R} = -\pi$ . In general, as indicated in Fig. 13.5(a),  $\mathbf{k}(\mathbf{M}) \cdot \mathbf{R} = n\pi$ , where  $n$  is the number of lines away from the line containing the origin.

Consider the  $B_{1u}$  mode with unit-cell symmetry function

$$\frac{1}{\sqrt{2}} (z_1 - z_2 e^{i\phi}) = \frac{1}{\sqrt{2}} \left[ z_1 - z_2 \cos\left(\frac{\pi}{3}\right) - i z_2 \sin\left(\frac{\pi}{3}\right) \right]. \quad (13.30)$$

The amplitudes of the displacements at the atomic sites for the sum of the Bloch waves from  $\mathbf{k}(\mathbf{M})$  and  $\mathbf{k}(-\mathbf{M})$  are proportional to

$$\left( z_1 - \frac{z_2}{2} \right) \cos[\mathbf{k}(\mathbf{M}) \cdot \mathbf{R}] = \left( z_1 - \frac{z_2}{2} \right) (-1)^n, \quad (13.31)$$

where  $n$  is the line number as illustrated in Fig. 13.5(a). The displacement pattern is shown in Fig. 13.5(b).

### 13.3.4 Lattice vibrations of graphene at $\mathbf{K}$

The group of the wavevector is  $D_{3h}$ . The operations can be selected from those in Table 13.2 that leave  $\mathbf{k}(\mathbf{K}_1) = (4\pi/(3a))\mathbf{e}_y$  unchanged or that convert it to an equivalent  $\mathbf{k}$ -vector. The equivalent  $\mathbf{k}$ -vectors are  $\mathbf{k}(\mathbf{K}_3) = (2\pi/(3a))(3\mathbf{e}_x - \mathbf{e}_y)$  and  $\mathbf{k}(\mathbf{K}_5) = (2\pi/(3a))(-3\mathbf{e}_x - \mathbf{e}_y)$ . They are shown in Fig. 13.6. The operations are

Table 13.8 The character table for  $D_{3h}$ . The upper labels for the operations are those from Table 13.2. The lower labels are the conventional operations used for the  $D_{3h}$  character table.

			$E$	$iC_2$	$2C_3$	$2iC_6$	$3C'_2$	$3iC''_2$
$D_{3h} = D_3 \times \sigma_h(\bar{6}m2)$			$E$	$\sigma_h$	$2C_3$	$2S_3$	$3C'_2$	$3\sigma_v$
$x^2 + y^2, z^2$	$R_z$	$A'_1$	1	1	1	1	1	1
		$A'_2$	1	1	1	1	-1	-1
		$A''_1$	1	-1	1	-1	1	-1
$(x^2 - y^2, xy)$	$z$	$A''_2$	1	-1	1	-1	-1	1
		$\mathcal{E}'$	2	2	-1	-1	0	0
$(xz, yz)$	$(R_x, R_y)$	$\mathcal{E}''$	2	-2	-1	1	0	0

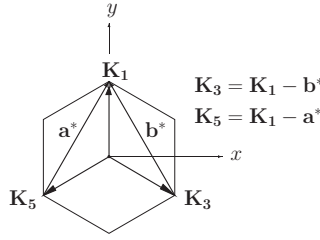


Figure 13.6 Equivalent  $\mathbf{K}$ -points in the Brillouin zone.  $\mathbf{K}_1$ ,  $\mathbf{K}_3$ , and  $\mathbf{K}_5$  are related by reciprocal-lattice vectors. The wavevector  $\mathbf{k} = \mathbf{K}_1$ .

$E$ ,  $C_3$ ,  $C_3^{-1}$ ,  $C_2^{(1)'}$ ,  $C_2^{(2)'}$ ,  $C_2^{(3)'}$  and the inversion operations  $iC_2$ ,  $iC_6$ ,  $iC_6^{-1}$ ,  $iC_2^{(1)''}$ ,  $iC_2^{(2)''}$ , and  $iC_2^{(3)''}$ . This collection of operations is isomorphic to  $D_{3h}$ . Typically,  $D_{3h}$  is presented in terms of other operators. The correspondence is shown at the top of the character table in Table 13.8. The action table for the group applied to graphene is shown in Tables 13.9 and 13.10.

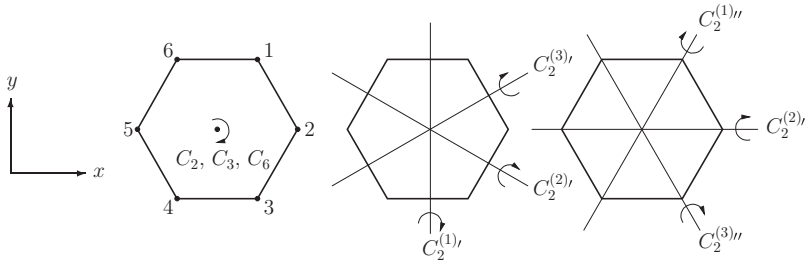
A representation of  $D_{3h}$ ,  $\Gamma(\mathbf{K}_1)$ , with bases  $x_1$ ,  $x_2$ ,  $y_1$ ,  $y_2$ ,  $z_1$ , and  $z_2$  has the following characters:  $\chi(E) = 6$ ,  $\chi(iC_2) = 2$ ,  $\chi(2C_3) = 0$ ,  $\chi(iC_6) = 2$ , and 0 for all other operators. For example, let us calculate the character for  $iC_6$ . Using Table 13.9 we have

$$\begin{aligned}
 P(iC_6)x_1 &\rightarrow \left(-\frac{1}{2}x_5 + \frac{\sqrt{3}}{2}y_5\right) \rightarrow \left(-\frac{1}{2}x_1 + \frac{\sqrt{3}}{2}y_1\right) e^{-2\pi i/3}, \\
 P(iC_6)y_1 &\rightarrow \left(-\frac{1}{2}y_5 - \frac{\sqrt{3}}{2}x_5\right) \rightarrow \left(-\frac{1}{2}x_1 - \frac{\sqrt{3}}{2}y_1\right) e^{-2\pi i/3}, \\
 P(iC_6)z_1 &\rightarrow -z_5 \rightarrow -z_1 e^{-2\pi i/3},
 \end{aligned}$$

Table 13.9 The action table for  $D_{3h}$ 

	$E$	$iC_2$	$C_3$	$C_3^{-1}$	$iC_6$	$iC_6^{-1}$	$C_2^{(1)''}$	$C_2^{(2)''}$	$C_2^{(3)''}$	$iC_2^{(1)''}$	$iC_2^{(2)''}$	$iC_2^{(3)''}$
$x$	$x$	$x$	$\xi_{--}$	$\xi_{-+}$	$\xi_{-+}$	$\xi_{--}$	$-x$	$\xi_{+-}$	$\xi_{++}$	$\xi_{+-}$	$-x$	$\xi_{++}$
$y$	$y$	$y$	$\zeta_{+-}$	$\zeta_{--}$	$\zeta_{--}$	$\zeta_{+-}$	$y$	$\zeta_{--}$	$\zeta_{+-}$	$\zeta_{--}$	$y$	$\zeta_{+-}$
$z$	$z$	$-z$	$z$	$z$	$-z$	$-z$	$-z$	$-z$	$-z$	$z$	$z$	$z$
1	1	1	3	5	5	3	6	4	2	4	6	2
2	2	2	4	6	6	4	5	3	1	3	5	1
3	3	3	5	1	1	5	4	2	6	2	4	6
4	4	4	6	2	2	6	3	1	5	1	3	5
5	5	5	1	3	3	1	2	6	4	6	2	4
6	6	6	2	4	4	2	1	5	3	5	1	3

$\xi_{ss'} \equiv s \frac{1}{2}x + s' \frac{\sqrt{3}}{2}y$  and  $\zeta_{ss'} \equiv s \frac{\sqrt{3}}{2}x + s' \frac{1}{2}y$  with  $s, s' = \pm$



$$P(iC_6)x_2 \rightarrow \left(-\frac{1}{2}x_6 + \frac{\sqrt{3}}{2}y_6\right) \rightarrow \left(-\frac{1}{2}x_2 + \frac{\sqrt{3}}{2}y_2\right) e^{2\pi i/3},$$

$$P(iC_6)y_2 \rightarrow \left(-\frac{1}{2}y_6 - \frac{\sqrt{3}}{2}x_6\right) \rightarrow \left(-\frac{1}{2}y_2 - \frac{\sqrt{3}}{2}x_2\right) e^{2\pi i/3},$$

$$P(iC_6)z_2 \rightarrow -z_6 \rightarrow -z_2 e^{2\pi i/3}.$$

The character for the operation is then  $-2(e^{-2\pi i/3} + e^{2\pi i/3}) = +2$ . The decomposition of  $\Gamma(\mathbf{K}_1)$  into the IRs of  $D_{3h}$  gives

$$\Gamma(\mathbf{K}_1) = A'_1 + A'_2 + \mathcal{E}' + \mathcal{E}''. \quad (13.32)$$

From the decomposition we see that no two modes belong to the same row of the same IR and therefore the symmetry functions will also be the normal modes (eigenvectors). The symmetry functions can be obtained by use of the symmetry-function-generating machine, taking care to include the phase factors for equivalent atoms.

The symmetry functions for the lattice vibrations at  $\mathbf{k}(\mathbf{K}_1)$  are

$$A'_1(\mathbf{K}_1^+) = \frac{1}{2}(x_1 - iy_1 - x_2 - iy_2), \quad (13.33a)$$

$$A'_2(\mathbf{K}_2^-) = \frac{1}{2}(x_1 - iy_1 + x_2 + iy_2), \quad (13.33b)$$



Table 13.10 *Phase angles and phase factors between carbon atoms for  $\mathbf{k}(\mathbf{K}_1)$* 

Translation $\mathbf{R}_j - \mathbf{R}_i$	Phase angle $\mathbf{k} \cdot (\mathbf{R}_j - \mathbf{R}_i)$	Phase factor $\exp[i\mathbf{k} \cdot (\mathbf{R}_j - \mathbf{R}_i)]$
$\mathbf{R}_2 - \mathbf{R}_1$	$-\theta$	$-\frac{1}{2} - (\sqrt{3}/2)i$
$\mathbf{R}_3 - \mathbf{R}_1$	$-2\theta$	$-\frac{1}{2} + (\sqrt{3}/2)i$
$\mathbf{R}_4 - \mathbf{R}_1$	$-2\theta$	$-\frac{1}{2} + (\sqrt{3}/2)i$
$\mathbf{R}_5 - \mathbf{R}_1$	$-\theta$	$-\frac{1}{2} - (\sqrt{3}/2)i$
$\mathbf{R}_6 - \mathbf{R}_1$	0	1
$\mathbf{R}_3 - \mathbf{R}_2$	$-\theta$	$-\frac{1}{2} - (\sqrt{3}/2)i$
$\mathbf{R}_4 - \mathbf{R}_2$	$-\theta$	$-\frac{1}{2} - (\sqrt{3}/2)i$
$\mathbf{R}_5 - \mathbf{R}_2$	0	1
$\mathbf{R}_6 - \mathbf{R}_2$	$\theta$	$-\frac{1}{2} + (\sqrt{3}/2)i$

$\theta = 2\pi/3$ ,  $\exp(\pm 3i\theta) = 1$ ,  $n - m$  phase angle is the negative of  $m - n$ .

$$\begin{aligned}\mathcal{E}'(\mathbf{K}_3^+) &= \frac{1}{2}(x_1 + iy_1 + x_2 - iy_2) & (\text{row 1}), \\ \mathcal{E}'(\mathbf{K}_3^+) &= \frac{1}{2}(x_1 + iy_1 - x_2 + iy_2) & (\text{row 2}),\end{aligned}\tag{13.33c}$$

$$\begin{aligned}\mathcal{E}''(\mathbf{K}_3^-) &= \frac{1}{\sqrt{2}}(z_1 + z_2) & (\text{row 1}), \\ \mathcal{E}''(\mathbf{K}_3^-) &= \frac{1}{\sqrt{2}}(z_1 - z_2) & (\text{row 2}).\end{aligned}\tag{13.33d}$$

The time-reversed state has  $\mathbf{k} = -\mathbf{K}_1$ , so the cell symmetry functions are the complex conjugates of those in (13.33a)–(13.33d). Symmetry functions with real amplitudes of displacement can be formed by taking combinations of the states with  $\mathbf{K}_1$  and  $-\mathbf{K}_1$ . For example, if we take the sum of the two Bloch waves for  $\mathcal{E}''(\mathbf{K}_3^-)$  we have

$$\mathcal{E}''(\mathbf{K}_3^-)(\text{row 1}) \propto (z_1 + z_2) \cos(\mathbf{K}_1 \cdot \mathbf{R}).\tag{13.34}$$

If we take the difference of the two Bloch waves we have for the  $A'_2(\mathbf{K}_2^-)$  stationary state, we obtain

$$A'_2(\mathbf{K}_2^-) \propto (x_1 + x_2) \sin(\mathbf{K}_1 \cdot \mathbf{R}) + (y_1 - y_2) \cos(\mathbf{K}_1 \cdot \mathbf{R}).\tag{13.35}$$

Sketches of the displacements are shown in Fig. 13.7.

Since  $\mathbf{K}_1$  is oriented along the  $y$ -axis, the hexagon centers parallel to the  $x$ -axis have constant phase. The line containing the origin has phase  $\mathbf{K}_1 \cdot \mathbf{R} = 0$ , the line

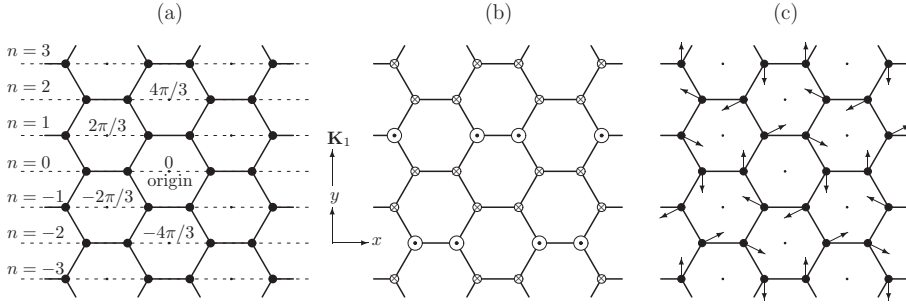


Figure 13.7 (a) The graphene lattice showing the constant-phase lines and locations of the carbon atoms. (b) The  $\mathcal{E}''$  (row 1) stationary state. The large circles indicate a displacement twice as large as that for the small circles. The circles with the dot in the center represent positive displacement perpendicular to the plane of the paper and the circles with “x” in the center represent negative displacement perpendicular to the surface of the paper. (c) The  $A_2'$  stationary state. The displacement vector makes a  $30^\circ$  angle with the adjacent side of the hexagon.

above has  $\mathbf{K}_1 \cdot \mathbf{R} = \theta = 2\pi/3$ , and for the line below  $\mathbf{K}_1 \cdot \mathbf{R} = -\theta = -2\pi/3$ . In general,  $\mathbf{K}_1 \cdot \mathbf{R} = n(2\pi/3)$ , where  $n$  labels the lines as shown in Fig. 13.7(a).

#### Matrix elements of the $\mathcal{E}''$ IR

The basis functions for the  $\mathcal{E}''$  IR are  $xz$  and  $yz$ . Using Table 13.2 together with Table 13.8, we find

$$\begin{aligned}
 E &= \begin{pmatrix} 1 & 0 \\ 0 & 1 \end{pmatrix}, & iC_2 &= \begin{pmatrix} 1 & 0 \\ 0 & -1 \end{pmatrix}, \\
 C_3 &= \begin{pmatrix} -\frac{1}{2} & -\sqrt{3}/2 \\ \sqrt{3}/2 & -\frac{1}{2} \end{pmatrix}, & C_3^{-1} &= \begin{pmatrix} -\frac{1}{2} & \sqrt{3}/2 \\ -\sqrt{3}/2 & -\frac{1}{2} \end{pmatrix}, \\
 iC_6 &= \begin{pmatrix} \frac{1}{2} & -\sqrt{3}/2 \\ \sqrt{3}/2 & \frac{1}{2} \end{pmatrix}, & C_6^{-1} &= \begin{pmatrix} \frac{1}{2} & \sqrt{3}/2 \\ -\sqrt{3}/2 & \frac{1}{2} \end{pmatrix}, \\
 C_2^{(1)'} &= \begin{pmatrix} 1 & 0 \\ 0 & -1 \end{pmatrix}, & C_2^{(2)'} &= \begin{pmatrix} -\frac{1}{2} & \sqrt{3}/2 \\ \sqrt{3}/2 & \frac{1}{2} \end{pmatrix}, \\
 C_2^{(3)'} &= \begin{pmatrix} -\frac{1}{2} & -\sqrt{3}/2 \\ -\sqrt{3}/2 & \frac{1}{2} \end{pmatrix}, & C_2^{(1)''} &= \begin{pmatrix} \frac{1}{2} & -\sqrt{3}/2 \\ -\sqrt{3}/2 & -\frac{1}{2} \end{pmatrix}, \\
 C_2^{(2)''} &= \begin{pmatrix} -1 & 0 \\ 0 & 1 \end{pmatrix}, & C_2^{(3)''} &= \begin{pmatrix} \frac{1}{2} & \sqrt{3}/2 \\ \sqrt{3}/2 & -\frac{1}{2} \end{pmatrix}.
 \end{aligned}$$

These matrices can be used to generate the  $\mathcal{E}''$  symmetry functions by means of the symmetry-function-generating machine,

$$f(\mathcal{E}'', \text{row } i) = \sum_R D_{ii}(P_R)^* P_R z_1.$$

The results are given in (13.33d).

In concluding this section we note that in the case of graphene all of the vibrational eigenvectors at high-symmetry points in the Brillouin zone are determined by symmetry alone.

### 13.3.5 Finite sheets of graphene

The analysis of the electronic states and lattice vibrations given above is for an infinite sheet of two-dimensional graphene. Under experimental conditions graphene samples are often quite small. Furthermore, the manner in which the sample is secured to the substrate becomes relevant. For example, if two edges of the sheet are pinned by a massive holder, the displacements of the edge atoms will be attenuated. To deal with this circumstance, boundary conditions may be imposed on the propagating-wave solutions obtained for the infinite sheet. For example, the wave and its time-reversed partner can be combined with certain amplitudes to satisfy appropriate boundary conditions. This procedure will lead to stationary states with a finite number of “allowed” wavevectors and hence discrete frequencies (or energies). Even for a “free”, finite sheet there are many different possible boundary conditions, depending on how the edges terminate. In addition, unsaturated bonds at the edges may form bonds with foreign atoms (hydrogen or oxygen, for example). On the other hand, if the sheet is larger than about 20 atoms on a side, the eigenvalues will be reasonably represented by the energies of the infinite sheet evaluated at the “allowed” (quantized) wavevectors.

### References

- [13.1] J. P. Hobson and W. A. Nierenberg, “The statistics of a two-dimensional, hexagonal net”, *Phys. Rev.* **89**, 662 (1953).
- [13.2] S. Pancharatnam “Generalized theory of interference, and its applications. Part I. Coherent pencils”, *Proc. Indian Acad. Sci.* **44**, 247–262 (1956).
- [13.3] M. V. Berry, “Quantal phase factors accompanying adiabatic changes”, *Proc. Roy. Soc. London A* **392**, 45–57 (1984).
- [13.4] J. W. McClure, “Diamagnetism of graphite”, *Phys. Rev.* **104**, 666–671 (1956).
- [13.5] C. W. J. Beenakker, “Colloquium: Andreev reflection and Klein tunneling in graphene”, *Rev. Mod. Phys.* **80**, 1337–1354 (2008).

### Exercises

- 13.1 Consider the Bloch wave with a Dirac wavevector,  $\exp(i\mathbf{K}_i \cdot \mathbf{r})$ , and show that the time-reversed state is of the form  $\exp(i\mathbf{K}_j \cdot \mathbf{r})$ , where  $\mathbf{K}_i$  and  $\mathbf{K}_j$  are inequivalent Dirac points.

- 13.2 Use Eq. (13.21) to show that the graphene effective Hamiltonian for  $\mathbf{k}$  near a Dirac point can be written as

$$\mathbb{H} = \hbar v_F \boldsymbol{\sigma} \cdot \mathbf{k}$$

where  $\boldsymbol{\sigma}$  is the Pauli spin operator,  $\mathbf{k} = k_x \mathbf{e}_x + k_y \mathbf{e}_y$  is the two-dimensional wavevector near a Dirac point, and  $v_F$  is the group velocity at the Fermi level (i.e., at  $\Omega = 0$ ). The operator  $\boldsymbol{\sigma}$  appearing in the Hamiltonian above is called the pseudo-spin.

- 13.3 (a) Find an expression for the energy of the graphene energy bands including the overlap integral,  $S_\pi$ , between nearest-neighbor  $p_z$  orbitals. Assume  $S_\pi > 0$  and  $(pp\pi) < 0$ .  
 (b) Find the energy for  $\mathbf{k}$  near a Dirac point.  
 (c) Plot a graph of  $(E - \epsilon_p)$  versus  $ka$  along the lines  $\Gamma \rightarrow \text{M} \rightarrow \text{K}$  in the Brillouin zone. Use  $S_\pi = 0.13$ ,  $(pp\pi) = -3 \text{ eV}$ , and  $\epsilon_p = 0$ .
- 13.4 For Exercise 13.3, show that the radial effective mass,  $m_r^*$ , and the group velocity near a Dirac point do not depend on the overlap integral.  $r = (\delta k_x^2 + \delta k_y^2)^{1/2}$  and  $\hbar^2/m_r^* = \partial^2 E / \partial r^2 + (\partial E / \partial r) / r$ .
- 13.5 Consider the Z-modes (out-of-plane lattice vibrations) of graphene. Assume the restoring force is of the form  $f_{ij} = -f(\delta z_i - \delta z_j)$ , where  $\delta z_i$  is the displacement of the  $i$ th carbon atom in the  $z$ -direction from its equilibrium position.  
 (a) Considering only nearest-neighbor interactions show that the lattice vibration eigenvalue equation is

$$\det \begin{vmatrix} 3f - m\omega^2(\mathbf{k}) & -fL(\mathbf{k}) \\ fL(\mathbf{k})^* & 3f - m\omega^2(\mathbf{k}) \end{vmatrix} = 0,$$

where  $L(\mathbf{k}) = [\exp(i\mathbf{K}_i \cdot \mathbf{R}_a) + \exp(i\mathbf{K}_i \cdot \mathbf{R}_b) + \exp(i\mathbf{K}_i \cdot \mathbf{R}_c)]$  and  $\mathbf{R}_a$ ,  $\mathbf{R}_b$ , and  $\mathbf{R}_c$  are the nearest-neighbor vectors.

- (b) Find dispersion formulas for the two branches and the eigenvectors for the modes. Identify the acoustic and optical branches and any degeneracies. Give the symmetry labels of the branches at  $\Gamma$ .  
 (c) Plot a graph of  $m\omega^2(\mathbf{k})/f$  versus the wavevector,  $\mathbf{k}$ , for the path  $\Gamma \rightarrow \text{M} \rightarrow \text{K} \rightarrow \Gamma$ .
- 13.6 (a) For Exercise 13.5 find the lattice vibration eigenvectors for  $\mathbf{k}$  along the  $\Lambda$  symmetry line.  
 (b) Give the frequencies in terms of the dynamic matrix.
- 13.7 For Exercise 13.5 sketch the relative displacements for the row-2  $\mathcal{E}'$  lattice vibration mode at  $\mathbf{K}_1$  using the sum of the lattice wave and its time-reversed state.

# 14

## Carbon nanotubes

The structure of a “single-walled” carbon nanotube (SWCNT) can be formed by rolling up a graphene sheet into a seamless tube as shown in Fig. 14.1. Multi-walled carbon nanotubes consist of two or more concentric SWCNTs or scroll-wrapped graphene sheets. Typical SWCNTs have diameters around 2 nm, but the range is from 0.7 to 50 nm. Some tubes are open at the ends and some are capped with a bucky hemisphere.

Nanostructures are produced by many different methods, including arc discharge, chemical vapor deposition, laser ablation, and flame burning of carbon-containing gases and solids. Some of these methods are becoming commercially practical for producing large quantities of carbon nanotubes.

Carbon nanotubes are of great scientific and technological interest because of their unique properties [14.1]. The  $sp^2$  carbon–carbon bond is stronger than the  $sp^3$  carbon–carbon bond of diamond. The tensile strength of an SWCNT is 10 to 100 times stronger than that of steel. Perhaps the most important potential application is in electronics, since SWCNTs can be grown as metallic threads that can carry an electrical current density that is 1,000 times greater than that of copper. The energy gaps between the valence and conduction bands in SWCNTs range from 0 to 2 eV. Semiconducting nanotubes have been fabricated as transistors that operate at room temperature and are capable of digital switching using just a single electron. Light-emitting diodes and photodetectors using single SWCNTs have been demonstrated under laboratory conditions. Multi-walled carbon nanotubes with connected inner tubes are superconducting, with  $T_c$  as high as 12 K. Carbon nanotubes have high thermal conductivity, about a factor of 10 greater than that of copper, along the tube axis, but have low thermal conductivity across the diameter. They are stable up to 3,800 °C.

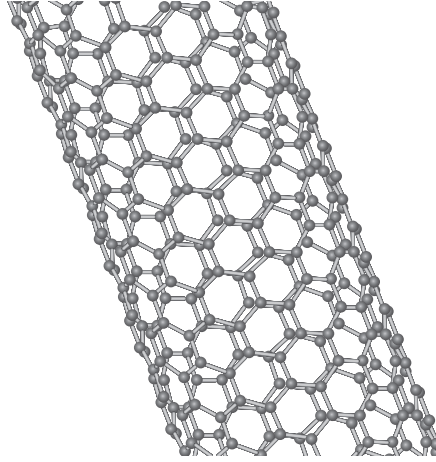


Figure 14.1 A single-walled carbon nanotube.

### 14.1 A description of carbon nanotubes

There are many different ways in which a graphene sheet can be rolled into a nanotube. The various nanotubes so produced have different properties. Therefore it is important to develop a systematic method for characterizing any nanotube structure in a relatively simple manner [14.2].

Figure 14.2 illustrates a portion of a long, unrolled nanotube superimposed on a graphene lattice. When the area is rolled up to form a tube the “chiral” vector  $\mathbf{C}_h$  lies on the tube circumference and  $\tau$  is parallel to the tube axis. The angle labeled  $\varphi$  is the chiral angle. This is the angle between  $\mathbf{C}_h$  and  $\mathbf{a}_1$ . At the top of the diagram the two inequivalent carbons in the unit cell, 1 and 2, are shown, together with the primitive-lattice vectors,  $\mathbf{a}$  and  $\mathbf{b}$ . The chiral vector initiates and terminates on lattice centers, and therefore can be expressed as a lattice vector. Following convention, we use primitive vectors  $\mathbf{a}_1 = \mathbf{a}$  and  $\mathbf{a}_2 = -\mathbf{b}$ . Then we have

$$\mathbf{C}_h = n\mathbf{a}_1 + m\mathbf{a}_2 \equiv (n, m), \quad (14.1)$$

where  $n$  and  $m$  are integers. The vector  $\tau$  is perpendicular to  $\mathbf{C}_h$ . It can be expressed as

$$\tau = r\mathbf{a}_1 + s\mathbf{a}_2 \equiv (r, s). \quad (14.2)$$

If  $d_t$  is the diameter of a single wall nanotube, then we have

$$\pi d_t = |\mathbf{C}_h| = a\sqrt{n^2 + nm + m^2}, \quad (14.3)$$

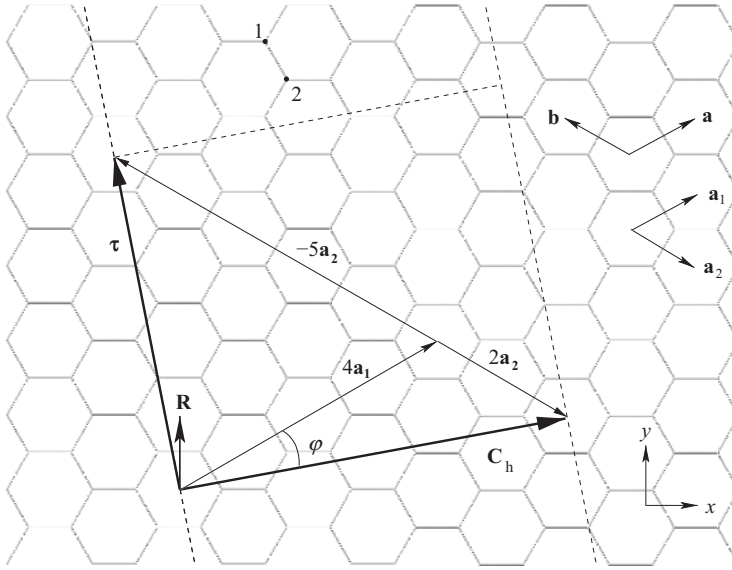


Figure 14.2 A sketch of a portion of an unrolled (4, 2) carbon nanotube in the  $x$ - $y$  plane. The full nanotube is enclosed by  $\tau$ ,  $\mathbf{C}_h$ , and the dashed lines. The nanotube is superimposed on a planar graphene array. The chiral angle is the angle between  $\mathbf{C}_h$  and  $\mathbf{a} = \mathbf{a}_1$ . When the area (cell) is rolled up to form a tube the “chiral” vector  $\mathbf{C}_h$  lies on the tube circumference and  $\tau$  is parallel to the tube axis.  $\tau$  is the primitive translation vector for the cell. The angle labeled  $\varphi$  is the chiral angle. At the top of the diagram two inequivalent carbons, 1 and 2, are shown, together with the primitive-lattice vectors for graphene,  $\mathbf{a}_1 = \mathbf{a}$  and  $\mathbf{a}_2 = -\mathbf{b}$ . Near the bottom  $\mathbf{R}$  is the graphene lattice vector with the smallest (non-zero) projection onto  $\mathbf{C}_h$ .

where  $a$  is the lattice spacing ( $|\mathbf{a}_1| = |\mathbf{a}_2| = a$ ). The tangent of the angle the chiral vector,  $\mathbf{C}_h$ , makes with the  $x$ -axis is

$$\tan \theta_x = \frac{n - m}{\sqrt{3}(n + m)}. \quad (14.4)$$

For the chiral angle,  $\varphi$ ,

$$\tan \varphi = \tan(30^\circ - \theta_x) = \frac{\sqrt{3}m}{2n + m}. \quad (14.5)$$

The SWCNTs having  $n = m$  ( $\varphi = 30^\circ$ ) are called “armchair” nanotubes, whereas those with  $m = 0$  ( $\varphi = 0$ ) are referred to as “zigzag” nanotubes. The names refer to the bond patterns seen on circling the circumference of the tube as illustrated in Fig. 14.3. These two structures are achiral because these nanotubes possess mirror symmetry elements. All other  $(n, m)$  nanotubes have chirality. Because of the symmetry, we need only consider  $0 \leq m \leq n$  to describe all chiral nanotubes.

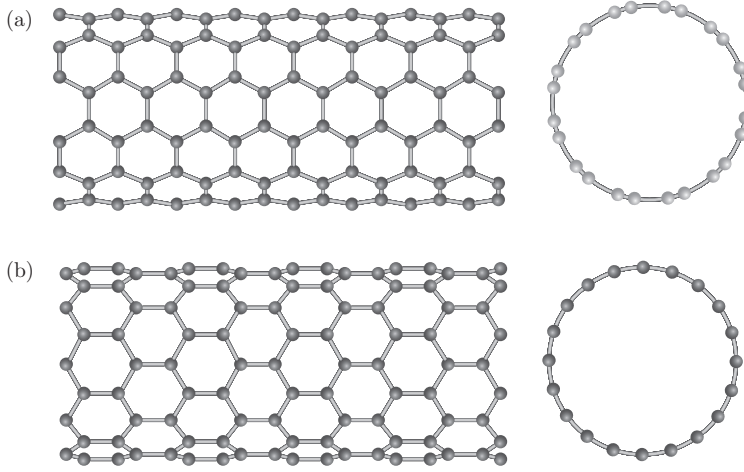


Figure 14.3 Single-walled carbon nanotubes. (a) A single-walled carbon nanotube with the armchair structure. The chiral angle is  $30^\circ$ . (b) A single-walled carbon nanotube with the zigzag structure. The chiral angle is zero.

The indices  $m$  and  $n$  determine the properties of a nanotube. As will be shown later, if  $n - m = 3p$ , where  $p$  is an integer, then the SWCNT is metallic. If  $n - m = 3p \pm 1$ , the nanotube is semiconducting.

## 14.2 Group theory of nanotubes

A single-walled carbon nanotube can be described group-theoretically as a one-dimensional system. In essence we treat the area in Fig. 14.2 determined by  $\mathbf{C}_h$  and  $\tau$  as the unit cell. The vector  $\tau$  is the primitive-lattice vector for the one-dimensional unit cell. Given the chiral vector,  $(n, m)$ , we can determine  $\tau$ . We have  $\mathbf{C}_h = (n + m)(\sqrt{3}a/2)\mathbf{e}_x + (n - m)(a/2)\mathbf{e}_y$ . A vector perpendicular to  $\mathbf{C}_h$  extending in the positive  $y$ -direction is

$$\begin{aligned} \mathbf{V} &= -(n - m)a\mathbf{e}_x + (n + m)(\sqrt{3}a)\mathbf{e}_y \\ &\propto (2n + m)\mathbf{a}_1 - (2m + n)\mathbf{a}_2. \end{aligned} \quad (14.6)$$

The vector  $\tau$  must be parallel to  $\mathbf{V}$ , and  $|\tau|$  must be equal to the smallest distance between lattice points along the axis defined by  $\mathbf{V}$ . With these requirements, we may write

$$\tau = \frac{(2m + n)\mathbf{a}_1 - (2n + m)\mathbf{a}_2}{D(n, m)}, \quad (14.7)$$

with

$$D(n, m) = \text{gcd of } (2n + m) \text{ and } (2m + n), \quad (14.8)$$

where “gcd” stands for “greatest common denominator”.



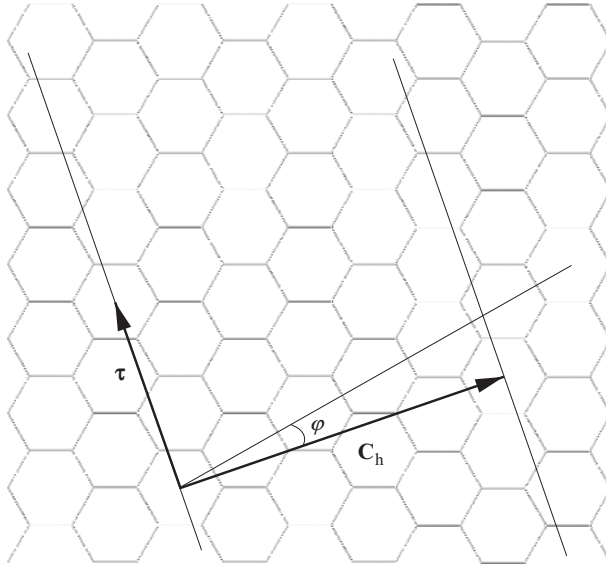


Figure 14.4  $\mathbf{C}_h = (4, 1)$ ,  $D(4, 1) = 3$ , and  $\boldsymbol{\tau} = (2, -3)$ .

In Fig. 14.2,  $\mathbf{C}_h = (4, 2)$ ,  $d = 2$ , and  $D(4, 2) = 2$ , so we have that  $\boldsymbol{\tau} = [(4 + 4)\mathbf{a}_1 - (8 + 2)\mathbf{a}_2]/2 = (4, -5)$ . This result may be verified visually on Fig. 14.2 (recall that  $\mathbf{a}_1 = \mathbf{a}$  and  $\mathbf{a}_2 = -\mathbf{b}$ ). Figure 14.4 shows another example with  $\mathbf{C}_h = (4, 1)$ . In this case  $d = 1$ ,  $n - m = 3$ , so  $D(4, 1) = 3$  and we have that  $\boldsymbol{\tau} = (2, -3)$ .

Some useful results for nanotubes are the following ( $a$  is the lattice spacing, and  $a/\sqrt{3}$  is the C–C distance):

$$\mathbf{a}_1 = \frac{a}{2}(\sqrt{3}\mathbf{e}_x + \mathbf{e}_y) = \frac{a^2}{4\pi}(2\mathbf{b}_1 + \mathbf{b}_2),$$

$$\mathbf{a}_2 = \frac{a}{2}(\sqrt{3}\mathbf{e}_x - \mathbf{e}_y) = \frac{a^2}{4\pi}(\mathbf{b}_1 + 2\mathbf{b}_2),$$

$$\mathbf{b}_1 = \frac{2\pi}{a}\left(\frac{1}{\sqrt{3}}\mathbf{e}_x + \mathbf{e}_y\right) = \frac{4\pi}{3a^2}(2\mathbf{a}_1 - \mathbf{a}_2),$$

$$\mathbf{b}_2 = \frac{2\pi}{a}\left(\frac{1}{\sqrt{3}}\mathbf{e}_x - \mathbf{e}_y\right) = \frac{4\pi}{3a^2}(-\mathbf{a}_1 + 2\mathbf{a}_2),$$

$$\mathbf{e}_x = \frac{\mathbf{a}_1 + \mathbf{a}_2}{\sqrt{3}a} = \frac{\sqrt{3}a}{4\pi}(\mathbf{b}_1 + \mathbf{b}_2),$$

$$\mathbf{e}_y = \frac{\mathbf{a}_1 - \mathbf{a}_2}{a} = \frac{a}{4\pi}(\mathbf{b}_1 - \mathbf{b}_2),$$

$$\mathbf{a}_1 \cdot \mathbf{a}_1 = \mathbf{a}_2 \cdot \mathbf{a}_2 = a^2,$$

$$\mathbf{b}_1 \cdot \mathbf{b}_1 = \mathbf{b}_2 \cdot \mathbf{b}_2 = \frac{16\pi^2}{3a^2},$$

$$\mathbf{a}_1 \cdot \mathbf{a}_2 = \frac{a^2}{2},$$

$$\mathbf{b}_1 \cdot \mathbf{b}_2 = -\frac{b^2}{2},$$

$$N_h = \frac{2(n^2 + m^2 + nm)}{D(n, m)},$$

$$\mathbf{C}_h = n\mathbf{a}_1 + m\mathbf{a}_2 = (n, m),$$

$$|\mathbf{C}_h| = a\sqrt{n^2 + m^2 + nm} = a\sqrt{\frac{N_h D(n, m)}{2}},$$

$$\boldsymbol{\tau} = r\mathbf{a}_1 + s\mathbf{a}_2 = (r, s) = \frac{a^2}{4\pi}[(2r + s)\mathbf{b}_1 + (2s + r)\mathbf{b}_2],$$

$$r = \frac{2m + n}{D(n, m)},$$

$$s = -\frac{2n + m}{D(n, m)},$$

$$|\boldsymbol{\tau}| = \frac{\sqrt{3}|\mathbf{C}_h|}{D(n, m)} = \frac{\sqrt{3}a\sqrt{n^2 + m^2 + nm}}{D(n, m)} = \sqrt{\frac{3a^2 N_h}{2D(n, m)}},$$

$$\kappa_1 = \frac{2\pi}{|\mathbf{C}_h|^2} \mathbf{C}_h = \frac{4\pi}{a^2 N_h D(n, m)} (n\mathbf{a}_1 + m\mathbf{a}_2)$$

$$= \frac{1}{N_h} (-s\mathbf{b}_1 + r\mathbf{b}_2),$$

$$|\kappa_1|^2 = \frac{8\pi^2}{a^2 N_h D(n, m)},$$

$$\kappa_2 = \frac{2\pi}{|\boldsymbol{\tau}|^2} \boldsymbol{\tau} = \frac{4\pi D(n, m)}{3a^2 N_h} (r\mathbf{a}_1 + s\mathbf{a}_2)$$

$$= \frac{1}{N_h} (-m\mathbf{b}_1 + n\mathbf{b}_2),$$

$$|\kappa_2|^2 = \frac{8\pi^2}{3a^2 N_h},$$

$$\mathbf{R} = c\mathbf{a}_1 + d\mathbf{a}_2 = (c, d), rc - sd = 1, 0 < mc - nd \leq N_h,$$

where the greatest common denominator of  $(c, d)$  must be 1, and  $N_h$  is the number of hexagons.

The Dirac points are given by

$$\begin{aligned}\mathbf{K}_1 &= \frac{4\pi}{3a} \mathbf{e}_y = \frac{4\pi}{3a^2} (\mathbf{a}_1 - \mathbf{a}_2) = \frac{1}{3} (\mathbf{b}_1 - \mathbf{b}_2), \\ \mathbf{K}_2 &= \frac{2\pi}{3a} (\sqrt{3} \mathbf{e}_x + \mathbf{e}_y) = \frac{4\pi}{3a^2} \mathbf{a}_1 = \frac{1}{3} (2\mathbf{b}_1 + \mathbf{b}_2).\end{aligned}$$

The number of atoms in an SWCNT can be calculated in terms of  $n$  and  $m$ . The unit cell for the SWCNT is the rectangle whose sides are  $\mathbf{C}_h$  and  $\tau$ . The area of the cell is

$$|\mathbf{C}_h| |\tau| = \frac{\sqrt{3} |\mathbf{C}_h|^2}{D(n, m)} = \frac{\sqrt{3} a^2 (n^2 + nm + m^2)}{D(n, m)}. \quad (14.9)$$

The area of one of the hexagons is  $\sqrt{3}a^2/2$ , and the number of carbon atoms is twice the number of hexagons, so the number of atoms in the SWCNT is

$$N(n, m) = 2N_h = \frac{4(n^2 + nm + m^2)}{D(n, m)}. \quad (14.10)$$

For Fig. 14.2, with  $\mathbf{C}_h = (4, 2)$ , and Fig. 14.4, with  $\mathbf{C}_h = (4, 1)$ , the unit cells defined by  $\mathbf{C}_h$  and  $\tau$  contain  $4(16 + 4 + 8)/2 = 56$  and  $4(16 + 4 + 1)/3 = 28$  carbon atoms, respectively.

If we regard the nanotube as a one-dimensional system then the primitive-lattice vector is  $\tau$ . Any translation by an integral multiple of  $\tau$  is a translation symmetry operation if the tube is of infinite length. For a tube of finite length we may impose periodic boundary conditions.

When rolled up into a tube, translations along the chiral vector,  $\mathbf{C}_h$ , become rotations about the tube axis. In the unrolled state we can define reciprocal-lattice vectors  $\kappa_1$  and  $\kappa_2$  analogous to those of graphene by the requirements that  $\kappa_1 \cdot \mathbf{C}_h = 2\pi$ ,  $\kappa_2 \cdot \tau = 2\pi$ ,  $\kappa_1 \cdot \tau = 0$ , and  $\kappa_2 \cdot \mathbf{C}_h = 0$ . Since  $\mathbf{C}_h$  and  $\tau$  are perpendicular,  $\kappa_1$  is parallel to  $\mathbf{C}_h$  and  $\kappa_2$  is parallel to  $\tau$ . A wave propagating along  $\kappa_1$  must return to its original phase and amplitude after having made one or multiple trips around the tube circumference; therefore, an allowed wavevector will satisfy  $\mathbf{k}_1 \cdot \mathbf{C}_h = 2\pi\eta$ , where  $\eta$  is an integer.

We can write

$$\kappa_1 = \frac{2\pi \mathbf{C}_h}{|\mathbf{C}_h|^2} = \frac{2\pi}{|\mathbf{C}_h|} \mathbf{e}_1, \quad (14.11)$$

where  $\mathbf{e}_1$  is a unit vector parallel to  $\mathbf{C}_h$ . For  $\kappa_2$  we find

$$\kappa_2 = \frac{2\pi \tau}{|\tau|^2} = \frac{2\pi}{|\tau|} \mathbf{e}_2, \quad (14.12)$$

where  $\mathbf{e}_2$  is a unit vector parallel to  $\tau$ .

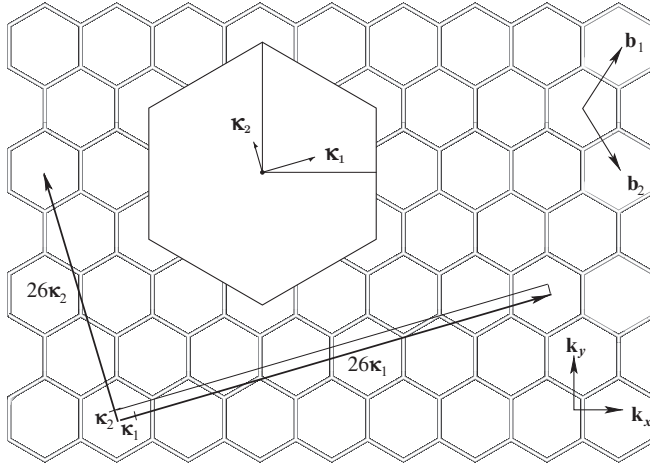


Figure 14.5 An unrolled (3,1) nanotube with  $\kappa_1 = (7\mathbf{b}_1 + 5\mathbf{b}_2)/26$  and  $\kappa_2 = (\mathbf{b}_1 - 3\mathbf{b}_2)/26$ . The Brillouin zone of the nanotube is the segment  $\kappa_2$ . For the rolled-up nanotube,  $\kappa_1$  becomes an angular quantum number.  $(4\pi/a^2)|\mathbf{C}_h|/|\kappa_1| = N_h = 26$  for the example shown. The inset shows the vectors in the first Brillouin zone of the graphene sheet.

It is useful to express the reciprocal-lattice vectors for the SWCNT in terms of the reciprocal-lattice vectors for the graphene sheet. To be consistent with the literature, we use the graphene reciprocal-lattice vectors  $\mathbf{b}_1$  and  $\mathbf{b}_2$ , where  $\mathbf{b}_1 = \mathbf{a}^* = (2\pi/a)(\mathbf{e}_x/\sqrt{3} + \mathbf{e}_y)$  and  $\mathbf{b}_2 = -\mathbf{b}^* = (2\pi/a)(\mathbf{e}_x/\sqrt{3} - \mathbf{e}_y)$ . The result is that

$$\kappa_1 = \frac{1}{N_h}(m\mathbf{b}_1 - n\mathbf{b}_2), \quad (14.13)$$

$$\kappa_2 = \frac{1}{N_h}(-s\mathbf{b}_1 + r\mathbf{b}_2), \quad (14.14)$$

where  $r$  and  $s$  are the coefficients of  $\tau = (r, s)$ , and  $n$  and  $m$  are the coefficients of  $\mathbf{C}_h = (n, m)$ . Figure 14.5 shows schematically the reciprocal-lattice vectors for  $\mathbf{C}_h = (3, 1)$  on the reciprocal lattice for graphene.

In developing a more complete group theory of the nanotube we need to consider all of the possible symmetry operations. For an infinitely long tube, translation by any graphene lattice vector is a symmetry operation that corresponds to a translation-and-rotation operation. Such an operation can be written in the space-group notation as  $\{R(\theta)|t\}$ . We wish to express  $\{R(\theta)|t\}$  in terms of  $\mathbf{C}_h$  and  $\tau$ . We can solve for the primitive-lattice vectors,  $\mathbf{a}_1$  and  $\mathbf{a}_2$ , in terms of  $\mathbf{C}_h$  and  $\tau$ . This gives

$$\mathbf{a}_1 = \frac{1}{N_h} \left[ \beta \mathbf{C}_h + m D(n, m) \tau \right], \quad (14.15)$$

$$\mathbf{a}_2 = \frac{1}{N_h} \left[ \alpha \mathbf{C}_h - n D(n, m) \tau \right], \quad (14.16)$$

where  $N_h = 2(n^2 + m^2 + mn)/D(n, m)$ ,  $\alpha = 2m + n$ , and  $\beta = 2n + m$ .

Let  $\mathbf{t}$  be a lattice vector for the unrolled tube,  $\mathbf{t}(c, d) = c\mathbf{a}_1 + d\mathbf{a}_2$ . Then, in terms of  $\mathbf{C}_h$  and  $\tau$ ,

$$\mathbf{t}(c, d) = \frac{c\beta + d\alpha}{N_h} \mathbf{C}_h + \frac{mc - nd}{N_h} \tau \equiv \frac{u}{N_h} \mathbf{C}_h + \frac{v}{N_h} \tau, \quad (14.17)$$

where  $u = (c\beta + d\alpha)/D(n, m)$  and  $v = mc - nd$ .

In the rolled-up tube configuration,  $(v/N_h)\tau$  represents a translation along the tube axis, and  $(u/N_h)\mathbf{C}_h$  represents a rotation about the tube axis. Clearly, if  $u/N_h = 1$  the rotation is one trip around the diameter or a rotation of  $2\pi$ . Therefore  $u/N_h$  is a measure of the rotation angle in units of  $2\pi$ . In space-group notation, we define a rotation by the notation  $C_N^u$ ,

$$C_N^u = 2\pi \frac{u}{N_h}. \quad (14.18)$$

In space-group notation,  $\mathbf{t}(c, d)$  is a screw operation,

$$\mathbf{t}(c, d) \rightarrow \left\{ C_N^u \left| \frac{v}{N_h} \tau \right. \right\}. \quad (14.19)$$

Given  $\mathbf{C}_h = (n, m)$ , the smallest angle of rotation for a symmetry operation corresponds to the values of  $c$  and  $d$  that result in a vector  $\mathbf{R} = c\mathbf{a}_1 + d\mathbf{a}_2$  that has the smallest projection onto  $\mathbf{C}_h$ . For the example in Fig. 14.2,  $\mathbf{R} = a\mathbf{e}_y$ . Since  $a\mathbf{e}_y = \mathbf{a}_1 - \mathbf{a}_2$ , it follows that the smallest projection onto  $\mathbf{C}_h$  occurs for  $c = 1$  and  $d = -1$ . With  $(n, m) = (4, 2)$  in Fig. 14.2, we find that the projection of  $\mathbf{R}$  onto  $\mathbf{C}_h$ ,  $C(\mathbf{R})$ , is given by

$$C(\mathbf{R}) = \frac{\mathbf{R} \cdot \mathbf{C}_h}{|\mathbf{C}_h|} = \frac{a}{\sqrt{28}}. \quad (14.20)$$

If we divide this result by  $|\mathbf{C}_h|$ , we obtain  $C(\mathbf{R})/|\mathbf{C}_h| = 1/28$ , meaning that the rotation about the tube axis is  $2\pi/28$ . We can also calculate this rotation angle using  $2\pi(u/N_h)$ . For the example we are considering,  $n = 4$ ,  $m = 2$ ,  $c = 1$ ,  $d = -1$ , and  $D(4, 2) = 2$ , we have

$$u = \frac{c\beta + d\alpha}{D(n, m)} = 1, \quad (14.21)$$

$$N_h = 28, \quad (14.22)$$

$$\frac{u}{N_h} 2\pi = \frac{2\pi}{28}. \quad (14.23)$$

In general, the minimum  $C(\mathbf{R})$  is such that the corresponding rotation is  $2\pi/N_h$ . This requires that  $\mathbf{R} = c\mathbf{a}_1 + d\mathbf{a}_2$  satisfies the equation

$$c(2n + m) + d(2m + n) = D(n, m). \quad (14.24)$$

For example, for  $\mathbf{C}_h = (4, 2)$ , we have  $10c + 8d = 2$ , which is satisfied by  $c = 1$  and  $d = -1$ . For  $\mathbf{C}_h = (8, 3)$  we have  $19c + 14d = 1$ , which is satisfied by  $c = 3$  and  $d = -4$ .

Since  $\{C_{N_h}^u|(v/N_h)\tau\}$  is a symmetry operation, it leaves the (infinitely long) nanotube unchanged. Therefore,  $\{C_N^u|(v/N_h)\tau\}^q$  (with  $q$  an integer) is also a symmetry operation.  $N_h$  such screw operations correspond to a rotation of  $2\pi$ , so  $\{C_N^u|(v/N_h)\tau\}^{N_h} = \{E|v\tau\}$ , where  $E$  is the identity operation.

In addition to these screw operations, for achiral tubes ( $m = 0$  or  $m = n$ ), rotations about axes perpendicular to the tube axis are also symmetry operations

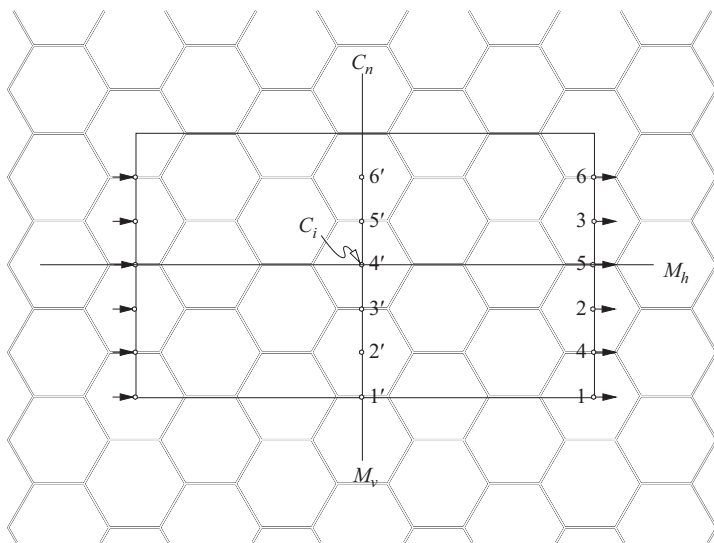


Figure 14.6 An achiral (3,3) nanotube unfolded. The center of inversion of the unit cell is indicated by  $C_i$ . The axis of the rolled tube is a  $C_n$  axis of symmetry. A vertical plane containing the  $C_n$ – $M_v$  line is a mirror plane. A horizontal plane containing the  $C_i$ – $M_h$  line is another mirror plane. When rolled up the arrows labeled 1 through 6 match up with the arrows on the opposite side of the unrolled tube. The axes through the tube connecting the primed and unprimed numbers are two-fold rotation axes perpendicular to the tube axis. Since  $n$  is 3, there are three axes passing through the centers of hexagons (1, 3, and 5) and three axes bisecting C–C bonds (2, 4, and 6).

(Fig. 14.6). If  $\mathbf{C}_h = (n, 0)$  or  $(n, n)$ , there are  $n$  axes through the center of a hexagon and carbon atoms on either side of the tube and  $n$  axes bisecting a C–C bond on either side of the tube. In the case of the achiral tubes, inversion is also a symmetry operation. The point group for the nanotube is obtained from the space group by setting the translation part of each operation to zero. Therefore, the point group of the achiral nanotubes is  $D_n \times i$ .

For an achiral tube the nature of the group depends on whether  $n$  is even or odd. For  $n$  even,  $D_n \times i = D_{nh}$ , whereas when  $n$  is odd  $D_n \times i = D_{nd}$ . Some character tables for the space groups and point groups are given in Appendix C. A more complete discussion of the space groups of nanotubes can be found in references [14.2] and [14.4].

### 14.3 One-dimensional nanotube energy bands

The one-dimensional energy bands for a nanotube can be deduced from those of graphene. For an infinitely long, single-walled nanotube the wavevector  $\mathbf{k}_2$  in the direction of  $\kappa_2$  is a continuous wavevector. The vector  $\mathbf{k}_1$  along the  $\kappa_1$  direction is quantized, taking on the values  $|\mathbf{k}_1| = \eta|\kappa_1|$ , where  $\eta = 1, 2, \dots, N_h$ . If we express the graphene energy bands  $\Omega^\pm(k_x, k_y)$  as  $\Omega^\pm(\mathbf{k}_1, \mathbf{k}_2)$  and impose the discrete values of  $|\mathbf{k}_1|$ , we obtain a series of one-dimensional energy bands, one ( $\pm$ ) pair for each value of  $\eta$  or a total of  $2N_h$  bands. That is, there is one energy band for each carbon atom in the nanotube unit cell. The process is illustrated in Fig. 14.7, which shows the graphene energy surface intersected by a plane passing through one of the quantized  $\mathbf{k}_1$  values and parallel to the  $\mathbf{k}_2$  vector. The intersection of the plane with the graphene energy surface produces a pair of one-dimensional energy bands.

The slices through the energy surface are along the lines  $\mathbf{k}_1(\eta) + \mathbf{k}_2$ , where

$$\mathbf{k}_1(\eta) = \eta \kappa_1 = k_1 \mathbf{e}_1 \quad (\eta = 1, 2, \dots, N_h) \quad (14.25)$$

and

$$\mathbf{k}_2 \equiv k_2 \frac{\tau}{|\tau|} = k_2 \mathbf{e}_2 \quad (-\kappa_2/2 \leq k_2 \leq \kappa_2/2), \quad (14.26)$$

where  $\mathbf{e}_1$  and  $\mathbf{e}_2$  are unit vectors in the  $\kappa_1$  and  $\kappa_2$  directions, respectively.

The energy bands for graphene (13.10) are given by

$$\Omega_{\mathbf{k}}^\pm = \pm |H_{AB}|/(pp\pi) = \pm \sqrt{e^{i\mathbf{k} \cdot \mathbf{R}_1} + e^{i\mathbf{k} \cdot \mathbf{R}_2} + e^{i\mathbf{k} \cdot \mathbf{R}_3}}, \quad (14.27)$$

where  $\mathbf{R}_1 = -(a/\sqrt{3})\mathbf{e}_x$ ,  $\mathbf{R}_2 = (a/2)[(\mathbf{e}_x/\sqrt{3}) + \mathbf{e}_y]$ , and  $\mathbf{R}_3 = (a/2) \times [(\mathbf{e}_x/\sqrt{3}) - \mathbf{e}_y]$ .

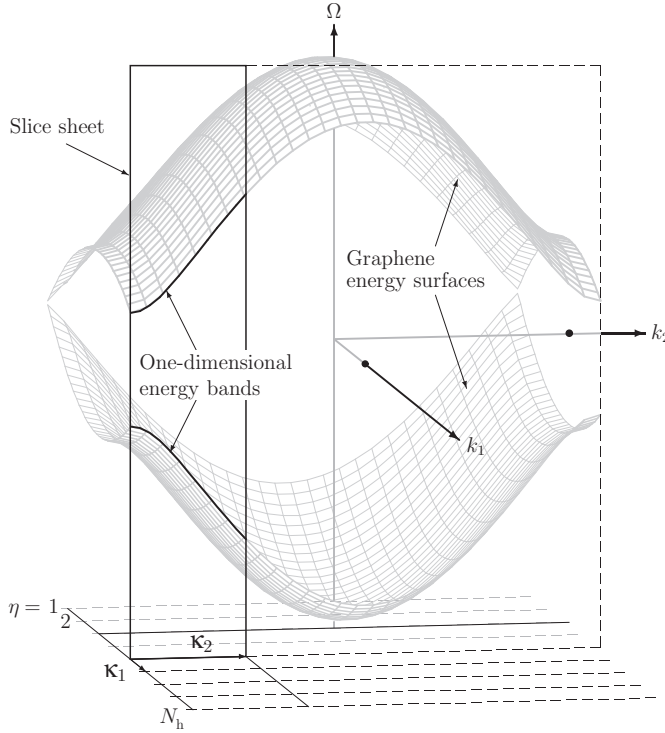


Figure 14.7 Intersection of the plane  $\mathbf{k}_1 = \kappa_1 \eta = \text{constant}$  ( $\eta = 1, 2, \dots, N_h$ ) with the graphene energy surface,  $\Omega(\mathbf{k}_1, \mathbf{k}_2)$ . The nanotube energy bands are shown by the heavy curves between 0 and  $+\kappa_2/2$ .

To find the nanotube's one-dimensional bands, we express the scalar products  $\mathbf{k} \cdot \mathbf{R}_i$  in the system of orthogonal coordinates in which the unit vectors are  $\mathbf{e}_1 = \mathbf{C}_h/|\mathbf{C}_h|$  and  $\mathbf{e}_2 = \boldsymbol{\tau}/|\boldsymbol{\tau}|$ . We have

$$\mathbf{e}_1 = \frac{a}{2} \frac{\sqrt{3}(n+m)\mathbf{e}_x + (n-m)\mathbf{e}_y}{|\mathbf{C}_h|}, \quad (14.28)$$

$$\mathbf{e}_2 = \frac{a}{2} \frac{(m-n)\mathbf{e}_x + \sqrt{3}(n+m)\mathbf{e}_y}{|\mathbf{C}_h|}, \quad (14.29)$$

$$|\mathbf{C}_h| = \sqrt{m^2 + n^2 + mn}, \quad (14.30)$$

$$\mathbf{R}_i = (\mathbf{e}_1 \cdot \mathbf{R}_i)\mathbf{e}_1 + (\mathbf{e}_2 \cdot \mathbf{R}_i)\mathbf{e}_2 \quad (i = 1, 2, \text{ or } 3), \quad (14.31)$$

$$\mathbf{k} = k_1 \mathbf{e}_1 + k_2 \mathbf{e}_2. \quad (14.32)$$

The scalar products are then

$$\mathbf{k} \cdot \mathbf{R}_i = k_1(R_{i1}) + k_2(R_{i2}), \quad (14.33)$$



where  $R_{ij} = \mathbf{R}_i \cdot \mathbf{e}_j$ . We find that

$$\mathbf{k} \cdot \mathbf{R}_1 = k_1(R_{11}) + k_2(R_{12}) = \frac{a^2 - k_1(m+n) + k_2(n-m)/\sqrt{3}}{2|\mathbf{C}_h|}, \quad (14.34)$$

$$\mathbf{k} \cdot \mathbf{R}_2 = k_1(R_{21}) + k_2(R_{22}) = \frac{a^2 k_1 n + k_2(2m+n)/\sqrt{3}}{2|\mathbf{C}_h|}, \quad (14.35)$$

$$\mathbf{k} \cdot \mathbf{R}_3 = k_1(R_{31}) + k_2(R_{32}) = \frac{a^2 k_1 m - k_2(2n+m)/\sqrt{3}}{2|\mathbf{C}_h|}. \quad (14.36)$$

The reciprocal-lattice vectors for a nanotube are

$$\kappa_1 = \frac{2\pi}{|\mathbf{C}_h|} \mathbf{e}_1, \quad \kappa_2 = \frac{2\pi D(n, m)}{\sqrt{3}|\mathbf{C}_h|} \mathbf{e}_2, \quad (14.37)$$

and the quantized values of  $\mathbf{k}_1 = \mathbf{k}_1(\eta)$  are

$$\mathbf{k}_1 a = \kappa_1 a \eta \quad (\eta = 1, 2, \dots, N_h). \quad (14.38)$$

If the results of (14.34) through (14.38) are substituted into (14.27), one obtains the one-dimensional energy bands for an arbitrary nanotube,

$$\begin{aligned} \Omega^\pm(n, m, \eta, k_2) = & \pm \left| \exp \left\{ i \frac{a^2}{2|\mathbf{C}_h|} \left[ -k_1(n-m) + \frac{k_2(n-m)}{\sqrt{3}} \right] \right\} \right. \\ & + \exp \left\{ i \frac{a^2}{2|\mathbf{C}_h|} \left[ k_1 n + k_2(2n+m)/\sqrt{3} \right] \right\} \\ & \left. + \exp \left\{ i \frac{a^2}{2|\mathbf{C}_h|} \left[ k_1 m + k_2(2n+m)/\sqrt{3} \right] \right\} \right|. \quad (14.39) \end{aligned}$$

In (14.39)  $\eta = 1, 2, \dots, N_h$ , and  $k_2$  is confined to the range  $\pm|\kappa_2/2|$  so that  $\mathbf{k}_2$  always lies within the first Brillouin zone. On the other hand, the quantized values of  $\mathbf{k}_1$  may span several Brillouin zones as illustrated in Figs. 14.5 and 14.8.

As simple examples consider the armchair and zigzag nanotubes. A schematic diagram of the armchair,  $(n, n)$ , nanotube on the extended graphene Brillouin zone is shown in Fig. 14.8. The parameters for the  $(n, n)$  armchair nanotube are as follows:

$$\begin{aligned} \mathbf{C}_h &= \sqrt{3}na \mathbf{e}_x, \\ D(n, n) &= 3n, \\ \mathbf{R} &= (1, 0), \\ \tau &= a \mathbf{e}_y, \\ \kappa_1 &= \frac{2\pi}{\sqrt{3}na} \mathbf{e}_x, \end{aligned}$$

$$\begin{aligned}
\kappa_2 &= \frac{2\pi}{a} \mathbf{e}_y, \\
N_h &= 2n, \\
b &= \frac{4\pi}{\sqrt{3}a}, \\
|\Gamma - \mathbf{K}_1| &= \frac{b}{\sqrt{3}} = \frac{4\pi}{3a}, \\
|\Gamma - \mathbf{M}| &= \frac{b}{2} = \frac{2\pi}{\sqrt{3}a}, \\
k_1(\eta) &= \kappa_1 \eta = \frac{2\pi\eta}{\sqrt{3}na} = \frac{b\eta}{4n} \quad (\eta = 1, 2, \dots, 2n), \\
N_h k_1(2n) &= \frac{4\pi}{\sqrt{3}a} = b,
\end{aligned}$$

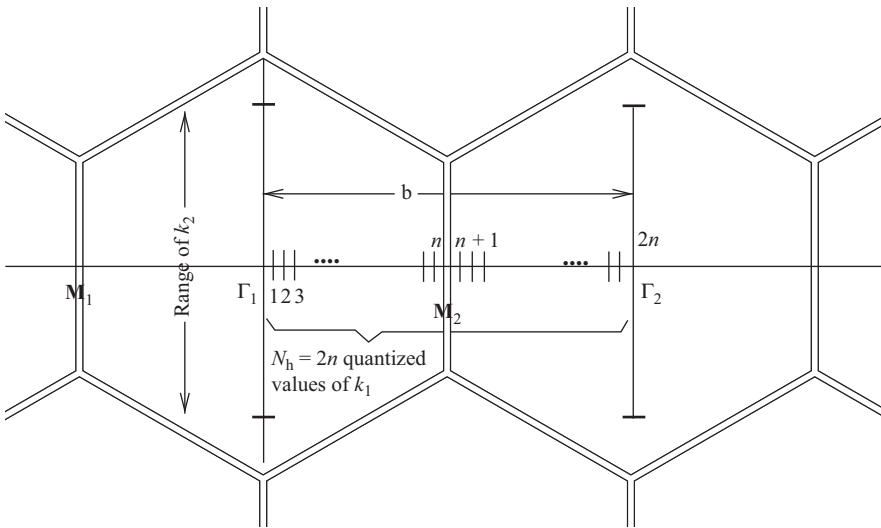


Figure 14.8 The armchair  $(n, n)$  nanotube on the graphene extended Brillouin zone, showing the range of the wavevector  $k_2$  and the  $N_h = 2n$  quantized  $k_1$  values (indicated by the short vertical lines), with  $k_1(\eta) = \eta\kappa_1$ ,  $\eta = 1, 2, \dots, 2n$ , and  $-\pi/a \leq k_2 \leq \pi/a$ . Since  $\cos(p\pi/n) = \cos[(2n - p)\pi/n]$ ,  $\eta = p$  and  $\eta = 2n - p$  (excluding the cases  $p = n$  and  $p = 2n$ ) are degenerate energy bands. For  $\eta = n$  and also  $\eta = 2n$  the bands are non-degenerate. All of the one-dimensional energy bands can be obtained by taking  $\eta = 1, 2, \dots, n$ . The bands corresponding to  $\eta = 0$  (equivalent to  $\eta = 2n$ ) and  $\eta = n$  give non-degenerate bands. The points  $\eta = n$  and  $k_2 = \pm b/(2\sqrt{3}) = \pm(2/3)\pi/a$  are Dirac  $\mathbf{K}$ -points, and therefore the armchair nanotube is always a conductor (has no gap between the valence and conduction bands).

and

$$-\frac{\pi}{a} \leq k_2 \leq \frac{\pi}{a},$$

where  $b$  is the magnitude of  $\mathbf{b}_1$  or  $\mathbf{b}_2$ .

Using the armchair parameters in (14.39) yields the one-dimensional energy bands,

$$\Omega^\pm(n, n, \eta, k_2) = \pm \sqrt{1 + 4 \cos^2 \left( \frac{k_2 a}{2} \right) + 4 \cos \left( \frac{\pi \eta}{n} \right) \cos \left( \frac{k_2 a}{2} \right)} \\ (\eta = 1, 2, \dots, 2n \text{ and } -\pi/a \leq k_2 \leq \pi/a). \quad (14.40)$$

Since  $\cos(\pi p/n) = \cos[(2n - p)\pi/n]$  it follows that the bands corresponding to  $\eta = p$  and  $\eta = 2n - p$  ( $p = 1, 2, \dots, n-1$ ) are degenerate. Note that  $\eta = n$  and  $\eta = 2n$  are non-degenerate. All of the bands can be obtained by taking  $\eta = 1, 2, \dots, n$ , with the understanding that  $\eta = n$  and  $\eta = 2n$  are non-degenerate and all other bands are doubly degenerate. The slice line for  $\eta = n$  passes through the Dirac  $\mathbf{K}_1$ - and  $\mathbf{K}_2$ -points for  $k_2 a = \pm 2\pi/3$  and therefore the valence and conduction bands touch at  $\Omega = 0$ . The armchair nanotubes are therefore metallic. Figure 14.9 shows the energy bands for the (3, 3) case.

The parameters for the  $(n, 0)$  achiral, zigzag, tube (Fig. 14.10) are as follows:

$$\begin{aligned} \mathbf{C}_h &= na \mathbf{e}_1, \\ D(n, 0) &= n, \\ \mathbf{R} &= (1, -1), \\ \tau &= \sqrt{3} a \mathbf{e}_2, \\ \kappa_1 &= \frac{2\pi}{na} \mathbf{e}_1, \\ \kappa_2 &= \frac{2\pi}{\sqrt{3}a} \mathbf{e}_y, \\ N_h &= 2n, \\ b &= \frac{4\pi}{\sqrt{3}a}, \\ \Gamma - \mathbf{K}_1 &= \frac{b}{\sqrt{3}} = \frac{4\pi}{3a}, \\ \Gamma - \mathbf{M} &= \frac{b}{2} = \frac{2\pi}{\sqrt{3}a}, \\ k_1(\eta) &= \kappa_1 \eta = \frac{2\pi \eta}{na} = \frac{\sqrt{3}b\eta}{2n} \quad (\eta = 1, 2, \dots, 2n), \\ |\kappa_2| &= \frac{b}{2}, \\ |\kappa_1| N_h &= \sqrt{3}b, \end{aligned}$$

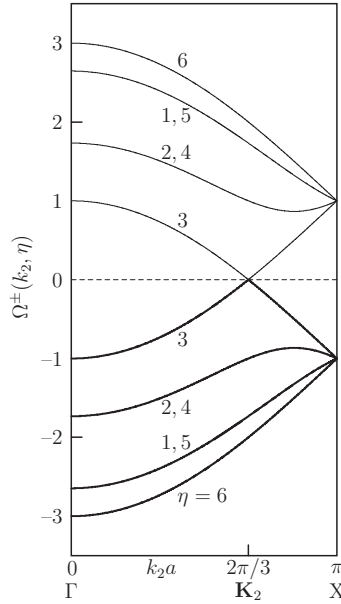


Figure 14.9 One-dimensional, armchair, energy bands along the  $\Gamma$ -X direction for  $C_h = (3, 3)$ . Curves with  $\eta = 5$  and  $\eta = 1$  are degenerate and also those with  $\eta = 4$  and  $\eta = 2$  are degenerate. The slice line for  $\eta = 3$  passes through the Dirac  $\mathbf{K}_2$ -point, and therefore the valence and conduction bands touch at  $\Omega = 0$ . The  $(3, 3)$  nanotube is metallic. The one-dimensional Brillouin zone extends from  $-\kappa_2/2$  to  $\kappa_2/2$ , which corresponds to  $-\pi \leq k_2a \leq \pi$ . The energy bands are symmetric in  $k_2a$ . (Note that X denotes the X-point of the nanotube Brillouin zone, not the X-point of the two-dimensional graphene zone.)

and

$$-\frac{\pi}{\sqrt{3}a} \leq k_2 \leq \frac{\pi}{\sqrt{3}a}.$$

Using (14.39) gives the energy dispersion curves for this case,

$$\Omega^\pm(n, 0, \eta, k_2) = \pm \sqrt{1 + 4 \cos^2 \left( \frac{\pi \eta}{n} \right) + 4 \cos \left( \frac{\sqrt{3} k_2 a}{2} \right) \cos \left( \frac{\pi \eta}{n} \right)} \\ \left( \eta = 1, 2, \dots, 2n \quad \text{and} \quad -\frac{\pi}{\sqrt{3}a} \leq k_2 \leq \frac{\pi}{\sqrt{3}a} \right). \quad (14.41)$$

The zigzag energy bands are also symmetric in  $k_2$  and, again,  $\cos(\pi p/n) = \cos[(2n - p)\pi/n]$ , so  $\eta = p$  and  $\eta = 2n - p$  ( $\eta = 1, 2, \dots, n - 1$ ) are degenerate. The bands for  $\eta = n$  and  $2n$  are non-degenerate.

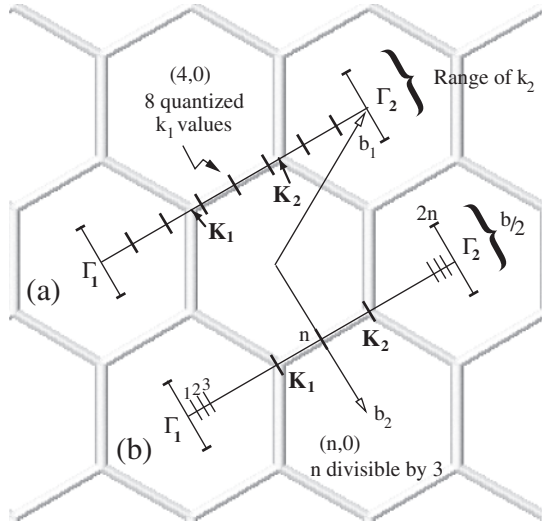


Figure 14.10 The Brillouin zone of a zigzag  $(n, 0)$  nanotube on extended graphene zones. (a) A  $(4, 0)$  zigzag tube with eight quantized values for  $k_1$ , none of which passes through the Dirac points,  $K_1$  and  $K_2$ . (b) When  $n$  is divisible by 3 the slice lines pass through  $K_1$  for  $\eta = 2n/3$  and through  $K_2$  for  $\eta = 4n/3$ . In both (a) and (b),  $|\kappa_1| = \sqrt{3}b/(2n)$  and  $|\kappa_2| = b/2$ , where  $b$  is the length of a graphene reciprocal-lattice vector nanotube.

As a last example we consider the chiral nanotube  $(4, 2)$ . The parameters for this SWCNT are as follows:

$$\begin{aligned}
 |C_h| &= \sqrt{28}a, \\
 D(4, 2) &= 2, \\
 |\tau| &= \sqrt{21}a, \\
 \kappa_1 &= \frac{2\pi}{\sqrt{28}a} \mathbf{e}_1, \\
 \kappa_2 &= \frac{2\pi}{\sqrt{21}a} \mathbf{e}_2, \\
 N_h &= 28, \\
 k_1 &= \eta|\kappa_1| \quad (\eta = 1, 2, \dots, 28),
 \end{aligned}$$

and

$$-\frac{\pi}{\sqrt{21}} \leq k_2 a \leq \frac{\pi}{\sqrt{21}}.$$

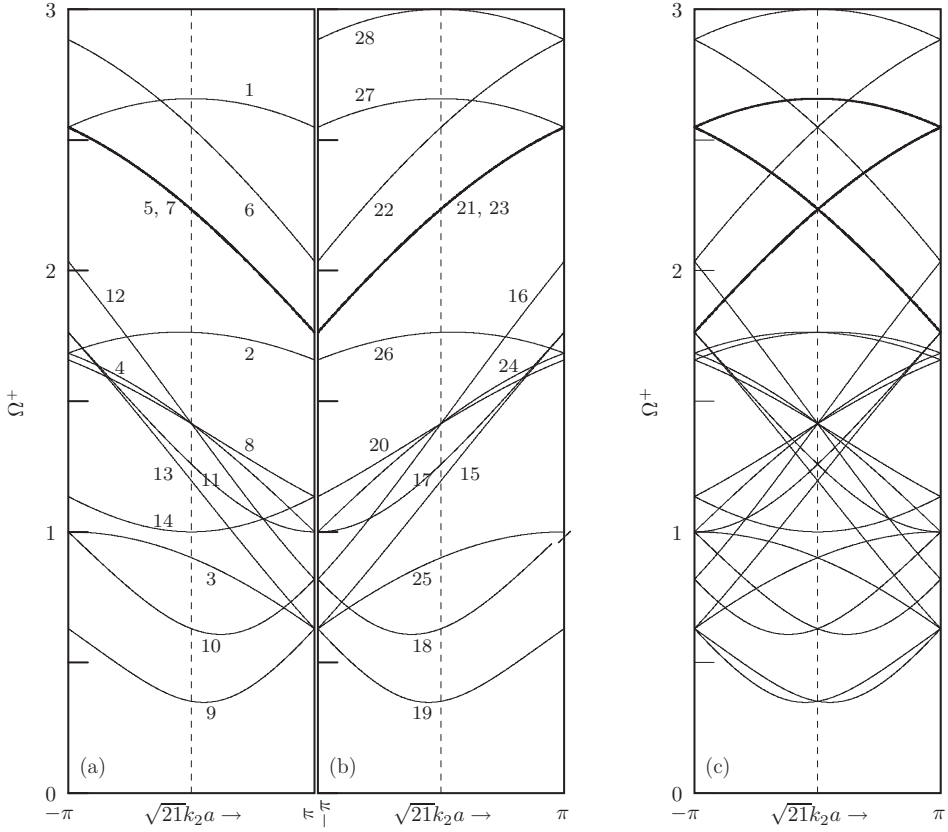


Figure 14.11 One-dimensional conduction energy bands for the (4, 2) chiral nanotube. (a) The first 14 bands ( $\eta = 1$  to 14) and (b) the bands for  $\eta = 15$  to 28. (c) All 28 conduction bands. For Löwdin orbitals the valence bands are mirror reflections through  $\Omega = 0$ .

The dimensionless energy,  $\Omega^\pm(n, m, \eta, k_2)$ , determined by use of (14.39) for the one-dimensional energy bands (the conduction bands are shown in Fig. 14.11), is given by

$$\Omega^\pm(4, 2, \eta, k_2) = \pm \left| \exp\left(\frac{-i3\pi\eta}{14} + \frac{ik_2a}{2\sqrt{21}}\right) + \exp\left(\frac{i\pi\eta}{7} + \frac{i2k_2a}{\sqrt{21}}\right) + \exp\left(\frac{i\pi\eta}{14} - \frac{i5k_2a}{2\sqrt{21}}\right) \right|. \quad (14.42)$$

To convert from  $\Omega$  to  $(E - \epsilon_p)$  we need only multiply by  $|(pp\pi)|$ . Various calculations show that  $|(pp\pi)|$  is in the range from 2.4 to 3.2 eV.

### 14.4 Metallic and semiconducting nanotubes

If the slice line determined by  $\eta\kappa_1\mathbf{e}_1 + k_2\mathbf{e}_2$  cuts through any of the  $\mathbf{K}$ -points in the graphene Brillouin zone the one-dimensional valence and conduction energy bands will touch at  $\Omega^\pm = 0$ . That is, there will be no energy gap between the lower and upper bands, and the nanotube will be metallic. If none of the slices through the energy surface cut through a  $\mathbf{K}$ -point, then all the one-dimensional energy bands will have an energy gap between the valence and conduction bands. In this case the nanotube will be semiconducting. Nanotube parameters are given in Table 14.1.

The Dirac points for the graphene Brillouin zone have the vectors  $\mathbf{V}_1 = \mathbf{K}_1 + \mathbf{K}_r$ , and  $\mathbf{V}_2 = \mathbf{K}_2 + \mathbf{K}_r$ , where  $\mathbf{K}_1$  and  $\mathbf{K}_2$  are Dirac vectors in the central unit cell, and  $\mathbf{K}_r$  is any reciprocal-lattice vector,  $\mathbf{K}_r = p\mathbf{b}_1 + q\mathbf{b}_2$ , where  $p$  and  $q$  are arbitrary integers. We need only consider the Dirac points  $\mathbf{K}_1$  and  $\mathbf{K}_2$ , where

$$\mathbf{K}_1 = \frac{4\pi}{3a}\mathbf{e}_y = \frac{\mathbf{b}_1 - \mathbf{b}_2}{3},$$

$$\mathbf{K}_2 = \frac{2\pi}{3a}(\sqrt{3}\mathbf{e}_x + \mathbf{e}_y) = 2\mathbf{b}_1 + \mathbf{b}_2.$$

If we express  $\mathbf{V}_i$  ( $i = 1$  or  $2$ ) as the vector  $A\kappa_1 + B\kappa_2$ , then  $A = (\mathbf{K}_i \cdot \kappa_1)/\kappa_1^2$ . A necessary condition for a slice line to pass through a Dirac point is that  $A$  must be a positive integer. For  $\mathbf{V}_1$  we find that

$$A = \frac{(\mathbf{K}_1 + \mathbf{K}_r) \cdot \kappa_1}{\kappa_1^2} = \frac{n - m}{3} + (pn + qm) = \text{integer}. \quad (14.43)$$

The condition is satisfied if  $n - m$  is divisible by 3. For  $\mathbf{V}_2$  we find that

$$A = \frac{(\mathbf{K}_2 + \mathbf{K}_r) \cdot \kappa_1}{\kappa_1^2} = \frac{2n + m}{3} + (pn + qm) = \text{integer}. \quad (14.44)$$

Again the condition is satisfied if  $n - m$  is divisible by 3.

It is expedient to use the abbreviation NBZ (nanotube Brillouin zone) to refer to the rectangle in the reciprocal-lattice space of graphene. This area is bounded by  $0 \leq k_1 \leq N_h\kappa_1$  and  $-\kappa_2/2 \leq k_2 \leq \kappa_2/2$ . The requirement that  $n - m$  be divisible by 3 is necessary but not sufficient because the vector  $\mathbf{V}_1$  or  $\mathbf{V}_2$  must also lie in or on the boundary of the NBZ. It turns out that in all cases at least one Dirac point lies within the NBZ if  $n - m$  is divisible by 3. As a consequence this condition is necessary and sufficient to insure that  $\Omega^\pm = 0$  within the NBZ and that the nanotube is metallic. In the case of  $(n, n)$  armchair nanotubes,  $n - m = 0$ , so they are all metallic. For the  $(n, 0)$  zigzag nanotubes,  $n - m = n$ , and hence they are metallic only if  $n$  is a multiple of 3. Figure 14.12 shows the bands for  $(2, 0)$  and  $(3, 0)$ . (The X points in Fig. 14.12 refer to the one-dimensional Brillouin zone of the carbon nanotube.) For the armchair  $\kappa_1$  is parallel to the  $x$ -axis, whereas for the

Table 14.1 Nanotube parameters

$C_h = (n, m)$ $n\mathbf{a}_1 + m\mathbf{a}_2$ units of $a$	$ C_h $	$D(n, m)$ $N_h$	$\tau$ $ \tau $	$\kappa_1$ $ \kappa_1 $	$\kappa_2$ $ \kappa_2 $
$(n, n)$	$\sqrt{3}na$	$3n$	$\mathbf{a}_1 - \mathbf{a}_2$	$(\mathbf{b}_1 + \mathbf{b}_2)/(2n)$	$(\mathbf{b}_1 - \mathbf{b}_2)/2$
armchair		$2n$	$a$	$b/(2n)$	$\sqrt{3}b/2$
$(n, 0)$	$na$	$n$	$\mathbf{a}_1 - 2\mathbf{a}_2$	$(2\mathbf{b}_1 + \mathbf{b}_2)/(2n)$	$-\mathbf{b}_2/2$
zigzag		$2n$	$\sqrt{3}a$	$\sqrt{3}b/(2n)$	$b/2$
$(2, 1)$	$\sqrt{7}a$	1	$4\mathbf{a}_1 - 5\mathbf{a}_2$	$(5\mathbf{b}_1 + 4\mathbf{b}_2)/14$	$(\mathbf{b}_1 - 2\mathbf{b}_2)/14$
		14	$\sqrt{21}a$	$\sqrt{21}b/14$	$\sqrt{7}b/14$
$(3, 1)$	$\sqrt{13}a$	1	$5\mathbf{a}_1 - 7\mathbf{a}_2$	$(7\mathbf{b}_1 + 5\mathbf{b}_2)/26$	$(\mathbf{b}_1 - 3\mathbf{b}_2)/26$
		26	$\sqrt{39}a$	$\sqrt{39}b/26$	$\sqrt{13}b/26$
$(3, 2)$	$\sqrt{19}a$	1	$7\mathbf{a}_1 - 8\mathbf{a}_2$	$(8\mathbf{b}_1 + 7\mathbf{b}_2)/38$	$(2\mathbf{b}_1 - 3\mathbf{b}_2)/38$
		38	$\sqrt{57}a$	$\sqrt{57}b/38$	$\sqrt{19}b/38$
$(4, 1)$	$\sqrt{21}a$	3	$2\mathbf{a}_1 - 3\mathbf{a}_2$	$(3\mathbf{b}_1 + 2\mathbf{b}_2)/14$	$(\mathbf{b}_1 - 4\mathbf{b}_2)/14$
		14	$\sqrt{7}a$	$\sqrt{7}b/14$	$\sqrt{21}b/14$
$(4, 2)$	$\sqrt{28}a$	2	$4\mathbf{a}_1 - 5\mathbf{a}_2$	$(5\mathbf{b}_1 + 4\mathbf{b}_2)/28$	$(2\mathbf{b}_1 - 4\mathbf{b}_2)/28$
		28	$\sqrt{21}a$	$\sqrt{21}b/28$	$b/\sqrt{28}$
$(4, 3)$	$\sqrt{37}a$	1	$10\mathbf{a}_1 - 11\mathbf{a}_2$	$(11\mathbf{b}_1 + 10\mathbf{b}_2)/74$	$(3\mathbf{b}_1 - 4\mathbf{b}_2)/74$
		74	$\sqrt{111}a$	$\sqrt{111}b/74$	$\sqrt{37}b/74$
$(5, 1)$	$\sqrt{31}a$	1	$7\mathbf{a}_1 - 11\mathbf{a}_2$	$(7\mathbf{b}_1 + 11\mathbf{b}_2)/62$	$(\mathbf{b}_1 - 5\mathbf{b}_2)/62$
		62	$\sqrt{93}a$	$\sqrt{93}b/62$	$\sqrt{31}b/62$
$(5, 2)$	$\sqrt{39}a$	3	$3\mathbf{a}_1 - 4\mathbf{a}_2$	$(4\mathbf{b}_1 + 3\mathbf{b}_2)/26$	$(2\mathbf{b}_1 - 5\mathbf{b}_2)/26$
		26	$\sqrt{13}a$	$\sqrt{13}b/26$	$\sqrt{39}b/26$
$(5, 3)$	$7a$	1	$11\mathbf{a}_1 - 13\mathbf{a}_2$	$(13\mathbf{b}_1 + 11\mathbf{b}_2)/98$	$(3\mathbf{b}_1 - 5\mathbf{b}_2)/98$
		98	$\sqrt{147}a$	$\sqrt{147}b/98$	$7b/98$
$(5, 4)$	$\sqrt{61}a$	1	$13\mathbf{a}_1 - 14\mathbf{a}_2$	$(14\mathbf{b}_1 + 13\mathbf{b}_2)/122$	$(4\mathbf{b}_1 - 5\mathbf{b}_2)/122$
		122	$\sqrt{183}a$	$\sqrt{183}b/122$	$\sqrt{61}b/122$

$a = |\mathbf{a}_1| = |\mathbf{a}_2|$ ,  $b = |\mathbf{b}_1| = |\mathbf{b}_2|$ ,  $b^2 = 16\pi^2/(3a^2)$ ,  $\mathbf{a}_1 \cdot \mathbf{a}_2 = a/2$ ,  $\mathbf{b}_1 \cdot \mathbf{b}_2 = -b/2$ ,  
 $D(n, m) = \text{gcd of } (2n + m) \text{ and } (2m + n)$ ,  $r = (2m + n)/D(n, m)$ ,  
 $s = -(2n + m)/D(n, m)$ ,  $\tau = r\mathbf{a}_1 + s\mathbf{a}_2$ ,  $\kappa_1 = (-s\mathbf{b}_1 + r\mathbf{b}_2)/N_h$ ,  
 $\kappa_2 = (m\mathbf{b}_1 - n\mathbf{b}_2)/N_h$ .



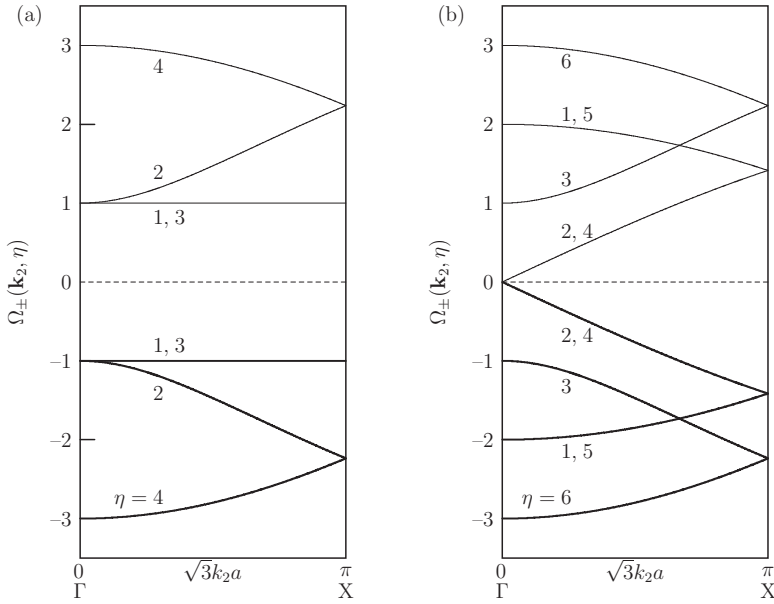


Figure 14.12 (a) One-dimensional, zigzag, energy bands for  $(2, 0)$ . None of the slice lines cut through a Dirac point ( $n$  is not a multiple of 3). Two degenerate, flat bands ( $\eta = 1$  and  $\eta = 3$ ) are produced. (b) One-dimensional, zigzag, energy bands for  $(3, 0)$ . One of the slice lines cuts through the  $\mathbf{K}_2$  Dirac point in the Brillouin zone, and therefore the valence and conduction bands touch at  $\Omega = 0$  for  $\mathbf{k}_2 = 0$ . Here  $\kappa_2 = 2\pi/(\sqrt{3}a)$  and  $-\pi/\sqrt{3} \leq k_2a \leq \pi/\sqrt{3}$ .

zigzag  $\kappa_1$  is parallel to the  $\mathbf{a}_1$  axis. All other nanotubes have  $\kappa_1$  oriented between the  $x$ -axis and the  $\mathbf{a}_1$  axis.

### 14.5 The nanotube density of states

The density of states (DOS),  $\rho(E)$ , is defined so that  $\rho(E) dE$  is the number of states in the range between  $E$  and  $E + dE$ . The function  $\rho(E)$  has dimensions of  $(\text{energy})^{-1}$ . If the energy,  $E$ , is a function of  $\mathbf{k}_2$  only, as it is for the one-dimensional nanotube energy bands, then

$$\rho(E(\mathbf{k}_2)) dE = \rho(\mathbf{k}_2) dk_2. \quad (14.45)$$

The density of  $\mathbf{k}_2$ -points,  $\rho(\mathbf{k}_2)$ , is a constant,

$$\rho(\mathbf{k}_2) = \frac{1}{|\kappa_2|}. \quad (14.46)$$

It follows that

$$\rho(E(\mathbf{k}_2)) = \frac{1}{|\kappa_2| |dE(\mathbf{k}_2)/dk_2|}. \quad (14.47)$$

The absolute value of  $dE(\mathbf{k}_2)/dk_2$  is introduced into (14.47) because the density of states is positive irrespective of the sign of the slope of the energy band. The length of the unit cell along the  $\kappa_2$ -direction is  $|\tau|$  and if we consider the density of states per unit length (along the axis of the nanotube),  $\rho_1$ , we obtain

$$\rho_1(E(\mathbf{k}_2)) = \frac{1}{|\kappa_2||\tau||dE(\mathbf{k}_2)/dk_2|} = \frac{1}{2\pi|dE(\mathbf{k}_2)/dk_2|}, \quad (14.48)$$

where we have used the fact that  $|\kappa_2||\tau| = 2\pi$ .

In the previous sections on graphene we showed that near a Dirac  $\mathbf{K}$ -point the dimensionless energy,  $\Omega^\pm(\mathbf{K} + \delta\mathbf{k})$ , behaved as

$$\Omega^\pm(\mathbf{K} + \delta\mathbf{k}) = \pm \frac{\sqrt{3}a}{2} |\delta\mathbf{k}|, \quad (14.49)$$

describing a conical energy surface centered at the Dirac  $\mathbf{K}$ -points. For a metallic nanotube one of the slice lines passes through two inequivalent  $\mathbf{K}$ -points. The one-dimensional energy band near a  $\mathbf{K}$ -point is given by

$$\Omega^\pm(\mathbf{K} + \delta\mathbf{k}_2) = \pm \frac{E^\pm(\mathbf{K} + \delta\mathbf{k}_2)}{(pp\pi)} \rightarrow \pm \frac{\sqrt{3}a}{2} |\delta\mathbf{k}_2|. \quad (14.50)$$

The situation for the conduction band is illustrated in Fig. 14.13.

We can restrict our attention to the right-hand side of the energy band where  $\delta k_2 \geq 0$ , remembering that there will be a factor of 2 multiplying  $\rho_1$  to account for

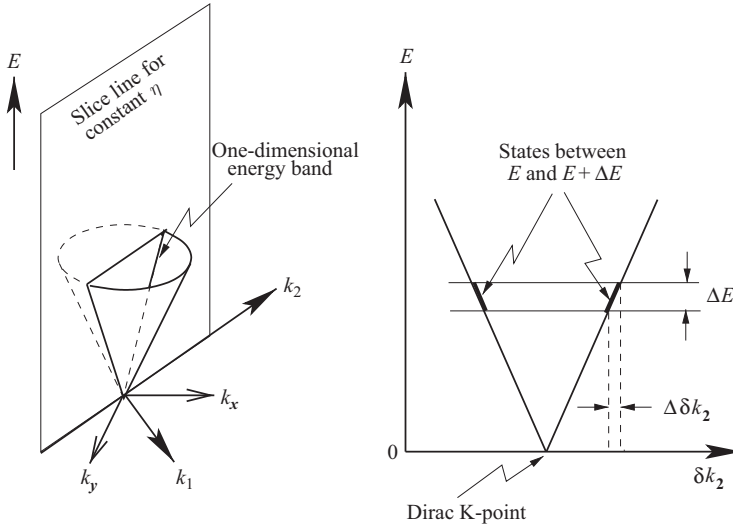


Figure 14.13 (a) A slice through a Dirac cone. (b) Linear dispersion near a Dirac  $\mathbf{K}$ -point;  $\Delta E/\Delta\delta k_2 = \text{constant}$  is the slope of the one-dimensional energy band.

the left-hand side of the dispersion curve in Fig. 14.13. Using (14.48) and (14.49), we obtain

$$\frac{dE(\mathbf{k}_2)}{dk_2} = \frac{dE(\mathbf{K} + \delta\mathbf{k}_2)}{d(\delta k_2)} = \frac{d\{(\sqrt{3}a/2)(pp\pi)\delta k_2\}}{d(\delta k_2)} = \frac{\sqrt{3}a}{2}(pp\pi), \quad (14.51)$$

for  $\Omega$  near zero, and

$$\rho_1(E) = \frac{8}{2\pi(\sqrt{3}a/2)(pp\pi)} = \frac{8}{\pi\sqrt{3}a(pp\pi)}. \quad (14.52)$$

The factor of 8 arises from three considerations: (1) a factor of 2 because both the right- and the left-hand side of the energy curve in Fig. 14.13 contribute, (2) a factor of 2 because the slice line for a metallic nanotube always passes through two inequivalent Dirac  $\mathbf{K}$ -points (see Figs. 14.9 and 14.10), and (3) a factor of 2 to account for the two spin states. The density of states (DOS) near the top of the valence band at a Dirac  $\mathbf{K}$ -point will also be described by (14.52) for small negative values of  $E$ .

The DOS for graphene (the background curves in Fig. 14.14) vanishes at the Dirac  $\mathbf{K}$ -points. In contrast, Eq. (14.52) shows that the DOS for a metallic nanotube is a non-zero constant over the range of  $E$  for which the energy band can be considered as linear in  $\delta k_2$ . The DOS for graphene has a single peak (logarithmic singularity) but the nanotube DOS has many spikes (singularities). These spikes result whenever a one-dimensional energy band has a minimum or maximum, since at such points  $dE/dk_2$  vanishes. To see the spiky nature of the nanotube DOS consider the achiral,  $(n, 0)$  nanotube whose dimensionless energy is

$$\Omega^\pm(\mathbf{k}_2, \eta) = \pm \sqrt{1 + 4\cos^2\left(\frac{\pi\eta}{n}\right) + 4\cos\left(\frac{\sqrt{3}k_2a}{2}\right)\cos\left(\frac{\pi\eta}{n}\right)}. \quad (14.53)$$

We may limit discussion to the upper branch since  $\rho(\Omega) = \rho(|\Omega^\pm|)$ . For simplicity we drop the superscript, with the understanding that  $\Omega = \Omega^+$ . We have

$$\left|\frac{d\Omega(\mathbf{k}_2, \eta)}{dk_2}\right| = \left|\frac{1}{2\Omega}(2\sqrt{3}a)\sin\left(\frac{\sqrt{3}k_2a}{2}\right)\cos\left(\frac{\pi\eta}{n}\right)\right|, \quad (14.54)$$

and

$$\cos\left(\frac{\sqrt{3}k_2a}{2}\right) \equiv f(\Omega) = \frac{\Omega^2 - 1 - 4A_\eta^2}{4A_\eta}, \quad (14.55)$$

where

$$A_\eta \equiv \cos(\pi\eta/n). \quad (14.56)$$

The DOS is then described by

$$\rho_l(\Omega) = \frac{8(1/(2\pi))\Omega}{|(\sqrt{3}a)A_\eta\sqrt{1-f(\Omega)^2}|}, \quad \Omega_{\min}(\eta) \leq \Omega \leq \Omega_{\max}(\eta), \quad (14.57)$$

where  $\Omega_{\min}$  and  $\Omega_{\max}$  are, respectively, the minimum and maximum values of the energy band described by  $\Omega(\eta)$ . The factor of 8 was explained above.

For numerical calculations of the DOS for  $(n, 0)$  nanotubes a more efficient method is to use the expression

$$\rho_l(\Omega) = \frac{16}{\sqrt{3}\pi a} \Re \left\{ \frac{\Omega}{\sqrt{(\alpha^2 - \Omega^2)(\Omega^2 - \beta^2)}} \right\}, \quad (14.58)$$

where  $\alpha = 2A_\eta + 1$  and  $\beta = 2A_\eta - 1$ . (a) Choose  $k_2$  in the range  $0 \leq k_2 a \leq \pi/\sqrt{3}$ , (b) compute  $\Omega(\mathbf{k}_2)$  from (14.53), and (c) compute  $\rho_l(\Omega)$  using (14.58). This procedure gives  $\rho_l(\Omega)$  versus  $\Omega$  and converges well at the Dirac points. If  $n$  is even, the band for  $\eta = n/2$  and  $(3/2)n$  will have a delta-function DOS at  $\Omega = 1$ . This band can not be numerically computed from (14.57) or (14.58). A disadvantage of this method is that each band has a different range of  $\Omega$ , so calculating the total of all bands is more difficult.

Several features are apparent. First, (14.52) shows that if  $n$  is even the band for  $\eta = n/2$  and  $(3/2)n$  has  $\Omega^+ = 1$  irrespective of  $k_2$ . That is, the band is flat, and therefore the DOS tends to infinity (a delta-function DOS). Second, (14.56) shows that the DOS will have a spike (square-root singularity) at the value of  $\Omega^+$  for which  $1 - f(\eta)^2$  or  $\sin(\sqrt{3}k_2 a/2) = 0$ . From (14.54) we see that this occurs for every band (every  $\eta$ ) at  $\Gamma(\mathbf{k}_2 = 0)$  except for bands that include Dirac points. In the case for which  $\Omega^+ = 0$ , the DOS must be determined by a limiting process since both the numerator and the denominator in (14.55) tend to zero. The limiting process yields  $8/(\sqrt{3}\pi a)$ . Since  $\rho_l(E) = \rho_l(\Omega)|(pp\pi)|$ , we regain the results of (14.52).

Figure 14.14 shows the total DOS for the metallic zigzag nanotube  $(6, 0)$ , and the semiconducting nanotube  $(7, 0)$ .

## 14.6 Curvature and energy gaps

When a graphene sheet is rolled into a nanotube, the angles between the C–C bonds are altered. Two effects result from this. First, the  $p_z$  orbitals on nearest-neighbor carbon atoms are slightly tilted with respect to one another. This leads to a small sigma interaction between the  $p_z$  orbitals. Second, and more importantly, the  $sp^2$  bonds are twisted, leading to an interaction between the  $2s$  and  $p_z$  orbitals. Except for the armchair nanotubes [14.2], both these effects lead to the formation of a small energy gap (of the order of meVs) between the conduction and valence

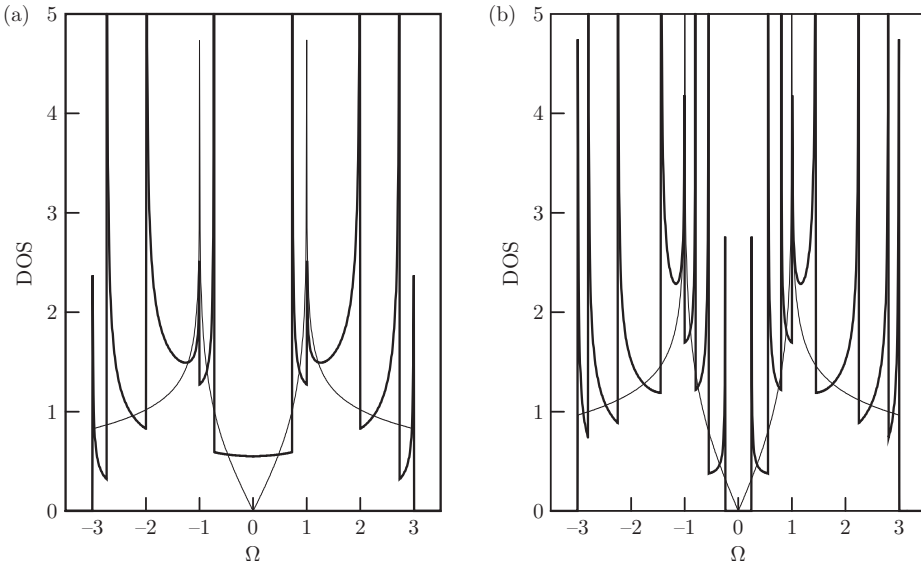


Figure 14.14 The total DOS for (a) the metallic zigzag nanotube (6, 0), and (b) the semiconducting zigzag nanotube (7, 0). The background curve is the DOS for graphene.

bands near the Dirac points. Clearly, the hybridization is more pronounced for small-diameter tubes than for large-diameter tubes. The gap induced by the tube curvature is proportional to  $1/d_t^2$ , where  $d_t$  is the diameter of the nanotube [14.3]. The gap is important for nanotubes that would otherwise be metallic, but not for semiconducting nanotubes, whose energy gap is already much larger than that due to curvature.

## References

- [14.1] Carbon nanotube: [en.wikipedia.org/wiki/Carbon\\_nanotube](http://en.wikipedia.org/wiki/Carbon_nanotube).
- [14.2] R. Saito, G. Dresselhaus, and M. S. Dresselhaus, *Physical Properties of Carbon Nanotubes* (London: Imperial College Press, 1998).
- [14.3] A. Kleiner and S. Eggert, “Curvature, hybridization, and STM images of carbon nanotubes”, *Phys. Rev. B* **64**, 113402 (2001) (4 pages).
- [14.4] M. S. Dresselhaus, G. Dresselhaus, and A. Jorio, *Group Theory and Applications to the Physics of Condensed Matter* (Berlin: Springer-Verlag, 2007), pp. 538–542.

## Exercises

- 14.1 (a) For armchair nanotube energy bands show that  $\Omega = \pm 1$  at the one-dimensional zone boundary irrespective of  $\eta$  ( $2n$ -fold degeneracy).

- (b) Show that the valence band touches the conduction band for  $\eta = n$  and  $k_2 a/2 = \pi/3$ .
- (c) Show that the touching point is at the Dirac point,  $\mathbf{K}_2 = (2\pi/a) \times (\mathbf{e}_x/\sqrt{3} + \mathbf{e}_y/3)$ .
- 14.2 (a) Derive a formula for the one-dimensional energy bands for  $\mathbf{C}_h = (2, 1)$ .
- (b) Find  $\kappa_1$  and  $\kappa_2$  and specify the first Brillouin zone for the nanotube.
- (c) Make a graph of the energy bands for  $-\kappa_2/2 \leq \mathbf{k}_2 \leq \kappa_2/2$  for  $\eta = 1, 2, \dots, N_h$ .
- (d) Are the bands symmetric in the variable  $k_2$ ?
- (e) Characterize the degeneracies at  $\mathbf{k}_2 = 0$  and  $\mathbf{k}_2 = \pm\kappa_2/2$ .
- 14.3 (a) For the  $(2, 1)$  nanotube express  $\mathbf{C}_h$ ,  $\kappa_1$ , and  $\kappa_2$  in terms of the reciprocal-lattice vectors  $\mathbf{b}_1$  and  $\mathbf{b}_2$ .
- (b) Construct a graph in reciprocal-lattice space that shows the quantized  $\mathbf{k}_1$  vectors and the  $\mathbf{k}_2$  vector.
- 14.4 (a) For an  $(n, m)$  nanotube show that the reciprocal-lattice vector  $p\mathbf{b}_1 + q\mathbf{b}_2 = (np + mq)\kappa_1 + (pr + qs)\kappa_2$ , where  $p$  and  $q$  are arbitrary integers.
- (b) Show that an arbitrary vector from the origin to a  $\mathbf{K}_2$  Dirac point anywhere in the reciprocal-lattice space ( $\mathbf{b}_1$ ,  $\mathbf{b}_2$  space) is given by  $\mathbf{V}_2 = [(2n + m)/3](np + mq)\kappa_1 + (1/D)[m + p(2m + n) - q(2n + m)]\kappa_2$ .
- (c) Show that  $D(n, m)$  is a multiple of 3 if  $n - m$  is divisible by 3.
- 14.5 (a) For the  $(7, 4)$  nanotube, use the results of Exercise 14.4 to show that the slice line with  $\eta = 17$  passes through a  $\mathbf{K}_2$  Dirac point.
- (b) What is the value of  $\mathbf{k}_2$  when the slice line intersects  $\mathbf{K}_2$ ?
- 14.6 Consider an  $(n, n)$  armchair nanotube and two nearest-neighbor carbon atoms on the rim as shown in Fig. 14.15.

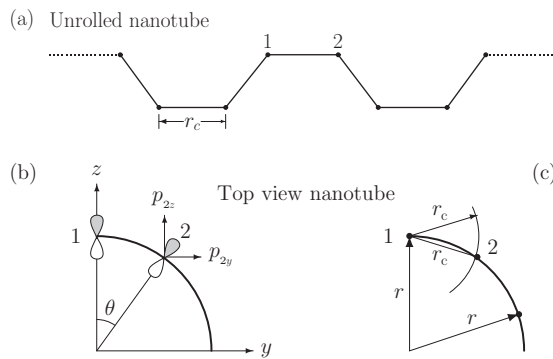


Figure 14.15

Take the origin at the tube center in the  $y$ - $z$  plane. Carbon atoms 1 and 2 lie in the  $y$ - $z$  plane, and the  $x$ -direction is perpendicular to the plane of the paper (along the tube axis). Figure (a) is a portion of the  $(n, n)$  tube unrolled in the  $y$ - $z$  plane. Figures (b) and (c) are top views of the rolled nanotube showing the locations of carbon atoms 1 and 2. Assume that the distance between carbon atoms 1 and 2,  $r_c$ , is fixed.

- (a) Show that the direction cosines for the vector from carbon atom 2 to carbon atom 1 are  $\alpha = 0$ ,  $\beta = (1 - r_c^2/(4r^2))^{1/2}$  and  $\gamma = -r_c/(2r)$ .
- (b) The  $2s$ - $2p$  interaction vanishes by symmetry for graphene. Show that the  $2s_1$ - $2p_2$  interaction for carbon atoms 1 and 2 of the nanotube is given by

$$(sp\sigma)[\beta(\sin \theta) + \gamma \cos \theta] = (sp\sigma) \left[ -\sqrt{1 - \frac{r_c^2}{4r^2}} \sin \theta + \frac{r_c}{2r} \cos \theta \right],$$

where  $\theta = 2\pi/n$ .

- (c) Show that, for large  $n$ , the interaction is inversely proportional to the tube diameter.

# Appendix A

## Vectors and matrices

### A.1 Vectors

A vector in  $n$ -dimensional space is specified by  $n$  components that give the projections of the vector onto the  $n$  unit vectors of the space:  $\mathbf{V} = (v_1, v_2, v_3, \dots, v_n)$ . Two vectors are equal if all of the components are equal. The components may be real or complex numbers. Vectors obey the following rules:

$$\begin{aligned}\mathbf{U} + (\mathbf{V} + \mathbf{W}) &= (\mathbf{U} + \mathbf{V}) + \mathbf{W}, \\ \mathbf{U} + \mathbf{V} &= \mathbf{V} + \mathbf{U}, \\ r\mathbf{U} + s\mathbf{U} &= (r + s)\mathbf{U}, \\ r\mathbf{U} + r\mathbf{V} &= r(\mathbf{U} + \mathbf{V}), \\ r(s\mathbf{U}) &= rs\mathbf{U}\end{aligned}$$

( $r$  and  $s$  are any real or complex numbers). The inner product or (Hermitian) scalar product of two  $n$ -dimensional vectors  $\mathbf{U}$  and  $\mathbf{V}$  is

$$\sum_{i=1}^n u_i^* v_i = (\mathbf{U}, \mathbf{V}) = (\mathbf{V}, \mathbf{U})^*.$$

The magnitude, or length, of  $\mathbf{V}$  is  $|\mathbf{V}| = (\mathbf{V}, \mathbf{V})^{1/2}$ . It is a positive number. It is zero if and only if  $\mathbf{V} = 0$ , and  $\mathbf{V} = 0$  if and only if  $v_i = 0$  for all  $i$ . A “normalized” vector has  $|\mathbf{V}| = 1$ .

The scalar product,  $(\mathbf{U}, \mathbf{V})/|\mathbf{V}|$ , is the projection of  $\mathbf{U}$  onto  $\mathbf{V}$ , and the cosine of the angle,  $\phi$ , between two vectors is

$$-1 \leq \cos \phi = \frac{(\mathbf{U}, \mathbf{V})}{|\mathbf{U}||\mathbf{V}|} \leq 1.$$

If  $\cos \phi = 1$ ,  $\mathbf{U}$  and  $\mathbf{V}$  are parallel vectors. If  $\cos \phi = 0$ ,  $\mathbf{U}$  and  $\mathbf{V}$  are orthogonal. The scalar product of two vectors is unchanged if both vectors are subjected to the



same symmetry operation. For example, if  $\mathbf{U}$  and  $\mathbf{V}$  are subjected to a rotation  $R$  or operator  $P_R$ ,

$$(P_R \mathbf{U}, P_R \mathbf{V}) = (R\mathbf{U}, R\mathbf{V}) = (\mathbf{U}, \mathbf{V}).$$

A set of  $m$  normalized, mutually orthogonal,  $n$ -dimensional vectors,  $\mathbf{U}_1, \mathbf{U}_2, \dots, \mathbf{U}_m$ , is an *orthonormal* set. If  $m = n$  then the set “spans” the  $n$ -dimensional vector space, and each  $\mathbf{U}_i$  ( $i = 1, 2, \dots, n$ ) is a basis vector for the space. Any vector  $\mathbf{W}$  in this  $n$ -dimensional vector space can be constructed from a linear combination of basis vectors:  $\mathbf{W} = \sum_{i=1}^n r_i \mathbf{U}_i$ , where  $r_i$  is a constant coefficient.

If a set of  $m$  vectors is such that no vector in the set can be expressed as a linear combination of the other vectors, then the vectors of the set are said to be *linearly independent*. An  $n$ -dimensional vector space has exactly  $n$  linearly independent vectors.

## A.2 Properties of matrices

### A.2.1 Rectangular matrices

A rectangular matrix is an array of elements with  $l_r$  rows and  $l_c$  columns. Taking the product of two rectangular matrices  $\mathbb{A}$  and  $\mathbb{B}$  requires that  $l_c(\mathbb{A}) = l_r(\mathbb{B})$ , and the resultant matrix,  $\mathbb{A}\mathbb{B}$ , is an  $l_r(\mathbb{A}) \times l_c(\mathbb{B})$  matrix. The product is

$$(\mathbb{A}\mathbb{B})_{ik} = \sum_{j=1}^{l_c(\mathbb{A})} A_{ij} B_{jk} \quad (l_c(\mathbb{A}) = l_r(\mathbb{B})).$$

Rectangular matrices and allowed products obey the *associative* law, but the *trace*, *determinant*, and *inverse* are not defined for non-square matrices.

The scalar product of two vectors is equivalent to matrix multiplication of a  $(1 \times l)$  matrix by an  $(l \times 1)$  matrix to produce a  $1 \times 1$  matrix (a scalar).

Rectangular matrices can be partitioned into rectangular submatrices. For example, let  $\mathbb{U}$  and  $\mathbb{V}$  be matrices that can be multiplied in the order  $\mathbb{U}\mathbb{V}$ . Partition these matrices as shown below:

$$\mathbb{U} = \begin{pmatrix} u_{11} & u_{12} & u_{13} \\ u_{21} & u_{22} & u_{23} \end{pmatrix}, \quad \mathbb{V} = \begin{pmatrix} v_{11} \\ v_{12} \\ v_{13} \end{pmatrix}.$$

The product is

$$\mathbb{U}\mathbb{V} = \begin{pmatrix} u_{11}v_{11} + u_{12}v_{12} + u_{13}v_{13} \\ u_{21}v_{11} + u_{22}v_{12} + u_{23}v_{13} \end{pmatrix},$$

where the  $us$  and  $vs$  are themselves matrices of appropriate dimensions. That is, the partitioned matrices follow the same multiplication law as regular rectangular matrices. The partitioning is rather arbitrary, provided that all of the products of the submatrices meet the requirement that the number of columns of the left submatrix is equal to the number of rows of the right submatrix. For example, the number of columns of  $u_{11}$  and  $u_{21}$  must equal the number of rows of  $v_{11}$ . Partitioned matrices are sometimes called *supermatrices*.

### A.2.2 Definitions and properties of square matrices

Some of the properties of square matrices are listed below.

1. Let the elements of  $\mathbb{A}$  be  $A_{ij}$ . The *transpose* of  $\mathbb{A}$ , denoted by  $\mathbb{A}^T$ , is obtained by interchanging the rows and columns of  $\mathbb{A}$ :  $[\mathbb{A}^T]_{ij} = A_{ji}$ .
2. The Hermitian conjugate of  $\mathbb{A}$  is  $\mathbb{A}^\dagger = [\mathbb{A}^T]^*$ .
3. A matrix is unitary if  $\mathbb{A}^{-1} = \mathbb{A}^\dagger = [\mathbb{A}^T]^*$ .
4. The rows (or the columns) of a unitary matrix form a set of  $n$  orthogonal vectors.
5. The product of two unitary matrices is a unitary matrix.
6. A matrix for which  $\mathbb{A} = \mathbb{A}^\dagger$  is called *self-adjoint* or *Hermitian*. The eigenvalues of a Hermitian matrix are real numbers.
7. The *trace*, *spur*, or *character* of a matrix is the sum of its diagonal elements:  $\mathfrak{Tr}\{\mathbb{A}\} = \sum_i A_{ii}$ . Also,  $\mathfrak{Tr}\{\mathbb{A}\mathbb{B}\} = \mathfrak{Tr}\{\mathbb{B}\mathbb{A}\}$ , where “ $\mathfrak{Tr}\{ \}$ ” denotes the trace of the enclosed matrix.
8. The trace of  $\mathbb{A}$  is invariant under a similarity transformation:  $\mathfrak{Tr}\{\mathbb{A}\} = \mathfrak{Tr}\{\mathbb{S}^{-1}\mathbb{A}\mathbb{S}\}$ .
9. The determinant of the product of two square matrices is the product of the individual determinants:  $\det\{\mathbb{A}\mathbb{B}\} = \det\{\mathbb{A}\}\det\{\mathbb{B}\}$ . Therefore the determinant is invariant under a similarity transformation:  $\det\{\mathbb{S}^{-1}\mathbb{A}\mathbb{S}\} = \det\{\mathbb{A}\}$ . (The determinant of  $\mathbb{A}$  is often denoted by  $|\mathbb{A}|$ .)
10. The *identity* matrix, also called  $\mathbb{E}$ ,  $\mathbf{1}$ ,  $\mathbb{I}$ , or the *unit matrix* is a diagonal matrix with elements  $E_{ij} = \delta_{ij}$ .
11. If a square matrix has a non-zero determinant, then a unique inverse matrix,  $\mathbb{A}^{-1}$ , can be constructed that has the property that  $\mathbb{A}\mathbb{A}^{-1} = \mathbb{A}^{-1}\mathbb{A} = \mathbb{E}$ . The inverse of a product of two matrices is the product of the inverses in the opposite order:  $(\mathbb{A}\mathbb{B})^{-1} = \mathbb{B}^{-1}\mathbb{A}^{-1}$ .
12. If the elements of  $\mathbb{A}$  are  $A_{ij}$  and those of  $\mathbb{B}$  are  $B_{ij}$ , then the elements of  $\mathbb{A} + \mathbb{B}$  are  $(\mathbb{A} + \mathbb{B})_{ij} = A_{ij} + B_{ij}$ .
13. If  $c$  is a number, the elements of  $c\mathbb{A}$  are  $cA_{ij}$ .  $\mathfrak{Tr}\{c\mathbb{A}\} = c\mathfrak{Tr}\{\mathbb{A}\}$ , but  $\det\{c\mathbb{A}\} = c^n \det\{\mathbb{A}\}$ , where  $n$  is the dimensionality of  $\mathbb{A}$ .

14. The form of a matrix equation remains unchanged by a similarity transformation of all of the matrices. If  $\mathbb{A} = f(\mathbb{B})$ , then  $\mathbb{A}' = f(\mathbb{B}')$  with  $\mathbb{A}' = \mathbb{S}^{-1}\mathbb{A}\mathbb{S}$  and  $\mathbb{B}' = \mathbb{S}^{-1}\mathbb{B}\mathbb{S}$ , where  $f$  is a function. For example, if  $\mathbb{A} = \sin(\mathbb{B})$ , then  $\mathbb{A}' = \sin(\mathbb{B}')$ .
15. The secular equation for an  $n$ -dimensional matrix  $\mathbb{A}$  is  $\det\{\mathbb{A} - \lambda\} = 0$ . This equation has  $n$  eigenvalues,  $\lambda_k$  ( $k = 1, 2, \dots, n$ ), which are the only values of  $\lambda$  for which the secular equation can be satisfied. For  $\lambda = \lambda_k$ , the matrix equation  $\mathbb{A} \xi^k = \lambda_k \xi^k$  has a non-trivial solution for the  $n$ -dimensional eigenvector  $\xi^k$ . When normalized, the eigenvectors form an orthonormal set of vectors that span an  $n$ -dimensional space.
16. *Diagonalizing a matrix.* Transforming a matrix to a diagonal form. This is usually accomplished by a similarity transformation:  $\mathbf{d} = \mathbb{V}^{-1}\mathbb{A}\mathbb{V}$ , where  $\mathbf{d}$  is a diagonal matrix whose elements are the eigenvalues of  $\mathbb{A}$ . That is,  $d_{ij} = \lambda_i \delta_{ij}$ . The *normalized eigenvectors*,  $\xi^k$ , arranged as columns of an  $n \times n$  matrix produce a *unitary* transformation,  $\mathbb{V}$ , that diagonalizes  $\mathbb{A}$ :  $\mathbb{V}^{-1}\mathbb{A}\mathbb{V} = \mathbf{d}$ , where  $V_{ij} = (\xi^j)_i$ .
17. Since the determinant of a matrix is invariant under similarity transformation, it follows from item 13 in this list that  $\det\{\mathbb{A}\} = \prod_k \lambda_k$ .
18. If  $f(\mathbb{A})$  is a function of the matrix  $\mathbb{A}$ , then  $f(\mathbb{A}) = \mathbb{V}f(\lambda)\mathbb{V}^{-1}$ , where  $f(\lambda)_{ij} = f(\lambda_i)\delta_{ij}$  and  $\mathbb{V}$  is the transformation that diagonalizes  $\mathbb{A}$  (see item 16 in this list). As examples,

$$\begin{aligned} [\cos(\mathbb{A})]_{ij} &= \sum_k V_{ik}^{-1} \cos(\lambda_k) V_{kj}, \\ [\mathbb{A} - \omega]_{ij}^{-1} &= \sum_k V_{ik}^{-1} (\lambda_k - \omega)^{-1} V_{kj}, \\ \ln[\det\{\mathbb{A}\}] &= \ln\left(\prod_k \lambda_k\right) = \sum_k \ln(\lambda_k). \end{aligned}$$

19. The *direct product* of two square matrices  $\mathbb{A}$  and  $\mathbb{B}$  is denoted by  $\mathbb{A} \otimes \mathbb{B}$  or  $\mathbb{A} \times \mathbb{B}$ . The matrix elements of  $\mathbb{A} \times \mathbb{B}$  use two sets of indices,

$$(\mathbb{A} \times \mathbb{B})_{ik,jl} = A_{ij} B_{kl}.$$

If  $\mathbb{A}$  and  $\mathbb{B}$  are square matrices then  $\mathbb{A} \times \mathbb{B}$  is a square matrix. However,  $\mathbb{A}$  and  $\mathbb{B}$  need not have the same dimensions.<sup>1</sup> If  $\mathbb{A}$  has  $l_A$  rows and columns and  $\mathbb{B}$  has  $l_B$  rows and columns then  $\mathbb{A} \times \mathbb{B}$  has  $l_A l_B$  rows and columns.

<sup>1</sup> The concept of the direct product of two matrices can be extended to rectangular matrices with appropriate dimensionalities.

20. Direct-product matrices multiply in the same manner as ordinary matrices if subscripts  $i$  and  $k$  are considered the “row” indices, with  $j$  and  $l$  the “column” indices,

$$[(\mathbb{A} \times \mathbb{B})(\mathbb{C} \times \mathbb{D})]_{ik,jl} = \sum_{mn} [\mathbb{A} \times \mathbb{B}]_{ik,mn} [\mathbb{C} \times \mathbb{D}]_{mn,jl}.$$

Here the number of columns of  $(\mathbb{A} \times \mathbb{B})$  should equal the number of rows of  $(\mathbb{C} \times \mathbb{D})$ .

21. From the rule of multiplication, it follows that

$$(\mathbb{A} \times \mathbb{B})(\mathbb{C} \times \mathbb{D}) = (\mathbb{A}\mathbb{C}) \times (\mathbb{B}\mathbb{D}).$$

22. The direct product of two diagonal matrices is a diagonal matrix.

# Appendix B

## Basics of point-group theory

### B.1 Definitions

Group theory is a very broad field of study. We shall look only at a narrow part of the field. We are concerned here with the application of group theory to the analysis of physical and chemical systems. For our discussions a group consists of elements (or operators) that mathematically represent operations that leave a system in an equivalent state. For our purposes group multiplication is the sequential application of symmetry operations or the multiplication of square matrices representing two symmetry operations. The *point group* of interest in the analysis of atoms, molecules, and solids is the *covering group*, which consists of the elements (or operators) of rotation, reflection, and inversion under which the atom, molecule, or solid remains invariant. For crystalline solids the group (*space group*) is enlarged to include rotations, reflections, and inversion combined with translations under which the crystalline solid remains invariant.

A *group* is a collection of distinct elements that possess the following four characteristics.

- (1) *Closure*. The product of any two elements is an element of the group. If  $A$  and  $B \in G$  and  $AB = C$ , then  $C \in G$  (the symbol  $\in$  means “belongs to” or “is a member of the set that follows”).
- (2) Every group must contain the *identity element*,  $E$ , which commutes with all elements of  $G$ :  $EA = AE = A$  for all  $A \in G$ .
- (3) Elements of the group obey the *associative* law:  $A(BC) = (AB)C$ .
- (4) Each element has an *inverse*. If  $A \in G$ , then  $A^{-1} \in G$ , where  $AA^{-1} = A^{-1}A = E$ .

The *order* of a group is the number of elements in the group, usually denoted by  $h$ .

A *subgroup*,  $\mathcal{G}$ , is a collection of elements of  $G$  (less than  $h_G$  in number) that satisfy the four requirements listed above. The subgroup  $\mathcal{G}$  is an *invariant* or *normal subgroup* if  $X_i \mathcal{G} X_i^{-1} = \mathcal{G}$ , for every  $X_i$  in  $G$ . If this is the case,  $\mathcal{G}$  consists of entire classes of elements. (The ordering of the elements appearing in  $X_i \mathcal{G} X_i^{-1}$  is irrelevant as long as all of the elements of  $\mathcal{G}$  occur once and only once.)

*Rotations.* A rotation of a system or object about an axis by  $2\pi/n$  that leaves the system or object in a configuration indistinguishable from its original configuration is a symmetry operation usually denoted by  $C_n$ . Here  $n$  denotes the number of such rotations resulting in the identity:  $(C_n)^n = E$ . The axis of rotation is said to be an  $n$ -fold axis of symmetry.

*Center of symmetry and inversion.* If a system or object possesses a center of symmetry, then it is invariant under the transformation of coordinates  $(x, y, z) \rightarrow (-x, -y, -z)$ . That is, the system or object is invariant under the operation,  $i$ , of inversion.

*Reflection.* If a system reflected through a line or plane of symmetry results in an equivalent system, the system is symmetric under the reflection. Such a reflection operation is an element of the covering group of the system. Elements of reflection are usually denoted by the symbol,  $\sigma$ .  $\sigma_h$  denotes reflection in a plane that bisects a principal rotation axis.  $\sigma_v$  denotes a reflection in a plane that includes a principal axis of rotation.  $\sigma_d$  denotes a reflection in a diagonal plane that includes the principal axis and bisects a pair of two-fold axes perpendicular to the principal axis. A reflection operation is its own inverse; that is,  $\sigma^2 = E$ .

*Improper rotation.* A rotation by  $2\pi/n$  followed by a reflection in a plane perpendicular to the rotation axis is an improper rotation denoted by  $S_n$ .

*Group multiplication table.* The rows and columns of a group multiplication table are labeled by the group elements. The table entries list the products of the row element times a column element in the order row  $\times$  column, as illustrated:

	$E$	$A_1$	$A_2$	$\dots$	$A_h$
$E$		$\downarrow$		$\dots$	
$A_1$		$\downarrow$		$\dots$	
$A_2$	$\rightarrow \rightarrow$	$A_2 A_1$		$\dots$	$A_2 A_h$
$\vdots$		$\vdots$		$\vdots$	
$A_h$		$A_h A_1$		$\dots$	

*Rearrangement theorem.* If all of the elements of  $G$  are multiplied by any element of  $G$  the result is  $G$  (ignoring the order of the elements so produced). That is,  $AG = G$  if  $A \in G$ .

*Proof.* Show that every element in  $G$  is also in  $AG$ . Show that no element of  $G$  occurs more than once in  $AG$ . Let  $C$  be an arbitrary element of  $G$ , then  $A^{-1}C \in G$ . Therefore  $A(A^{-1}C) = C$  is in  $AG$ . Suppose  $D$  occurs twice in  $AG$ , that is, there exist two distinct elements of  $G$ , say  $B_1$  and  $B_2$ , for which  $AB_1 = AB_2 = D$ . Multiplying by  $A^{-1}$  on the left gives  $B_1 = B_2$ . This contradicts the assumption that  $B_1$  and  $B_2$  are distinct. As a result of the rearrangement theorem, it follows that every row of the multiplication table contains each element of  $G$  once and only once. Also, every column of the multiplication table contains each element of  $G$  once and only once.  $\square$

### Conjugate elements and classes

Let  $A, B, C \in G$ . If  $C = B^{-1}AB$ , then  $A$  is conjugate to  $C$ . If  $C$  is conjugate to  $A$  and  $D$  is conjugate to  $A$ , then  $C$  is conjugate to  $D$ .

*Proof.* If  $C = B^{-1}AB$  and  $D = X^{-1}AX$ , then  $A = (BCB^{-1})$  and  $D = (X^{-1}B)C(B^{-1}X) = T^{-1}CT$ , where  $T \in G$ . Therefore  $C$  is conjugate to  $D$ .  $\square$

A complete set of distinct elements that are mutually conjugate forms a *class*. The identity is in a class by itself. An element can not be in more than one class.

*Proof.* Let  $K_1$  and  $K_2$  be two different classes of  $G$ . Assume that  $A \in K_1$  and also  $A \in K_2$ . For some element  $X \in G$ , we have  $X^{-1}AX = B \in K_1$ , and for some element  $Y \in G$ ,  $Y^{-1}AY = D \in K_2$ . Then,  $B$  and  $D$  are conjugates, and therefore belong to the same class. This contradicts the assumption that  $K_1$  and  $K_2$  are different classes. It follows that in the collection of all of the distinct classes of  $G$  every element of  $G$  occurs once and only once.  $\square$

If  $\mathcal{G}$  is an invariant subgroup of  $G$  then  $X_i\mathcal{G}X_i^{-1} = \mathcal{G}$  for every  $X_i$  in  $G$ . To prove this we show that every element of  $\mathcal{G}$  occurs once and only once in the product  $X_i\mathcal{G}X_i^{-1}$ . First we show that every element of  $\mathcal{G}$  is contained in the product  $X_i\mathcal{G}X_i^{-1}$ . Let  $C$  be an arbitrary element of  $\mathcal{G}$ , then  $B = X_i^{-1}CX_i$  must also be an element in  $\mathcal{G}$ , since  $C$  and  $B$  are conjugates and belong to the same class. Thus  $C = X_iBX_i^{-1} \in X_i\mathcal{G}X_i^{-1}$ . Therefore every element of  $\mathcal{G}$  occurs at least once in the product  $X_i\mathcal{G}X_i^{-1}$ . Since  $X_i\mathcal{G}X_i^{-1}$  has the same number of elements as  $\mathcal{G}$ , no element of  $X_i\mathcal{G}X_i^{-1}$  can occur more than once. Consequently, every element of  $\mathcal{G}$  occurs once and only once in  $X_i\mathcal{G}X_i^{-1}$ .

### Cosets

Let  $\mathcal{G}$  be a normal subgroup (invariant subgroup) of a group,  $G$ :  $\mathcal{G} = (S_1, S_2, S_3, \dots, S_n)$ , where the ordering of the elements is irrelevant. Multiplying  $\mathcal{G}$  by the elements  $X_i$  ( $i = 1, 2, \dots, h_G$ ) of the group  $G$  produces  $h_G$  left cosets (and  $h_G$  right cosets), where  $h_G$  is the number of elements in  $G$ :

$$L_i = X_i\mathcal{G} = \{X_iS_1, X_iS_2, X_iS_3, \dots, X_iS_n\} \quad (\text{left coset}),$$

$$R_i = \mathcal{G}X_i = \{S_1X_i, S_2X_i, S_3X_i, \dots, S_nX_i\} \quad (\text{right coset}).$$

If  $X_i$  is a member of  $\mathcal{G}$ , then  $L_i = R_i = \mathcal{G}$  by virtue of the rearrangement theorem. Therefore we now restrict our attention to  $X_i$  in  $G$  but not in  $\mathcal{G}$ . (Note that for a point group  $G$  this restriction means that no coset can be a subgroup, since none can contain the identity element.) In this case neither  $L_i$  nor  $R_i$  contains elements in common with those of  $\mathcal{G}$ . To show this for  $L_i$ , assume that some  $X_iS_j$  is a member of  $\mathcal{G}$ , say  $S_k$ . Then we have  $X_i = S_kS_j^{-1}$ , which belongs to  $\mathcal{G}$ . This contradicts our assumption that  $X_i$  is not in  $\mathcal{G}$ . A similar proof holds for a right coset.

It also follows that two cosets of  $\mathcal{G}$  are either identical or have no elements in common. Assume that two cosets  $L_i = X_i\mathcal{G}$  and  $L_j = X_j\mathcal{G}$  have a common element. Then,  $X_iS_k = X_jS_l$  for some elements  $S_k$  and  $S_l$  of  $\mathcal{G}$ . As a result  $X_j^{-1}X_i = S_lS_k^{-1}$  is then a member of  $\mathcal{G}$ , so  $X_j^{-1}X_i\mathcal{G} = \mathcal{G}$  by virtue of the rearrangement theorem. Multiplying on the left by  $X_j$  gives  $X_i\mathcal{G} = X_j\mathcal{G}$ , so the two cosets are identical if they have a common member. Among the  $h_G$  cosets generated by  $X_i\mathcal{G}$  ( $i = 1, 2, \dots, h_G$ ),  $h_s$  of them are identical to  $\mathcal{G}$  (except for the ordering of the elements), where  $h_s$  is the number of elements in  $\mathcal{G}$ . The remaining  $h_G - h_s$  left cosets have no elements of  $\mathcal{G}$ . However, some of these cosets may be identical. If we consider the collection of *distinct* cosets together with  $\mathcal{G}$ , every element of  $G$  can be found once and only once in the collection. Suppose there are  $n - 1$  distinct cosets, then we have

$$G = \{\mathcal{G}, L_1, L_2, L_3, \dots, L_{n-1}\}.$$

Note that each term on the right-hand side of the equation contains  $h_s$  elements. Therefore there are  $nh_s$  elements on the right-hand side. There are  $h_G$  terms on the left-hand side of the equation, so  $h_G = nh_s$  or  $h_G/h_s = n$  (an integer). (A similar proof can be constructed for right-hand cosets.) The above considerations show that the order,  $h_s$ , of an invariant (normal) subgroup is a divisor of the order of the full group.

### The factor group

Consider a group  $G$  with an invariant subgroup  $\mathcal{G}$  and  $n - 1$  distinct cosets so that

$$G = \{\mathcal{G}, L_1, L_2, L_3, \dots, L_{n-1}\}.$$

We may regard each  $\mathcal{G}$  and  $L_i$  as elements of a more complex group called the *factor group* of  $G$  with respect to the normal divisor  $\mathcal{G}$ .  $L_i = \{X_iS_1, X_iS_2, \dots, X_iS_{h_s}\}$  is regarded as a single complex element. Two complex elements are the same if they contain the same elements irrespective of the order of the elements. In addition, for the complex group multiplication  $L_iL_j$ ,  $\mathcal{G}L_i$ , or  $L_i\mathcal{G}$  *only the distinct terms are retained*. For this group of complexes  $\mathcal{G}$  plays the role of the identity,



since  $\mathcal{G} = \mathcal{G}^{-1}$ ,  $\mathcal{G}\mathcal{G} = \mathcal{G}$ , and  $L_i\mathcal{G} = (X_i\mathcal{G})\mathcal{G} = X_i\mathcal{G}\mathcal{G} = X_i\mathcal{G} = L_i$ . We define the inverse,  $L_i^{-1}$ , as  $\mathcal{G}^{-1}X_i^{-1}$  so that  $L_iL_i^{-1} = X_i\mathcal{G}\mathcal{G}^{-1}X_i^{-1} = X_i\mathcal{G}X_i^{-1} = X_iX_i^{-1}\mathcal{G} = \mathcal{G}$  (the identity). In a similar fashion  $L_i^{-1}L_i = \mathcal{G}$ . Finally we show that, for the elements of  $G$ ,  $X_iX_j = X_k$ , then  $L_iL_j = L_k$ , and  $L_k$  is a member of the factor group. That is, the factor group is closed under group multiplication. We have

$$L_iL_j = X_i\mathcal{G}L_j = X_iX_j\mathcal{G} = X_k\mathcal{G} = L_k.$$

If there are  $n - 1$  distinct cosets, then the factor group has  $n$  (complex) elements.

The number of elements in a class is a divisor of  $h_G$ , the number of elements in  $G$ .

Given two groups,  $G_1$  and  $G_2$ , whose elements commute, the *direct product* is denoted by  $G_1 \otimes G_2$  or  $G_1 \times G_2$ . If  $A_i$  ( $i = 1, 2, \dots, h_1$ ) denotes the elements of  $G_1$  and  $B_j$  ( $j = 1, 2, \dots, h_2$ ) the elements of  $G_2$ , then the  $h_1$  times  $h_2$  elements of  $G_1 \times G_2$  are all of the products,  $A_iB_j$ . The order of  $G_1 \times G_2$  is  $h_1h_2$ . See Appendix A, items 19–21 in the list in Section A.2.2.

### Point groups

*Abelian group.* All of the elements of an Abelian group commute with each other. That is, the order of the product of two elements is irrelevant:  $AB = BA$  for all  $A$  and  $B \in G$ .

*Cyclic group.* A cyclic group of order  $n$ , denoted as  $C_n$ , consists of the elements  $A, A^2, A^3, \dots, A^{n-1}, A^n$ , where  $A^n = E$ . All cyclic groups are Abelian.

*$C_i$  and  $C_s$ .* These are groups that have two elements:  $C_i = \{E, i\}$  and  $C_s = \{E, \sigma_d\}$

*$C_n$  groups.* A cyclic group of this type is the covering group of an  $n$ -sided, regular polygon. The elements include  $n$  rotations by  $2\pi/n$  about a perpendicular axis through the center of the polygon.

*$C_{nv}$  groups.* A group of this type is the covering group for a regular polygon prism. It contains the  $n$  rotations of  $C_n$  plus reflections in  $n$  vertical planes that contain the rotational axis and bisect the prism. For  $n$  odd, there are  $n$   $\sigma_v$  reflections. For  $n$  even there are  $n/2$   $\sigma_v$  and  $n/2$   $\sigma_d$  reflections. The planes make an angle of  $\pi/n$  with one another.

*$D_n$  groups.* A group of this type is also a covering group of an  $n$ -sided prism whose cross-section is a regular polygon. It includes the elements of  $C_n$ , and it has  $n$  polygon bisector lines through the center cross-section. If  $n$  is even, the elements include  $n/2$  rotations by  $\pi$  about bisector lines through vertices and  $n/2$  rotations by  $\pi$  about bisector lines through parallel sides. If  $n$  is odd, the elements include  $n$  rotations by  $\pi$  about the bisector lines through the vertices.

$C_{nh}$  groups. The elements of a group of this type are those of  $C_n$  and also  $n$  product elements,  $\sigma_h C_n$ .

$S_n$  groups. The group  $S_{2n+1}$  (odd number of elements) is the same as  $C_{nh}$ ;  $S_{2n}$  contains  $2n$  improper rotations.

$D_{nd}$  groups. The elements of these groups include the  $2n$  rotations of  $D_n$  and the  $2n$  product elements  $\sigma_d$  times the elements of  $D_n$ .

$D_{nh}$  groups. The elements of these groups includes the  $2n$  rotations of  $D_n$  and the  $2n$  product elements  $\sigma_h$  times the elements of  $D_n$ .

Groups associated with polyhedra. The five polyhedra of importance are depicted in Fig. B.1. The covering groups of the cube, octahedron, and tetrahedron are most often encountered.

$O$  and  $O_h$  groups. There are 24 elements in the octahedral,  $O$ , group (see Appendix E):  $E$ ,  $8C_3$ ,  $6C_4$ ,  $3C_2$  ( $=C_4^2$ ), and  $6\bar{C}_2$ . The  $O_h$  group has 48 elements, namely the 24 elements of  $O$  and  $i$  times each of the  $O$  elements:  $O_h = O \times i$ . These two groups apply to the symmetries of the cube and the octahedron. An alternate definition for  $O_h$  is the elements of  $O$  plus  $i$ ,  $6S_4$ ,  $8S_6$ ,  $3\sigma_h$ , and  $6\sigma_d$ .

$T$ ,  $T_h$ , and  $T_d$  groups. The  $T$  group has 12 elements:  $E$ ,  $4C_3$ ,  $4C_3^2$ , and  $3C_2$ . The elements of  $T_h$  are the elements of  $T$  plus  $i$  times the elements of  $T$ :  $T_h = T \times i$ . The elements of  $T_d$  are the elements of  $T$  plus  $\sigma_d$  times the elements of  $T$ :  $T_d = T \times C_s$ . These groups apply to the symmetries of tetrahedra (see Appendix F).

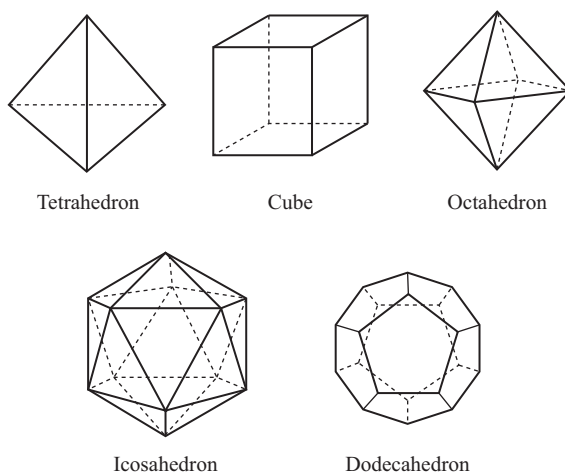


Figure B.1 The five regular convex polyhedra.

### B.1.1 Symmetry operators

Rotation, reflection, translation, or inversion of coordinates can be accomplished by a real, orthogonal transformation  $R$  such that  $\mathbf{r}' = R\mathbf{r}$  or, in terms of components,  $r'_i = \sum_j R_{ij}r_j$ . The inverse transformation is  $R^{-1}\mathbf{r}' = \mathbf{r}$ , where  $R^{-1} = R^T$  with superscript T denoting the transpose. With a group  $G = \{A_\alpha\}$  consisting of rotations, reflections, and inversion we may associate a transformation matrix  $R_\alpha$  that induces the operation corresponding to  $A_\alpha$ . The set of transformation matrices  $\{R_\alpha\}$  form a group isomorphic to  $G$ . These matrices transform (rotate, reflect, translate, or invert) the coordinates of a system.

We may also define operators that transform a function. These operators, denoted by  $P(R_\alpha)$ , transform a function,  $f(\mathbf{r})$ , in a manner defined by

$$P(R_\alpha)f(\mathbf{r}) = f(R_\alpha^{-1}\mathbf{r}). \quad (\text{B.1})$$

The set of operators  $\{P(R_\alpha)\}$  form a group that is isomorphic to  $G$ . Conceptually, we may think of  $P(R_\alpha)$  as an operator that rotates (reflects, translates, or inverts) the function but leaves the coordinate system unchanged.

## B.2 Matrix representations of groups

A matrix representation of a group  $G$  is a set of matrices  $\{\mathbb{D}(A_i)\}$  that obey the group multiplication table of  $G$ . That is, if  $A_i A_j = A_k$ , then  $\mathbb{D}(A_i)\mathbb{D}(A_j) = \mathbb{D}(A_k)$ . It follows that  $\mathbb{D}(A_i^{-1}) = [\mathbb{D}(A_i)]^{-1}$ . The representation matrices may be assumed to be square, unitary matrices with non-vanishing determinants. The number of distinct representation matrices is less than or equal to the number of elements,  $h$ , of  $G$ . If there is a one-to-one correspondence between  $A_i$  and  $\mathbb{D}(A_i)$  the representation is said to be faithful and the set of representation matrices is isomorphic to  $G$ . If the representation matrices obey the multiplication table of  $G$ , but their number is less than  $h$ , the set is homomorphic to  $G$ .

The character,  $\chi$ , of a representation matrix  $\mathbb{D}(A_i)$  is the sum of the diagonal elements, namely the trace of the matrix:  $\chi(A_i) = \sum_\alpha D_{\alpha\alpha}(A_i)$ . The character of a representation matrix is unchanged by a similarity transformation,  $\mathbb{S}$ .

Let  $\mathbb{D}'(A_i) = \mathbb{S}^{-1} \mathbb{D}(A_i) \mathbb{S}$  (similarity transformation). Then

$$\begin{aligned} \chi'(A_i) &= \sum_{\alpha\beta\gamma} S_{\alpha\beta}^{-1} D_{\beta\gamma}(A_i) S_{\gamma\alpha} = \sum_{\beta\gamma} \left[ \sum_{\alpha} S_{\gamma\alpha} S_{\alpha\beta}^{-1} \right] D_{\beta\gamma}(A_i) \\ &= \sum_{\beta\gamma} \delta_{\gamma\beta} D_{\beta\gamma}(A_i) = \sum_{\beta} D_{\beta\beta}(A_i) = \chi(A_i). \end{aligned}$$

Hence,  $\chi[\mathbb{D}(A_i)] = \chi[\mathbb{D}'(A_i)]$ . It follows that the characters of elements or operators belonging to the same class are equal.

A matrix representation that can be block-diagonalized (cast in a form consisting of smaller unconnected blocks along the diagonal) by a similarity transformation is “reducible”. A matrix representation that can not be reduced to smaller blocks by a similarity transformation is “irreducible”. The same block-diagonalization must be achieved *for all of the representation matrices by the same similarity transformation*.

For any group,  $G$ , it is always possible to find a similarity transformation,  $\mathbb{S}$ , that block-diagonalizes the representation matrices of  $G$  into blocks that are all irreducible. For physical systems whose states are characterized by eigenvectors and eigenvalues, the irreducible representations (IRs) are associated with quantities that are conserved in the dynamics of the system. The IRs of a quantum system are associated with the “good” quantum numbers.

Consider a set of functions  $\{f(\mathbf{r})_k\}$ ,  $k = 1, 2, \dots, n$ , that transform among themselves under the operators  $P(R_\alpha)$ . That is,

$$P(R_\alpha) f(\mathbf{r})_k = \sum_{m=1}^n f(\mathbf{r})_m D_{mk}(R_\alpha), \quad (\text{B.2})$$

where the set of  $D_{mk}(R_\alpha)$  are real constants. If we define an  $n$ -column vector,  $F$ , whose columns are the functions  $f(\mathbf{r})_1, f(\mathbf{r})_2, \dots, f(\mathbf{r})_n$ , then the  $D_{mk}(R_\alpha)$ s are the matrix elements of an  $n \times n$  matrix transformation,

$$P(R_\alpha)F = F\mathbb{D}(R_\alpha). \quad (\text{B.3})$$

In bra-ket notation the transformation that rotates the functions for fixed coordinate axes is  $P(R_\alpha)|f_1, f_2, f_3, \dots, f_n\rangle = \langle f_1, f_2, f_3, \dots, f_n|D(R_\alpha)$ .

Rotating the coordinate axes would give the transformation  $R_\alpha|f_1, f_2, f_3, \dots, f_n\rangle = D(R_\alpha)|f_1, f_2, f_3, \dots, f_n\rangle$ . The transformation  $R_\alpha^{-1}|f_1, f_2, f_3, \dots, f_n\rangle = D(R_\alpha^{-1})|f_1, f_2, f_3, \dots, f_n\rangle$  is equivalent to the transformation given in Eq. (B.2).

We have  $R_\alpha^{-1}f_k = \sum_m D(R_\alpha^{-1})_{km}f_m = \sum_m f_m D(R_\alpha)_{mk}$  or  $P(R_\alpha)F = FD(R_\alpha)$ , which is the same as Eq. (B.3). A clockwise rotation is the inverse of a counter-clockwise rotation, so we have that  $P(R_\alpha^{\text{R.H.}})f = R^{\text{L.H.}}f$ , where the superscripts R.H. and L.H. refer to right-hand and left-hand screw-rule conventions, respectively.

The set of matrices  $\mathbb{D}(R_\alpha)$  forms an  $n \times n$  matrix representation of  $G$  that may be reducible or irreducible, depending on the set of functions  $f(\mathbf{r})_k$ . The proof that  $\mathbb{D}(R_\alpha)$  forms a group is as follows. Let  $R$  and  $S$  be elements of  $G$ , then

$$\begin{aligned} P(S)P(R)f_k &= P(S)\sum_m f_m D_{mk}(R) = \sum_{m,n} D_{mk}(R)f_n D_{nm}(S) \\ &= \sum_n f_n \left[ \sum_m D_{nm}(S) D_{mk}(R) \right] = \sum_n f_n [\mathbb{D}(S)\mathbb{D}(R)]_{nk}. \end{aligned} \quad (\text{B.4})$$

On the other hand, since  $T = SR \in G$  according to (B.2),

$$P(T) f_k = \sum_n f_n D_{nk}(T) = \sum_n f_n D_{nk}(SR). \quad (\text{B.5})$$

On comparing (B.4) and (B.5) we can conclude that  $\mathbb{D}(SR) = \mathbb{D}(S)\mathbb{D}(R)$ , and therefore the matrices form a representation of  $G$ .

The functions  $\{f(\mathbf{r})_k\}$  are called the basis functions for the  $\mathbb{D}$  representation, and  $f(\mathbf{r})_m$  is called the basis for the  $m$ th row of the  $\mathbb{D}$  representation. The  $p$ -fold, degenerate wavefunctions of a quantum-mechanical system (solutions to Schrödinger's equation, for example) are basis functions for a  $p$ -dimensional representation of the group of the Hamiltonian.

Note that  $R_\alpha$  and  $P(R_\alpha)$  are defined differently.  $R_\alpha$  rotates the coordinate system with the function fixed, while  $P(R_\alpha)$  rotates the function with the coordinate system fixed.

### B.3 Properties of representations

1. Any two representations related by a similarity transformation are equivalent. If  $\mathbb{D}$  and  $\mathbb{D}'$  are matrix representations of  $G$ , they are equivalent if  $\mathbb{D}' = \mathbb{S}^{-1} \mathbb{D} \mathbb{S}$ . Equivalent here means that the matrices of  $\mathbb{D}$  and  $\mathbb{D}'$  satisfy the same group multiplication table, and have the same classes and characters.

2. For non-magnetic groups, any matrix representation with non-vanishing determinants is equivalent to a representation for which the matrices are all unitary and  $\mathbb{D}(R)^{-1} = \mathbb{D}(R)^*_T$ . Therefore we may assume that all of the representation matrices are square, unitary matrices with non-zero determinants.

3. The characters of the elements (operators) belonging to the same class are equal.

#### B.3.1 Irreducible representations

1. The number of inequivalent IRs of a group is equal to the number of classes of the group.

2. The sum of the squares of the dimensions of all the inequivalent IRs of a group is equal to the order of the group:  $\sum_i l_i^2 = h$ , where  $l_i$  is the dimension of the  $i$ th IR.

3. The characters of the elements (operators) of the IRs of a group are orthogonal:

$$\frac{1}{h} \sum_R \chi^i(R)^* \chi^j(R) = \delta_{ij}, \quad (\text{B.6})$$

where  $i$  and  $j$  label the IRs of the group.

4. *Schur's lemma.* Any matrix that commutes with all the matrices of an IR is a constant matrix, that is, a multiple of the unit matrix. Conversely, if a non-constant matrix commutes with all of the matrices of a representation, the representation is reducible.

5. Let  $\mathbb{D}^{(i)}$  and  $\mathbb{D}^{(j)}$  be two *inequivalent* IRs of the same group with dimensions  $l_1$  and  $l_2$ , respectively. Suppose that there exists a matrix  $\mathbb{H}$  with  $l_1$  rows and  $l_2$  columns that satisfies the condition

$$\mathbb{D}^{(j)}(R) \mathbb{H} = \mathbb{H} \mathbb{D}^{(i)}(R) \quad (\text{for all } R \text{ in the group}). \quad (\text{B.7})$$

Then (a) if  $l_1 \neq l_2$ ,  $\mathbb{H} = 0$  or (b) if  $l_1 = l_2$ , either  $\mathbb{H} = 0$  or  $\det(\mathbb{H}) \neq 0$ . If  $\det(\mathbb{H}) \neq 0$ ,  $\mathbb{H}$  has an inverse, and therefore  $\mathbb{D}^{(i)}$  and  $\mathbb{D}^{(j)}$  are equivalent representations, contradicting the initial assumption. Therefore a matrix  $\mathbb{H}$  satisfying (B.7) is a null matrix.

6. *The great orthogonality theorem.* Let  $\mathbb{D}^{(i)}$ ,  $i = 1, 2, \dots, N_c$ , represent the  $i$ th IR of a group, where  $N_c$  is the number of classes of the group. The matrix elements of different IRs are orthogonal,

$$\sum_R D_{mn}^{(i)}(R)^* D_{pq}^{(j)}(R) = \frac{h}{l_i} \delta_{ij} \delta_{mp} \delta_{nq}. \quad (\text{B.8})$$

We sketch the proof of this theorem here. Let  $\mathbb{D}^{(i)}$  and  $\mathbb{D}^{(j)}$  be two inequivalent IRs of  $G$ . The matrix

$$\mathbb{H} = \sum_R \mathbb{D}^{(j)}(R) \mathbb{K} \mathbb{D}^{(i)}(R^{-1}), \quad (\text{B.9})$$

where  $\mathbb{K}$  is an arbitrary, rectangular matrix of dimensions  $l_1$  rows  $\times$   $l_2$  columns, satisfying item 5 in the list above, namely that  $\mathbb{D}^{(j)}(P) \mathbb{H} = \mathbb{H} \mathbb{D}^{(i)}(P)$  for all  $P$  in the group. The proof is as follows:

$$\begin{aligned} \mathbb{D}^{(j)}(P) \mathbb{H} &= \sum_R \mathbb{D}^{(j)}(P) \mathbb{D}^{(j)}(R) \mathbb{K} \mathbb{D}^{(i)}(R^{-1}) \\ &= \sum_R \mathbb{D}^{(j)}(P) \mathbb{D}^{(j)}(R) \mathbb{K} \mathbb{D}^{(i)}(R^{-1}) \mathbb{D}^{(j)}(P^{-1}) \mathbb{D}^{(i)}(P) \\ &= \left\{ \sum_R \mathbb{D}^{(j)}(PR) \mathbb{K} \mathbb{D}^{(i)}(R^{-1}P^{-1}) \right\} \mathbb{D}^{(i)}(P) = \mathbb{H} \mathbb{D}^{(i)}(P). \end{aligned}$$

According to item 5 in the list above,  $\mathbb{H} = 0$ . Since the matrix  $\mathbb{K}$  is arbitrary, we can select its elements. Suppose  $\mathbb{K}$  has only one non-zero element,  $K_{rs} = \delta_{r\alpha} \delta_{s\beta}$ . Then we have

$$\begin{aligned} H_{\gamma\nu} &= \sum_R \sum_{m,n} D_{\gamma m}^{(j)}(R) \delta_{m\alpha} \delta_{n\beta} D_{n\nu}^{(i)}(R^{-1}) = \sum_R D_{\gamma\alpha}^{(j)}(R) D_{\beta\nu}^{(i)}(R^{-1}) \\ &= \sum_R D_{\nu\beta}^{(i)}(R)^* D_{\gamma\alpha}^{(j)}(R) = 0, \end{aligned} \quad (\text{B.10})$$

where the unitary feature  $\mathbb{D}^{(i)}(R^{-1}) = \mathbb{D}^{(i)}(R)_{\mathbb{T}}^*$  is used to arrive at the final result in (B.10). This establishes the orthogonality of the matrix elements of inequivalent IRs.

For equivalent IRs we use the matrix

$$\mathbb{H} = \sum_R \mathbb{D}^{(i)}(R) \mathbb{K} \mathbb{D}^{(i)}(R^{-1}), \quad (\text{B.11})$$

which commutes with all of the matrices of  $\mathbb{D}^{(i)}$ . Employing Schur's lemma (item 4 in the list above), we have  $\mathbb{H} = c \mathbb{I}$ , where  $c$  is a constant and  $\mathbb{I}$  is an  $l_i \times l_i$  unit matrix. Writing (B.11) in subscript form gives

$$H_{\gamma\nu} = \sum_R \sum_{m,n} D_{\gamma m}^{(i)}(R) K_{mn} D_{nv}^{(i)}(R^{-1}) = c \delta_{\gamma\nu}. \quad (\text{B.12})$$

Now choose the arbitrary matrix  $\mathbb{K}$  to have only a single non-zero element,  $K_{mn} = \delta_{m,\alpha} \delta_{n,\beta}$ , so that

$$\begin{aligned} H_{\gamma\nu} &= \sum_R \sum_m D_{\gamma m}^{(i)}(R) \delta_{m\alpha} \delta_{n\beta} D_{nv}^{(i)}(R^{-1}) \\ &= \sum_R D_{\gamma\alpha}^{(i)}(R) D_{\beta\nu}^{(i)}(R^{-1}) = c \delta_{\gamma\nu}. \end{aligned} \quad (\text{B.13})$$

For the diagonal element we have

$$H_{\gamma\gamma} = \sum_R D_{\gamma\alpha}^{(i)}(R) D_{\beta\gamma}^{(i)}(R^{-1}) = c. \quad (\text{B.14})$$

Choose  $\alpha = \beta$  and sum over the index  $\gamma$ . The right-hand side yields

$$\sum_R \sum_{\gamma} D_{\gamma\alpha}^{(i)}(R) D_{\alpha\gamma}^{(i)}(R^{-1}) = \sum_R D_{\alpha\alpha}^{(i)}(E) = \sum_R I = h. \quad (\text{B.15})$$

The left-hand side of (B.14) gives

$$\sum_{\gamma} c = l_i c,$$

where  $l_i$  is the dimensionality of the  $D^{(i)}$  IR. Using (B.15) and (B.16) gives  $c = h/l_i$ . Using this result in (B.14) with  $\alpha = \beta$  yields

$$\sum_R D_{\alpha\gamma}^{(i)}(R) D_{\gamma\alpha}^{(i)}(R^{-1}) = \sum_R [D_{\alpha\gamma}^{(i)}(R^{-1})]^* D_{\alpha\gamma}^{(i)}(R) = \frac{h}{l_i}. \quad (\text{B.16})$$

Equations (B.10) and (B.16) can be combined to give the general result

$$\sum_R D_{\nu\beta}^{(i)}(R)^* D_{\gamma\alpha}^{(j)}(R) = \frac{h}{l_i} \delta_{ij} \delta_{\beta\alpha} \delta_{\gamma\nu}. \quad (\text{B.17})$$

Renaming the indices in (B.17) as  $\nu = m$ ,  $\beta = n$ ,  $\gamma = p$ , and  $\alpha = q$  gives (B.8).

#### B.4 The projection operator (symmetry-function-generating machine)

Suppose we have a set of normalized basis functions  $\{f^{(\alpha)}(\mathbf{r})_k\}$  for the  $\alpha$ th IR of a group,  $G$ , where  $k = 1, 2, \dots, l_\alpha$ . The function  $f^{(\alpha)}(\mathbf{r})_m$ , hereafter denoted as simply  $f_m^{(\alpha)}$ , is a basis function for the  $m$ th row of the  $\alpha$ th IR. The functions in the set  $\{f_k^{(\alpha)}\}$  are called partners or partner basis functions. Under the operations of  $G$ ,  $f_m^{(\alpha)}$  transforms into linear combinations of the set of partner functions, and the coefficients are the matrix elements of the  $\alpha$ th IR of  $G$ :

$$P(R) f_m^{(\alpha)} = \sum_n f_n^{(\alpha)} D_{nm}^{(\alpha)}(R). \quad (\text{B.18})$$

If we multiply both sides of (B.18) by  $[D_{n'm'}^{(\beta)}(R)]^*$  and sum over all the operations of the group, we arrive at

$$\sum_R P(R) f_m^{(\alpha)} D_{n'm'}^{(\beta)}(R)^* = \sum_n f_n^{(\alpha)} \left[ \sum_R D_{nm}^{(\alpha)}(R) D_{n'm'}^{(\beta)}(R)^* \right]. \quad (\text{B.19})$$

Applying the orthogonality theorem, (B.8), to the right-hand side of (B.19) yields

$$\sum_n f_n^{(\alpha)} \frac{h}{l_\alpha} \delta_{\alpha\beta} \delta_{nn'} \delta_{mm'} = \frac{h}{l_\alpha} f_{n'}^{(\alpha)} \delta_{\alpha\beta} \delta_{mm'}. \quad (\text{B.20})$$

Equating the result of (B.20) to the left-hand side of (B.19) gives

$$\sum_R D_{n'm'}^{(\beta)}(R)^* P(R) f_m^{(\alpha)} = \frac{h}{l_\alpha} f_{n'}^{(\alpha)} \delta_{\alpha\beta} \delta_{mm'}. \quad (\text{B.21})$$

We define the projection operator,  $\mathcal{P}_{n'm'}^{(\beta)}$ , as

$$\mathcal{P}_{n'm'}^{(\beta)} = \sum_R D_{n'm'}^{(\beta)}(R)^* P(R), \quad (\text{B.22})$$

and have that

$$\mathcal{P}_{n'm'}^{(\beta)} f_m^{(\alpha)} = \frac{h}{l_\alpha} f_{n'}^{(\alpha)} \delta_{\alpha\beta} \delta_{mm'}. \quad (\text{B.23})$$

Consider a function that is an arbitrary linear combination of the basis functions of all of the IRs of a group,

$$F = \sum_\gamma \sum_q c_q^{(\gamma)} f_q^{(\gamma)}, \quad (\text{B.24})$$

where  $c_n^{(\gamma)}$  are constant coefficients. If we operate on  $F$  with  $\mathcal{P}_{n'm'}^{(\beta)}$ , we obtain

$$\begin{aligned} \mathcal{P}_{n'm'}^{(\beta)} F &= \sum_\gamma \sum_q c_q^{(\gamma)} \left[ \mathcal{P}_{n'm'}^{(\beta)} f_q^{(\gamma)} \right] \\ &= \sum_\gamma \sum_q c_q^{(\gamma)} \frac{h}{l_\gamma} f_{n'}^{(\gamma)} \delta_{\gamma\beta} \delta_{qm'} = c_{m'}^{(\beta)} \frac{h}{l_\beta} f_{n'}^{(\beta)}. \end{aligned} \quad (\text{B.25})$$



Equation (B.25) shows that when the operator  $\mathcal{P}_{n'm'}^{(\beta)}$  operates on an arbitrary linear combination of the basis functions it projects out a function that is proportional to a basis function that belongs to the  $n$ 'th row of the  $\beta$ th IR of  $G$ . The projection operator can therefore be used to generate the basis functions (symmetry functions) starting with an arbitrary function that  $\mathcal{P}_{n'm'}^{(\beta)}$  can operate on. To employ this tool, one assumes an arbitrary function, applies  $\mathcal{P}_{n'm'}^{(\beta)}$  to the arbitrary function, and then normalizes the result. The function so produced will be either a null function or a function that can serve as the basis function for the  $n$ 'th row of the  $\beta$ th IR of  $G$ . The operator  $\mathcal{P}_{n'm'}^{(\beta)}$  is sometimes referred to as *the symmetry-function-generating machine*. The diagonal projection operator

$$\mathcal{P}_{nn}^{(\beta)} = \sum_R D_{nn}^{(\beta)}(R)^* P(R) \quad (\text{B.26})$$

may also be used to generate symmetry functions. In the case that  $D^{(\beta)}$  is a one-dimensional IR,  $D_{nn}^{(\beta)}(R)^* = \chi^{(\beta)}(R)^*$ , and (B.26) becomes

$$\mathcal{P}_{nn}^{(\beta)} = \sum_R \chi^{(\beta)}(R)^* P(R), \quad (\text{B.27})$$

where  $\chi^{(\beta)}(R)$  is the character of the operation for the  $\beta$ th, one-dimensional IR of  $G$ .

## B.5 Character and action tables

The character table for a group presents many useful pieces of information regarding the properties of the group. A typical character table is shown in Fig. B.2. The character table contains six essential pieces of information, as indicated in Fig. B.2.

- (1) The name of the group ( $C_{4v}$  in this case).
- (2) Names of the IRs of the group.
- (3) Classes of the group as headings for the columns.
- (4) The number of elements in each class.
- (5) The character of the class for a particular IR shown as a row.
- (6) Some of the basis functions for the IRs. Included are  $x$ ,  $y$ ,  $z$ , and infinitesimal rotations about the major axis,  $R_x$ ,  $R_y$ , and  $R_z$ . Other bilinear bases may also be listed.

All one-dimensional IRs are named  $A_i$  or  $B_i$ , where the index  $i$  is used to distinguish various IRs when needed. Two-dimensional IRs are labeled  $\mathcal{E}_i$ . Three-dimensional IRs are most often labeled  $T_i$ . If the group has a center of inversion, the labels of the IRs carry an additional subscript, either “ $g$ ” for symmetric under inversion or “ $u$ ” for antisymmetric under inversion. For example, for the  $O_h$  group,

		$C_{4v}$	(3) Elements of the group by class				
			$E$	$C_2$	$2C_4$	$2\sigma_v$	$(2\sigma_d)$
(6) Basis functions	$x^2 + y^2, z^2$	$A_1$	1	1	1	1	1
	$z$	$A_2$	1	1	1	-1	-1
	$x^2 - y^2$	$B_1$	1	1	-1	1	-1
	$xy$	$B_2$	1	1	-1	-1	1
	$xz, yz$	$E$	2	-2	0	0	0
	$\left. \begin{matrix} x, y \\ R_x, R_y \end{matrix} \right\}$						

Figure B.2 The character table for  $C_{4v}$ , illustrating the types of information contained therein.

Basis functions		$C_5(5)$	$E$	$C_5$	$C_5^2$	$C_5^3$	$C_5^4$
$x^2 + y^2, z^2$	$z, R_z$	$A$	1	1	1	1	1
$xz, yz$	$\left. \begin{matrix} x, y \\ R_x, R_y \end{matrix} \right\}$	$E'$	1	$\omega$	$\omega^2$	$\omega^3$	$\omega^4$
$x^2 - y^2, xy$		$E''$	1	$\omega^4$	$\omega^3$	$\omega^2$	$\omega$
			1	$\omega^2$	$\omega^4$	$\omega$	$\omega^3$
			1	$\omega^3$	$\omega$	$\omega^4$	$\omega^2$

$\omega = e^{2\pi i/5}$

Pairs of one-dimensional IRs whose bases are degenerate due to time-reversal symmetry

Figure B.3 The character table for  $C_5$ , showing pairs of one-dimensional IRs grouped together to form  $E$  representations.

one of the three-dimensional IRs is  $T_{2g}$ , indicating a three-dimensional IR for basis functions that are symmetric under inversion.

For cyclic groups and direct products with cyclic groups, pairs of one-dimensional basis functions may be degenerate due to time-reversal symmetry. In these cases the two IRs are grouped together and listed as a two-dimensional,  $E$ -type, representation. This feature is illustrated for  $C_5$  in Fig. B.3.

Some groups are specified as a direct product. An example is  $O_h = O \times i$ . Let  $\{R_\alpha\}$  denote the elements of  $O$ . Then the elements of  $O_h$  are  $\{R_\alpha, iR_\alpha\}$ . For such groups, the character table can be divided into four sectors. Denote the table of characters for the  $O$  group as  $X$ , then the table of characters of  $O_h$  is

$$\begin{matrix} g \\ u \end{matrix} \begin{pmatrix} X & X \\ X & -X \end{pmatrix},$$

where  $g$  indicates that the basis functions for the upper rows of IRs are symmetric under inversion and  $u$  indicates that the basis functions for the lower rows of IRs are antisymmetric under inversion. For more detail see the character table for  $O_h$  in Appendix C.

### B.5.1 The action table

For molecular vibrations the covering-group operations transform both the displacements and the atomic position numbers relative to a fixed coordinate system. A representation,  $\Gamma$ , of the group that is based on atomic displacements and atomic position numbers will consist of  $3N_a \times 3N_a$  matrices, where  $N_a$  is the number of atoms in the molecule. The action of an operator on displacements can be determined by considering separately the way in which the vector  $\mathbf{r}$  transforms under the operators of the group and the way in which the atomic position numbers change relative to the fixed coordinate system. A representation based on atomic displacements and atomic position numbers is the direct product of a representation  $\Gamma^r$  based on  $r_x$ ,  $r_y$ , and  $r_z$ , and  $\Gamma^{(\text{ap})}$  based on the atomic position numbers. That is,  $\Gamma^{(\text{molecule})} = \Gamma^r \times \Gamma^{(\text{ap})}$  (“ap” stands for “atomic positions”).

A similar result holds for molecular electronic states, in which case  $\Gamma^r$  is a representation based on how the orbitals alone transform. For vibrations of crystalline solids,  $N_a$  is the number of atoms per unit cell. For the LCAO electronic states of a crystalline solid,  $\Gamma^r$  is a representation that is based on the way in which the orbitals in the central unit cell transform under the group of the wavevector.

An “*action table*” is a convenient, compact method for obtaining the information needed to construct  $\Gamma^r \times \Gamma^{(\text{ap})}$ . Use of an action table is first discussed in Chapter 1. Action tables for the octahedral and tetrahedral groups are given in Appendices E and F, respectively.

# Appendix C

## Character tables for point groups

$C_1(1)$	$E$
$A$	1

$h = 1$

$C_2(2)$		$E$	$C_2$
$x^2, y^2, z^2, xy$	$z, R_z$	$A$	1
$yz, zx$	$x, y$	$B$	1
	$R_x, R_y$		-1

$h = 2$

$C_3(3)$		$E$	$C_3$	$C_3^2$
$x^2 + y^2, z^2$	$z, R_z$	$A$	1	1
$yz, zx$	$x, y$	$\mathcal{E}$	$\omega$	$\omega^2$
$x^2 - y^2, xy$	$R_x, R_y$		$\omega^2$	$\omega$

$\omega = e^{2\pi i/3}$   
 $h = 3$

$C_4(4)$		$E$	$C_2$	$C_4$	$C_4^3$
$x^2 + y^2, z^2$	$z, R_z$	$A$	1	1	1
$x^2 - y^2, xy$		$B$	1	-1	-1
$yz, zx$	$x, y$	$\mathcal{E}$	$\begin{Bmatrix} 1 \\ 1 \end{Bmatrix}$	$\begin{Bmatrix} -1 \\ -1 \end{Bmatrix}$	$\begin{Bmatrix} i \\ -i \end{Bmatrix}$
	$R_x, R_y$				

$h = 4$

$C_5(5)$			$E$	$C_5$	$C_5^2$	$C_5^3$	$C_5^4$
$x^2 + y^2, z^2$	$z, R_z$	$A$	1	1	1	1	1
$xz, yz$	$x, y$	$\mathcal{E}'$	$\left\{ \begin{array}{c} 1 \\ 1 \end{array} \right.$	$\omega$	$\omega^2$	$\omega^3$	$\omega^4$
	$R_x, R_y$		$\left\{ \begin{array}{c} 1 \\ 1 \end{array} \right.$	$\omega^4$	$\omega^3$	$\omega^2$	$\omega$
$x^2 - y^2, xy$		$\mathcal{E}''$	$\left\{ \begin{array}{c} 1 \\ 1 \end{array} \right.$	$\omega^2$	$\omega^4$	$\omega$	$\omega^3$
			$\left\{ \begin{array}{c} 1 \\ 1 \end{array} \right.$	$\omega^3$	$\omega$	$\omega^4$	$\omega^2$

$$\omega = e^{2\pi i/5}$$

$$h = 5$$

$C_6(6)$			$E$	$C_6$	$C_3$	$C_2$	$C_3^2$	$C_6^5$
$x^2 + y^2, z^2$	$z, R_z$	$A$	1	1	1	1	1	1
		$B$	1	-1	1	-1	1	-1
$xz, yz$	$x, y$	$\mathcal{E}'$	$\left\{ \begin{array}{c} 1 \\ 1 \end{array} \right.$	$\omega$	$\omega^2$	$\omega^3$	$\omega^4$	$\omega^5$
	$R_x, R_y$		$\left\{ \begin{array}{c} 1 \\ 1 \end{array} \right.$	$\omega^5$	$\omega^4$	$\omega^3$	$\omega^2$	$\omega$
$x^2 - y^2, xy$		$\mathcal{E}''$	$\left\{ \begin{array}{c} 1 \\ 1 \end{array} \right.$	$\omega^2$	$\omega^4$	1	$\omega^2$	$\omega^4$
			$\left\{ \begin{array}{c} 1 \\ 1 \end{array} \right.$	$\omega^4$	$\omega^2$	1	$\omega^4$	$\omega^2$

$$\omega = e^{2\pi i/6}$$

$$h = 6$$

$C_{2v}(2mm)$			$E$	$C_2$	$\sigma_v$	$\sigma'_v$
$x^2, y^2, z^2$	$z$	$A_1$	1	1	1	1
$xy$	$R_z$	$A_2$	1	1	-1	-1
$xz$	$R_y, x$	$B_1$	1	-1	1	-1
$yz$	$R_x, y$	$B_2$	1	-1	-1	1

$$h = 4$$

$C_{3v}(3m)$			$E$	$2C_3$	$3\sigma_v$
$x^2 + y^2, z^2$	$z$	$A_1$	1	1	1
	$R_z$	$A_2$	1	1	-1
$yz, zx$	$x, y$	$\mathcal{E}$	$\left\{ \begin{array}{c} 1 \\ 1 \end{array} \right.$	$\left\{ \begin{array}{c} 2 \\ -1 \end{array} \right.$	$\left\{ \begin{array}{c} 1 \\ 1 \end{array} \right.$
$x^2 - y^2, xy$	$R_x, R_y$		$\left\{ \begin{array}{c} 1 \\ 1 \end{array} \right.$	$\left\{ \begin{array}{c} 2 \\ -1 \end{array} \right.$	$\left\{ \begin{array}{c} 1 \\ 1 \end{array} \right.$

$$h = 6$$

$C_{4v}(4mm)$			$E$	$C_2$	$2C_4$	$2\sigma_v$	$2\sigma_d$
$x^2 + y^2, z^2$	$z$	$A_1$	1	1	1	1	1
	$R_z$	$A_2$	1	1	1	-1	-1
$x^2 - y^2$		$B_1$	1	1	-1	1	-1
$xy$		$B_2$	1	1	-1	-1	1
$xz, yz$	$x, y$	$\mathcal{E}$	$\left\{ \begin{array}{c} 2 \\ -2 \end{array} \right.$	$\left\{ \begin{array}{c} 0 \\ 0 \end{array} \right.$	$\left\{ \begin{array}{c} 0 \\ 0 \end{array} \right.$	$\left\{ \begin{array}{c} 0 \\ 0 \end{array} \right.$	$\left\{ \begin{array}{c} 0 \\ 0 \end{array} \right.$
	$R_x, R_y$		$\left\{ \begin{array}{c} 2 \\ -2 \end{array} \right.$	$\left\{ \begin{array}{c} 0 \\ 0 \end{array} \right.$	$\left\{ \begin{array}{c} 0 \\ 0 \end{array} \right.$	$\left\{ \begin{array}{c} 0 \\ 0 \end{array} \right.$	$\left\{ \begin{array}{c} 0 \\ 0 \end{array} \right.$

$$h = 8$$

$C_{5v}(5m)$			$E$	$2C_5$	$2C_5^2$	$5\sigma_v$
$x^2 + y^2, z^2$	$z$	$A_1$	1	1	1	1
	$R_z$	$A_2$	1	1	1	-1
$yz, zx$	$\left. \begin{matrix} x, y \\ R_x, R_y \end{matrix} \right\}$	$\mathcal{E}_1$	2	$2\cos x$	$2\cos(2x)$	0
$x^2 - y^2, xy$		$\mathcal{E}_2$	2	$2\cos(2x)$	$2\cos(4x)$	0

$$\begin{aligned} x &= 2\pi/5 \\ h &= 10 \end{aligned}$$

$C_{6v}(6mm)$			$E$	$C_2$	$2C_3$	$2C_6$	$3\sigma_d$	$3\sigma_v$
$x^2 + y^2, z^2$	$z$	$A_1$	1	1	1	1	1	1
	$R_z$	$A_2$	1	1	1	1	-1	-1
		$B_1$	1	-1	1	-1	-1	1
		$B_2$	1	-1	1	-1	1	-1
$yz, zx$	$\left. \begin{matrix} x, y \\ R_x, R_y \end{matrix} \right\}$	$\mathcal{E}_1$	2	-2	-1	1	0	0
$x^2 - y^2, xy$		$\mathcal{E}_2$	2	2	-1	-1	0	0

$$h = 12$$

$C_{1h}(m)$			$E$	$\sigma_h$
$x^2, y^2, z^2, xy$	$x, y, R_z$	$A'$	1	1
$yz, zx$	$R_x, R_y, z$	$A''$	1	-1

$$h = 2$$

$C_{2h}(2/m)$			$E$	$C_2$	$\sigma_h$	$i$
$x^2, y^2, z^2, xy$	$R_z$	$A_g$	1	1	1	1
	$z$	$A_u$	1	1	-1	-1
$xz, yz$	$R_x, R_y$	$B_g$	1	-1	-1	1
	$x, y$	$B_u$	1	-1	1	-1

$$h = 4$$

$C_{3h} = C_3 \times \sigma_h(\bar{6})$			$E$	$C_3$	$C_3^2$	$\sigma_h$	$S_3$	$(\sigma_h C_3^2)$
$x^2 + y^2, z^2$	$R_z$	$A'$	1	1	1	1	1	1
	$z$	$A''$	1	1	1	-1	-1	-1
$x^2 - y^2, xy$	$x, y$	$\mathcal{E}'$	1	$\omega$	$\omega^2$	1	$\omega$	$\omega^2$
			1	$\omega^2$	$\omega$	1	$\omega^2$	$\omega$
$xz, yz$	$R_x, R_y$	$\mathcal{E}''$	1	$\omega$	$\omega^2$	-1	$-\omega$	$-\omega^2$
			1	$\omega^2$	$\omega$	-1	$-\omega^2$	$-\omega$

$$\begin{aligned} \omega &= e^{2\pi i/3} \\ h &= 6 \end{aligned}$$

$$C_{4h} = C_4 \times i(4/m)$$

$$C_{5h} = C_5 \times \sigma_h(\bar{1}0)$$

$$C_{6h} = C_6 \times i(6/m)$$

$$h = 8$$

$$h = 10$$

$$h = 12$$

$S_2(\bar{1})$			$E$	$i$
$x^2, y^2, z^2, xy, yz, zx$	$R_x, R_y, R_z$	$A_g$	1	1
	$x, y, z$	$A_u$	1	-1

$$h = 2$$

$S_4(\bar{4})$			$E$	$C_2$	$S_4$	$S_4^3$
$x^2 + y^2, z^2$	$R_z$	$A$	1	1	1	1
			$z$	$B$	-1	-1
$xz, yz$	$x, y$	$\mathcal{E}$	1	-1	$i$	$-i$
			$x^2 - y^2, xy$	$R_x, R_y$	-1	$-i$

$$h = 4$$

$$S_6 = C_3 \times i(\bar{3})$$

$$h = 6$$

$D_2(222)$			$E$	$C_2^z$	$C_2^y$	$C_2^x$
$x^2, y^2, z^2$		$A_1$	1	1	1	1
$xy$	$R_z, z$	$B_1$	1	1	-1	-1
$xz$	$R_y, y$	$B_2$	1	-1	1	-1
$yz$	$R_x, x$	$B_3$	1	-1	-1	1

$$h = 4$$

$D_3(32)$			$E$	$2C_3$	$3C_2'$
$x^2 + y^2, z^2$	$z, R_z$	$A_1$	1	1	1
			$A_2$	1	-1
$yz, zx$	$x, y$	$\mathcal{E}$	2	-1	0
			$x^2 - y^2, xy$	$R_x, R_y$	

$$h = 6$$

$D_4(422)$			$CE = C_4^2$	$2C_4$	$2C_2'$	$2C_2''$
$x^2 + y^2, z^2$	$R_z, z$	$A_1$	1	1	1	1
			$A_2$	1	1	-1
$x^2 - y^2$	$x, y$	$B_1$	1	1	-1	1
			$xy$	$B_2$	-1	-1
$xz, yz$	$x, y$	$\mathcal{E}$	2	-2	0	0
			$R_x, R_y$			

$$h = 8$$

$D_5(52)$		$E$	$2C_5$	$2C_5^2$	$5C_2'$
$x^2 + y^2, z^2$		$A_1$	1	1	1
$z, R_z$		$A_2$	1	1	-1
$yz, zx$	$\left. \begin{matrix} x, y \\ R_x, R_y \end{matrix} \right\}$	$\mathcal{E}_1$	2	$2\cos x$	$2\cos(2x)$
$x^2 - y^2, xy$		$\mathcal{E}_2$	2	$2\cos(2x)$	$2\cos(4x)$

$$\begin{aligned} x &= 2\pi/3 \\ h &= 10 \end{aligned}$$

$D_6(622)$		$E$	$C_2$	$2C_3$	$2C_6$	$3C_2'$	$3C_2''$
$x^2 + y^2, z^2$		$A_1$	1	1	1	1	1
$R_z, z$		$A_2$	1	1	1	-1	-1
		$B_1$	1	-1	1	-1	-1
		$B_2$	1	-1	1	-1	1
$xz, yz$	$\left. \begin{matrix} x, y \\ R_x, R_y \end{matrix} \right\}$	$\mathcal{E}_1$	2	-2	-1	1	0
$x^2 - y^2, xy$		$\mathcal{E}_2$	2	2	-1	-1	0

$$h = 12$$

$D_{2d}(\bar{4}2m)$		$E$	$C_2$	$2S_4$	$2C_2'$	$2\sigma_d$
$x^2 + y^2, z^2$		$A_1$	1	1	1	1
$R_z$		$A_2$	1	1	1	-1
$x^2 - y^2$		$B_1$	1	1	-1	1
$xy$	$z$	$B_2$	1	1	-1	-1
$xz, yz$	$\left. \begin{matrix} x, y \\ R_x, R_y \end{matrix} \right\}$	$\mathcal{E}$	2	-2	0	0

$$h = 8$$

$$\begin{aligned} D_{3d} &= D_3 \times i (\bar{3}m) \\ D_{2h} &= D_2 \times i (mmm) \end{aligned}$$

$$h = 12$$

$$h = 8$$

$D_{3h} = D_3 \times \sigma_h$	$(\bar{6}m2)$	$E$	$\sigma_h$	$2C_3$	$2S_3$	$3C_2'$	$3\sigma_v$
$x^2 + y^2, z^2$		$A_1'$	1	1	1	1	1
$R_z$		$A_2'$	1	1	1	-1	-1
		$A_1''$	1	-1	1	1	-1
		$A_2''$	1	-1	1	-1	1
$x^2 - y^2, xy$	$x, y$	$\mathcal{E}'$	2	2	-1	-1	0
$xz, yz$	$R_x, R_y$	$\mathcal{E}''$	2	-2	-1	1	0

$$h = 12$$

$$\begin{aligned} D_{4h} &= D_4 \times i (4/mmm) \\ D_{5h} &= D_5 \times \sigma_h (10m2) \\ D_{6h} &= D_6 \times i (6/mmm) \end{aligned}$$

$$h = 16$$

$$h = 20$$

$$h = 24$$



$T(23)$		$E$	$C_2$	$4C_3$	$4CS'_3$	
$r^2$	$A$	1	1	1	1	
$x^2 - y^2, 3z^2 - r^2$	$\mathcal{E}$	$\begin{Bmatrix} 1 \\ 1 \end{Bmatrix}$	$\begin{Bmatrix} 1 \\ 1 \end{Bmatrix}$	$\begin{Bmatrix} \omega \\ \omega^2 \end{Bmatrix}$	$\begin{Bmatrix} \omega^2 \\ \omega \end{Bmatrix}$	$h = 4$
$xy, yz, zx$	$\left. \begin{matrix} x, y, z \\ R_x, R_y, R_z \end{matrix} \right\}$	$T$	3	-1	0	0

$T_h = T \times i(m3)$		$E$	$4C_3$	$4C_3^2$	$3C'_2$	$i$	$4S_6$	$4S_6^5$	$3\sigma_h$
$x^2 + y^2 + z^2$	$A_g$	1	1	1	1	1	1	1	1
$x^2 - y^2, 3z^2 - r^2$	$\mathcal{E}_g$	$\begin{Bmatrix} 1 \\ 1 \end{Bmatrix}$	$\begin{Bmatrix} \omega \\ \omega^2 \end{Bmatrix}$	$\begin{Bmatrix} \omega^2 \\ \omega \end{Bmatrix}$	$\begin{Bmatrix} 1 \\ 1 \end{Bmatrix}$	$\begin{Bmatrix} 1 \\ 1 \end{Bmatrix}$	$\begin{Bmatrix} \omega \\ \omega^2 \end{Bmatrix}$	$\begin{Bmatrix} \omega^2 \\ \omega \end{Bmatrix}$	$\begin{Bmatrix} 1 \\ 1 \end{Bmatrix}$
$xy, xz, yz$	$\left. \begin{matrix} R_x, R_y, R_z \\ T_g \\ A_u \end{matrix} \right\}$	$\begin{Bmatrix} 3 \\ 1 \end{Bmatrix}$	$\begin{Bmatrix} 0 \\ 1 \end{Bmatrix}$	$\begin{Bmatrix} 0 \\ 1 \end{Bmatrix}$	$\begin{Bmatrix} -1 \\ 1 \end{Bmatrix}$	$\begin{Bmatrix} 3 \\ -1 \end{Bmatrix}$	$\begin{Bmatrix} 0 \\ -1 \end{Bmatrix}$	$\begin{Bmatrix} 0 \\ -1 \end{Bmatrix}$	$\begin{Bmatrix} -1 \\ -1 \end{Bmatrix}$
	$\mathcal{E}_u$	$\begin{Bmatrix} 1 \\ 1 \end{Bmatrix}$	$\begin{Bmatrix} \omega \\ \omega^2 \end{Bmatrix}$	$\begin{Bmatrix} \omega^2 \\ \omega \end{Bmatrix}$	$\begin{Bmatrix} 1 \\ 1 \end{Bmatrix}$	$\begin{Bmatrix} -1 \\ -1 \end{Bmatrix}$	$\begin{Bmatrix} -\omega \\ -\omega^2 \end{Bmatrix}$	$\begin{Bmatrix} -\omega^2 \\ -\omega \end{Bmatrix}$	$\begin{Bmatrix} -1 \\ -1 \end{Bmatrix}$
	$\left. \begin{matrix} x, y, z \\ T_u \end{matrix} \right\}$	$\begin{Bmatrix} 3 \\ 3 \end{Bmatrix}$	$\begin{Bmatrix} 0 \\ 0 \end{Bmatrix}$	$\begin{Bmatrix} 0 \\ 0 \end{Bmatrix}$	$\begin{Bmatrix} 1 \\ 1 \end{Bmatrix}$	$\begin{Bmatrix} -3 \\ -3 \end{Bmatrix}$	$\begin{Bmatrix} 0 \\ 0 \end{Bmatrix}$	$\begin{Bmatrix} 0 \\ 0 \end{Bmatrix}$	$\begin{Bmatrix} 1 \\ 1 \end{Bmatrix}$

$h = 48$

$O(432)$		$E$	$8C_3$	$3C_2$	$6\bar{C}_2$	$6C_4$
	$A_1$	1	1	1	1	1
	$A_2$	1	1	1	-1	-1
$x^2 - y^2, 3z^2 - r^2$	$\mathcal{E}$	2	-1	2	0	0
	$\left. \begin{matrix} R_x, R_y, R_z \\ x, y, z \end{matrix} \right\}$	$\begin{Bmatrix} T_1 \\ T_2 \end{Bmatrix}$	$\begin{Bmatrix} 3 \\ 3 \end{Bmatrix}$	$\begin{Bmatrix} 0 \\ 0 \end{Bmatrix}$	$\begin{Bmatrix} -1 \\ -1 \end{Bmatrix}$	$\begin{Bmatrix} 1 \\ -1 \end{Bmatrix}$
$xy, yz, xz$						

$h = 24$

$O_h = O \times i(m3m)$		$E$	$8C_3$	$3C_2$	$6C'_2$	$6C_4$	$i$	$8iC_3$	$3iC_2$	$6iC'_2$	$6iC_4$
$x^2 + y^2 + z^2$	$A_{1g}$	1	1	1	1	1	1	1	1	1	1
	$A_{2g}$	1	1	1	-1	-1	1	1	1	-1	-1
$x^2 - y^2, 3z^2 - r^2$	$\mathcal{E}_g$	2	-1	2	0	0	2	-1	2	0	0
$R_x, R_y, R_z$	$T_{1g}$	3	0	-1	-1	1	3	0	-1	-1	1
$xy, xz, yz$	$T_{2g}$	3	0	-1	1	-1	3	0	-1	1	-1
	$A_{1u}$	1	1	1	1	1	-1	-1	-1	-1	-1
	$A_{2u}$	1	1	1	-1	-1	-1	-1	-1	1	1
	$\mathcal{E}_u$	2	-1	2	0	0	-2	1	-2	0	0
$x, y, z$	$T_{1u}$	3	0	-1	-1	1	-3	0	1	1	-1
	$T_{2u}$	3	0	-1	1	-1	-3	0	1	-1	1

$h = 48$

$T_d(\bar{4}3m)$				$E$	$8C_3$	$3C_2$	$6\sigma_d$	$6S_4$
$r^2$				$A_1$	1	1	1	1
				$A_2$	1	1	1	-1
$x^2 - y^2, 3z^2 - r^2$				$\mathcal{E}$	2	-1	2	0
				$T_1$	3	0	-1	1
$xy, yz, xz$				$T_2$	3	0	-1	-1
				$R_x, R_y, R_z$				
				$x, y, z$				

 $h = 24$ 

$C_{\infty v}(\infty m)$				$E$	$2C_\phi$	$\sigma_v$
$x^2 + y^2, z^2$				$A_1(\Sigma^+)$	1	1
				$A_2(\Sigma^-)$	1	-1
$xz, yz$				$\mathcal{E}_1(\Pi)$	2	$2\cos\phi$
				$\mathcal{E}_2(\Delta)$	2	$2\cos(2\phi)$
$x^2 - y^2, xy$				...	...	...
				...	...	...

 $h = 4$ 

$D_{\infty h}(\infty/mm)$				$E$	$2C_\phi$	$C'_2$	$i$	$2iC_\phi$	$iC'_2$
$x^2 + y^2, z^2$				$A_{1g}(\Sigma_g^+)$	1	1	1	1	1
				$A_{1u}(\Sigma_u^-)$	1	1	-1	-1	-1
				$A_{2g}(\Sigma_g^-)$	1	1	-1	1	-1
				$A_{2u}(\Sigma_u^+)$	1	1	-1	-1	1
$xz, yz$				$\mathcal{E}_{1g}(\Pi_g)$	2	$2\cos\phi$	0	$2\cos\phi$	0
				$\mathcal{E}_{1u}(\Pi_u)$	2	$2\cos\phi$	0	$-2\cos\phi$	0
$x^2 - y^2, xy$				$\mathcal{E}_{2g}(\Delta_g)$	2	$2\cos(2\phi)$	0	$2\cos(2\phi)$	0
				$\mathcal{E}_{2u}(\Delta_u)$	2	$2\cos(2\phi)$	0	$-2\cos(2\phi)$	0
				...	...	...	...	...	...

 $h = 8$ 

$O'$	$E$	$R$	$8C_3$	$8RC_3$	$6C_2$	$12\sigma_d$	$6S_4$	$6RS_4$	Double group
$\Gamma_1(A_1)$	1	1	1	1	1	1	1	1	$h = 48$
$\Gamma_2(A_2)$	1	1	1	1	1	-1	-1	-1	
$\Gamma_3(\mathcal{E})$	2	2	-1	-1	2	0	0	0	
$\Gamma_4(T_1)$	3	3	0	0	-1	-1	1	1	
$\Gamma_5(T_2)$	3	3	0	0	-1	1	-1	-1	
$\Gamma_6$	2	-2	1	-1	0	0	$\sqrt{2}$	$-\sqrt{2}$	
$\Gamma_7$	2	-2	1	-1	0	0	$-\sqrt{2}$	$\sqrt{2}$	
$\Gamma_8$	4	-4	-1	1	0	0	0	0	

**C.1 Some character tables for nanotubes**

(See *Group Theory Applications to the Physics of Condensed Matter*, M. S. Dresselhaus, G. Dresselhaus, and A. Jorio, Springer 2008.)

Character table for the group of the wavevectors  $k = 0$  and  $k = \pi/\tau$  for achiral carbon nanotubes

$D_{2nh}$	$\{E 0\}$	...	$2S_p$	...	$2S_n$	$n\{C'_2 0\}$	$n\{C''_2 0\}$	$\{E 0\}$	...	$2S'_p$	...	$\{\sigma_h 0\}$	$n\{\sigma'_v 0\}$	$n\{\sigma''_v \tau/2\}$
$A_{1g}$	1	...	1	...	1	1	1	1	...	1	...	1	1	1
$A_{2g}$	1	...	1	...	1	-1	-1	1	...	1	...	1	-1	-1
$B_{1g}$	1	...	$(-1)^p$	...	$(-1)^n$	-1	1	1	...	$(-1)^p$	...	$(-1)^n$	-1	1
$B_{2g}$	1	...	$(-1)^p$	...	$(-1)^n$	1	-1	1	...	$(-1)^p$	...	$(-1)^n$	1	-1
$\vdots$	$\vdots$	$\vdots$	$\vdots$	$\vdots$	...	$\vdots$	$\vdots$	$\vdots$	$\vdots$	...	$\vdots$	$\vdots$	$\vdots$	$\vdots$
$\mathcal{E}_{\mu g}$	2	...	$2\cos(\mu p\pi/n)$	...	$2(-1)^\mu$	0	0	2	...	$2\cos(\mu p\pi/n)$	...	$2(-1)^\mu$	0	0
$\vdots$	$\vdots$	$\vdots$	$\vdots$	$\vdots$	...	$\vdots$	$\vdots$	$\vdots$	$\vdots$	$\vdots$	...	$\vdots$	$\vdots$	$\vdots$
$A_{1u}$	1	...	1	...	1	1	1	-1	...	-1	...	-1	-1	-1
$A_{2u}$	1	...	1	...	1	-1	-1	-1	...	-1	...	-1	1	1
$B_{1u}$	1	...	$(-1)^p$	...	$(-1)^n$	-1	1	-1	...	$-(-1)^p$	...	$-(-1)^n$	1	-1
$B_{2u}$	1	...	$(-1)^p$	...	$(-1)^n$	1	-1	-1	...	$-(-1)^p$	...	$-(-1)^n$	-1	1
$\vdots$	$\vdots$	$\vdots$	$\vdots$	$\vdots$	...	$\vdots$	$\vdots$	$\vdots$	$\vdots$	...	$\vdots$	$\vdots$	$\vdots$	$\vdots$
$\mathcal{E}_{\mu u}$	2	...	$2\cos(\mu p\pi/n)$	...	$2(-1)^\mu$	0	0	-2	...	$-2\cos(\mu p\pi/n)$	...	$-2(-1)^\mu$	0	0
$\vdots$	$\vdots$	$\vdots$	$\vdots$	$\vdots$	...	$\vdots$	$\vdots$	$\vdots$	$\vdots$	$\vdots$	...	$\vdots$	$\vdots$	$\vdots$

The values of  $p$  and  $\mu$  span the integer values between 1 and  $n - 1$ .  $S_m = \{C_{2n}^u|v\tau/(2n)\}^m$ ,  $S'_m = \{iC_{2n}^u|v\tau/(2n)\}^m$ .

*Character table for the group of the wavevectors  $k = 0$  and  $k = \pi/\tau$  for chiral carbon nanotubes*

$D_N$	$\{E 0\}$	$2S_1$	$2S_2$	$\dots$	$2S_{N/2-1}$	$2S_{N/2}$	$(N/2)\{C'_2 0\}$	$(N/2)\{C''_2 0\}$
$A_1$	1	1	1	$\dots$	1	1	1	1
$A_2$	1	1	1	$\dots$	1	1	-1	-1
$B_1$	1	-1	1	$\dots$	$(-1)^{(N/2-1)}$	$(-1)^{N/2}$	1	-1
$B_2$	1	-1	1	$\dots$	$(-1)^{(N/2-1)}$	$(-1)^{N/2}$	-1	1
$\mathcal{E}_1$	2	$2\cos(2\pi/N)$	$2\cos(4\pi/N)$	$\dots$	$2\cos[2(N/2-1)\pi/N]$	-2	0	0
$\mathcal{E}_2$	2	$2\cos(4\pi/N)$	$2\cos(8\pi/N)$	$\dots$	$2\cos[4(N/2-1)\pi/N]$	2	0	0
$\vdots$	$\vdots$	$\vdots$	$\vdots$	$\vdots$	$\dots$	$\vdots$	$\vdots$	$\vdots$
$\mathcal{E}_{N/2-1}$	2	$2\cos[2(N/2-1)\pi/N]$	$2\cos[4(N/2-1)\pi/N]$	$\dots$	$2\cos[2(N/2-1)^2\pi/N]$	$2\cos[(N/2-1)\pi]$	0	0

$$S_m = \{C_{2n}^u | v\tau/(2n)\}^m.$$

*Character table for the group of the wavevectors  $0 < k < \pi/\tau$  for achiral carbon nanotubes*

$C_{2nv}$	$\{E 0\}$	$2S_1$	$2S_2$	$\dots$	$2S_{n-1}$	$2S_n$	$n\{\sigma'_v r'\}$	$n\{\sigma''_v r''\}$
$A'$	1	1	1	$\dots$	1	1	1	1
$A''$	1	1	1	$\dots$	1	1	-1	-1
$B'$	1	-1	1	$\dots$	$(-1)^{(n-1)}$	$(-1)^n$	1	-1
$B''$	1	-1	1	$\dots$	$(-1)^{(n-1)}$	$(-1)^n$	-1	1
$\mathcal{E}_1$	2	$2\cos(\pi/n)$	$2\cos(2\pi/n)$	$\dots$	$2\cos[2(n-1)\pi/n]$	-2	0	0
$\mathcal{E}_2$	2	$2\cos(2\pi/n)$	$2\cos(4\pi/n)$	$\dots$	$2\cos[4(n-1)\pi/n]$	2	0	0
$\vdots$	$\vdots$	$\vdots$	$\vdots$	$\vdots$	$\dots$	$\vdots$	$\vdots$	$\vdots$
$\mathcal{E}_{n-1}$	2	$2\cos[(n-1)\pi/n]$	$2\cos[2(n-1)\pi/n]$	$\dots$	$2\cos[(n-1)^2\pi/n]$	$2\cos[(n-1)\pi]$	0	0

For zigzag nanotubes with  $n$  odd,  $r' = r'' = \tau/2$ .  $S_m = \{C_{2n}^u | v\tau/(2n)\}^m$ .

Character table for the group of the wavevectors  $0 < k < \pi/\tau$  for chiral carbon nanotubes

$C_N$	$\{E 0\}$	$S_1$	$S_2$	$S_3$	$\dots$	$S_t$	$\dots$	$S_{N-1}$
$A$	1	1	1	1	$\dots$	1	$\dots$	1
$B$	1	-1	1	-1	$\dots$	$(-1)^t$	$\dots$	-1
$\mathcal{E}_1^+$	1	$\omega$	$\omega^2$	$\omega^3$	$\dots$	$\omega^t$	$\dots$	$\omega^{N-1}$
$\mathcal{E}_1^-$	1	$\omega^*$	$\omega^{*2}$	$\omega^{*3}$	$\dots$	$\omega^{*t}$	$\dots$	$\omega^{*(N-1)}$
$\mathcal{E}_2^+$	1	$\omega^2$	$\omega^4$	$\omega^6$	$\dots$	$\omega^{2t}$	$\dots$	$\omega^{2(N-1)}$
$\mathcal{E}_2^-$	1	$\omega^{*2}$	$\omega^{*4}$	$\omega^{*6}$	$\dots$	$\omega^{*2t}$	$\dots$	$\omega^{*2(N-1)}$
$\vdots$	$\vdots$	$\vdots$	$\vdots$	$\vdots$	$\dots$	$\vdots$	$\dots$	$\vdots$
$\mathcal{E}_{N/2-1}^+$	1	$\omega^{(N/2-1)}$	$\omega^{2(N/2-1)}$	$\omega^{3(N/2-1)}$	$\dots$	$\omega^{t(N/2-1)}$	$\dots$	$\omega^{(N/2-1)(N-1)}$
$\mathcal{E}_{N/2-1}^-$	1	$\omega^{*(N/2-1)}$	$\omega^{*2(N/2-1)}$	$\omega^{*3(N/2-1)}$	$\dots$	$\omega^{*t(N/2-1)}$	$\dots$	$\omega^{*(N/2-1)(N-1)}$

$$S_m = \{C_N^u | v\tau/N\}^m, \omega = e^{2\pi i/N}.$$

# Appendix D

## Tensors, vectors, and equivalent electrons

A tensor may be described as a multidimensional array of components (numbers). The *rank* of a tensor is the number of indices required to specify a particular component. A zeroth-rank tensor is a scalar. A first-rank tensor is a vector with components  $V_i$ . A second-rank tensor is a matrix with elements  $M_{ij}$ . An  $n$ th-rank tensor has components labeled by  $n$  indices:  $\mathbf{T}_{i(1)i(2)i(3)\dots i(n)}$ .

In science tensors are used to express relationships between vectors and combinations of vectors. For example, in electromagnetic theory the relationship between the dielectric displacement,  $\mathbf{D}$ , and the electric intensity,  $\mathbf{E}$ , is the dielectric tensor,  $D_i = \sum_j \epsilon_{ij} E_j$ , where  $\epsilon_{ij}$  is a second-rank tensor.

The coupling of two quantum systems of angular momenta  $\mathbf{J}_1$  and  $\mathbf{J}_2$  can be characterized by eigenfunctions whose quantum numbers are  $\mathbf{J}^2 = (\mathbf{J}_1 + \mathbf{J}_2)^2 = j(j+1)$  and  $J_z = j_{1z} + j_{2z}$ . These quantum numbers label the representation  $D^{(j_1)} \times D^{(j_2)}$  based on the product of the eigenfunctions of the two isolated systems. The decomposition of the direct-product representation is

$$D^{(j_1)} \times D^{(j_2)} = \sum_{k=|j_1-j_2|}^{|j_1+j_2|} D^{(k)}. \quad (\text{D.1})$$

The vector  $\mathbf{r}$  transforms according to  $D^{(1)}$  so that the product of the components of two vectors  $\mathbf{r}_1$  and  $\mathbf{r}_2$  transforms as a second-rank tensor. The component  $T_{ij}$  transforms as the product  $r_{1i} r_{2j}$ , which in turn transforms according to  $D^{(1)} \times D^{(1)}$ . The direct product  $D^{(1)} \times D^{(1)}$  is a reducible representation that decomposes into the IRs  $D^{(0)} + D^{(1)} + D^{(2)}$  of the full rotation group. Similarly, a second-rank tensor can be decomposed into a sum of irreducible tensors,

$$T = T^{(1)} + T^{(2)} + T^{(3)}, \quad (\text{D.2})$$

which transform as  $S$ ,  $P$ , and  $D$  functions, respectively. The parts of the decomposition  $T^{(i)}$  ( $i = 1, 2$ , and  $3$ ) are called irreducible tensors because they transform



according to the IRs of the full rotation group. The total second-rank tensor described above (Cartesian coordinates) is a sum of parts that transform as a scalar and as an axial vector, and a set of five degenerate  $d$ -orbitals. This type of decomposition allows the determination of selection rules. For example, the matrix element of  $T$  between two atomic-like states,  $\psi^{(\alpha)}$  and  $\psi^{(\beta)}$ ,

$$\langle \alpha | T | \beta \rangle = \int \psi^{(\alpha)*} T \psi^{(\beta)} d\tau, \quad (\text{D.3})$$

vanishes unless  $D^{(\alpha)} \times D^{(\beta)}$  contains  $D^{(0)}$ ,  $D^{(1)}$ , or  $D^{(2)}$ . If  $\alpha = \beta$ , then the matrix element does not vanish because of symmetry considerations since  $D^{(\alpha)} \times D^{(\alpha)}$  contains  $D^{(0)}$ .

Combinations of the Cartesian components can be used to express the irreducible forms of the tensor. For example, the scalar product  $\mathbf{r}_1 \cdot \mathbf{r}_2 = \sum_k r_{1k} r_{2k}$  is invariant under all of the operations of the full rotation group, and  $T^{(1)}$  may be taken as  $\mathfrak{T}\{\mathbf{T}\} = T_{11} + T_{22} + T_{33}$ .

The cross product,  $\mathbf{r}_1 \times \mathbf{r}_2$ , is an axial vector. Its components are  $(r_{1y} r_{2z} - r_{1z} r_{2y})$ ,  $(r_{1x} r_{2z} - r_{1z} r_{2x})$ , and  $(r_{1x} r_{2y} - r_{1y} r_{2x})$ , which are symmetric under inversion, but antisymmetric in the interchange of  $\mathbf{r}_1$  and  $\mathbf{r}_2$ . The elements  $(T_{13} - T_{31})$ ,  $(T_{12} - T_{21})$ , and  $(T_{23} - T_{32})$  constitute the part of  $\mathbf{T}$  that transforms as  $D^{(1)}$ . The remaining elements that transform as  $D^{(2)}$  may be patterned after the five angular functions of the  $d$ -orbitals (the spherical harmonics for  $l = 2$ ),

$(T_{12} + T_{21})$	(analogous to $xy$ )
$(T_{13} + T_{31})$	(analogous to $xz$ )
$(T_{23} + T_{32})$	(analogous to $yz$ )
$(T_{11} - T_{22})$	(analogous to $x^2 - y^2$ )
$(2T_{33} - T_{11} - T_{22})$	(analogous to $2z^2 - x^2 - y^2$ ).

It is useful to define  $T^{(2)}$  in such a way that it is traceless. The components are then taken as

$$T_{ij}^{(2)} \equiv S_{ij} = \frac{1}{2}(T_{ij} + T_{ji}) - \frac{1}{3}\mathfrak{T}\{T\},$$

where the last term ensures that  $\mathfrak{T}\{S\} = 0$ . Only five of the six components are independent, since we have required the trace to vanish.

Higher-rank tensors can be constructed in a similar fashion by considering the transformation properties of higher-order products of the components such as  $r_{1i} r_{2j} r_{3k}$ . A third-rank tensor,  $T_{ijk}$ , with 27 components transforms as  $D^{(1)} \times D^{(1)} \times D^{(1)}$ , so it decomposes into  $D^{(0)} + 3D^{(1)} + 2D^{(2)} + D^{(3)}$ . Thus it decomposes into seven distinct tensors, namely one scalar, three first-rank, two second-rank, and one

third-rank irreducible tensor. A fourth-rank tensor has 81 components and decomposes into  $3D^{(0)} + 6D^{(1)} + 6D^{(2)} + 3D^{(3)} + D^{(4)}$ . From the decomposition rule it is clear that an  $n$ th-rank tensor in Cartesian coordinates will always contain exactly one  $n$ th-rank, irreducible tensor.

### D.1 Spherical component vectors

It is often convenient to use vectors specified by their spherical-like components rather than their Cartesian components. To this end we define a vector,  $\mathbf{V}$ , and orthogonal unit vectors,  $\mathbf{e}_0$ ,  $\mathbf{e}_{-1}$ , and  $\mathbf{e}_1$ , that form the basis vectors for the  $D^{(1)}$  IR:

$$\mathbf{V} = -V_{-1} \mathbf{e}_1 + V_0 \mathbf{e}_0 - V_1 \mathbf{e}_{-1}, \quad (\text{D.4})$$

$$\mathbf{e}_0 = \mathbf{e}_z, \quad (\text{D.5})$$

$$\mathbf{e}_1 = -\frac{1}{\sqrt{2}}(\mathbf{e}_x + i\mathbf{e}_y), \quad (\text{D.6})$$

$$\mathbf{e}_{-1} = \frac{1}{\sqrt{2}}(\mathbf{e}_x - i\mathbf{e}_y), \quad (\text{D.7})$$

$$\mathbf{e}_\mu \cdot \mathbf{e}_\nu = (-1)^\mu \delta_{\mu, -\nu}. \quad (\text{D.8})$$

Equation (D.4) can be written as

$$\mathbf{V} = \sum_{\nu} (-1)^\nu V_{-\nu} \mathbf{e}_\nu, \quad (\text{D.9})$$

so that the scalar product between two vectors  $\mathbf{V}$  and  $\mathbf{X}$  is

$$\mathbf{V} \cdot \mathbf{X} = \sum_{\mu} \sum_{\nu} (-1)^{\mu+\nu} V_{-\mu} X_{-\nu} (\mathbf{e}_\mu \cdot \mathbf{e}_\nu) = \sum_{\mu} (-1)^\mu V_{-\mu} X_\mu. \quad (\text{D.10})$$

Vectors defined in this way are basis functions for the  $D^{(1)}$  IRs of the full rotation group and transform as

$$P_R V_\mu(r) = \sum_{\nu} D_{\nu\mu}^{(1)}(R^{-1}) V_\nu(r) \quad (\nu = 0, \pm 1).$$

The spherical vectors can be used to construct irreducible tensors of any rank. In particular, irreducible tensor operators can be defined by their transformation properties. If  $j$  denotes the angular quantum number then a tensor operator,  $T_m^{(j)}$ , is of rank  $(2j + 1)$  (the magnetic quantum number,  $m$ , takes on  $2j + 1$  values). These tensors transform among themselves as

$$P_R T_m^{(j)} = \sum_{m'} T_{m'}^{(j)} D_{m'm}^{(j)}(R)$$

when subjected to a rotation,  $R$ . Analogous to case of the Cartesian tensors, the transformation properties correspond to those of products of components of the spherical vectors.

## D.2 Representations based on products of wavefunctions

Consider the product of two equivalent, one-electron wavefunctions for a spherically symmetric system,  $\Psi_{mm'}^{j \times j} = \phi_m^j(\mathbf{r}) \phi_{m'}^j(\mathbf{r}')$ , where  $j$  and  $m$  denote the angular-momentum and magnetic quantum numbers. The  $\Psi_{mm'}^{j \times j}$  functions are bases for a direct-product representation,

$$\begin{aligned} P_R \Psi_{mm'}^{j \times j} &= (P_R \phi_m^j(\mathbf{r}))(P_R \phi_{m'}^j(\mathbf{r}')) \\ &= \left( \sum_{\lambda} D_{\lambda m}^{(j)}(R^{-1}) \phi_{\lambda}^j \right) \left( \sum_{\omega} D_{\omega m'}^{(j)}(R^{-1}) \psi_{\omega}^j \right) \\ &= \sum_{\lambda} \sum_{\omega} \left( D_{\lambda m}^{(j)}(R^{-1}) \times D_{\omega m'}^{(j)}(R^{-1}) \right)_{\lambda m, \omega m'} \Psi_{\lambda \omega}^{j \times j}, \end{aligned} \quad (\text{D.11})$$

where

$$\left( D_{\lambda m}^{(j)}(R^{-1}) \times D_{\omega m'}^{(j)}(R^{-1}) \right)_{\lambda m, \omega m'} = D_{\lambda m}^{(j)}(R^{-1}) D_{\omega m'}^{(j)}(R^{-1}) \quad (\text{D.12})$$

and  $D^{(j)}(R)$  is the IR matrix for the rotation  $R$  and angular momentum  $J^2 = j(j+1)$ .

We can define basis functions that are symmetric or antisymmetric in the interchange of indices  $m$  and  $m'$  (equivalent to interchanging  $\mathbf{r}$  and  $\mathbf{r}'$ ):

$$\Psi_{mm'}^{j \times j \pm} = \frac{1}{2} \left[ \Psi_{mm'}^{j \times j} \pm \Psi_{m'm}^{j \times j} \right]. \quad (\text{D.13})$$

Under the operations of the full rotation group these functions transform as

$$P_R \Psi_{mm'}^{j \times j \pm} = \frac{1}{2} \sum_{\lambda} \sum_{\omega} \left[ D_{\lambda m}^{(j)} D_{\omega m'}^{(j)} \pm D_{\lambda m'}^{(j)} D_{\omega m}^{(j)} \right] \Psi_{\lambda \omega}^{j \times j} \quad (\text{D.14})$$

(for simplicity in notation we omit the operation symbol  $R^{-1}$  in  $D(R^{-1})$ ).

For the upper (+) sign the quantity in brackets is symmetric in the interchange of  $\lambda$  and  $\omega$ . For the lower (−) sign the quantity in brackets is antisymmetric in the interchange of  $\lambda$  and  $\omega$ . Therefore we may write

$$\begin{aligned} P_R \Psi_{mm'}^{j \times j +} &= \frac{1}{2} \sum_{\lambda} \sum_{\omega} \left[ D_{\lambda m}^{(j)} D_{\omega m'}^{(j)} + D_{\lambda m'}^{(j)} D_{\omega m}^{(j)} \right] \frac{1}{2} \left[ \Psi_{mm'}^{j \times j} + \Psi_{m'm}^{j \times j} \right] \\ &= \frac{1}{2} \sum_{\lambda} \sum_{\omega} \left[ D_{\lambda m}^{(j)} D_{\omega m'}^{(j)} + D_{\lambda m'}^{(j)} D_{\omega m}^{(j)} \right] \Psi_{mm'}^{j \times j +}. \end{aligned} \quad (\text{D.15})$$

Similarly,

$$\begin{aligned} P_R \Psi_{mm'}^{j \times j-} &= \frac{1}{2} \sum_{\lambda} \sum_{\omega} \left[ D_{\lambda m}^{(j)} D_{\omega m'}^{(j)} - D_{\lambda m'}^{(j)} D_{\omega m}^{(j)} \right] \frac{1}{2} \left[ \Psi_{mm'}^{j \times j} - \Psi_{m'm}^{j \times j} \right] \\ &= \frac{1}{2} \sum_{\lambda} \sum_{\omega} \left[ D_{\lambda m}^{(j)} D_{\omega m'}^{(j)} - D_{\lambda m'}^{(j)} D_{\omega m}^{(j)} \right] \Psi_{mm'}^{j \times j-}. \end{aligned} \quad (\text{D.16})$$

We can combine (D.15) and (D.16) in the form

$$P_R \Psi_{mm'}^{j \times j \pm} = \sum_{\lambda} \sum_{\omega} D_{\lambda \omega, mm'}^{j \times j \pm} \Psi_{\lambda \omega}^{j \times j \pm}, \quad (\text{D.17})$$

where

$$D_{\lambda \omega, mm'}^{j \times j \pm} = \frac{1}{2} \left[ D_{\lambda m}^{(j)} D_{\omega m'}^{(j)} \pm D_{\lambda m'}^{(j)} D_{\omega m}^{(j)} \right].$$

Equation (D.15) shows that the functions  $\Psi_{mm'}^{j \times j+}$  transform among themselves under the operations of the group and do not mix with the antisymmetric functions. Equation (D.16) confirms that the functions  $\Psi_{mm'}^{j \times j-}$  do not mix with the symmetric functions. Therefore, the  $\Psi_{mm'}^{j \times j \pm}$  functions are bases for a symmetric (antisymmetric) representation of the full rotation group, and the IR matrices are  $D_{\lambda \omega, mm'}^{j \times j \pm}$ .

Let  $S = R^{-1}$ , then the characters of these representations are

$$\begin{aligned} \chi^j(S)^{\pm} &= \sum_{\lambda} \sum_{\omega} D_{\lambda \omega, \lambda \omega}^{j \times j \pm}(S) \\ &= \frac{1}{2} \sum_{\lambda} \sum_{\omega} \left[ D_{\lambda \lambda}^{(j)}(S) D_{\omega \omega}^{(j)}(S) \pm D_{\lambda \omega}^{(j)}(S) D_{\omega \lambda}^{(j)}(S) \right]. \end{aligned} \quad (\text{D.18})$$

For the left-hand side of (D.18) we have

$$\begin{aligned} \frac{1}{2} \sum_{\lambda} \sum_{\omega} \left[ D_{\lambda \lambda}^{(j)}(S) D_{\omega \omega}^{(j)}(S) \right] &= \frac{1}{2} \left\{ \sum_{\lambda} D_{\lambda \lambda}^{(j)}(S) \right\} \left\{ \sum_{\lambda} D_{\lambda \lambda}^{(j)}(S) \right\} \\ &= \frac{1}{2} [\chi^j(S)]^2, \end{aligned} \quad (\text{D.19})$$

and

$$\frac{1}{2} \sum_{\lambda} \sum_{\omega} \left[ D_{\lambda \omega}^{(j)}(S) D_{\omega \lambda}^{(j)}(S) \right] = \frac{1}{2} \sum_{\lambda} D_{\lambda \lambda}^{(j)}(S^2) = \frac{1}{2} [\chi^j(S^2)]. \quad (\text{D.20})$$

Substituting (D.19) and (D.20) into (D.18) gives

$$\chi^j(S)^{\pm} = \frac{1}{2} [\chi^j(S)]^2 \pm \frac{1}{2} \chi^j(S^2). \quad (\text{D.21})$$

This may be written as

$$\chi^j(\theta)^\pm = \frac{1}{2}[\chi^j(\theta)]^2 \pm \frac{1}{2}\chi^j(2\theta), \quad (\text{D.22})$$

$$\chi^j(\theta) = \frac{\sin[(j + \frac{1}{2})\theta]}{\sin(\theta/2)}, \quad (\text{D.23})$$

where  $\theta$  is the angle of rotation of the operation  $S$ .

Equation (D.23) can be rewritten as

$$\chi^0(\theta) = 1, \quad (\text{D.24})$$

$$\chi^j(\theta) = 1 + \sum_{n=1}^j 2\cos(n\theta), \quad \text{for } j \geq 1. \quad (\text{D.25})$$

Equation (D.21) leads to restrictions on the direct-product decompositions. For example, for  $j = 1$ ,

$$\chi^1(\theta)^\pm = \frac{1}{2}[\chi^1(\theta)]^2 \pm \frac{1}{2}\chi^1(2\theta) = \frac{1}{2}[1 + 2\cos(\theta)]^2 \pm \frac{1}{2}[1 + 2\cos(2\theta)]. \quad (\text{D.26})$$

With the plus sign we find

$$\chi^1(\theta)^+ = 1 + [1 + 2\cos(\theta) + 2\cos(2\theta)] = \chi^0(\theta) + \chi^2(\theta), \quad (\text{D.27})$$

whereas with the minus sign we obtain

$$\chi^1(\theta)^- = 1 + 2\cos(\theta) = \chi^1(\theta). \quad (\text{D.28})$$

Equations (D.27) and (D.28) indicate the decompositions of the IRs  $D^{j \times j \pm}$  as

$$D^{(1 \times 1)+} = D^{(0)} + D^{(2)}, \quad (\text{D.29})$$

$$D^{(1 \times 1)-} = D^{(1)}. \quad (\text{D.30})$$

These results express the vector coupling model for a (spinless) two-electron wavefunction. Equation (D.29) shows that two  $p$ -states can be combined to form a symmetric  $S$  and  $D$  state, but not a symmetric  $P$  state. Equation (D.30) shows that the only antisymmetric state that can be formed is a  $P$  state. The direct-product rule gives

$$D^{(1 \times 1)} = D^{(0)} + D^{(1)} + D^{(2)}, \quad (\text{D.31})$$

but gives no information about the parity of the two-electron states that can be formed. The notation  $D^{(i \times i)}$  or  $D_{(i \times i)}$  is often used to indicate a symmetric representation and  $D^{[i \times i]}$  or  $D_{[i \times i]}$  to indicate an antisymmetric representation. Also, the decomposition may be written as, for example,

$$D^{(1 \times 1)} = D^{(0)} + [D^{(1)}] + D^{(2)}, \quad (\text{D.32})$$

where the square brackets indicate that  $D^{(1)}$  has odd parity.

Next we consider the case where  $j = 2$  (a pair of electrons in  $d$ -states). Equations (D.21) and (D.25) give

$$\begin{aligned}\chi^{(2 \times 2)}(\theta)^\pm &= \frac{1}{2}[\chi^{(2)}(\theta)]^2 \pm \frac{1}{2}\chi^2(2\theta) \\ &= \frac{1}{2}[1 + 2\cos(\theta) + 2\cos(2\theta)]^2 \pm \frac{1}{2}[1 + 2\cos(2\theta) + 2\cos(4\theta)].\end{aligned}\tag{D.33}$$

Using the minus sign in (D.33) gives

$$\begin{aligned}\chi^{(2 \times 2)}(\theta)^- &= 2 + 4\cos(\theta) + 2\cos(2\chi^{(2 \times 2)}(\theta)^+) + 2\cos(3\theta) \\ &= [1 + 2\cos(\theta)] + [1 + 2\cos(\theta) + 2\cos(3\theta)] \\ &= \chi^{(1)} + \chi^{(3)}.\end{aligned}\tag{D.34}$$

The plus sign yields

$$\begin{aligned}\chi^{(2 \times 2)}(\theta)^+ &= 1 + [1 + 2\cos(\theta) + 2\cos(2\theta)] \\ &\quad + [1 + 2\cos(\theta) + 2\cos(2\theta) + 2\cos(3\theta) + 2\cos(4\theta)] \\ &= \chi^{(0)} + \chi^{(2)} + \chi^{(4)}.\end{aligned}\tag{D.35}$$

Equations (D.34) and (D.35) indicate the decomposition as

$$D^{(2 \times 2)+} = D^{(0)} + D^{(2)} + D^{(4)},\tag{D.36}$$

$$D^{(2 \times 2)-} = D^{(1)} + D^{(3)},\tag{D.37}$$

or

$$D^{(2 \times 2)} = D^{(0)} + [D^{(1)}] + D^{(2)} + [D^{(3)}] + D^{(4)},\tag{D.38}$$

where the square brackets indicate antisymmetric representations. In general, in the decomposition formulas, an odd  $j$  does not have a symmetric representation.

# Appendix E

## The octahedral group, $O$ and $O_h$

### E.1 Elements of the $O$ group

The octahedral or  $O$  group consists of the 24 rotations about various axes that leave a cube or octahedron unchanged. The symmetry axes are shown in Fig. E.1. The symmetry elements are listed below.

- (1) Four  $C_3$  axes: 120- and 240-degree rotations about cube body diagonals. These symmetry axes are shown in Fig. E.1(a). We label the elements  $C_3^k$  and  $(C_3^2)^k$ ,  $k = 1, 2, 3$ , and 4, where the superscript  $k$  identifies the particular axis. There are in total eight such rotations, and these eight elements form a class.
- (2) Three  $C_4$  axes: 90-, 180-, and 270-degree rotations about the  $x$ -,  $y$ -, and  $z$ -axes in Fig. E.1. We label these elements as  $C_4^k$ ,  $C_2^k$ , and  $(C_4^3)^k$ ,  $k = 1, 2$ , and 3. The six elements  $C_4^k$  and  $(C_4^3)^k$ ,  $k = 1, 2$ , and 3, form a class. The three elements  $C_2^k$ ,  $k = 1, 2$ , and 3, form a separate class. The axes are shown in Fig. E.1(b).
- (3) Six  $\bar{C}_2$  axes: 180-degree rotations about axes through the origin bisecting face edges. We label these elements as  $\bar{C}_2^k$ ,  $k = 1, 2, \dots, 6$ . The six elements form a class. The axes are shown in Fig. E.1(c).

The  $O_h$  group is the direct-product group  $O \times i$ . All rotations are clockwise (left-hand screw rule) so that they correspond to operations rather than elements of the group. The rotations and matrices representing them are appropriate for the operators  $P_R$  applied to a function.

### E.2 The character table for $O$

The character table for the group  $O$  is given in Table E.1.

Table E.1 The character table for  $O$ .  $O_h = O \times i$  ( $m3m$ ).

	$O(432)$	$E$	$8C_3$	$3C_2$	$6\bar{C}_2$	$6C_4$
	$A_1$	1	1	1	1	1
	$A_2$	1	1	1	-1	-1
$(x^2 - y^2, 3z^2 - r^2)$	$\mathcal{E}$	2	-1	2	0	0
$(R_x, R_y, R_z), (x, y, z)$	$T_1$	3	0	-1	-1	1
$(xy, yz, xz)$	$T_2$	3	0	-1	1	-1

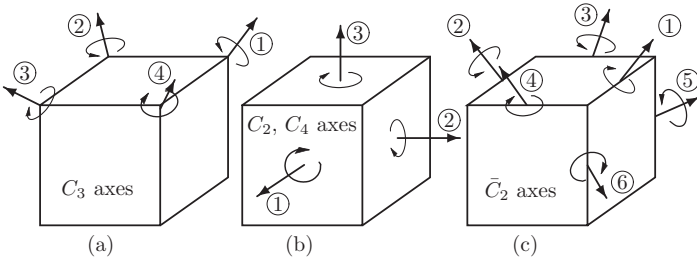


Figure E.1 Symmetry axes and operations of the  $O$  group.

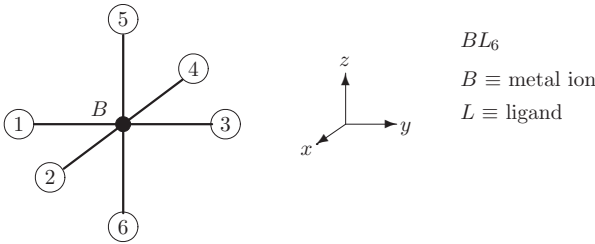


Figure E.2 An octahedrally coordinated ion. The ligands are labeled 1 through 6.

E.3 The action table for octahedral coordination

The geometry for a central ion surrounded by an octahedron of ligands is shown in Fig. E.2. The ligands are labeled 1 through 6. The action table for the octahedral complex is shown in Table E.2.

E.4 The irreducible-representation matrices of the  $O$  group

The individual matrices for the IRs of the  $O$  group are given in Tables E.3, E.4, and E.5. Denote the operators of the  $O$  group as the set  $\{R\}$ , then the operators of  $O_h$  are  $\{R, iR\}$ , where  $i$  is the inversion operator. If the matrices  $\{M^\alpha(R)\}$  form the  $\Gamma^\alpha$  IR of the  $O$  group, then for the  $O_h$  group  $\Gamma_g^\alpha$  has  $M^\alpha(iR) = M^\alpha(R)$  and  $\Gamma_u^\alpha$  has  $M^\alpha(iR) = -M^\alpha(R)$ .



Table E.2 The action table for the octahedral complex in Fig. E.2 for the  $O$  group. The first section shows how the coordinates,  $x$ ,  $y$ , and  $z$ , transform under the group operations. The entries in **boldface roman** indicate coordinates that transform into a multiple of themselves. The second sections shows how the ligand positions are transformed under the group operations. The entries in **boldface roman** indicate the ligands that are unchanged by the operation. The third and fourth sections show how the  $d$ -orbitals transform under the group operations.

$E$	$C_3^1$	$C_3^{1^2}$	$C_3^2$	$C_3^{2^2}$	$C_3^3$	$C_3^{3^2}$	$C_3^4$	$C_3^{4^2}$	$C_2^1$	$C_2^2$	$C_2^3$	$\bar{C}_2^1$	$\bar{C}_2^2$	$\bar{C}_2^3$	$\bar{C}_2^4$	$\bar{C}_2^5$	$\bar{C}_2^6$	$C_4^1$	$C_4^{1^3}$	$C_4^2$	$C_4^{2^3}$	$C_4^3$	$C_4^{3^3}$
<b>x</b>	$-y$	$-z$	$-z$	$y$	$-y$	$z$	$z$	$y$	<b>x</b>	<b>-x</b>	<b>-x</b>	<b>-x</b>	<b>-x</b>	$-z$	$z$	$-y$	$y$	<b>x</b>	<b>x</b>	$z$	$-z$	$-y$	$y$
<b>y</b>	$z$	$-x$	$x$	$-z$	$-z$	$-x$	$x$	$z$	<b>-y</b>	<b>y</b>	<b>-y</b>	$z$	$-z$	<b>-y</b>	<b>-y</b>	$-x$	$x$	$-z$	$z$	<b>y</b>	<b>y</b>	$x$	$-x$
<b>z</b>	$-x$	$y$	$-y$	$-x$	$x$	$-y$	$y$	$x$	<b>-z</b>	<b>-z</b>	<b>z</b>	$y$	$-y$	$-x$	$x$	<b>-z</b>	<b>-z</b>	$y$	$-y$	$-x$	$x$	<b>z</b>	<b>z</b>
<b>1</b>	6	2	4	5	5	2	4	6	3	<b>1</b>	3	6	5	3	3	2	4	5	6	<b>1</b>	<b>1</b>	4	2
<b>2</b>	1	6	6	3	1	5	5	3	<b>2</b>	4	4	4	4	6	5	1	3	<b>2</b>	<b>2</b>	5	6	1	3
<b>3</b>	5	4	2	6	6	4	2	5	1	<b>3</b>	1	5	6	1	1	4	2	6	5	<b>3</b>	<b>3</b>	2	4
<b>4</b>	3	5	5	1	3	6	6	1	<b>4</b>	2	2	2	2	5	6	3	1	<b>4</b>	<b>4</b>	6	5	3	1
<b>5</b>	4	3	1	4	2	1	3	2	6	6	<b>5</b>	3	1	4	2	6	6	3	1	4	2	<b>5</b>	<b>5</b>
<b>6</b>	2	1	3	2	4	3	1	4	5	5	<b>6</b>	1	3	2	4	5	5	1	3	2	4	<b>6</b>	<b>6</b>
<b>xy</b>	$-yz$	$xz$	$-xz$	$-yz$	$yz$	$-xz$	$xz$	$yz$	<b>-xy</b>	<b>-xy</b>	<b>xy</b>	$-xz$	$xz$	$yz$	$-yz$	<b>xy</b>	<b>xy</b>	$-xz$	$xz$	$yz$	$-yz$	<b>-xy</b>	<b>-xy</b>
<b>xz</b>	$xy$	$-yz$	$yz$	$-xy$	$-xy$	$-yz$	$yz$	$xy$	<b>-xz</b>	<b>xz</b>	<b>-xz</b>	$-xy$	$xy$	<b>xz</b>	<b>xz</b>	$yz$	$-yz$	$xy$	$-xy$	<b>-xz</b>	<b>-xz</b>	$-yz$	$yz$
<b>yz</b>	$-xz$	$-xy$	$-xy$	$xz$	$-xz$	$xy$	$xy$	$xz$	<b>yz</b>	<b>-yz</b>	<b>-yz</b>	<b>yz</b>	<b>yz</b>	$xy$	$-xy$	$xz$	$-xz$	<b>-yz</b>	<b>-yz</b>	$-xy$	$xy$	$xz$	$-xz$
$\frac{3z^2-r^2}{2\sqrt{3}}=b$	$\frac{x^2-y^2}{2}=a$	$-\frac{1}{2}b+\frac{\sqrt{3}}{2}a$	$-\frac{1}{2}b-\frac{\sqrt{3}}{2}a$	$-\frac{1}{2}b+\frac{\sqrt{3}}{2}a$	$-\frac{1}{2}b-\frac{\sqrt{3}}{2}a$	$-\frac{1}{2}b+\frac{\sqrt{3}}{2}a$	$-\frac{1}{2}b-\frac{\sqrt{3}}{2}a$	$-\frac{1}{2}b+\frac{\sqrt{3}}{2}a$	$b$	$a$	$b$	$-\frac{1}{2}b-\frac{\sqrt{3}}{2}a$	$-\frac{1}{2}b-\frac{\sqrt{3}}{2}a$	$-\frac{1}{2}b+\frac{\sqrt{3}}{2}a$	$-\frac{1}{2}b+\frac{\sqrt{3}}{2}a$	$b$	$-a$	$-\frac{1}{2}b-\frac{\sqrt{3}}{2}a$	$-\frac{1}{2}b-\frac{\sqrt{3}}{2}a$	$-\frac{1}{2}b+\frac{\sqrt{3}}{2}a$	$-\frac{1}{2}b+\frac{\sqrt{3}}{2}a$	$b$	$-a$

Table E.3 The  $\mathcal{E}$  representation

---



---

$E = \begin{pmatrix} 1 & 0 \\ 0 & 1 \end{pmatrix}$	$C_3^1 = \begin{pmatrix} -\frac{1}{2} & -\sqrt{3}/2 \\ \sqrt{3}/2 & -\frac{1}{2} \end{pmatrix}$	$C_3^{1^2} = \begin{pmatrix} -\frac{1}{2} & \sqrt{3}/2 \\ -\sqrt{3}/2 & -\frac{1}{2} \end{pmatrix}$
$C_3^2 = \begin{pmatrix} -\frac{1}{2} & \sqrt{3}/2 \\ -\sqrt{3}/2 & -\frac{1}{2} \end{pmatrix}$	$C_3^{2^2} = \begin{pmatrix} -\frac{1}{2} & -\sqrt{3}/2 \\ \sqrt{3}/2 & -\frac{1}{2} \end{pmatrix}$	$C_3^3 = \begin{pmatrix} -\frac{1}{2} & -\sqrt{3}/2 \\ \sqrt{3}/2 & -\frac{1}{2} \end{pmatrix}$
$C_3^{3^2} = \begin{pmatrix} -\frac{1}{2} & \sqrt{3}/2 \\ -\sqrt{3}/2 & -\frac{1}{2} \end{pmatrix}$	$C_3^4 = \begin{pmatrix} -\frac{1}{2} & \sqrt{3}/2 \\ -\sqrt{3}/2 & -\frac{1}{2} \end{pmatrix}$	$C_3^{4^2} = \begin{pmatrix} -\frac{1}{2} & -\sqrt{3}/2 \\ \sqrt{3}/2 & -\frac{1}{2} \end{pmatrix}$
$C_2^1 = \begin{pmatrix} 1 & 0 \\ 0 & 1 \end{pmatrix}$	$C_2^2 = \begin{pmatrix} 1 & 0 \\ 0 & 1 \end{pmatrix}$	$C_2^3 = \begin{pmatrix} 1 & 0 \\ 0 & 1 \end{pmatrix}$
$\bar{C}_2^1 = \begin{pmatrix} \frac{1}{2} & -\sqrt{3}/2 \\ -\sqrt{3}/2 & -\frac{1}{2} \end{pmatrix}$	$\bar{C}_2^2 = \begin{pmatrix} \frac{1}{2} & -\sqrt{3}/2 \\ -\sqrt{3}/2 & -\frac{1}{2} \end{pmatrix}$	$\bar{C}_2^3 = \begin{pmatrix} \frac{1}{2} & \sqrt{3}/2 \\ \sqrt{3}/2 & -\frac{1}{2} \end{pmatrix}$
$\bar{C}_2^4 = \begin{pmatrix} \frac{1}{2} & \sqrt{3}/2 \\ \sqrt{3}/2 & -\frac{1}{2} \end{pmatrix}$	$\bar{C}_2^5 = \begin{pmatrix} -1 & 0 \\ 0 & 1 \end{pmatrix}$	$\bar{C}_2^6 = \begin{pmatrix} -1 & 0 \\ 0 & 1 \end{pmatrix}$
$C_4^1 = \begin{pmatrix} \frac{1}{2} & -\sqrt{3}/2 \\ -\sqrt{3}/2 & -\frac{1}{2} \end{pmatrix}$	$C_4^{1^3} = \begin{pmatrix} \frac{1}{2} & -\sqrt{3}/2 \\ -\sqrt{3}/2 & -\frac{1}{2} \end{pmatrix}$	$C_4^2 = \begin{pmatrix} \frac{1}{2} & \sqrt{3}/2 \\ \sqrt{3}/2 & -\frac{1}{2} \end{pmatrix}$
$C_4^{2^3} = \begin{pmatrix} \frac{1}{2} & \sqrt{3}/2 \\ \sqrt{3}/2 & -\frac{1}{2} \end{pmatrix}$	$C_4^3 = \begin{pmatrix} -1 & 0 \\ 0 & 1 \end{pmatrix}$	$C_4^{3^3} = \begin{pmatrix} -1 & 0 \\ 0 & 1 \end{pmatrix}$

---



---

For  $\mathcal{E}_u$ ,  $M(iR) = -M(R)$ . For  $\mathcal{E}_g$ ,  $M(iR) = M(R)$ . The basis functions are  $x^2 - y^2$  and  $(3z^2 - r^2)/\sqrt{3}$ .

Table E.4 The  $T_1$  representation

---



---

$E = \begin{pmatrix} 1 & 0 & 0 \\ 0 & 1 & 0 \\ 0 & 0 & 1 \end{pmatrix}$	$C_3^1 = \begin{pmatrix} 0 & -1 & 0 \\ 0 & 0 & 1 \\ -1 & 0 & 0 \end{pmatrix}$	$C_3^{1^2} = \begin{pmatrix} 0 & 0 & -1 \\ -1 & 0 & 0 \\ 0 & 1 & 0 \end{pmatrix}$
$C_3^2 = \begin{pmatrix} 0 & 0 & -1 \\ 1 & 0 & 0 \\ 0 & -1 & 0 \end{pmatrix}$	$C_3^{2^2} = \begin{pmatrix} 0 & 1 & 0 \\ 0 & 0 & -1 \\ -1 & 0 & 0 \end{pmatrix}$	$C_3^3 = \begin{pmatrix} 0 & -1 & 0 \\ 0 & 0 & -1 \\ 1 & 0 & 0 \end{pmatrix}$
$C_3^{3^2} = \begin{pmatrix} 0 & 0 & 1 \\ -1 & 0 & 0 \\ 0 & -1 & 0 \end{pmatrix}$	$C_3^4 = \begin{pmatrix} 0 & 0 & 1 \\ 1 & 0 & 0 \\ 0 & 1 & 0 \end{pmatrix}$	$C_3^{4^2} = \begin{pmatrix} 0 & 1 & 0 \\ 0 & 0 & 1 \\ 1 & 0 & 0 \end{pmatrix}$
$C_2^1 = \begin{pmatrix} 1 & 0 & 0 \\ 0 & -1 & 0 \\ 0 & 0 & -1 \end{pmatrix}$	$C_2^2 = \begin{pmatrix} -1 & 0 & 0 \\ 0 & 1 & 0 \\ 0 & 0 & -1 \end{pmatrix}$	$C_2^3 = \begin{pmatrix} -1 & 0 & 0 \\ 0 & -1 & 0 \\ 0 & 0 & 1 \end{pmatrix}$
$\bar{C}_2^1 = \begin{pmatrix} -1 & 0 & 0 \\ 0 & 0 & 1 \\ 0 & 1 & 0 \end{pmatrix}$	$\bar{C}_2^2 = \begin{pmatrix} -1 & 0 & 0 \\ 0 & 0 & -1 \\ 0 & -1 & 0 \end{pmatrix}$	$\bar{C}_2^3 = \begin{pmatrix} 0 & 0 & -1 \\ 0 & -1 & 0 \\ -1 & 0 & 0 \end{pmatrix}$
$\bar{C}_2^4 = \begin{pmatrix} 0 & 0 & 1 \\ 0 & -1 & 0 \\ 1 & 0 & 0 \end{pmatrix}$	$\bar{C}_2^5 = \begin{pmatrix} 0 & -1 & 0 \\ -1 & 0 & 0 \\ 0 & 0 & -1 \end{pmatrix}$	$\bar{C}_2^6 = \begin{pmatrix} 0 & 1 & 0 \\ 1 & 0 & 0 \\ 0 & 0 & -1 \end{pmatrix}$
$C_4^1 = \begin{pmatrix} 1 & 0 & 0 \\ 0 & 0 & -1 \\ 0 & 1 & 0 \end{pmatrix}$	$C_4^{1^3} = \begin{pmatrix} 1 & 0 & 0 \\ 0 & 0 & 1 \\ 0 & -1 & 0 \end{pmatrix}$	$C_4^2 = \begin{pmatrix} 0 & 0 & 1 \\ 0 & 1 & 0 \\ -1 & 0 & 0 \end{pmatrix}$
$C_4^{2^3} = \begin{pmatrix} 0 & 0 & -1 \\ 0 & 1 & 0 \\ 1 & 0 & 0 \end{pmatrix}$	$C_4^3 = \begin{pmatrix} 0 & -1 & 0 \\ 1 & 0 & 0 \\ 0 & 0 & 1 \end{pmatrix}$	$C_4^{3^3} = \begin{pmatrix} 0 & 1 & 0 \\ -1 & 0 & 0 \\ 0 & 0 & 1 \end{pmatrix}$

---



---

For  $T_{1u}$ ,  $M(iR) = -M(R)$ . For  $T_{1g}$ ,  $M(iR) = M(R)$ . The basis functions are  $x(z^2 - y^2)$  (row 1),  $y(z^2 - x^2)$  (row 2), and  $z(x^2 - y^2)$ .

Table E.5 The  $T_2$  representation

---



---

$E = \begin{pmatrix} 1 & 0 & 0 \\ 0 & 1 & 0 \\ 0 & 0 & 1 \end{pmatrix}$	$C_3^1 = \begin{pmatrix} 0 & 0 & -1 \\ 1 & 0 & 0 \\ 0 & -1 & 0 \end{pmatrix}$	$C_3^{1^2} = \begin{pmatrix} 0 & 1 & 0 \\ 0 & 0 & -1 \\ -1 & 0 & 0 \end{pmatrix}$
$C_3^2 = \begin{pmatrix} 0 & -1 & 0 \\ 0 & 0 & 1 \\ -1 & 0 & 0 \end{pmatrix}$	$C_3^{2^2} = \begin{pmatrix} 0 & 0 & 1 \\ -1 & 0 & 0 \\ 0 & 1 & 0 \end{pmatrix}$	$C_3^3 = \begin{pmatrix} 0 & 0 & 1 \\ -1 & 0 & 0 \\ 0 & -1 & 0 \end{pmatrix}$
$C_3^{3^2} = \begin{pmatrix} 0 & -1 & 0 \\ 0 & 0 & -1 \\ 1 & 0 & 0 \end{pmatrix}$	$C_3^4 = \begin{pmatrix} 0 & 1 & 0 \\ 0 & 0 & 1 \\ 1 & 0 & 0 \end{pmatrix}$	$C_3^{4^2} = \begin{pmatrix} 0 & 0 & 1 \\ 1 & 0 & 0 \\ 0 & 1 & 0 \end{pmatrix}$
$C_2^1 = \begin{pmatrix} -1 & 0 & 0 \\ 0 & -1 & 0 \\ 0 & 0 & 1 \end{pmatrix}$	$C_2^2 = \begin{pmatrix} -1 & 0 & 0 \\ 0 & 1 & 0 \\ 0 & 0 & -1 \end{pmatrix}$	$C_2^3 = \begin{pmatrix} 1 & 0 & 0 \\ 0 & -1 & 0 \\ 0 & 0 & -1 \end{pmatrix}$
$\bar{C}_2^1 = \begin{pmatrix} 0 & -1 & 0 \\ -1 & 0 & 0 \\ 0 & 0 & 1 \end{pmatrix}$	$\bar{C}_2^2 = \begin{pmatrix} 0 & 1 & 0 \\ 1 & 0 & 0 \\ 0 & 0 & 1 \end{pmatrix}$	$\bar{C}_2^3 = \begin{pmatrix} 0 & 0 & 1 \\ 0 & 1 & 0 \\ 1 & 0 & 0 \end{pmatrix}$
$\bar{C}_2^4 = \begin{pmatrix} 0 & 0 & -1 \\ 0 & 1 & 0 \\ -1 & 0 & 0 \end{pmatrix}$	$\bar{C}_2^5 = \begin{pmatrix} 1 & 0 & 0 \\ 0 & 0 & 1 \\ 0 & 1 & 0 \end{pmatrix}$	$\bar{C}_2^6 = \begin{pmatrix} 1 & 0 & 0 \\ 0 & 0 & -1 \\ 0 & -1 & 0 \end{pmatrix}$
$C_4^1 = \begin{pmatrix} 0 & -1 & 0 \\ 1 & 0 & 0 \\ 0 & 0 & -1 \end{pmatrix}$	$C_4^{1^3} = \begin{pmatrix} 0 & 1 & 0 \\ -1 & 0 & 0 \\ 0 & 0 & -1 \end{pmatrix}$	$C_4^2 = \begin{pmatrix} 0 & 0 & 1 \\ 0 & -1 & 0 \\ -1 & 0 & 0 \end{pmatrix}$
$C_4^{2^3} = \begin{pmatrix} 0 & 0 & -1 \\ 0 & -1 & 0 \\ 1 & 0 & 0 \end{pmatrix}$	$C_4^3 = \begin{pmatrix} -1 & 0 & 0 \\ 0 & 0 & -1 \\ 0 & 1 & 0 \end{pmatrix}$	$C_4^{3^3} = \begin{pmatrix} -1 & 0 & 0 \\ 0 & 0 & 1 \\ 0 & -1 & 0 \end{pmatrix}$

---



---

For  $T_{2u}$ ,  $M(iR) = -M(R)$ . For  $T_{2g}$ ,  $M(iR) = M(R)$ . The basis functions are  $xy$ ,  $yz$ , and  $zx$ .

# Appendix F

## The tetrahedral group, $T_d$

### F.1 Elements of the $T_d$ group

The octahedral or  $T_d$  group consists of the 24 rotations, rotations, and reflections that leave a tetrahedron unchanged. For visual purposes it is useful to show the tetrahedron inscribed within a cube as illustrated in Fig. F.1. The symmetry axes are also shown. The symmetry elements in addition to the identity are listed below.

- (1)  $C_3$ . Four three-fold axes: 120- and 240-degree clockwise rotations about cube body diagonals. We label the elements  $C_3^{(k)}$  and  $(C_3^{(k)})^2$ ,  $k = 1, 2, 3$ , and 4, where the superscript  $k$  identifies the particular axis. There are in total eight such rotations, and these eight elements form the  $C_3$  class. The  $C_3$  axes are shown in Fig. F.1(a).
- (2)  $\sigma_d$ . Six reflections. The reflection planes are defined by a pair of face diagonals on opposite sides of the circumscribed cube. We label these elements as  $\sigma_d^{(k)}$ ,  $k = 1, \dots, 6$ . The six elements form the  $\sigma_d$  class. The  $\sigma_d$  reflection planes are shown in Fig. F.1(b).
- (3)  $C_2$ . Three two-fold axes: 180-degree clockwise rotations about the  $x$ -,  $y$ -, and  $z$ -axes. We label these elements as  $C_2^{(k)}$ ,  $k = 1, 2$ , and 3. The three elements  $C_2^k$ ,  $k = 1, 2$ , and 3, form the  $C_2$  class. The  $C_2$  axes are shown in Fig. F.1(c).
- (4)  $S_4$ . Six improper rotations. Clockwise rotations by 90 and 270 degrees about a  $C_2$  axis followed by a reflection in the plane perpendicular to the axis of rotation. These elements are labeled as  $S_4^{(k)}$  and  $(S_4^{(k)})^3$ ,  $k = 1, 2$ , and 3. These six elements form the  $S_4$  class. The rotation axes and reflection planes are shown in Fig. F.1(d).

### F.2 Character table for $T_d$

The character table for the  $T_d$  group is given in Table F.1.

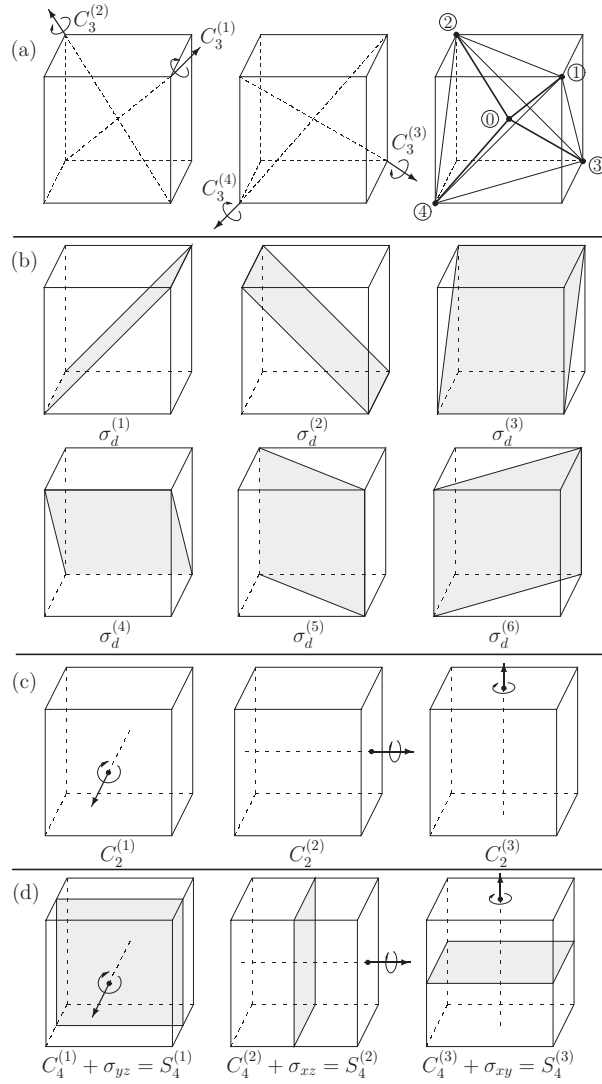


Figure F.1 Symmetry elements for the  $T_d$  group. (a)  $C_3$  rotation axes and (in the last column on the right) a tetrahedron inscribed within a cube. (b)  $\sigma_d$  reflection planes. (c)  $C_2$  rotation axes. (d) Axes and reflection planes for  $S_4$  elements.

Table F.1 The character table for  $T_d$

Basis functions	$T_d$	$E$	$8C_3$	$3C_2$	$6S_4$	$6\sigma_d$
	$A_1$	1	1	1	1	1
	$A_2$	1	1	1	-1	-1
$(3z^2 - r^2, x^2 - y^2)$	$\mathcal{E}$	2	-1	2	0	0
$[x(z^2 - y^2), y(z^2 - x^2), z(x^2 - y^2)]$	$T_1$	3	0	-1	1	-1
$(xy, xz, yz)$	$T_2$	3	0	-1	-1	1

**F.3 The action table for tetrahedral coordination**

The geometry for a central ion surrounded by a tetrahedron of ligands is shown in Fig. F.1(a). The ligands are labeled 1 through 4. The action table is shown in Table F.2.

**F.4 The irreducible-representation matrices of the  $T_d$  group**

The individual matrices for the  $\mathcal{E}$ ,  $T_1$ , and  $T_2$  IRs are given in Tables F.3, F.4, and F.5.

Table F.2 *The action table for ligands. The symmetry operations are listed across the top row. The first column lists the functions. Subsequent columns list the function produced when a symmetry operation is applied to the function.*

$E$	$C_3^1$	$C_3^{1^2}$	$C_3^2$	$C_3^{2^2}$	$C_3^3$	$C_3^{3^2}$	$C_3^4$	$C_3^{4^2}$	$C_2^1$	$C_2^2$	$C_2^3$	$\sigma_d^1$	$\sigma_d^2$	$\sigma_d^3$	$\sigma_d^4$	$\sigma_d^5$	$\sigma_d^6$	$S_4^1$	$S_4^{1^3}$	$S_4^2$	$S_4^{2^3}$	$S_4^3$	$S_4^{3^3}$
$x$	$z$	$y$	$-z$	$y$	$z$	$-y$	$-x$	$-y$	$x$	$-x$	$-x$	$x$	$x$	$-z$	$z$	$y$	$-y$	$-x$	$-x$	$z$	$-z$	$-y$	$y$
$y$	$x$	$z$	$x$	$-z$	$-x$	$-z$	$-z$	$z$	$-y$	$y$	$-y$	$z$	$-z$	$y$	$y$	$y$	$-x$	$-z$	$z$	$-y$	$-y$	$x$	$-x$
$z$	$y$	$x$	$-y$	$-x$	$-y$	$x$	$y$	$-x$	$-z$	$-z$	$z$	$y$	$-y$	$-x$	$x$	$z$	$z$	$y$	$-y$	$-x$	$x$	$-z$	$-z$
1	1	1	4	3	4	2	3	2	4	3	2	1	4	3	1	1	2	3	2	2	4	4	3
2	1	6	6	3	1	5	5	3	2	4	4	4	4	6	5	1	3	2	2	5	6	1	3
3	4	2	1	4	3	3	2	1	2	1	4	2	3	1	3	4	3	4	1	4	2	1	2
4	2	3	3	1	2	1	4	4	1	2	3	4	1	4	2	3	4	2	3	1	3	2	1
$xy$	$xz$	$yz$	$-xz$	$-yz$	$yz$	$-xz$	$-yz$	$xz$	$-xy$	$-xy$	$xy$	$xz$	$-xz$	$-yz$	$yz$	$xy$	$xy$	$xz$	$-xz$	$-yz$	$yz$	$-xy$	$-xy$
$xz$	$yz$	$xy$	$yz$	$-xy$	$-xy$	$-yz$	$xy$	$-yz$	$-xz$	$xz$	$-xz$	$xy$	$-xy$	$xz$	$xz$	$yz$	$-yz$	$-xy$	$xy$	$xz$	$-yz$	$yz$	$-yz$
$yz$	$xy$	$xz$	$-xy$	$xz$	$xz$	$xy$	$-xz$	$-xy$	$yz$	$-yz$	$-yz$	$yz$	$yz$	$-xy$	$xy$	$xz$	$-xz$	$-yz$	$-yz$	$-xy$	$-xy$	$-xz$	$xz$
$3z^2-r^2$	$\frac{2\sqrt{3}}{-\frac{1}{2}b-\frac{1}{2}a}$	$-\frac{1}{2}b+\frac{\sqrt{3}}{2}a$	$-\frac{1}{2}b-\frac{\sqrt{3}}{2}a$	$-\frac{1}{2}b+\frac{\sqrt{3}}{2}a$	$-\frac{1}{2}b-\frac{\sqrt{3}}{2}a$	$-\frac{1}{2}b+\frac{\sqrt{3}}{2}a$	$-\frac{1}{2}b-\frac{\sqrt{3}}{2}a$	$-\frac{1}{2}b+\frac{\sqrt{3}}{2}a$	$b$	$b$	$b$	$-\frac{1}{2}b-\frac{\sqrt{3}}{2}a$	$-\frac{1}{2}b-\frac{\sqrt{3}}{2}a$	$-\frac{1}{2}b+\frac{\sqrt{3}}{2}a$	$-\frac{1}{2}b+\frac{\sqrt{3}}{2}a$	$b$	$b$	$-\frac{1}{2}b-\frac{\sqrt{3}}{2}a$	$-\frac{1}{2}b-\frac{\sqrt{3}}{2}a$	$-\frac{1}{2}b+\frac{\sqrt{3}}{2}a$	$-\frac{1}{2}b+\frac{\sqrt{3}}{2}a$	$b$	$b$
$\frac{x^2-y^2}{2}$	$-\frac{1}{2}a+\frac{\sqrt{3}}{2}b$	$-\frac{1}{2}a-\frac{\sqrt{3}}{2}b$	$-\frac{1}{2}a+\frac{\sqrt{3}}{2}b$	$-\frac{1}{2}a-\frac{\sqrt{3}}{2}b$	$-\frac{1}{2}a+\frac{\sqrt{3}}{2}b$	$-\frac{1}{2}a-\frac{\sqrt{3}}{2}b$	$-\frac{1}{2}a+\frac{\sqrt{3}}{2}b$	$-\frac{1}{2}a-\frac{\sqrt{3}}{2}b$	$a$	$a$	$a$	$\frac{1}{2}a-\frac{\sqrt{3}}{2}b$	$\frac{1}{2}a-\frac{\sqrt{3}}{2}b$	$\frac{1}{2}a+\frac{\sqrt{3}}{2}b$	$\frac{1}{2}a+\frac{\sqrt{3}}{2}b$	$-a$	$-a$	$\frac{1}{2}a-\frac{\sqrt{3}}{2}b$	$\frac{1}{2}a-\frac{\sqrt{3}}{2}b$	$\frac{1}{2}a+\frac{\sqrt{3}}{2}b$	$\frac{1}{2}a+\frac{\sqrt{3}}{2}b$	$-a$	$-a$



Table F.3 The  $\mathcal{E}$  representation

---



---

$E = \begin{pmatrix} 1 & 0 \\ 0 & 1 \end{pmatrix}$	$C_3^{(1)} = \begin{pmatrix} -\frac{1}{2} & \sqrt{3}/2 \\ -\sqrt{3}/2 & -\frac{1}{2} \end{pmatrix}$	$C_3^{(1)^2} = \begin{pmatrix} -\frac{1}{2} & -\sqrt{3}/2 \\ \sqrt{3}/2 & -\frac{1}{2} \end{pmatrix}$
$C_3^{(2)} = \begin{pmatrix} -\frac{1}{2} & -\sqrt{3}/2 \\ \sqrt{3}/2 & -\frac{1}{2} \end{pmatrix}$	$C_3^{(2)^2} = \begin{pmatrix} -\frac{1}{2} & \sqrt{3}/2 \\ -\sqrt{3}/2 & -\frac{1}{2} \end{pmatrix}$	$C_3^{(3)} = \begin{pmatrix} -\frac{1}{2} & -\sqrt{3}/2 \\ \sqrt{3}/2 & -\frac{1}{2} \end{pmatrix}$
$C_3^{(3)^2} = \begin{pmatrix} -\frac{1}{2} & \sqrt{3}/2 \\ -\sqrt{3}/2 & -\frac{1}{2} \end{pmatrix}$	$C_3^{(4)} = \begin{pmatrix} -\frac{1}{2} & -\sqrt{3}/2 \\ \sqrt{3}/2 & -\frac{1}{2} \end{pmatrix}$	$C_3^{(4)^2} = \begin{pmatrix} -\frac{1}{2} & \sqrt{3}/2 \\ -\sqrt{3}/2 & -\frac{1}{2} \end{pmatrix}$
$C_2^{(1)} = \begin{pmatrix} 1 & 0 \\ 0 & 1 \end{pmatrix}$	$C_2^{(2)} = \begin{pmatrix} 1 & 0 \\ 0 & 1 \end{pmatrix}$	$C_2^{(3)} = \begin{pmatrix} 1 & 0 \\ 0 & 1 \end{pmatrix}$
$\sigma_d^{(1)} = \begin{pmatrix} \frac{1}{2} & -\sqrt{3}/2 \\ -\sqrt{3}/2 & -\frac{1}{2} \end{pmatrix}$	$\sigma_d^{(2)} = \begin{pmatrix} \frac{1}{2} & -\sqrt{3}/2 \\ -\sqrt{3}/2 & -\frac{1}{2} \end{pmatrix}$	$\sigma_d^{(3)} = \begin{pmatrix} \frac{1}{2} & \sqrt{3}/2 \\ \sqrt{3}/2 & -\frac{1}{2} \end{pmatrix}$
$\sigma_d^{(4)} = \begin{pmatrix} \frac{1}{2} & \sqrt{3}/2 \\ \sqrt{3}/2 & -\frac{1}{2} \end{pmatrix}$	$\sigma_d^{(5)} = \begin{pmatrix} -1 & 0 \\ 0 & 1 \end{pmatrix}$	$\sigma_d^{(6)} = \begin{pmatrix} -1 & 0 \\ 0 & 1 \end{pmatrix}$
$S_4^{(1)} = \begin{pmatrix} \frac{1}{2} & -\sqrt{3}/2 \\ -\sqrt{3}/2 & -\frac{1}{2} \end{pmatrix}$	$(S_4^{(1)})^3 = \begin{pmatrix} \frac{1}{2} & -\sqrt{3}/2 \\ -\sqrt{3}/2 & -\frac{1}{2} \end{pmatrix}$	$S_4^{(2)} = \begin{pmatrix} \frac{1}{2} & \sqrt{3}/2 \\ \sqrt{3}/2 & -\frac{1}{2} \end{pmatrix}$
$(S_4^{(2)})^3 = \begin{pmatrix} \frac{1}{2} & \sqrt{3}/2 \\ \sqrt{3}/2 & -\frac{1}{2} \end{pmatrix}$	$S_4^{(3)} = \begin{pmatrix} -1 & 0 \\ 0 & 1 \end{pmatrix}$	$(S_4^{(3)})^3 = \begin{pmatrix} -1 & 0 \\ 0 & 1 \end{pmatrix}$

---



---

The basis functions are  $(x^2 - y^2)$  (row 1), and  $(3z^2 - r^2)$  (row 2).

Table F.4 The  $T_1$  representation

---



---

$E = \begin{pmatrix} 1 & 0 & 0 \\ 0 & 1 & 0 \\ 0 & 0 & 1 \end{pmatrix}$	$C_3^{(1)} = \begin{pmatrix} 0 & 0 & -1 \\ -1 & 0 & 0 \\ 0 & 1 & 0 \end{pmatrix}$	$(C_3^{(1)})^2 = \begin{pmatrix} 0 & -1 & 0 \\ 0 & 0 & 1 \\ -1 & 0 & 0 \end{pmatrix}$
$C_3^{(2)} = \begin{pmatrix} 0 & -1 & 0 \\ 0 & 0 & -1 \\ 1 & 0 & 0 \end{pmatrix}$	$(C_3^{(2)})^2 = \begin{pmatrix} 0 & 0 & 1 \\ -1 & 0 & 0 \\ 0 & -1 & 0 \end{pmatrix}$	$C_3^{(3)} = \begin{pmatrix} 0 & 1 & 0 \\ 0 & 0 & -1 \\ -1 & 0 & 0 \end{pmatrix}$
$(C_3^{(3)})^2 = \begin{pmatrix} 0 & 0 & -1 \\ 1 & 0 & 0 \\ 0 & -1 & 0 \end{pmatrix}$	$C_3^{(4)} = \begin{pmatrix} 0 & 1 & 0 \\ 0 & 0 & 1 \\ 1 & 0 & 0 \end{pmatrix}$	$(C_3^{(4)})^2 = \begin{pmatrix} 0 & 0 & 1 \\ 1 & 0 & 0 \\ 0 & 1 & 0 \end{pmatrix}$
$C_2^{(1)} = \begin{pmatrix} 1 & 0 & 0 \\ 0 & -1 & 0 \\ 0 & 0 & -1 \end{pmatrix}$	$C_2^{(2)} = \begin{pmatrix} -1 & 0 & 0 \\ 0 & 1 & 0 \\ 0 & 0 & -1 \end{pmatrix}$	$C_2^{(3)} = \begin{pmatrix} -1 & 0 & 0 \\ 0 & -1 & 0 \\ 0 & 0 & 1 \end{pmatrix}$
$\sigma_d^{(1)} = \begin{pmatrix} -1 & 0 & 0 \\ 0 & 0 & -1 \\ 0 & -1 & 0 \end{pmatrix}$	$\sigma_d^{(2)} = \begin{pmatrix} -1 & 0 & 0 \\ 0 & 0 & -1 \\ 0 & 1 & 0 \end{pmatrix}$	$\sigma_d^{(3)} = \begin{pmatrix} 0 & 0 & -1 \\ 0 & -1 & 0 \\ -1 & 0 & 0 \end{pmatrix}$
$\sigma_d^{(4)} = \begin{pmatrix} 0 & 0 & 1 \\ 0 & -1 & 0 \\ 1 & 0 & 0 \end{pmatrix}$	$\sigma_d^{(5)} = \begin{pmatrix} 0 & 1 & 0 \\ 1 & 0 & 0 \\ 0 & 0 & -1 \end{pmatrix}$	$\sigma_d^{(6)} = \begin{pmatrix} 0 & -1 & 0 \\ -1 & 0 & 0 \\ 0 & 0 & -1 \end{pmatrix}$
$S_4^{(1)} = \begin{pmatrix} 1 & 0 & 0 \\ 0 & 0 & 1 \\ 0 & -1 & 0 \end{pmatrix}$	$(S_4^{(1)})^3 = \begin{pmatrix} 1 & 0 & 0 \\ 0 & 0 & -1 \\ 0 & 1 & 0 \end{pmatrix}$	$S_4^{(2)} = \begin{pmatrix} 0 & 0 & 1 \\ 0 & 1 & 0 \\ -1 & 0 & 0 \end{pmatrix}$
$(S_4^{(2)})^3 = \begin{pmatrix} 0 & 0 & -1 \\ 0 & 1 & 0 \\ 1 & 0 & 0 \end{pmatrix}$	$S_4^{(3)} = \begin{pmatrix} 0 & -1 & 0 \\ 1 & 0 & 0 \\ 0 & 0 & 1 \end{pmatrix}$	$(S_4^{(3)})^3 = \begin{pmatrix} 0 & 1 & 0 \\ -1 & 0 & 0 \\ 0 & 0 & 1 \end{pmatrix}$

---



---

The basis functions are  $x(z^2 - y^2)$  (row 1),  $y(z^2 - x^2)$  (row 2), and  $z(x^2 - y^2)$ .

Table F.5 The  $T_2$  representation

---



---

$E = \begin{pmatrix} 1 & 0 & 0 \\ 0 & 1 & 0 \\ 0 & 0 & 1 \end{pmatrix}$	$C_3^{(1)} = \begin{pmatrix} 0 & 0 & 1 \\ 1 & 0 & 0 \\ 0 & 1 & 0 \end{pmatrix}$	$(C_3^{(1)})^2 = \begin{pmatrix} 0 & 1 & 0 \\ 0 & 0 & 1 \\ 1 & 0 & 0 \end{pmatrix}$
$C_3^{(2)} = \begin{pmatrix} 0 & 0 & -1 \\ 1 & 0 & 0 \\ 0 & -1 & 0 \end{pmatrix}$	$(C_3^{(2)})^2 = \begin{pmatrix} 0 & 1 & 0 \\ 0 & 0 & -1 \\ -1 & 0 & 0 \end{pmatrix}$	$C_3^{(3)} = \begin{pmatrix} 0 & 0 & 1 \\ -1 & 0 & 0 \\ 0 & -1 & 0 \end{pmatrix}$
$(C_3^{(3)})^2 = \begin{pmatrix} 0 & -1 & 0 \\ 0 & 0 & -1 \\ 1 & 0 & 0 \end{pmatrix}$	$C_3^{(4)} = \begin{pmatrix} 0 & 0 & -1 \\ -1 & 0 & 0 \\ 0 & 1 & 0 \end{pmatrix}$	$(C_3^{(4)})^2 = \begin{pmatrix} 0 & -1 & 0 \\ 0 & 0 & 1 \\ -1 & 0 & 0 \end{pmatrix}$
$C_2^{(1)} = \begin{pmatrix} 1 & 0 & 0 \\ 0 & -1 & 0 \\ 0 & 0 & -1 \end{pmatrix}$	$C_2^{(2)} = \begin{pmatrix} -1 & 0 & 0 \\ 0 & 1 & 0 \\ 0 & 0 & -1 \end{pmatrix}$	$C_2^{(3)} = \begin{pmatrix} -1 & 0 & 0 \\ 0 & -1 & 0 \\ 0 & 0 & 1 \end{pmatrix}$
$\sigma_d^{(1)} = \begin{pmatrix} 1 & 0 & 0 \\ 0 & 0 & 1 \\ 0 & 1 & 0 \end{pmatrix}$	$\sigma_d^{(2)} = \begin{pmatrix} 1 & 0 & 0 \\ 0 & 0 & -1 \\ 0 & -1 & 0 \end{pmatrix}$	$\sigma_d^{(3)} = \begin{pmatrix} 0 & 0 & -1 \\ 0 & 1 & 0 \\ -1 & 0 & 0 \end{pmatrix}$
$\sigma_d^{(4)} = \begin{pmatrix} 0 & 0 & 1 \\ 0 & 1 & 0 \\ 1 & 0 & 0 \end{pmatrix}$	$\sigma_d^{(5)} = \begin{pmatrix} 0 & 1 & 0 \\ 1 & 0 & 0 \\ 0 & 0 & 1 \end{pmatrix}$	$\sigma_d^{(6)} = \begin{pmatrix} 0 & -1 & 0 \\ -1 & 0 & 0 \\ 0 & 0 & 1 \end{pmatrix}$
$S_4^{(1)} = \begin{pmatrix} -1 & 0 & 0 \\ 0 & 0 & -1 \\ 0 & 1 & 0 \end{pmatrix}$	$(S_4^{(1)})^3 = \begin{pmatrix} -1 & 0 & 0 \\ 0 & 0 & 1 \\ 0 & -1 & 0 \end{pmatrix}$	$S_4^{(2)} = \begin{pmatrix} 0 & 0 & 1 \\ 0 & -1 & 0 \\ -1 & 0 & 0 \end{pmatrix}$
$(S_4^{(2)})^3 = \begin{pmatrix} 0 & 0 & -1 \\ 0 & -1 & 0 \\ 1 & 0 & 0 \end{pmatrix}$	$S_4^{(3)} = \begin{pmatrix} 0 & -1 & 0 \\ 1 & 0 & 0 \\ 0 & 0 & -1 \end{pmatrix}$	$(S_4^{(3)})^3 = \begin{pmatrix} 0 & 1 & 0 \\ -1 & 0 & 0 \\ 0 & 0 & -1 \end{pmatrix}$

---



---

The basis functions are  $xy$  (row 1),  $xz$  (row 2), and  $yz$  (row 3).

# Appendix G

## Identifying point groups

Applying group theory requires identifying the point group appropriate to the symmetry of the system or molecule. There are many schemes using flow charts to identifying the point group of a molecule (see, for example, reference [G.1]).

### G.1 Definitions of symmetry elements

$E$ : The identity.

$C_n^p$ : Rotation by  $2\pi p/n$  ( $p = 1, 2, \dots, n$ ),  $C_n^n = E$ .

$S_n$ : Improper rotation. A rotation of  $2\pi/n$  followed by a reflection in a plane perpendicular to the rotation axis.  $S_1 = S$  is a reflection through a plane.  $S_2 = i$  (inversion).

$\sigma$ : Reflection through a plane.

$\sigma_h$ : Reflection through a horizontal plane that is perpendicular to the principal axis of rotation. The principal axis is  $C_n$  with the largest value of  $n$ .

$\sigma_v$  or  $\sigma_d$ : Reflection through a plane that contains the principal axis of rotation and is perpendicular to a  $\sigma_h$  plane if one exists. For molecules, if both  $\sigma_v$  and  $\sigma_d$  planes exist, the  $\sigma_v$  planes are assigned to the planes containing the most atoms and the  $\sigma_d$  contain the bisectors of the bond angles.

$i$ : The inversion operation. A center of symmetry (of inversion). If all  $C_n$  and  $S_n$  axes pass through a common point, the point is a center of symmetry or center of inversion.

### G.2 Special point groups

**Cubic:** Tetrahedral, octahedral/cubic, isohedral, and dodecahedral. *A molecule with two or more  $C_n$  axes with  $n > 2$  is a member of the cubic group.*

**Tetrahedral:** Four three-fold axes and no four-fold axes.

$T$ : Three two-fold axes (no reflection planes, no center of inversion).

$T_h$ : Three two-fold axes and a center of inversion.  $T_h = T \times i$ .

$T_d$ : Three two-fold axes and six reflection planes.

**Cubic/octahedral:** Four three-fold axes and three four-fold axes.

$O$ : No center of inversion.

$O_h$ : A center of inversion.  $O_h = O \times i$ .

**Icosahedral:** Six five-fold axes.

$I$ : No center of inversion.

$I_h$ : A center of inversion.  $I_h = I \times i$ .

Linear molecules have an axis about which any rotation is a symmetry element. Any plane containing this axis is a reflection plane. The groups are

$C_{4\infty}$ : No center of inversion.

$D_{4\infty}$ : A center of inversion.

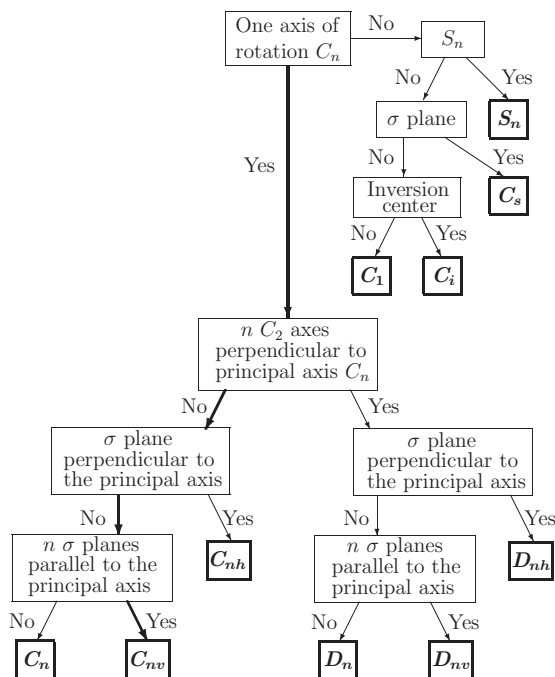


Figure G.1 A flow chart for identifying point groups with no more than one  $C_n$  with  $n > 2$ . The thick arrows show the identification of a  $C_{nv}$  group.

### G.3 Other point groups

If the group has two or more  $C_n$  axes ( $n > 2$ ) it is a member of one of the special groups. A flow chart for identifying other point groups not listed in Section G.2 above is shown in Fig. G.1.

As an example of the use of the flow chart, consider a molecule (e.g.,  $\text{NH}_3$ ). It has only a  $C_3$  axis and three  $\sigma$  reflection (mirror) planes. The thick arrows in Fig. G.1 indicate the flow ending at  $C_{nv}$ . Since  $n = 3$ , in this case the group is  $C_{3v}$ .

*The identification of the elements of a group is not always unique. There can be equivalences among rotations, inversion, and improper rotations, depending on the geometry of the system.* For example,  $D_{6h} = D_6 \times i$  has the operations (a)  $E$ ,  $C_2$ ,  $2C_3$ ,  $2C_6$ ,  $3C'_2$ ,  $3C''_2$ , and  $i$  times these operators. The operations can also be taken as (b)  $E$ ,  $C_2$ ,  $2C_3$ ,  $2C_6$ ,  $3C'_2$ ,  $3C''_2$ ,  $i$ ,  $2S_3$ ,  $2S_6$ ,  $\sigma_h$ ,  $3\sigma_d$ , and  $3\sigma_v$ . In the analysis of a system the choice of the group elements for  $D_{6h}$  as (a) or (b) yields the same results.

### References

- [G.1] D. C. Harris and M. D. Bertolucci, *Symmetry and Spectroscopy: An Introduction to Vibrational and Electronic Spectroscopy* (New York: Dover Publications, Inc., 1978).

# Index

- Abelian groups, 251, 419
- accidental degeneracy, 255
- action table
  - $AB_2$  molecule, 41, 63, 190
  - diatomic molecules electronic states, 195–197, 207
  - graphene energy bands, 369–372, 377, 378, 427, 429
  - $H_2O$  electronic states, 183, 184
  - octahedral complex, 213, 214, 222, 223, 450
  - perovskite energy bands, 281, 285, 286
  - plane wave energy bands, 270, 271
  - square electronic states, 170, 172
  - square vibrations, 7–9, 23, 169
  - tetrahedral complex, 228, 230, 238, 457, 458
- angular momentum
  - crystal field, 93, 112
  - diatomic molecules, 198, 202, 203, 205
  - double group, 150, 198–199, 202, 203, 205
  - multi-electron systems, 95, 98–100
  - nuclear-shell model, 150
  - operators, 100, 112, 129, 131, 133, 155, 338
  - quantum numbers, 66–67, 93, 100, 112, 135, 140, 150, 198–199, 442, 444
  - rotation group, 67, 85
  - spin, 123, 127, 129–132, 135, 138, 140
  - tensors and vectors (Appendix D), 442, 444
  - time reversal, 337, 338
- antiferromagnetic structures, 346, 351–352
- anti-Stokes transitions, 33
- antisymmetric, 79, 99–100, 181, 427, 428, 443
  - representations, 447, 448
  - functions, 96, 98, 99, 101, 109, 131, 132, 145, 156, 172–174, 195, 445, 447
  - vibration, 32–33, 94
- antiunitary operators, 342, 348–350, 354, 356
- axial vector, 89, 443
- band, *see* energy bands
- basis functions
  - $AB_2$  molecules, 39–42
  - Bloch-wave states, 254, 259, 261
  - character table, 428
  - co-representations, 353
  - crystal field, 96, 97, 101–103
  - $D_{4h}$  splitting, 273, 302
  - $D_{\infty h}$ , 195
  - definition, 423
  - diatomic molecules, 195, 197, 210
  - direct product, 82–85, 98, 99, 428
  - double group, 151
  - $^3F$  ground state, 99, 101, 102, 108
  - generation of (symmetry-function-generating machine), 22, 23, 36, 47, 48, 63, 83, 84, 89, 108, 180, 213, 223, 264, 269, 270, 272, 288, 291, 302, 370, 372, 374, 378, 380, 426
  - graphene, 371, 372, 380
  - half-integer angular momentum, 104, 127, 140
  - $H_2O$ , 182–184
  - hybrid, 167
  - irreducible representation for  $O$  group, 451–454, 456
  - irreducible representation for  $T_d$  group, 459–461
  - Jahn–Teller, 117, 118
  - Löwdin orbitals, 165
  - multi-electron, 97, 99, 101
  - octahedral complex, 212, 213, 217, 222
  - perovskite (vibrations), 284, 285, 296
  - phonon, 310, 315, 318
  - plane-wave states, 268, 270, 273, 274
  - product wavefunction, 444
  - projection operator, 426
  - rotation group, 66, 71, 74–76, 78, 79, 85, 88, 89, 99, 108
  - space groups, 250, 254, 259
  - square (electronic states), 168–171
  - square (vibrational states), 5, 7–10, 12, 14, 15, 17, 20, 21, 23–26, 32, 33
  - tetrahedral complex, 229, 233, 238
  - vector model, 97–99
- basis vectors, *see* basis functions
- Bloch theorem, 249–250

- Bloch waves (functions), 249–252, 255, 259, 260, 263, 381  
 Brillouin zone, 250  
 character, 338–339  
 compatibility, 260, 264  
 graphene, 368, 375, 379  
 lattice vibrations, 283  
 plane waves, 264, 268, 270–272  
 point-group symmetry, 252–254  
 representation by, 255, 259, 263  
 space group, 283  
 time reversal, 307, 308, 364  
 block-diagonal matrices, 15, 21, 22, 26–28, 37, 43, 50, 175, 229, 295, 317, 323, 334, 422  
 block-diagonalized secular equation, 175, 184, 198, 213, 238, 288, 290, 297, 302, 320, 322  
 bonds, 31, 117, 168, 184, 199, 204, 208, 209, 213, 307, 383, 385, 393, 462  
 Bragg condition, reflection, 247, 278  
 Bravais lattice, 239–247, 249, 253, 259, 260, 267, 278, 281, 314, 363  
 Brillouin zone, 249, 250, 252, 253, 260, 267, 270, 290, 304  
   cubic, 248, 260  
   graphene, 364, 366, 367, 369, 377, 381, 382, 395, 401  
   hexagonal, 247, 257–258, 260, 266, 271, 276, 283–284, 310–313, 318  
   nanotube, 390, 395, 396, 398, 399, 401–403, 408  
   perovskite, 290, 302  
   square, 243  
 Cartesian, 5, 9, 31, 305  
 cell, *see* unit cell  
 center of mass, 29, 45, 64, 315, 326  
 character  
    $C_{4v}$  group, 16, 19, 22, 23, 32, 248, 262  
   crystal field, 96, 107, 108  
   crystal double group, 150, 151  
    $D^{(l)}$ , 75, 76, 85, 121  
   definition, 16, 18, 412, 428  
   diatomic molecule, 196, 197, 209  
   direct product, 11, 79, 82, 96, 97, 446  
   graphene, 373, 377, 393  
    $H_2O$ , 62, 183, 188  
   Herring rules, 345  
   inversion, 78, 213  
   irreducible representations, 18  
   magnetic groups, 350, 357  
   non-symmorphic group, 264  
    $O_h$ , 78, 79, 88, 108, 211, 261, 273, 287  
   octahedral complex, 213, 222, 223, 228  
   orthogonality, 16, 18, 20  
   perovskite (electronic), 284–286, 289, 291, 293, 296  
   plane wave, 270, 272, 273  
   projection operator, 427  
   rotations, 73, 74  
   same class, 423  
   similarity transformation, 421, 422  
   square (electronic), 183  
   time reversal, 342, 344, 345  
 character tables  
   description of, 427–428  
   for all point groups (Appendix C), 430–437  
   for nanotubes, 437  
    $C_2$ , 42, 360  
    $C_{2v}$ , 187, 297, 310, 320  
    $C_3$ , 346  
    $C_{3v}$ , 171, 261, 263  
    $C_{4v}$ , 16, 26, 33, 190, 261, 262, 293, 310, 428  
    $C_5$ , 374  
    $C_{\infty h}$ , 193, 194  
    $D^{(1/2)}-D^{(2)}$ , 87  
    $D_2$ , 374  
    $D_4$ , 89, 117, 118  
    $D_{3h}$ , 376, 377  
    $D_{4h}$ , 272, 273  
    $D_6$ , 369, 370  
    $D_{\infty h}$ , 193–196, 205  
    $O$ ,  $O_h$  groups, 76, 107, 108, 211, 212, 261, 287, 310, 449, 450  
    $O'$  crystal double group, 152, 153  
    $T_d$ , 229, 456  
 chiral nanotubes, 385, 386  
 class, 15–18, 73, 75, 81, 85, 151, 170, 215, 246, 251, 257, 280, 286, 361, 417–418, 421, 423, 427, 428, 455  
   character of, 17, 20  
   definition of, 15  
   elements of, 17, 418, 449  
 co-representations, 350, 356, 357  
 conduction band, 301, 366, 368, 404, 408  
 configuration  
   bond order, 204  
   crystal field, 98, 111  
    $d^1$ , 91, 92, 94, 117, 226  
    $d^2$ , 95, 96, 99, 103, 107, 114–116, 226  
    $d^3$ , 121, 153, 155, 226, 236  
    $d^4$ , 92, 95, 226, 227, 236  
    $d^5$ ,  $d^6$ , 94, 227, 236  
    $d^7$ , 236  
    $d^8$ , 107, 227, 236  
    $d^9$ , 94, 95, 117  
    $d^{10}$ , 94  
   diatomic molecule, 204  
   double group, 152, 153  
   graphene, 363  
    $H_2O$  electronic states, 186  
   heteronuclear molecule, 208  
   high/low-spin states, 226, 227, 236, 238  
   molecular, 199, 201–202, 204, 209, 220  
   nanotubes, 391  
   octahedral complex, 220  
   perovskite energy bands, 300  
   spin–orbit interaction, 144, 149



- squarene electronic states, 179
  - Zeeman effect, 155
- conjugate-group elements, 338, 375
- correlation diagram, 179, 192, 201
- covering group, 62, 64, 77, 83, 96, 166, 190, 193, 198, 200, 206, 211, 244, 349, 416, 419, 422, 429
- covering operations, 3, 75, 77, 168, 227
- crystal double group, 150–153
- crystal field, 90, 93–96, 99, 152, 153, 211, 222
  - potential, 92, 103–105, 109
  - splitting, 91, 107, 109, 120, 153, 219, 260
- cyclic groups, 419, 428
- decomposition
  - of a representation, 14, 15, 17, 20–22, 27, 28, 35, 36, 42, 43, 75, 79, 83–85, 96, 108, 117, 118, 121, 125, 132, 140, 144, 145, 151–153, 170, 172, 183, 184, 213, 231, 260, 270–273, 287, 288, 291, 293, 297, 311, 315, 321–323, 370, 371, 374, 378
  - of a tensor, 442–444, 447–448
- degeneracy, 27, 90, 116, 148, 154, 198, 221, 263, 268, 271, 275, 340, 342, 344–346, 357, 408
  - accidental, 254
  - energy bands, 396
  - time reversal, 99
- diagonal matrix, 21, 23, 26, 40, 47, 50, 52, 109, 171, 176, 224, 244, 266, 271, 288–290, 295, 331, 413, 414
- diagonalization of a matrix, 2, 43, 198
- diamagnetic, 226, 238, 347, 348
- dimensionality of a representation, 19, 72, 354, 362, 412, 425
- Dirac
  - points, 368, 381, 401, 408
  - relativistic quantum theory, 139
- direct product, 76–83, 89, 96–98, 108, 119, 120, 140, 144, 145, 157, 193, 202, 205, 252, 259, 283, 369, 413, 419, 428, 442, 445, 447, 449
- double groups, 150–153, 346
- double-valued representation, 87
- effective mass, 368, 382
- eigenvalues, 1–2, 21, 26–31, 39, 43, 52, 99–102, 105, 107, 113, 114, 124–125, 129, 130, 136, 139–143, 145, 156, 165, 167, 175, 176, 179, 185, 189, 191, 194, 206, 213, 219, 232, 235, 244, 266, 288, 295, 296, 306, 312, 319–321, 327, 329, 330, 333, 340, 381, 412, 413, 422
- eigenvectors/eigenfunctions, 23, 27, 32, 37, 46, 48, 64, 111, 126, 184, 198, 293, 312, 323, 332, 342, 375, 413
- electric-dipole transition, 187, 205, 237
- electron, 86, 94, 107, 113, 117, 123, 126, 144, 187, 190, 199, 201, 203, 215, 220, 225–227, 231, 236, 241, 265, 276, 277, 301, 341, 368, 383
  - crystal-field splitting of, 90, 91, 93, 96, 98, 109
  - electron–electron interactions, 103, 107–109, 159, 280
  - lone pair, 184
  - multi-electron systems, 66, 74, 82, 95, 96, 98, 129–131, 138–140, 143, 153, 158–160, 171, 181, 195, 339, 340
  - one-electron approximation, 66, 74, 82, 282, 338, 339
  - spin, 123, 125, 129, 131, 138–139, 143, 144
  - two-electron wavefunctions, 82, 96–101, 103–105, 132, 447
- empty-lattice approximation, 266, 276
- energy bands, 243, 244, 254, 260, 262–264, 266–270, 272–282, 284, 286, 294, 296–303
  - bcc, 278
  - cubic, 362
  - degeneracy, 268, 272, 275, 278, 345, 396–398
  - graphene, 363–368, 382, 393
  - LCAO or tight-binding, 291, 293, 304, 320, 363
  - LDA, 299–300
  - nanotube, 393–400, 403–409
  - theory, 261, 280
  - time reversal, 342, 344
  - wavefunctions/states, 275, 288, 290–291, 294
- equivalent
  - atomic sites, 77, 285–287, 289, 314, 318, 334, 372, 378
  - electrons, 98, 136, 145–149, 156, 294, 296, 442–447
  - groups, 4, 347
  - irreducible co-representations, 356
  - irreducible representation, 15, 252, 372, 423
  - oxygen sites, 228, 290, 322
  - representations, 12, 121, 356, 362, 423, 424
  - wavevectors, 253–254, 256, 258, 261, 272, 283, 290, 345, 364, 368, 369, 372, 375
- Euler angles, 72
- even modes, 34
- exclusion principle, 96, 98, 99, 145, 150, 221
- face-centered cubic, 247–249, 276, 278, 313
- factor group, 259, 418, 419
- faithful representation, 421
- Fermi, 150, 366, 382
- ferromagnetic, 346, 359
- force constant, 40, 50, 54, 59–60, 305–307, 327
- Frobenius–Schur test, 357, 359, 361, 362
- full rotation group, 66, 68, 71, 75, 85, 442–444
  - representations of, 71, 85, 87, 444
- glide plane, 246, 350
- group, 11, 32, 73, 117, 168, 169, 182, 263, 270, 289, 290, 295, 296, 302, 310–312, 314, 318–321, 325, 345, 350, 353, 355, 356, 362, 368–370, 372–374, 377, 382, 389, 417, 420–428, 438–441, 445, 450–452, 456, 457
  - Abelian, 251, 419
  - classes of a, 15, 18
  - covering, 62, 63, 77, 83, 96, 166, 190, 193, 198, 200, 206, 211, 227, 244

- cyclic, 251, 252, 419, 428
  - definition/properties of, 4, 5, 15
  - direct-product, 76, 79, 81, 82, 96
  - double, 150–153
  - elements of  $a$ , 4, 8, 10, 16, 17, 33, 38, 41, 68
  - factor, 259, 418
  - full rotation, 66, 68, 71, 75, 85, 87
  - inversion, 77, 78
  - magnetic, 337, 346–351, 357–359, 361
  - multiplication table, 8, 10, 16, 37
  - octahedral, 74–77, 79, 83–85, 88, 99, 108, 117, 121, 151, 152, 211, 212, 221, 224, 259, 260, 361, 449
  - operators, 7, 10, 15, 19, 21, 38
  - order of, 10, 171, 362, 415, 418, 423
  - point, 3, 12, 17, 39, 245, 252, 259, 346, 348, 349, 351, 353, 356, 357, 393, 415, 430, 462–464
  - representations of  $a$ , 12, 443
  - rotation, 70, 95, 97, 127, 150, 151
  - space, 239, 241, 244–246, 252–260, 264, 268, 269, 280, 282, 304, 333, 342–344, 346, 353, 357, 362, 393, 415
  - symmorphic, 249, 250, 252, 255, 258, 259
  - theory, 1, 2, 4, 10, 14, 17, 18, 20, 29, 30, 34, 39, 79, 88, 95, 98, 156, 165, 200, 386
  - tetrahedral, 455
  - of the wavevector ( $\mathbf{g}_k$ ), 253–255, 258–261, 264, 269, 271, 279, 283–384
- Hamiltonian, 15, 75, 76, 79, 82, 83, 91, 95, 158, 337–344, 423
- atomic, 282
  - crystal-field, 91, 109
  - effective, 382
  - eigenfunctions of, 249, 254
  - electronic, 245
  - group of, 82, 96, 98
  - Hartree–Fock, 161, 162
  - hydrogen-like, 93, 98, 129
  - many-electron, 339
  - matrix elements of, 163–165, 174–177, 189, 194, 198, 206, 244
  - molecular, 198
  - one-electron, 66, 282, 338, 339
  - perturbation, 209
  - spin–orbit, 338
  - spinless, 343
  - two-electron, 96, 103, 108
- Hartree–Fock equations, 159–160
- Hermitian, 21, 27, 29, 35, 37, 83, 309, 341, 410, 412
- adjoint, 412
  - matrix, 309
- hole, 92, 95, 107, 117, 368
- homomorphic, 421
- Hund’s rules, 98, 99, 107, 120, 204, 210, 222, 223, 225, 226, 237
- hybrid orbitals, 167, 168, 217, 232
- hydrogen, 39, 54, 123, 140, 157, 183–185, 208, 381
- angular symmetry of orbitals, 161
  - hydrogen-like orbitals/hydrogenic orbitals, 130, 161, 167, 193
- improper rotation, 416
- inequivalent
- carbons, 384, 385
  - electrons, 145, 304
  - irreducible representations, 72, 356, 362, 423, 424
  - wavevectors, 256–257, 364, 368, 382, 404, 405
- integral
- Green’s function, 331
  - interaction, 162, 178, 215, 217, 233
  - overlap, 162–164, 167, 179, 189, 191, 215, 233, 237, 238, 289, 291, 382
- internal coordinates, 5, 31
- invariant, 96, 111, 238
- under full rotation group, 66, 95, 443
  - under  $\mathbf{g}_k$ , 270, 283–284, 369, 372
  - under inversion, 172, 203
  - under  $O_h$ , 296, 314
  - under point group, 253, 415
  - under reflection, 203, 243
  - under similarity transformation, 412, 413
  - under space group, 245, 320
  - under subgroups, 346–349, 351, 353, 356–360, 362, 416–418
  - under time reversal, 346
  - under translation, 241, 249, 263, 346
- inverse, 5, 10, 16, 26, 70, 167, 245, 254, 316, 331, 409, 411, 412, 415, 416, 419, 421, 422, 424
- inversion, 4, 33, 34, 66, 77–79, 89, 94, 99, 100, 114, 117, 168, 172–174, 180, 195, 196, 199, 203–206, 213, 227, 245, 272, 302, 310, 337, 343–346, 350, 358, 369–372, 377, 392, 393, 415, 416, 421, 427–428, 462–464
- irreducible
- representations, 14, 17, 22, 25, 42, 72, 197, 198, 268, 310, 360, 362, 450, 457
  - tensors, 442, 444
- isotope, 3, 327, 328, 331–333
- isotopic substitution, 54, 56, 58
- Jahn–Teller effects, 116
- Koopman’s theorem, 160
- lattice, 241, 243, 249–255, 259, 262–264, 278, 280–285, 290, 294, 295, 299, 302, 304, 305, 307, 309–313, 317, 320, 322, 327–331, 333, 336, 350, 358, 378, 380–382, 384–387, 390
- Bravais, 239, 241, 242, 259, 260, 312
  - reciprocal, 243–244, 246–247, 252–254, 257, 258, 265–268, 276, 277, 283, 335, 343–345, 363, 364, 368, 376, 389, 395, 399, 401, 402, 408
- LCAO method, 161, 162, 282, 290
- longitudinal, 311–313, 317, 319, 334–336, 375

- magnetic, 67, 72, 74, 75, 90, 100, 112, 138, 150, 153–155, 226, 280, 337, 338, 341–344, 346–350, 353, 356–359, 361, 367, 444
- matrix elements, 2, 10, 21–23, 27, 28, 34, 43, 50–55, 58, 60, 79, 83, 84, 88, 89, 99, 103–104, 109, 111, 113, 114, 120, 127, 129, 139, 161–165, 171, 174, 176, 179, 185, 189, 206, 215, 224, 237, 238, 255, 259, 270, 271, 275, 283, 289, 294, 296, 306, 309, 312, 317, 319, 327, 335, 336, 361, 371, 413, 422, 425, 426
- matrix representations, 8, 10, 41, 80, 81, 85, 170, 421
- Miller indices, 277
- mirror plane, 257, 350, 392, 464
- molecular, 9, 59, 158, 182, 183, 211, 223, 327, 361
  - bond, 163, 168, 179, 185, 222
  - complex, 90, 116, 227, 228
  - configurations, 192, 199–201, 204, 209, 210, 227
  - Green's function, 52–54
  - orbitals, 192, 193, 198, 199, 202, 209, 210, 219–222, 225, 236, 237
  - state/level, 32, 159, 161, 171, 179–181, 185–188, 190, 192, 193, 195, 198–203, 205, 209–210, 212, 213, 219–221, 224, 225, 233, 236–238, 282, 429
  - vibrations, 1–3, 5, 15, 23, 29, 32, 35, 40, 52, 53, 165, 219, 304, 429
- nanotube, 363, 383–407
  - curvature and energy gap, 406, 407
  - density of states, 403–406
  - energy bands, 393–401
  - metallic and semiconducting, 401
- Néel temperature, 358
- neutron scattering, 313, 317
- normal divisor (factor subgroup), 347, 418
- normal modes of vibration
  - AB<sub>2</sub> molecules, 39, 44–51, 53
  - AB<sub>3</sub> molecules, 64
  - crystalline solids, 304–328
  - graphene, 370–381
  - infrared-active, 31, 34, 42
  - parity, 32
  - Raman-active, 33
  - square, 1–30
- octahedral complex
  - correlation diagram, 115
  - $d^1$  crystal-field theory, 90
  - $d^2$  crystal-field theory, 94
  - $d^4$  splitting of energy levels, 117
  - $e_g$ – $t_{2g}$  splitting, 76, 94
  - high- and low-spin states, 226
  - Jahn–Teller effects, 116
  - ligand-field theory, 211
- octahedral group ( $O$  and  $O_h$ ), 74–77, 83, 361, 449–454
  - action table, 450
  - character table, 449
  - elements and operators, 449
- optical
  - infrared absorption, 31–34, 42, 314
  - modes, 316–317, 324, 326, 333
  - properties, 31, 158, 301
  - Raman scattering, 33, 34, 43, 84
- optical modes of vibration
  - optical branches, CsCl structure, 314, 327
  - optical branches, graphene, 372
  - optical branches, perovskite structure, 320
- order
  - bond order, 204, 205
  - group, of, 10, 170, 415, 418
  - levels of a transition-metal complex, 235
  - magnetic, 346–350
  - molecular levels, 222
- orthogonal/orthogonality of
  - atomic/atomic-like orbitals, 93
  - characters of different irreducible representations, 16, 423
  - Löwdin orbitals, 166
  - matrix elements between different irreducible representations, 21, 111, 275
  - matrix elements of different irreducible representations, 423–425
- orthonormal vectors, 411, 413
- overlap integral/matrix, 162–167, 174, 176, 179, 189, 191, 194, 198, 215, 233, 237, 238, 289, 291, 382
- oxygen
  - ABO<sub>3</sub> phase factor, 285, 286
  - atoms, 183, 185
  - bands in perovskites, 299–301
  - H<sub>2</sub>O molecules, 184
  - LCAO interactions, 294
  - $\pi$  and  $\zeta$  orbitals, 286, 287
  - sites in perovskites, 190, 191
- paramagnetic, 226
  - type II magnetic group, 347
  - type III magnetic group, 348
- parity, 32, 94, 150, 199, 261, 447
- partner basis functions, 173, 343, 375, 426
- Pauli, 155
  - exclusion principle, 96, 98, 99, 145, 150, 159, 221
  - spin matrices, 123–128, 130, 339, 382
- periodic boundary conditions, 239, 245, 251, 264, 381, 389
- point groups
  - basic theory (Appendix B), 415
  - character tables (Appendix C), 430
  - covering group, 3, 62, 64, 415, 416, 419, 420, 422, 429
  - irreducible representation, 12–20, 42, 72, 127
  - irreducible representations for  $O$ ,  $O_h$  (Appendix E), 449
  - irreducible representations for  $T$ ,  $T_d$  (Appendix F), 455
- polarizability, 33, 317
- primitive

- lattice vector, 239–243, 246–248, 251, 276, 277, 363, 364, 384–386, 390, 391
- reciprocal-lattice vector, 246–248, 257, 276, 277, 363
- projection operator, 22, 426–427
- proper rotation, 66
- quantum
  - coupling of two systems, 442
  - phonon, 304
  - probability, 32, 33
  - theory, 126, 139, 304, 341
  - tunneling, 118
- quantum numbers, 66, 72, 82, 93, 100, 112, 122, 422, 442, 444
  - diatomic molecules, 198
  - $j$ – $m_j$  coupling, 140, 141
  - $L$ – $S$  coupling, 130, 135
- rearrangement theorem, 38, 345, 417, 418
- reciprocal lattice, 243–244, 246–249, 343, 344
  - body-centered cubic, 247, 276, 278
  - Brillouin zone, 247
  - energy bands, 265–268
  - face-centered cubic, 248, 278
  - graphene, 363, 364, 366, 372, 389
  - Herring rules, 345
  - hexagonal, 247, 248, 257, 259, 276
  - nanotube, 395, 401, 402, 408
  - simple cubic, 248, 276, 277, 284, 335
- representations
  - $C_{4v}$ , 9–11, 126, 318, 428, 431
  - character of, 16, 17, 170
  - compatibility, 260
  - constructing, 8–12
  - co-representation, 350–357
  - $D_{4h}$ , 116, 272, 363
  - decomposition of, 13–15, 27, 28, 42, 75, 76, 83–84, 173, 183, 191, 213, 229, 269, 286–287
  - dimensionality, 423–424
  - direct product, 76, 79–83, 96, 97, 121
  - equivalent, 4, 9, 12, 72, 121, 211, 252, 356, 423, 425
  - faithful, 421
  - full rotation group, 68–72, 85
  - half-integer, for, 86, 127, 130, 150–152, 359
  - irreducible, 12, 17, 22, 25, 47, 75, 197, 198, 268, 315, 360, 362, 450, 453
  - matrix, 8–12, 19, 41, 85, 170, 195, 250, 421
  - non-symmorphic, 264
  - number and type of irreducible representations, 15–19
  - $O$  and  $O_h$ , 310, 450–454
  - orthogonality, 17–20, 423–425
  - perovskite, 284
  - plane-wave, 265–267
  - regular, 37–38
  - reducible, 12–15, 72
  - space group, 258, 268
  - symmorphic group, 255
  - $T_d$ , 459–461
  - unitary  $D^{(l)}$  matrices, 72–86
- rotation group, 66–72, 75
  - characters of a rotation, 76
  - decomposition, 97
  - representations of, 70, 71, 85, 87, 127, 446–448
- Russell–Saunders coupling ( $L$ – $S$  coupling), 95, 96, 99, 129–132, 135
- scalar
  - constant, 2, 35, 41
  - operator, 125, 253
  - product, 18, 125, 341, 394, 410, 411, 444
  - tensor, 442–444
- Schrödinger equation, 123, 150
- Schröfnies notation, 350
- Schur's lemma, 424, 425
- screw
  - axis, 246, 350
  - operation, 391, 392
  - rule, 422, 449
- selection rules, 33–34, 82–85, 94, 113, 205, 302, 312, 443
- similarity transformation, 12–16, 19, 21, 26, 29, 30, 50, 165, 227, 316, 421–423
- simple cubic lattice, 262, 266, 269, 283, 309, 310, 312
- singularity, 332, 405, 406
- Slater determinant, 74, 98, 101, 106, 107, 121, 131, 159, 161, 182
- space groups, 239, 242, 244–246, 248, 249, 268, 282, 304, 333, 342, 343, 346, 353, 358, 369, 391, 393, 415
  - definition of, 244
  - non-symmorphic, 246, 264
  - symmorphic, 246, 249, 252, 255, 258, 283
- spherical harmonics, 67, 76, 85, 88, 104, 119, 121, 150, 158, 161, 443
- spin–orbit
  - Hund's rules, 98, 99
  - interaction, 67, 138–140
  - $j$ – $j$  states, 95, 143–149
  - $j$ – $m_j$  states, 140
  - $L$ – $S$  states, 129
  - molecular orbitals, 199
  - nuclear-shell model, 149
  - splitting, 140
  - time reversal, 338–340
  - Zeeman effect, 153
- spinors, 124, 125, 127, 129
- square, 1–3, 6, 7, 11, 15, 16, 20, 22–23, 26, 28–30, 32, 33, 36, 38, 68, 168–171, 175, 179, 180
- star of the wavevector (of  $\mathbf{k}$ ), 255–258, 261
- Stokes transition, 33
- subgroup, 246, 250–256, 258–260, 267, 283, 346–349, 362, 416, 418
  - factor group, 259, 418

- invariant, 346–349, 351, 353, 356–358, 360, 362, 417–418
- symmetry-function-generating machine
  - crystal field, 108
  - direct product, 84
  - graphene, 370, 372, 375, 378, 380
  - H<sub>2</sub>O, 46, 49
  - LCAO model, 181
  - octahedral complex, 215, 223
  - perovskite energy bands, 288
  - plane wave, 269, 270
  - projection operator, 426, 427
  - space group, 264, 272, 288
  - square, 22, 23
  - tetrahedral complex, 231
- tensor, 33, 83, 442–448
- tetrahedral
  - group, 455–461
  - splitting in crystal field, 235
- time-reversal symmetry
  - antiunitary operators, 342
  - band theory, 342–345
  - C<sub>5</sub>, 428
  - co-representation, 350
  - external field, 341
  - Frobenius–Schur test, 357
  - Herring test, 344–346
  - Kramers’ theorem, 427–428
  - magnetic group, 346–352
  - MnF<sub>2</sub>, 357–358
  - operator, 338–342
  - partners, 375
  - quantum systems, 337–340
- trace of a matrix, *see* character
- transformation
  - AB*<sub>2</sub> molecule, 50, 51, 60
  - ABO*<sub>3</sub>, 323
  - Bloch waves, 272
  - graphene, 370
  - inversion, 240
  - LCAO model, 165, 176, 180
  - matrices, 421
  - point group, 421–423
  - rotation group, 66, 69
  - similarity, 121, 412, 413
  - spin, 128, 145
  - square, 12–16, 19, 21, 26, 30
  - tensor, 443, 444
  - time reversal, 354
  - two atoms per unit cell, 316
- translation
  - AB*<sub>2</sub> vibration modes, 43, 44, 49
  - perovskite vibration modes, 323, 325
- space-group operations, 241, 244–246
- square electronic states, 170
- square vibration modes, 2, 23–33
- unit cell, 239, 241, 243, 247, 262, 266, 276, 280–282, 284–286, 289–292, 295, 296, 298, 301, 302, 304–312, 314–315, 320–322, 324, 327, 333, 334, 336, 358, 363, 364, 371, 375, 376, 384, 386, 389, 392–393, 401, 404, 429
- unitary
  - co-representations, 353–357
  - Hamiltonian, 166
  - magnetic group, 346–349
  - matrices, 12, 59, 330, 356, 362, 412, 413, 421, 423, 425
  - rotation group, 85
  - time reversal, 337, 341–342
- valence
  - graphene bands, 364, 366, 408
  - H<sub>2</sub>O states, 186
  - ML*<sub>4</sub> complex, 228
  - nanotube bands, 383, 396–398, 400, 401, 405, 407
  - perovskite bands, 300–301
- variational principle, 159
- vector
  - angular momentum, 86, 95
  - basis, 21
  - displacement, 2, 5–9, 21–23, 26, 40, 41, 44–45
  - electric dipole, 32
  - inversion, 77
  - normalized, 24
  - orthogonal, 17–20, 25, 31
  - rotation group, 68, 70–73
- vibrations (lattice vibrations)
  - axially symmetric model, 307–308
  - eigenvalue equation, 305
  - graphene, 369–381
  - localized modes, 327–337
  - perovskites, 320–327
  - simple cubic crystal, 314
  - two atoms per unit cell, 316–320
- vibrations (molecular vibrations)
  - AB*<sub>2</sub> molecules, 39–52
  - isotopically substituted *AB*<sub>2</sub> molecules, 52–60
  - isotopically substituted H<sub>2</sub>O molecules, 60, 61
  - square, 1–34
- water (H<sub>2</sub>O molecule)
  - force constants, 61
  - isotopically substituted vibrational frequencies, 60
  - vibrational frequencies, 61
- Zeeman effect, 153–155